COALESCENCE OF A SINGLE DROPLET AT A LIQUID - LIQUID INTERFACE

by

M.Greaves B.Tech.

A thesis submitted in partial fulfilment of the requirements for the Degree of Doctor of Philosophy of Loughborough University of Technology.

Department of Chemical Engineering

Director of Research — Professor D.C.Freshwater

Supervisor — Dr.R.M.Edge

Co-Supervisor — Mr.W.F.Calus

September, 1970

ACKNOWLEDGEMENTS

The author wishes to express his thanks to the following:

Professor D.C.Freshwater,Director of Research,Department of Chemical Engineering,Loughborough University of Technology,for the use of Departmental facilities.

The Ministry of Technology,Warren Spring Laboratory,for financial support of the project.

Dr. R.M.Edge,Supervisor of this project,for his guidance and encouragement throughout the course of this work and for his contribution to the theoretical treatment in Chapter 3.

Mr. W.F.Calus,Co-Supervisor of this project,for his helpful criticism of the contents of this thesis.

Dr. D.Muir,for useful discussion on statistics.

Members of the Computing Centre and other Departments of the University.

The technical staff of the Department of Chemical Engineering for their generous assistance.

SUMMARY

The coalescence of single drops at a plane liquid-liquid interface has been studied both theoretically and experimentally.

Experiments were carried out with a wide range of drop size using two and three component systems. The drops coalesced in a partial manner and the drop size ratios between stages were determined. A detailed examination is made of the rest-time distributions for each stage of coalescence. Generally,coalescence rest-times increased with increase in size of drop and fall height of the primary drop. Reasonable agreement between theory and experiment is approached for small drops. Coalescence rest-times of large drops were considerably less than predicted,presumably because of the deformation of the "trapped" film and uneven drainage. The variables affecting the coalescence are analysed and an empirical correlation is formulated to permit prediction of coalescence rest-times.

Observations of the motion of the droplet fluid and the disturbed interface were carried out using schlieren photography. The way in which wave disturbances at the interface can influence the coalescence process is examined. It is shown that that such wave disturbances may be responsible for the existence of the residence time distribution observed in all single drop coalescence studies.

CONTENTS

PHOTOGRAPHIC PLATES

CHAPTER 1

INTRODUCTION

As chemical engineering knowledge develops,increasingly more complex and sophisticated process designs are implemented. One area that has benefited from this advance is the process of liquid-liquid extraction. In this unit operation the recovery and separation of materials is accomplished by transfer between two liquid phases. The process may be one of simple physical transfer of a component,or it may include the more complex aspects of chemical reaction and ion transfer. It is quite understandable therefore,that the range of equipment available for carrying out such operations is extensive. Inevitably, the choice of specific equipment is often a difficult one.

One of the most important factors to be considered in the selection of liquid-liquid extraction equipment is the ease of separation of the dispersion. The rate at which separation occurs is dependent on many physical and chemical factors,but predominant among these is the coalescence behaviour of the drops constituting the dispersion. The separation of most liquid-liquid dispersions can be divided into two stages: (i) the primary stage,during which most of the dispersed drops coalesce to form a continuous phase,and (ii) the secondary stage when the haze of very small drops,left behind from the first stage,finally coalesces and disappears. These two stages can in most cases be clearly distinguished unless the volume fraction of the dispersed phase is very small. It has been shown (83) that in principle,two quite different mechanisms of phase separation in the primary stage can be distinguished. These mechanisms have been termed the interdroplet and interfacial modes of phase separation. The behaviour of an actual dispersion may be a combination of these mechanisms. If the interdroplet mode of phase separation predominates,coalescence within the dispersion layer takes

place primarily between two or more drops. Generally,this mode of coalescence is marked by a wide range of drop sizes in the dispersion. When the interfacial mode of phase separation predominates,coalescence occurs mainly at the interface between the layer of dispersed phase already separated and the dispersion layer.

The study of coalescence in technical equipment is complicated by the large number and wide size range of drops present in such circumstances; furthermore,the hydrodynamics of the process is difficult to define. For this reason considerable attention has been directed towards simple systems in order to obtain fundamental information about coalescence. Hydrodynamically,one of the simplest situations is that provided by the approach of a single drop to a plane interface,and it is to this situation that the present work was confined.

When a drop of liquid (phase-1) falls through a second immiscible liquid (phase-2) on to the bulk interface separating the two phases,it may rest at the interface for a period of time before coalescing. The drop is separated from the interface by a thin film of phase-2 liquid and coalescence occurs when this film ruptures. Coalescence of the drop (primary drop) with the bulk phase-1 liquid may take place wholly or partially. Partial coalescence results in a second smaller drop of phase-1 liquid being formed from the drop. Frequently,the drop may coalesce in several stages,with a smaller drop being produced at each successive stage. The coalescence rest-time* is defined as the time between the arrival of the drop at the interface and its coalescence. This time may include just the first stage of coalesence (first stage coalescence rest-time) or any subsequent stages which occur. The coalescence time of a drop,even for a given system (i.e. phase-1/phase-2) and fixed conditions,is not constant and may take any of a wide range of values. The coalescence time may also

* This is also referred to simply as the coalescence time

be greatly affected by small changes in conditions of the system.

Although a great deal of interest has been shown in recent years in coalescence,many important problems still remain unsolved. In an attempt to consolidate and extend the understanding of coalescence,the aim of the present work was:

(i) To develop an apparatus in which the coalescence rest-times of single droplets at a plane interface could be measured for a wide range of drop size,with minimum disturbance of the bulk interface.

(ii) To determine the coalescence rest-time distributions for all visible stages of coalescence,for a number of liquid-liquid systems.

(iii) To investigate the effect of length of fall of the drop on the coalescence rest-time.

(iv) To develop a correlation between the coalescence rest-time and physical variables.

(v) To observe the motion of the droplet fluid immediately after the rupture of the continuous phase film.

(vi) To investigate the way in which induced disturbances at the interface can influence the drainage of the continuous phase film.

As part of a research contract with the Ministry of Technology, Warren Spring Laboratory,the coalescence in similar systems to those used by Fletcher and Flett (37) was investigated.

Throughout this thesis,a two-component system is regarded as comprising two purified liquids (phase-1 and phase-2),and a three-component,as a two-component system containing a third component in the phase-2 liquid.

CHAPTER 2

LITERATURE SURVEY

Coalescence at a Flat Interface

When a drop of liquid (phase-1) falls gently through a lighter immiscible liquid (phase-2) on to a flat interface* separating the two bulk phases,it rests on the interface for a time t before coalescing with the underlying homophase (phase-1) (16). Osborne Reynolds (111) and other early investigators (46,92,110) attributed this temporary stability to the presence of a residual film of phase-2 liquid,trapped between the drop and the interface. This film is drained out under the combined action of gravity and surface forces (79). When the film reaches a critical thickness,mechanical,thermal,Marangoni instability,or other disturbances arriving randomly in time,rupture the phase-2 film (83). The coalescence begins with the formation by film rupture,of hole in the phase-2 film. The hole expands,whilst the droplet liquid simultaneously drains through in to the lower bulk phase,or homophase (16,28).

2.1 Coalescence Rest-Time

A number of investigators (16,19,33,44,67,79,97) have established that t,the coalescence rest-time,is not constant in either stabilised (i.e. with surfactant present),or unstabilised systems (i.e. without surfactant).

One of the first fundamental experimental investigations concerning coalescence rest-times was carried out by Cockbain and McRoberts (19). These workers studied the coalescence of liquid drops in stabilised systems. They state that if thirty or more identical drops are examined independently,then a reproducible coalescence rest-time

* The interface between the phase-1 and phase-2 liquids is not to be regarded as a simple geometric plane,upon either side of which extend the homogeneous liquid phases,but rather as a thin lamina;the material in this lamina exhibits properties differing from those of either the phase-1 or phase-2 liquids (20).

distribution curve can be obtained and that the distribution curve is approximately Gaussian. Because of the wide spread associated with these distributions the reproducibility of results is an important factor to be considered. In the light of more recent investigations, it is doubtful whether 30 drops are a sufficient population to give good reproducibility of these curves. Cockbain and McRoberts expressed the first stage coalescence time distributions as plots of log N/N_o versus t (Figure 2.1) where N is the number of drops which had not coalesced in time t, and N_o the total number of drops assessed. The shape of the distribution curves expressed in this fashion, suggested to the authors

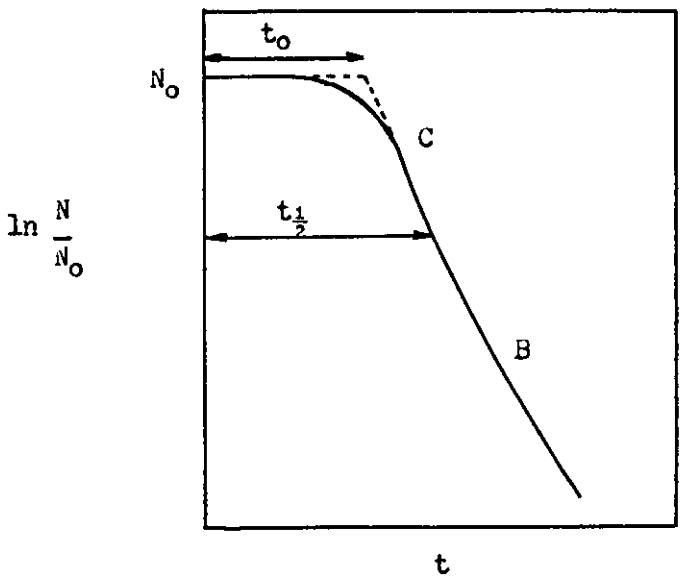

Figure 2.1 Rest-Time Distribution Curve

that coalescence was occurring by drainage and rupture of the film trapped between the drop and the interface. They considered that localised displacement of the surfactant molecules from the interface, was responsible for the rupture of the trapped film. This concept, although accepted by a number of workers (97,134) cannot account for the similar coalescence time distribution curves found in pure two-component systems (16,33,44,68, 79,97). It was found (19) that the portion of the distribution curve BC (Figure 2.1) could be described by the equation:

$$\ln N = kt + \text{constant} \qquad (2.1.1)$$

where k is a constant for the film rupture process.

Gillespie and Rideal (44) proposed an alternative theory for the rupture part of the process, based on irregular thinning of the phase-2 film. They attributed the latter condition to the existence of capillary waves, generated by thermal and mechanical disturbances. Their semi-theoretical analysis, which is somewhat obscure and difficult to follow and assumes an increased probability of rupture as the film thins beyond a critical thickness, produced the following equation:

$$\ln \frac{N}{N_o} = -k(t - t_o)^{3/2} \qquad (2.1.2)$$

where k is a rate constant and t_o and initial drainage period. Gillespie and Rideal, and Charles and Mason (16) were able to correlate their results for unstabilised systems using Eqn. (2.1.2). Other investigators (97), who employed surfactants in their systems, found that their results did not agree with Eqn. (2.1.2). Jeffreys and Hawksley (67), who studied the systems kerosine-water and benzene-water, found that their results were correlated instead by $\ln N/N_o$ vs. $(t - t_o)^{5/2}$ and $(t - t_o)^2$, respectively. The inability to correlate their results for unstabilised systems using Eqn. (2.1.2) was attributed to the presence of a blue dye in the kerosine. This impurity may well have been surface active and it is recognised that the presence of quite a small amount of surface active impurity can considerably modify the behaviour of a system. Agreement with Eqn. (2.1.2) was obtained by these authors for the liquid paraffin-water and redistilled kerosine-water systems.

Elton and Picknett (33), who studied the stability of single drops in the presence of electrolyte, could not correlate their results with Eqn. (2.1.2). Instead they proposed the following equation:

$$\ln \frac{N}{N_o} = -ct^{n_2} \qquad (2.1.3)$$

and found that the exponent n_2 was 2 for concentrated solutions of electrolyte,and 3 for dilute solutions. Eqn. (2.1.3),and equations of the general form:

$$\ln \frac{N}{N_o} = -k(t - t_o)^{n_1} \qquad (2.1.4)$$

have been used to correlate coalescence time distributions for coalescence with mass transfer occurring (66). The effect of mass transfer on coalescence will be treated later in this chapter (see Section 2.12). Jeffreys and Hawksley (68) found that the exponent n_2 in Eqn. (2.1.3) was independent of the system studied and was equal to 4. By substituting $t = (t_{\frac{1}{2}})_1$ and $N/N_o = 0.5$ into Eqn. (2.1.3),they obtained the relationship:

$$c = 0.3(t_{\frac{1}{2}})_1^{-4} \qquad (2.1.5)$$

where $(t_{\frac{1}{2}})_1$ is the half-life of the first stage coalescence. These authors were able to obtain an estimate for $(t_{\frac{1}{2}})_1$ using an empirical correlation based on the physical properties of the system (see Chapter 7 for further details). The correlation is quite complex but the agreement between experimental and predicted points was apparently good. However,one must be critical of the graphical assessment used,because the logarithmic scale for N/N_o tends to smooth the distributions.

Sheludko (116,117) has presented a somewhat obscure modification of the theory of Gillespie and Rideal (44),based on statistical fluctuations in temperature. The following relationship was presented to account for this:

$$f = Ae^{-Bh^2} \qquad (2.1.6)$$

where A and B are constants which are characteristic of the system,and f is the fraction of droplets which have coalesced before the film thins to a certain thickness,h. It should be appreciated,that for random variations in temperature to affect the stability of the draining film,the film thickness would need to be very small,probably less than 25 $\overset{o}{A}$. The idea that a van der Waals force of attraction can cause instability in the film, has also been advanced by Sheludko (118). This would seem to be a more reasonable concept than the one based on temperature fluctuations. Contrary to the author's own results,those of Charles and Mason (16) failed to agree with Eqn. (2.1.6).

Recently,Jeffreys and Hawksley (68),and Hartland (53),have observed that the drop tilts as it approaches the interface. The latter author has proposed that this behaviour may,in part,explain the scatter in the coalescence rest-time. He suggests that tilting of the drop causes unsymmetrical film drainage,which results in preferential film thinning in certain areas of the trapped film. Thus the different times taken to thin down to a critical thickness are responsible for the residence time distribution. One aspect that is difficult to reconcile in this explanation,is the difference between large and small drops. Hartland only examined large drops. We would expect small drops,which are practically spherical,to approach the interface without tilting. It is well known though,that small drops exhibit the same scatter in the rest-time.

Coalescence Phenomena

The process of coalescence,whether it involves a single drop and a plane interface,or two or more drops,takes place by drainage and final rupture of the thin film trapped between them. In practice,the thin film is really a liquid mixture,although in experimental work the liquids are often referred to as being 'pure'.

In the sections which follow various models of the coalescence

process are discussed. These models are very idealised and they assume that the fluid or film drains by creeping flow between two rigid surfaces. Also included is a discussion of the various physical phenomena which affect the drainage process but which have not been accounted for in the idealised models of coalescence.

2.2 Film Shape

The shape of the film trapped between a single drop and an interface is dependent on the pressure distribution within the film and outside the film. To incorporate an exact mathematical description of the film shape in to an analysis of the film flow, would be an extremely complicated matter, and therefore a number of idealised models have been developed (see Fig. 2.2).

If the drop boundary adjacent to the interface deforms in the direction of the drop interior so that a cavity is formed, then the drop is said to be dimpled. The existence of dimpling in gas bubbles has been investigated by Derjaguin and Kussakov (23). The film thickness between a bubble and a flat glass plate was measured using an optical interference technique. They found that the bubble was dimpled and that the phase-2 film was plano-convex in shape and thinnest along a circle of radius R about the axis of symmetry. This position of minimum thickness is often referred to as the barrier ring. Lacking a satisfactory theoretical treatment of this profile, the measured values of R were nevertheless found to be in agreement with the relationship:

$$R = b^2 \left(\frac{2\Delta\rho}{3\gamma} \right)^{\frac{1}{2}} \qquad (2.2.1)$$

where b is the spherical drop radius, $\Delta\rho$ the density diference between the phases, and γ the interfacial tension. The work of Derjaguin and Kussakov has been verified by many workers (17,34,45). It is interesting to note that the position of the barrier ring, for the case of a film formed between two small identical sized drops, is given by the same equation (83*).

A.

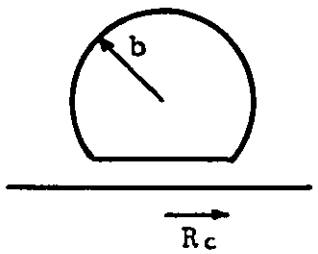

Deformed drop, Rigid interface, Uniform film

B.

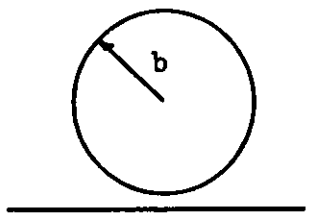

Rigid drop and interface, non-uniform film

C.

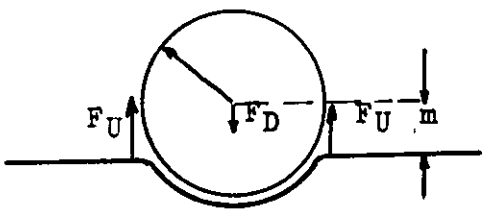

Rigid drop, deformable interface, uniform film

D.

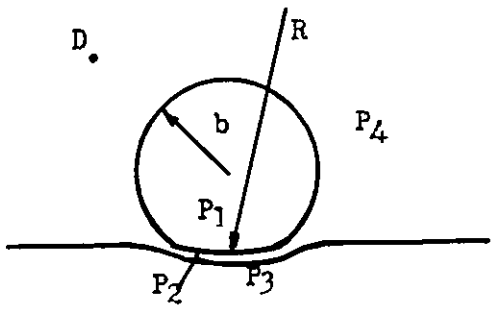

Deformable drop and interface
P_1 -Pressure inside drop
P_2 -Pressure inside film
P_3 -Pressure below interface
P_4 -Pressure above interface

E.

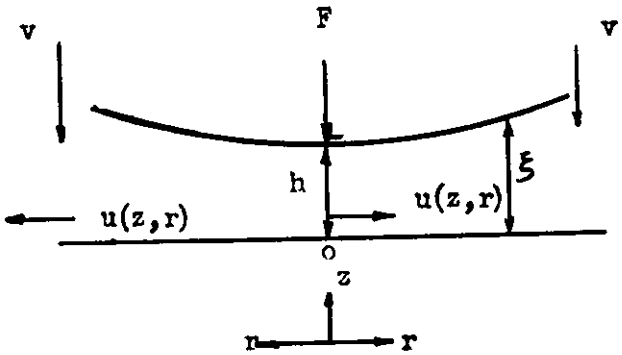

F.

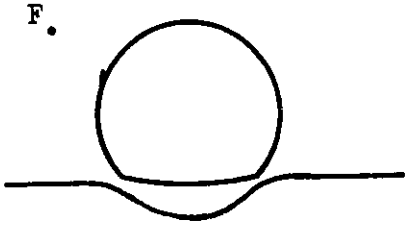

G.

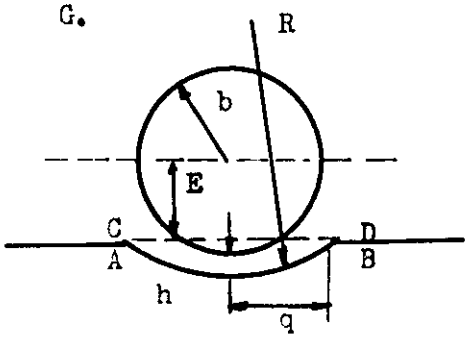

(i)

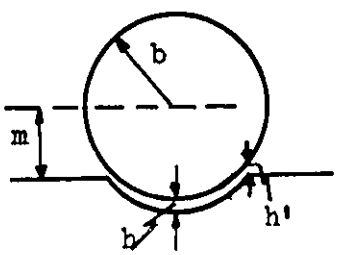

(ii)

Figure 2.2 Idealised Film Drainage Models

The approach of small nitrogen bubbles to a gas-liquid interface has been studied by Allan et al. (2). These workers observed, that after the formation of the barrier ring, thinning took place at a greater rate near the edge of the film than at the centre and that the liquid at the centre was temporarily immobilized. At a film thickness of about 1500 Å there was a bulk movement of the liquid at the centre of the film and the film shape became more uniform. Thereafter, the rate of film thinning was more uniform in all areas of the film, except for occasional high rates observed near the centre. These observations thus illustrate how the film shape must be changing considerably during the film drainage.

MacKay and Mason (89) have investigated the film profiles for electrically charged and uncharged liquid drops approaching a flat liquid interface. For drops of diameter less than about 1 mm., they noticed that the film thickness at the periphery, for the uncharged case, was occasionally 500 - 1000 Å less than at the centre. At coalescence, the trapped film was apparently curved and of uniform thickness. Therefore it seems that dimpling in both gas bubbles and liquid drops, occurs in similar manner. It was discovered that for the charged drop, the film retained the plano-convex shape until rupture occurred. This of course, may have been due to the greatly reduced rest-time, in comparison with the uncharged drop. For both uncharged and charged drops, above about 1 mm. in diameter, film thinning was uneven, some sections thinning more rapidly than others. The fluid dynamics of the coalescence of large drops is complex, and we would expect therefore, some difference in film thinning behaviour, but perhaps in this instance, the problem is mainly associated with the tilting effect mentioned previously.

Jeffreys and Hawksley (68) have carried out pressure drop calculations for the draining film, which indicate that there can be a dimple in the drop and a cavity in the interface. High speed photographic work by these authors has revealed, that frequently, coalescence was initiated at the periphery of the film. Thus, it was entirely reasonable

for them to suggest that this position corresponded to the thinnest part of the film. This is further evidence of possible dimple formation.

Fairly conclusive evidence (photographic) has been presented by MacKay and Mason (89) for the existence of a dimple in a large (1.0 cm. diameter) silicon oil drop. The recent work of Hartland (56,57,58),who used electrical capacitance and photographic techniques to measure the film profile,demonstrates quite conclusively,the occurrence of dimple formation in large liquid drops.

In conclusion,it is reasonably certain that the film trapped between the drop and the interface is non-uniform in thickness. However, further work is required to establish how the film thickness varies during the coalescence process. The importance of this work is readily apparent when it is realised that our ability to develop a satisfactory model for the coalescence process,is very dependent on knowledge of film shape.

2.3 Film Drainage

Over a narrow range of film thickness,MacKay and Mason (89) found good agreement between the observed rate of film thinning and that predicted by Model A (see Fig. 2.2). This occurred only at low values of the film thickness,usually less than 1 micron. In the region where the film thickness was less than 0.2 microns,the rate of film thinning was much greater than that predicted by the theory,suggesting that interface movement was taking place. Thus,it is apparent that the parallel discs model (Model A in Fig. 2.2) does not represent a limiting case,but applies only over some intermediate range of film thickness. In MacKay and Mason's case,this was between 1.0 and 0.2 microns,but the extent of applicability will obviously vary according to the properties of the system.

In attempting to assess the usefulness of particular drainage model, the method of plotting relationships should be examined carefully. MacKay and Mason,using the parallel plates equation (see Eqn. (2.3.9)),

plotted their results in the form $\frac{dh}{dt}$ versus h^3, where h is the film thickness. This plot is very insensitive at low values of h and is not therefore recommended.

Van den Temple (126), who pressed together two oil drops in aqueous solution, found that film thinning approximated to the prediction of model A, if the separation was less than 1000 Å. At separations in excess of this value, the rate of drainage was greater than predicted. Temple suggested that this was because the barrier ring (i.e. the extent of dimple formation) had not reached a sufficiently advanced stage. The reasoning would appear to be, that as the barrier ring moves outwards from the centre of the drop, the resistance to flow within the film increases. Recent work by Hodgson and Lee (83*) has shown that two drops of the same size resting against one another, are equally deformed. This mutual deformation results in a smaller area of contact than between a drop and a plane interface, and by symmetry, the overall shape of the intervening film is plane instead of being a spherical cap. This evidence would therefore tend to support van den Temple's finding that the rate of approach of two drops approximates that predicted by the parallel plates model.

Representing a draining film by a model in which two plane parallel discs approach each other, is valuable because it provides a simplified model more amenable to exact analysis than the dimpled film case. Hodgson (63) has shown, that for small drops, the surfaces of the film are almost plane. Even in the case of larger drops, surface movements from the centre may make the deformed film more uniform in thickness. Since use is made of the parallel discs drainage equation in the present work, it is instructive to present its derivation. Following the treatment of Hodgson (63), the Navier-Stokes equations are used as a starting point:

Viscous flow between immobile interfaces.

A cylindrical coordinate system as indicated in Fig. 2.3, is adopted to suit the symmetry of the problem.

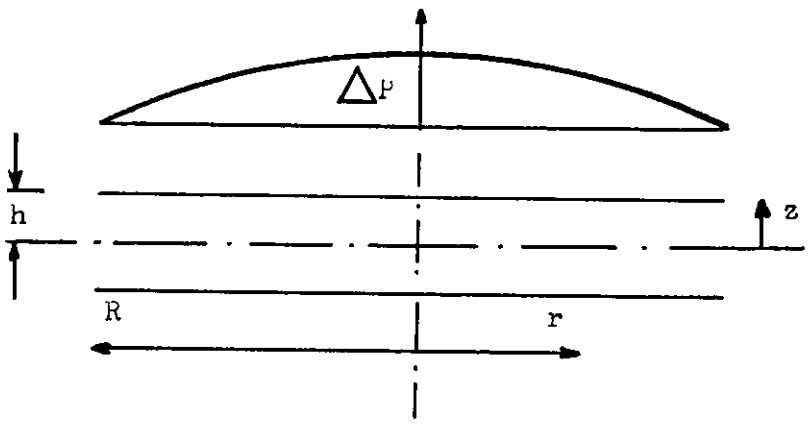

Figure 2.3 Pressure Distribution for Approach of Parallel Plates

(i) Continuity Equation (9):

$$\frac{\partial \rho}{\partial t} + \frac{1}{r}\frac{\partial}{\partial r}(\rho r u_r) + \frac{1}{r}\frac{\partial}{\partial \theta}(\rho u_\theta) + \frac{\partial}{\partial z}(\rho u_z) = 0 \qquad (2.3.1)$$

ρ is constant for the liquid and the $\frac{\partial}{\partial \theta}$ term is zero by symmetry. Therefore:

$$\frac{1}{r}\frac{\partial}{\partial r}(r u_r) + \frac{\partial u_z}{\partial z} = 0 \qquad (2.3.2)$$

(ii) The equation of motion for a liquid of constant density (9) is,

(r component):

$$\rho\left(\frac{\partial u_r}{\partial t} + u_r\frac{\partial u_r}{\partial r} + \frac{u_\theta}{r}\frac{\partial u_r}{\partial \theta} - \frac{u_\theta^2}{r} + u_z\frac{\partial u_r}{\partial z}\right)$$

$$= -\frac{\partial P_f}{\partial r} + \mu\left\{\frac{\partial}{\partial r}\left[\frac{1}{r}(r u_r)\frac{\partial}{\partial r}\right] + \frac{1}{r^2}\frac{\partial^2 u_r}{\partial \theta^2} - \frac{2}{r^2}\frac{\partial u_\theta}{\partial \theta} + \frac{\partial^2 u_r}{\partial z^2}\right\} \qquad (2.3.3)$$

where P_f is the pressure in the film and μ is the viscosity.

θ component: zero by symmetry

z component: assumed to be negligible

In the above r component equation the $\partial/\partial\theta$ and u_θ terms are zero by symmetry, and it is assumed that:

(i) $u_z \approx 0$ but $\frac{\partial u_z}{\partial z} \neq 0$

(ii) $\frac{\partial u_r}{\partial t} = 0$ i.e. a pseudo steady-state.

(iii) $u_r \frac{\partial u_r}{\partial r} \simeq 0$ i.e. inertial terms neglected, valid for creeping flow.

The distribution of the velocity u_r will now be investigated. Since the discs are parallel and remain parallel, it is assumed that $\partial u_z / \partial z$ is f(z) only, i.e. is independent of r. Let $\frac{\partial u_z}{\partial z} = -\omega$. The continuity equation (2.3.2) then becomes:

$$\frac{1}{r} \frac{\partial}{\partial r} (r u_r) - \omega = 0$$

with boundary conditions $u_r = 0$; $r = 0$. Integrating:

$$u_r = \tfrac{1}{2} \omega r \qquad (2.3.4)$$

The implication of this equation is that the velocity profiles at various radial positions are geometrically similar. The equation of motion (2.3.3), with the above simplifications, is:

$$\mu \frac{\partial^2 u_r}{\partial z^2} = \frac{\partial P_f}{\partial r} \qquad (2.3.5)$$

If z is measured from the mid plane (fig. 2.3) then $\partial u_r / \partial z = 0$, $z = 0$ for all r. A further boundary condition in the case of immobile interfaces is:

$$u_r = 0 , \quad z = \frac{h}{2} \text{ for all r.}$$

Integrating Eqn. (2.3.5) subject to these conditions:

$$u_r = -\frac{1}{2\mu} \left(\frac{\partial P_f}{\partial r}\right) \left[\left(\frac{h}{2}\right)^2 - z^2 \right] \qquad (2.3.6)$$

Equating u_r from Eqns. (2.3.4) and (2.3.6), $(\partial P_f / \partial r) = -K_z r$, where $K_z = \mu \omega / \left[\left(\frac{h}{2}\right)^2 - z^2 \right]$ and is a function of z only. Integrating with respect to r and setting $P_f = 0$ when $r = 0$ for all z:

$$\triangle P_f = -\tfrac{1}{2} K_z r^2 \qquad (2.3.7)$$

The distribution of P_f with r is thus parabolic. However, the pressure on the drop side of the interface is virtually uniform. This is a

fundamental inconsistency in the plane discs model. To circumvent this difficulty, we equate the total forces on either side of the interface:

$$F = \int_0^R - \Delta P_f . 2\pi r \, dr$$

where F is the force acting on the discs. Hence, $K_z = 4F/\pi R^4$ and is independent of r as required. Substituting above for K_z and hence ω, we obtain:

$$u_r = \frac{2}{\pi} \frac{F}{\mu} \frac{r}{R^4} \left[\left(\frac{h}{2} \right)^2 - z^2 \right] \qquad (2.3.8)$$

The rate of approach of the discsfollows from equating the total rate of outflow to the rate at which the liquid is displaced from the film:

$$Q = \int_{-h/2}^{h/2} u_r . 2\pi R \, dz = - \pi R^2 \frac{dh}{dt} \qquad (2.3.9)$$

i.e.

$$- \frac{dh}{dt} = \frac{2}{3} \frac{F}{\mu} . \frac{h^3}{\pi R^4}$$

This equation is identical with that previously quoted in the literature (16). Eqn. (2.3.9) was first derived by Osborne Reynolds (111). However, the methods that he used do not readily give the shear stress distribution at the surface. For drainage of the film from thickness h_1 to thickness h_2, the drainage time is:

$$t_2 - t_1 = \left(\frac{3\pi \mu_2 R^4}{4F} \right) \left(\frac{1}{h_2^2} - \frac{1}{h_1^2} \right) \qquad (2.3.10)$$

Assuming that a liquid drop of radius b approaches a flat liquid interface under its own weight, and deforms only slightly, the expression for F is (16):

$$F = \frac{2\pi \gamma R^2}{b} \qquad (2.3.11$$

where R is given by Eqn. (2.2.1). Substituting into Eqn. (2.3.10):

$$t_2 - t_1 = \frac{\mu_2}{4} \left(\frac{\Delta\rho g b^5}{\gamma^2}\right) \left(\frac{1}{h_2^2} - \frac{1}{h_1^2}\right) \qquad (2.3.12)$$

which reduces to:

$$t_2 - t_1 = \frac{\mu_2}{4} \left(\frac{\Delta\rho g b^5}{\gamma^2}\right) \left(\frac{1}{h_2^2}\right) \qquad (2.3.13)$$

when $h_1 >> h_2$.

Charles and Mason (16) considered the case of a sphere of radius b approaching an unbounded plane. This is sometimes called the spherical-planar model (see Fig. 2.2B). The space between the surface and the plane contained a liquid of viscosity μ_2. The distance between the surface and the plane at the vertical mid-axis was h, and at any radius r, ξ. ξ was a function of r. They assumed that the velocity of the liquid being squeezed out, u, was a function of r and z, and that the velocity profile was parabolic. Equating the work done by the force F to the energy dissipated by viscous forces, Charles and Mason obtained the expression:

$$V = -\frac{dh}{dt} = \frac{F}{6\pi\mu_2 \int_0^r \frac{r^3}{\xi^3} dr} \qquad (2.3.14)$$

To render their approach tractable, they substituted for the sphere, a parabola of the same radius of curvature at the apex (see Fig. 2.2.E), and therefore:

$$\xi = h + \frac{r^2}{2b} \qquad (2.3.15)$$

which on substitution into Eqn. (2.3.14) and integration from r = 0 to r = b, gave:

$$\frac{dh}{dt} = -\frac{Fh}{6\pi\mu_2 b^2} \qquad (2.3.16)$$

for $b >> h$.

Further integration between the limits h_1 and h_2 yielded the following equation:

$$t_2 - t_1 = \left(\frac{6\pi\mu_2 b^2}{F}\right) \ln\left(\frac{h_1}{h_2}\right) \qquad (2.3.17)$$

It is pertinent to report that both the equations (2.3.14) and

(2.3.17) were earlier derived by Taylor (122). Eqn. (2.3.17) was previously given without derivation by Hardy and Bircumshaw (52). We see in the film thickness term of Eqn. (2.3.17) the fundamental difference between this non-uniform film model (spherical-planar) and the uniform film model (parallel plates). The numerical value of the term $\ln (h_1/h_2)$ will always be very small in comparison with the $(1/h_2^2)$ term in Eqn. (2.3.13). Therefore, in the case of drops which retain a spherical shape (or deform only slightly), e.g. very small drops or moderately sized drops in high interfacial tension systems, Eqn. (2.3.17) will predict a very small rest-time.

Using an approach similar to that employed by Charles and Mason, McAvoy and Kintner (93) derived an equation for the approach of two solid spheres in a liquid field:

$$t_2 - t_1 = \frac{3\pi\mu_2 b^2}{F} \ln \left(\frac{H_1}{H_2} \right) \qquad (2.3.18)$$

where $H = 2h$ is the minimum separation distance, and $b >> h$. It is interesting to compare this equation with Eqn. (2.3.17) obtained by Charles and Mason. We see that the only difference between the time of approach for a sphere to a flat plane, and to another sphere, is a numerical constant.

The case of a rigid drop and a deformable interface, Model 2.2C, where the interfacial film has a spherical shape, was proposed by Lang (79). The force balance, first obtained by Nielsen (98) was:

$$m\left(1 + 2\gamma m/(\rho_1 - \rho_2)gb^2 - m^2/3b^2 \right) = 2\gamma/(\rho_1 - \rho_2)gb - \frac{2}{3} b \qquad (2.3.19)$$

where m is the distance from the centre of the drop to the flat undisturbed interface. The time require to thin to a film thickness h_2, based on parallel discs equal in area to the spherical segments was:

$$t_2 - t_1 = 9/\mu_2 b^2 (b - m)^2 / (2b^3 + 3b^2 m - m^3) (\rho_1 - \rho_2) g h^2 \quad (2.3.20)$$

provided that $h_1 \gg h_2$. Eqns. (2.3.19) and (2.3.20) have been solved simultaneously by Chappelear (18). The results were presented in terms of dimensionless groups and it was found that the relative equilibrium deformation is only a function of the dimensionless group:

$$\Pi_5 = \frac{\gamma}{b^2} (\rho_1 - \rho_2) g \quad (2.3.21)$$

It is of course hardly unexpected, that the shape of the deformed drop and bulk interface is dependent on the variables contained in Eqn, (2.3.21). This is explained in more detail by Princen (103). The results of the numerical solutions for small deformations, approach those of model 2.2A, given by Eqn. (2.3.13).

Lang (79), who derived the time of approach for Model 2.2C to be:

$$t_2 - t_1 = \left[12 \pi b^4 / \mu_2 (\cos p - 1 - 4 \ln \cos(\tfrac{p}{2}) / F) \left(\frac{1}{h_2^2} - \frac{1}{h_1^2} \right) \right] \quad (2.3.22)$$

incorrectly assumed that the force causing drainage was $F_D + F_U$ (see Fig. 2.2C). It is apparent from a consideration of the simple drainage mechanics, that the correct drainage force is $F = F_D = F_U$. Hartland (53) has derived a similar equation to Lang for the same conditions:

$$t_2 - t_1 = \frac{6 \pi R^4 / \mu_2 Q}{F} \left(\frac{1}{h_2^2} - \frac{1}{h_1^2} \right) \quad (2.3.23)$$

where $Q = 1 - \cos\theta_c - \frac{1}{2}\sin\theta_c^2$, R is the overall radius of curvature of the film and θ_c is the inclination of the edge of the film to the horizontal axis. It is to be expected that these two equations will produce very similar drainage times.

Schotland and Hale (114) using Lang's model, found the time for liquid drops falling through a gaseous phase to a flat interface to be:

$$t = \pi \left(\frac{\rho_1}{12\gamma} \right)^{\frac{1}{2}} \cdot a^{3/2} \qquad (2.3.24)$$

This work, which has a meteorological background, serves to demonstrate to the reader the wide range of topics where a basic understanding of coalescence phenomena is important.

The two previous models which have been discussed (2.2A and C) are limiting cases (in terms of physical geometry) where $R_1 = \infty$ and $R_1 = b$, respectively; R_1 being the radius of curvature of the film. A more general model would have a constant but arbitrary radius of curvature at the surface of contact. If one assumes small spherical deformations and equal deformations on both sides of the film:

$$P_1 - P_2 = \frac{2\gamma}{R_1} = P_2 - P_3 \qquad (2.3.25)$$

(see Fig. 2.2). Neglecting the hydrostatic head, which would be satisfactory for a very small drop, then $P_1 - P_3$ is equal to the pressure drop across the free surface of the drop. Thus:

$$P_1 - P_3 = \frac{4\gamma}{R_1} = \frac{2\gamma}{b} \qquad (2.3.26)$$

This is the deformable drop and interface model presented by Chappelear (18). This model would appear to be the most realistic of the uniform film models, especially for large drops which are greatly deformed. For a sufficiently small drop, the following approximate equation can be derived:

$$t_2 - t_1 = \frac{\mu_2}{i} \cdot \left(\frac{\Delta\rho g b^5}{\gamma^2} \right) \left(\frac{1}{h_2^2} \right) \qquad (2.3.27)$$

Eqn. (2.3.13), as derived by Charles and Mason (16), may be put in the same form as Eqn. (2.3.27). The only difference between these two equations would then be the value of i. For Eqn. (2.3.13) $i = 4$ and Eqn. (2.3.27) $i = 1$. This means that the area required to support the drop according to Eqn. (2.3.27) is only half as much as for Charles and Mason's model. It would appear then that small drops present proportionately less area for

film formation than do larger drops.

All uniform film models predict that the rest-time increases as b^5 and with increasing density difference. However, these predictions require some qualification in the light of experimental findings. The rather surprising effect of increasing density difference can be explained on the basis of increased film area. This opposes the direct effect of increased drainage force due to increased density difference, but a number of workers have contested this point In practice, the effect of drop radius has been observed to be much less than b^5. Therefore Model 2.2B might be a better approximation in the case of very small drops since this model predicts that the rest-time decreases with increasing radii and density difference. Intermediate radii would then require a 'mixed' model.

To satisfy their results for the benzene-water system, for which t was proportional to the drop diameter, Jeffreys and Hawksley (68) proposed a 'mixed' model possessing a drainage film of non-uniform thickness (see Fig. 2.2G). For their model (i), the film was thinnest at the centre, and for model (ii) thinnest at the periphery. The distance m was obtained from a force balance. The upward force F_U due to the surface tension, given by:

$$F_U = \frac{2\pi (b^2 - m^2)\gamma}{b} \qquad (2.3.28)$$

was equated with the downward force, equal to the weight of that part of the drop above the interface, given by:

$$F_D = \frac{4}{3}\pi b^2 (\Delta\rho)g - \left(\frac{2}{3}b^2 - bm^2 + \frac{m^3}{3}\right)$$

In a similar manner to that of Charles and Mason (16), and substituting appropriately in Eqn. (2.3.14), Jeffreys and Hawksley (68) derived the following equation for their model (i):

$$t_2 - t_1 = \frac{-6\pi\mu_2}{4F\phi^2}\left[\ln\frac{h_2}{h_1} + \ln\frac{(h_1+\theta)}{(h_2+\theta)} + \frac{\theta}{h_2+\theta} - \frac{\theta}{h_1+\theta}\right] \qquad (2.3.29)$$

where, $\phi = \frac{1}{2b}(1 - \lambda)$, $\theta = (\lambda - 1)(b - m)$ and $R = \lambda b$. The drainage equation derived for model (ii) was similar to Eqn. (2.3.29).

The application of the equations derived for the respective models above, by Jeffreys and Hawksley, requires that arbitrary limits of h_1 and h_2 be chosen and an appropriate value of λ selected. This is not altogether satisfactory, since although the value of h_1 was shown to be not very critical the value of t is extremely sensitive to the chosen value of h_2. Jeffreys and Hawksley were unable to use their model (ii) to predict experimental results. This is disappointing, all the more so because model (ii) is the most realistic of the two cases considered. Although the agreement obtained between the experimental results and those predicted by the model (i) equation was good, the real value of these semi-empirical equations is subject to some doubt.

Princen has derived equations which give the pressure inside the film and the drop (102). These enable one to calculate the excess pressure across the surface of the drop, and hence determine the drop-interface profile or shape. Details of Princen's method are contained in Appendix 4, together with drop shape characteristics for a wide range of liquid-liquid systems. He has also shown that the drainage equation for the case of an infinitely large drop (assuming a uniform film thickness) is:

$$t_2 - t_1 = \frac{3\mu_2 b^3}{\gamma} \cdot \left(\frac{1}{h_2^2}\right) \qquad (2.3.30)$$

where $h_1 \gg h_2$. This is a very interesting equation since it predicts a dependency on the drop radius b to the third power, whereas all other uniform film models predict a dependency to the fifth power. To date, coalescence rest-time experiments have been mainly concerned with drops having a diameter greater than about 0.5 mm. The drop size dependency in these cases, has been shown to be considerably less than b^5. Charles and Mason (16), found that for the benzene-water system and a drop size greater than 0.1 cm.

the dependency on drop was $b^{3.15}$, approximately. This is remarkably close to that predicted by Princen's equation (2.3.30).

So far, the discussion has only been concerned with the process of film thinning. It is necessary at this point to consider some aspects of film drainage which are not explainable soley in terms of fluid mechanics.

MacKay and Mason (89) have observed (using an optical interference technique) that the average rupture thickness of the film beneath liquid drops was less than 500 Å, when the drop diameter was less than 0.1 cm. At larger drop diameters than this, film thinning was uneven, but part of the film was usually observed to have a critical thickness less than 500 Å. Using Eqn. (2.3.10) as an example, the calculated drainage time required to approach a film thickness of 500 Å would be at least an order of magnitude greater than the experimental rest-time. If fluctuations in temperature are responsible for the rupture of the film, which as Ewers and Sutherland (35) have pointed out will only occur if the film thickness is less than 50 Å, then the situation is even worse. Therefore we should conclude that other forces, in addition to gravity and surface forces, become important as the film thins.

It must be emphasised that the equations describing the approach of drops to liquid-liquid interfaces are subject to many limitations. It is assumed that the electrical double layer interaction (28), the electro-viscous effect (31,32), disjoining and London-van der Waals forces of attraction (28,73,99) are negligible. Furthermore, it is assumed that the interfaces are rigid and thus resist shear stresses due to finite velocity gradients at each surface. If liquid drops and bubbles are unable to resist imposed tangential surface stresses, they will have internal circulation (40-43,49,86,112). Infact, it is a common acceptance that a free interface in a pure system cannot support a shear stress. Hodgson (63) has stated, that a more satisfactory concept is that free movement, retarded mobility, and complete mobility of the interface are all possible modes of behaviour

in film flow. Rigid behaviour is reported to occur only with low velocity gradients,high interfacial tension (greater than 30dyne $cm.^{-1}$),and in the presence of surfactants (40,86).

2.4 Interface Curvature and Pressure Drop in the Draining Film

In a liquid-liquid system,inwhich a drop of liquid is resting on a liquid-liquid interface,both the drop and the interface are distorted. If the film is thin,it has the general shape of a spherical cap (18,53,79, 102,103). The film profile,i.e. the variation of film thickness with distance from the centre of the film,is dependent on the pressure distribution in the flowing film. It is important therefore,to present some of the more important details of an analysis of the pressure drop in the draining film as carried out by Jeffreys and Hawksley (68).

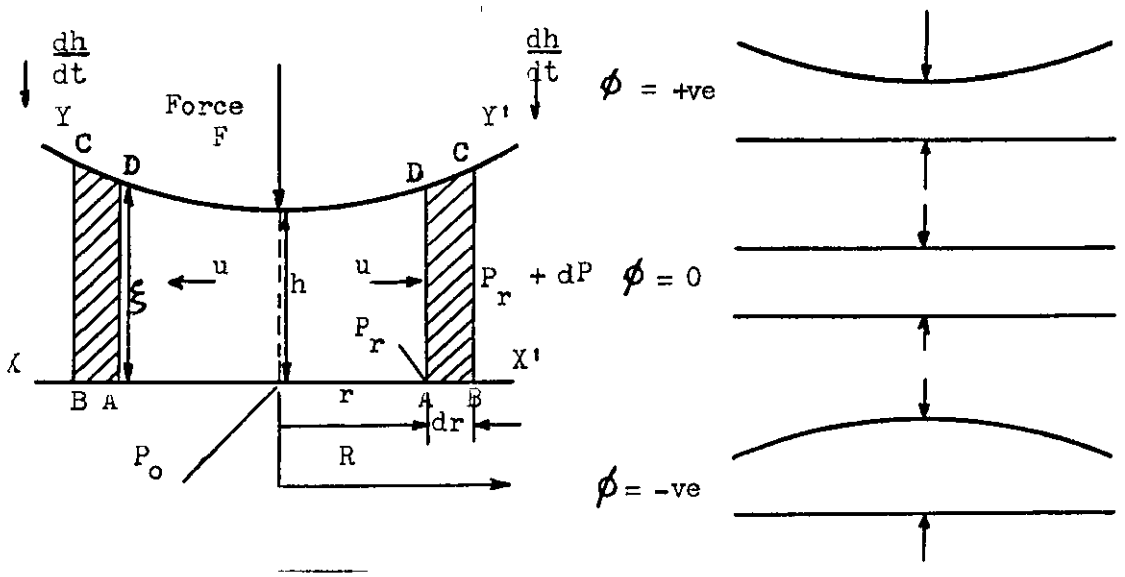

Figure 2.4 Film Pressure Drop Models (68)

The continuity equation for flow through the element ABCD is:

$$\frac{\partial}{\partial r}\left[r \int_0^{\xi} u.dz \right] = r \frac{dh}{dt} \qquad (2.4.1)$$

and assuming that the velocity profile is parabolic,and u is a function of r:

$$u = z\,(\xi - z)\,f(r) \qquad (2.4.2)$$

A rate of momentum balance over the element ABCD gave:

$$-4\pi r\mu_2\left(\frac{\partial u}{\partial z}\right)\Big|_{z=0} \cdot dr - \frac{\partial}{\partial r}\left[2\pi r\rho_2\int_0^{\xi} u^2\,dz\right]dr$$

$$-2\pi r\xi\,dP = 0 \qquad (2.4.3)$$

The solution of these equations produced a relationship for calculating the pressure at any radial distance r. For films of uniform thickness, $\xi = h$ and $\phi = 0$, the full equation reduced to the following form:

$$\Delta P_f = -\frac{2F}{\pi R^2} - \frac{F^2\rho_2 h^4}{15\pi^2\mu_2^2 R^6} \qquad (2.4.9)$$

Therefore, for thin films, when h is small, ΔP_f is independent of viscosity and film thickness. This conclusion may be misleading. The term $-2F/\pi R^2$ suggests that the parallel plates and spherical planar models would infact be limiting cases for film flow. If the change in film shape, from one of these extremes to the other, was not dependent simply on R, the parallel plates model would no longer represent a limiting case.

In order to evaluate the system completely, it is necessary to know the pressure distribution at the surface of the drop. Jeffreys and Hawksley calculated this from measurements of the radii of curvature of the drop obtained from projected photographs. Direct measurement of radii of curvature in this way, is not very precise, and MacDonald (94) has emphasised the difficulties involved. However, we would expect the analysis to indicate those aspects which are most likely to affect film drainage. Jeffreys and Hawksley concluded that the film was of non-uniform thickness and least thick at the periphery. A number of investigators have shown this to be true, at least for pure systems.

Hodgson (63) has attempted to explain the phenomenon of dimple formation by considering changes in interface shape, in terms of departure from the model of parallel plates. Frankel and Mysels (38) have treated the

the problem and its effect on film drainage, by consideration of a two-dimensional analysis. Assuming that the departure from parallel plates was small, Hodgson neglected the higher order powers of $\frac{dz}{dr}$ in the differential equations describing the principal radii of curvature. Thus:

$$\frac{1}{\beta_1} = \frac{d^2z}{dr^2} \quad \text{and} \quad \frac{1}{\beta_2} = \frac{1}{r}\frac{dz}{dr} \tag{2.4.5}$$

Then:

$$P = -\frac{\gamma}{r}\frac{d}{dr}\left(r\frac{dz}{dr}\right) \tag{2.4.6}$$

and,

$$\frac{dP}{dr} = -\frac{d}{dr}\left[\frac{1}{r}\frac{d}{dr}\left(r\frac{dz}{dr}\right)\right] \tag{2.4.7}$$

for a pressure gradient in the r-direction only. By assuming the same pressure gradient as pertaining in the plane discs model, it is possible to integrate Eqn. (2.4.7) and hence calculate the deformation from parallel plates. Hodgson concluded that if the deformation was small compared with the film thickness, then the model would give a fair approximation to the rate of film drainage. He found the deformation to be:

$$d = \frac{a^3 \Delta\rho\, g}{6\gamma} \tag{2.4.8}$$

Except for very small drops, d will only be very small in comparison with the film thickness, at relatively large separations. It may also partly explain why small drops (less than 0.05 cm. diameter), which are almost spherical, have coalescence times which are much greater than those predicted by the spherical-planar model equation.

The shape of the drop interface was given by (see Fig. 2.5):

$$(h_o - h_r) = \frac{d}{R^4}(2R^2 - r^2)r^2 \tag{2.4.9}$$

The value of R was found to be identical with the value of R calculated for model A in Fig. 2.2, but with allowance for interface deformation, i.e.

$$R^2 = \frac{Fb}{2\pi\gamma} \tag{2.4.10}$$

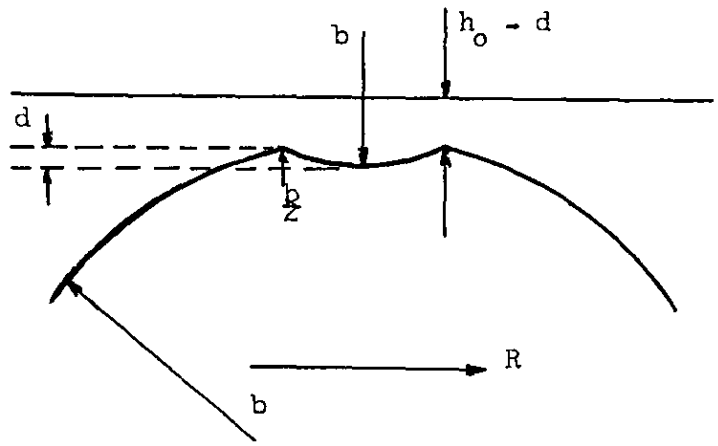

Figure 2.5 Drop Dimpling at a Rigid Interface (63)

Once the interface has deformed to the shape given by Eqn. (2.4.9), drainage will be similar to that predicted by the parallel disc model, with virtually no change in interface shape until d becomes comparable with the film thickness. When the film thickness varies appreciably with r, the rate of film drainage must deviate significantly from that of parallel discs.

Frankel and Mysels analysis (38) considered the film periphery only. Since the interface here is flat, there is no curvature, and:

$$P_{nn}^{(1)} - P_{nn}^{(2)} = \gamma \left(\frac{1}{\beta 1} + \frac{1}{\beta 2} \right) \qquad \text{(After Levich (84))}$$

reduces to:

$$P_{nn}^{(1)} - P_{nn}^{(2)} = \gamma \frac{d^2 z}{dr^2} \qquad (2.4.11)$$

and since the pressure on the drop side of the interface is constant:

$$\frac{dP}{dr} = \frac{d^3 z}{dr^3} \qquad (2.4.12)$$

Considering small drops and rigid interfaces, the flow at any radius r is given by:

$$Q_r = \int_{-h/2}^{h/2} 2\pi r u_r = \frac{1}{12} \mu \left(- \frac{dP}{dr} \right) h_r^3 \, 2\pi r \qquad (2.4.13)$$

The following equation was given by Frankel and Mysels, and may be obtained by substitution of Eqn. (2.4.12) in Eqn. (2.4.13):

$$Q_r = \frac{\gamma}{12\mu} \left(\frac{d^3 h_r}{dr^3} \right) h_r^3 \qquad (2.4.14)$$

By assuming the flow per unit length of periphery to be constant, they were able to integrate Eqn. (2.4.19). From the shape of the dimple thus obtained, they predicted the rate of drainage (assuming the flow at the periphery to be $\pi R^2 \frac{dh_o}{dt}$). Not surprisingly, they found the rate of approach of the interfaces (at the periphery), to be close to that of parallel plates. This treatment is inadequate because, although it predicts that the dimple becomes more pronounced as the film thickness decreases, no allowance is made for the variation in flow with radius, brought about by the changing film shape.

For large drops it is conceivable that the value of d calculated from Eqn. (2.4.8) will be greater than the separation distance at which the barrier first forms. It is obvious that the film drainage must then be very different from that predicted by the usual parallel plates equation. Considering one interface to be rigid, reference to the corresponding observations (32,38,44) shows that while the barrier ring is still developing, the entrapped film is still substantially uniform (see Fig. 2.6).

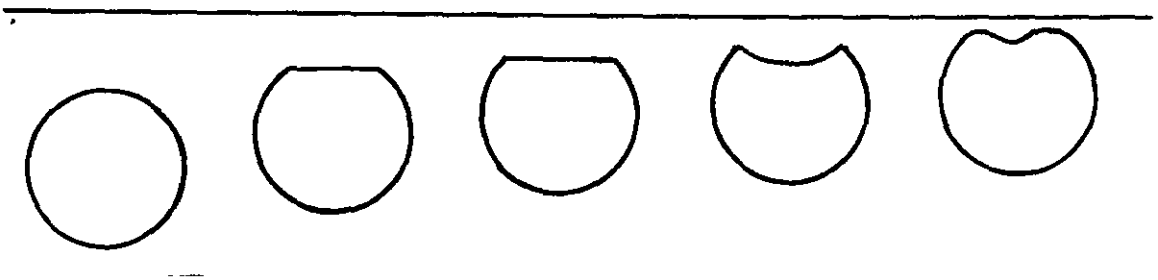

Figure 2.6 Observed Changes in Film Shape for a Bubble Approaching a Flat Rigid Interface (34)

Once the barrier ring is completed, the film thins abruptly at its periphery. After this, there follows a slow adjustment to a more uniform shape.

The equations describing the above phenomena are complicated, but Hodgson (63) put forward a qualitative explanation which essentially can be

summarised as follows: "At the moment of completion of the barrier ring there is a large driving force for drainage outside the film but none inside. However,the drainage outside the barrier ring has then to be matched by corresponding drainage inside the ring. The interface therefore deforms so there is a pressure drop and flow inside the film". A simplified analysis of the pressure drop gradient in the film during dimple formation was made. Using an equation of the form $\frac{dP}{dr} = Kr^n$,where K and n are constant with respect to r,it was found that this was inconsistent with film thinning occurring at the film edge only. This indicated quite clearly,the necessity for matching the changing interface shape with the pressure gradient.

Further evidence of dimpling behaviour (for large drops) presented by Hartland (56),seems to indicate that dimpling and tilting of the drop are closely related events. This suggest that the tilting ability of drops at liquid-liquid interfaces should be examined in more detail.

2.5 Film Thickness

Before a drop may coalesce,the film separating it from the homophase must rupture,and before rupture can occur,the film must drain to a certain critical thickness (44,79). The effect other factors may be judged by their effect on either,or both of these two processes of film rupture and film drainage.

Hartland (53) conducted electrical capacitance measurements of the phase-2 film. For a given system and at a given time,the thickness of the film varied from drop to drop. The standard deviation of the film thickness distribution was approximately 30%. It is pertinent to report that this figure is approximately the same magnitude as the standard deviation of rest-times for single drops. Hartland's results are of undeniable value, though the systems chosen must attract some criticism. The very high viscosity liquids were chosen to confer a high degree of stability on the drops and so greatly facilitated the taking of physical measurements.

These substances are of low purity and therefore it is doubtful whether the drainage process observed with pure systems will be the same as that observed by Hartland.

The thickness of the draining film at rupture will depend on the liquids employed and also the temperature and pressure of the system. There is little,if any,positive agreement between experimental and theoretical values of the film thickness at rupture. Bearing in mind the inadequacies of the drainage models so far contained in the literature, it is certain that the estimates obtained will not be very satisfactory.

The thickness at which a film becomes in some way unstable is still a matter of conjecture (see also Section 2.18). However,it is certain that the initial onset of rupture occurs at the thinnest point of the film. MacKay and Mason's measurements,which are probably the most reliable,indicate that the film thickness at this location could be considerably less than 500 $\mathring{A}$. In addition,the auguments advanced by de Vries (28) suggest that an incipient hole will only grow if the film thickness is less than about 25 $\mathring{A}$ at the point in question. His calculations show,that at this thickness,the surfaces must be approaching each other quite rapidly,and that the hole grows quite quickly once it has passed a critical size. The precise local film thickness at which a hole develops, may not therefore be very important in determining the lifetime of the film.

The state of knowledge in this vital area of coalescence studies is far from complete. It is essential therefore,that a greater effort be employed to expand the understanding of the behaviour of thin liquid films. A first requirement is accurate,reliable data on the film thickness during the drainage of the film and at the rupture of the film.

2.6 Temperature

A number of investigators (13,16,33,44,60,81,82) have found,that in general,the coalescence rest-time decreases with increase in temperature

of the system. This is explained as being due to the reduction of the viscosity of the phase-2 film causing it to drain faster.

Convection currents, caused by temperature gradients in the coalescence apparatus, were reported by Cockbain and McRoberts (19) and Gillespie and Rideal (44) to decrease the rest-time. The importance of a well-thermostatted apparatus has thus been indicated quite clearly to future workers. Adams et al. (97) produced a decrease in drop rest-times by keeping the drop liquid at a lower temperature than the interface. But these authors and Cockbain and McRoberts (19), in some cases found no effect on rest-time due to temperature gradients. This may be partly due to the fact that they were using surfactants in all of their coalescence studies.

An increase in temperature will cause the mutual solubility of the two liquid phases to increase. This will result in a higher interfacial bulk concentration of one phase in the other and increased interface-bulk concentration gradient. Prokhorov (104) has shown that such conditions favour premature coalescence.

2.7 Drop Size

Many investigators have found that the coalescence rest-time increased with increasing drop size (13,16,33,44,60,79,81,82). All the investigators discovered this trend to hold for t_{max} (the maximum rest-time), t_m and $t_{\frac{1}{2}}$. However, the variation in t_{min} (the minimum rest-time), was very erratic. Charles and Mason (16) attributed this to the large relative error involved in the measurement of small intervals of time, with a limited drop population. However, the times involved are usually between 0.1 and 1 second and are definitely measurable. Realistic measuring errors are unlikely to produce the large deviations that have been found, therefore some other cause must be responsible.

In contradiction to the trends normally observed, Nielsen, Wall and Adams (97) found that increasing the drop size could either increase or decrease the stability. Similar findings were reported by Keith and

Hixon (72),studying the same system. Lang (79) remarks that the only systems showing this type of behaviour are those complicated by falling drop disturbances and contamination. Since Keith and Hixon conducted their experiments in a liquid-liquid spray column,they undoubtedly had falling drop disturbances. The erratic results of Nielsen,Wall and Adams may be attributed to the presence of surfactants in all of their experiments.

To maintain a clean interface in the systems which he investigated, Hodgson (63) developed a novel method of interface cleaning,which he called the "Teflon-Glass" method. The principal element used consists of a slim glass tube in the end of which is mounted a small piece of "Teflon" (referred to by the author as a "Teflon-Whisker"). The principle involved, is that the glass is water-wetted and the "Teflon is organic phase-wetted. Thus,by inserting the tube in to an oil-water interface,it was possible to suck liquid from both sides. This technique,according to Hodgson,is superior to other methods of interface cleaning. Although there is no doubt that this method allows liquid to be drawn from both sides of the interface,it is questionable whether its performance is superior to the usual method of "spilling over" the interface.

Using the "Teflon-Glass" method,Hodgson (63) carried out experiments on oil and water drops at liquid-liquid interfaces. Generally, the coalescence rest-time increased with increasing size of drop. Rest-times increased from apparently instantaneous,for oil drops below 0.1 mm. diameter,to about 1.5 seconds for a 5 mm. diameter oil drop. The rest-times were surprisingly reproducible,but very small and much less scattered than before interface cleaning. At a certain interface age after cleaning the interface,the rest-times increased sharply to give very long rest-times. The behaviour of very small water drops befor cleaning the interface, was strikingly different to that of similar sized oil drops. The rest-times were virtually instantaneous,irrespective of the age of the system. In addition,water drops as large as 2 mm. diameter tended to give virtually zero rest-times.particularly when the drop was not aged. Surprisingly,the

secondary drops (see Section 2.20 for a discussion of this phenomenon) then gave distinct rest-times. Hodgson's interpretation is that there exists a very small resistance to coalescence which can be readily overcome by the momentum of the drop. Although the momentum force of the drop is quite capable of overcoming the small "energy barrier" to coalescence, a large percentage of the energy must be imparted to the interface. This effect is discussed in the following section.

2.8 Mechanical Disturbances

The effect of distance of fall of the drop to the interface was investigated by Jeffreys and Hawksley (68). Increasing the fall height of the drop increases the energy carried by the drop. Thus, the disturbance produced finally at the interface, also increases with fall height of the drop (up to the point where the terminal velocity is reached). It might be thought that an increase in disturbance at the interface would cause the drop stability to be reduced. This is not the case in practice. The disturbance causes the drop to bounce at the interface, thereby increasing the thickness of the trapped film. By continual renewal and depletion of the film in this manner (for as long as the disturbance lasts) the coalescence rest-time is effectively increased. Lang (79) has also presented an explanation for this phenomenon.

2.9 Electrolytes

Electrolytes when added to the water phase in small concentrations, have been shown to greatly reduce the rest-time (12,33). Brown (12), who has studied the effect of high concentrations of electrolyte, observed that the drops became more stable with increasing concentration. The effects were most pronounced when strong sodium hydroxide was used (N/1.0 solution). This is hardly surprising in view of the strong surface active character of the hydroxyl ion, relative to the hydronium ion. Enhanced stability was also noted for N/1.0 hydrochloric acid.

Lang has confirmed experimentally (79), that low molecular weight

materials will decrease the rest-time if they are present in non-equilibrium quantities in the two phases. He attributed this effect to interfacial disturbances due to the Marangoni Effect (to be discussed later).

2.10 Surfactants and Interface Mobility

A number of workers (12,19,63,79,97,129) have studied the effect of surface-active agents on coalescing drops. It is reported that even trace amounts of surfactant are sufficient to confer remarkable stability on drops. Watanabe and Kusui (129) have proposed a mechanism for coalescence, based on the formation of a "defect" in the surfactant layer on the surface of the drop, in the vicinity of the trapped phase-2 film. The "defect" is visualised as being a portion of the interfacial film which is not covered by the surfactant. The proposed mechanism is thus: (i) drainage first takes place in the manner described by Gillespie and Rideal (44); (ii) once a "defect" forms in the adsorbed surfactant layer, the liquid from the drop drains into it, due to the excess pressure within the drop. It is difficult to visualise exactly what the authors mean by a "defect". The proposed mechanism is obviously over simplified, since it does not take into account secondary droplet formation, nor does it explain the phenomenon of coalescence in pure binary systems.

Hodgson (63) has investigated the effect of both ionic and non-ionic surfactants on the coalescence of oil and water drops. It was shown that the presence of a surfactant could set up interfacial forces capable of resisting interface expansion. If interface mobility was severely restricted, the continuous phase film drained as if it were between two immobile interfaces. Thus, the rest-time was increased considerably, due to the reduced rate of film drainage.

The surfactant in a film will be swept out unless it reaches a certain critical interfacial concentration. This critical concentration was shown by Hodgson (63) to be very small. Thus, it is entirely possible for these interfacial concentrations of surfactant to be attained by the

adsorption of impurities,even though their concentration in the bulk liquid is extremely low. Once the critical concentration is exceeded,the interface mobility will be controlled by the rate at which surfactant is transferred to the expanded areas. Material can be transferred tothese areas along the interface or from the bulk phases. Transfer from the bulk phase is most likely to be important when the ratio of interfacial to bulk concentration is small. If the transfer is rapid,the expanded areas are readily replenished with surfactant. This causes relaxation of the tangential forces in the interface,thus maintaining interface mobility. This is usually the case if the surfactant is present in the dispersed phase. When the surfactant is contained in the continuous phase only,the film is likely to become denuded of surfactant in the early stages of drainage. Any material which is transferred from the bulk phase has then to diffuse along the narrow film. This transfer path behaves as a barrier to adsorption.

The postulation of Hodgson's (63),that free movement,retarded mobility and incomplete mobility are all possible modes of behaviour in film flow,seems likely to resolve some of the anomalies between the predictions of rigid interface models and experimental results.

Hodgson (63) has developed an analysis of the criteria for interface mobility,based on the parallel plates film drainage model. He considered the case of an insoluble surfactant. Because of its insolubility, diffusion of the surfactant in the bulk of the liquid film is negligible. Therefore,an insoluble non-diffusing surfactant represents the simplest possible case,because no account needs to be taken of the diffusion equation. The radial velocity of the film was given as:

$$u_r = \frac{2Fr}{\pi \mu_R^4} \left[\left(\frac{h}{2}\right)^2 - (z)^2 \right] \qquad (2.10.1)$$

(see Eqn. (2.3.6)).

By differentiating Eqn. (2.10.1),the shear stress τ_r due to viscous motion at any point on the surface,is found to be:

$$\tau_r = \mu \left(\frac{\partial u_r}{\partial z} \right)\Big|_{z=\frac{h}{2}} = - \frac{2 Frh}{\pi R^4} \qquad (2.10.2)$$

Thus, τ_r is proportional to r, and the maximum shear stress occurs at the periphery of the film, at r = R. If one substitutes for R from Eqn. (2.2.1) and also $F = \frac{4}{3} b^3 \Delta \rho g$, the following relationship is obtained:

$$\tau_r = \frac{4h}{b^3} \cdot \left(\frac{3\gamma^2}{2\Delta \rho g} \right) \qquad (2.10.3)$$

Thus, it is seen that the shear stress increases very rapidly with decreasing drop radius.

(i) Criterion for Complete Immobility:

The insoluble surface active material is considered to be present in the interface, initially as a uniform layer. If a shearing action is applied, the material becomes redistributed so that the shear stresses are just opposed by the gradients in surface tension. This will only happen if a sufficiently large difference in surface tension exists between the centre of the film and the periphery, and therefore, only if the surfactant material is present in sufficient quantity. The smallest difference in surface tension, which will immobilise the film completely, can be established by using the result obtained for the parallel discs model. If $\Delta\gamma_o$ is taken as the difference in surface tension between the centre of the film r = 0, and the periphery r = R, then:

$$\Delta\gamma_o = \int_o^R \tau_R dr \qquad (2.10.4)$$

Substituting for τ_r from Eqn. (2.10.2):

$$\Delta\gamma_o = - \frac{2h}{b} \qquad (2.10.5)$$

It is interesting to note that $\Delta\gamma_o$ is proportional to $\frac{1}{b}$. Therefore Eqn. (2.10.5) predicts an increased tendency for the surfactant to be swept away as the drop size decreases. It is therefore to be expected that small drops will have a much greater ability to resist the effects of surfactant

in the film. The film trapped beneath a large drop however, will no doubt strongly influenced by even quite small concentrations of surfactant.

(ii) Criterion for Complete Mobility:

In the limiting case, the discs are completely free of surfactant. At the edge of the discs, the surfactant concentration and hence the surface tension, changes sharply. In his analysis, Hodgson equated the pressure drop at the edge of the discs ΔP_R to the change in surface tension round the periphery, $\Delta \gamma_R$, to obtain:

$$\Delta \gamma_R = - \frac{h\gamma}{b} \qquad (2.10.6)$$

Therefore, this is just half the value which gives complete immobility to the film.

When an adsorbed material is present in the interface, expansion causes the interfacial concentration Γ to fall and simultaneously, (i) the local interfacial tension rises and opposes the interfacial motion, (ii) mass transfer of the surfactant material from the bulk of the liquid, or other parts of the surface, tends to restore the surface concentration to its static value. The rate of mass transfer controls the rate of interface expansion, so that the two are in balance.

If the surfactant material is soluble in the film phase only, and its concentration in the liquid trapped in the film is high, the interface is fed by diffusion and bulk flow in a direction normal to the interface. As described by Andrews (4), this occurs without the film becoming denuded of surfactant. If however, the concentration of the surfactant material, or strictly the ratio c/Γ, is not high, the thin film will very soon be depleted by diffusion into the interfaces. Further material must be transferred in a radial direction from the main bulk of the liquid, which lies outside the film altogether. Since the diffusion path is relatively long (see Fig. 2.7), mass transfer is relatively slow. The surface movement is a controlled slip rather than a rapid expansion.

This latter case was developed by Hodgson (63) and is outlined here.

The equation for bulk diffusion in the radial direction is, in cylindrical symmetry (9):

$$(u_r)_{av.} \cdot \frac{\partial c}{\partial r} = D \frac{1}{r} \frac{\partial}{\partial r}\left[r \cdot \frac{\partial c}{\partial r} \right] + R_A \qquad (2.10.7)$$

where R_A is the molar rate of production of A per unit volume. In Hodgson's example, unit volume was associated with an area 2/h. Thus, if this area was expanding with a specific surface expansion rate S_r, the area per unit volume was increasing at a rate $2S_r/h$. When the local surface concentration is Γ mole/unit area, $R_A = -2S_r\Gamma/h$. $S_r = \frac{1}{r}\frac{\partial}{\partial r}(ru_s)$ and substitution of $(u_r)_{av.}$ gives the following equation:

$$\frac{r}{2h}\frac{dh}{dt}\frac{\partial c}{\partial r} = D \frac{1}{r}\frac{\partial}{\partial r}\left[r \cdot \frac{\partial c}{\partial r} \right] - \frac{2\Gamma}{h} \cdot \frac{1}{r}\frac{\partial}{\partial r}(ru_s) \qquad (2.10.8)$$

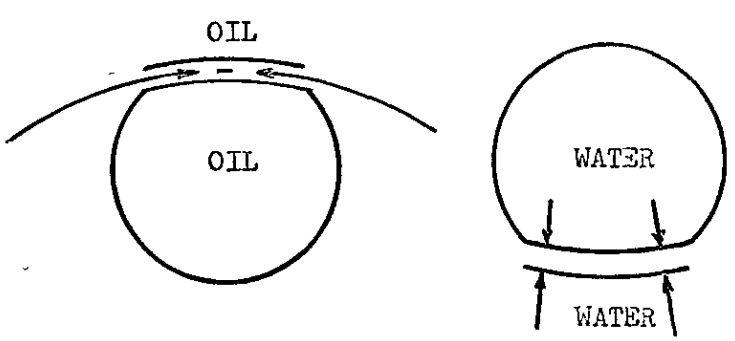

Figure 2.7 Adsorption at the interface within the Barrier Ring when the Surfactant is present in the water phase only.

In these equations, the quantity D is strictly a diffusion coefficient. However, Hodgson's development in this context suggests that D is really some form of dispersion coefficient. This is because of the effect of the partly parabolic profile.

If surface diffusion alone were supplying the surfactant to the expanding interface, an equation very similar to the above would apply:

$$u_s \frac{\partial \Gamma}{\partial r} = D_s \frac{1}{r}\frac{\partial}{\partial r}\left[r \frac{\partial \Gamma}{\partial r} \right] - \frac{\Gamma}{r}\frac{\partial}{\partial r}(ru_s) \qquad (2.10.9)$$

(Surface Flow) (Surface Diffusion) (Interface Diffusion)

or, to correspond exactly with the diffusion equation:

$$u_s \frac{\partial (2/h)}{\partial r} = D_s \frac{1}{r}\frac{\partial}{\partial r}\left[r \frac{\partial (2\Gamma/h)}{\partial r} \right] - \frac{2\Gamma}{h}\frac{1}{r}\frac{\partial}{\partial r}(ru_s) \qquad (2.10.10)$$

It was further assumed that in the surface flow term, $u_s \simeq (u_r)_{av.}$, and $D_s = D$. Thus, it is possible to write an equation which combines the effects of both bulk diffusion and surface diffusion:

$$\frac{r}{2h}\cdot\frac{dh}{dt}\frac{\partial (c + 2\Gamma/h)}{\partial r} = D\frac{1}{r}\frac{\partial}{\partial r}\left[\frac{r\partial (c + 2\Gamma/h)}{\partial r} \right] - \frac{2}{h}\frac{1}{r}\frac{\partial}{\partial r}(ru_s) \qquad (2.10.11)$$

or,

$$\frac{r}{2h}\cdot\frac{dh}{dt}\frac{\partial a}{\partial r} = D\frac{1}{r}\left[\frac{\partial}{\partial r}\cdot r\frac{\partial a}{\partial r} \right] - \frac{2\Gamma}{h}\cdot\frac{1}{r}\frac{\partial}{\partial r}(ru_s) \qquad (2.10.12)$$

where $a = c + 2\Gamma/h$. They act together to feed the expanding interface. Now the local surface tension gradient (i.e. $\tau = \text{grad}\,\gamma$) provides the basic coupling between the Flow Equation and the Diffusion Equation. Thus:

$$\tau_r = \frac{\partial \gamma}{\partial r} = \frac{\partial \gamma}{\partial c}\cdot\frac{\partial c}{\partial r} = \frac{\partial \gamma}{\partial c}\cdot\frac{\partial c}{\partial a}\cdot\frac{\partial a}{\partial r} \qquad (2.10.13)$$

Writing $\beta = \frac{\partial \gamma}{\partial c}\cdot\frac{\partial c}{\partial a}$, where β was assumed to be a function of concentration, $\tau_r = \beta\frac{\partial a}{\partial r}$. If β is not strongly dependent on r, comparison between the Flow and Diffusion Equations is possible. Hodgson presented the final equations:

$$\text{Flow:} \quad \frac{1}{h}\cdot\frac{dh}{dt} = \frac{1}{r}\frac{\partial}{\partial r}(ru_s) - \frac{h}{6}\frac{\beta}{\mu}\cdot\frac{1}{r}\frac{\partial}{\partial r}\cdot r\left(\frac{\partial a}{\partial r}\right) \qquad (2.10.14)$$

$$\text{Diffusion:} \quad \frac{1}{h}\cdot\frac{dh}{dt}\frac{r}{2}\frac{\partial a}{\partial r} = -\frac{2\Gamma}{h}\cdot\frac{1}{r}\frac{\partial}{\partial r}(ru_s) + D\frac{1}{r}\frac{\partial}{\partial r}\cdot r\left(\frac{\partial a}{\partial r}\right) \qquad (2.10.15)$$

These two equations must hold at each and every point in the film. A completely determinate solution is obtained by using the boundary conditions; $a = a_b$ when $r = R$; $u_s = 0$ when $r = 0$. An examination of Eqns. (2.10.14) and (2.10.15) reveals that since Γ is an arbitrary function of concentration, a numerical solution will, in general, be necessary. An approximate trial

solution of these equations was carried out by Hodgson and this is conveniently summarised in Fig. 2.8 below.

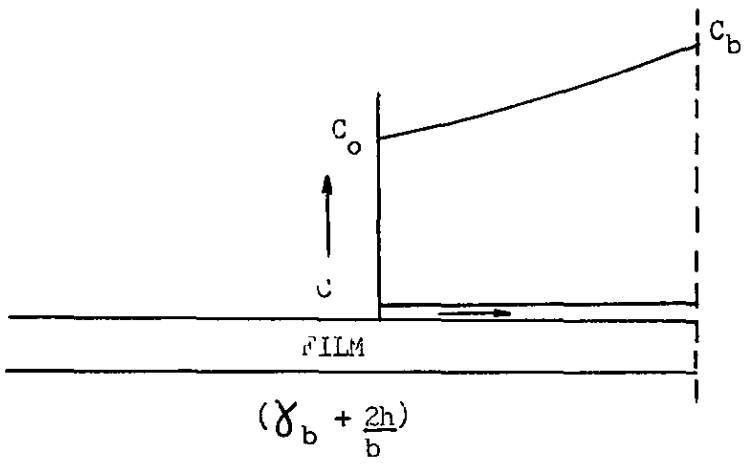

Figure 2.8 Distribution of c and γ in the film when slip is controlled by radial diffusion (63)

2.11 Dirty Interfaces

Traces of dirt, which may be airborne dust or other material, when present at the interface, have been found to promote coalescence (16,44,79). Usually, results obtained in these circumstances produce low rest-times. The presence of foreign particles may:

(i) Absorb heat from external sources. This will cause local temperature gradients which may be sufficient to rupture the film.

(ii) Form a hydrophobic, or partly hydrophobic particle in the film. This would form part of a "bridge" which could reduce, or even eliminate the energy barrier to coalescence.

The true nature of any contaminative dirt is in most cases impossible to determine. It is imperative therefore, that the experimental environment be well designed to prevent accidental contamination of the experimental equipment. Whilst extreme care has been taken by some workers, others have not been very careful in this regard. It is probable in the latter instances, that many unexplained results were caused by

accidental contamination of the liquid systems or apparatus.

2.12 Mass Transfer and the Marangoni Effect

When transfer of a solute takes place across a liquid-liquid interface, localised variations in concentration occur. These in turn produce changes in interfacial tension along the interface. The interface then seeks a lower state of free energy. This takes place through expansion of regions of low interfacial tension, at the expense of regions of high tension (the Marangoni Effect (92)). Sawistowski and Goltz (113), who employed a schlieren technique, produced some remarkable photographs of interfacial movement caused in this fashion. The Marangoni Effect has also been studied theoretically by Sternling and Scriven (120).

Charles and Mason (16) have studied the coalescence of chloroform drops at a chloroform-water interface. When the drops contained ethanol, they were found to coalesce almost immediately. It was concluded that this was due to the diffusion of the ethanol across the phase interface. Experiments conducted with water drops containing p-dioxane, also showed some interesting trends. The rest-time was observed to decrease with increasing amounts of p-dioxane. Thus, at a concentration greater than 10% p-dioxane, the coalescence was instantaneous. This is quite a high concentration, but even much smaller concentrations had a very noticeable effect on the rest-time.

Smith, Caswell, Larson and Cavers (125) have presented an explanation of the effects mentioned above. The model which they used to develop their hypothesis, was that of two drops in close proximity. This was also the arrangement which they employed in their experimental investigations. When the transfer of solute material is taking place from the dispersed phase to the continuous phase, the direction of interfacial movement was observed to be away from the zone of closest approach of the two drops. Circulation occurs within the drops and this serves to continue the process by bringing fresh solute to the drop interface. Under these conditions

streaming of continuous phase fluid out of this zone occurs and drop coalescence is promoted. However,when solute transfer is in the reverse direction,a considerably different pattern of behaviour is observed. This time,the direction of interfacial movement is towards the zone of closest approach. Continuous phase fluid is drawn into this region thereby keeping the drops apart. Hence,coalescence is prevented from taking place. The method used by these authors to predict the ease of coalescence in different systems,is of some value. They employed equilibrium data and interfacial tension diagrams for this purpose. This approach should have many useful practical applications,providing of course,that the requisite data is available.

2.13 Interfacial Tension

Appel and Elgin (5) concluded that high interfacial tension promoted coalescence. In contradiction to this finding,Keith and Hixon (72), and a number of other investigators (48,119) have found that coalescence is promoted by low interfacial tension. An explanation is that high interfacial tension promotes film thinning,whilst low interfacial tension promoted film rupture. Therefore,if film thinning is the rate controlling factor,then high interfacial tension is desirable to promote coalescence. If film rupture is important,then low interfacial tension is desirable.

In most of the systems studied by Lang (79),film rupture was found to be the rate determining step. Thus,he arrived at the conclusion, that in an environment with few and weak disturbances,rapid coalescence will occur with systems having physical properties,such that the film ruptures easily. Conversely,in an environment with many strong disturbances, rapid coalescence will occur with systems having physical properties that cause the film to thin rapidly. In other words,the one mechanism of several,that occurs most slowly,will be the rate determining step.

2.14 Density

A low density difference will cause the phase-2 film to thin rapidly, but a high density difference will cause the film to rupture more easily. This is the conclusion reached by Lang (79). In view of the difficulties experienced by Lang in some of his experimentation one should treat this finding with caution. It is true to say that the effect of density difference on coalescence has not been fully established.

2.15 Viscosity

Mahajan (90,91) as long ago as 1930 investigated the effect of the surrounding medium on the lifetime of drops. His finding was, that the stability of drops increased as the viscosity of the surrounding medium (phase-2 fluid) increased. The relationship between the rest-time and the viscosity of the phase-2 fluid was claimed to be linear. Later workers have also established this fact (16,23,53,85). They all contend that the increased drop stability arises from the longer time required for the more viscous films to drain to their critical thickness.

2.16 Electrostatic Phenomena

The Double Layer in Liquid-Liquid Systems

If two immiscible liquids in mutual contact contain electrolytes, even in very small amounts, a potential differerence will be set up between the interiors of the liquids. This potential arises because of the generally unequal distribution coefficients of the positive and negative ions, and is known as the distribution potential γ. Each electrolyte present gives rise to a potential determined by the properties of the ions. Near the interface, the ionic concentration of one ion increases and that of the other decreases. This occurs in such a way that the total charge on both sides of the interface is equal but has opposite signs. This distribution of charge is known as the electrical double layer. The electrolytes may have been deliberately added to the system. On the other hand, the liquids

used generally contain sufficient electrolytic impurities to build up a double layer at the interface (NH_4^+, H^+, HCO_3^- ions in water, organic acids in organic liquids, etc.)

The partition of the double layer potential between two liquids, depends upon the ratio of the ionic concentration in each phase, c_1/c_2, the ratio of the dielectric constants, ϵ_1/ϵ_2, and the actual potential. If $c_1\epsilon_1$ is much greater than $c_2\epsilon_2$, then the potential drop in phase-1 is less than in phase-2. Infact, the potential drop in the phase with the largest ionic concentration, becomes rather small as soon as $c_1\epsilon_1$ differs considerably from $c_2\epsilon_2$. This is especially true for low values of the total potential (127). Thus, in oil-water systems, and especially with slightly polar oils, when the ionic concentrations differ by several orders of magnitude, the potential drop occurs mainly in the oil phase.

The Interaction of Two Double Diffuse Layers

If two interfaces are brought so close together that their double layers interact, these double layers cannot develop fully (see Fig. 2.9).

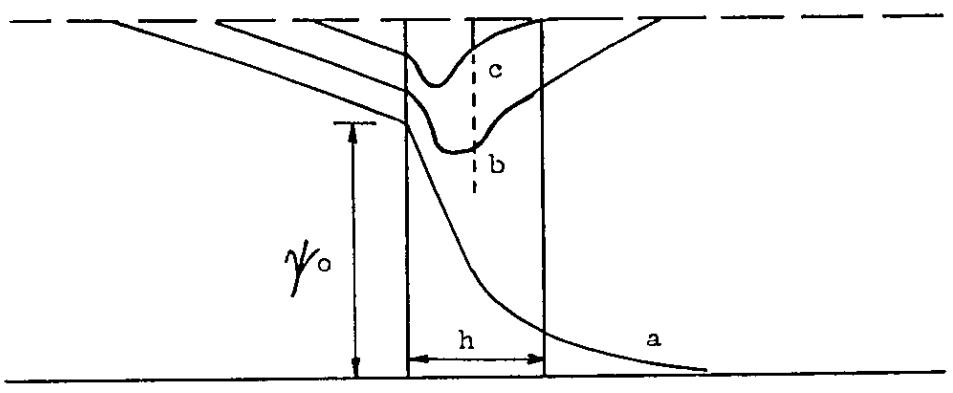

Figure 2.9 The interaction of two double layers at the liquid-liquids (127). (a) interface separation at infinity, (b) and (c) show the effect of decreasing interface separation, h.

When the dispersed phase is oil, only a small part of the double layer potential occurs in the continuous phase. The double layer repulsion between the two interfaces of the dispersed phase is therefore always weak. It is a general observation that such dispersions are unstable. In the reverse situation, the greatest part of the potential drop is in the

continuous phase (oil). However,the ionic concentration in the continuous phase is now very small. Thus the double layer repulsion between the two interfaces of dispersed phase is again,always weak.

The Double Layer in Oil-Water Systems and the Presence of Surfactants

The presence of a surface active material,concentrated at the interface,can change the potential pattern of the double layer considerably. The magnitude of the potential difference between the interiors of thetwo phases,remains unchanged as long as the ionic concentrations in the bulk phases are not affected by the adsorption process. However,the adsorption of surfactant causes a change in the surface potential,which must be compensated by a rearrangement in the dissolved ions across the interface. The presence of a surface active charge pushes the potential drop into the phase with greater concentration of counter ions. Thus,for oil-water systems, the potential drop is pushed into the aqueous layer. As a result of this, there is a greatly increased repulsion when oil is the dispersed phase. In fact,the double layer repulsion will be determined mainly by the surface charge due to the surfactant,and the ionic concentration in the aqueous phase. Under these circumstance,it is possible to apply to liquid-liquid systems,the theory of double layer interactions which has been developed for solid-liquid systems.

The repulsive force due to the interaction of two double layers, has been calculated by several workers (24,127). For the case of a symmetrical electrolyte,the double layer thickness is found to be proportional to $1/n^{\frac{1}{2}}$,where n is the total ionic concentration in the bulk phase. Thus, the thickness decreases as the ionic concentration increases (e.g. by the addition of electrolyte). In the presence of non-ionic surfactant,the additional counter ions will crowd in around the surfactant molecules (which are oriented because they contain electrical dipoles). This decreases the double layer thickness,producing a layer of uniform thickness. To be

absolutely certain of the contribution of double layer repulsion in coalescence,direct measurement will be required.

Reduced Film Tension

If at some film thickness,the repulsive force exceeds the attractive force between the interfaces,film drainage will be halted. There then exists a minimum in the free energy of the system. A typical example of the variation of free energy with separation for soap films is shown in Fig. 2.10. The secondary minimum is determined by the double layer repulsion,the van der Waals attraction and the pressure in the film (due to drop buoyancy). The primary minimum occurs at very small film thicknesses,when the film consists of a bimolecular leaflet of surfactant molecules. At such small separations,a very short range repulsive force

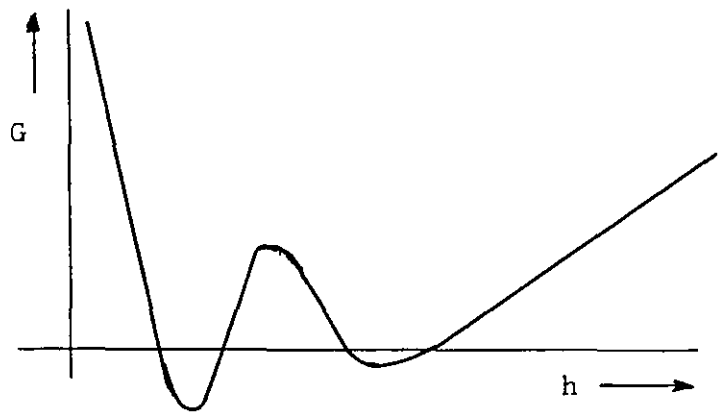

Figure 2.10 Typical plot of the Free Energy versus Film Thickness for a Soap Film

(Born repulsion) exists between the electron shells of the surfactant molecules or ions. When the above forces are significant compared with gravitational forces,the interfacial tension is effectively altered. Thus, Derjaguin defines a reduced film tension as (25,26):

$$\gamma_f = 2\gamma + G_{min} \qquad (2.16.1)$$

γ_f is the apparent interfacial tension of the interfaces of an equilibrium film. G_{min} is the value of the free energy in the primary or secondary minimum.

The case of a drop in a state of equilibrium, resting at a liquid-liquid interface has been considered by Princen and Mason (103). The interfacial tension outside of the barrier ring remains unaltered, but inside it is given by Eqn. (2.16.1). These authors have shown that this situation must lead to an expansion of the barrier ring. One must presume that this tends to make the film more uniform and hence slower to drain. Further, it was shown that the effect is greater as the drop size decreases.

Electroviscosity

If an electrical double layer is sheared, for example, by causing a flow relative to the interface, a potential known as the streaming potential is set up in the plane of shear. The streaming potential arises because part of the double layer is mobile and is carried away by the flow. It tends to resist the flow because of the electrical retarding force acting in the ions of the double layer. The effect is likely to be important in thin films and appears as an increased viscosity.

Electroviscosity has been investigated in some detail by Elton (31, 32). To study the importance of the effect, he examined the physical situation of two approaching parallel discs contained in an ionic liquid. He also examined experimentally, the rate of approach of an air bubble to a flat glass plate. The approximate form of the electroviscous equation predicted by Elton is:

$$\mu_a = \mu + \frac{3\epsilon^2 \zeta^2}{32\pi^2 K h^2} \qquad (2.16.2)$$

where K is the specific conductivity of the liquid and ζ is the electrokinetic potential. The latter is usually a little less than the surface potential ψ_o. μ_a is the apparent viscosity of the liquid.

The rate of approach of two parallel plates (or discs) in an ionic liquid is:

$$\frac{dh_2}{dt} = -\frac{2F}{3\pi\mu_a R^4} \cdot h_2^2 \qquad (2.16.3)$$

where R is the radius of the discs, F the force pressing them together, and $\mu_a = \mu + A\epsilon^2\zeta^2/h^2K$, A being a constant. h_2 is the distance of separation of the two plates at time time t_2. Integrating Eqn. (2.16.3) from h_1 to h_2:

$$t_2 - t_1 = \frac{3\pi\mu R^4}{4F}\left(\frac{1}{h_2^2} - \frac{1}{h_1^2}\right) + \frac{C\epsilon^2\zeta^2}{K}\left(\frac{1}{h_2^4} - \frac{1}{h_1^4}\right) \quad (2.16.4)$$

where C is a constant.

Some idea of the orderof the electroviscous effect, can be obtained by considering the following example. The times of approach for discs of 1 cm. radius under a foce of 1000 dynes, (a) in a non-ionic liquid of viscosity 0.01 poise, and (b) in an ionic liquid (ζ = 100 mv, ϵ = 80 and $K = 10^{-6}$ ohm^{-1} cm.$^{-1}$) of the same bulk viscosity are:

Distance of Fall	non-ionic liquid	ionic liquid
1.0×10^{-5} cm. to 9×10^{-6} cm.	5.4×10^4 sec. (about 15 hr.)	1.6×10^6 sec. (about 450 hr.)

The results of the approximate calculations presented above indicate that the electroviscous effect is likely to be an important consideration in coalescence. Particularly so when the surface potential is high and the ionic concentration very low.

In summary, it is pertinent to mention that although Elton's findings were justified by his experimental results, his reasoning of the electroviscous effect has been contested by other workers (97). Finally, it may be pointed out that there is an additional mechanism whereby the viscosity of the draining film may be increased. It has been demonstrated experimentally, that the viscosity of the liquid immediately next to the interface is greater than that of the bulk liquid (20). This is because of a strong attraction between layers of molecules which are induced to orientate at the interface. Again this phenomenon must act to decrease the rate of film drainage.

Disjoining Pressure

When a fluid is squeezed out between two bodies, a resisting force can be measured which is not due to the viscosity of the liquid. This force is a measure of the long range attraction of the molecules (79). It is significant only when the film is very thin, i.e. because it arises by repulsive action due to electric charges in close proximity (16). Derjaguin and Kussakov (23) have named this force "disjoining pressure" and have measured its magnitude in a number of systems, as a function of film thickness. A typical value of the disjoining pressure is 500 dynes/cm.^{2}, corresponding to a film thickness of 10^{-5} cm.

Elton has suggested that the disjoining pressures that have been measured were really due to the fact that the film had not reached an equilibrium state. But since in coalescence work we are rarely concerned with equilibrium states (if at all), this does not give us concern to doubt its existance. However, Lang has reported (79), that the disjoining pressure has very little effect on the drop rest-time. If the existence of the disjoining pressure is assumed to be valid, then Lang's finding would suggest that the film does not drain to a sufficiently thin value. This seems a little bit perplexing, since as already mentioned in Section 2.5, the phase-2 film can reach very low film thicknesses before it rupture.

London - van der Waals Forces

Molecular attraction due to long range London-van der Waals forces have been observed by many investigators (27,99,126,127). These forces act to decrease the film thickness. Van den Temple has stated (126) that the contribution of these forces is only significant when the film thickness is below 1000 Å. This has been further substantiated by MacKay and Mason (89). Their finding was that the contribution was negligible if the film thickness was greater than 500 Å. Since the measurements of film thickness during coalescence by these authors were in most cases less than 500 Å, we must conclude that the London-van der Waals force is important in coalescence.

Unfortunately, the precise form of the equation representing a

London-van der Waals force is subject to some doubt (10,73,75,118). Theoretically,the short range unretarded forces,which operate over a distance of the order of 100 Å,are proportional to $1/h^3$. At distances greater than about 1000 Å,the forces are of the retarded kind and are proportional to $1/h^4$. The most realistic values for the calculation of the van der Waals force lie in the retarded range. Since the film thickness at rupture is likely to be considerably below the retarded range,calculations of the van der Waals force should be treated cautiously.

The understanding of electrostatic phenomena pertaining to liquid-liquid systems is not completely reliable. This is mainly because very few experimental measurements have been carried out for liquid-liquid systems. Whilst valid interpretations may be made from the theory,the true significance of any findings will remain obscured until reliable data is available.

2.17 Electric Fields

The use of electrical fields to promote coalescence has proved to be one of the few practical successes in this field of endeavour. This is all the more remarkable,considering the scant knowledge of the principles involved.

As long ago as 1879 Rayleigh (106) produced easy coalescence of parallel jets by charging one to a higher potential than the other. Charles and Mason (16) have investigated the coalescence of single drops when subjected to an electrical field. The electrical field was produced by placing electrodes (aluminium discs) on either side of the interface. With increasing potential,the rest-times of primary and secondary drops decreased,finally producing instantaneous coalescence. Thus,the coalescence problem reduces to one of very simple magnitude if sufficient electrical potential is applied.

Without entering into great detail on this subject,the more important findings may be summarised as follows:

(i) For a D.C. field,an inverse linear relationship exists between the strength of the applied electrical field and the mean rest-time of a single drop;Allan and Mason (1).

(ii) Almost identical effects to those listed in (i) are found if A.C. fields are used;Brown and Hanson (13).

(iii) The field inside the drop,rather than the charge it carries, is responsible for premature coalescence (13).

(iv) The potential drop across the aqueous phase is negligible compared with the organic phase (87,130).

Item (iv) describes the important principle behind the development of electrical coalescence units for oil-water systems,used in the petroleum industry. It is important enough to merit more extensive investigation so that the principle can be applied in other liquid-liquid systems.

In examining the coalescence of two aqueous drops,Allan and Mason (3) found that there was a variation in coalescence angle with field strength. The coalescence angle is defined as the angle between the symmetric drop axis (about the vertical axis) and the vertical axis. In addition,the contact time was greatly reduced at high field strengths. The latter phenomenon is analogous to decreased rest-time found with single drops at a plane interface. The overall effect is one of increased film thinning, which may be explained in terms of electrostatic attraction.

Stewart and Thornton (121) have applied D.C. fields to single drops moving through a non-conducting liquid. Theory predicts that such drops will have reduced interfacial tensions and higher terminal velocities. Both of these effects are likely to produce drop oscillation. Using high speed photography,it was observed that the terminal velocity of charged drops could be twice that of uncharged drops. This type of investi gation should prove to be extremely valuable in obtaining fundamental information about the effect of electic fields on liquid-liquid systems.

2.18 Film Instability

Early workers (16,33,44) used the parallel plates model and the observed rest-times to calculate the film thickness at rupture. Thus, Gillespie and Rideal (44) were led to the conclusion that the film thickness at rupture was of the order 1000 to 10,000 $\mathring{A}$. The variation in this value correponds to the observed scatter in the rest-times. These relatively large film thicknesses at rupture then led workers (16,33,44) to the conclusion that rupture was brought about by mechanical and thermal disturbances. Thus,a detailed investigation of the effects of mechanical disturbances on coalescence was undertaken by Lang (79). He considered two possible ways inwhich a disturbance can grow in a film so that it might become large enough to cause rupture.

(i) Rayleigh Instability: (105,107,108). Rayleigh demonstrated that a disturbance can grow in a cylinder of ideal fluid provided that the disturbance produces a decrease in surface area. The driving force for the final breakup of the cylinder is surface tension. However,Lang concluded that such a disturbance cannot grow in a film with spherical surfaces.

(ii) Taylor Instability: In this case (80,122),the driving force for the growth of a disturbance is gravity. The instability can arise whenever a more dense fluid overlies a less dense fluid. This must be the situation at one interface of the continuous phase film between the drop and the bulk interface. The Taylor instability was chosen by Lang (79) as being responsible for film rupture in coalescence.

Lang considered the case of a layer of fluid,density ρ_2 and thickness 2h,lying between two semi-infinite layers of fluid. The upper layer was of density ρ_1 and the lower one of density ρ_3. He assumed for simplicity that $\rho_1 = \rho_3$,which is the actual situation in coalescence,and reasoned that if $\rho_1 > \rho_2$,then from Taylor's instability,the upper interface will be unstable and the lower one stable. Lang summarised two important conclusions: "First,in a system containing two free interfaces,two wave

systems can exist corresponding to a single wave number. If the interfaces are far apart,the wave systems act independently of one another,each in a separate interface. If the two interfaces are close together,however,both wave systems exist in each interface. The relative initial amplitude of the waves in the upper and lower interfaces depending on the kinematic viscosity. Second,if a denser phase overlies a less dense phase in a layered system,the system will be inherently unstable".

In his experimental investigations,Lang employed all sorts of sonic disturbances but found they did not increase the rest-time appreciably. Thus,the importance of instability in determining the film rupture process in coalescence was not established. A comment concerning Lang's experimental coalescence rest-time results is in order. It was noticed that a number of sets of results appeared to have very erratic trends. If contamination was responsible for these trends,it is worth pointing out the damping effect which surfactants are known to have on surface disturbances (21).

It seems most probable from prior discussion,that rupture of the phase-2 film occurs at film thicknesses of a few hundred Angstroms or less. At interface separations of the order of 250 $\mathring{A}$,van der Waals forces are increasing very rapidly to create a significant attractive force between the interfaces. In view of this,and the doubts expressed above,the relevance of classical instability criteria in determining the stability of the phase-2 film,is open to question. Thus,in practice its importance may not be as great as suggested by idealised models.

2.19 Hydrodynamic Stability and the Marangoni Effect

The onset of interfacial movement or interfacial turbulence caused by local variations of interfacial tension (Marangoni Effect),has been studied by Sternling and Scriven (115,120). They proposed that interfacial turbulence is a manifestation of hydrodynamic instability,which is "touched-off" by ever present small random fluctuations of pressure and temperature.

The model used by Sternling and Scriven consisted of two semi-

infinite fluid phases in contact along a plane interface. The phases were considered to be in thermal but not in chemical equilibrium. Because very low concentrations of solute were used,the fluid properties were taken to be constant. Sternling and Scriven obtained solutions by first solving the hydrodynamic equations and then the diffusion equation describing the concentration disturbance. The two solutions were combined by means of the interfacial shear-stress boundary conditions. It was concluded that the stability of the disturbed system depended on the viscosity ratio,the diffusivity ratio,the direction of solute transfer and the sign of the rate of change on interfacial tension.

The analysis of Marangoni instability by Sternling and Scriven has led to some creditable explanations of a number of phenomenon. Thus,it explains why some systems are unstable with solute transfer in one direction, yet stable with transfer in the opposite direction,and others to be stable with transfer in either direction. Elegant as the analysis is,it is too simplified to be reproduced in the laboratory.

It is important to realise that the factors which promote interfacial turbulence and hence hydrodynamic instability ,also promote coalescence. However,direct measurement of these complex effects will obviously be necessary in order to determine their particular significance.

2.20 Rupture and Collapse of the Phase-2 Film

Lang (79) has shown that the probability of rupture of the phase-2 film is zero until it has thinned to a certain critical thickness. With the formation of a hole in the film,the interfacial tension acts to reduce the interfacial area and therefore to expand the hole. An analysis of the hole expansion in thin soap films was carried out by Dupré (30). The surface free energy released was assumed to be completely converted into kinetic energy in the film,and for motion within the film itself. Dupré proposed the following equation for the velocity of hole expansion:

$$v = \frac{dr}{dt} = \left(\frac{4\gamma}{\rho_2 h}\right)^{\frac{1}{2}} \qquad (2.20.1)$$

where r is the hole radius at time t, and ρ_2 the film density.

Obviously, Eqn. (2.20.1) can give only an upper limit for v. This is because energy will also be required for overcoming the viscous drag on the receding edge of the film and for the incoming phase-1 replacement liquid. Charles and Mason (15) carried out a similar analysis to that of Dupre, to derive the following equation for a coalescing system:

$$v = \left[\frac{4\gamma}{(\rho_1 + \rho_2)h}\right]^{\frac{1}{2}} \qquad (2.20.2)$$

This equation is only an approximation, since the whole of the incoming fluid does not move at the velocity v. It follows from Eqn. (2.20.2) that v is independent of r and constant for a film of uniform thickness.

Assuming the spherical-planar approach to be the appropriate film model, Charles and Mason derived the following equation:

$$\frac{1}{v_r^2} = \frac{1}{v_o^2} + kr^2 \qquad (2.20.3)$$

where $k = \left(\frac{\rho_1 + \rho_2}{4\gamma}\right)\left(\frac{1}{2R}\right)$, and R is the radius of curvature of the film. v_o is the initial velocity and v_r the velocity at hole radius r. In this derivation it was assumed that the film remains stationary until reached by the receding edge. Considering the rapid expansion of the hole, which initially may be as high as 1000 cm./sec. and up to 300 cm./sec. afterwards (15), this is to be expected. Thus, according to Eqn. (2.20.3), the velocity of hole expansion decreases as the hole radius increases. Both Charles and Mason and Hartland (53) have provided photographic evidence of this event. Experimental results plotted according to Eqn. (2.20.3), in the form $\frac{1}{v_r^2}$ versus r^2, showed a surprisingly good fit considering the simplicity of the analysis. A much more complicated expression, relating the hole expansion to the system properties, was formulated by Hartland (53). Here

again,a reasonable correlation was obtained,but not more so than for the simpler equation.

The location of the initial rupture point in the draining film needs to be considered. High speed photography has shown that central rupture is the most common occurrence in systems contaminated by surfactant material. The only explanation for this would seem to be that the film is thinnest at the centre. In pure systems,the film ruptures at,or near the edge. If dimple formation is important,then rupture would be expected to occur at the barrier ring which is the thinnest part of the film. Tilting of the drop may also occur causing preferential thinning on one side of the film. Another more spectacular type of rupture has been observed by Hartland (55). When the film is very thin (glycerol drop: liquid paraffin-glycerol system),instead of receding in the normal way,it shatters when rupture occurs. The film thickness at rupture was quite high compared with values obtained for less viscous systems,so that this event may not be very common.

2.21 Partial Coalescence

Coalescence is seldom a simple single-staged process. It is a common observation that coalescence takes place in a stage-wise manner (15,51,62,67,70,71,82,95). When the primary drop coalesces it produces a smaller secondary drop,which in turn produces a smaller tertiary drop and so on. Mahajan (91) and others have observed as many as eight successive stages to occur in certain systems. These observations were made with the naked eye so that it is possible that many more actual stages exist, although the size of the drops produced will be exceedingly small.

The viscosity ratio of the dispersed phase to the continuous phase p,is an important variable determining whether or not partial coalescence will take place. Charles and Mason (15) observed that coalescence became single-staged (no secondary drop formed) when p was less than 0.02 or greater than 11. We would infer from this that partial coalescence is

indeed a widely occurring phenomenon. It was also discovered by these workers that lowering of the interfacial tension (by the addition of small amounts of surfactants) had very little effect on the size of secondary drop produced. It is well to point out though,that the addition of a sufficiently high concentration of surfactant can suppress secondary drop formation altogether. Application of an electric field will also bring about the same effect.

With the aid of high speed photography,using film speeds as high as 3500 frames per second,Charles and Mason (15) were able to observe in detail the partial coalescence process. After the phase-2 film had ruptured, the drop liquid was observed to form a liquid column. The height of this column was approximately equal to the diameter of the original drop. During the drainage period the height of the column did not change appreciably. It was deduced that the excess pressure (γ/R) across the surface of the cylindrical column was responsible for causing drainage into the lower phase. Charles and Mason proposed a partial coalescence mechanism based on a Rayleigh disturbance. It was assumed that when the height of the liquid column becomes equal to its circumference ($2\pi R$),a Rayleigh disturbance grows in amplitude,resulting in a "necking down" at the base of the column. From here on there is a race between between the drainage and the "necking down" process,the outcome of which determines the size of the secondary drop. When the amplitude of the disturbance becomes equal to the radius of the column,the column breaks up and the undrained liquid forms the secondary drop.

The size of the secondary drop produced by partial coalescence can be found from the following equation. Charles and Mason (15) derived this equation by making use of Rayleigh's theory (108):

$$r_n = \left(\frac{a_{n+1}}{a_n}\right) = \left(\frac{3}{2 z_o^2}\right)^{\frac{1}{3}} \qquad (2.21.1)$$

where, r_n = drop diameter ratio

a_{n+1} = diameter of secondary drop

a_n = diameter of primary drop

z_o = 4.508 = optimum value of the dimensionless parameter (/2R)

Also,

$$r_o = \frac{a_{n+1}}{(12z_o)^{1/3}} \qquad (2.21.2)$$

where,

r_o = radius of column at breakup.

For z_o = 4.508, the calculated value of r_n from Eqn. (2.21.1) is 0.42. Considering the limitations of the original Rayleigh theory, which are considerable in the present circumstances, and those of Charles and Mason's own analysis, this predicted value is quite excellent. It is well within the accuracy of Charles and Mason's own experimental results. One significant restriction of their analysis of this process is the assumption that no drainage takes place after instability has occurred. This means that the volume of the secondary drop will be the same as that of the column at instability. Considering the high rate of drainage during the partial coalescence process, further drainage must occur after this point. This may cause a significant difference in the size of secondary drop which is predicted.

The Weber extension of Rayleigh's analysis yields the following equation for the breakup of the liquid column (131):

$$t_b = \left(\frac{1}{q} + \frac{6\mu_r}{\gamma}\right) \ln \frac{r}{\alpha_o} \qquad (2.21.3)$$

where t_b is the time required for the column to reach an amplitude r after instability has set in. Estimates for t_b have been obtained from high speed photographs by Charles and Mason, and Brown and Hanson (14) have measured t_b directly using an electrical technique. The latter authors, using a

simplified analysis incorporating Charles and Mason's theory of partial coalescence,developed a pair of equations for the prediction of the secondary drop diameter from the experimental value of t_b. The predicted values were in good agreement with those found from experiment. Their method overcomes the limitation of Charles and Mason's assumption mentioned previously. However,the fluid mechanics picture of the drainage of the liquid column,is obviously not as simple as they have assumed.

Mainly because of the work of Jeffreys and Hawksley (68) and Jeffreys and Lawson (66),doubt has arisen concerning the validity of the Rayleigh analysis as applied to the partial coalescence process. An extensive high speed photographic study of partial coalescence has been conducted by Lawson (82). Two important observations have resulted from this work:

(a) That movement of liquid back into the liquid column takes place from below the bulk interface. During the time this upward surge is taking place,material is still draining from the regions of the drop (liquid column) adjacent to the phase boundary.

The evidence for this event is: (i) a maximum in the height of the liquid column is reached during the period described above,and (ii) both Jeffreys and Lawson (66) and Brown and Hanson (14) have reported that liquid from the homophase is present in the secondary droplet. The latter authors report that the extent of mixing is in the region of 20 to 30%.

(b) Break-off of the liquid column was observed to take place very low down,almost near the base of the column.

According to the Rayleigh theory,if the liquid column is assumed to have a length greater than its circumference,this means that the disturbance should cause breakup at its mid-point. Thus,the actual break-off point is entirely in the wrong position for it to be caused by a Rayleigh disturbance.

A suggestion originally made by Wark and Cox (128) concerning the

formation of a secondary drop,now appears to be reasonable. The suggestion was,that there is such a rapid deflation within the drop (i.e. liquid column) that its 'tail' is sheared-off. The following possible mechanism for secondary droplet formation has been advanced by Lawson (82). "There is a balance between the upward force and the drop deflation,which depending on the relative magnitude of the former,describes whether or not there will be a finite secondary drop". The physical evidence certainly makes this explanation attractive,but the vagueness of the terms "upward force" and "deflation" requires some qualification. There does not seem to be a direct equality between these two terms. It would appear that more study is required to present the mechanism in a more quantitative fashion.

Partial coalescence is an extensively occurring phenomenon in liquid-liquid systems. Its mechansim deserves to be understood if many practical problems are to be solved.

CHAPTER 3

FILM DRAINAGE THEORY

Introduction

When a liquid drop falls onto a plane interface it is separated from that interface, prior to coalescence by a film of continuous phase fluid. It has been suggested that the residence time of the drop at the interface is equal to the time for this film to thin to a thickness at which it is unstable.

Several authors have made a hydrodynamic study of the drainage of the film and attempted to calculate the film thickness as a function of time. As the shape of the film is not known, their approach has been to select a drainage model which is geometrically simple and can be examined mathematically, but does have some similarity to the shapes of drop and interface which are observed during the coalescence process. The models which are used are discussed fully in Chapter 2. The two extremes are a spherical-planar model and a parallel-plates model and the other models have surfaces which lie somewhere between these two.

The Navier-Stokes equation has been solved for the flow of fluid in the film which is trapped between the surfaces described by the above models. The equations so obtained relate the film thickness at some time with viscosity, density, interfacial tension and drop diameter.

MacKay and Mason (88) who studied the parallel-plates model, found that their drainage equation could be used to describe the drainage of the film when the film thickness was between 1 micron and 0.2 microns. However, there is no evidence to suggest that the spherical-planar model gives an adequate description of the drainage.

The drainage equations may also be used to calculate the time required for the film to thin from h_1 to h_2, where h is the distance of separation of the two surfaces at some particular point. If h_2 and h_1 are taken as the respective values of h at film rupture and at some zero time

then $t_2 - t_1$ will be the coalescence time, provided that this coalescence time is measured from the same zero time at which h_1 is measured. However, neither h_2 or h_1 are easy to determine. Present techniques do not allow h_2 to be measured. Moreover, the zero time is taken as the moment when the drop first arrives at the interface and so does not take into account the oscillation of the plane surface which occurs. This may result in the drop bouncing from the surface before finally coming to rest on it.

Limited success has been obtained with the parallel-plates model and with a non-uniform film model. The non-uniform film model was used by Jeffreys and Hawksley (68) to explain their experimental relationship.

In the following sections, an attempt is made to calculate the shape of the film at the interface and to solve the Navier-Stokes equation for flow in this film.

Before attempting a mathematical analysis it is worth while considering a few general features associated with drainage of the phase-2 film; notably, the pressure distribution.

3.1 Pressure Distribution

A. Consider the case of a thin spherical film, closely resembling the phase-2 film(79,102), which is draining slowly (see Fig. (3.1)).

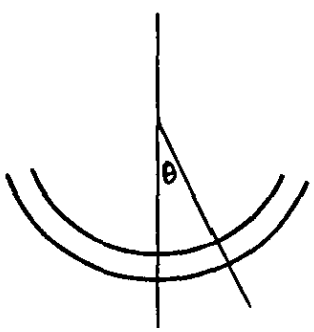

Fig. 3.1

If the principal radii of curvature of the drop and the main surfaces, are, respectively, R_{D1}, R_{D2} and R_{M1}, R_{M2}, then:

$$\gamma\left[\frac{1}{R_{D1}} + \frac{1}{R_{D2}} + \frac{1}{R_{M1}} + \frac{1}{R_{M2}}\right] = \frac{4\gamma}{R_o} \qquad (3.1.1)$$

where R_o = radius of curvature at $\theta = 0$ and γ = interfacial tension. Provided the film is thin (i.e. $h \ll R$) a solution is:

$$R_{D1} = R_{D2} = R_{M1} = R_{M2} = R_o \qquad (3.1.2)$$

B. For a similar situation (see Fig. 3.2) we may write the appropriate boundary conditions. Looking at the principal radii of curvature:

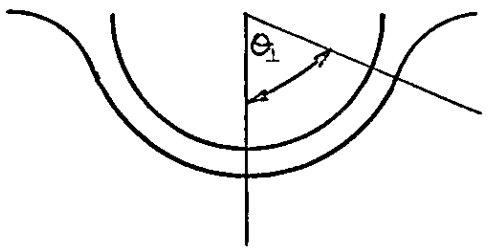

Fig. 3.2

(i) At $\theta = 0$ both surfaces are spherical with radii of curvature $\approx R_o$.

(ii) At θ = some value θ_i, which changes with time, the main surface has radii of curvature $\approx R_o, 0$, and therefore the drop surface has radii of curvature $\approx R_o$ and $R_o/2$.

(iii) Between $\theta = 0$ and $\theta = \theta_i$ the radii of curvature of the main surface will be R_o, (some value between 0 and R_0) and the drop surface R_o and some value between R_o and $R_o/2$, such that, $\frac{\gamma}{R_{D2}} + \frac{\gamma}{R_{M2}} = \frac{2\gamma}{R_o}$. R_{D2}, R_{M2} are the principal radii of curvature of the two surfaces which are varying with θ.

Provided there are no ripples in the film, it is obvious that where the film is thin, Eqn. (3.1.1) applies, except that near $\theta = \theta_i$, R_{D2}, R_{M2} will be changing noticeably. This assumes that the film is still thin at θ_i. If it is not, then Eqn. (3.1.1) applies up to a value of θ where the film can no longer be considered thin. Since the film is thin, any slow changes of h with θ will not affect the pressure distribution noticeably. Their only

effect will be on the momentum and on the shear forces.

C.

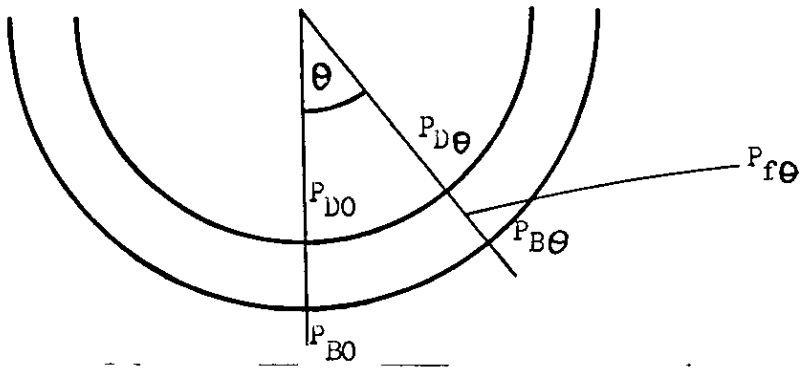

Figure 3.3

Following on from part A, provided that the film is very thin, then:

$$P_{DO} - P_{BO} = \frac{4\gamma}{R_o}, \quad P_{D\theta} - P_{B\theta} = \frac{4\gamma}{R_o} \quad \text{,and}$$

$$P_{f\theta} = P_{D\theta} - \frac{2\gamma}{R_o} = P_{DO} - \frac{2\gamma}{R_o} - R_o(1 - \cos\theta)\rho_1 g$$

$$P_{f\theta} = P_{fO} - R_o(1 - \cos\theta)\rho_1 g$$

where ρ_1 is the density of the dispersed phase and P the pressure. Now,

$$P_f(\theta + d\theta) = P_{fO} - R_o(1 - \cos(\theta + d\theta))\rho_1 g$$

$$\therefore \quad P_{f\theta} - P_{f(\theta + d\theta)} = R_o\rho_1 g \sin\theta\, d\theta.$$

Above the static pressure,

$\Delta P_{f \to \theta + d\theta} = (\rho_1 - \rho_2)R_o g \sin\theta\, d\theta$ where ρ_2 is the density of the continuous phase. Note that near θ_i (i.e. where $R_{M1} \to 0$) the pressure will decrease more rapidly than is shown by the above equation.

3.2 Flow Out of the Phase-2 Film

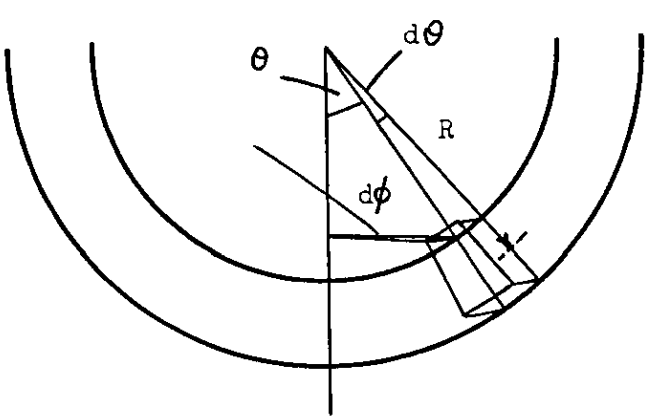

Figure 3.4

It is assumed that $\frac{dh}{dt}$ is independent of θ in the region where the

film is thin. The rate at which fluid is displaced from the film between $\theta = 0$ and $\theta = \theta$ is:

$$\left[\frac{4}{3}\pi\left(R + \frac{h}{2}\right)^3 - \frac{4}{3}\pi\left(R - \frac{h}{2}\right)^3 - \frac{4}{3}\pi\left(R + \frac{h}{2} - \frac{dh}{dt}\frac{1}{2}\right)^3 + \right.$$

$$\left. + \frac{4}{3}\pi\left(R - \frac{h}{2} + \frac{dh}{dt}\frac{1}{2}\right)^3\right]\frac{(1 - \cos\theta)}{2}$$

$$= 2\pi\frac{dh}{dt}\left[\left(R - \frac{h}{2}\right)^2 + \left(R + \frac{h}{2}\right)^2\right](1 - \cos\theta)/2$$

$$= 2\pi R^2(1 - \cos\theta)\frac{dh}{dt}, \text{since } R \gg h. \qquad (3.2.1)$$

Between 0 and $\theta + d\theta$ the rate of displacement of fluid is:

$$2\pi R^2(1 - \cos(\theta + d\theta))\frac{dh}{dt}$$

$$= 2\pi R^2(1 - \cos\theta + \sin\theta\, d\theta)\frac{dh}{dt}.$$

It is assumed that the two surfaces are rigid and that the velocity profile in the film is parabolic. Thus, $V = V_o(1 - 4x^2/h^2)$ where x is the distance from the centre of the film and V_o the velocity at $x = 0$. Thus the flow rate

$$= \int_{-\frac{h}{2}}^{+\frac{h}{2}} V_o\left(1 - \frac{4x^2}{h^2}\right)dx \cdot 2\pi R\sin\theta$$

$$= 2V_o h \cdot 2\pi R\sin\theta,$$

and $$V_o = \frac{2\ R^2(1 - \cos\theta)\ dh/dt}{\frac{2}{3}\,h\ 2\pi R\sin\theta},$$

so that $$V = \frac{3R}{2h}\left(\frac{1 - \cos\theta}{\sin}\right)\frac{dh}{dt}\left(1 - \frac{4x^2}{h^2}\right) \qquad (3.2.2)$$

The shear stresses at the interface are equal to:

$$-\mu_2\left[\frac{\partial V}{\partial x}\right]_{x = \pm h/2}$$

$$= \pm\frac{3}{2}\mu_2\frac{R}{h}\frac{(1 - \cos\theta)}{\sin\theta}\frac{dh}{dt}\left[\frac{4}{h}\right]$$

$$= \pm \frac{6R\mu_2}{h^2} \frac{(1 - \cos\theta)}{\sin\theta} \frac{dh}{dt} \qquad (3.2.3)$$

where μ_2 is the phase-2 viscosity. Therefore the shear force acting on the element (as shown in Fig. 3.4)

$$= - \frac{6R\mu_2}{h^2} \frac{(1 - \cos\theta)}{\sin\theta} \frac{dh}{dt} \left[2\pi R(R\cos\theta - R\cos(\theta + d\theta)) \right] . \; .2\frac{d\phi}{2\pi} \qquad (3.2.4)$$

$$= - 12R^3 \frac{\mu_2}{h^2} . \frac{dh}{dt} (1 - \cos\theta)\, d\theta\, .d\phi \qquad (3.2.5)$$

Pressure Force on the Element

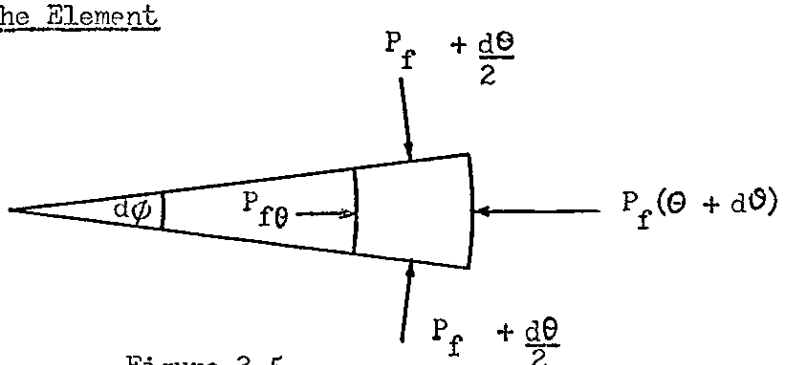

Figure 3.5

The pressure force =

$$-\frac{\partial P_f}{\partial\theta} .d\theta (2\pi R \sin(\theta + d\theta))h + \frac{\partial P_f}{\partial\theta} . \frac{d\theta}{2} (2\pi R\sin(\theta + d\theta) - 2\pi R \sin\theta) . \; .h \frac{d\phi}{2\pi}$$

$$= - \frac{\partial P_f}{\partial\theta} .d\theta (2\pi R \sin\theta)h \frac{d\phi}{2\pi}$$

$$= R\rho_1 g \sin\theta .d\theta (2\pi R \sin\theta)h . \frac{d\phi}{2\pi}$$

$$= 2\pi R^2 \rho_1 g \sin^2\theta .d\theta .h \frac{d\phi}{2\pi} ,$$

this includes the static pressure. Taking the pressure above the static value, to take into account the weight of the element, the effective force in fluid flow

$$= R^2 (\rho_1 - \rho_2) g \sin^2\theta .d\theta .h .d\phi \qquad (3.2.6)$$

Momentum

The momertum into the element per second

$$= \int_{-h/2}^{+h/2} \frac{3}{2}\rho \left(\frac{2R}{h} \frac{(1 - \cos\theta)}{\sin\theta} \frac{dh}{dt} (1 - \frac{4x^2}{h^2}) R \sin\theta .d\phi \right).$$

$$\cdot\frac{3}{2}\frac{R}{h}\left(\frac{1-\cos\theta}{\sin\theta}\right)\frac{dh}{dt}\left(1-\frac{4x^2}{h^2}\right)$$

$$= \frac{6}{5}\rho 2\frac{R^3}{h}\left(\frac{dh}{dt}\right)^2\left(\frac{1-\cos\theta}{\sin\theta}\right)^2 .d\phi$$

The rate of momentum out

$$= \frac{6}{5}\rho 2\frac{R^3}{h}\left(\frac{dh}{dt}\right)^2\left(\frac{1-\cos(\theta+d\theta)}{\sin(\theta+d\theta)}\right)^2 .d\phi$$

$$= \frac{6}{5}\rho 2\frac{R^3}{h}\left(\frac{dh}{dt}\right)^2\left(\frac{1-\cos\theta+\sin\theta d\theta}{\sin\theta+\cos\theta .d\theta}\right)^2 .d\phi$$

The rate of change of momentum

$$= \frac{6}{5}\rho 2\frac{R^3}{h}\left(\frac{dh}{dt}\right)^2\left[2(1-\cos\theta)-(1-\cos\theta)^2\frac{\cos\theta}{\sin^2\theta}\right]d\theta .d\phi \qquad (3.2.7)$$

Momentum Balance

$$\frac{6}{5}\rho 2\frac{R^3}{h}\left(\frac{dh}{dt}\right)^2\left[2(1-\cos\theta)-(1-\cos\theta)^2\frac{\cos\theta}{\sin^2\theta}\right]d\theta .d\phi$$

$$= R^2(\rho_1-\rho_2)g\sin^2\theta\, h\, d\theta .d\phi + 12R^3\frac{\mu_2}{h^2}\cdot\frac{dh}{dt}(1-\cos\theta)d\theta .d\phi \qquad (3.2.8)$$

When dh/dt is very small,

$$h^3 = -\frac{12\mu_2\frac{dh}{dt}(1-\cos\theta)R}{(\rho_1-\rho_2)g\sin^2\theta} \qquad (3.2.9)$$

and the film thickness,h,increases very slowly with increase in θ. This solution also gives,at a given value of θ:

$$-\frac{dh}{dt} = k\,h^3$$

$$\therefore \quad \frac{1}{2h^2} = kt + C$$

where $k = k'R\frac{\mu_2}{\Delta\rho}$ and C is a constant of integration. Looking at the inertial term, the assumption requires that Rh^5 is very small in comparison with R^2h, i.e. for small values of h. The full equation for film thickness versus time is:

$$(t_2 - t_1) = t = \frac{6\mu_2 R}{\Delta\rho g(1 + \cos\theta)} \cdot \frac{1}{h_2^2} \qquad (3.2.10)$$

for $h_1 \gg h_2$.

3.3 Comparison of Calculated Drainage Time and Experimental Mean Rest-Time

It is useful to compare the predicted value of the theoretical drainage time, t, for a given separation, h, with the experimental mean rest-time, t_m. For this purpose two examples have been taken from the Series 2 results which are described in Chapter 5 (see Appendix 3 for details of the results). The equations representing the various drainage models are as follows:

Model 1 Spherical-Planar

$$(t_2 - t_1) = t = \frac{2}{9}\frac{\mu_2}{\Delta\rho gb} \ln\frac{h_1}{h_2}$$

where h_1, h_2 = initial and final film thickness, respectively.

t_1, t_2 = initial and final drainage time, corresponding to h_1 and h_2, respectively.

μ_2 = phase-2 viscosity.

$\Delta\rho = (\rho_1 - \rho_2)$ = phase density difference.

b = droplet radius.

Model 2 (i) Parallel-Plates (Two Approaching Flat Discs)

$$(t_2 - t_1) = t = \frac{3\pi\mu_2 R^2}{mg} \frac{1}{h_2^2}$$

for $h_1 \gg h_2$, where

mg = force pressing the two discs together.

R = radius of disc $\cong x_c$.

It should be noted that in the above and subsequent models, the value of t is

based on an equivalent drainage force condition. In order to make a valid comparison between the parallel discs model and other models, it is necessary for the drainage force on the phase-2 film to be the same in all cases. When calculating this force the radius of the film in the parallel discs model is equal to the radius of the discs. In the other cases, the horizontal distance from the mid-axis to the periphery of the film is taken to be equivalent to R. This distance is the value x_c which can be calculated by the method due to Princen (102). Details of calculated drop shape characteristics for a number of different systems are contained in Appendix 4.

Model 2(ii) Deformable Drop - Rigid Interface (Charles and Mason's Uniform Film Model (16)).

$$(t_2 - t_1) = t = i\left[\frac{\mu_2}{4}\right]\left[\frac{\Delta\rho\, g\, b^5}{\gamma^2}\right]\frac{1}{h_2{}^2}$$

for $h_1 \gg h_2$, where γ = interfacial tension, and i = 1.

Model 2 (iii) Deformable Drop - Deformable Interface (Elton and Picknett's Uniform Film Model (33)). Small Drops.

$$(t_2 - t_1) = t = i\left[\frac{\mu_2}{4}\right]\left[\frac{\Delta\rho\, g\, b^5}{\gamma^2}\right]\frac{1}{h_2{}^2}$$

for $h_1 \gg h_2$, where i = 4.

Model 2(iv) Deformable Drop - Deformable Interface. Large Drops.

$$(t_2 - t_1) = t = \frac{3}{4}\frac{\mu_2 A^2}{\pi F_D}\frac{1}{h_2{}^2}$$

for $h_1 \gg h_2$, where,

F_D = drainage force (see Appendix 4)

A = area of "spherical cap" (see Appendix 4)

Model 3 Equation (3.2.10).

$$(t_2 - t_1) = t = \frac{6R\mu_2}{\Delta\rho\, g(1 + \cos\theta_c)} \cdot \frac{1}{h_2^2}$$

for $h_1 \gg h_2$.

On the basis of experimental evidence (16), and provided that t is sufficiently large, it can be assumed that coalescence will occur at the edge of the phase-2 film, i.e. at θ_c (see Appendix 4 for values of θ_c).

The following experimental results will serve as examples in the case of a large drop and a small drop.

Example 1 Large Drop. System: Heptane-Water.

b	= 0.2525 cm.	$\Delta\rho$	= 0.3158 gm.cm.$^{-3}$
R	= 0.4405 cm.	γ	= 50.75 dynes cm.$^{-1}$
x_c	= 0.1608 cm.	μ_2	= 0.4158 c.p.
θ_c	= 21° 23'	F_D	= 18.81 dynes (deformed drop)
t_{m1}	= 7.95 secs.	F_S	= 20.81 dynes (spherical drop)

Example 2 Small Drop. System: Heptane-Water.

b	= 0.03175 cm.	F_S	= 0.0414 dynes
θ_c	= 1° (assumed)		
t_{m3}	= 1.53 secs.		

The predicted values of t for a range of film separations $(h_2 - h_1)$ are presented in Tables 3.1 and 3.2.

3.4 Discussion

In Section 3.2 the Navier-Stokes equation was solved for the flow of the film fluid in the case where dh/dt is independent of θ. This assumption is valid over the region where the film is thin, since any slow changes of h with θ will not affect the pressure distribution noticeably. Their only effect will be on the momentum forces in the flowing fluid and the shear forces at the approaching interfaces. It is noticed that as $(1 - \cos\theta)/\sin^2\theta$, i.e. $1/(1 + \cos\theta)$, does not change rapidly with θ, the

assumption concerning dh/dt is consistent with Eqn. (3.2.9).

According to Eqn. (3.2.9),the rate of film thinning is proportional to h^3. Eqn. (3.2.10) predicts that the drainage time t,increases with increase in μ_2 and R,and decreases with increase in $\Delta\rho$. The fact that the dependency on the drop size is to the first power,suggests that the model is a "mixed model",i.e. that the predicted rest-time lies between the values predicted by the parallel plates model and the spherical-planar model. This is shown to be true in Table 3.2,for the case of a small drop (b = 0.03175). It is interesting to note,that as θ becomes very small, the term $(1 + \cos\theta)$ in Eqn. (3.2.10),approaches the value 2. This suggests that very small drops are spherical but large drops are deformed. In the latter case,the lower deformed part of the drop has a radius R whilst the upper part has a different radius.

The case of a large drop is considered in Table 3.1 and it is seen that the predicted drainage times lie outside the range between the parallel plates model and the spherical-planar model. In purified systems, it is likely that considerable movement occurs at the interfaces and this is not accounted for the present analysis. This will result in considerable increase in the rate of film thinning and hence the experimental rest-times will be much lower than the predicted values.

Table 3.2 suggests that the drainage model represented by Eqn. (3.2.10) will provide a better estimate than any of the other models for the case of very small drops. Without an exact knowledge of the film thickness, it is not possible to obtain a realistic estimate ,however.

General Reference

Longwell,P.A.,"Mechanics of Fluid Flow",McGraw Hill,1966.

TABLE 3.1

LARGE DROP

Distance of Separation cm.	Time for Model 1 secs.	Time for Model 2(i) secs.	Time for Model 2(ii) secs.	Time for Model 2(iv) secs.	Time for Model 3 secs.
0	0	0	0	0	0
1.10^{-1}	$5.53.10^{-4}$	$3.42.10^{-5}$	$1.51.10$	$3.69.10^{-5}$	$1.84.10^{-3}$
1.10^{-2}	$1.11.10^{-3}$	$3.42.10^{-3}$	$1.51.10^{3}$	$3.69.10^{-3}$	$1.84.10^{-1}$
1.10^{-3}	$1.66.10^{-3}$	$3.42.10^{-1}$	$1.51.10^{5}$	$3.69.10^{-1}$	$1.84.10$
1.10^{-4}	$2.21.10^{-3}$	$3.42.10$	$1.51.10^{7}$	$3.69.10$	$1.84.10^{3}$
1.10^{-5}	$2.76.10^{-3}$	$3.42.10^{3}$	$1.51.10^{9}$	$3.69.10^{3}$	$1.84.10^{5}$
1.10^{-6}	$2.32.10^{-3}$	$3.42.10^{5}$	$1.51.10^{11}$	$3.69.10^{5}$	$1.84.10^{7}$

TABLE 3.2

SMALL DROP

Distance of Separation cm.	Time for Model 1 secs.	Time for Model 2(i) secs.	Time for Model 2(iii) secs.	Time for Model 3 secs.
0	0	0	0	0
1.10^{-1}	$4.38.10^{-3}$	$3.82.10^{-2}$	$1.92.10$	$2.55.10^{-4}$
1.10^{-2}	$8.76.10^{-3}$	$3.82.10^{0}$	$1.92.10^{3}$	$2.55.10^{-2}$
1.10^{-3}	$1.31.10^{-2}$	$3.82.10^{2}$	$1.92.10^{5}$	2.55
1.10^{-4}	$1.75.10^{-2}$	$3.82.10^{4}$	$1.92.10^{7}$	$2.55.10^{2}$
1.10^{-5}	$2.19.10^{-2}$	$3.82.10^{6}$	$1.92.10^{9}$	$2.55.10^{4}$
1.10^{-6}	$2.63.10^{-2}$	$3.82.10^{8}$	$1.92.10^{11}$	$2.55.10^{6}$

** (1.10^{-1} means 1×10^{-1}, etc.)

CHAPTER 4

EQUIPMENT AND EXPERIMENTAL PROCEDURE

4.1 Purpose of Investigation

The purpose of the experimental investigation was to extend and consolidate the understanding of the coalescence of single drops at a plane liquid-liquid interface. The main objectives were:

(i) To determine the rest-times of single drops for all stages of coalescence in purified liquid systems.

(ii) To study the behaviour of a wide range of drop size and effect of important variables on the coalescence.

4.2 Choice of System

The use of liquid-liquid extraction techniques for the recovery and separation of metal-ions from solution has received much attention (36). Extractants such as tributylphosphate (TBP) and methyl isobutyl ketone (MIBK) have been used for the recovery and separation of Uranium/Plutonium and rare earth metals.

In recent years there have been attempts to find cheaper extractants which could be used for the recovery and separation of commoner metals. Fletcher and Flett (37) of the Warren Spring Laboratory studied the use of commercially available naphthenic* and Versatic* acids for this purpose. This type of extractant is suitable for the extraction of divalent and rare earth metal cations from aqueous solutions.

The uncertain purity and composition of the organic components used by Fletcher and Flett precluded their use in this investigation. However, components were selected which closely approximated the average properties of the liquid components used by Fletcher and Flett. Instead of Versatic 911 (a mixture of C_9 - C_{11} acids) n-decanoic acid was used as the extractant,

* Shell Chemical Co. Ltd.

and the solvent,kerosine (a mixture of C_6 - C_9 paraffins),was replaced by n-heptane.

4.3 Preliminary Experiments

In the binary system heptane-water,and the ternary system decanoic acid-heptane-water,single water drops were observed to coalesce at the interface in a stagewise manner. Depending on the size of the primary drop,the coalescence was usually complete by the fifth or sixth stage. The size of the drop beyond the fourth stage of coalescence was extremely small (estimated to be less than 0.01 cm.,approximately).

The process of partial coalescence thus provides a convenient method of forming single drops in the system. Equally important,the size of drops formed in this way can be adjusted for a given system,by altering the size of the primary drop.

4.4 Scope of Experiments

In order to achieve the main objectives,and to avoid unnecessary experimentation,the coalescence of single water drops was studied in the following systems:

Type	System
binary	heptane-water
ternary	0.05M decanoic acid-heptane-water
ternary	0.5M decanoic acid-heptane-water
ternary	1.0M decanoic acid-heptane-water

The range of properties exhibited by these systems allowed a systematic investigation of the important variables affecting coalescence to be carried out. The effect of temperature was excluded because as Ipsen (65) has shown, its influence is implicitly accounted for. All the experiments were therefore carried out at 25°C.

Two principal items of apparatus were required for the experiments:

(a) A cell in which the coalescence of the single drops could be observed and its rest-time measured.

(b) A cell in which the partial coalescence process could be photographed for the purpose of drop size measurement.

4.5 Coalescence Rest-Time Studies

Design Requirements

(i) The coalescence cell should be well thermostatted.

(ii) The purified liquid components should be free from contamination.

(iii) The drops should be easily seen whilst they are at the interface.

(iv) A method of interface renewal to remove impurity which accumulates at the interface.

(v) A method of forming large drops accurately.

(vi) A method of adjusting the height of fall of the drop to the interface.

Apparatus

The apparatus used for the coalescence rest-time studies was made of glass and its construction is shown in Fig. 4.1. To prevent seizure of the glass to glass surfaces, PTFE sleeves were fitted to all ground glass joints and stopcock plugs were made of PTFE.

The coalescence cell, A, consisted of a Pyrex tube 42 cm. long and 5 cm. diameter, fitted at each end with B55 ground glass joints. The arrangement was such that the operation of the cell could be reversed to allow the study of rising drops at a plane interface. A method of interface renewal, similar to that used by Charles and Mason (16) was employed. The interface was maintained at the top of the tube, B, which was ground flat. Various lengths of the tube B were available to allow the interface to be positioned at a convenient height in the cell, A. Drops were formed on a fine, drawn-out, glass capillary, C, approximately 18 cm. long, the tip of which was ground flat and square. The flow of liquid from the reservoir, D, to the capillary was controlled by an 'Alga' micrometer syringe connected to the reservoir by the PTFE tube, G. The reservoir assembly was attached to a sliding frame which could be moved in a vertical direction. A perspex cabinet was used to enclose the coalescence apparatus and the whole assembly was mounted on an antivibration mounting.

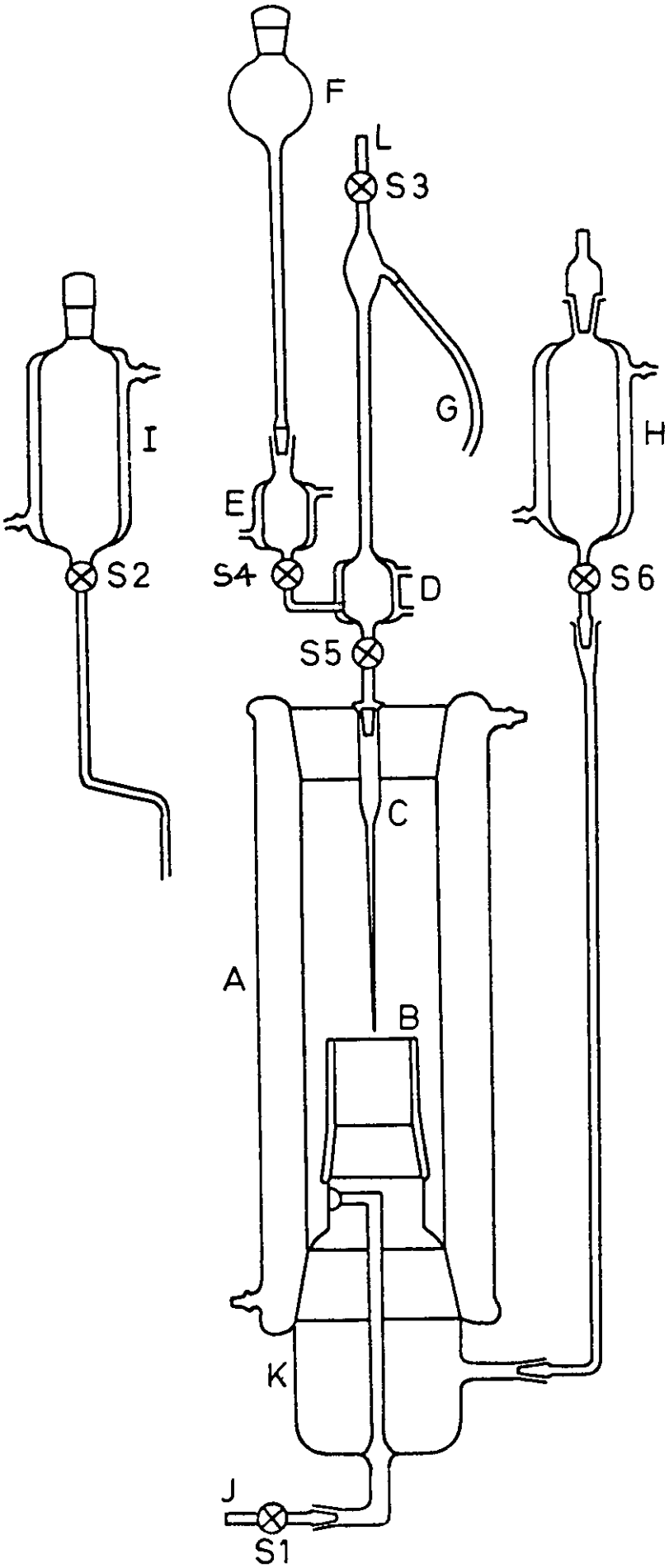

Fig. 4.1 Coalescence Time Apparatus

The cell,A, and the various heavy and light phase reservoirs were enclosed in jackets maintained at 25°C ± 0.01°C. In addition,fan-circulated air inside the cabinet was controlled at 25°C ± 0.25°C. Photograph 4.P.1 shows the unit fully assembled.

Cleaning

Prior to each series of experimental runs,the apparatus was thoroughly cleaned in the following manner:

(i) All the items of glassware and PTFE were degreased with acetone and rinsed with copious supplies of hot water.

(ii) The apparatus was filled with warm concentrated chromic acid, freshly prepared,and allowed to stand for approximately 24 hrs.

(iii) The apparatus was drained of chromic acid and vigorously rinsed with warm,freshly-distilled water for a prolonged period. It was then dried in a hot-air oven. During all the washing procedures and subsequent assembly,great care was taken in handling the apparatus so as to prevent contamination.

(iv) Lastly,the apparatus was assembled in the Perspex cabinet, filled with double-distilled water and left to stand overnight. A close fitting sheet of PTFE was used to seal the top of the cell,A.

Preparation of Materials

The water used in all the experiments was double distilled from potassium permanganate solution and stored in glass receivers. The n-heptane used was to I.P. specification and was redistilled (the fraction boiling between 98 and 100°C was collected) except for those experiments specifically indicated in Appendix 3.

Two grades of decanoic acid were used. The "Specially Pure" grade used in the Series 1 experiments was obtained in crystalline form from British Drug Houses Ltd. For the Series 2 and 3 experiments a purer form of decanoic acid was obtained from Eastman Kodak,N.Y. In each case,the decanoic

PHOTOGRAPH 4.P.1

Coalescence Time Apparatus

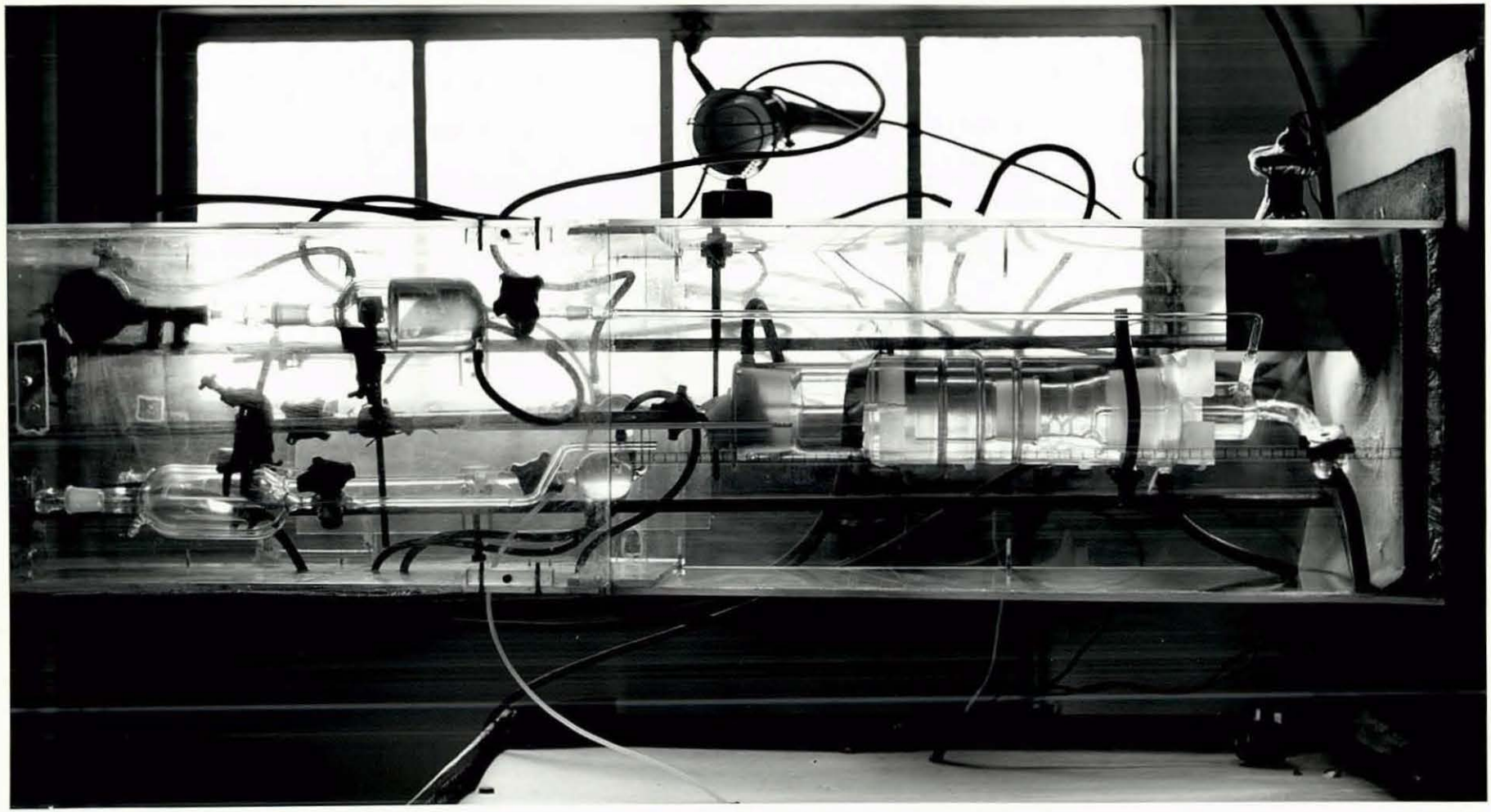

acid was used without further preparation. All of the systems were mutually saturated in glass receivers at 25°C.

Experimental Procedure

After the double-distilled water had been drained from the apparatus, the saturated water phase was admitted to the reservoir,H. A quantity was run through the coalescence cell,A,in order to purge any unsaturated water. The drop forming arrangement was then lowered so that the tip of the glass capillary was just below the top of B. With a suction bulb attached to L and S4 closed,the heavy phase liquid was drawn up to a level just above S5. The suction bulb was removed and the drop forming arrangement was completely filled with liquid from the reservoir,F. With S5 and S3 closed,the PTFE tube, G,and the micrometer syringe attached to it were also filled with liquid. Light phase liquid was then admitted to the coalescence cell from reservoir I. A flat PTFE cover was moved into position so that it was flush with the top rim of the cell,A. Theinterface was cleaned by allowing heavy phase liquid from H to overflow at B. The accumulation was removed through S1.

The shape of the interface was adjusted by means of a suction bulb attached to H. A water droplet was formed at the tip of the capillary by adjusting the micrometer syringe. The hight of the pendant drop above the flat interface was adjusted to that required by moving the frame supporting the drop forming device. S5 was then closed and the contents of the apparatus were allowed to come to equilibrium over a period of approximately 4 hours.

Before a series of readings was commenced,the interface was renewed and made plane,after which a short period was allowed for attainment of equilibrium. Just before taking readings,the air-circulating fan was switched off.

The interface was adjusted after about 10 primary drops had been investigated. In the case of the Series 1 experiments the interface was renewed from time to time during a run. Thispractice was not adopted in the Series 2 and 3 experiments.

The coalescence rest-time was recorded on magnetic tape using a Ferguson "Model 3214" tape recorder, each stage of coalescence being registered by a manually produced input signal. The time between a drop arriving at the interface and the first stage of coalescence, and the times taken between subsequent stages of coalescence, were determined with a stopwatch on playback of the tape.

4.6 Drop Size Ratio Studies

Design Requirements

(i) A simple glass cell to allow the drop to be photographed whilst resting at the interface.

(ii) A thermostatted enclosure to maintain the liquid contents of the cell at 25°C.

Apparatus

The layout of the equipment is shown schematically in Fig. 4.2. A 'tall form' 250 ml. glass beaker, E, was used to contain the two liquid phases. The beaker was placed in a thermostatically controlled tank, G, which was maintained at 25°C. Droplets were formed on the end of a glass capillary, B, which was connected to an 'Alga' micrometer syringe, C, by PTFE tubing. This connection was made via the reservoir arrangement used for the coalescence time experiments.

Observations of the partial coalescence process were recorded on 16 mm film. For this purpose a 16 mm Bolex cine camera, A, was used and it was mounted vertically above the 250 ml. beaker. Lighting was provided by a 200W tungsten filament bulb, F, positioned close to the bottom of the glass tank and directly below E.

Photographic Detail

Camera:	Paillhard-Bolex, Reflex, 16 mm cine.
lens:	Kern-Paillhard, 'Pizar', f 2.8/50 mm, fitted with 20 mm. extention tube and lens hood.
Exposure:	1/40 second at f22.
Film:	Kodak 'Plus X'.
Film Speed:	16 fps.

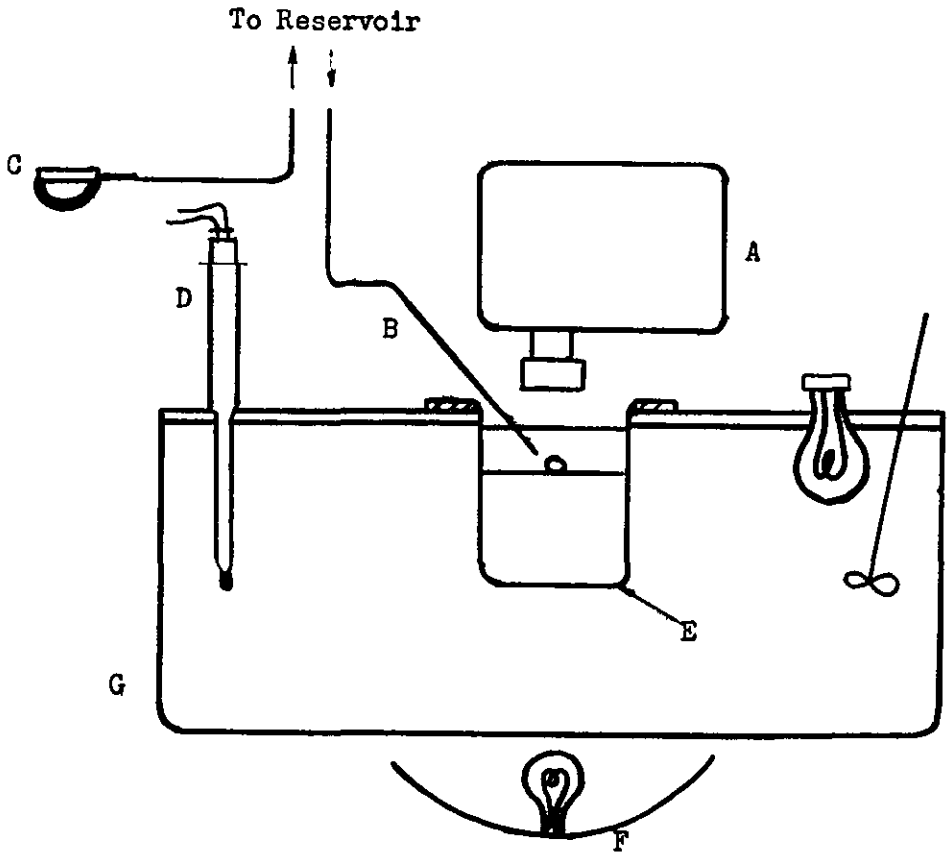

Fig. 4.2 Apparatus for Drop Size Ratio Studies

Experimental

All the pieces of PTFE and glass equipment were thoroughly cleaned in the manner described in Section 4.5. The preparation of the liquid components was also carried out as previously described in Section 4.5.

Two systems were investigated; the two-component system heptane-water and the three component system 0.5% decanoic acid-heptane-water. The study covered a range of primary dropsizes and lengths of fall of the drop to the interface.

Experimental Procedure

Heavy phase liquid was admitted directly into the 250 ml. beaker, E. A quantity of light phase liquid was then gently poured onto the top of the heavy phase liquid. The drop forming capillary, B, was immersed below the level of the interface separating the heavy and light phases. By means of a suction bulb attached to the heavy phase reservoir, a quantity of heavy phase liquid was drawn up through the glass capillary. The PTFE line connecting the glass capillary to the three-way tap was completely filled with liquid. The position of the three-way tap was reversed and the line to the micrometer syringe was filled by flowing liquid from the reservoir.

The camera, A, was brought into position, the lighting, F, was switched-on, and the three-way tap turned to connect the micrometer syringe to the capillary. A number of trial drops were allowed to fall to the interface so that the camera could be focussed.

Fresh liquid components were used in a clean beaker for each different drop size studied. The primary drop was formed very slowly on the end of the glass capillary so as to allow it to come to equilibrium with the bulk phase liquid. The fall height of the drop to the interface was conveniently adjusted by altering the height of the lower heavy phase liquid in the beaker.

The primary drop volume was obtained directly from the micrometer reading and the spherical drop diameter calculated from this. The drop diameters at the second, third and fourth partial coalescence stages were

obtained from the projected image recorded on the cine film. A magnification of approximately 12X was employed and the projected drops were measured with a transparent mm. rule.

4.7 Effect of Interface Age on Coalescence Rest-Time

The 'Teflon-Glass' method of cleaning the interface was reported by Hodgson (63) to be more effective than the method of overflowing the interface. It involves sucking-off the interface by means of a drawn-out glass tube which is fitted with a small Teflon 'whisker'. Since the Teflon is organic phase wetted and the glass water wetted, the principle is that both sides of the interface are swept clean.

Two groups of experiments were carried out to investigate the effect of interface age and the effects reported by Hodgson.

Experimental

The coalescence cell shown in Fig. 4.1 was used and it was fitted with a sucking probe similar to that used by Hodgson. Preparation of the equipment was carried out in the manner described previously in Section 4.5. The interface was only cleaned with the Teflon-Glass probe prior to a run. When the interface cleaning was complete, the interface age was designated to be zero and timing was commenced. The interface age was subsequently recorded when a drop had completely coalesced, and between such recordings the rest-times for each partial coalescence stage was registered on the recorder.

Two runs at a single drop size were carried out for each of the systems heptane-water and 0.5M decanoic acid-heptane-water. The fall height condition of the drop in each run was L = 0 cms* For each system, one run was performed with the primary drop aged for 1 minute prior to its release and the other without the drop being aged.

4.8 Determination of Physical Properties of Liquid Components

The density, viscosity and interfacial tension for all solutions were

* In this experiment, and all other experiments reported in this work, L = 0 cm. refers to the case where the drop was released from a position very close to the interface. In all cases, the distance was estimated to be between 0.1 and 0.3 cm.

determined at 25°C.

The density of solutions was determined using standard specific gravity bottlescalibrated with double-distilled water. The absolute density of water was taken to be 0.997074 gm./ml. at 25°C (100).

The viscosities were determined by using Cannon-Fenske glass viscometers. These were calibrated with double-distilled water and the absolute viscosity of water was taken to be 0.8937 cp. (8).

The interfacial tensions were determined by the drop volume method. This method is described in detail by Davies and Rideal (21).

The determinations of the interfacial tension were carried out in the coalescence cell described in Section 4.5. A glass nozzle with a carefully ground end was used to form the drops. The drops were formed very slowly over a period of about 3 minutes and the final detachment was approached extremely slowly.

The average volume reading for 8 drops was used to calculate the interfacial tension from the equation:

$$\gamma_i = \frac{\phi V (\rho_1 - \rho_2) g}{2\pi a}$$

where V = volume of drop, cm^3.

ρ_1, ρ_2 = density of heavy and light phase, respectively, $gm./cm.^3$

$2a$ = outside diameter of nozzle tip, cm.

g = gravitational constant, 981 $cm.^2/sec.$

γ_i = interfacial tension, dynes $cm.^{-1}$

ϕ = correction factor (58).

CHAPTER 5

EXPERIMENTAL RESULTS

Partial Coalescence and Drop Size Ratio

5.1 Partial Coalescence

Observations of the coalescence of single water drops were made visually (as part of the investigation of coalescence rest-time) and photographically (as part of the drop size ratio investigation). In each of the systems studied *, the drops were observed to coalesce in a partial manner. From the experimental point of view this is a very useful property (see Section 4.3). The process of partial coalescence has been discussed in detail by Charles and Mason (17) and Lawson (82). Picknett (101) and Jeffreys and Hawksley (67) have suggested that the formation of sub-micron drops by this process may be responsible for the secondary 'haze' commonly experienced in settler units. However, the attention in this work was focussed on those partial coalescence stages which were readily visible at the interface. This restricted the lower limit on drop size to about 0.01 cm.

Photograph 5.P.1 shows the partial coalescence of a primary water drop in the systems A and C. The left-hand sequence is for a 0.445 cm. drop in system C and the right-hand sequence for a 0.5995 cm. drop in system A.

In the centre sequence of 5.P.1 a small "satellite" drop can be seen adjacent to the secondary drop (system A, 0.414 cm. primary drop). This phenomenon is refferred to as "double-drop" coalescence (see Fig. 5.1).

* For reference the systems have been designated as:

Series	System
A	Heptane-Water
B	0.05M Decanoic Acid-Heptane-Water
C	0.5M Decanoic Acid-Heptane-Water
D	1.0M Decanoic Acid-Heptane-Water

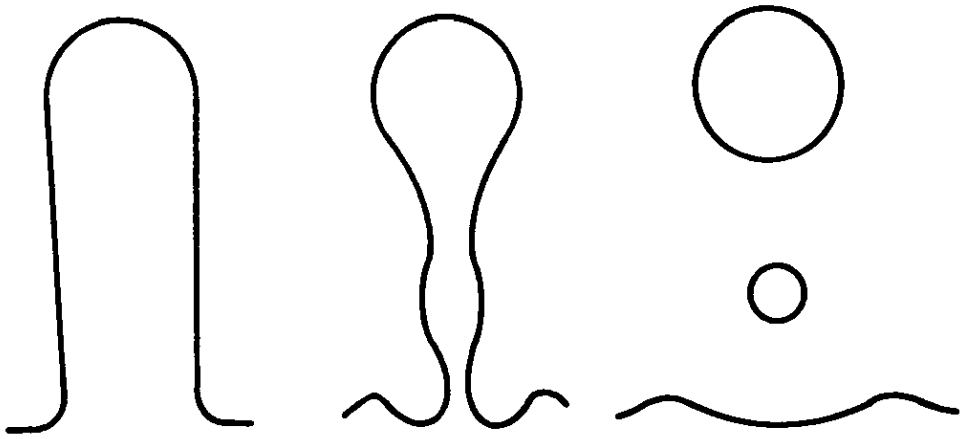

Fig. 5.1 Simultaneous formation of two secondary droplets during partial coalescence process (schematic), (17).

PHOTOGRAPH 5.P.1

Partial Coalescence in the System Heptane-Water and 0.5M Decanoic Acid-Hepatane-Water

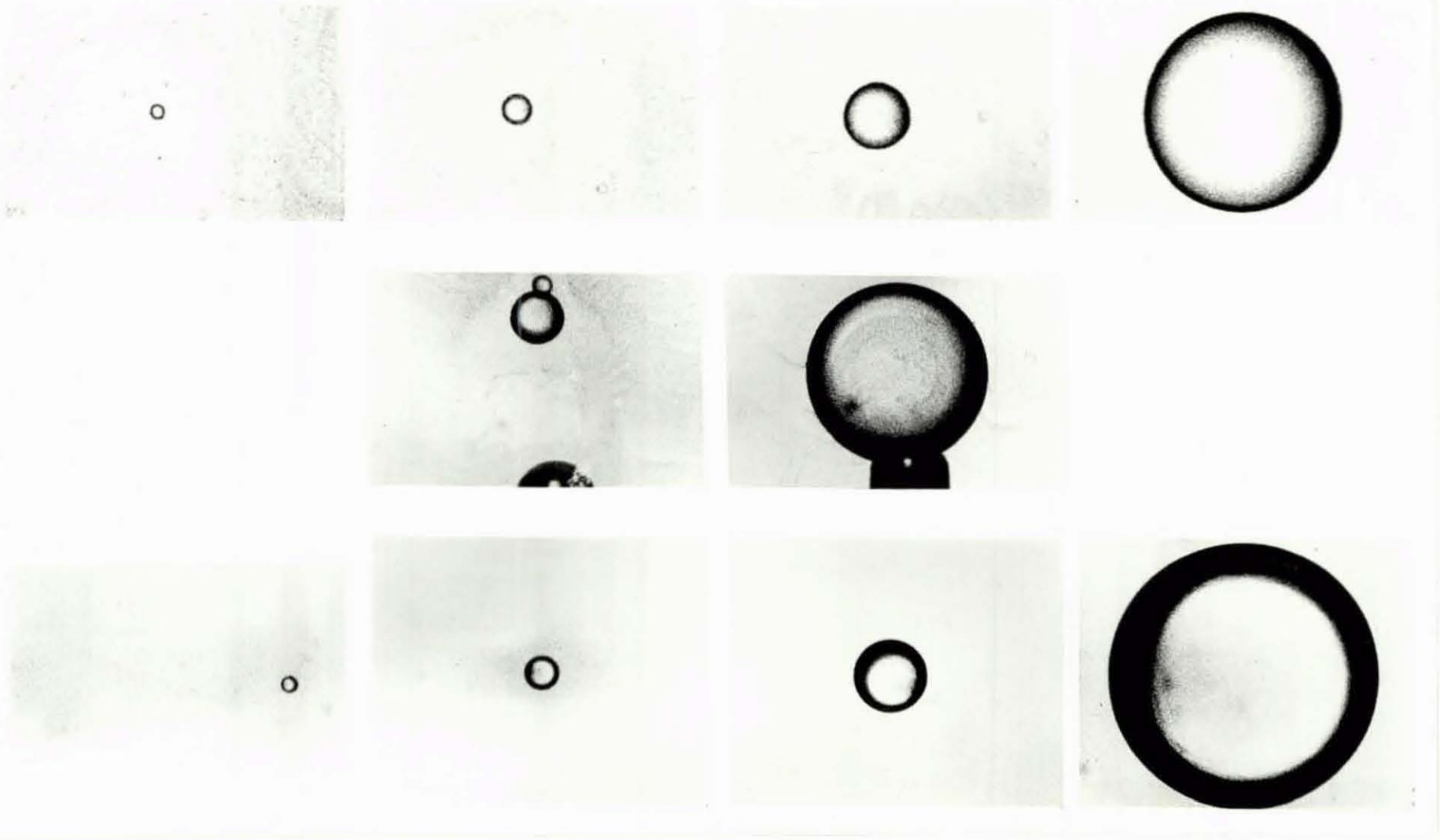

It was also observed to occur in the coalescence rest-time experiments,but only for the systems A and B. In these systems,the"satellite" drop coalesced very rapidly with the bulk interface and did not appear to interfere with the coalescence of the primary drop. The "satellite" drop shown in 5.P.1 possessed remarkable stability and persisted at the interface for a period of about 3 minutes. Again,the "satellite" drop did not appear to interfere with the secondary drop,which coalesced in the normal way (see right-hand sequence of 5.P.1).

Since the coalescence cell (i.e. 250 ml. beaker) was not totally enclosed,the interface became contaminated slightly during the photographic run. Therefore,the rest-time of the "satellite drop was obviously influenced by the contaminant. Considering the very long rest-times which were observed,it is probable that the contaminant was surface active. However,the secondary and succeeding drops were not greatly influenced by the contaminant.

5.2 Drop Size Ratio

The drop size ratio r_n,is defined as a_{n+1}/a_n,where a is the spherical drop diameter and n the number of the coalescence stage. In the manner described in Section 4.6,the drop sizes at the first,second,third and fourth stages of coalescence were determined. A range of primary drop size was investigated from fall heights of L = 0 to 7.5 cm. Only the systems A and C were studied.

The drop size ratio results are presented in Figs. 5.2 to 5.9 as plots of r_1,r_2 and r_3 versus a_1. Individual points on the graphs may represent single or multiple results. The weighting of each point is indicated by the number adjacent to it. Those points without a number are single determinations. The method of least squares was used to obtain the best fit to the experimental results.

5.3 Coalescence Rest-Time

The coalescence rest-time t,was measured for the primary drop (first stage) and three succeeding drops at the second,third and fourth

stages of coalescence, respectively. It is defined as the time between the arrival of the drop at the interface and its eventual disappearance (or release of a secondary drop). The drops which were produced at the fifth and sixth stages of coalescence were extremely small (probably of the order of 0.01 cm., and less). These rest-times were very short and could not be measured manually. Therefore, the overall rest-time $\hat{t}$, previously calculated by a number of workers (12,16,19,44,55,60) can be calculated to a good approximation by:

$$\hat{t} = t_1 + t_2 + t_3 + t_4 \qquad (5.2.1)$$

where t_1, t_2, t_3 and t_4 are, respectively the coalescence rest-time at the first, second, third and fourth stages.

5.4 Reproducibility of Coalescence Rest-Times

Initial experiments revealed that the coalescence rest-time for any stage in the partial coalescence process was not constant, but had a range of values. This is in agreement with the findings of other workers in the field, who studied $\hat{t}$ and t_1 (16,33,44,60,63,66-68,79,81,82).

Sample sizes containing up to 200 drops were examined. The ratio of the mean rest-time to the time for 50% coalescence of the drops $t_m/t_{\frac{1}{2}}$, was found to be the most reproducible characteristic of the rest-time distribution. This was so for sample sizes as low as 50. However, it did not guarantee the constancy of the distribution curve, which really suggests that this ratio is of little use in assessing the reproducibility. A sample size of 75 drops was found to be more reproducible than 50. Therefore, a sample count of 75 was adopted for the purpose of experiments and generally, sample sizes of this order have been used by other workers.

5.5 Experimental Coalescence Rest-Times

The main body of the results is contained in the Series 1 and Series 2 groups of experiments. In all of the cases considered in these groups, the release of the drop was very close to the interface (reported as

L = 0 cms.). Thus,the effect of all height was excluded from these experiments. In addition,the experimental technique used in Series 2 was slightly different to that employed in Series 1. This is explained fully in Section 4.6. It is not expected that this slight difference in technique will cause any marked differencesin the results of the two groups of experiments. Therefore,Series 1 and Series 2 may effectively be considered as one large group of experimental results,including the systems A,B,C and D.

The Series 3 results are concerned primarily with the effect of fall height on the drop rest-time. They are a direct extension of the Series 2 experiments since they were carried out under exactly the same experimental conditions,apart from the fall height. Only the systems A and C were investigated.

In this section,the main features of the results are presented, whilst the results themselves are given in detail in Appendix 2. Here the results are presented in the form of tables of t versus N/N_o,where:

N = Number of drops which have not coalesced in time t.

N_o = Total number of drops assessed.

Series 1 Results

Typical results,in the form ln N/N_o vs. t,are presented in Fig. 5.10 for system A and in Figs. 5.11 to 5.15 for system C. The relationship between the mean rest-time t_m,and the primary drop size,is presented in Figs. 5.16 (A and B),5.17 and 5.18. For the system decanoic acid-heptane-water,the effect of increasing the concentration of third component, decanoic acid,is shown in Figs. 5.19 to 5.22. The concentrations used were 0.05M,0.5M and 1.0M and the primary drop sizes were respectively, 0.312,0.314 and 0.304 cm.

Series 2 Results

A representative selection of the results in the form ln N/N_o

versus t is presented for all the systems,A,B,C and D,in Figs. 5.23 to 5.38. These cover the drop size range for four stages of coalescence as follows:

(i) 0.028 to 0.596 cm. for system A,in Figs. 5.23 to 5.26.

(ii) 0.0228 to 0.509 cm. for system B,in Figs. 5.27 to 5.31.

(iii) 0.0204 to 0.449 cm. for system C,in Figs.5.32 to 5.35.

(iv) 0.022 to 0.385 cm. for system D,in Figs. 5.36 to 5.38.

The relationship between the mean rest-time t_m,and the drop size is presented for each individual stage in the heptane-water system in Fig. 5.39. The slopes of the first,second and third stages are respectively, 28.6 secs./cm.,117.8 secs./cm. and 157.8 secs./cm. For the system 1.0M decanoic acid-heptane-water,the relationship between t_m and a (the drop diameter) is presented for each stage of coalescence in Figs. 5.40 to 5.42. The form of the relationship for the systems B and C is similar to that exhibited by D,but is not so well defined for these cases.

Series 3 Results

This set of results,with the inclusion of result A2/2,investigates the effect of fall height of the primary drop on the coalescence rest-time for the four stages of coalescence. In Figs. 5.43 to 5.46,the individual stage distributions,in the form $\ln N/N_o$ vs. t,are given for L = 0,2.5,5.0, 7.5 and 10.0 cms. The curve for L = 7.5 cm. is omitted from Fig. 5.43 because the value for t_{m1} (see Appendix 3) is suspect,being less than the corresponding value at L = 5.0 cm.

Effect of Interface Age on Coalescence Rest-Time

The results of the individual stage rest-times with interface age (τ) are presented for the four separate groups in Table 5.1. In Studies 1 and 3 the drop was aged for 1 minute prior to release,and in Studies 2 and 4 the drop was not aged. Since the interface age was recorded at the completion of coalescence of a drop,the interface age at the time of arrival of the primary drop at the interface is given by:

$$\left[\tau - (t_1 + t_2 + t_3 + t_4)\right] = (\tau - \hat{t})$$

TABLE 5.1

COALESCENCE TIME (t) VERSUS INTERFACE AGE (τ) EMPLOYING THE TEFLON-GLASS METHOD OF INTERFACE CLEANING

Study 1

System: Heptane-Water, a_1 = 0.416 cm., L = 0 cm.

Drop aged for 1 minute prior to release.

Drop Number	t_1 secs.	t_2 secs.	t_3 secs.	t_4 secs.	τ mins.
1	2.6	9.7	2.2	0.4	2.95
2	26.5	7.8	2.0	0.3	4.93
3	8.1	8.6	2.3	0.3	6.53
4	11.2	6.0	2.1	0.4	8.17
5	10.8	8.5	2.3	0.4	9.83
6	21.8	9.2	2.1	0.3	13.05
7	18.6	7.5	2.0	0.3	15.04
8	3.9	9.4	2.3	0.4	16.40
9	5.4	9.2	2.3	0.4	18.15
10	16.4	7.8	2.0	0.4	20.00

Study 2

System: Heptane-Water, a_1 = 0.416 cm., L = 0 cm.

Drop not aged.

Drop Number	t_1 secs.	t_2 secs.	t_3 secs.	t_4 secs.	τ mins.
1	5.3	8.3	2.1	0.3	1.37
2	3.3	6.0	2.3	0.3	2.00
3	4.1	5.8	1.8	0.7	2.80
4	6.2	4.6	2.3	0.4	3.47
5	5.4	7.3	2.4	0.3	4.10
6	3.6	5.8	2.2	0.5	4.66
7	5.8	6.6	2.3	0.3	5.32
8	3.6	6.6	2.1	0.5	5.90
9	5.3	6.7	2.4	0.5	6.55
10	4.4	5.8	2.3	0.3	7.12
11	6.1	6.1	2.3	0.3	7.80
12	4.6	6.0	2.4	0.4	8.45
13	10.0	8.2	2.3	0.4	9.20
14	4.8	6.6	2.3	0.5	9.83
15	4.4	6.3	2.3	0.4	10.63
16	4.9	6.3	2.1	0.5	11.33
17	7.9	9.3	2.3	0.5	22.12
18	14.0	8.7	2.2	0.3	23.03
19	5.7	7.2	2.3	0.4	23.77
20	4.5	6.8	2.2	0.5	24.53
21	37.5	8.4	2.2	0.4	56.33
22	8.5	8.4	2.2	0.4	57.17

Study 3

System 0.5M Decanoic Acid-Heptane-Water, a_1 = 0.324 cm., L = 0 cm.

Drop aged for 1 minute prior to release.

Drop Number	t_1 secs.	t_2 secs.	t_3 secs.	t_4 secs.	τ mins.
1	29.5	18.4	3.9	0.6	2.8
2	9.5	17.3	4.1	0.6	7.18
3	15.5	9.4	4.0	0.6	9.73
4	33.2	17.1	3.8	0.6	12.08
5	18.1	13.5	4.0	0.7	13.97
6	24.4	6.4	3.8	0.7	16.10
7	21.2	4.5	3.8	0.8	17.93
8	7.9	4.9	2.3	0.4	20.93
9	8.2	11.2	3.4	0.5	22.57
10	8.5	4.6	3.2	0.8	24.47

Study 4

System: 0.5M Decanoic Acid-Heptane-Water, a_1 = 0.342 cms., L = 0 cm.

Drop not aged.

Drop Number	t_1 secs.	t_2 secs.	t_3 secs.	t_4 secs.	τ mins.
1	22.1	11.9	4.5	0.4	1.58
2	17.1	16.7	4.0	0.7	3.54
3	5.7	8.2	3.2	0.5	4.17
4	9.9	4.0	3.6	0.5	4.83
5	10.4	5.4	3.1	0.6	5.45
6	14.3	4.1	3.2	0.7	6.17
7	13.2	4.3	3.4	0.7	6.83
8	12.6	5.5	2.7	0.4	7.56
9	9.0	10.3	3.4	0.4	8.17
10	11.2	7.8	3.1	0.7	8.88
11	9.0	2.6	3.0	0.4	9.52
12	12.7	7.9	2.9	0.5	10.35

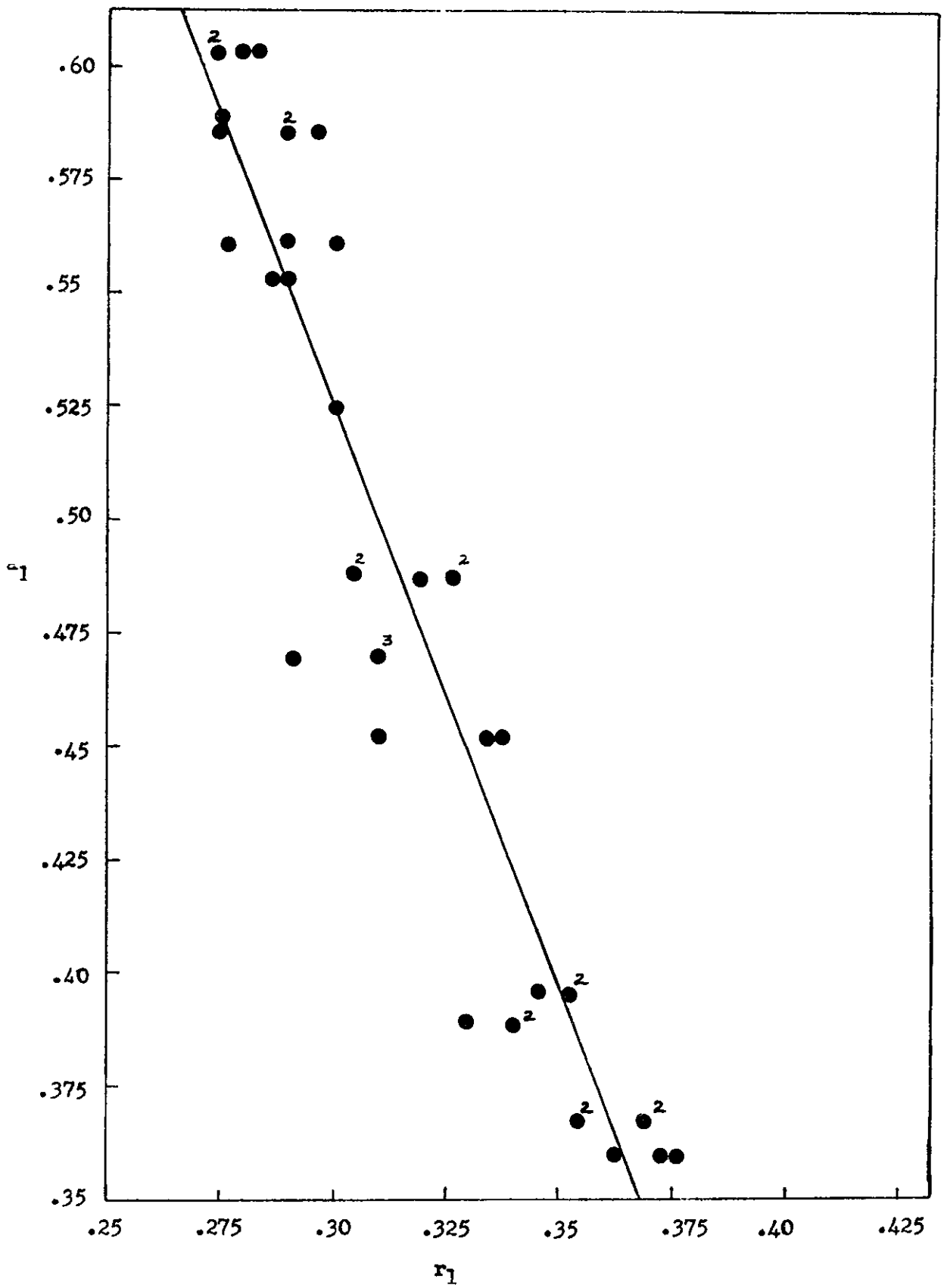

Fig. 5.2A Drop size ratio (r) versus primary drop diameter (a_1) for the system heptane-water L = 0 cms.

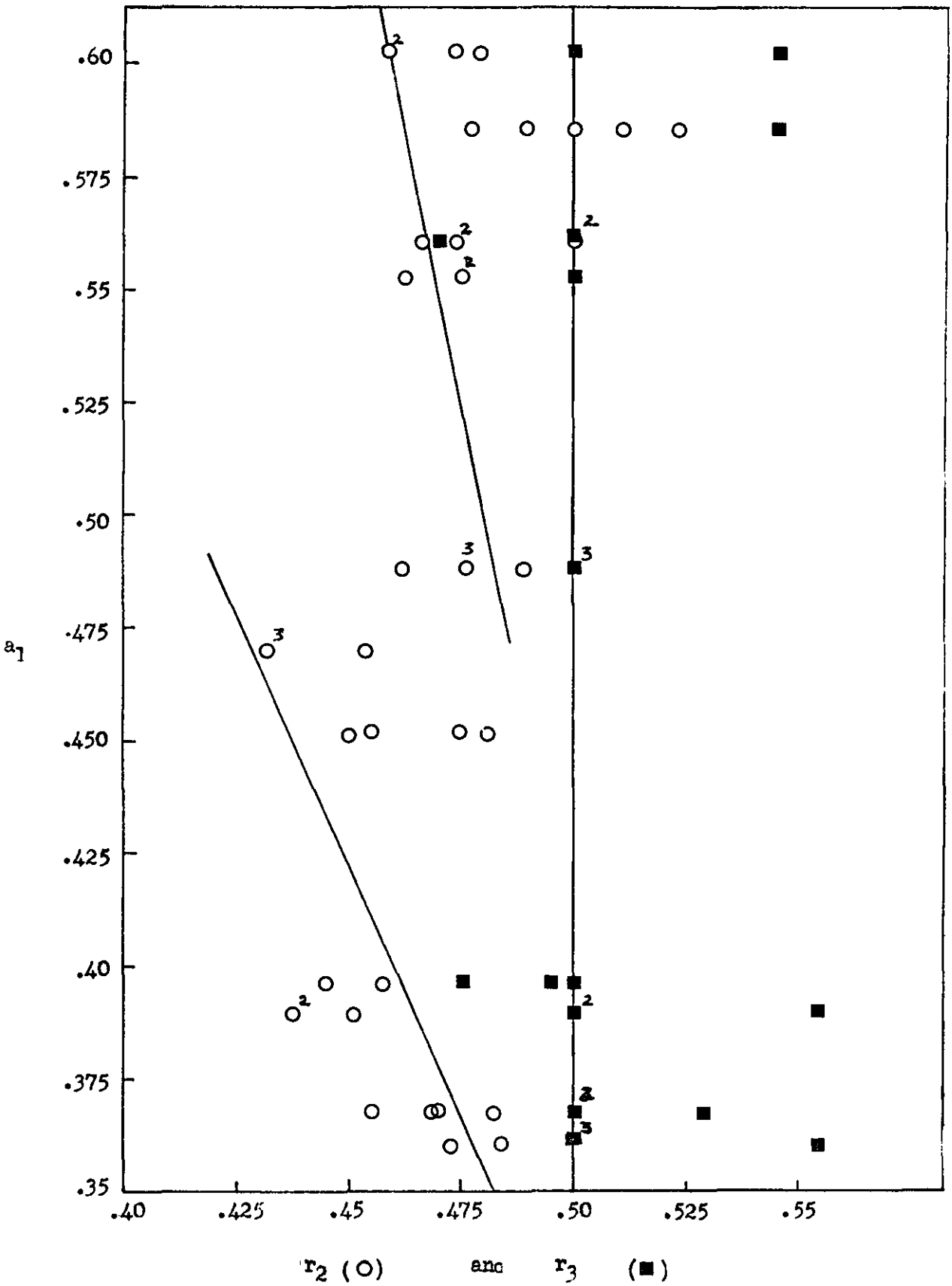

Fig. 5.2B Drop size ratio (r) versus primary drop diameter (a_1) for the system heptane-water L = 0 cms.

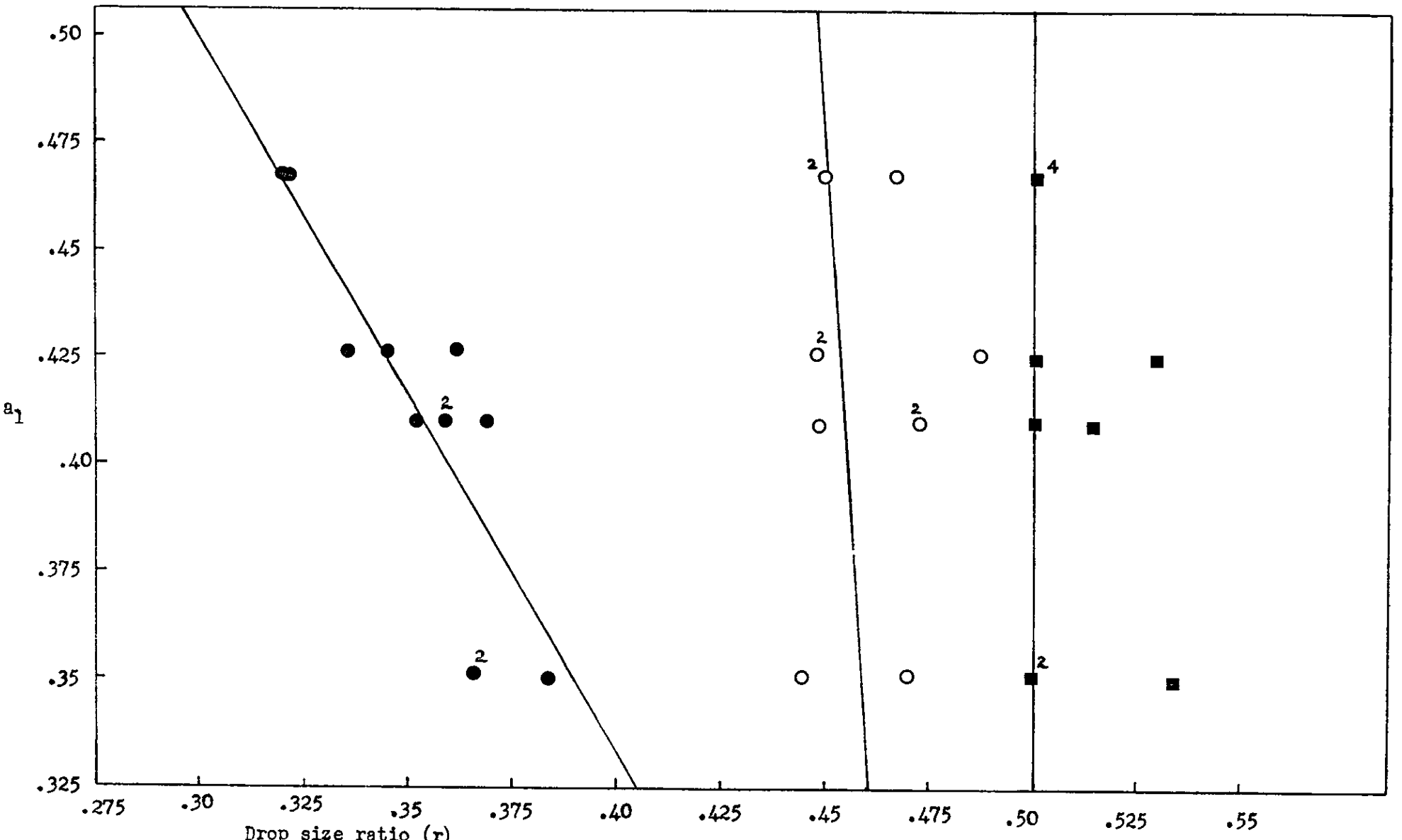

Fig. 5.3 versus primary drop diameter (a_1) for the system heptane-water r_1 (●), r_2 (○) and r_3 (■) L = 2.5 cms.

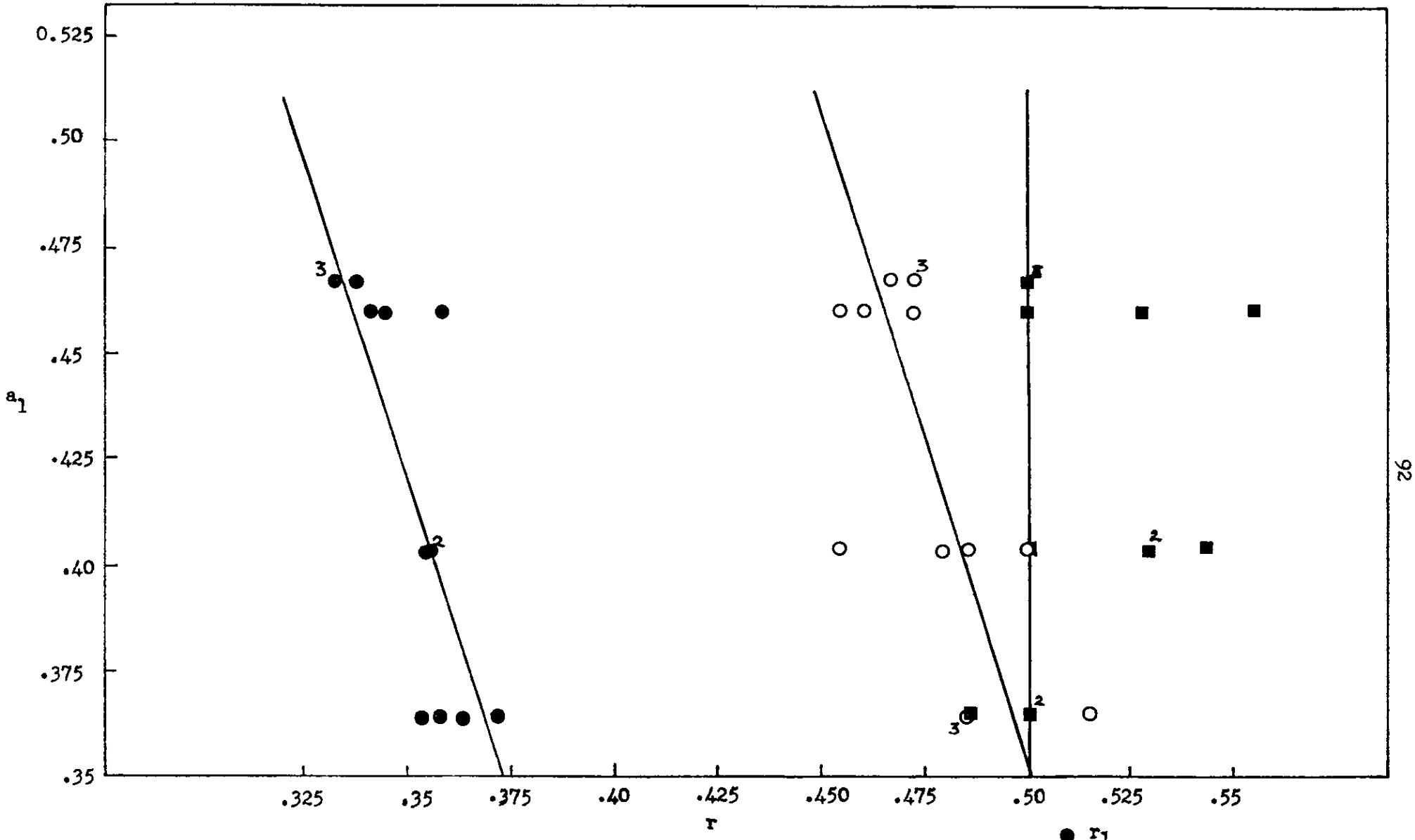

Fig. 5.4 Drop Size Ratio versus primary drop diameter for the system heptane-water

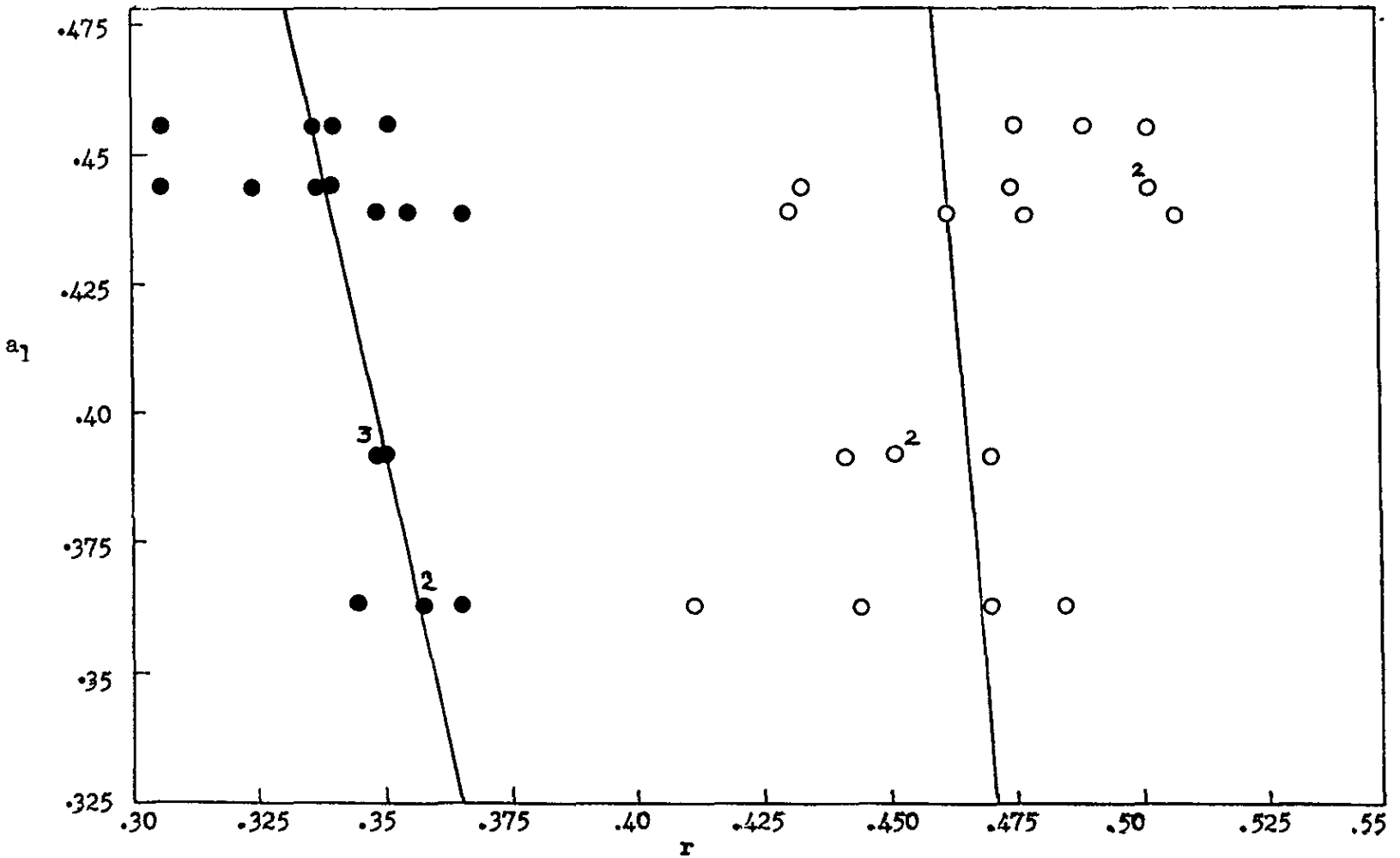

Fig.5.5 Drop size ratio(r) versus primary drop diameter (a_1) in the system heptane-water

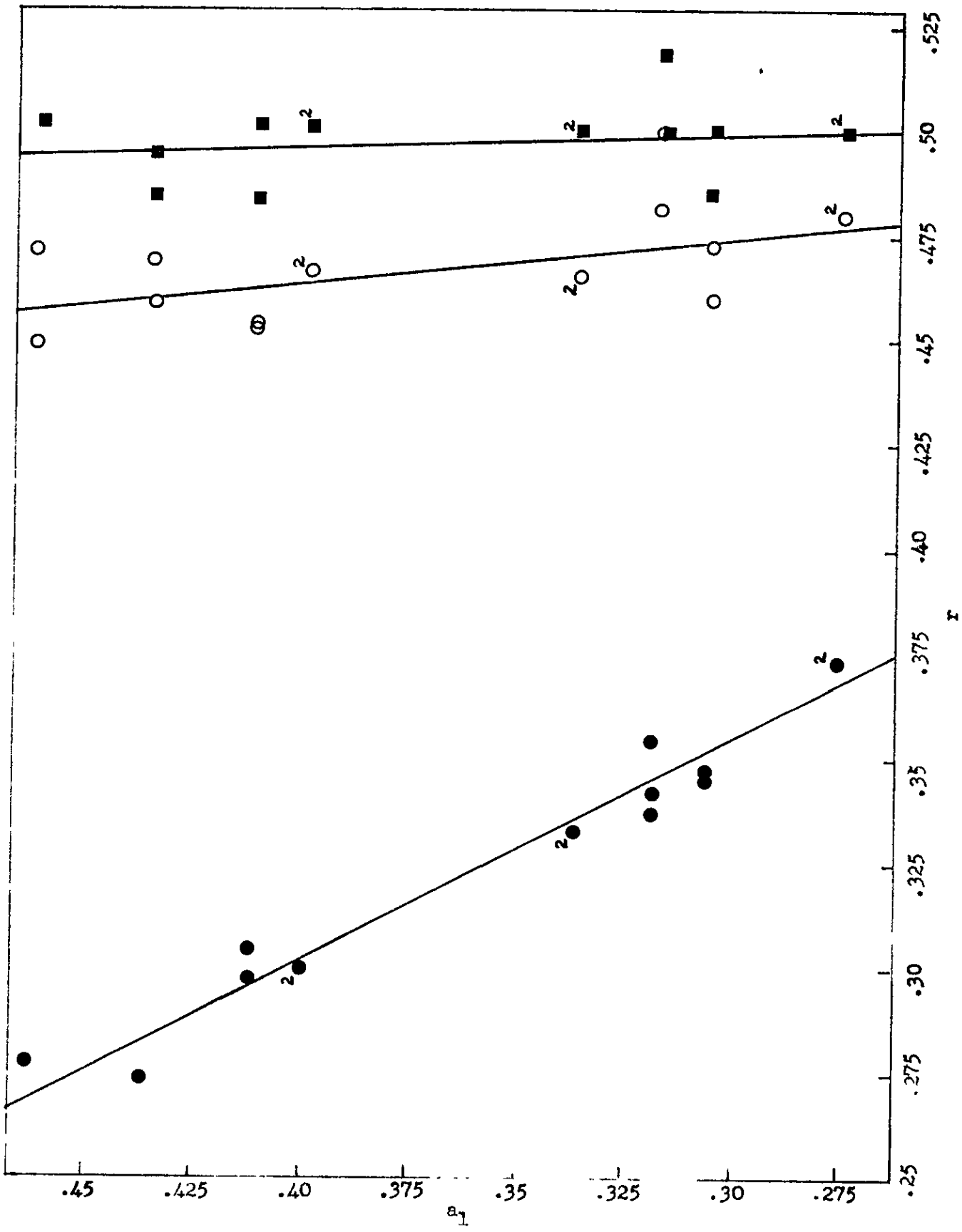

Fig. 5.6 Drop size ratio (r) versus Primary drop diameter (a_1) in the system 0.5M decanoic acid-heptane-water

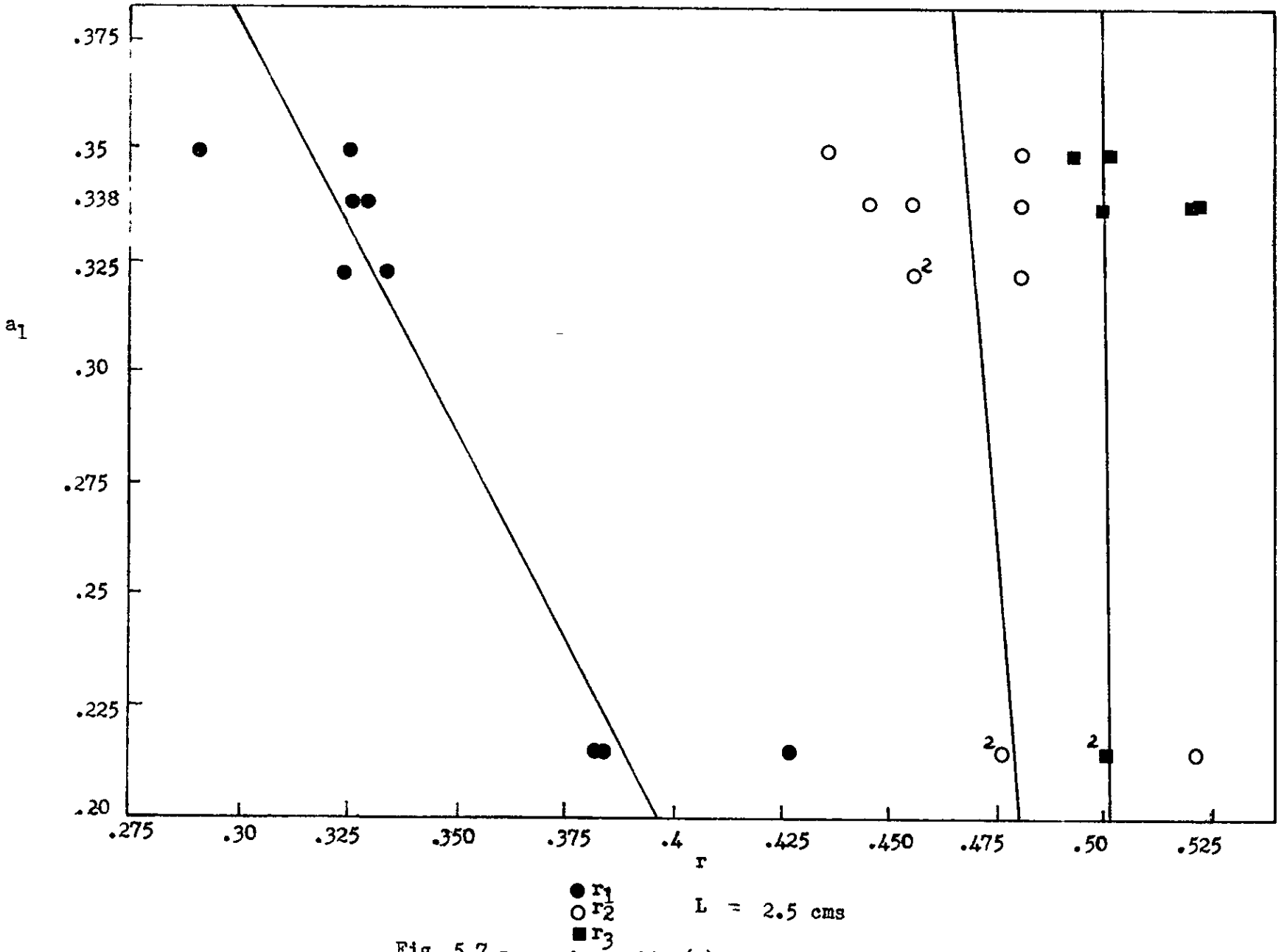

Fig. 5.7 Drop size ratio (r) versus primary drop diameter (a_1) in the system 0.5M decanoic acid-heptane-water

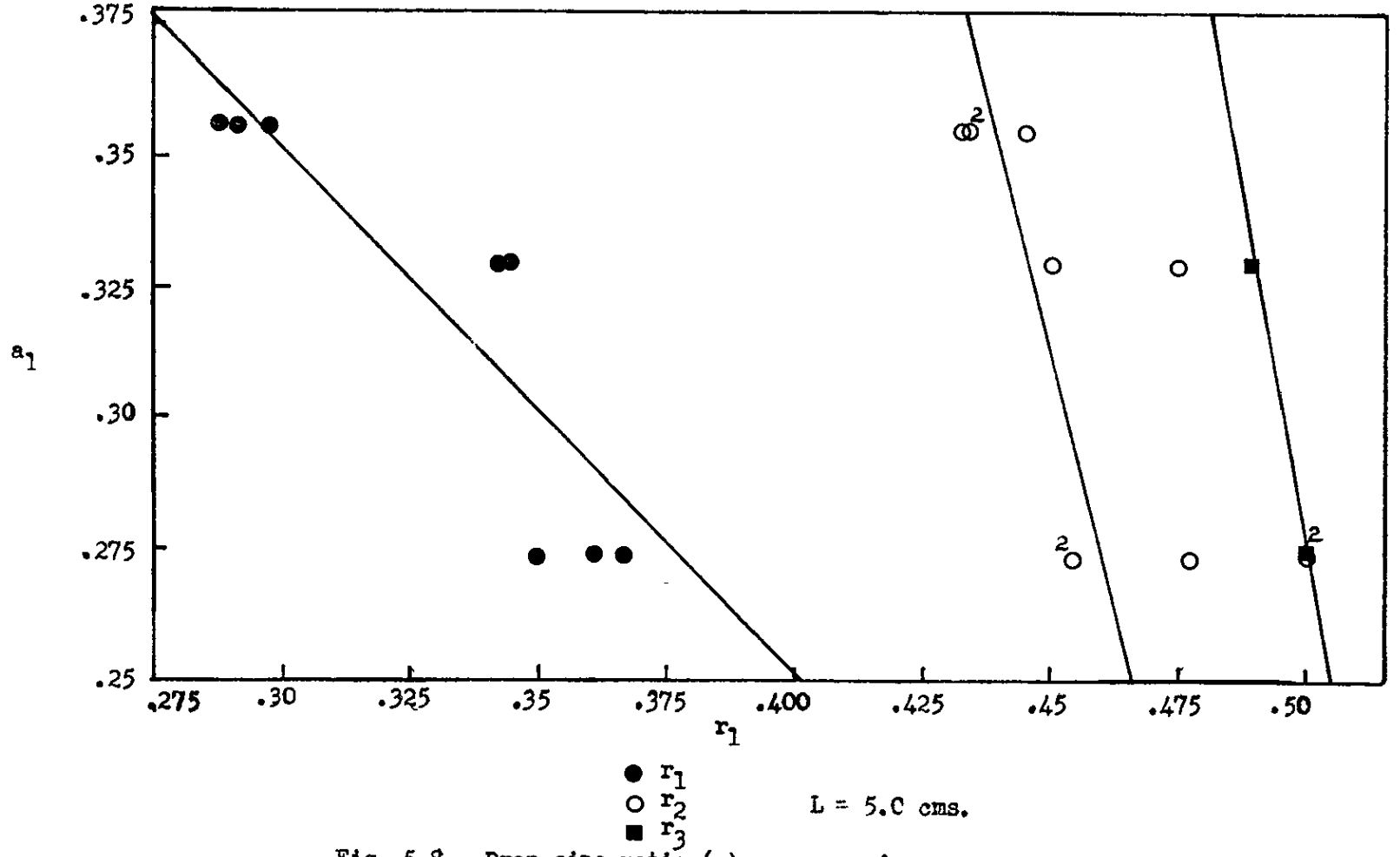

Fig. 5.8 Drop size ratio (r) versus primary drop diameter (a_1) in the system 0.5M decanoic acid heptane-water

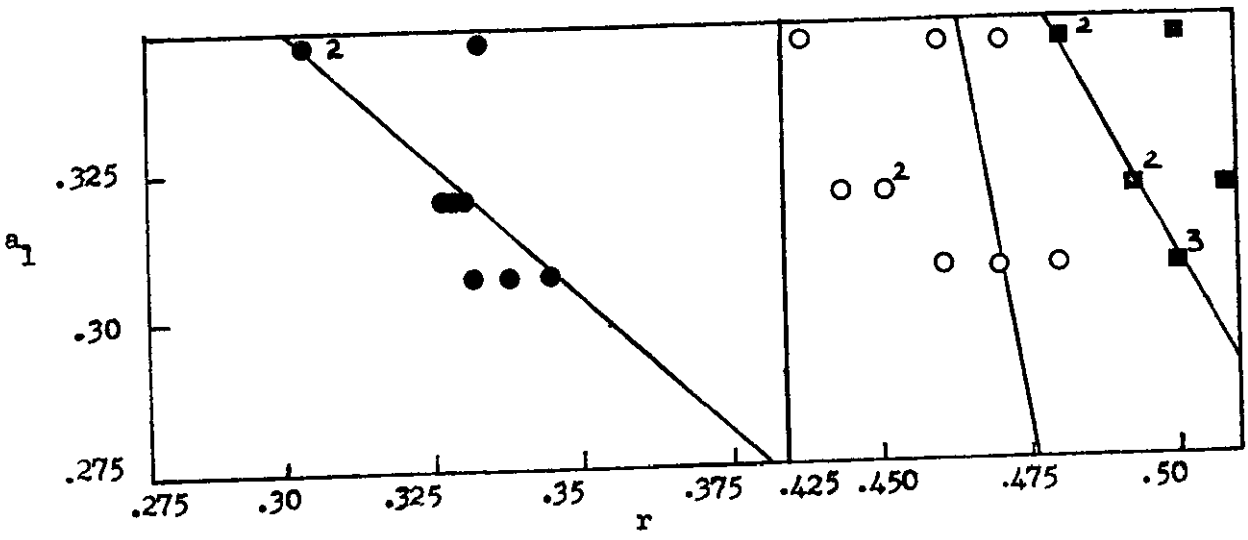

● r_1
○ r_2
■ r_3

L = 7.5 cms.

Fig. 5.9 Drop size ratio (r) versus primary drop diameter (a_1) in the system 0.5M decanoic acid-heptane-water

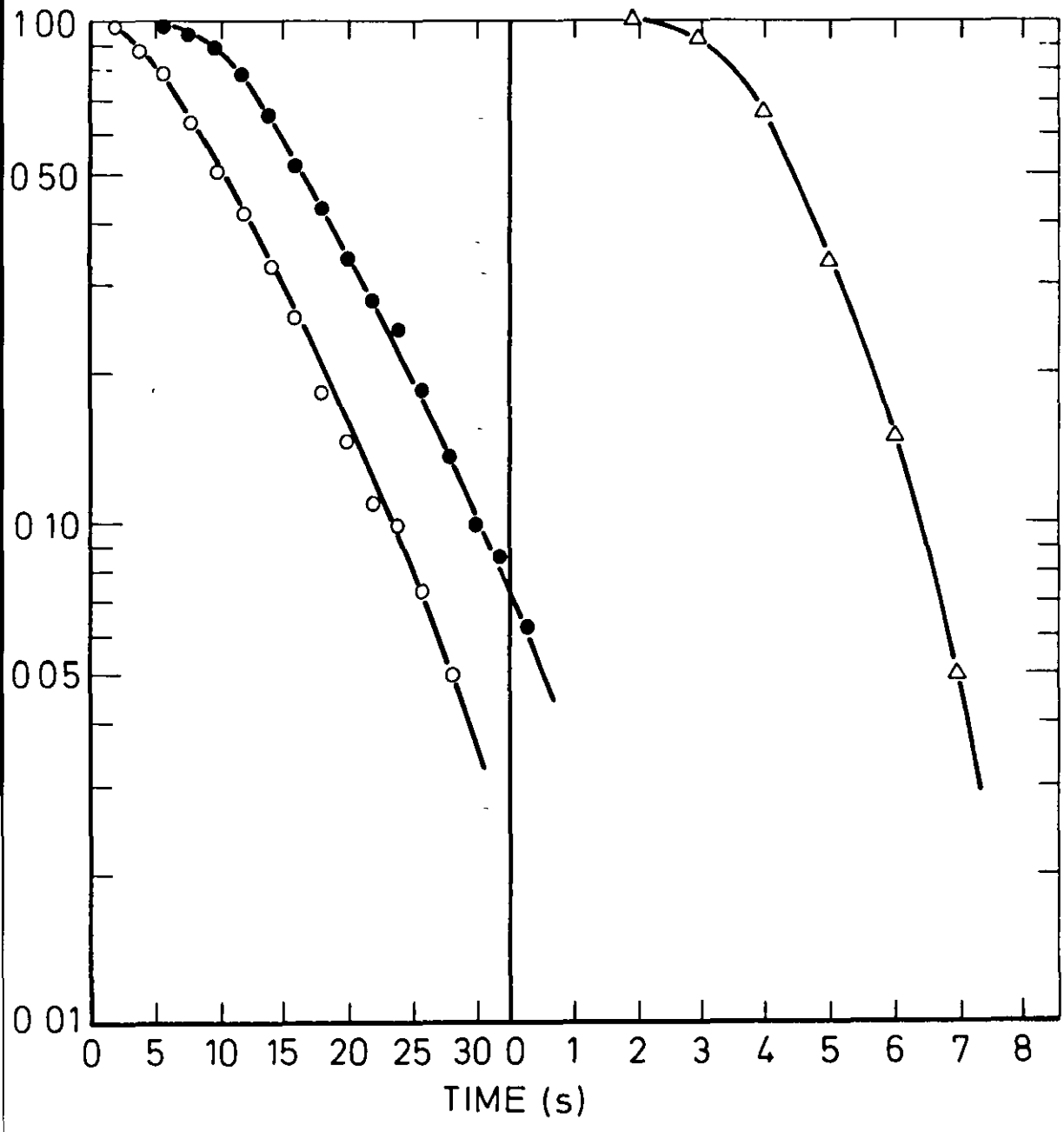

● overall stage
○ first stage
△ second stage

Drop size a_1 = 0.348 cms.

Series A1/6

Fig. 5.10A Partial coalescence time distribution for system heptane-water

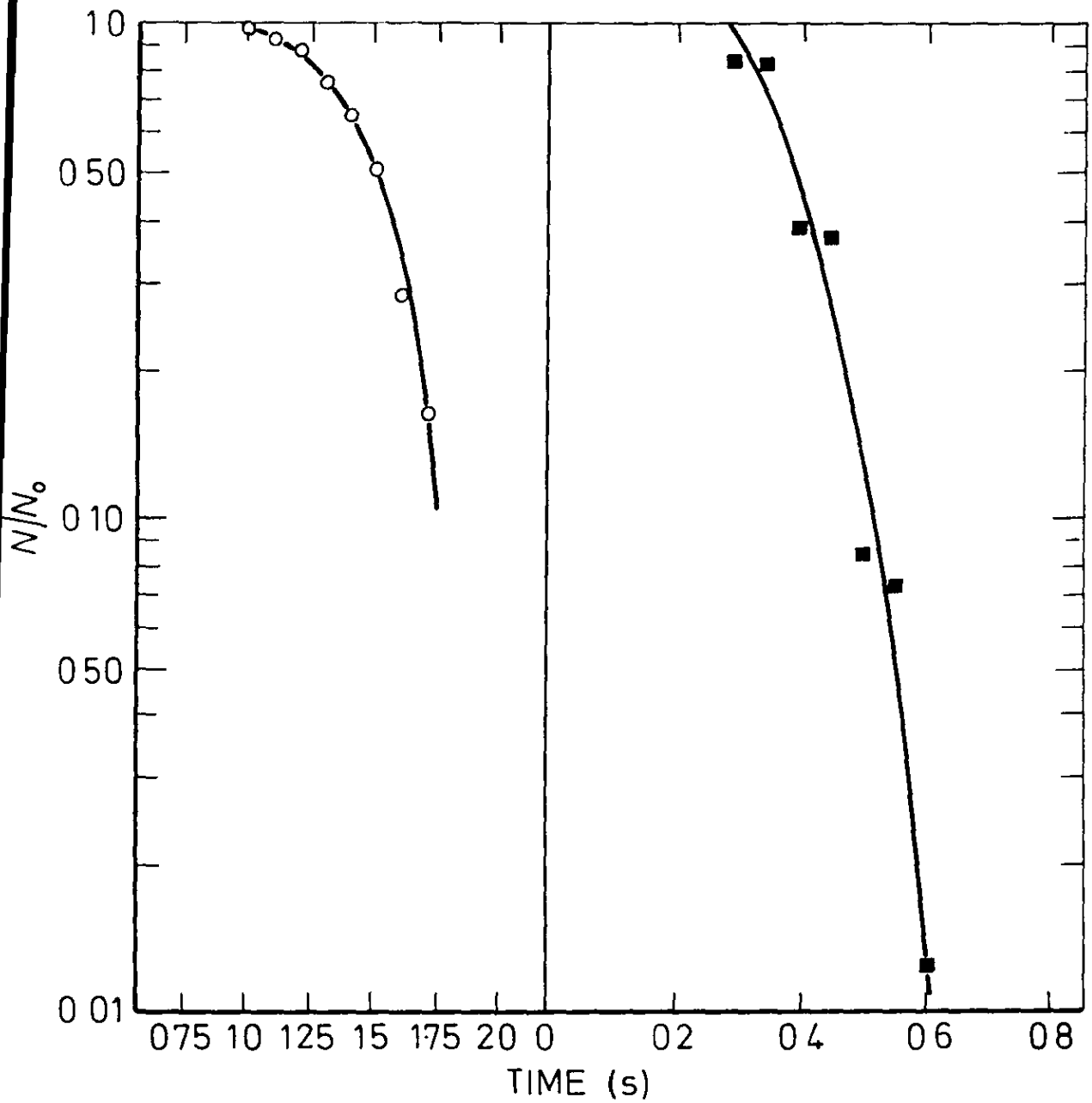

○ third stage
■ fourth stage

Drop size a_1 = 0.348 cms.

Fig. 5.10B Partial coalescence time distribution for system heptane-water

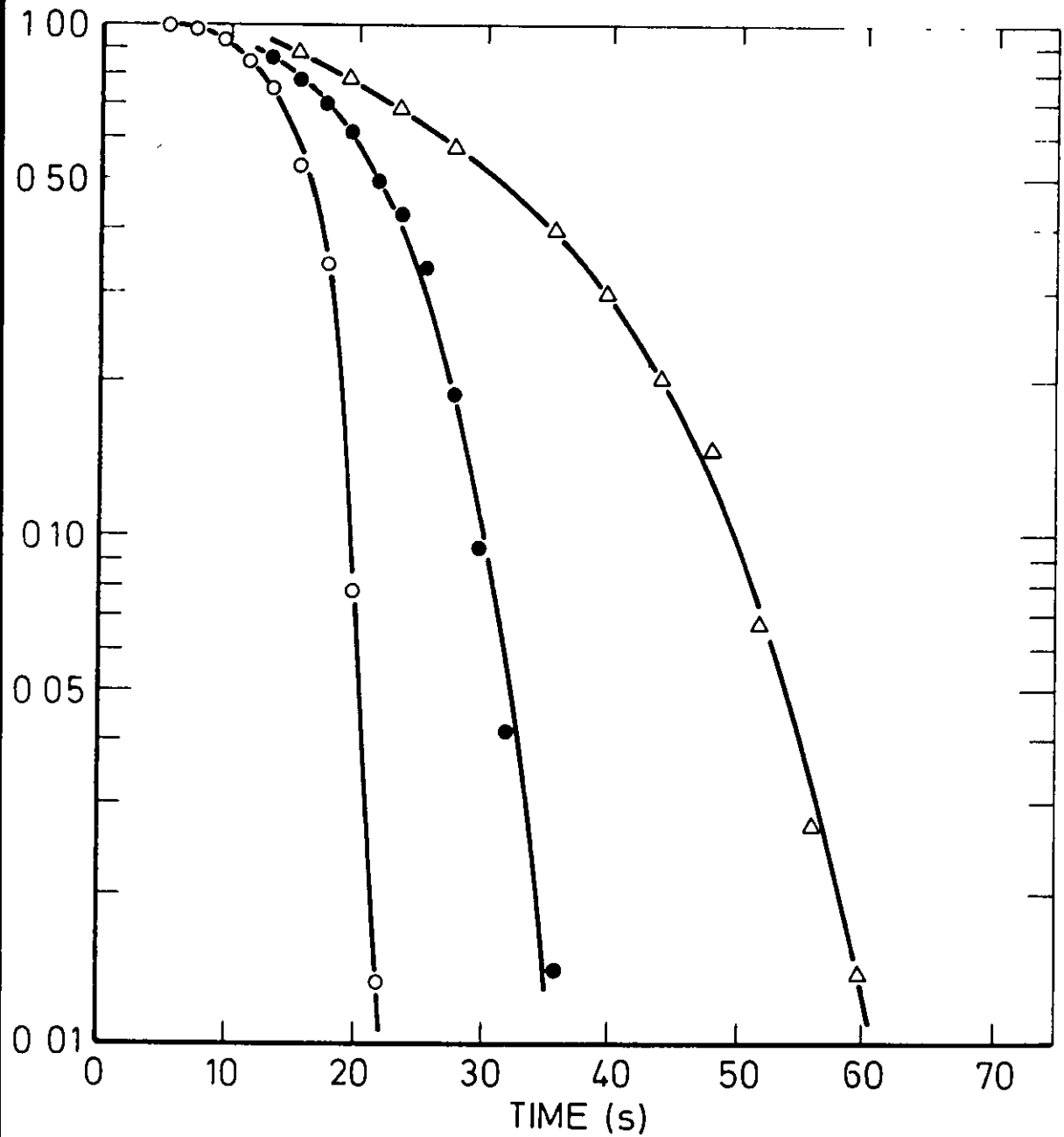

a_1 Drop size (cms)

○ 0.232
● 0.314
∧ 0.382

Series C1/1, C1/4, C1/5

Fig. 5.11 Overall coalescence time distributions for systems 0.5M decanoic acid-heptane-water

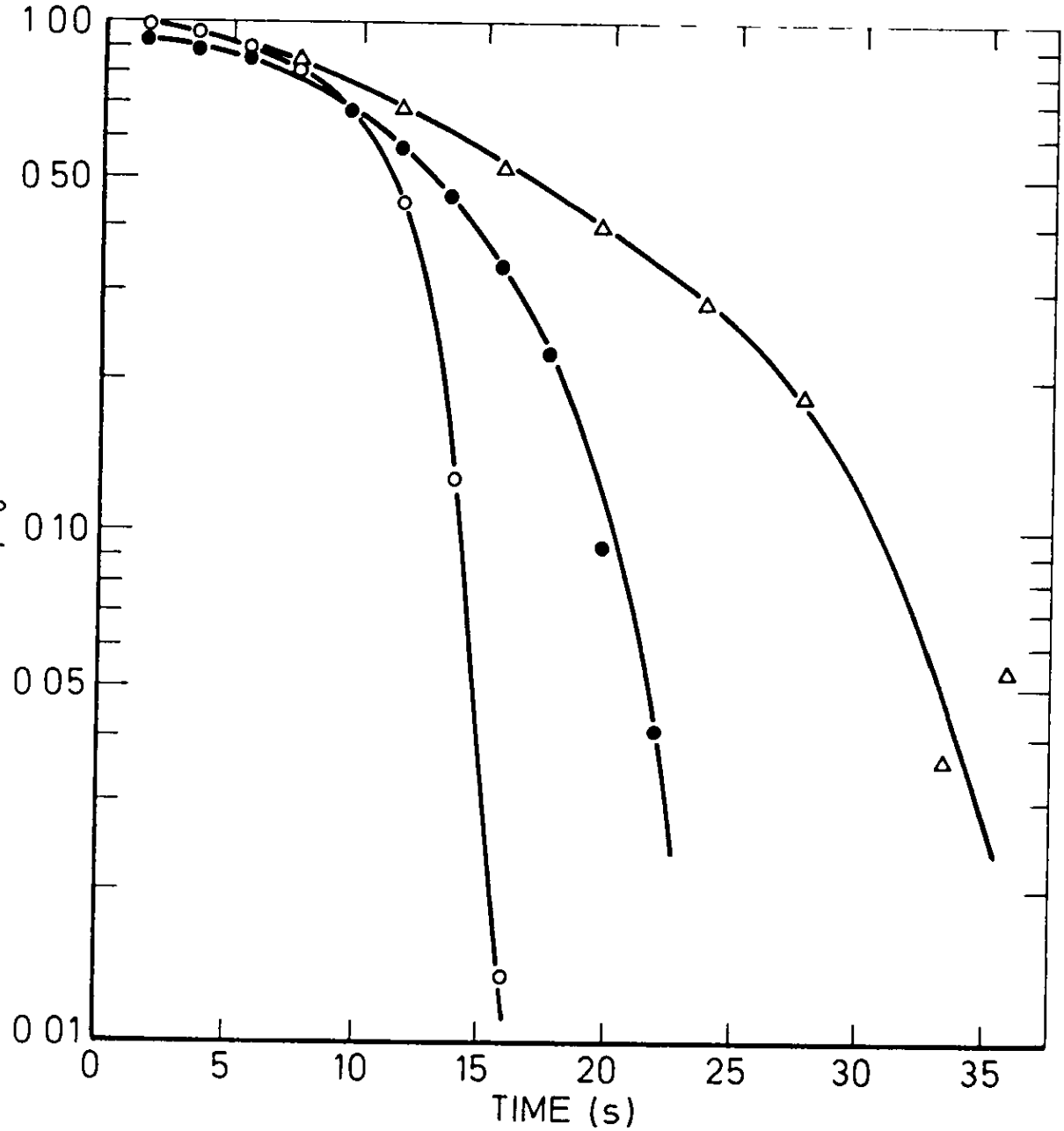

a_1 Drop Size (cms.)

○ 0.232
● 0.314
△ 0.382

Series C1/1, C1/4, C1/5

Fig. 5.12 First Stage coalescence time distributions for system 0.5M decanoic acid-heptane-water

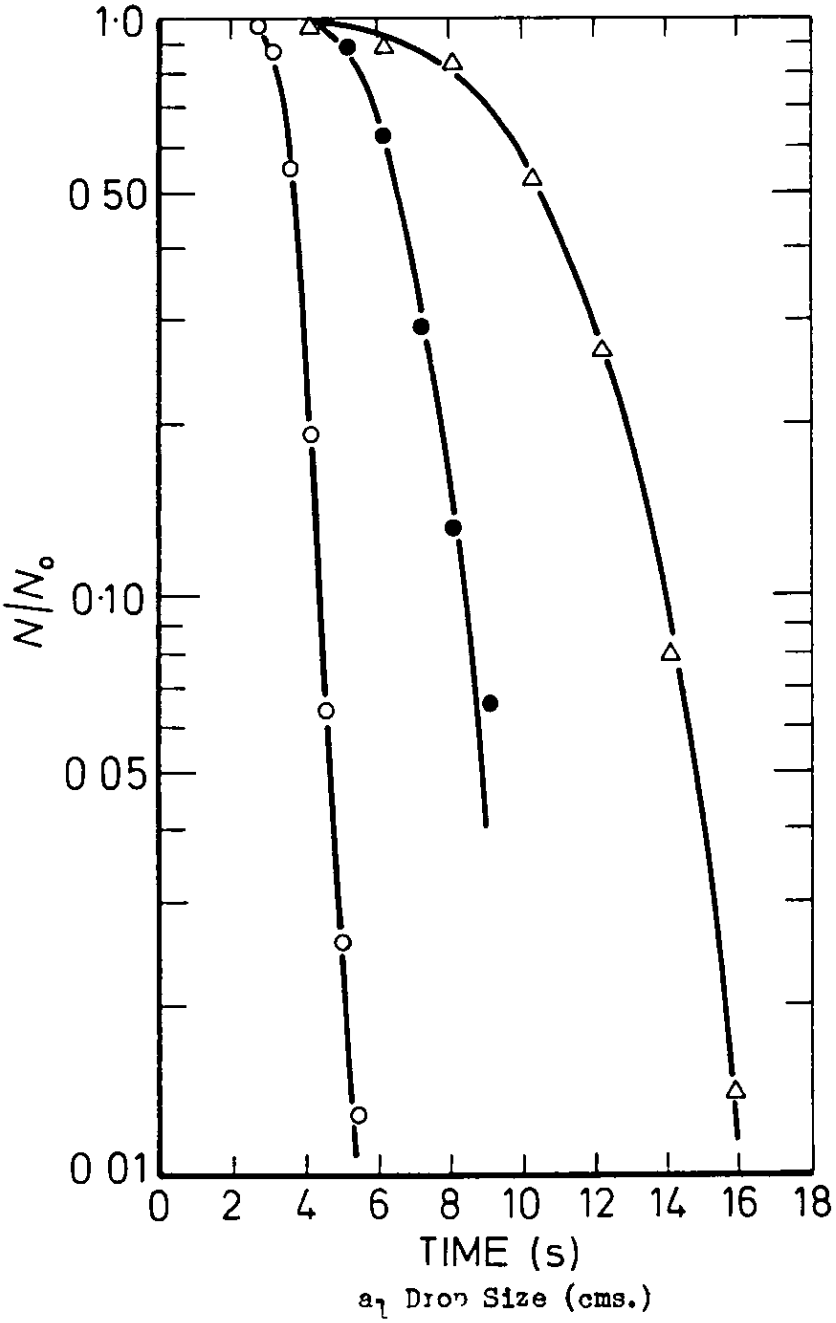

a_1 Drop Size (cms.)

○ 0.232
● 0.314
△ 0.382

Series C1/1, C1/4, C1/5

Fig. 5.13 Second Stage coalescence time distributions for systems 0.5M decanoic acid-heptane-water

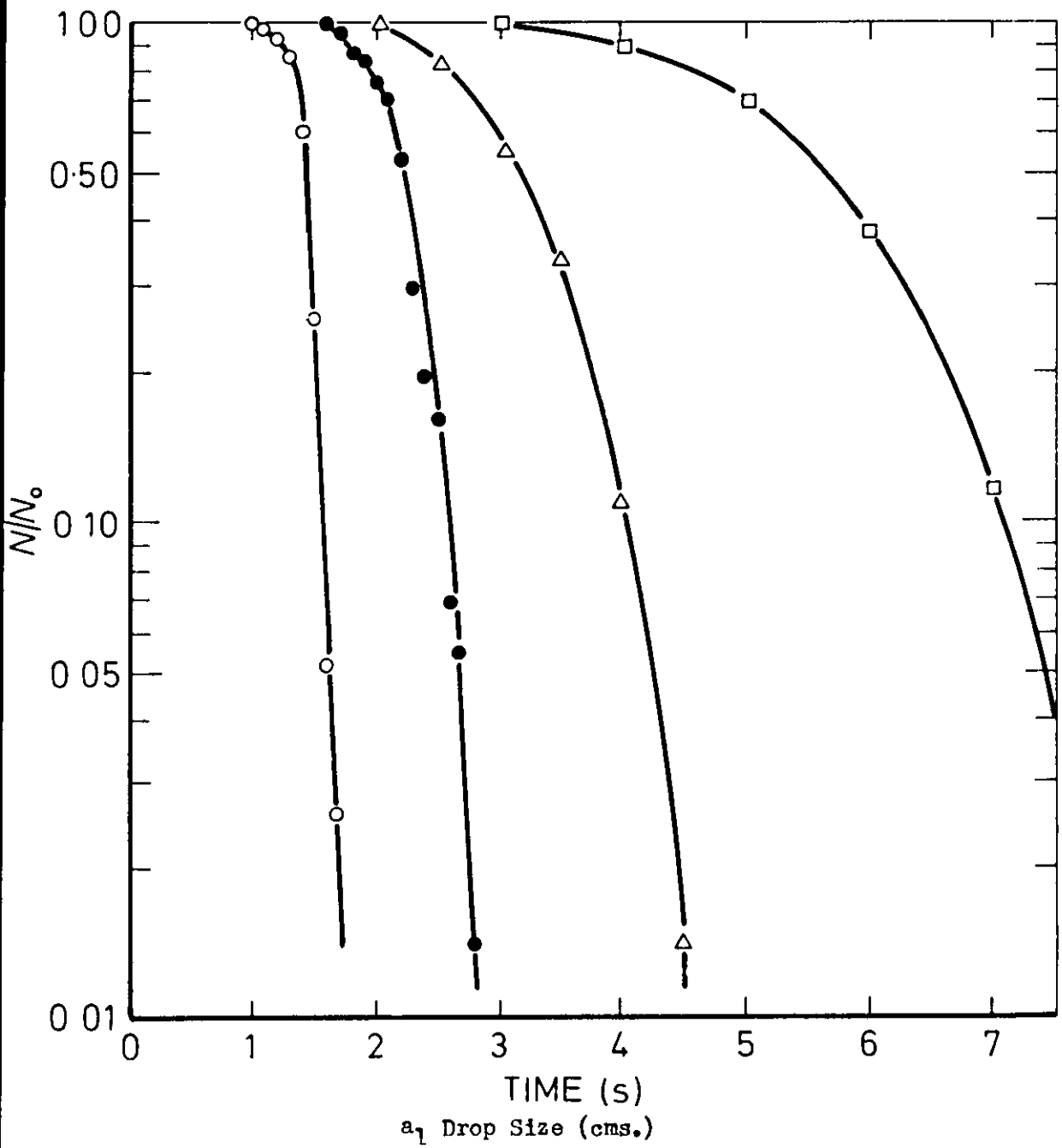

a_1 Drop Size (cms.)

○ 0.232
● 0.314
△ 0.382
□ 0.214

Series C1/1, C1/4, C1/5

Fig. 5.14 Third Stage coalescence time distributions for system 0.5M decanoic acid-heptane-water

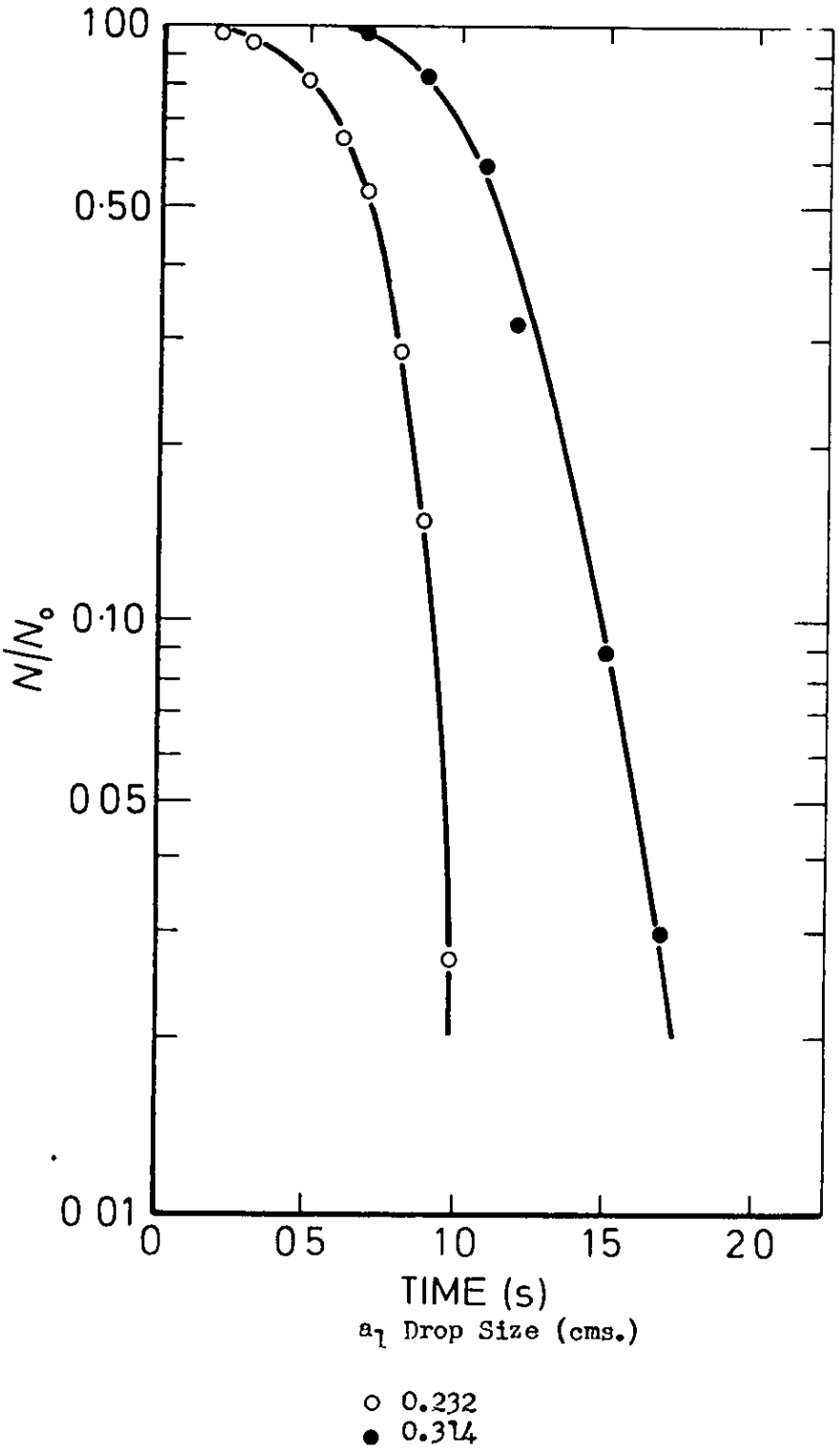

Series C1/1, C1/4

Fig. 5.15 Fourth Stage coalescence time distributions for system 0.5M decanoic acid-heptane-water

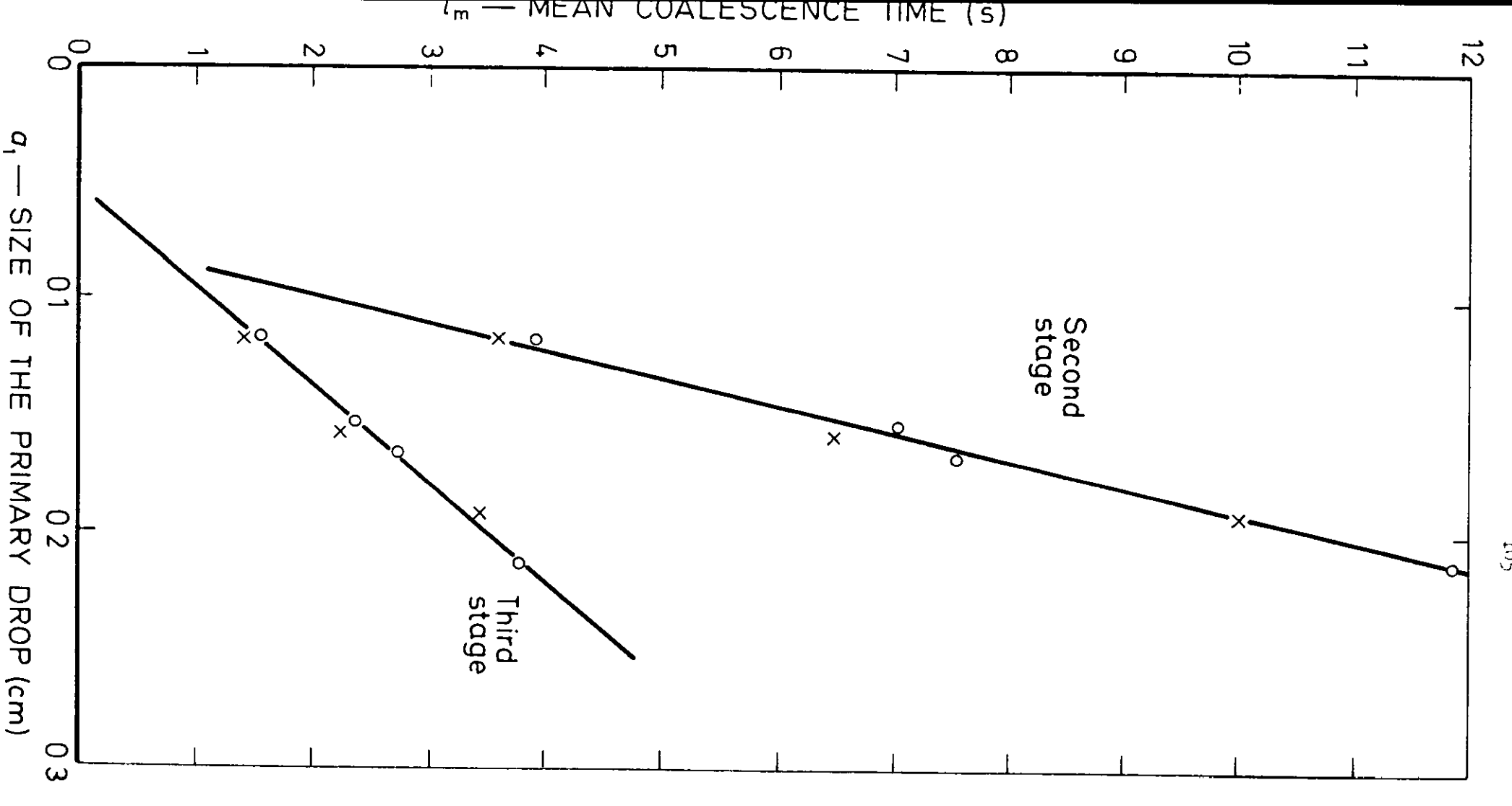

○ 1.0M decanoic acid × 0.5M decanoic acid

All drops formed at the interface
Series B1, C1/D1

Fig. 5.16A Mean coalescence times of second and third stage of coalescence as a function of the size of primary drop

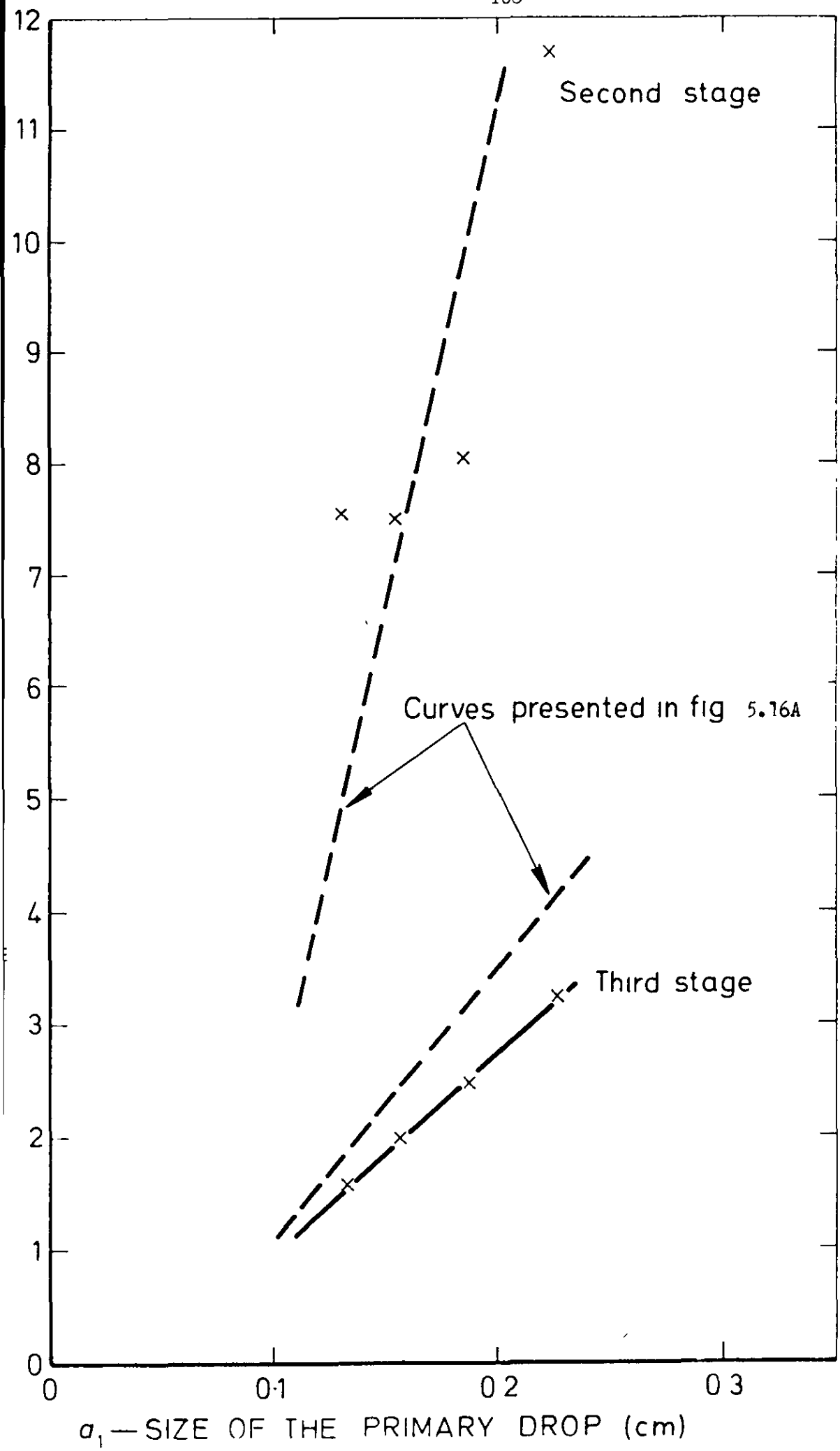

0.5M Decanoic Acid
All drops formed at the interface
Series B1, C1/D1

Fig. 5.16B Mean coalescence times of second and third stage of coalescence as a function of the size of primary drop

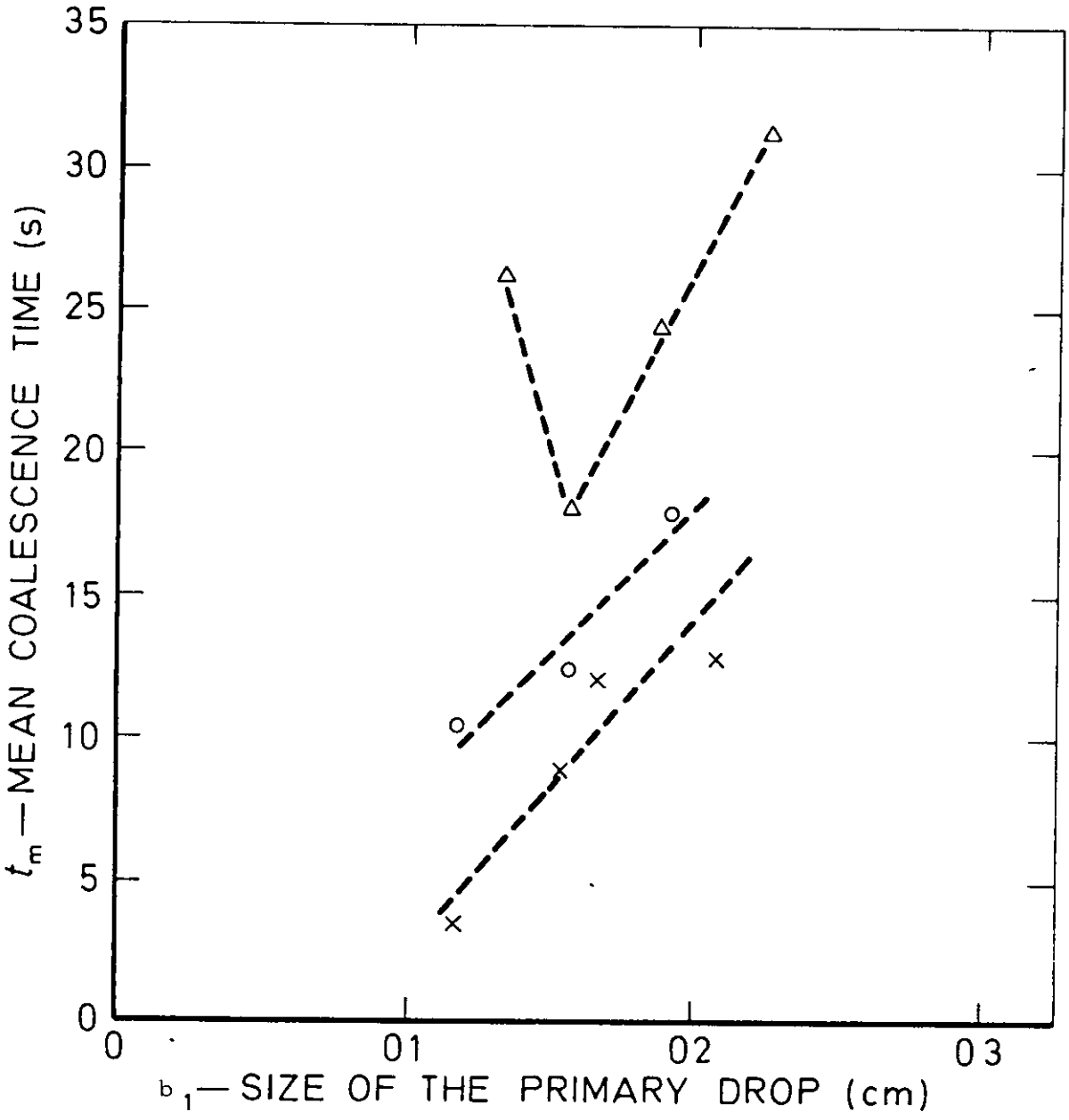

Fig. 5.17 Mean Coalescence time of the first stage of coalescence as a function of primary drop size

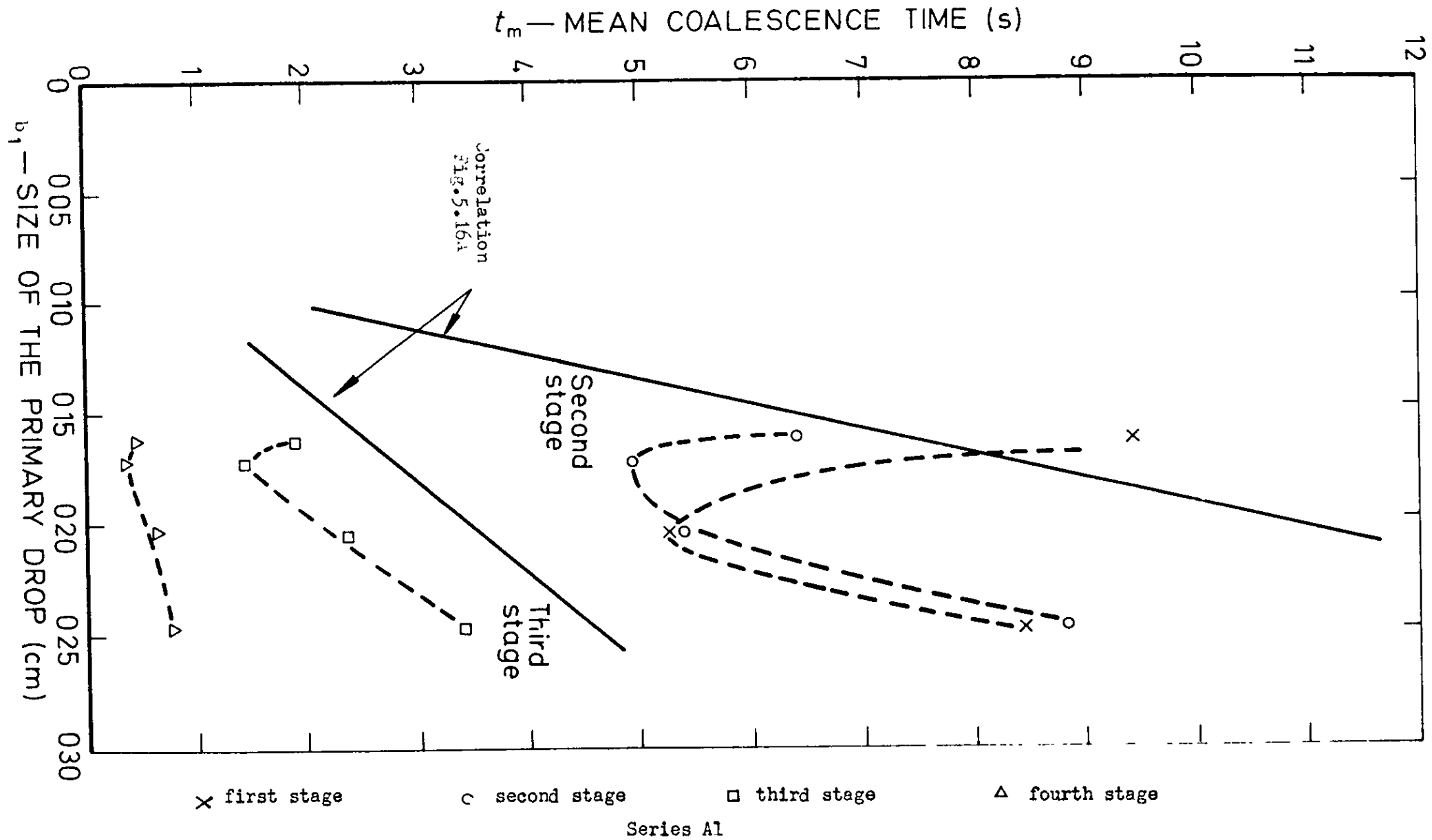

Fig. 5.18 Relationship between the mean coalescence time and the primary drop size for the system heptane-water

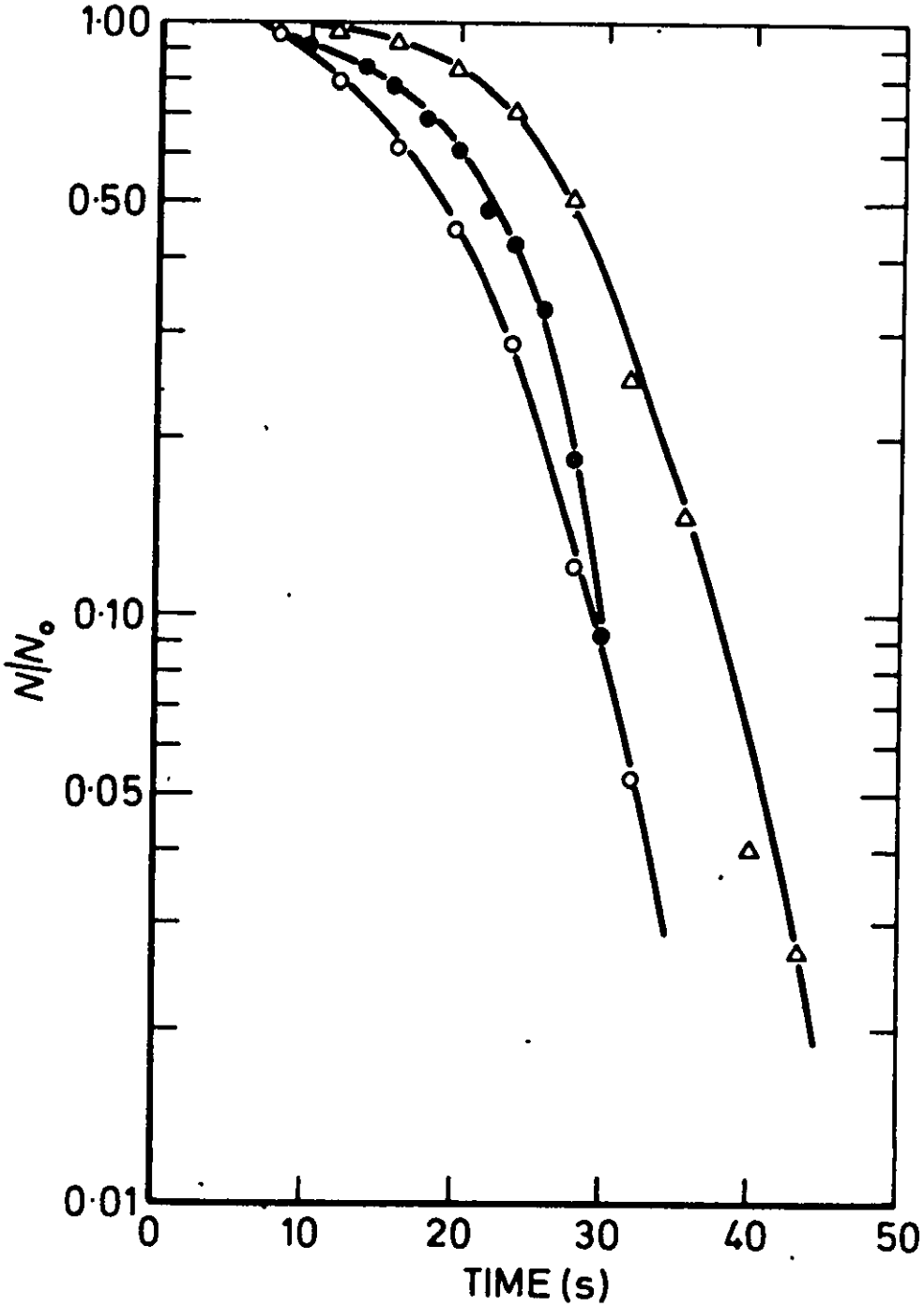

a_1	Drop Size (cms.)	Concentration of Decanoic acid
○	0.304	1.0M
●	0.314	0.5M
△	0.312	0.05M

Series B1/2, C1/4, D1/2

Fig. 5.19 Effect of Decanoic Acid concentration on the overall coalescence time distributions for the system decanoic acid-heptane-water

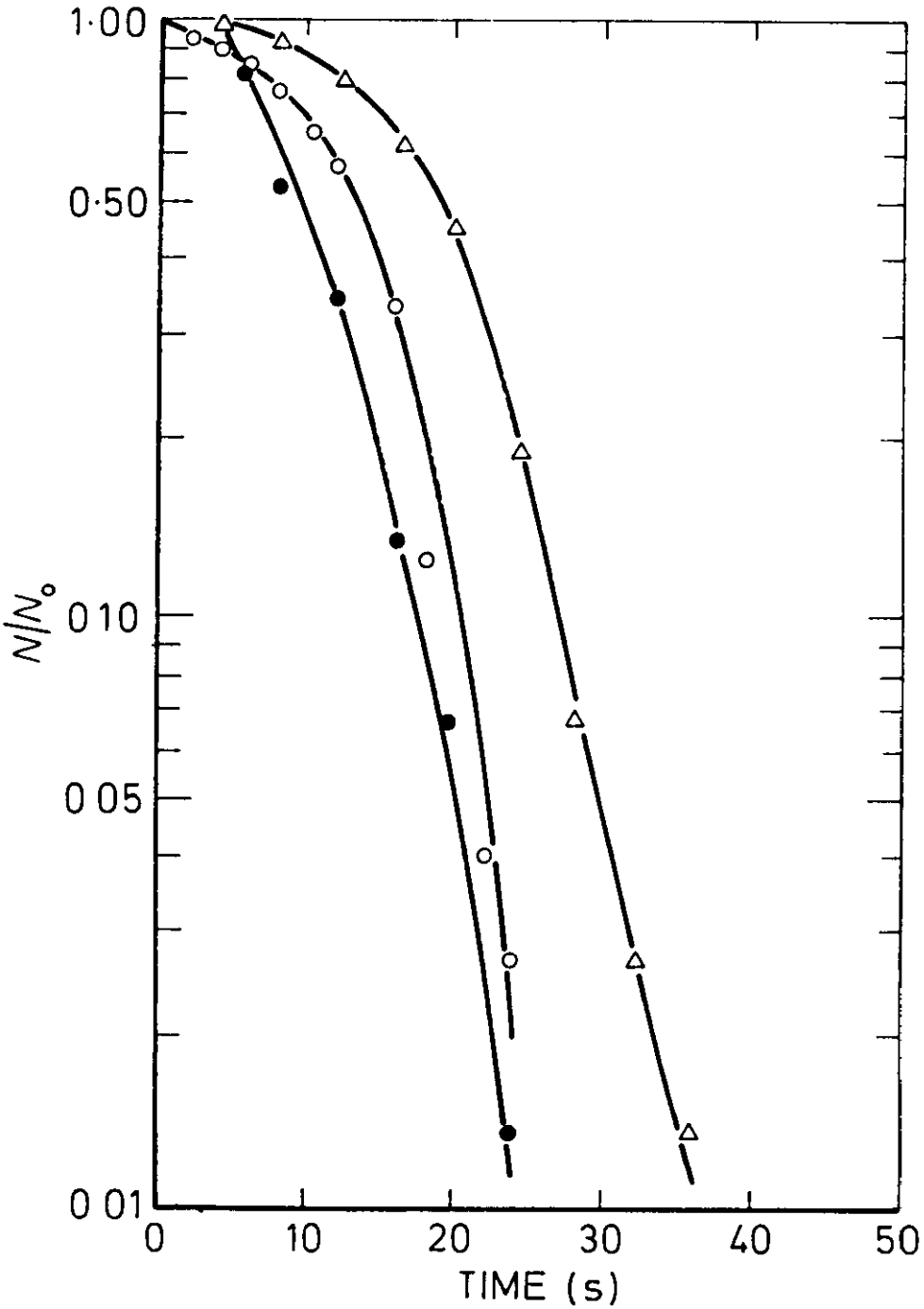

a_1	Drop Size (cms.)	Concentration of Decanoic acid
○	0.304	1.0M
●	0.314	0.5M
△	0.312	0.05M

Series B1/2, C1/4, D1/2

Fig. 5.20 Effect of Decanoic Acid concentration on the first stage coalescence time distributions for the system decanoic acid-heptane-water

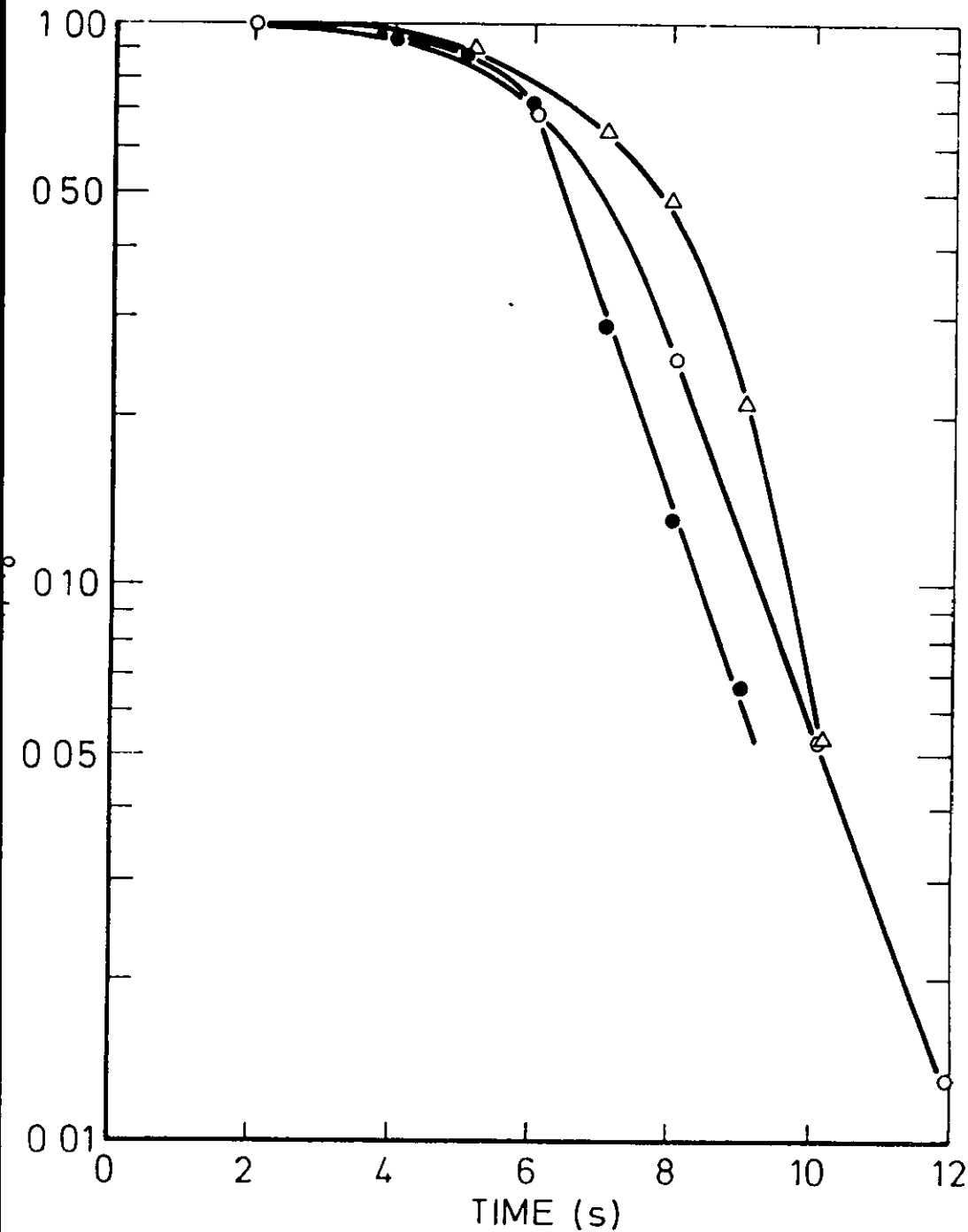

a_1	Drop Size (cms.)	Concentration of Decanoic Acid
○	0.304	1.0M
●	0.314	0.5M
△	0.312	0.05M

Series B1/2, C1/4, D1/2

Fig. 5.21 Effect of Decanoic Acid concentration on the second stage coalescence time distributions for the system decanoic acid-heptane-water

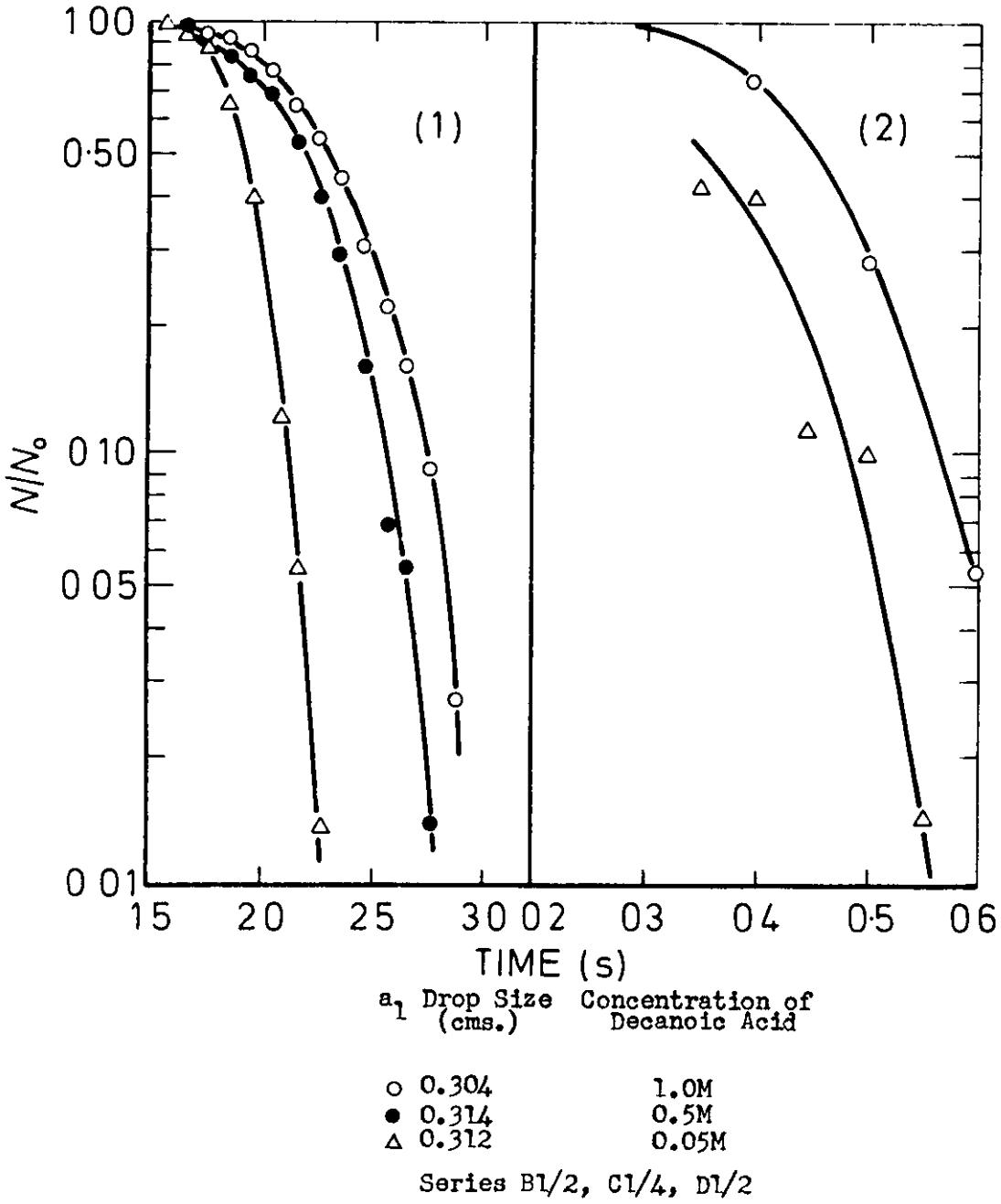

Fig. 5.22 Effect of Decanoic Acid concentration on the third (1) and fourth stage (2) coalescence time distributions for the system decanoic acid-heptane-water

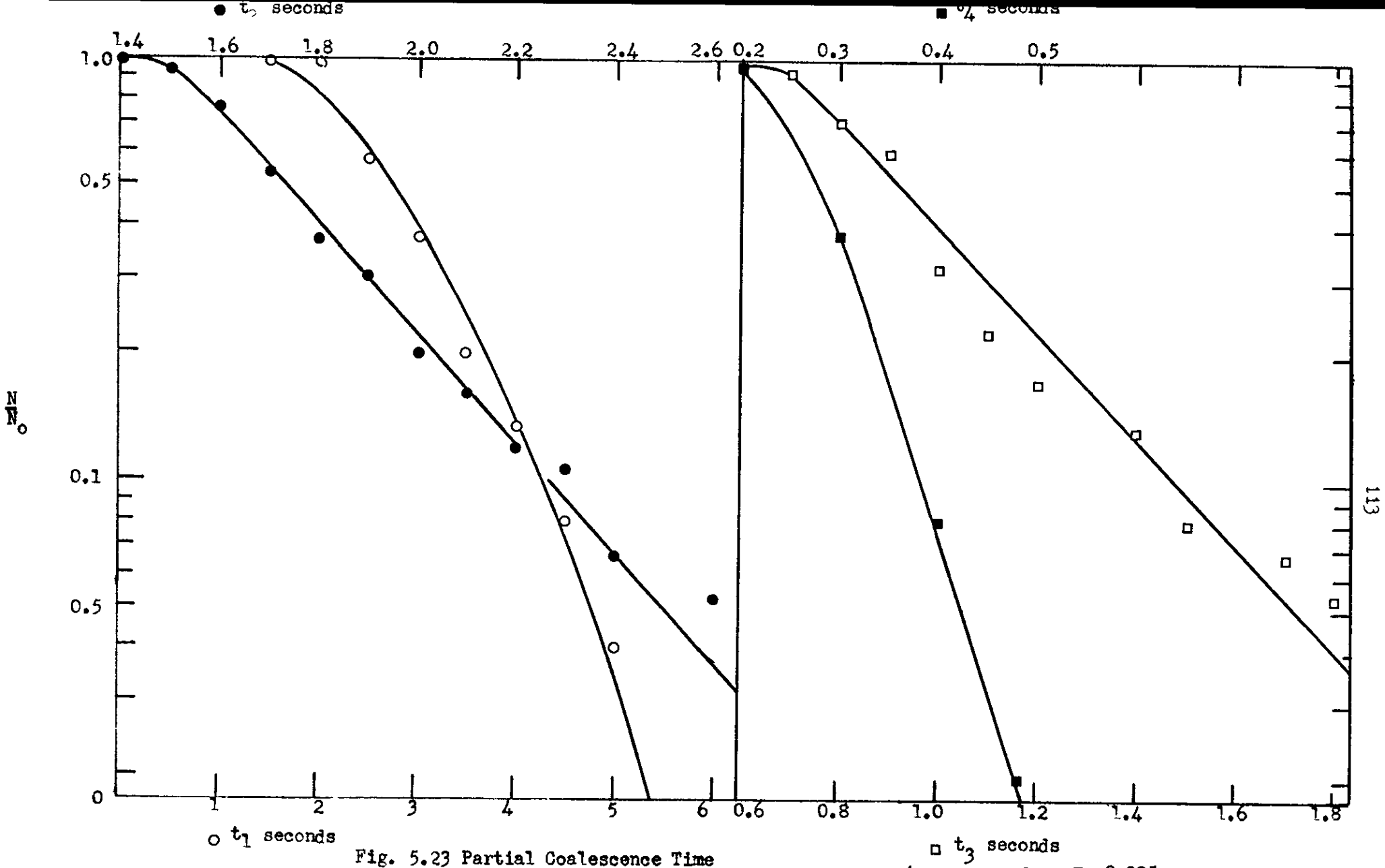

Fig. 5.23 Partial Coalescence Time distributions for the system heptane-water

Series A2/1
L = 0 cms.

a_1 = 0.325 cms.
a_2 = 0.1230 cms.
a_3 = 0.0573 cms.
a_4 = 0.0287 cms.

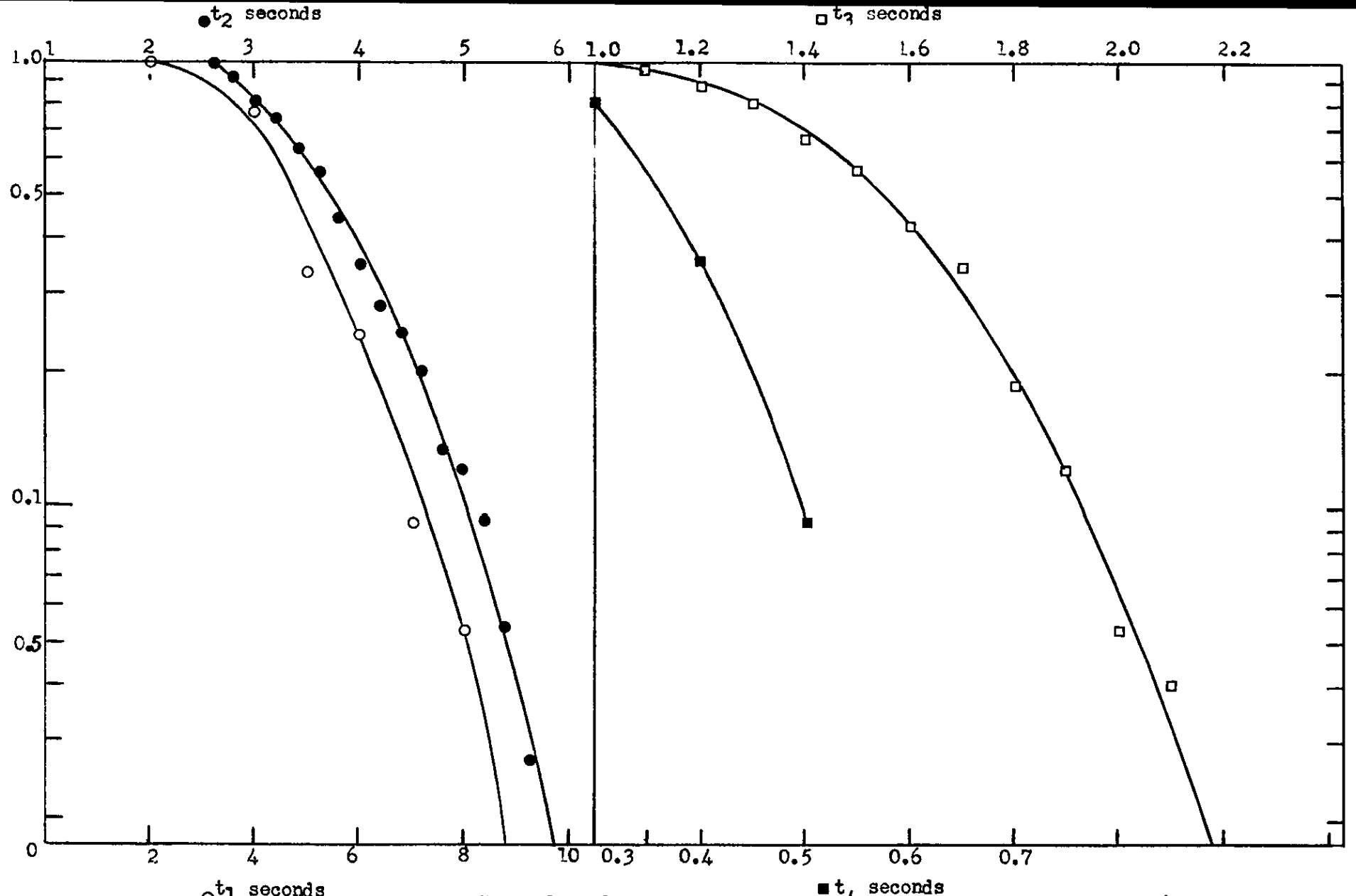

Fig. 5.24 Partial Coalescence Time distributions for system heptane-water

Series A2/2
L = 0 cms.

a_1 = 0.416 cms.
a_2 = 0.1426 cms.
a_3 = 0.0635 cms.
a_4 = 0.0318 cms.

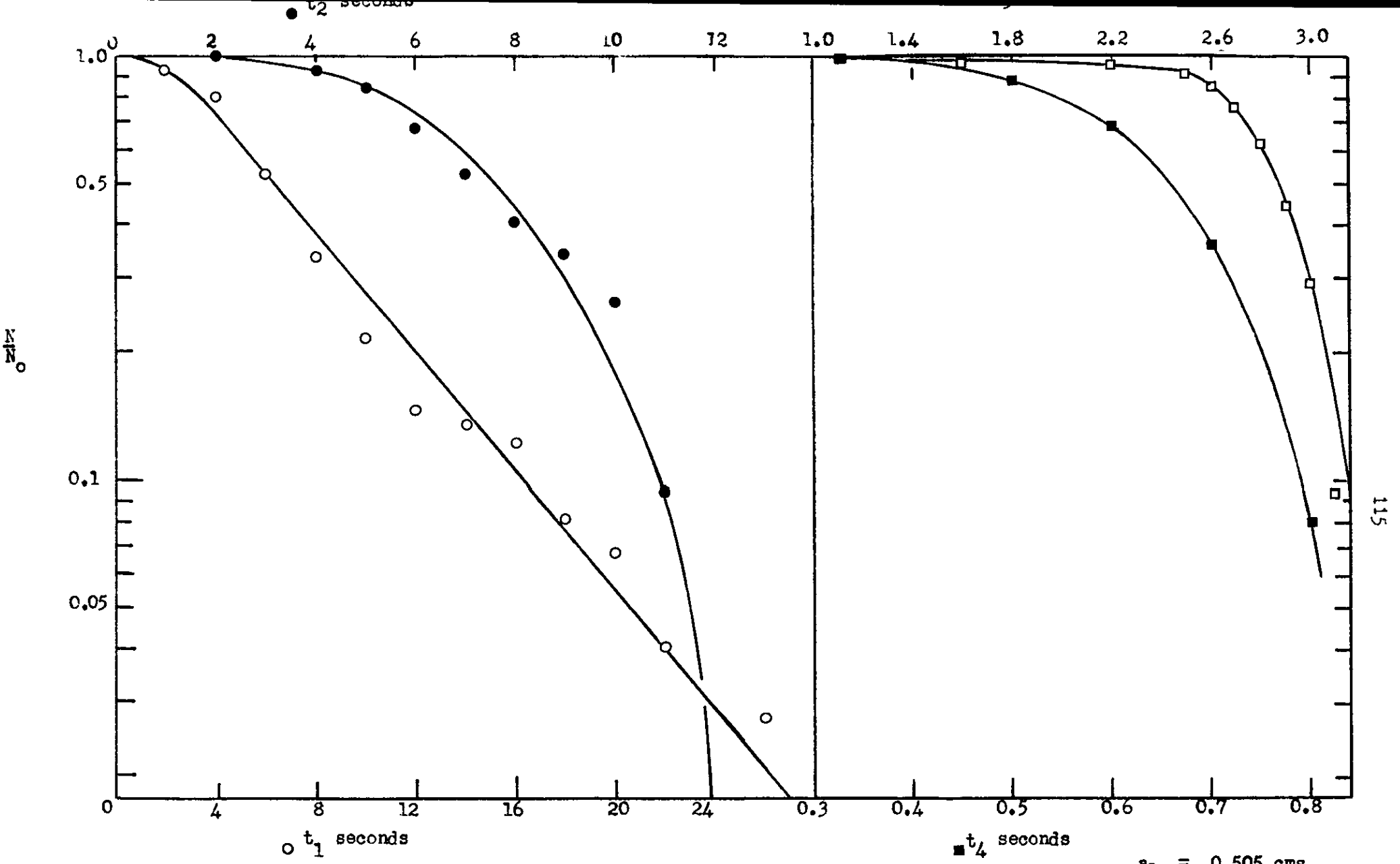

Fig. 5.25 Partial Coalescence Time distributions for system heptane-water

Series A2/3
L = 0 cms.

a_1 = 0.505 cms.
a_2 = 0.1558 cms.
a_3 = 0.0665 cms.
a_4 = 0.0333 cms.

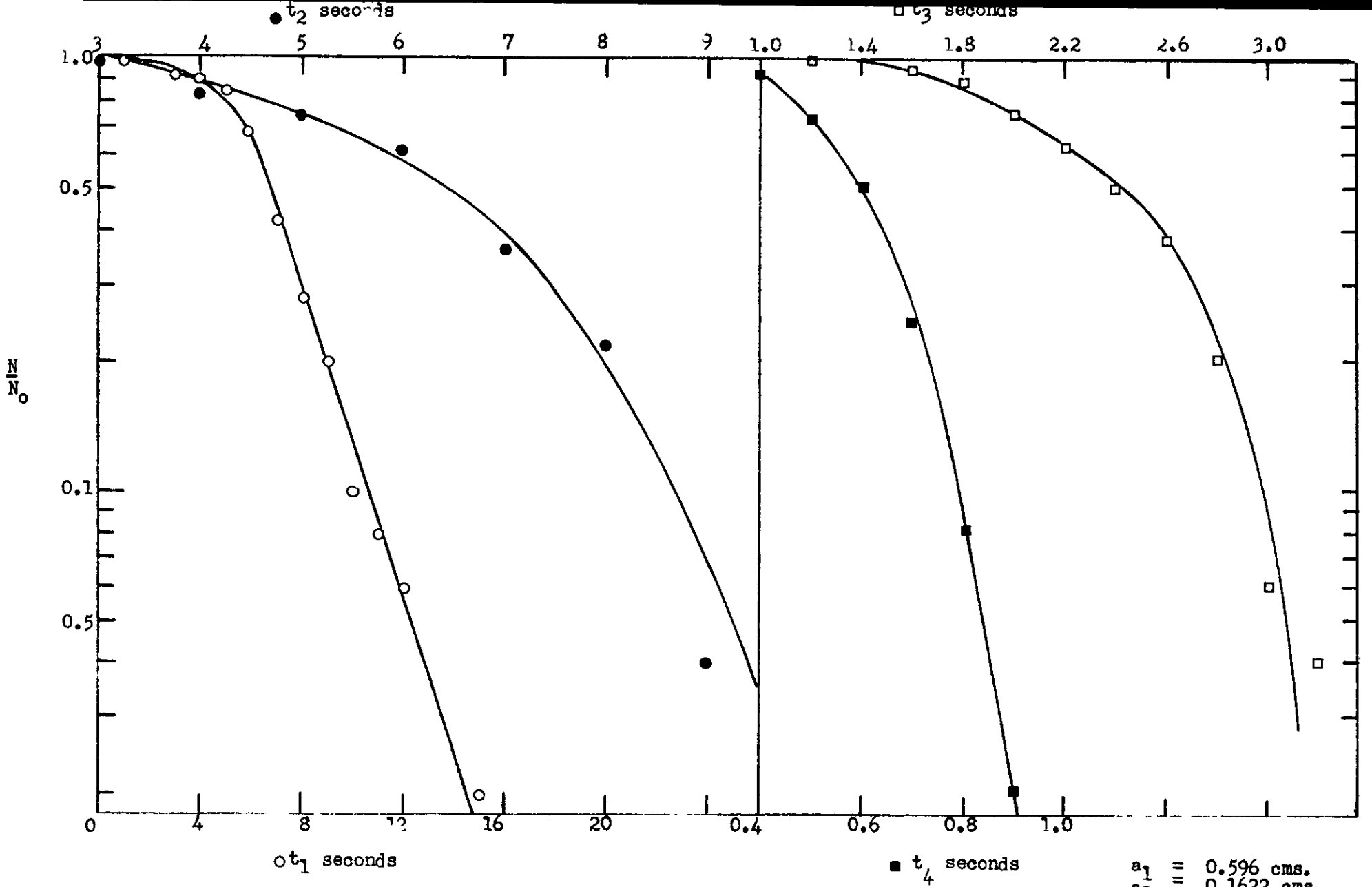

Fig. 5.26 Partial coalescence time distribution for system heptane-water

Series A2/4
L = 0 cms.

a_1 = 0.596 cms.
a_2 = 0.1622 cms.
a_3 = 0.0679 cms.
a_4 = 0.0339 cms.

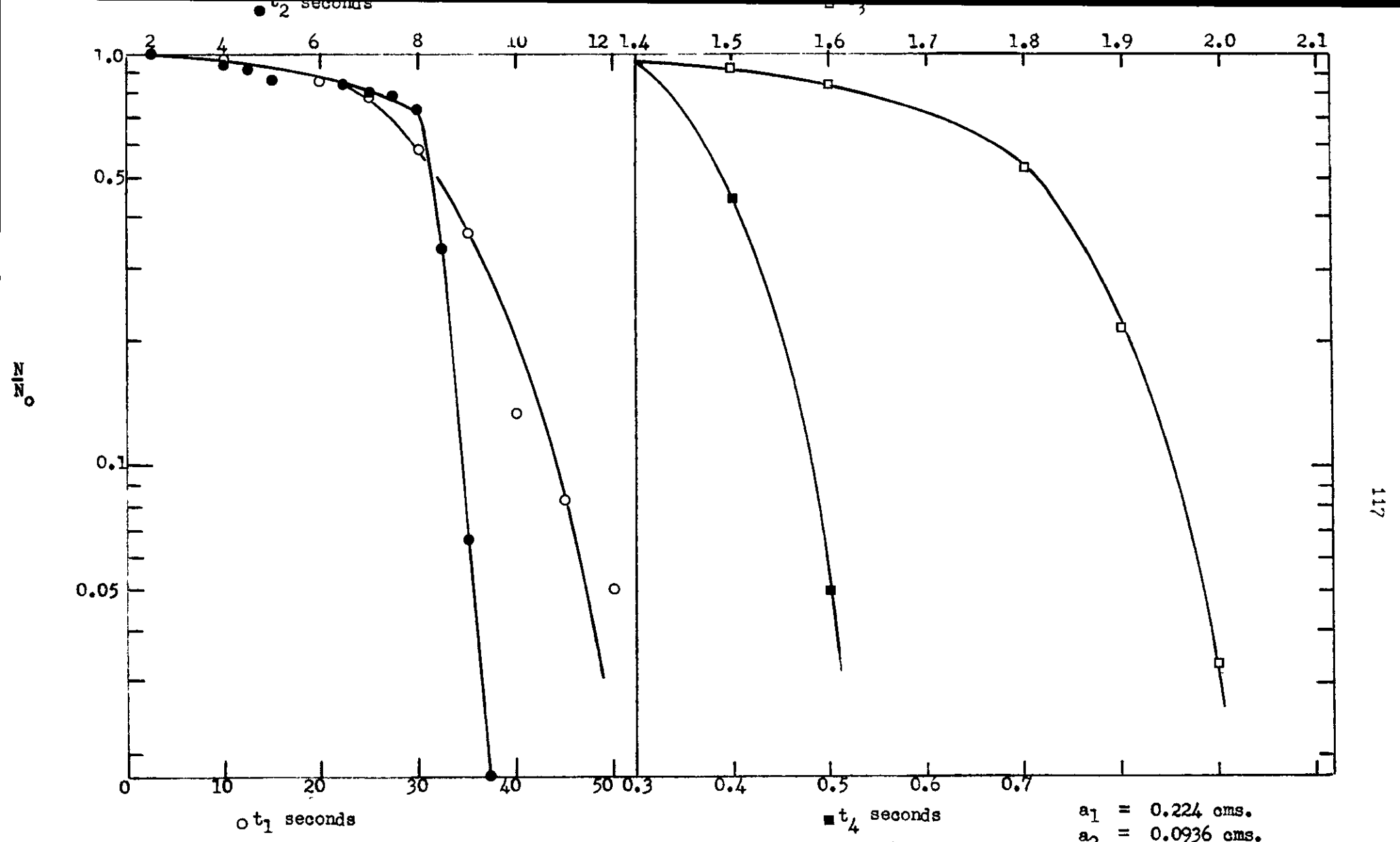

Series B2/1
L = 0 cms.

a_1 = 0.224 cms.
a_2 = 0.0936 cms.
a_3 = 0.0457 cms.
a_4 = 0.0228 cms.

Fig. 5.27 Partial Coalescence Time distributions for system 0.05M decanoic acid-heptane-water

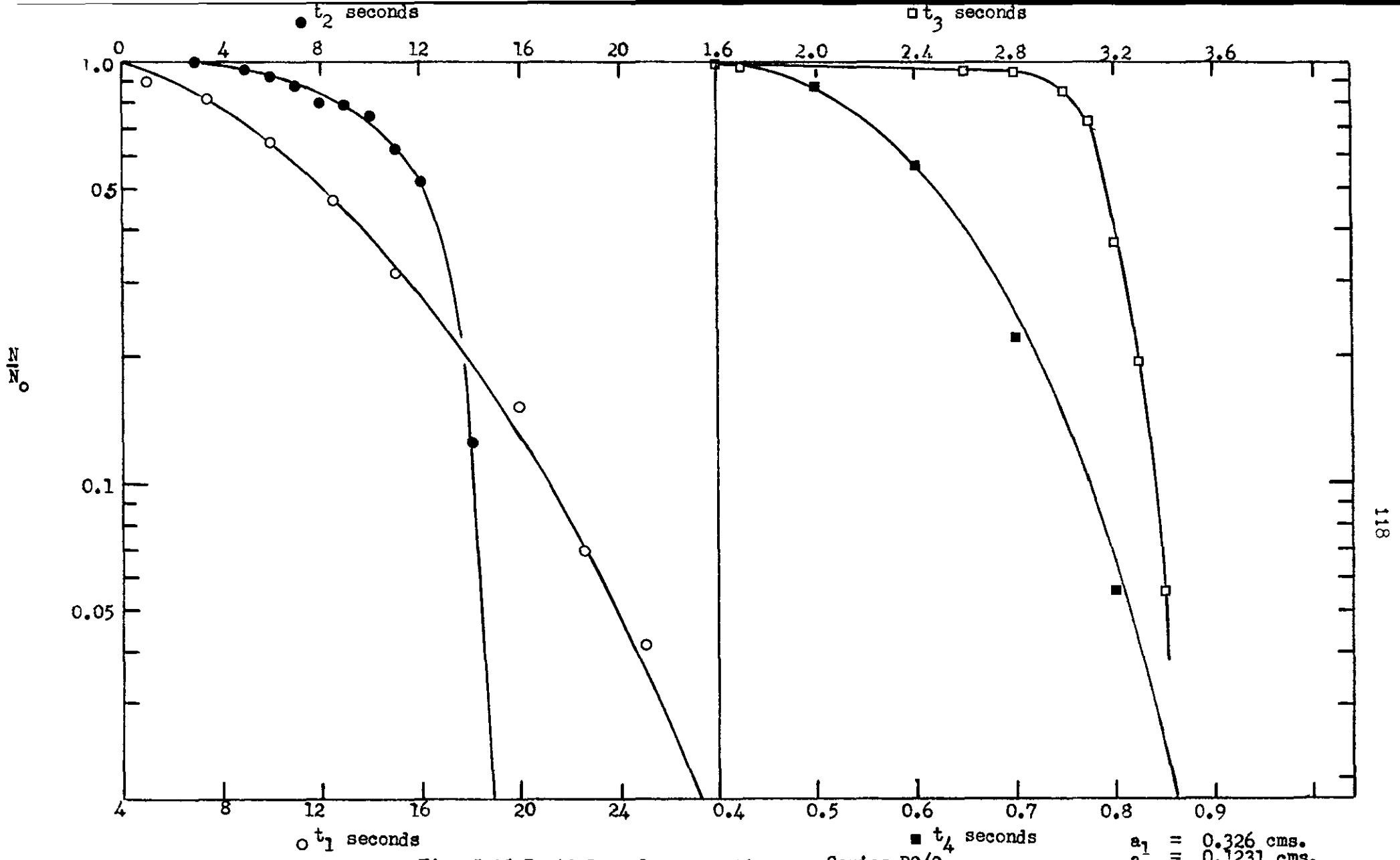

Fig. 5.28 Partial Coalescence Time distributions for system 0.05M decanoic acid- heptane-water

Series B2/2
L = 0 cms.

a_1 = 0.326 cms.
a_2 = 0.1231 cms.
a_3 = 0.0575 cms.
a_4 = 0.0288 cms.

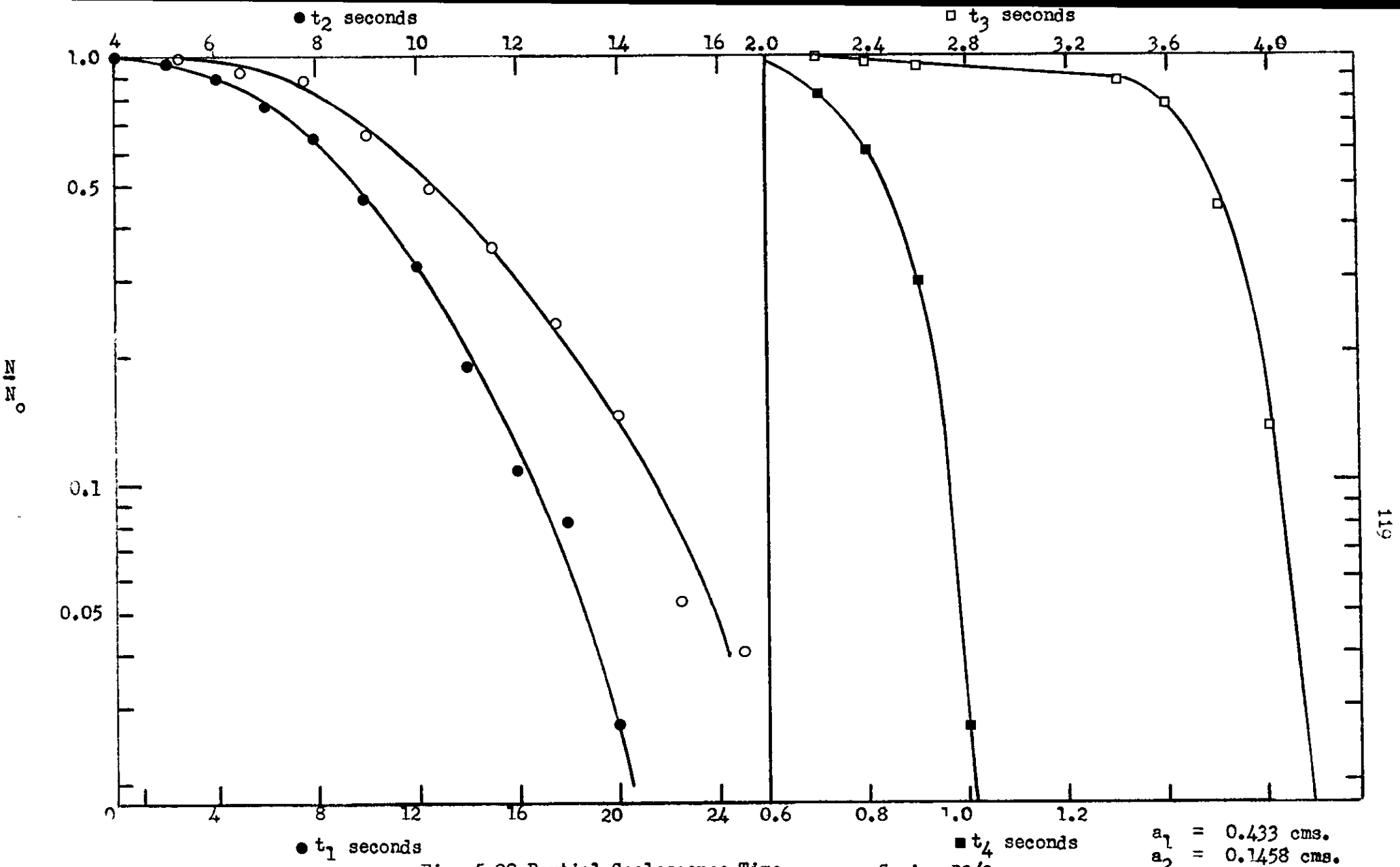

Fig. 5.29 Partial Coalescence Time distributions for system 0.05M decanoic acid-heptane-water

Series B2/3
L = 0 cms.

a_1 = 0.433 cms.
a_2 = 0.1458 cms.
a_3 = 0.0645 cms.
a_4 = 0.0323 cms.

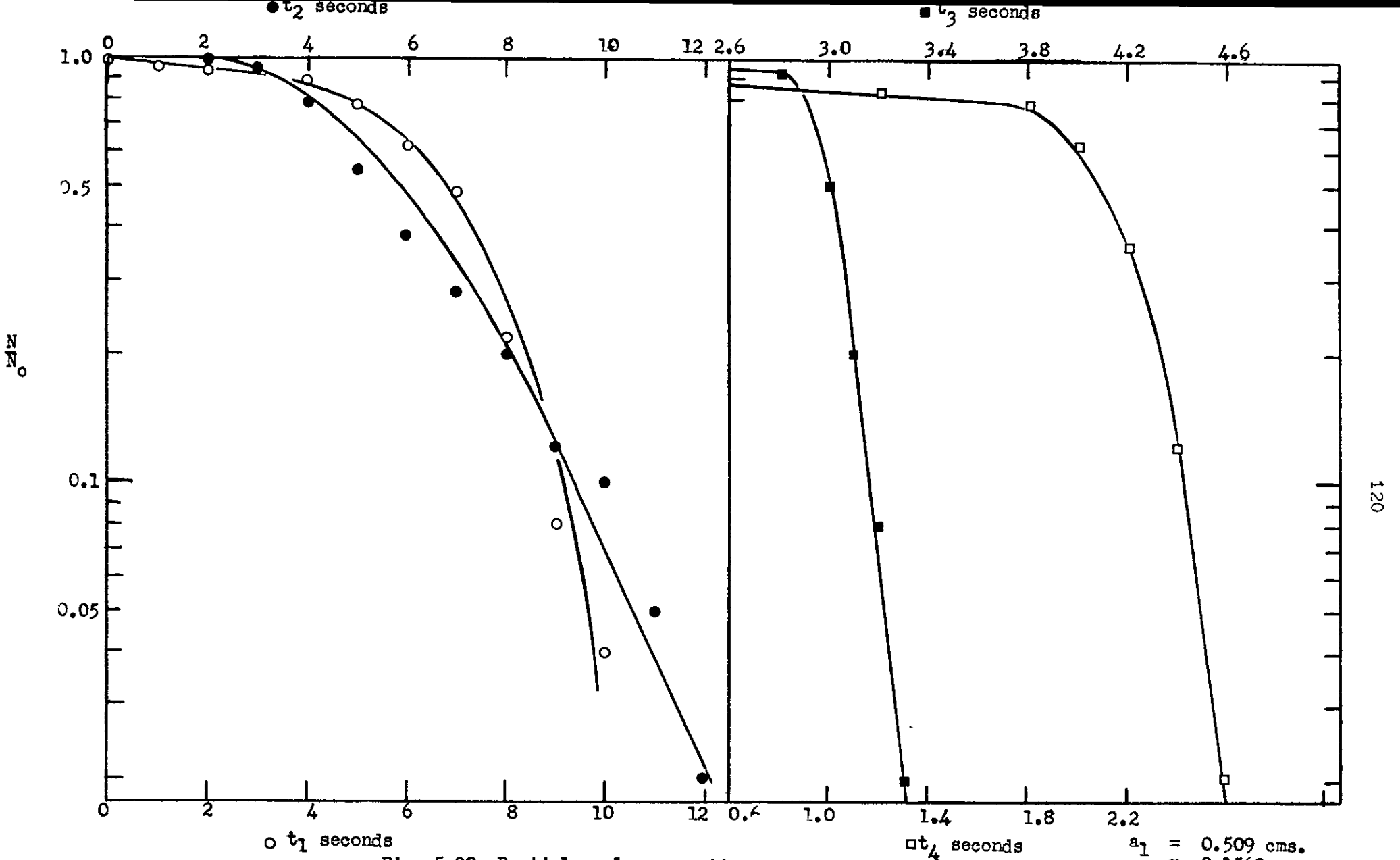

Fig. 5.30 Partial coalescence time distributions for system 0.05M decanoic acid-heptane-water

Series B2/4
L = 0 cms.

a_1 = 0.509 cms.
a_2 = 0.1560 cms.
a_3 = 0.0665 cms.
a_4 = 0.0333

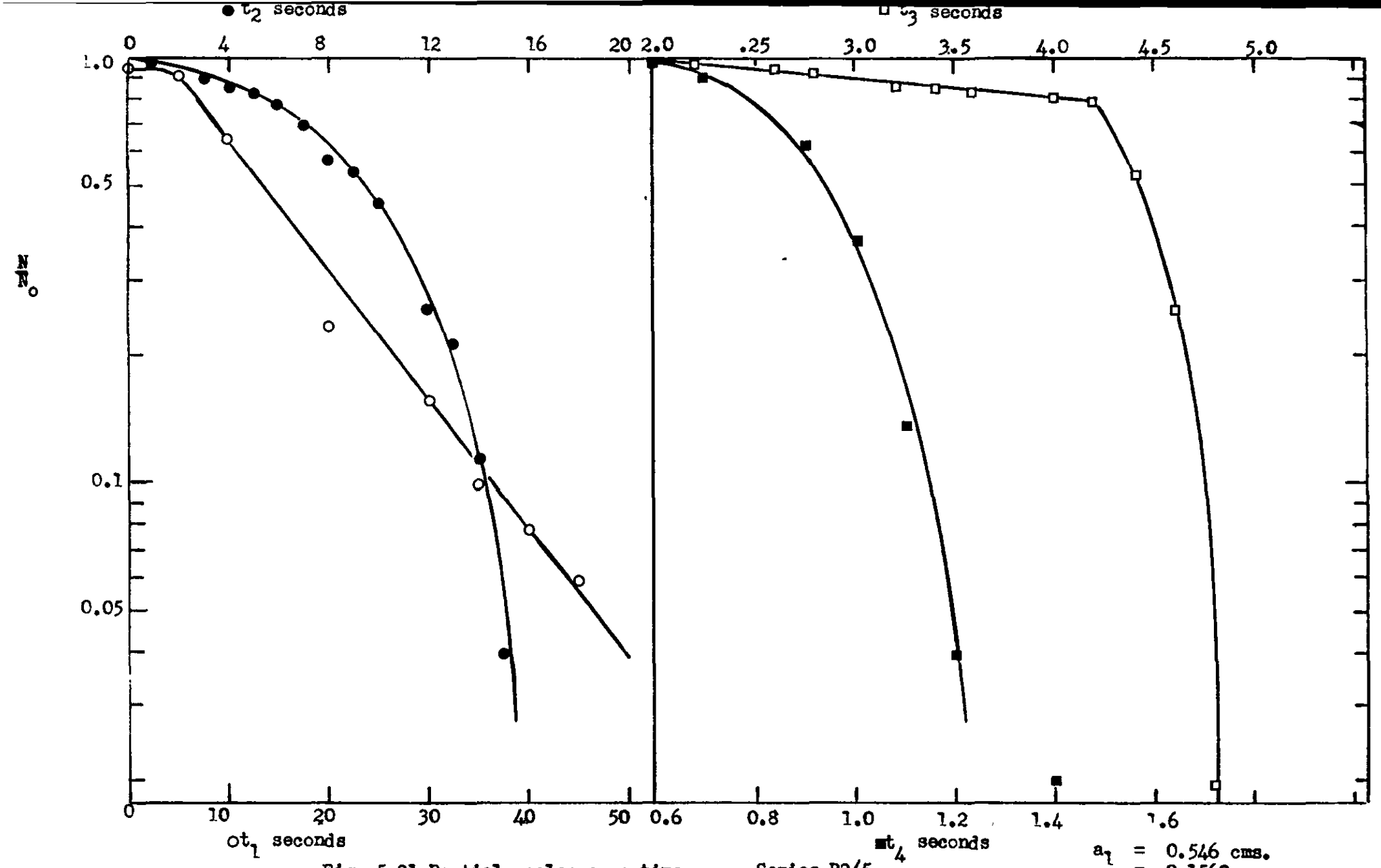

Fig. 5.31 Partial coalescence time distribution for system 0.05M decanoic acid-heptane-water

Series B2/5
L = 0 cms.

a_1 = 0.546 cms.
a_2 = 0.1560 cms.
a_3 = 0.0665 cms.
a_4 = 0.0333 cms.

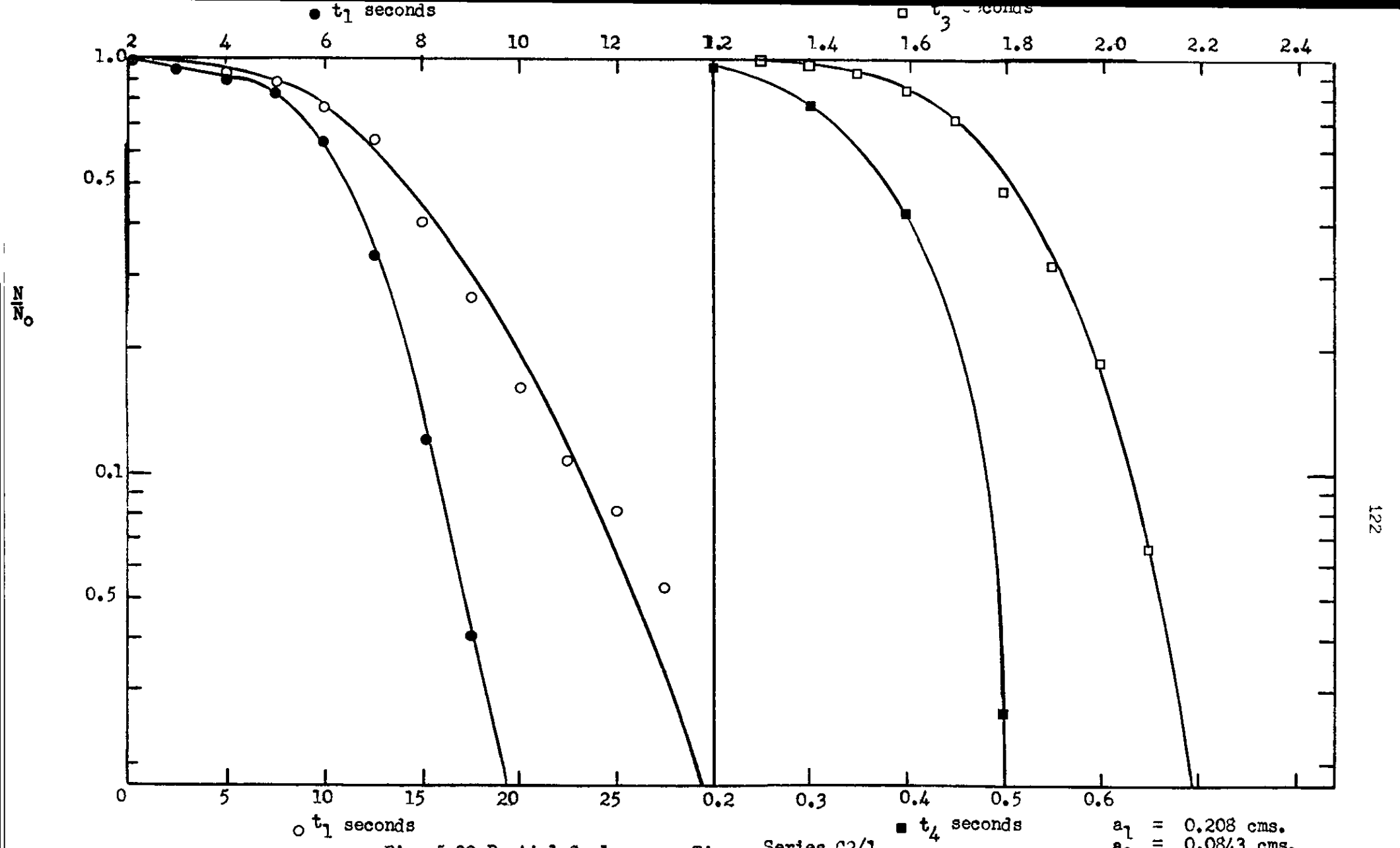

Fig. 5.32 Partial Coalescence Time distributions for system 0.5M decanoic acid-heptane-water

Series C2/1
L = 0 cms.

a_1 = 0.208 cms.
a_2 = 0.0843 cms.
a_3 = 0.0408 cms.
a_4 = 0.0204 cms.

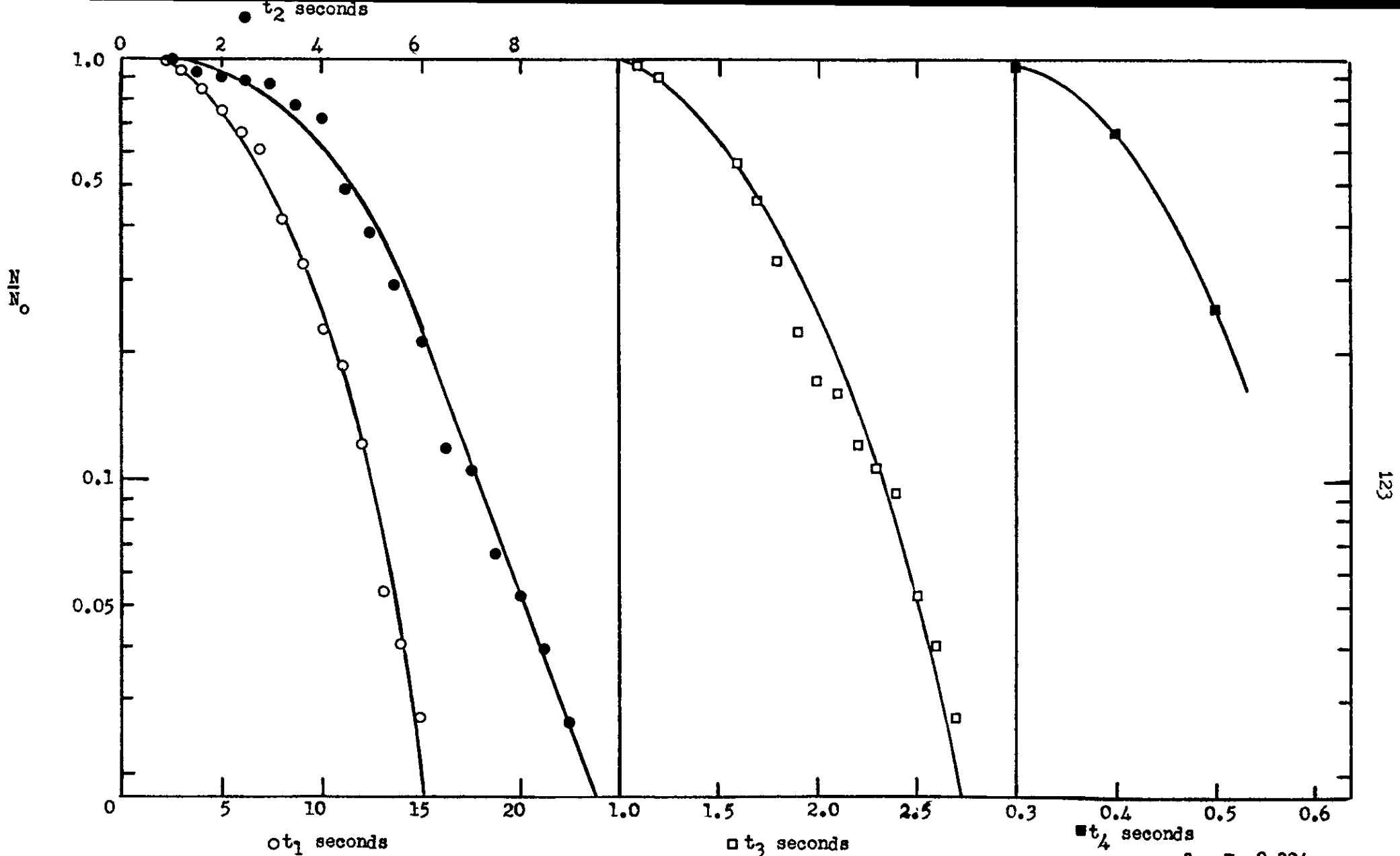

Fig. 5.33 Partial coalescence time distributions for system 0.5M decanoic acid-heptane-water

Series C2/2
L = 0 cms.

a_1 = 0.324 cms.
a_2 = 0.1110 cms.
a_3 = 0.0523 cms.
a_4 = 0.0266 cms.

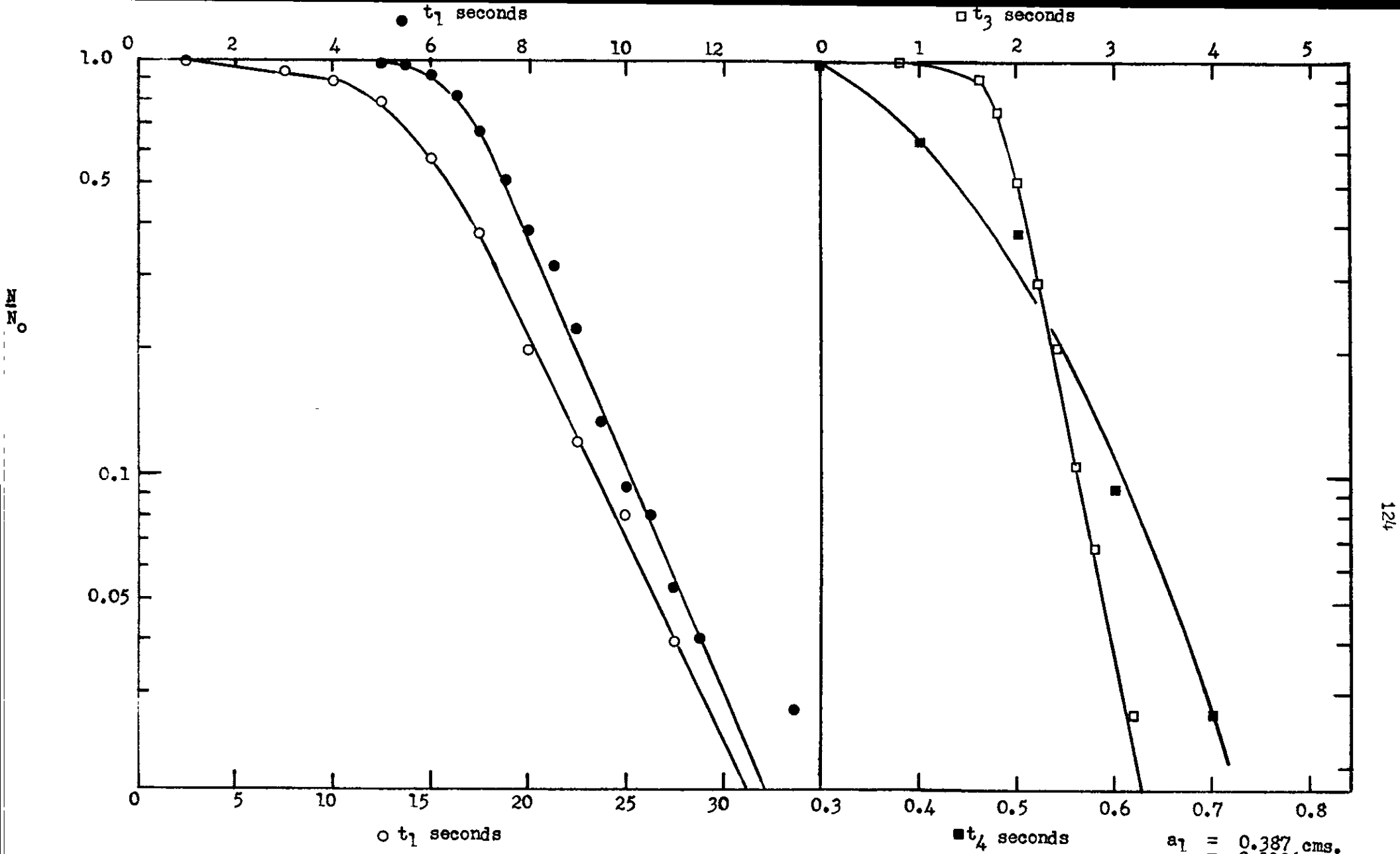

Fig. 5.34 Partial coalescence time distributions for system 0.5M decanoic acid-heptane-water

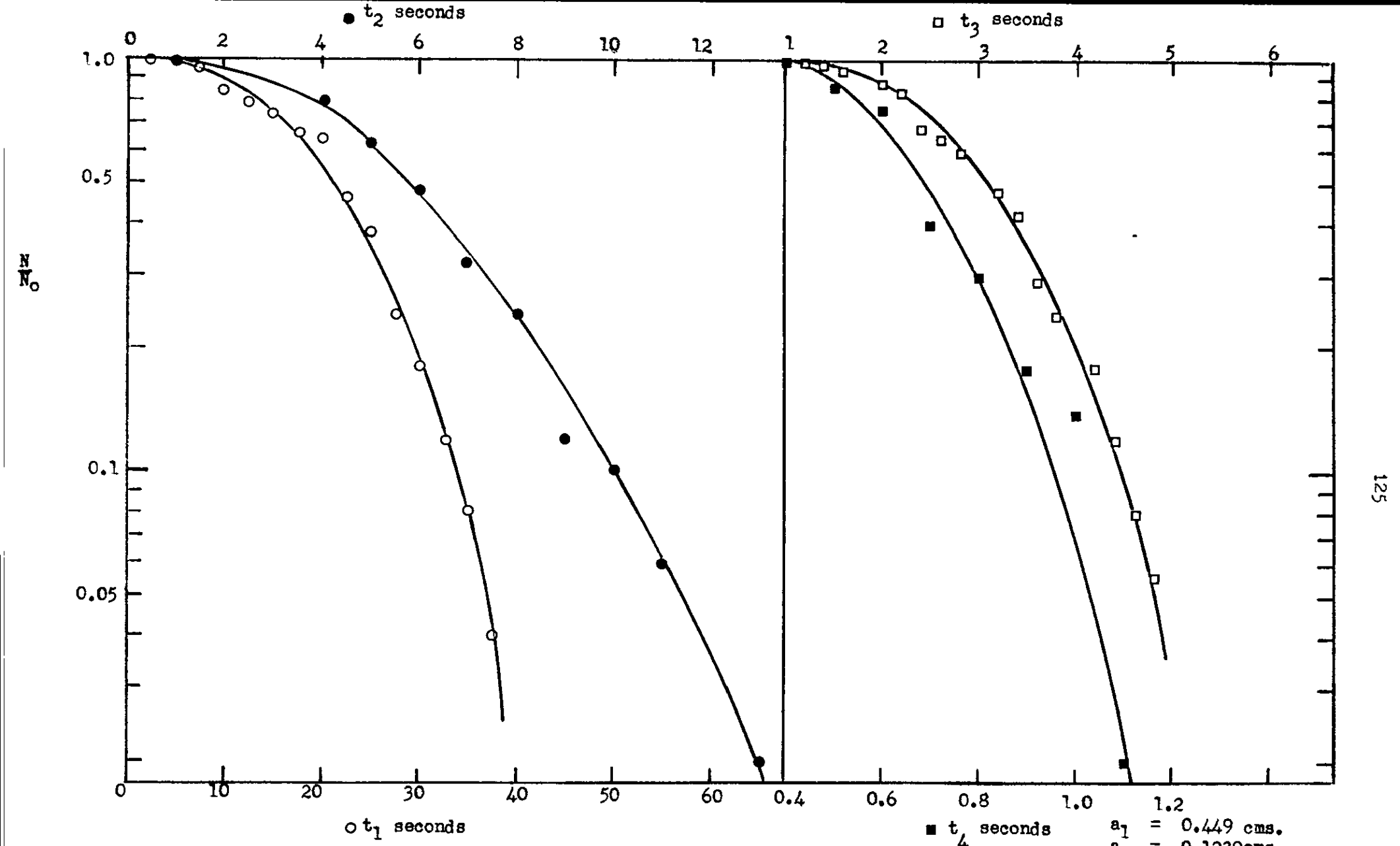

Fig. 5.35 Partial coalescence time distributions for system 0.5M decanoic acid-heptane-water

Series C2/4
L = 0 cms.

a_1 = 0.449 cms.
a_2 = 0.1239cms.
a_3 = 0.0564 cms.
a_4 = 0.0282 cms.

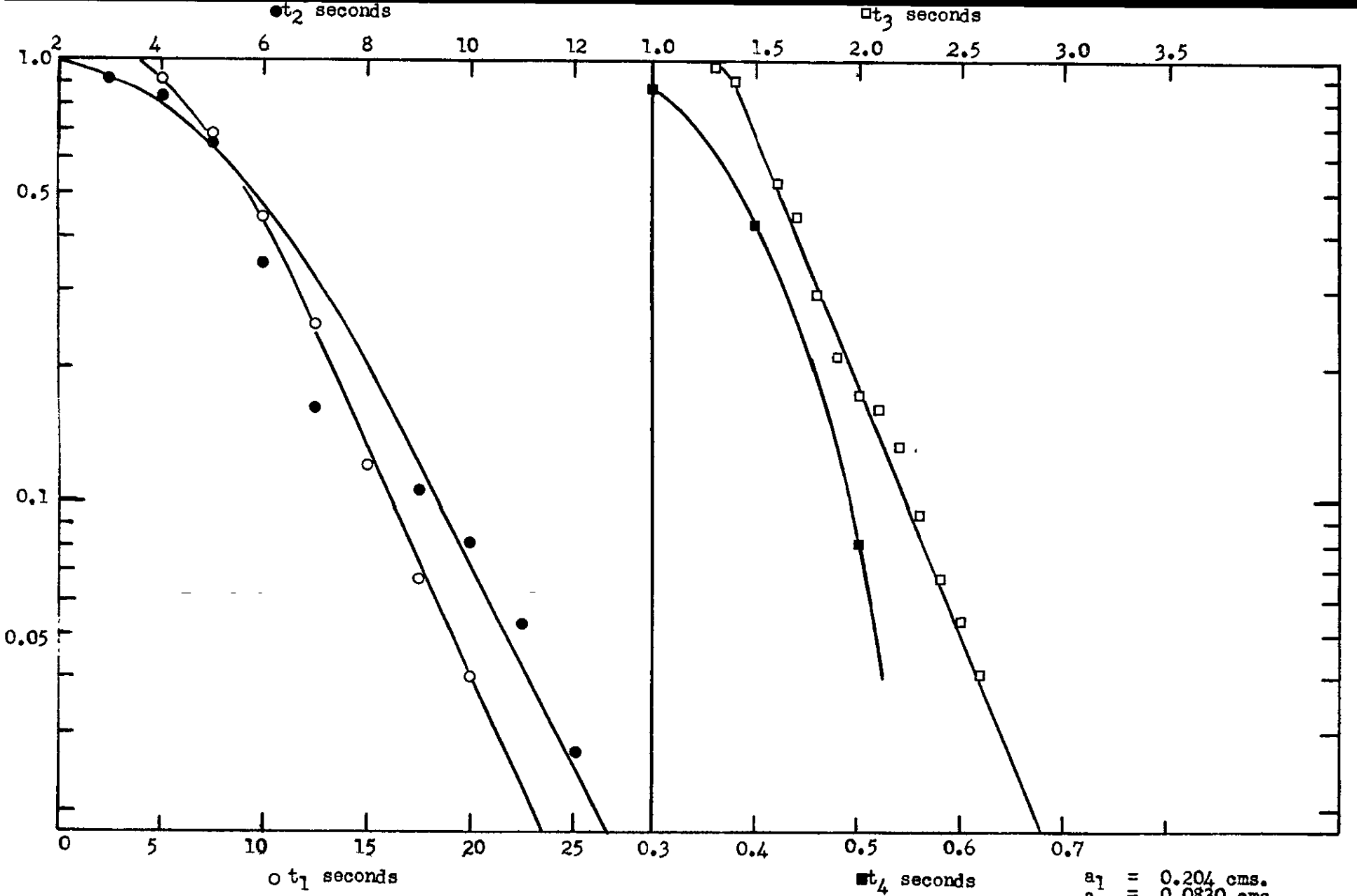

Series D2/1
L = 0 cms.

a_1 = 0.204 cms.
a_2 = 0.0830 cms.
a_3 = 0.0440 cms.
a_4 = 0.0220 cms.

Fig. 5.36 Partial coalescence time distributions for system 1.0M decanoic acid-heptane-water

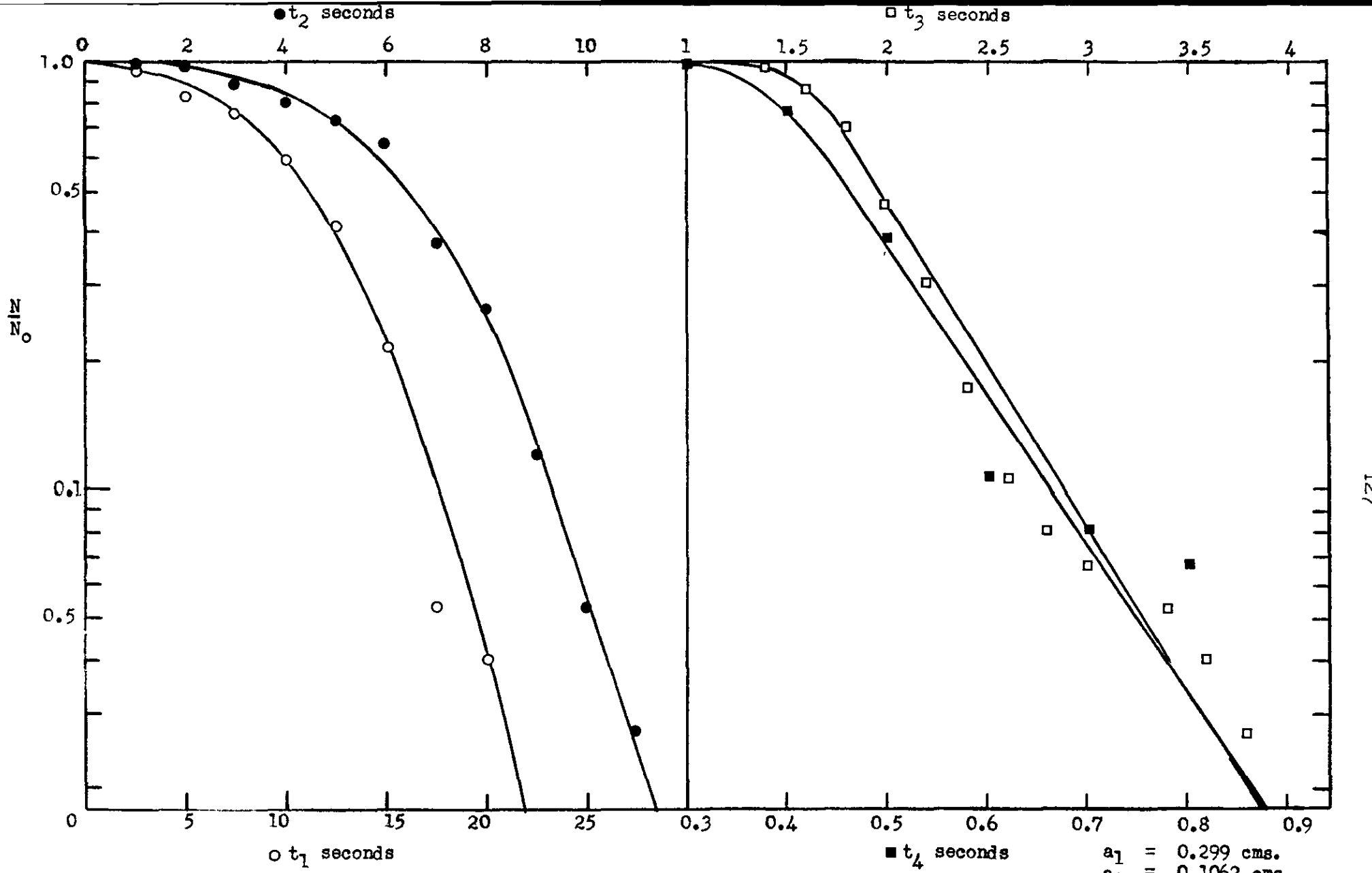

Fig. 5.37 Partial coalescence time distributions for system 1.0M decanoic acid-heptane-water

Series D2/2
L = 0 cms.

a_1 = 0.299 cms.
a_2 = 0.1062 cms.
a_3 = 0.0504 cms.
a_4 = 0.0252 cms.

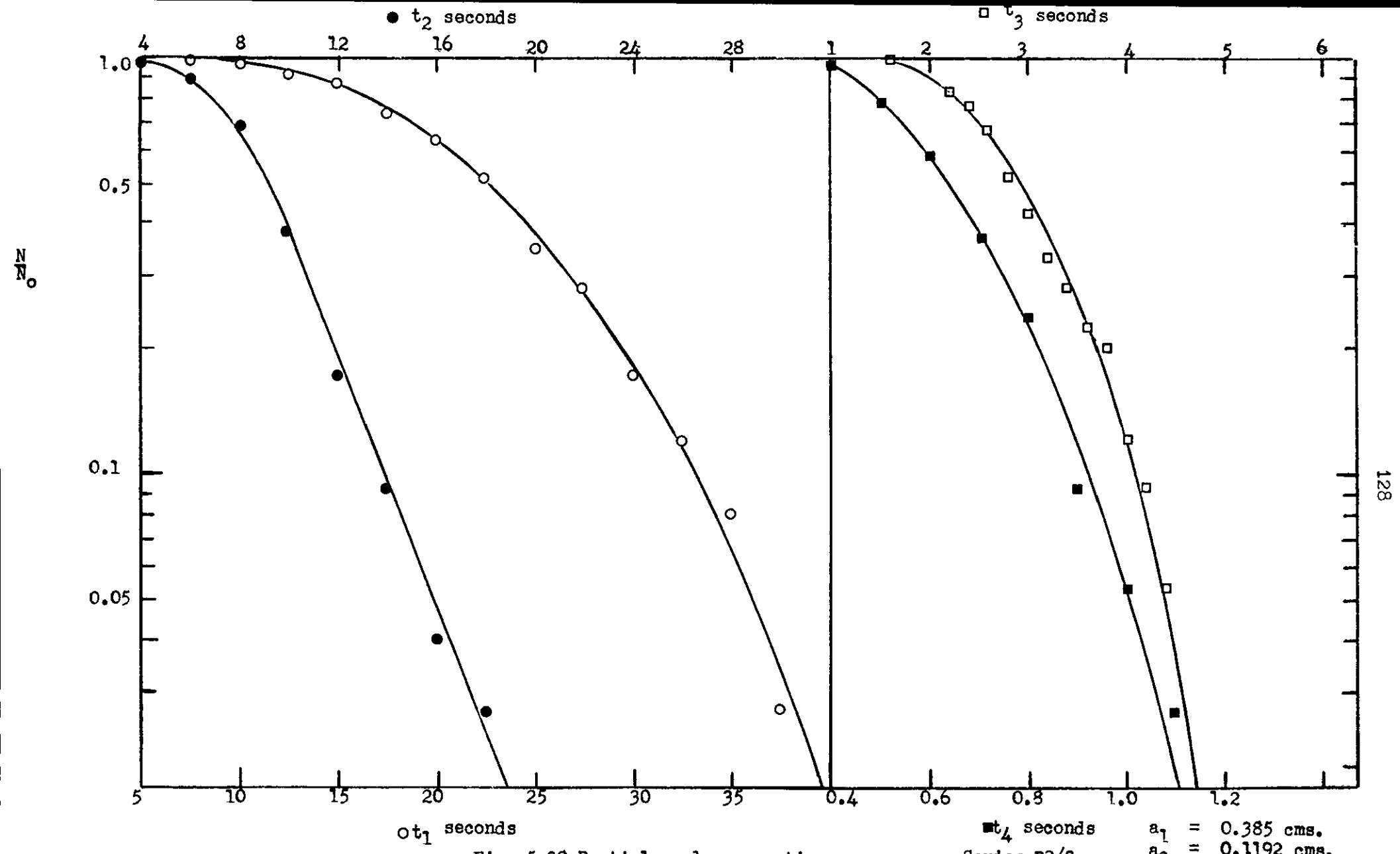

Fig. 5.38 Partial coalescence time distributions for system 1.0M decanoic acid-heptane-water

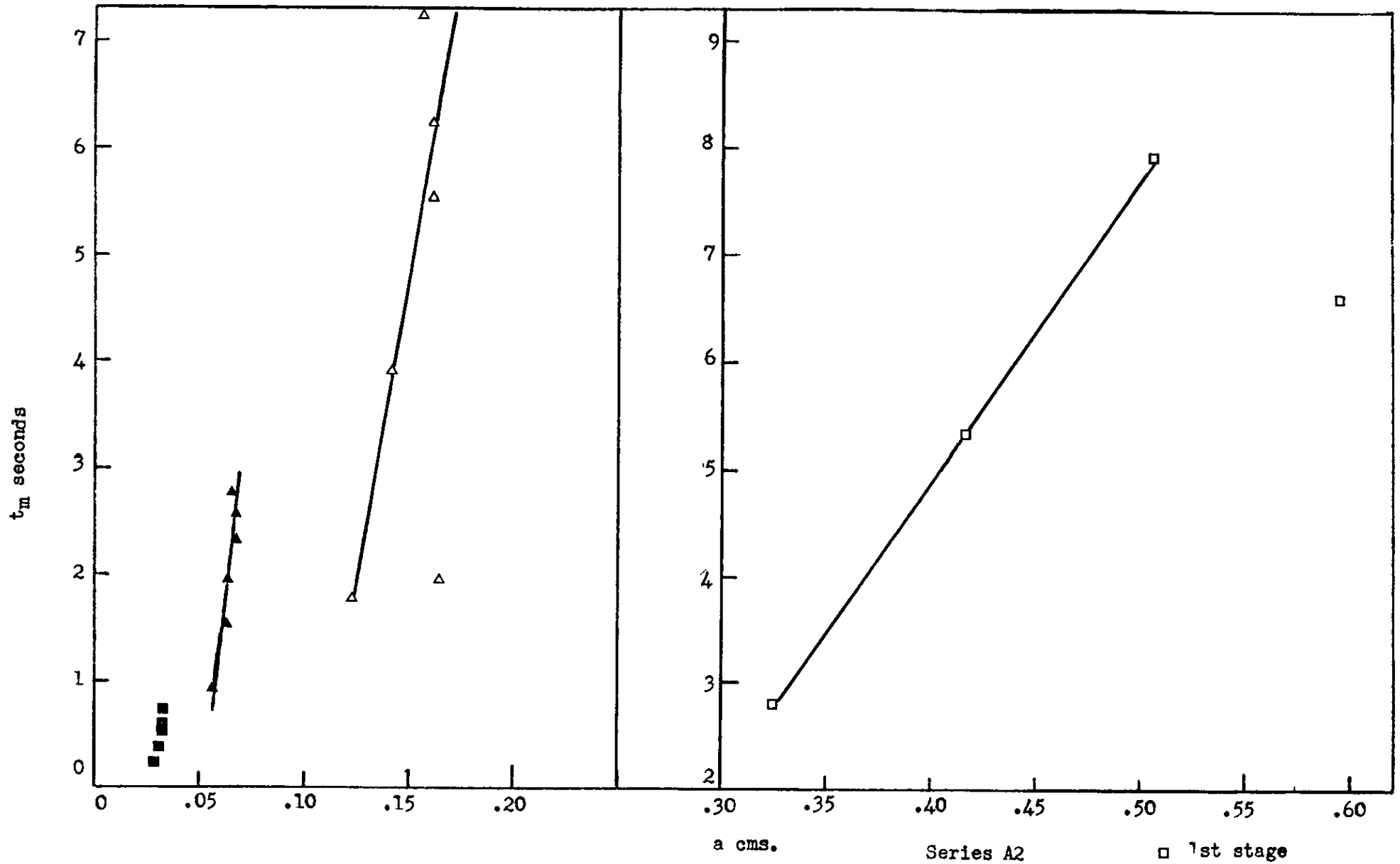

Fig. 5.39 Relationship between drop size (a) and mean coalescence time (t_m) for the system heptane-water

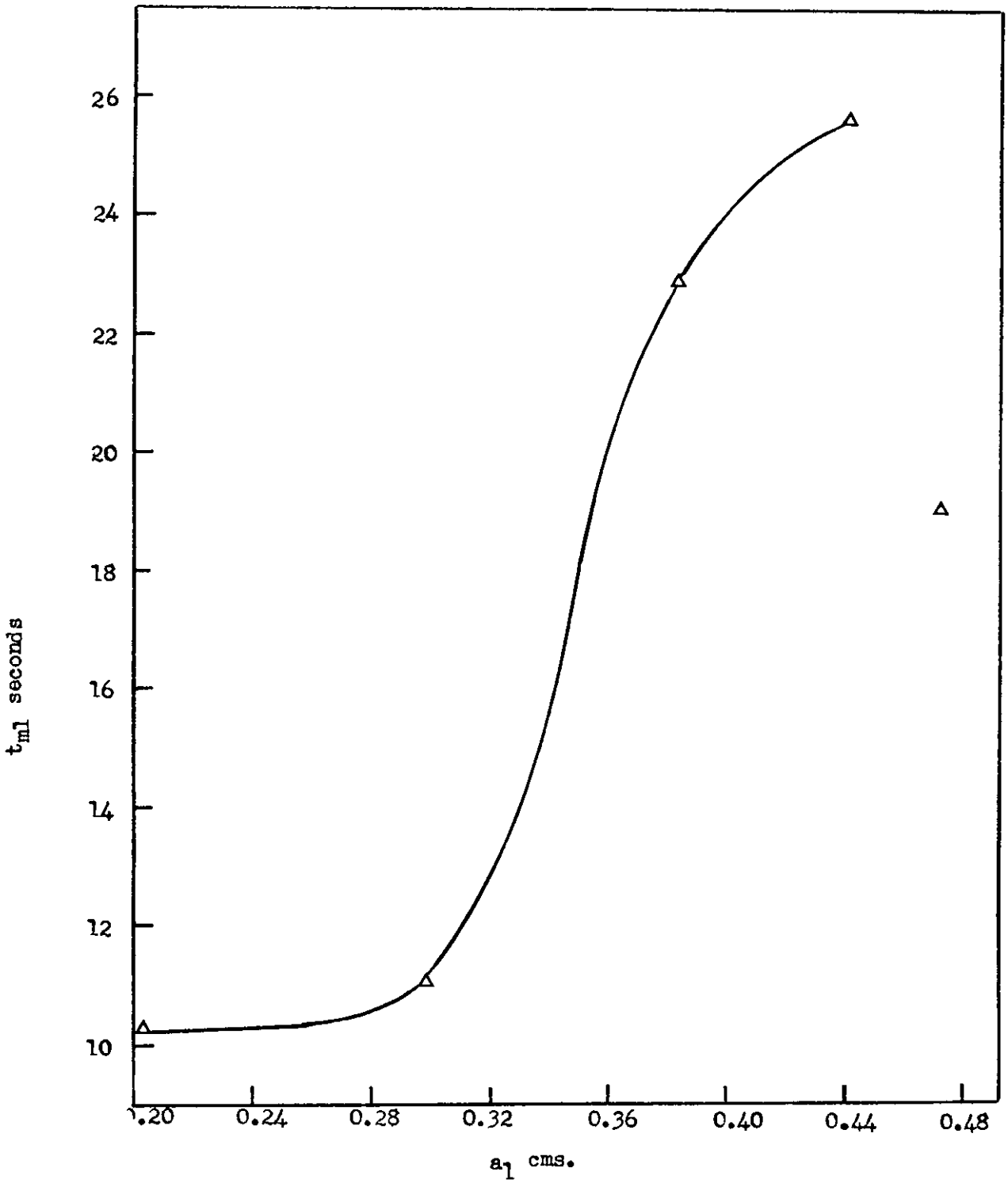

Series D2/1

Fig. 5.40 Relationship between primary drop size a_l, and mean coalescence time t_{ml}, for system 1.0M decanoic acid-heptane-water

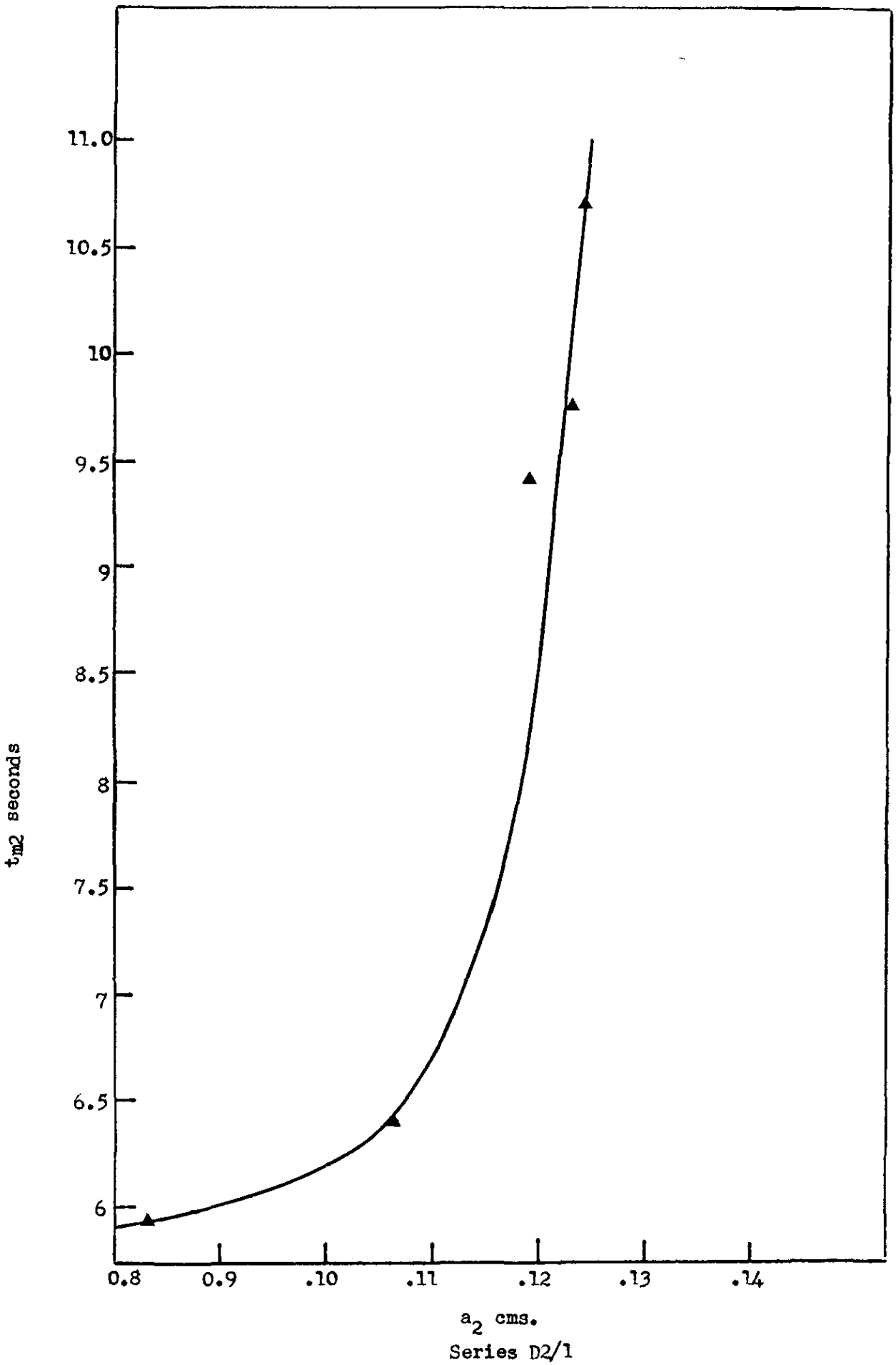

Series D2/1

Fig. 5.41 Relationship between secondary drop size, a_2, and mean coalescence time, t_{m2}, for system 1.0M decanoic acid-heptane-water

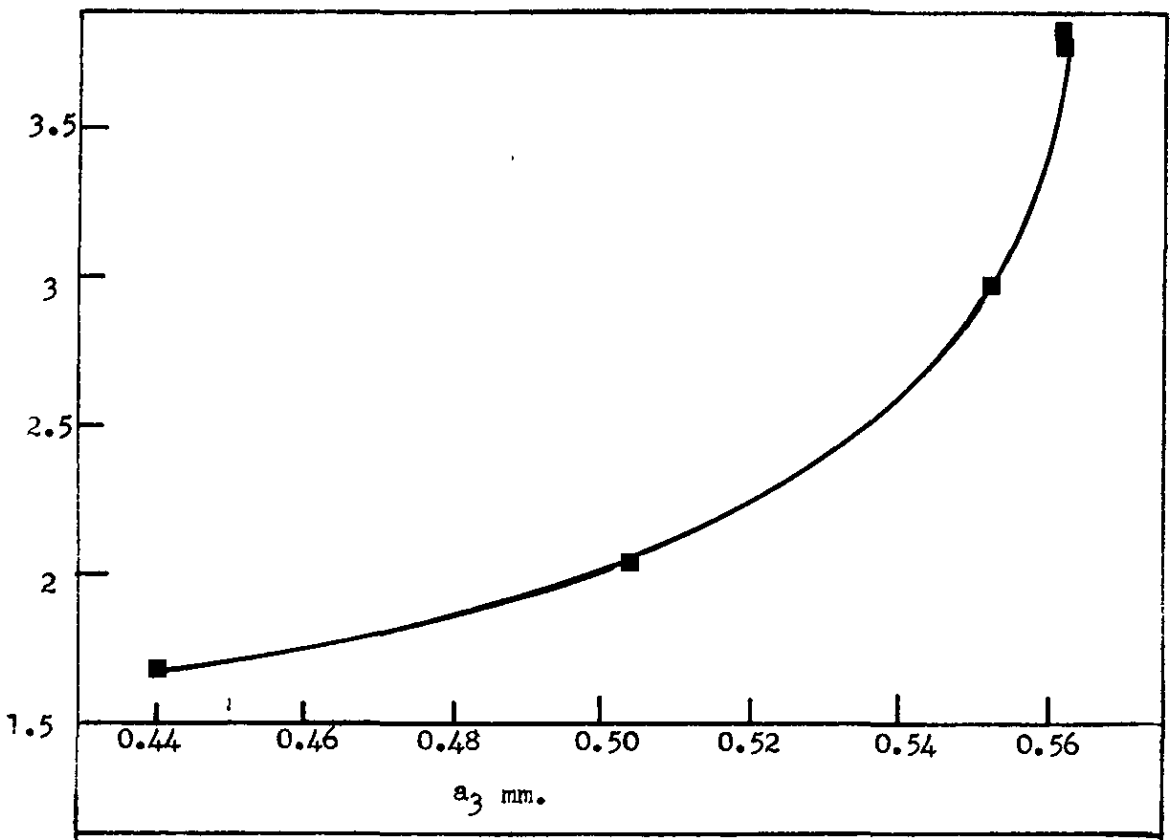

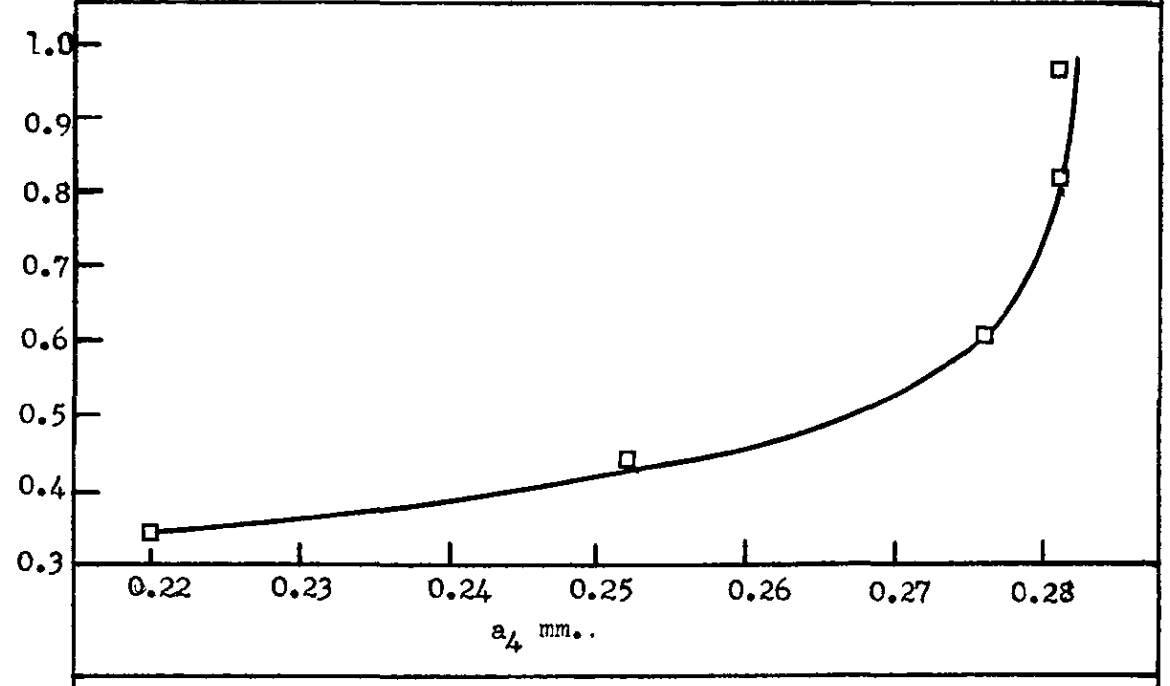

Series D2/1

Fig. 5.42 Relationship between mean rest-time and drop size for system 1.0M decanoic acid-heptane-water

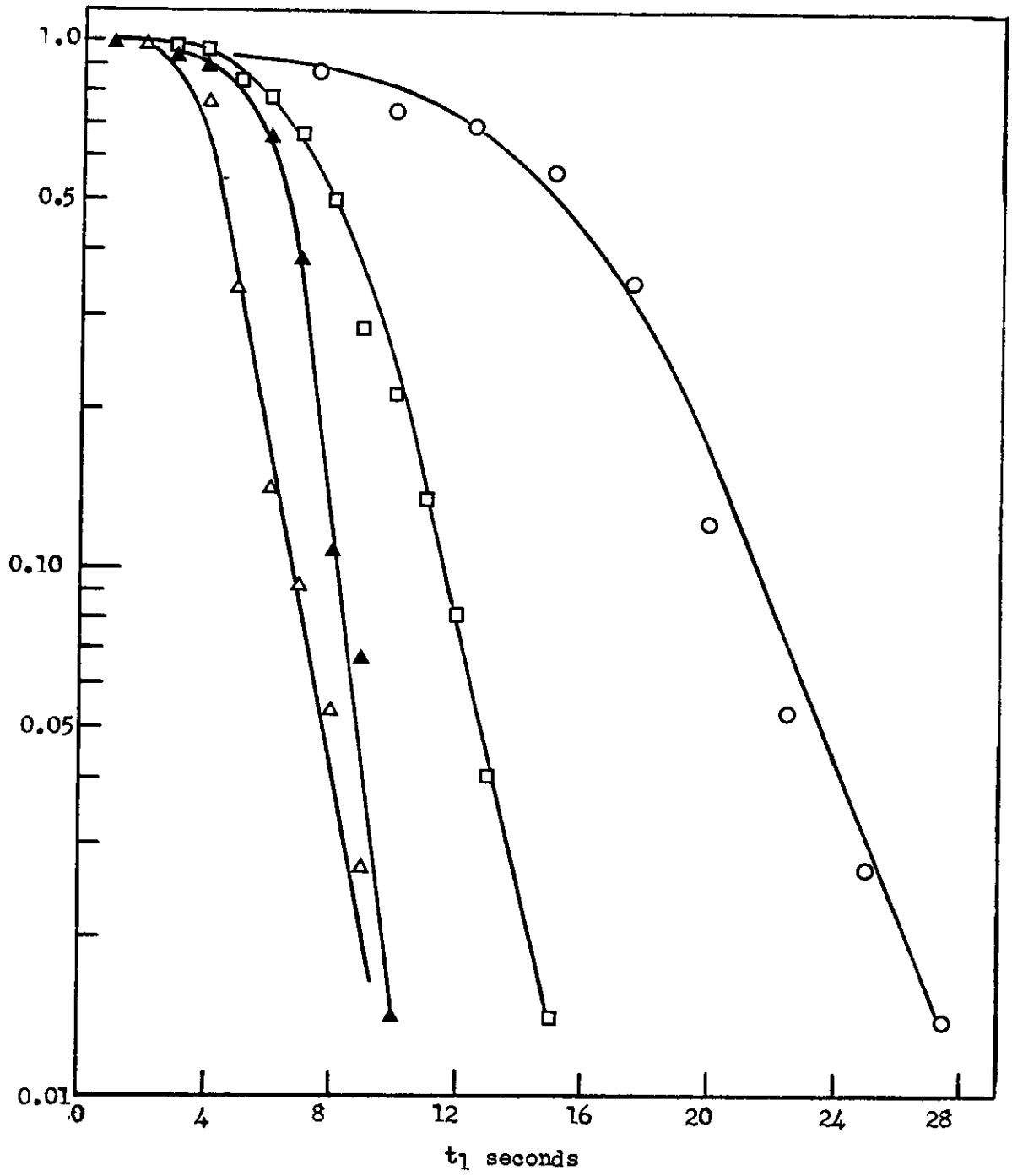

	L cms.	a_1 cms.
△	0	0.416
▲	2.5	0.416
□	5	0.416
○	10.0	0.416

Series A2/2 and A3

Fig. 5.43 Effect of fall height, L, on the first stage coalescence time distribution for system heptane-water

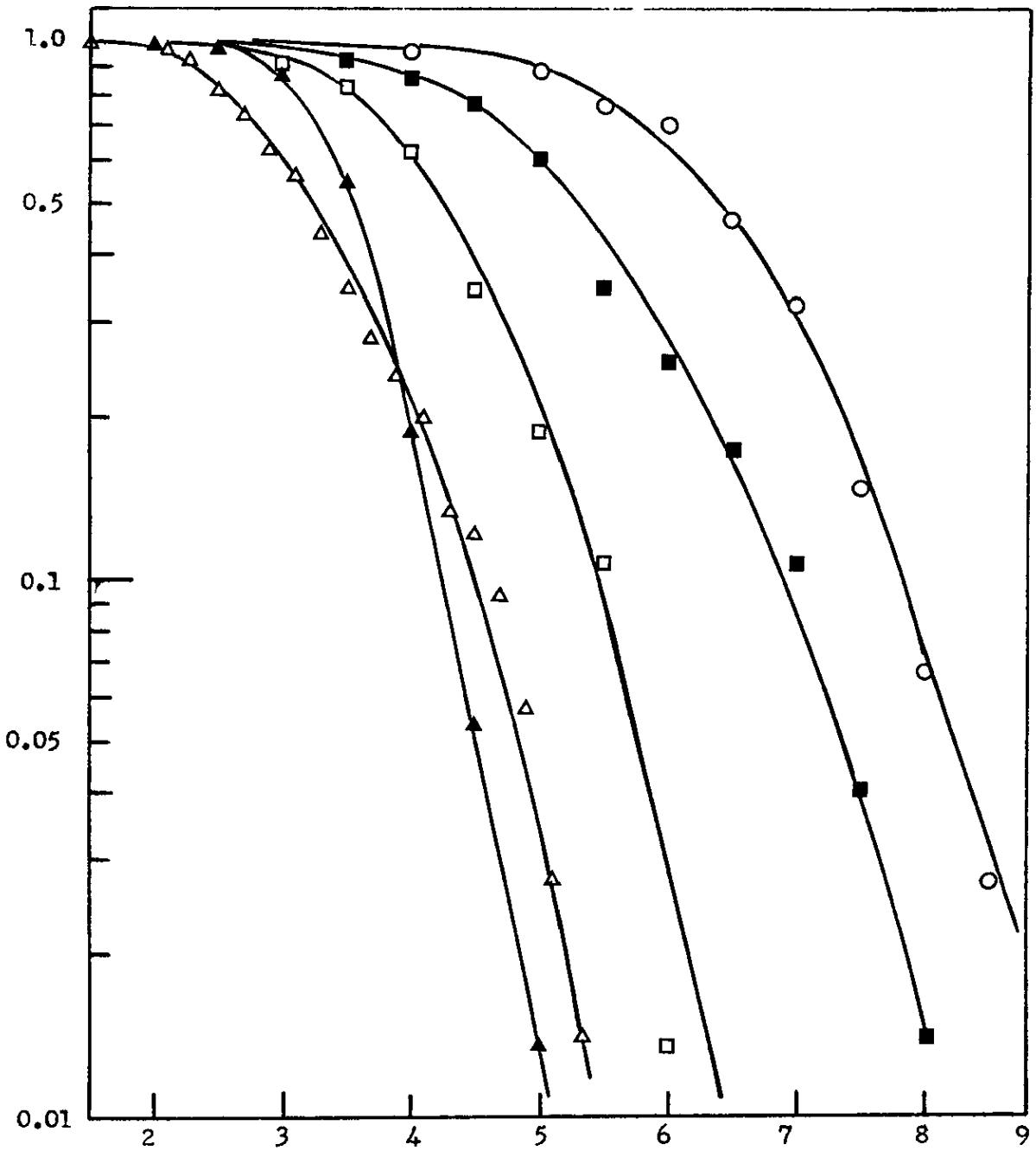

Fig. 5.44 Effect of fall height, L, on the second stage coalescence time distribution for system heptane-water

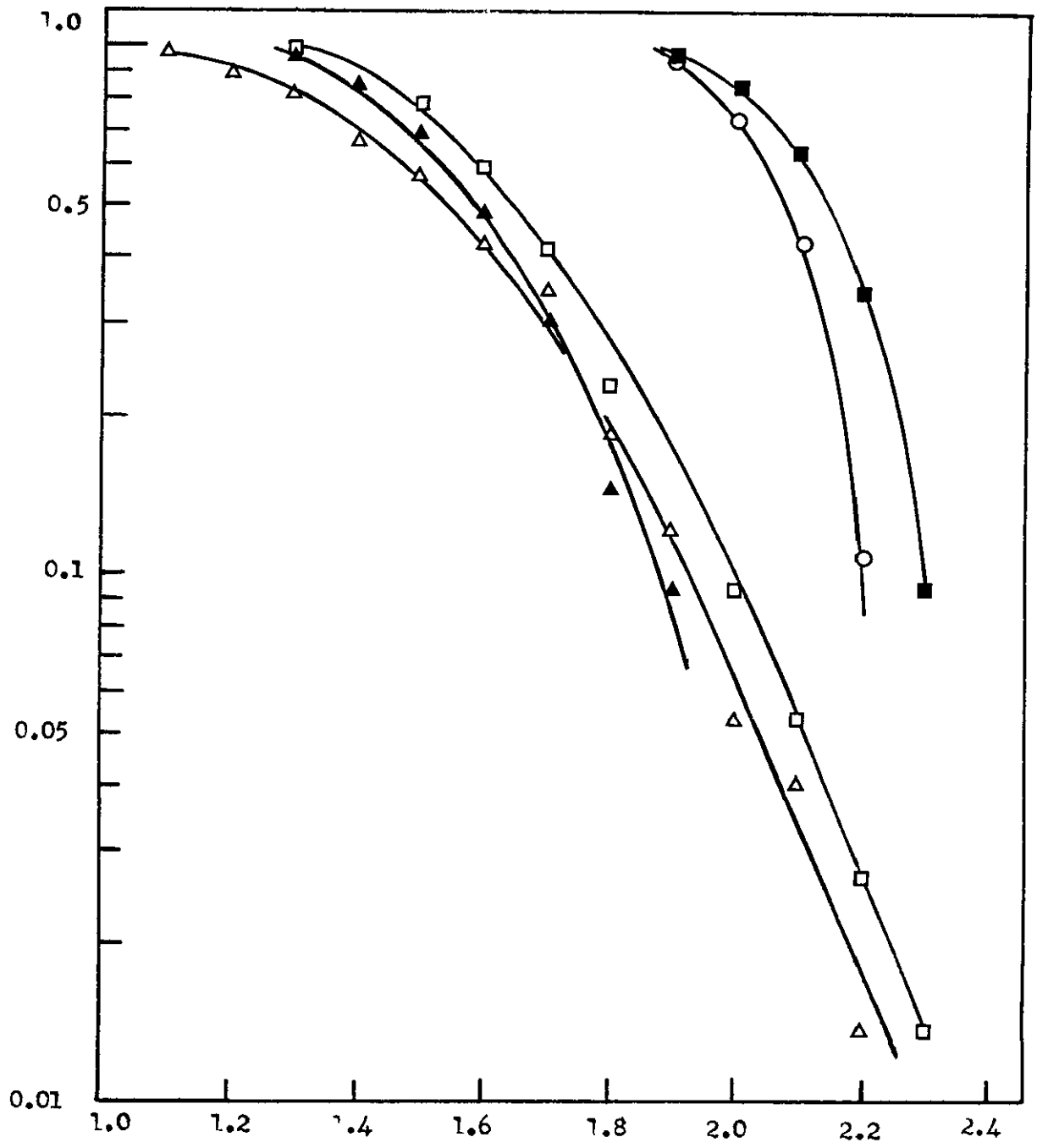

Fig. 5.45 Effect of fall height, L, on the third stage coalescence time distribution for system heptane-water

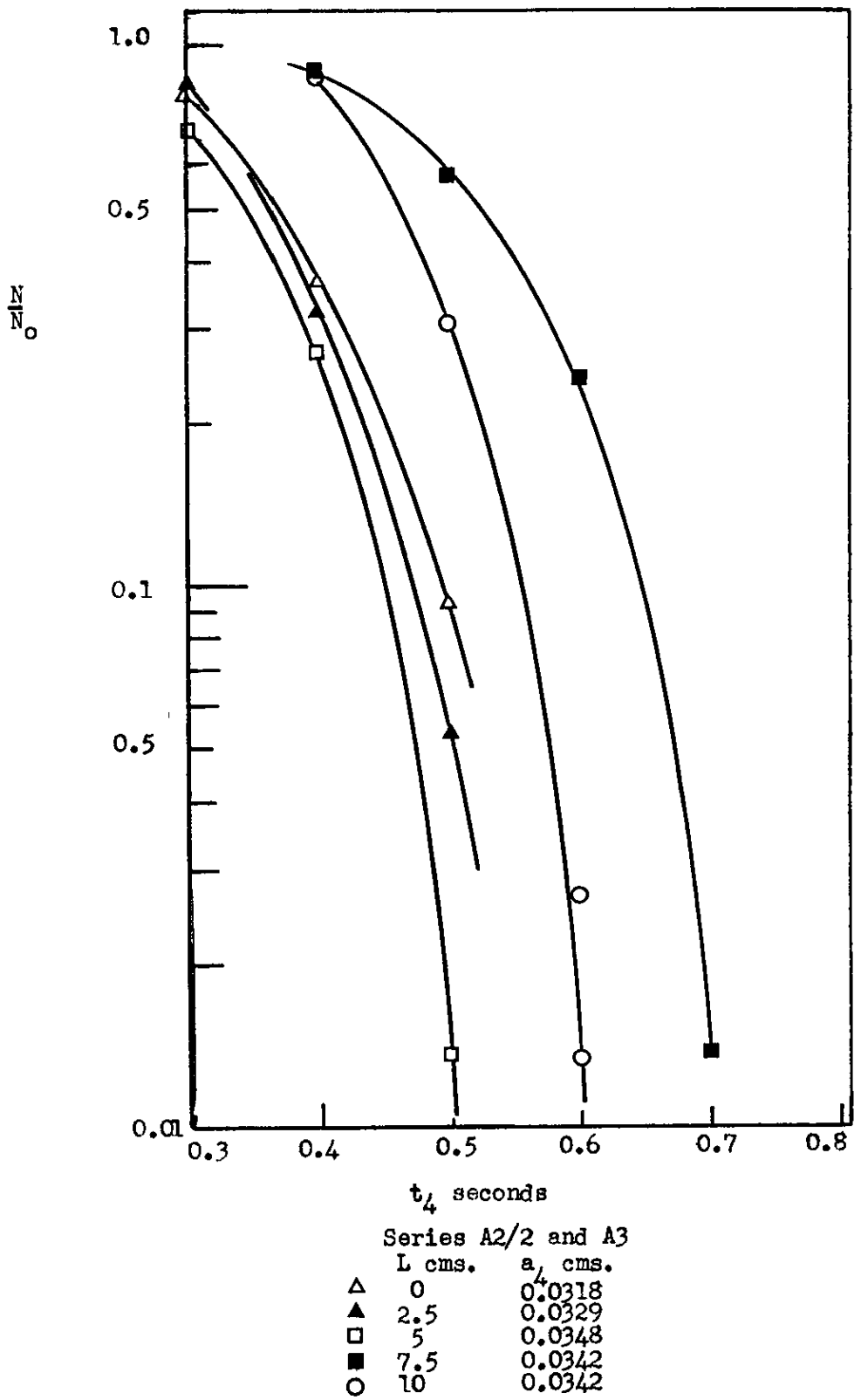

Fig. 5.46 Effect of fall height, L on the fourth stage coalescence time distribution for system heptane-water

CHAPTER 6

INTERPRETATION AND DISCUSSION OF RESULTS

The experimental results presented in Chapter 5 may now be examined.

6.1 Partial Coalescence and Drop Size Ratio

The phenomenon of "double drop" coalescence was observed to occur only in the systems for which redistilled heptane was used (see Appendix 3). It was not observed at all in the Series A1/1 and A1/5 for which undistilled heptane was used, nor in systems C and D. Hawksley (60) has suggested that contamination of the interface is responsible, but the above findings do not suggest this.

The results contained in Appendix 3 suggest that the formation of a "satellite" drop with the secondary drop only occurs when (i) the primary drop, and (ii) the interfacial tension, are sufficiently large. In the case of the two lower interfacial tension systems, C and D (γ = 22.54 and 18.62 dynes cm.$^{-1}$, respectively), a "satellite" drop did not result. However, in the two higher interfacial tension systems, A and B (γ = 50.75 and 32.41 dynes cm.$^{-1}$, respectively) a "satellite" drop was formed in each case when the primary drop size was greater than 0.348 cm. and 0.509 cm., respectively. This latter finding is in agreement with the observations of Charles and Mason (15).

The long rest-time of the "satellite" drop shown in 5.P.1. is almost certainly due to contamination of the interface. However, this did not appear to interfere with the coalescence of the secondary drop, or any other succeeding stages.

The relationship between primary drop size a_1 and the drop diameter ratios r_1, r_2 and r_3 is shown in Figures 5.2 to 5.9. A least squares fit has been carried out for r_1 and r_2 assuming a linear correlation, but it can be seen that this is often unsatisfactory. The linear correlation of r_1 versus a_1 is reasonable, but is less good as L

increases. With the exception of Fig. 5.2B, the straight line correlation is a fair indication of the results for r_2 and r_3. The following features are apparent from a consideration of Figs. 5.2 to 5.9:

For each stage of coalescence the drop size ratio increases as the drop size decreases. This increase is greatest for r_1 and is small for r_3, which is approximately constant and equal to 0.5. In the heptane-water system, larger secondary and tertiary drops are formed as the fall height of the primary drop is increased. The opposite result is found for the 0.5M decanoic acid system. To illustrate the latter point, values of a_2 and a_3 calculated from Figs. 5.2 to 5.9 are given below in Table 6.1.

TABLE 6.1

Effect of Fall Height of the Primary Drop on the Size of Secondary and Tertiary Drops

System	Fall Height L cm.	Drop Size cm. a_1	a_2	a_3
A	0	0.475	0.1496	0.0648
A	2.5	0.475	0.1509	0.0677
A	5	0.475	0.1590	0.0745
C	0	0.350	0.1151	0.0540
C	2.5	0.350	0.1097	0.0511
C	5	0.350	0.1062	0.0468

An explanation of the behaviour depicted in Table 6.1 is that the position of breakup of the liquid column when formed during coalescence, and hence the size of secondary drop, is affected by the disturbances in the interface. These disturbances increase with increased distance of fall of the droplet onto the interface.

Charles and Mason (15) showed that lowering the interfacial tension of the benzene-water system had virtually no effect on the drop size ratio. Since the change in the value of the viscosity between systems A and B, and between the systems C and D, is small, it is valid to calculate the drop size ratio for system B from the results obtained for system A, and similarly

for system D from system C.

6.2 Correlation of Coalescence Rest-Time Distributions

Previous workers have suggested that the distribution of $\hat{t}$, the overall coalescence rest-time, and t_1, the rest-time for the first stage of coalescence, may be correlated by equations which are of the form:

$$\ln \frac{N}{N_o} = -k(t - t_o)^{n_1} \qquad (6.2.1)$$

or

$$\ln \frac{N}{N_o} = -ct^{n_2} \qquad (6.2.2)$$

For both the heptane-water and decanoic acid systems, the distribution of the rest-times for each stage of coalescence can be represented by Eqn. (6.2.1). Examples of the correlation for heptane-water (A2/1) and decanoic acid (C1/5 and C2/1) are given in Figs. 6.1 to 6.3. However, with a sample size containing only 75 drops, it is not possible to select values of t_o and n_1 from a range of connected values of these parameters (see Fig. 6.4). All of the distributions are correlated satisfactorily by Eqn. (6.2.1) with $t_o = 0$, i.e. by Eqn. (6.2.2). An example of the correlation using Eqn. (6.2.2) is given in Fig. 6.5 (C1/5), with n_2 = 1.7, 3.57 and 5.1 for the first, second and third stages of coalescence, respectively. In addition, Table 6.2 lists the values of n_2 in Eqn. 6.2.2) for a number of cases for the Series 2 results. Fig. 6.4 indicates how wide is the range of values of t_o and n_1 which are possible when only 75 results are available. The high values of n_2 which are required to correlate the later stages of coalescence may limit the usefulness of Eqn. (6.2.2). Although the true values of n_1 and t_o in Eqn. (6.2.1) may not be determined with accuracy, it is apparent that n_1 increases with the stage of coalescence. This is also true for n_2 in Eqn. (6.2.2).

The distributions may also be correlated by using arithmetic probability plots and an example is given in Fig. 6.6. Although this test of normality is insensitive (39) and the sample size too small to allow any

firm conclusions to be made,a number of features not immediately discernable in Figs. 6.1 to 6.3 and Fig. 6.5 can be seen. Several distributions are best represented by two straight lines. Usually,the intersection of the lines is at $0.85 < N/N_o < 0.15$,and the one line exists in a region where the accuracy of N/N_o is not high,because of the small sample size on which it is based. However,it may be possible that certain distributions are best represented by the sum of two distributions. It should be mentioned,that if two normal distributions are involved,the two straight lines would infact be replaced by a curve lying near to these lines (see Fig. 6.7). Generally, Eqns. (6.2.1) and (6.2.2) correlate the results better than a normal distribution.

6.3 Properties of Coalescence Time Distributions

Correlation of Mean Coalescence Rest-Times

Firstly,we will discuss the Series 1 results and later extend this to include the Series 2 results.

The mean coalescence rest-times of the secondary and tertiary droplets are given in Figs. 5.16 at three decanoic acid concentrations as a function of the primary drop size,a_1. It can be seen,that within the accuracy of the results,the relationship is linear for the third stage at the three concentrations investigated,and also for the second stage at the two highest concentrations employed. The resultant curves for 0.5M and 1.0M solutions coincide for both the second and third stages of coalescence, whilst the third stage of of coalescence with a 0.05Msolution shows lower coalescence rest-times than do the curves for the 0.5M and 1.0M solutions. The resultsfor the third stage of coalescence,with a 0.05M solution,suggests a minimum corresponding to a_1 = 0.16 cm.,approximately. The graphs obtained for the first stage of coalescence (Fig. 5.17) are less well defined,but with both the 0.5M and 1.0M solutions the mean coalescence rest-time increases as the droplet size increases. With the 0.05M solution a minimumis again suggested at a drop size similar to that at which the minimum in the third

stage occurred. The curves obtained for the heptane-water system are given in Fig. 5.18, and for comparison Fig. 5.16 is superimposed. In this case, the curves for all stages indicate a minimum corresponding to a primary drop size a_1 = 0.18 cm., approximately.

TABLE 6.2

Values of n_2 in the Equation

$$\ln \frac{N}{N_o} = - ct^{n_2}$$

Study No.	a_1 cm.	n_2 1st Stage	2nd Stage	3rd Stage	4th Stage
A2/1	0.325	0.635	2 sections	3.83	6.78
A2/2	0.416	0.396	0.597	2.58	6.31
A2/3	0.505	0.228	0.252	1.73	4.04
B2/1	0.224	2 sections	0.1442	4.580	15.50
B2/2	0.326	0.0635	0.0915	4.000	6.40
B2/3	0.433	0.0830	0.2000	0.471	5.93
C2/1	0.208	0.109	0.293	1.880	7.98
C2/2	0.324	0.241	0.370	2.130	4.93
C2/3	0.387	0.122	0.421	1.108	10.10
D2/1	0.204	0.2490	0.440	1.341	12.35
D2/2	0.299	0.0560	0.216	2.000	5.35
D2/3	0.385	0.0498	0.214	0.955	5.35

The Series 2 results cover a wider range of drop size and also serve to explain some of the features associated with the Series 1 results. Within the accuracy of the results, the heptane-water system exhibits a linear relationship between the mean rest-time and drop size. This is shown in Fig. 5.39 for each of the four stages of coalescence. However, for the first stage coalescence, the primary drop becomes less stable at a value of approximately a_1 = 0.5 cm. The results given in Fig. 5.39 suggest that the minimum condition shown in Fig. 5.18 does not exist. Figs. 5.40 to 5.42 show the relationship between the mean rest-time and the drop size for each stage of coalescence in the system 1.0M decanoic acid. For each stage there is a firm trend for the mean rest-time to increase with increase in size of drop. Similar trends were exhibited by the 0.05M and 0.5M systems.

but they were not so well defined. The results for the 0.05M system suggest that the minimum condition encountered in the Series 1 results does not exist. A cautionary note is necessary when stressing the latter remark because "high" and "low" rest-time results (i.e. results which deviate from the normal trend) have been reported to occur by other workers (16,60). Both "high" and "low" results could give rise to a minimum condition in the drop size vs. mean rest-time relationship.

An interesting comparison can be made between the results shown in Fig. 5.39 and the results for the same system, heptane-water, presented by Allan and Mason (1). The values of t_{m1} in Allan and Mason's Fig.3 agree closely with those presented in Fig.5.39. The overall trend of the author's results, and this applies to the other systems B,C and D, is described by the series:

$$t_{m1} > t_{m2} > t_{m3} > t_{m4}$$

However, Allan and Mason's results describe the series:

$$t_{m1} < t_{m2} > t_{m3}$$, and also, their result at $a_1 = 0.29$ cm. yields:

$$t_{m1} < t_{m2} < t_{m3} .$$

A comparison of the results for the second and third stage coalescence reveals two important differences:

(i) Allan and Mason's values for t_{m2} and t_{m3} are much greater than those in Fig. 5.39.

(ii) Allan and Mason's results for t_{m2} and t_{m3} lie on a single curve, whereas those in Fig. 5.39 fall on separate curves.

The first finding suggests that the system used by Allan and Mason may have been contaminated, probably by a surfactant material.

Standard Deviation of Coalescence Rest-Time Distributions

For all the rest-time distributions obtained in this work, it was found that the standard deviation of adjacent stages mutually increased.

An example, for each coalescence stage for the 1.0% decanoic acid system, is presented in Fig. 6.8. It is seen that the relationships between the standard deviation of the first and second stage, the second and third stage, and the third and fourth stage, are linear. In the other systems A, B and C the relationships were also linear, but not so well defined as for system D.

The relationship between the standard deviation of adjacent partial coalescence stages may be defined as follows:

$$\sigma_{n+1} = \phi_{n+1/n} \cdot \sigma_n$$

where σ_n = standard deviation of the nth stage.

σ_{n+1} = standard deviation of the (n + 1)th stage.

$\phi_{n+1/n}$ = slope of the relationship between σ_n and σ_{n+1}.

Values of $\phi_{n+1/n}$ are given in Table 6.3 for the systems A, B, C and D (including the Series 1, 2 and 3 results).

TABLE 6.3

Relationship between the Standard Deviation of Adjacent Coalescence Stages

$$\sigma_{n+1} = \phi_{n+1/n} \cdot \sigma_n$$

System	ϕ_{21}	ϕ_{32}	ϕ_{43}
A	0.455	0.193	0.371
B	0.259	0.175	0.275
C	0.298	0.188	0.220
D	0.483	0.213	0.220

These findings, together with Fig. 5.16, suggest that with the system heptane-water and the system decanoic acid-heptane-water, there is a simple relationship between the size of drop before the coalescence and the size of drop which is subsequently produced by the coalescence.

Effect of Distance of Fall

The distributions for the heptane-water system in Fig. 5.43 show that the rest-time t_1 increases with increase in fall height L,of the primary drop. Furthermore,the corresponding rest-times of the second,third and fourth stages of coalescence (Figs. 5.44 to 5.46) also increase. The result concerning the first stage rest-time is in agreement with the findings of Jeffreys and Hawksley (67) and Lawson (81). It has recently been reported by Lawson (82) that little if any effect of fall height is transmitted beyond the first stage. This led Lawson to postulate that the effect of distance of fall on coalescence is merely a calibration of the experimental apparatus in which the study is conducted. In attempting to establish this hypothesis,he carried out observations of the periodic motion of the interface caused by a falling drop disturbance. If the total period of oscillation was subtracted from the measured mean rest-time,it was found that the difference was approximately constant. This was so for all the fall heights investigated.

The method adopted by Lawson to observe oscillations at the interface is one which is very liable to error. As Lawson frankly points out,"There is the possibility of error in measurement not only amongst different workers but even,also with the same observer"! The small oscillations occurring at the interface during the later stages of coalescence may not have been perceptible to the naked eye. It is extemely unlikely that these disturbances would have no effect on these later stages. Also the coalescence of the primary drop will create a disturbance sufficient to influence the secondary,and possibly succeeding drops.

The trends exhibited in Figs. 5.43 to 5.46 can be seen more clearly if the mean rest-time for each stage is plotted against the fall height as shown in Fig. 6.9. Whilst the results for the fourth stage of coalescence are a little scattered,the fall height effect for the coalescence stages is clearly defined.

The way in which the standard deviation of the coalescence rest-time distribution is affected by the fall height is shown in Table 6.4. It is interesting to observe that there is a considerable reduction in the percentage standard deviation for the first, second and third stages of coalescence, when the drop is released some distance from the interface (i.e. at L = 2.5, 5.0, 7.5 and 10.0 cm.). The reduction in the % standard deviation is most probably caused by the contribution of the periodic motion of the interface to the drop rest-time.

TABLE 6.4

Effect of Fall Height of the Primary Drop on the Standard Deviation of the Coalescence Rest-Time Distribution

Study	L cm.	% S.D. of 1st Stage	% S.D. of 2nd Stage	% S.D. of 3rd Stage	% S.D. of 4th Stage
A2/2	0	61.7	37.8	21.5	-
A3/1	2.5	29.7	15.9	12.3	25.8
A3/2	5	35.0	19.3	14.5	26.6
A3/3	7.5	*	21.6	6.22	21.4
A3/4	10	41.5	18.5	5.63	16.0

* Suspect Result

6.4 The Effect of Interface Age on Coalescence Rest-Time

The results in Table 5.1 for the heptane-water system and decanoic acid system do not reveal the same trends as were observed by Hodgson (63). The latter author found, that for water drops in purified systems, the rest-time for all coalescence stages was virtually instantaneous after cleaning the interface by the Teflon-Glass method. There is absolutely no indication of this behaviour in Table 5.1. This may suggest that Hodgson's results are of questionable value.

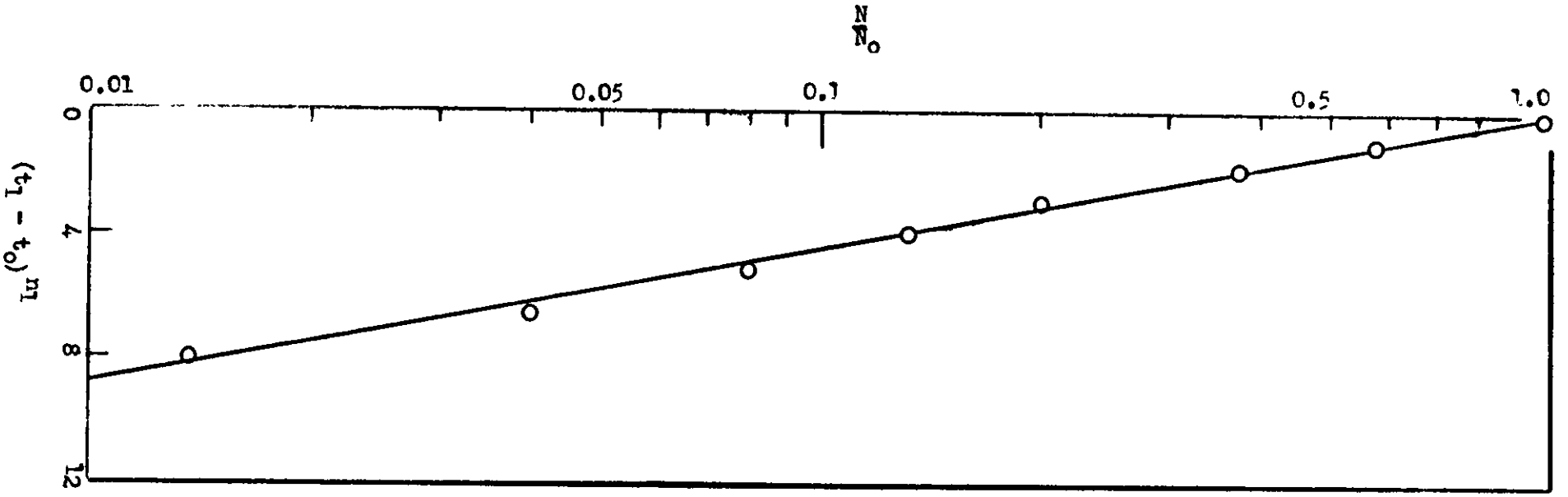

Drop size a_1 = 0.325 cms.
n = 1.5
t_o = 1.5 secs.

Series A2/1

Fig. 6.1A Correlation of first stage coalescence time distribution using Eqn. (6.2.1)

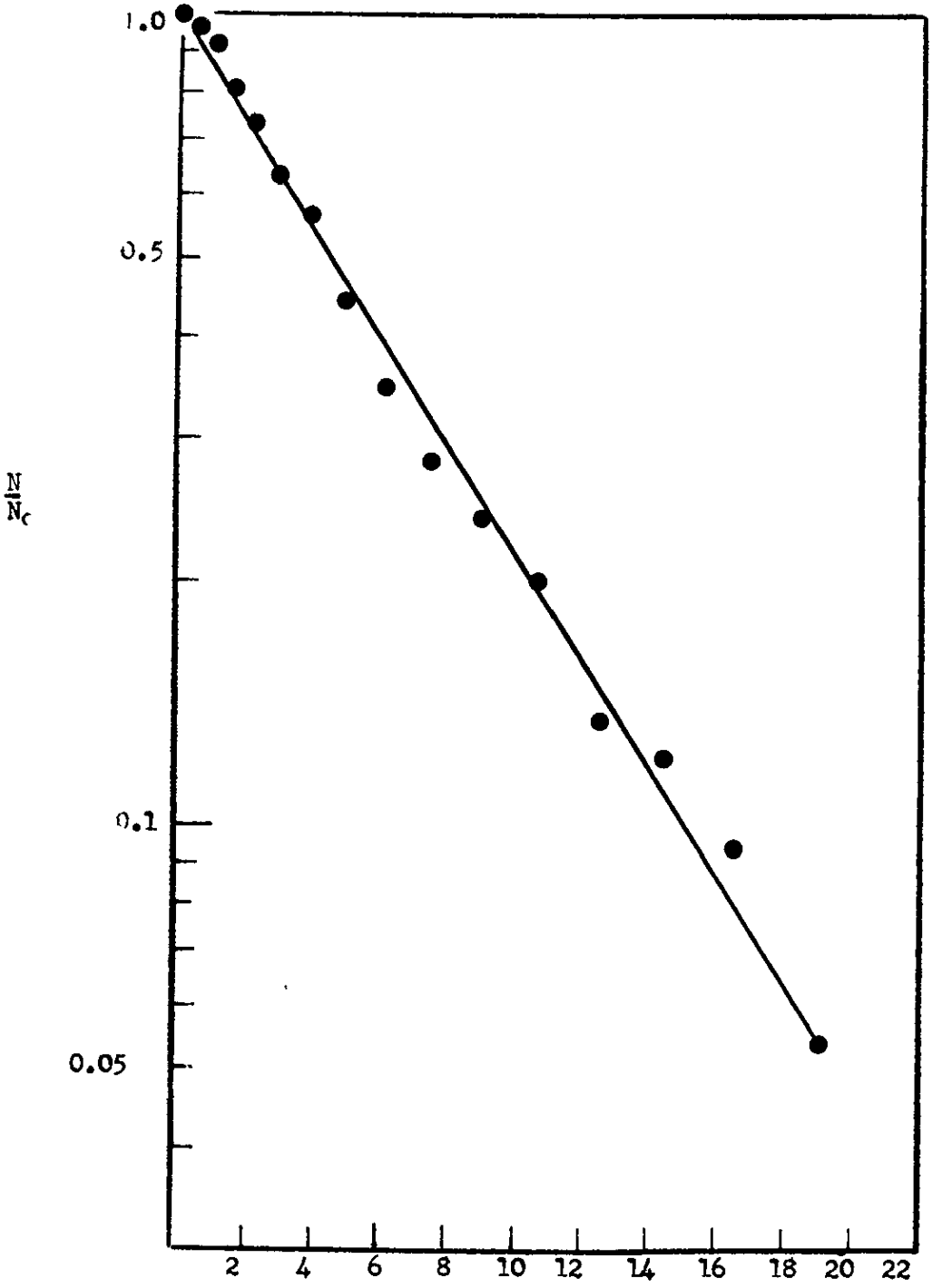

Fig. 6.1B Correlation of second stage coalescence time distribution using Eqn. (6.2.1)

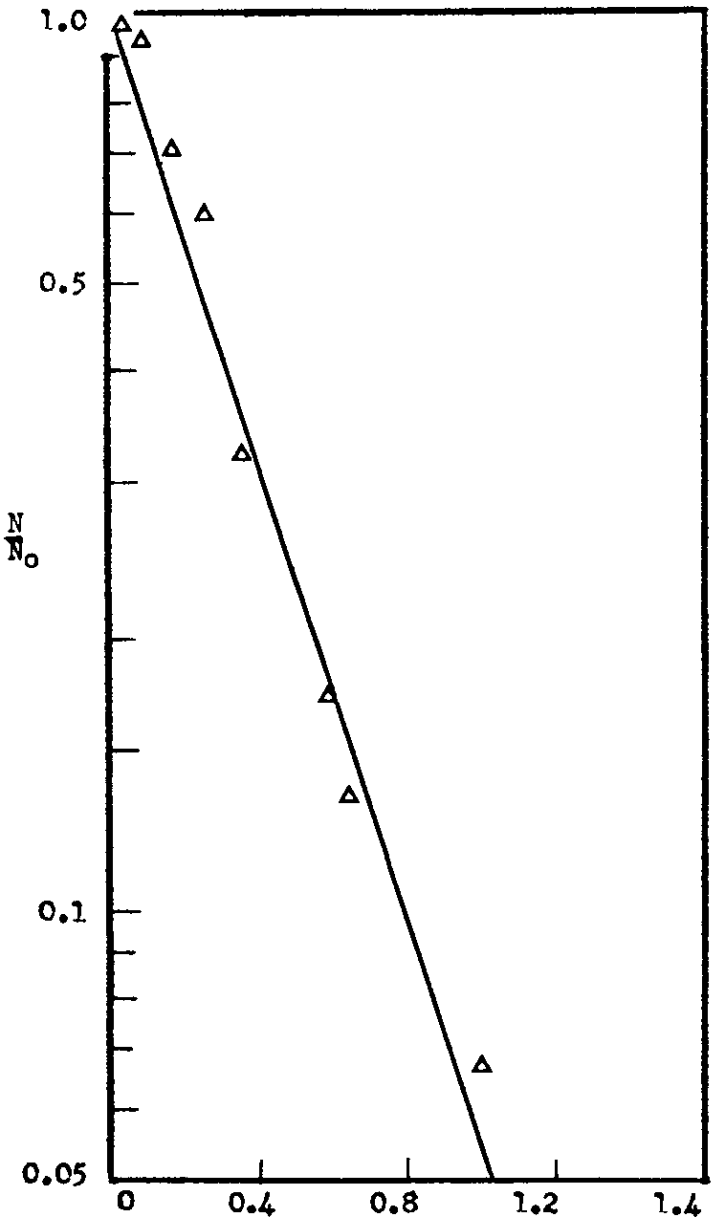

Series A2/1

Drop size a_3 = 0.0573 cms.
n = 1.5
t_o = 0.5 secs.

Fig. 6.1C Correlation of third stage coalescence time distribution using Eqn. (6.2.1)

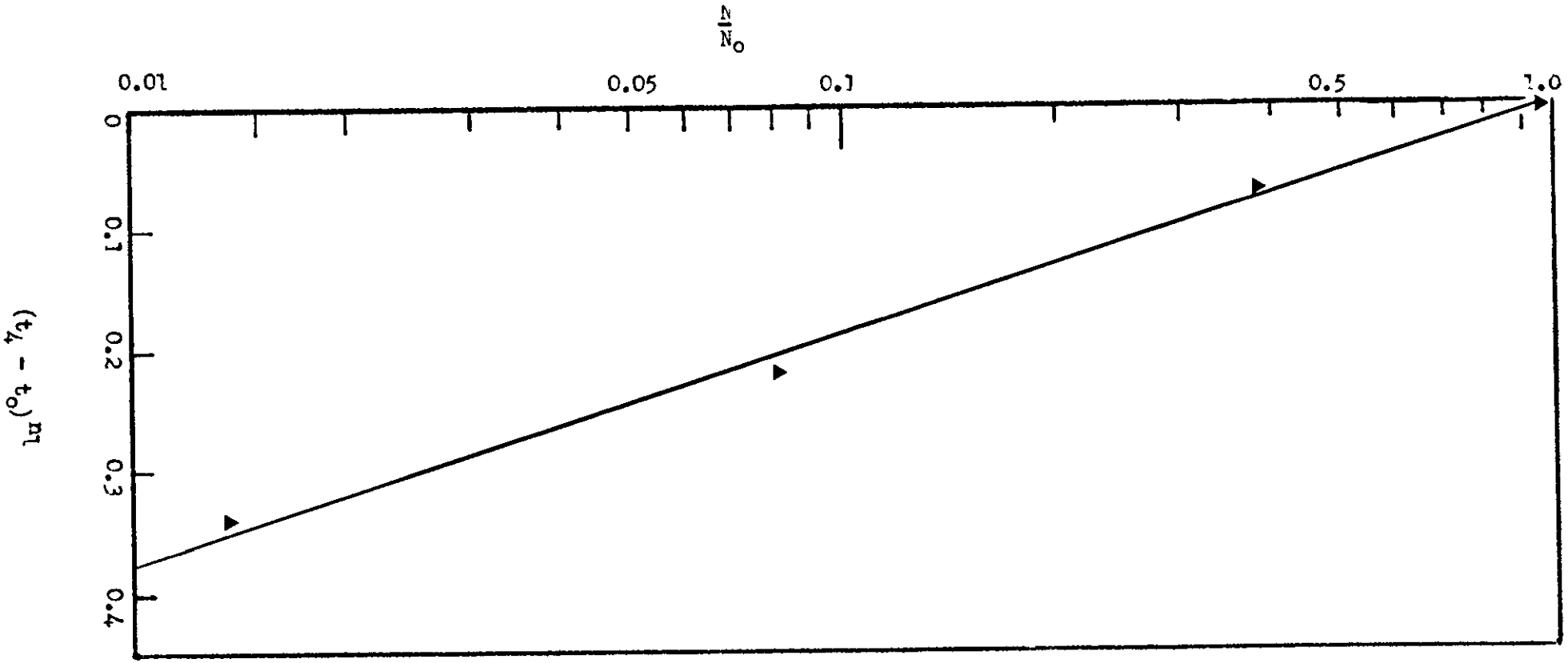

Series A2/1

Drop Size a_4 = 0.0287 cms.
n = 1.0
t_o = 0.18 secs.

Fig. 6.1D Correlation of fourth stage coalescence time distribution using Eqn. (6.2.1)

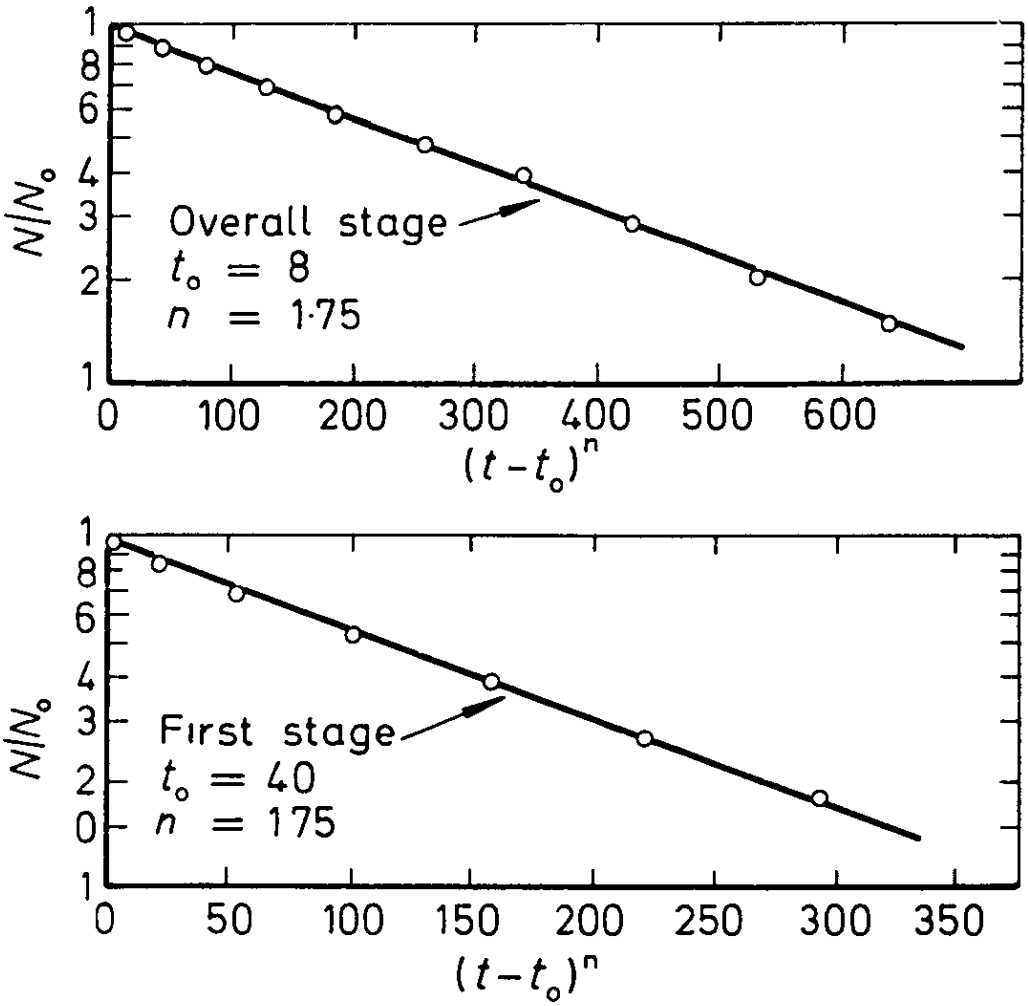

Series C1/5 Drop Size a_1 = 0.382 cms.

Fig. 6.2A Correlation of coalescence time distribution using Eqn. (6.2.1)

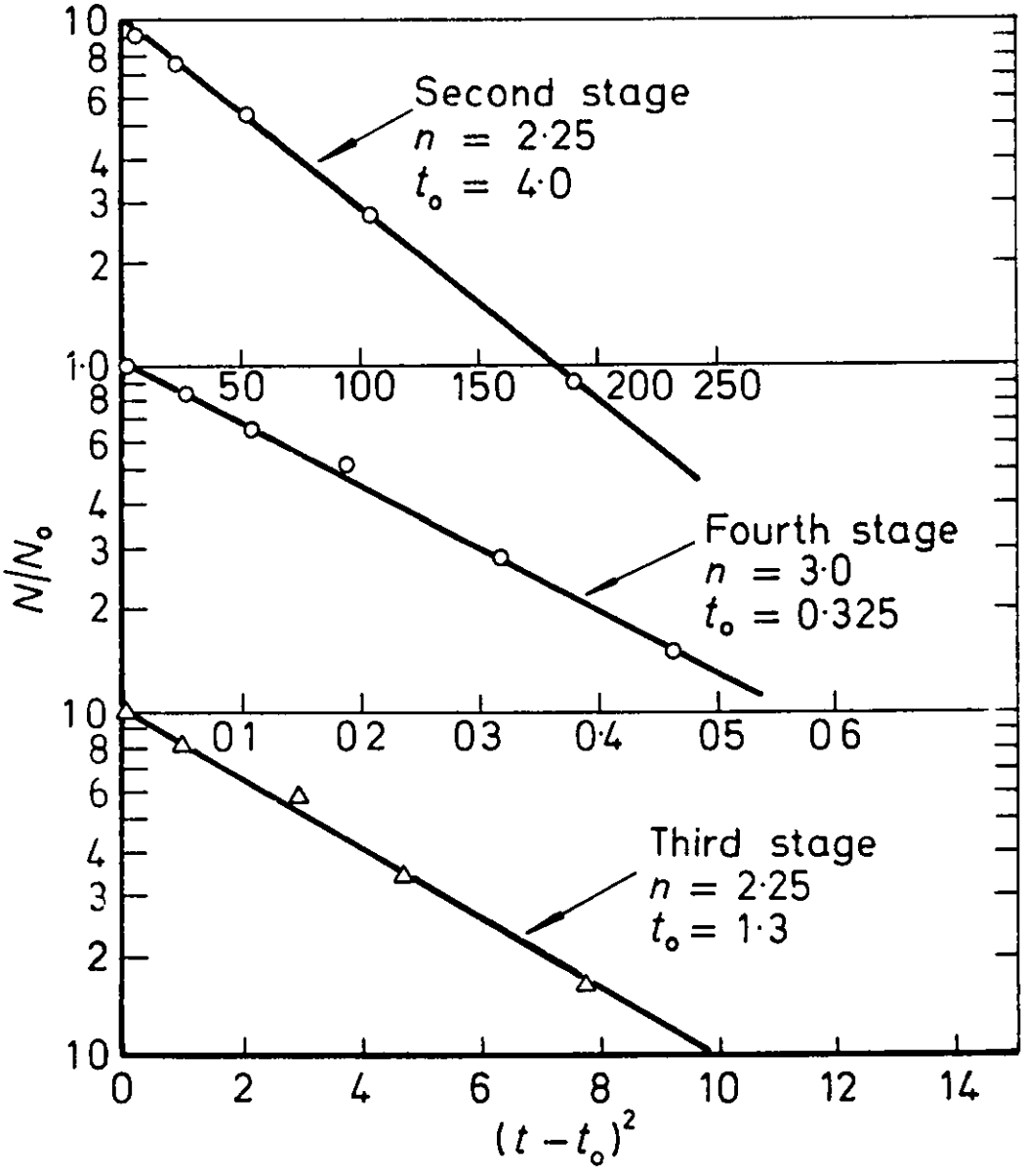

Series C1/5 Drop size a_1 = 0.382 cms.

Fig. 6.2.B Correlation of coalescence time distribution using Eqn. (6.2.1)

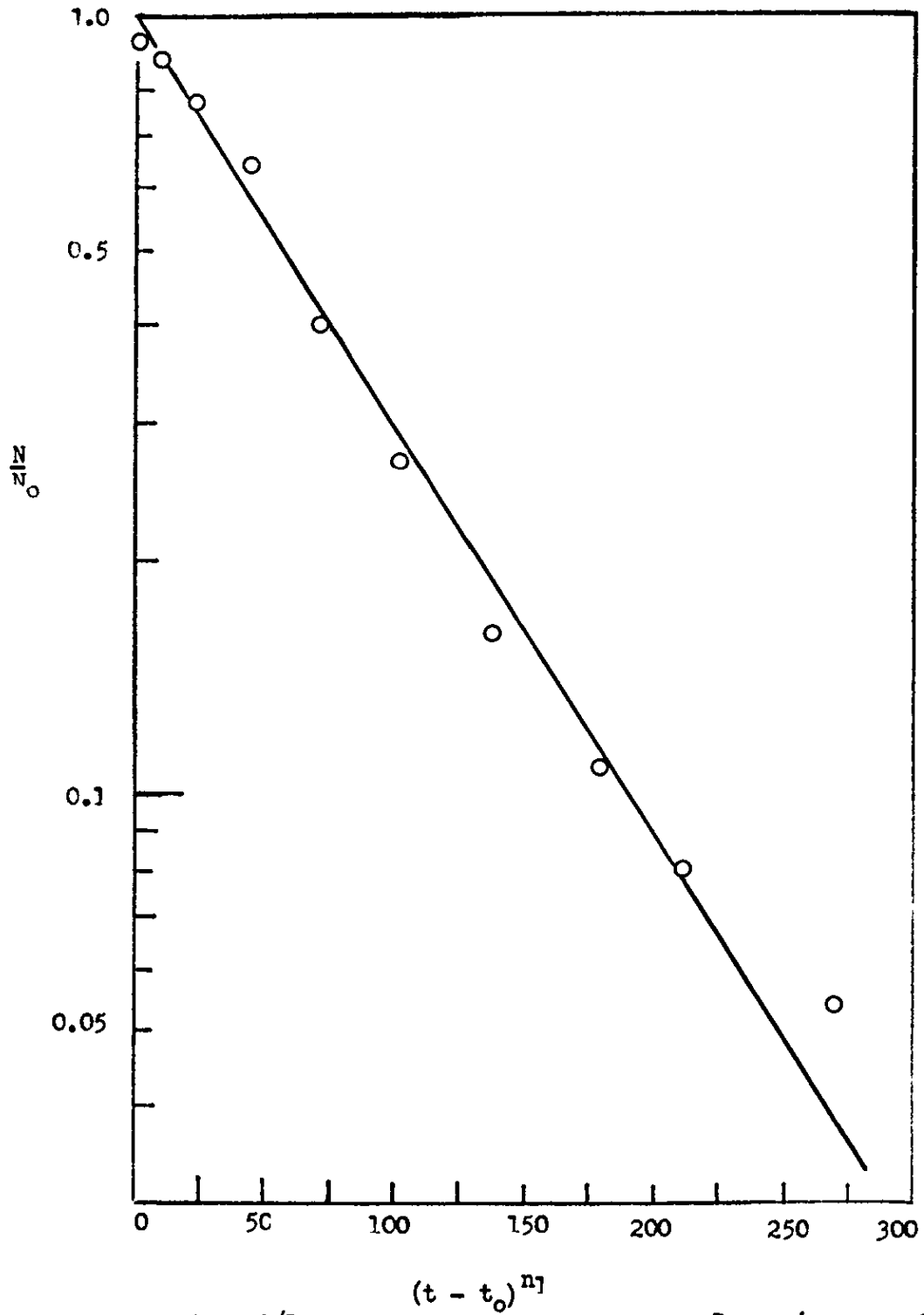

Series C2/1

Drop size a_1 = 0.208 cms.
n = 1.76
t_o = 4.0 secs.

Fig. 6.3A Correlation of first stage coalescence time distribution using Eqn. (6.2.1)

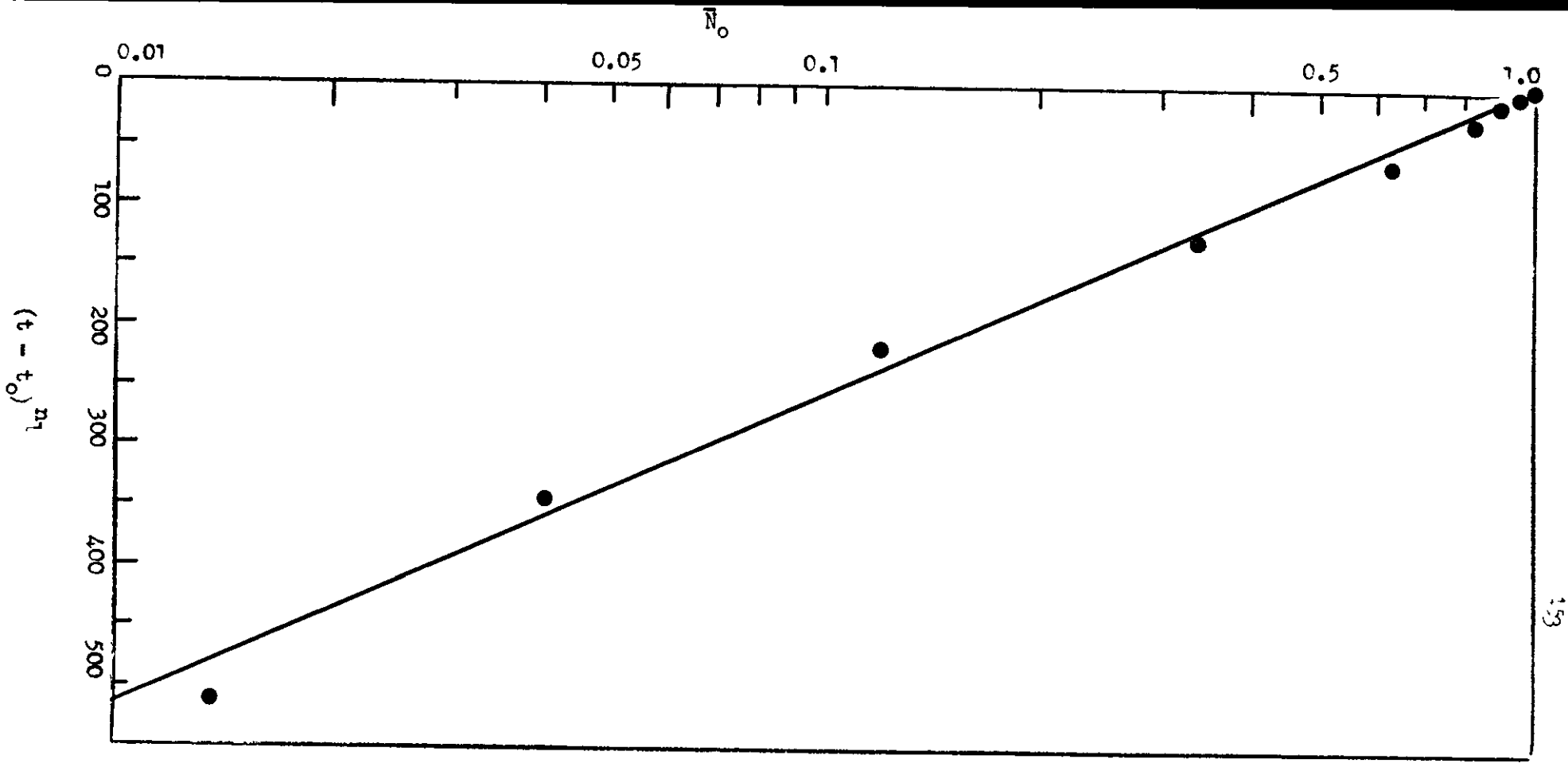

Series C2/1

Drop size a_2 = 0.0843 cms.
n = 3.0
t_o = 2.0 secs.

Fig. 6.3B Correlation of second stage coalescence time distribution using Eqn. (6.2.1)

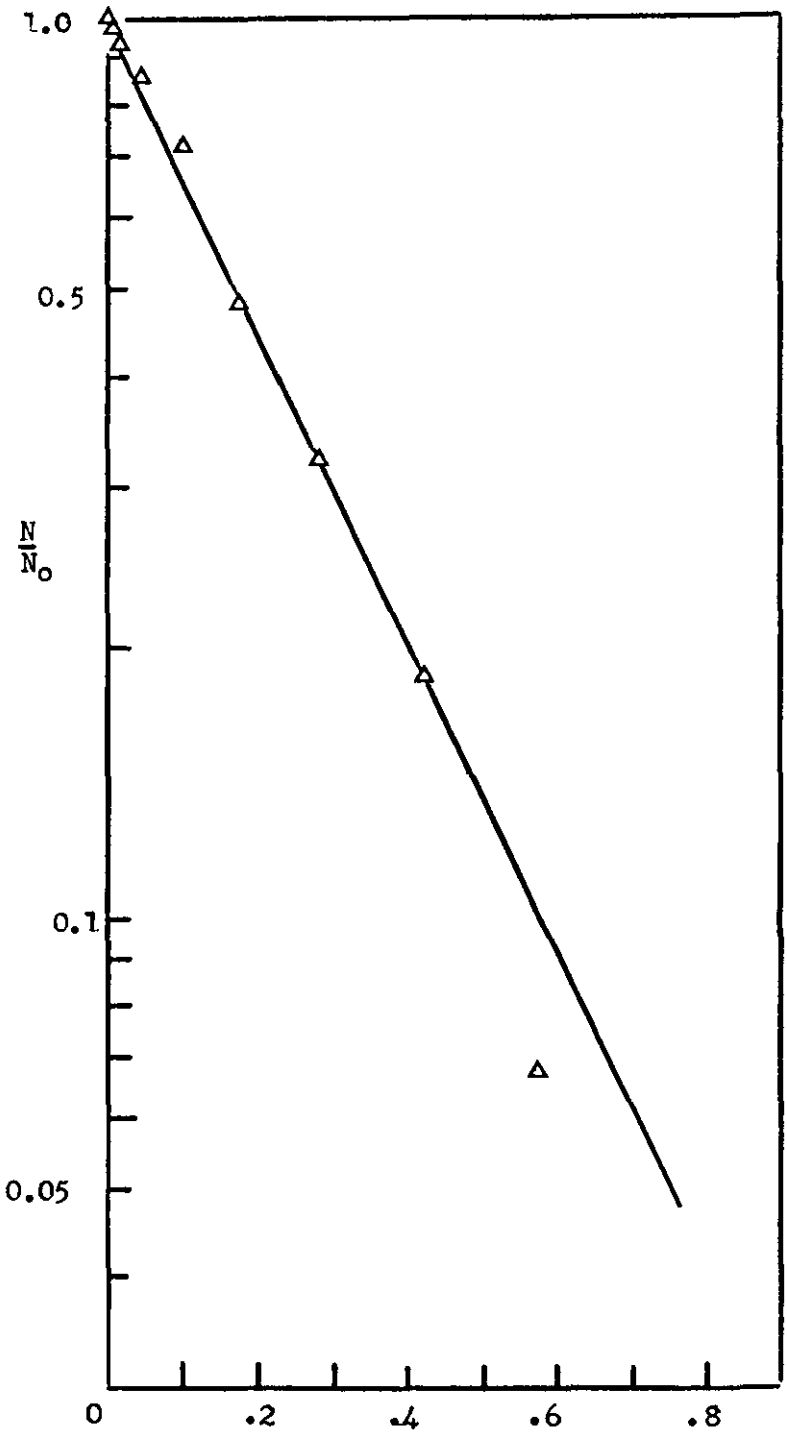

Series C2/1 $(t - t_o)^{n_1}$ Drop size a_3 = 0.0408 cms.
n = 3.0
t_o = 1.3 secs.

Fig. 6.3C Correlation of third stage coalescence time distribution using Eqn. (6.2.1)

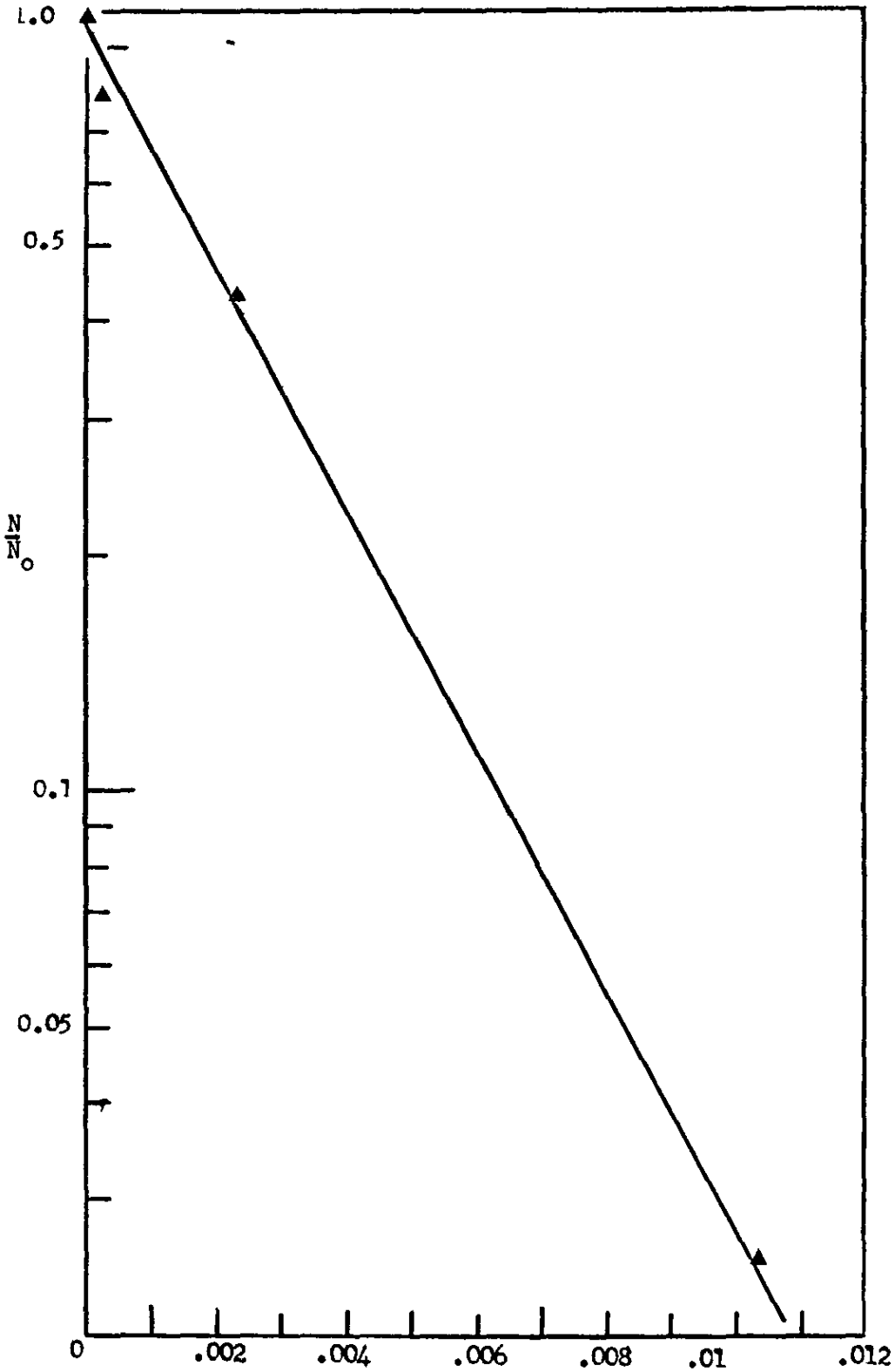

Series C2/1

Drop size a_4 = 0.0204 cms.
n = 4.0
t_o = 0.18 secs.

Fig. 6.3D Correlation of fourth stage coalescence time distribution using Eqn. (6.2.1)

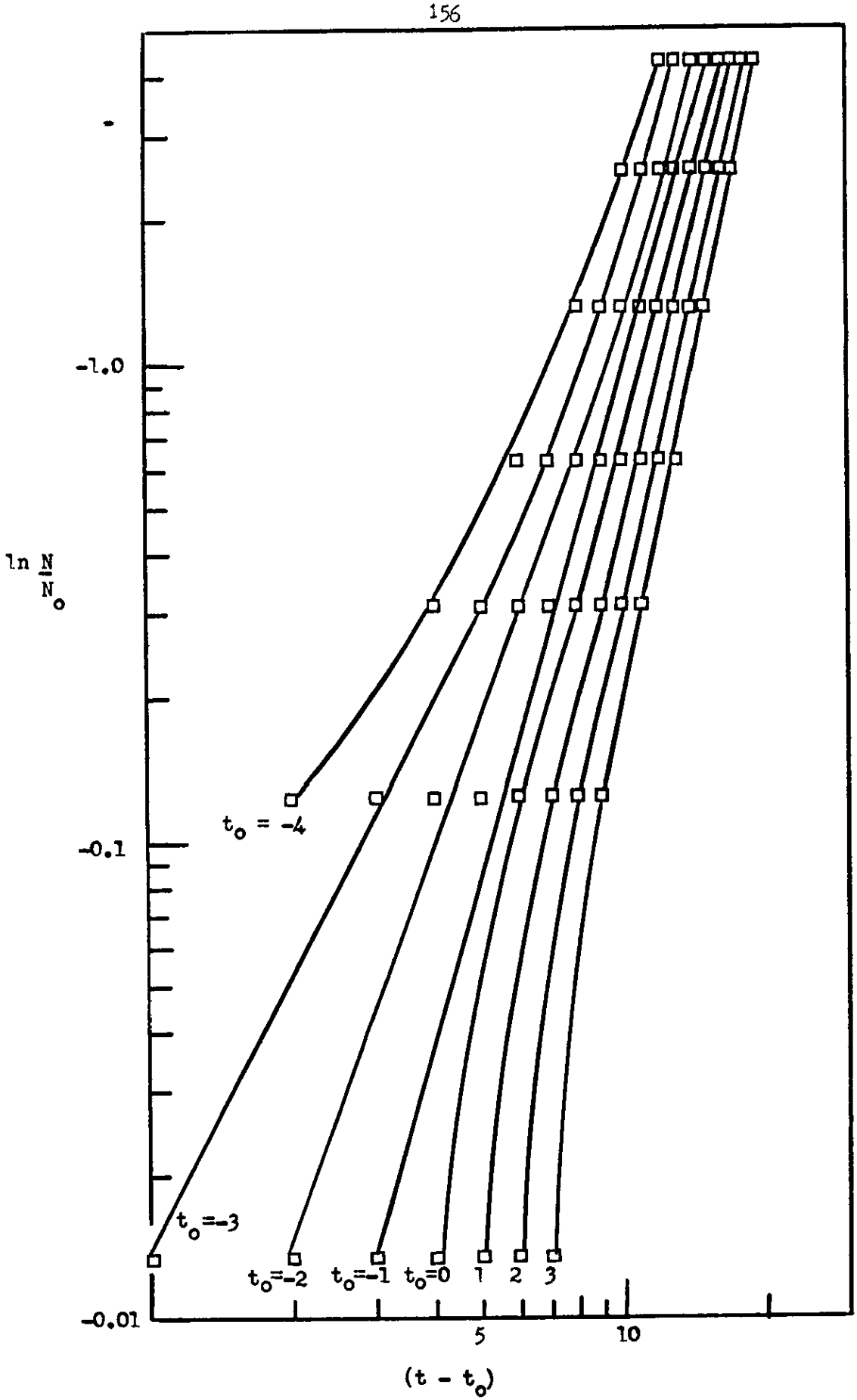

Series C1/5

a_1 = 0.382 cms.

Second Stage Coalescence

Fig. 6.4 Test of fit to Eqn. $\ln \frac{N}{N_o} = -k(t - t_o)^{n_1}$

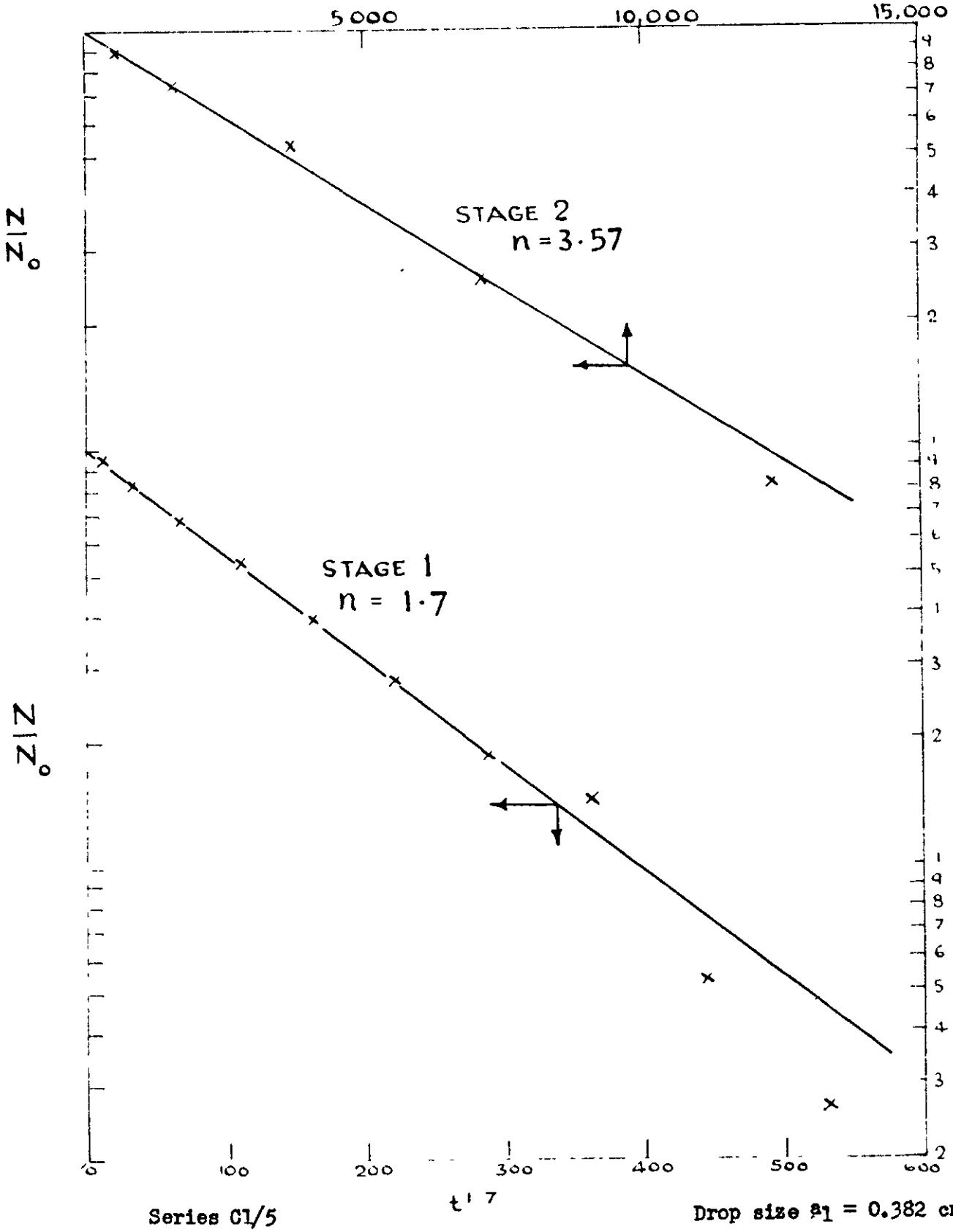

Fig. 6.5A Correlation of first and second stage coalescence time distributions using Eqn. (6.2.2)

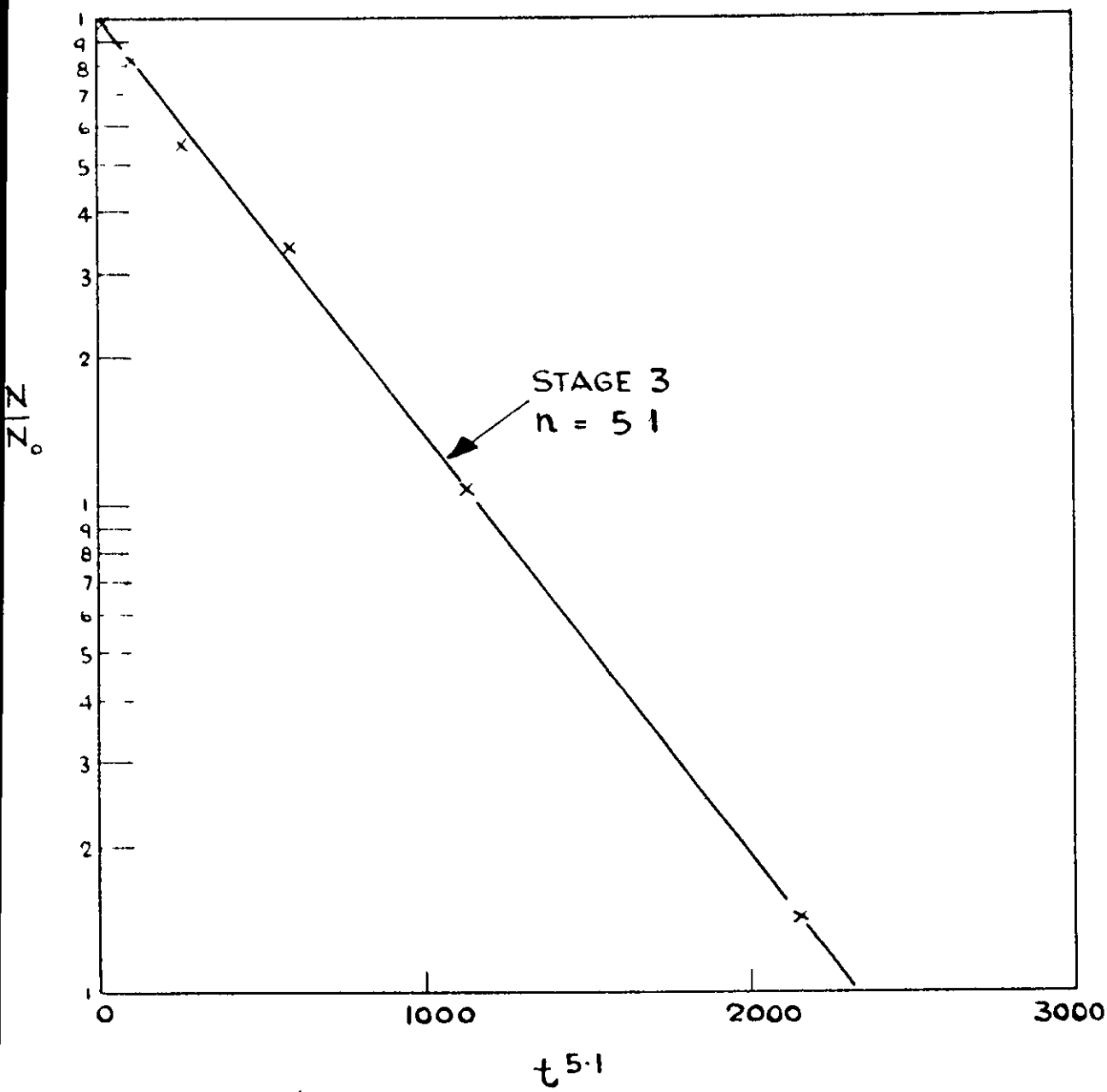

Series C1/5

Drop size a_1 = 0.382 cms.

Fig. 6.5B Correlation of third stage coalescence time distribution using Eqn. (6.2.2)

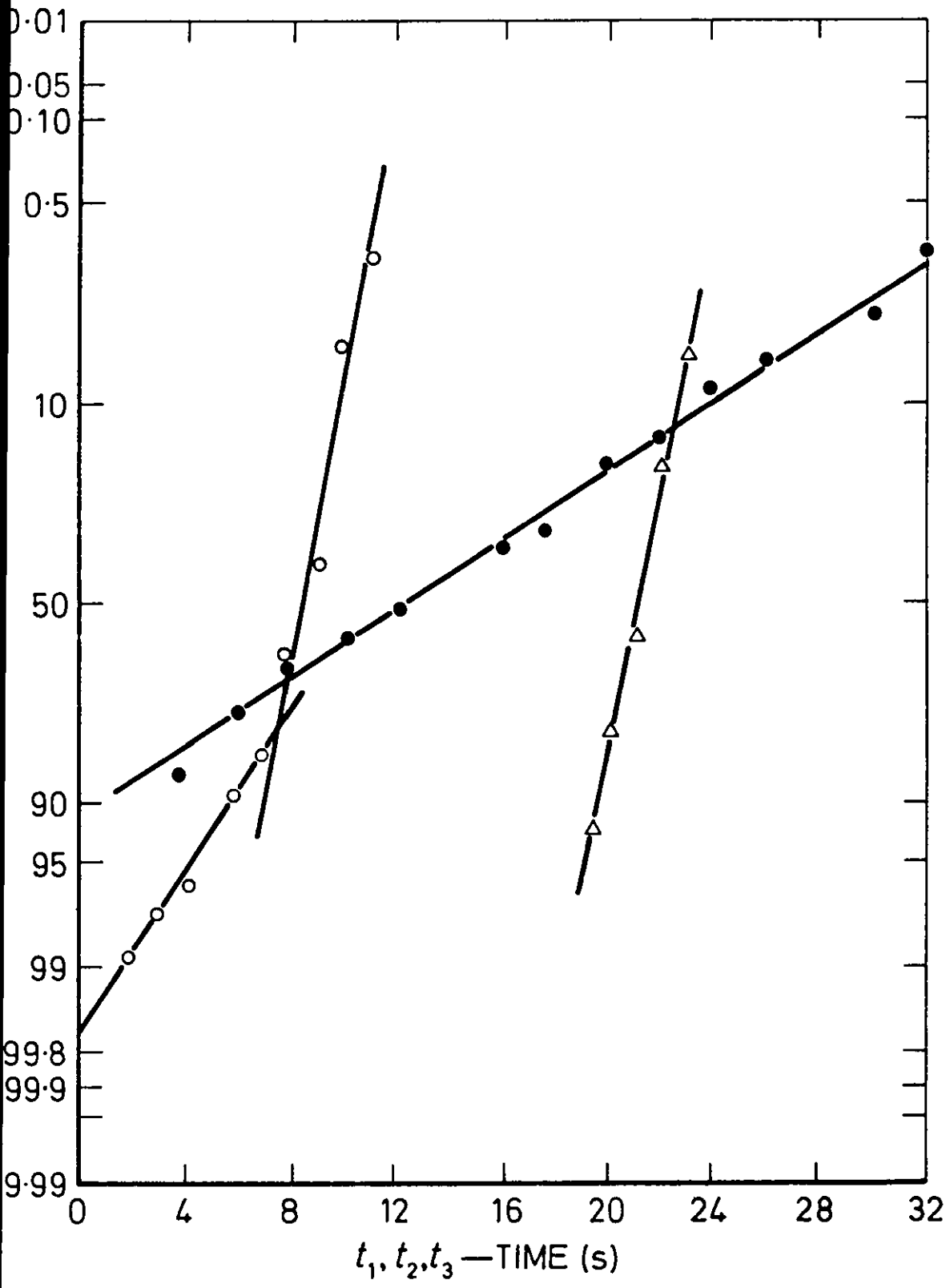

Fig. 6.6 Correlation of coalescence time distributions for the system heptane-water using probability paper

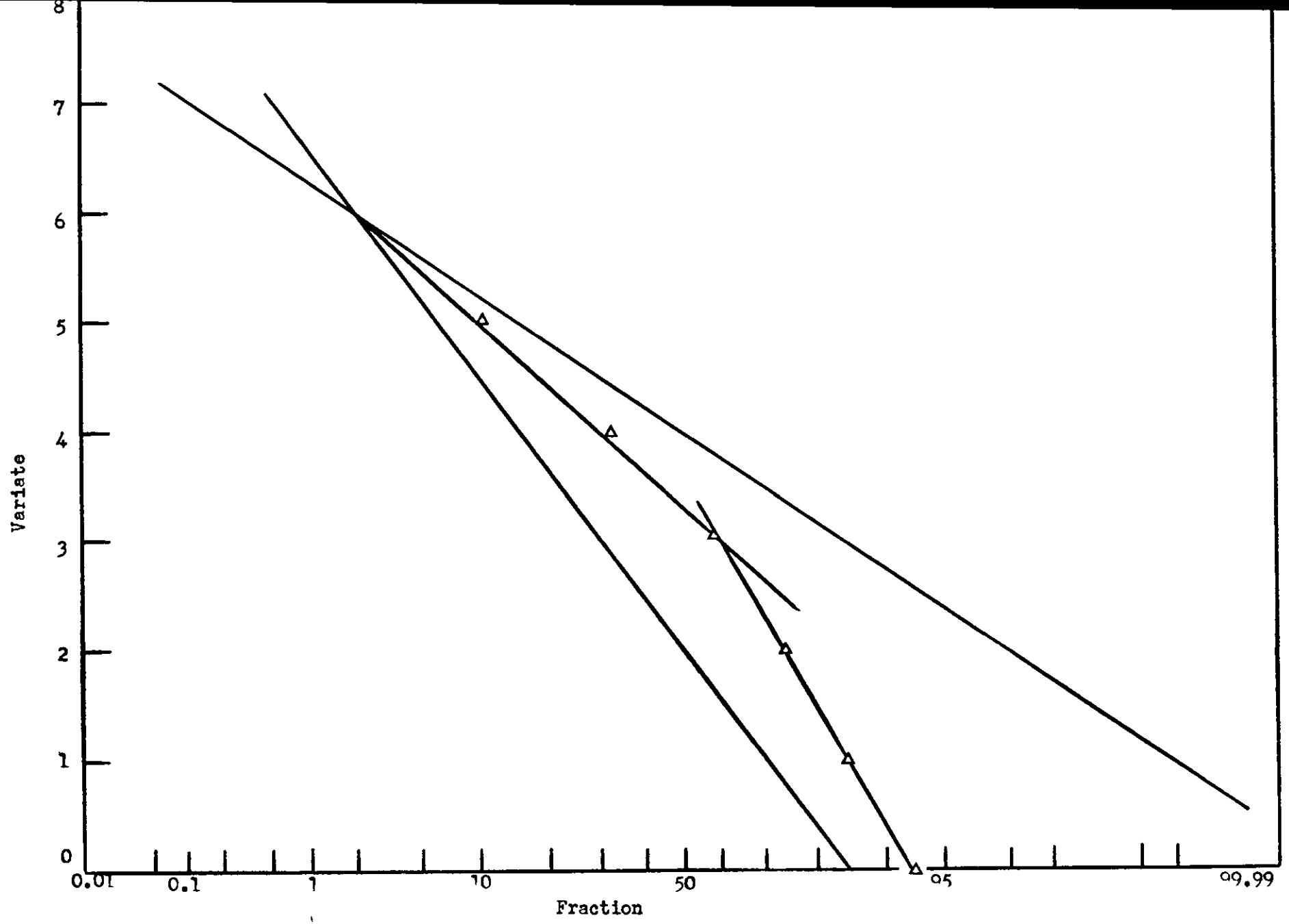

Fig. 6.7 Effect of Adding Two Normal Distributions

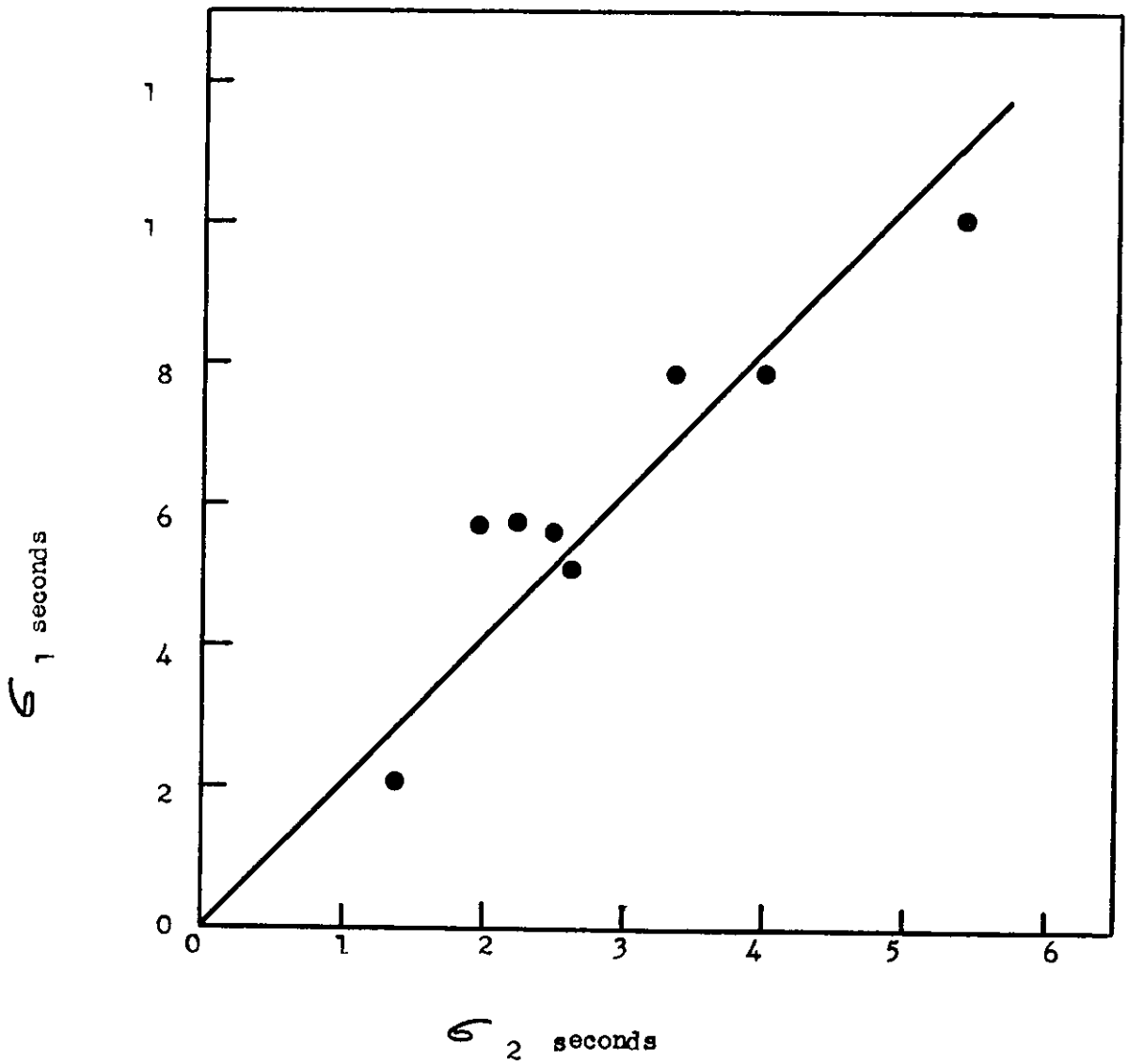

System 1.0M Decanoic Acid-Heptane/Water
(Series D1 and D2)

Fig. 6.8A Relationship between the standard deviations of the first and second stage coalescence time distributions

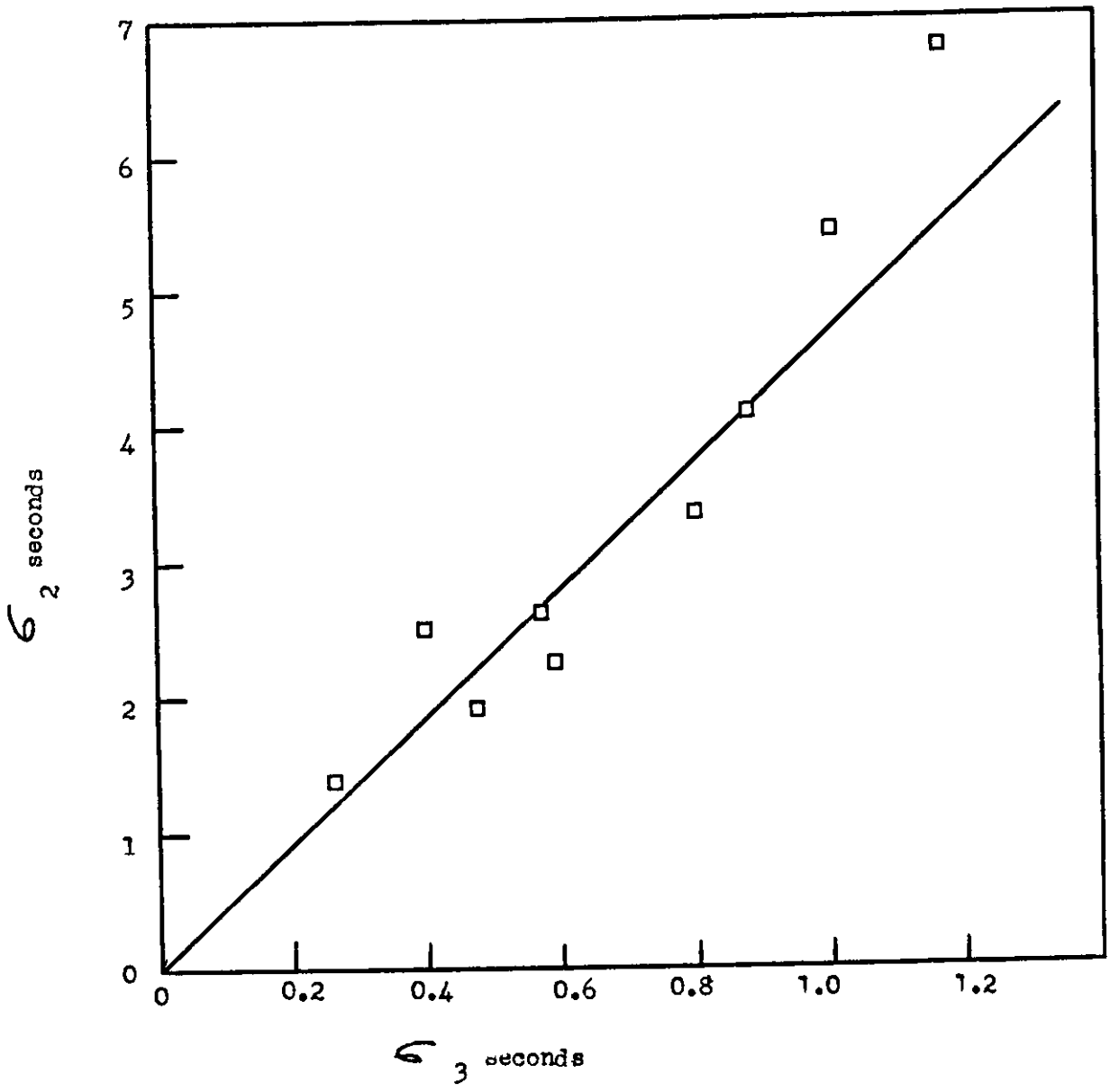

System: 1.0M Decanoic Acid-Heptane/Water
(Series D1 and D2)

Fig. 6.8B Relationship between standard deviations of the second and third stage coalescence time distributions

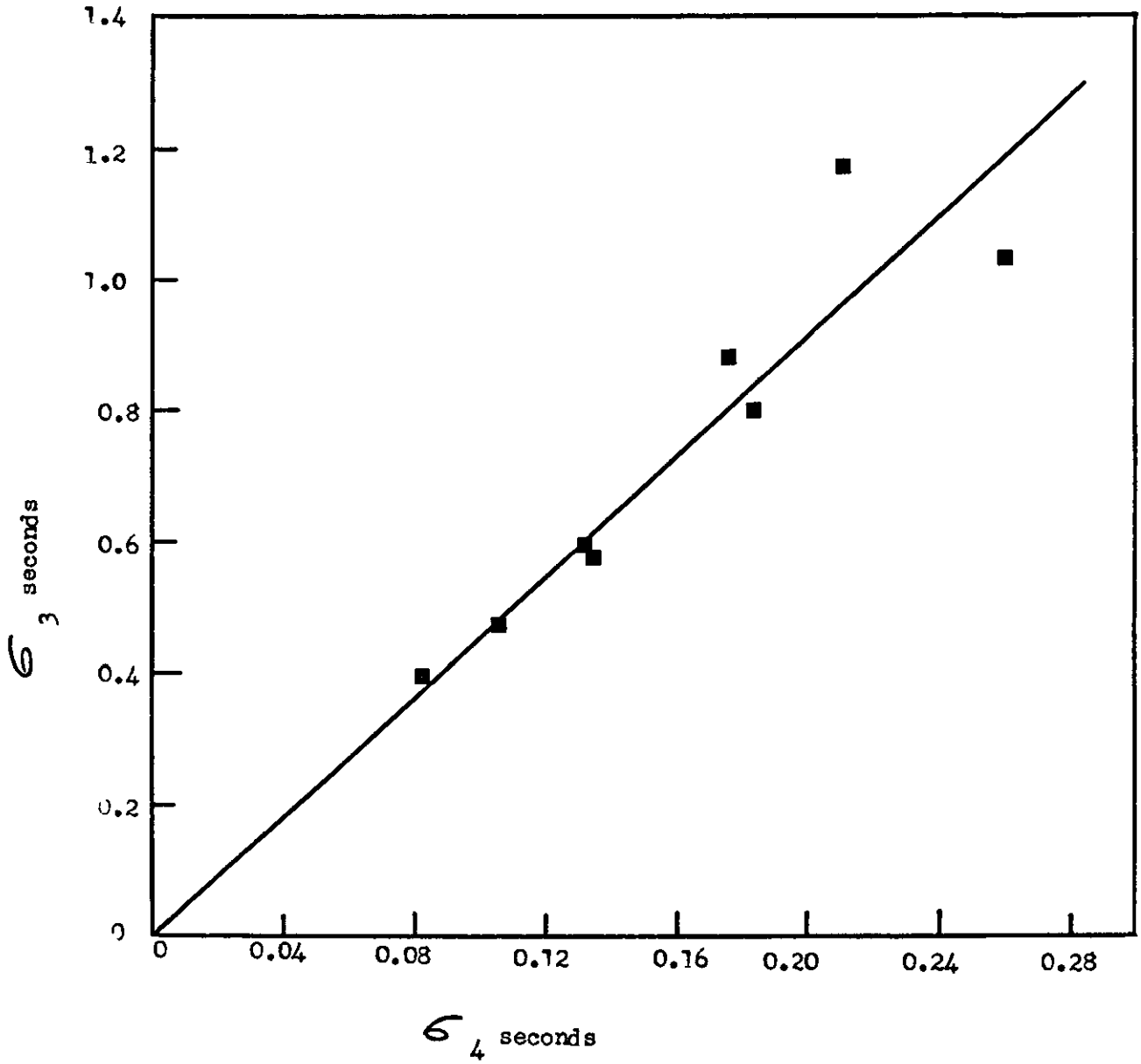

System: 1.0M Decanoic Acid-Heptane/Water
(Series D1 and D2)

Fig. 6.8C Relationship between standard deviations of the third and fourth stage coalescence time distributions

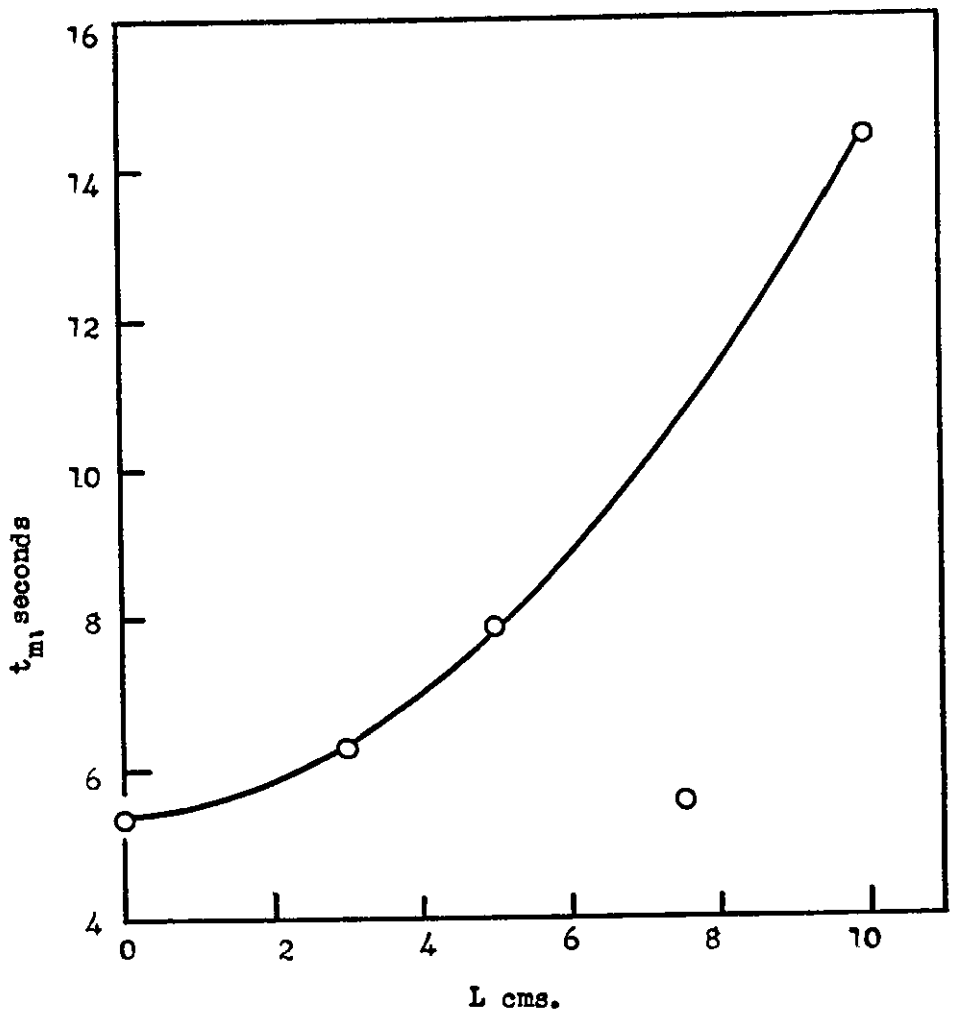

Drop Size a_1 = 0.416 cms.

System: Heptane-Water (Series A2)

Fig. 6.9A Relationship between first stage mean coalescence time and the fall height of the drop

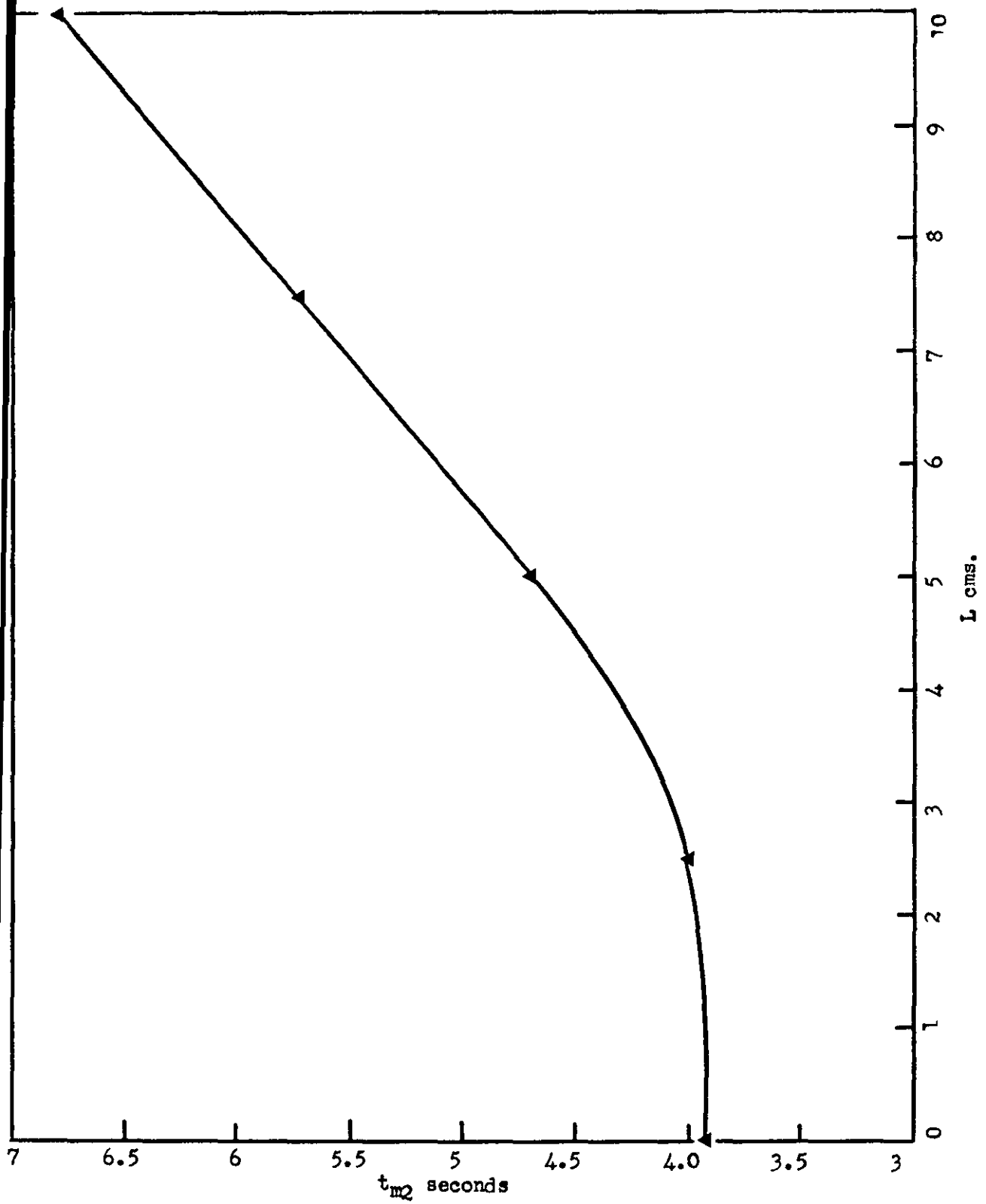

Drop size a_2 = 0.1426 to 0.1461 cms.

System: Heptane-Water (Series A2)

Fig. 6.9B Relationship between second stage mean coalescence time and fall height of the drop

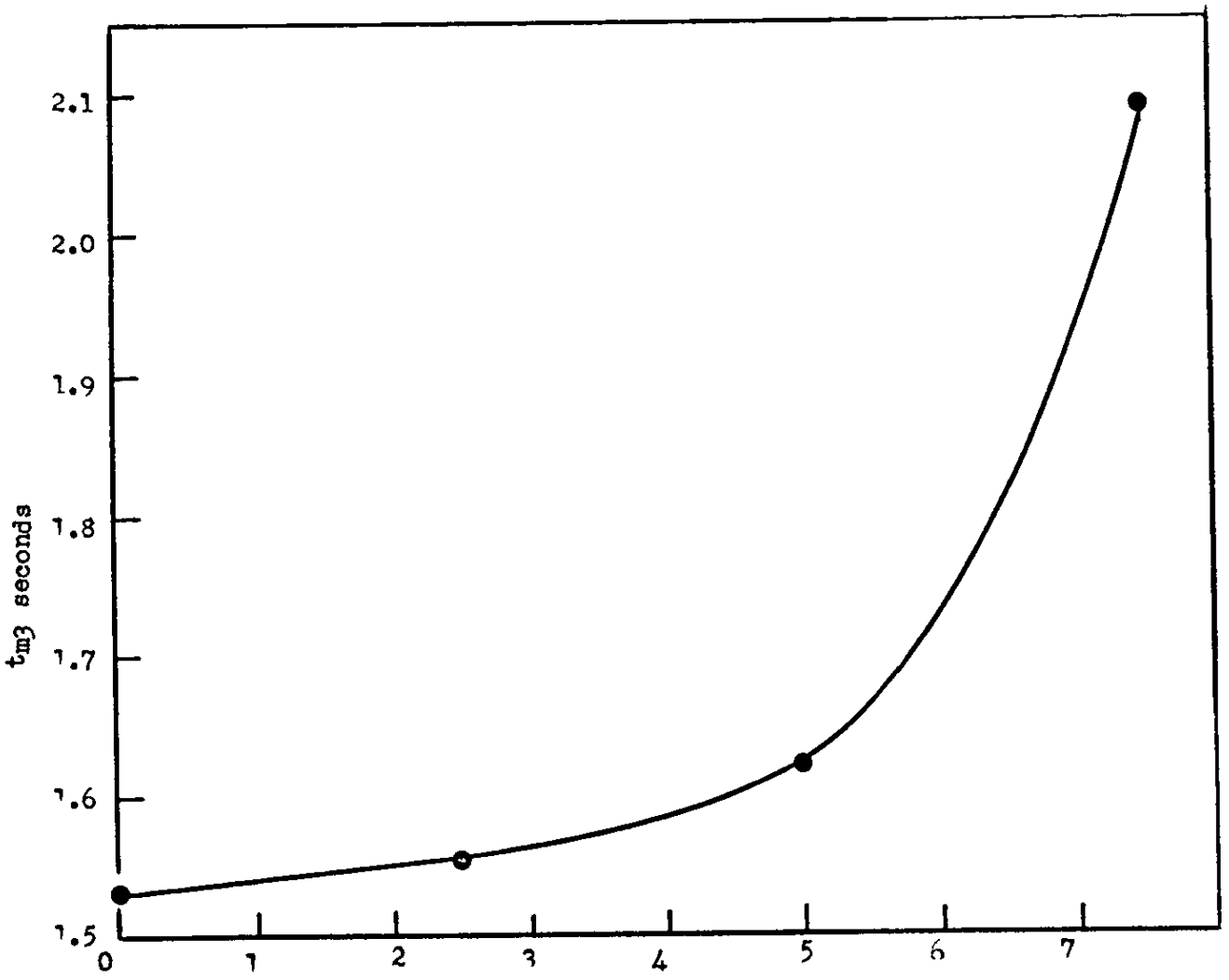

Drop size a_3 = 0.0635 to 0.0697 cms.

System: Heptane–Water (Series A2)

Fig. 6.9C Relationship between third stage mean coalescence time and fall height of the drop

CHAPTER 7

CORRELATION OF EXPERIMENTAL MEAN COALESCENCE REST-TIME WITH PHYSICAL VARIABLES

Introduction

The study of coalescence in technical equipment is difficult because of the complicated hydrodynamics involved. To understand the process of coalescence, the author and many other workers have studied the coalescence of single drops at a plane interface. A large number of experimental results on single drop systems are to be found in the literature.

Whilst the prediction of the behaviour of dispersions remains largely unsolved, the available experimental data on single drop coalescence should provide a useful guide in the design of technical equipment. The correlation of single drop rest-times using theoretically derived equations (previously discussed in Chapter 3) is far from satisfactory. An attempt is made in this Chapter to develop a more useful correlation. This is carried out in two parts:

(i) A dimensional analysis to obtain a relationship between the coalescence rest-time and the important variables.

(ii) A statistical analysis to fit the experimental data.

7.1 Dimensional Analysis

The coalescence of a single drop is mainly concerned with the drainage of the thin phase-2 film, which is trapped between the drop and the interface. It is therefore necessary to obtain a relationship between the film drainage time, the film thickness and other variables of the system.

The variables considered in this analysis are the ones which have been found to be important in creeping flow problems. However, since the pressure distribution in the film is unknown, the pressure is expressed as a function of the drop size, density difference between the phases and the

interfacial tension. Thus,the drainage time t,which is assumed to be equivalent to the coalescence rest-time,can be written as a function of the following variables:

$$t = \gamma(a, \Delta\rho, g, \mu_2, \gamma, h)$$

where,

t	=	coalescence rest-time	T
a	=	spherical drop diameter	L
$\Delta\rho$	=	phase density difference	ML^{-3}
g	=	gravitational constant	LT^{-2}
μ_2	=	continuous phase viscosity	$ML^{-1}T^{-1}$
γ	=	interfacial tension	MT^{-2}
h	=	film thickness	L

Following the procedure which is usually adopted in dimensional analysis it is assumed that this equation can be re-written as follows:

$$t = [a]^p[\Delta\rho]^q[g]^r[\mu_2]^s[\gamma]^t[h]^n \qquad (7.1.1)$$

Because both a and h have the same dimension of length,it is convenient to rearrange Eqn. (7.1.1) as follows:

$$t = [a]^p[\Delta\rho]^q[g]^r[\mu_2]^s[\gamma]^t\left[\frac{a}{h}\right]^n \qquad (7.1.2)$$

For this equation to be dimensionally consistent:

$$p = 2q + \frac{s}{2} + \frac{1}{2}$$

$$r = \frac{s}{2} + q - \frac{1}{2}$$

$$t = -q - s$$

Substituting for p,r and t in terms of q and s in Eqn. (7.1.2):

$$t = \left[a\right]^{(2q + \frac{s}{2} + \frac{1}{2})}\left[\Delta\rho\right]^{q}\left[g\right]^{(\frac{s}{2} + q - \frac{1}{2})}\left[\mu_2\right]^{s} \cdot$$

$$\cdot\left[\gamma\right]^{-q\ -s}\left[\frac{a}{h}\right]^{n} \qquad (7.1.3)$$

Rearranging Eqn. (7.1.3), the following equation is obtained:

$$t = \left[\frac{a}{g}\right]^{\frac{1}{2}} \phi \left[\frac{a^2 \Delta\rho\, g}{\gamma}\right]^{q} \left[\frac{a^{\frac{1}{2}}\, g^{\frac{1}{2}}\, \mu_2}{\gamma}\right]^{s} \left[\frac{a}{h}\right]^{n} \qquad (7.1.4)$$

The value of the constant ϕ must be determined experimentally.

Discussion

Jeffreys and Hawksley (68) have carried out a dimensional analysis of the above system but without the inclusion of the variable h. They obtained the two dimensionless groups:

$$\pi_1 = \left[\frac{(t_{\frac{1}{2}})_1\, b \Delta\rho\, g}{\gamma^2}\right] \quad \text{and} \quad \pi_2 = \left[\frac{\gamma}{b^2 \Delta\rho\, g}\right]$$

where $(t_{\frac{1}{2}})_1$ is the first stage half-life time and b the spherical drop radius. The group π_2 also occurs in Eqn. (7.1.4). Jeffreys and Hawksley's analysis infers the assumption that the film breaks when $(\frac{a}{h})$ is equal to a constant. Recent evidence however(54,79,89), indicates that in a given system, the film ruptures at a definite thickness.

If the exponent s in Eqn. (7.1.4) is set equal to 1, the following equation is obtained:

$$\frac{\gamma t}{\mu_2 a} = \phi \left[\frac{a^2 \Delta\rho\, g}{\gamma}\right]^{q} \left[\frac{a}{h}\right]^{n}$$

If it is now assumed that the film breaks after some time t_m, corresponding to a film thickness h_b, the above equation can be rewritten as:

$$\frac{\gamma t_m}{\mu_2 a} = \phi \left[\frac{a^2 \Delta\rho\, g}{\gamma}\right]^{q} \left[\frac{a}{h_b}\right]^{n}$$

By putting q = 1 and n = 2, the following equation is obtained:

$$t_m = \phi\left[\frac{\mu_2 \Delta\rho\, g\, a^5}{\gamma^2}\right]\frac{1}{h_b^2}$$

This is the exact form of the parallel plates equation, obtained by solving the Navier-Stokes equations (111), i.e. for the case of a deformable drop approaching a rigid flat plate. The parallel plates equation for this case is:

$$(t_2 - t_1) = t = \frac{\mu_2}{128}\left[\frac{\Delta\rho\, g\, a^5}{\gamma^2}\right]\frac{1}{h_2^2}\,.$$

7.2 Statistical Analysis

It is not possible to determine experimentally the value of the film thickness at breakage and consequently Eqn. (7.1.4) cannot be used directly. However, as a first assumption, the film thickness h_b will be considered to be a function of the variables μ_2, $\Delta\rho$, a and γ, only. The following equation is easily derived from Eqn. (7.1.4):

$$t_m = k\, a^p \mu_2^q \Delta\rho^r \gamma^s \qquad (7.2.1)$$

where k, p, q, r and s are constants. In studies where L is important, the following equation can be similarly derived:

$$t_m = k^*\, a^p \mu_2^q \Delta\rho^r \gamma^s\, L^t \qquad (7.2.2)$$

where k* and t are also constants.

The author's experimental data and the available data from the literature are correlated using Eqns. (7.2.1) and (7.2.2). This is achieved by fitting a Multiple Linear Regression by the method of least squares.

The mathematics of multiple linear regression and a computer program are described in Appendix 5. The computation for the analysis was performed on an I.C.T. 1905 computer.

7.3 Results and Discussion

Correlations were obtained for a variety of cases, and these are detailed in Appendix 5. They are presented in Figs. 7.1 to 7.13 in the form:

$$(\ln t_m)_{EXPERIMENTAL} \quad \text{vs.} \quad (\ln t_m)_{PREDICTED}, \text{ where:}$$

$(\ln t_m)_{EXPERIMENTAL}$ = experimentally determined value of $\ln t_m$.

$(\ln t_m)_{PREDICTED}$ = value predicted by the regression model.

The computer printout, giving details of the calculated statistics is contained in Appendix 5.

The 95% confidence limits for the true regression coefficients are given in Table 5.A.2 (Appendix 5). In a number of cases, certain of the regression coefficients are not precisely defined, e.g. the case PROL02:

$$\beta_2(\mu_2) = 2.0829 \pm 3.8400 \quad \text{and}$$
$$\beta_3(\Delta\rho) = 1.1271 \pm 2.9630$$

The calculated t values (t-test, see computer printout) for b_2 and b_3 similarly fail to reach the 0.05 significance level. It should be appreciated that the non-significance of a particular variable does not in anyway imply that the independent variable concerned does not affect, or is not related to the dependent variable. It implies merely, that at the level of significance adopted, the confidence limits for the estimated effect, or slope, include zero as a possible value.

The standard errors of the regression coefficients (see computer printout - Appendix 5) and the confidence limits measured therefrom, measure the overall uncertainty of each estimated regression coefficient taken separately. An estimate of the overall extent of association between the value of the dependent variable t, and the independent variables, is measured by the multiple correlation coefficient (see computer printout).

An examination of the residual errors (see Figs. 5.A.2 to 5.A.4, Appendix 5) for the correlations does not reveal any abnormalities. The

statistical analysis therefore indicates that a satisfactory correlation between the dependent variable t, and the independent variables a , μ_2, $\Delta\rho$, γ and L has been obtained.

KEY TO CORRELATIONS

	Symbol	System	Reference
SMALL SYMBOLS	○	Heptane–Water	Series A2, A3, (16)
	●	0.05M Decanoic Acid/Heptane–Water	Series B2
	△	0.5M Decanoic Acid/Heptane–Water	Series C2, C3
	▲	1.0M Decanoic Acid/Heptane–Water	Series D2
	□	Benzene–Water	(16, 60, 79, 81, 82)
	■	CCl_4–Water	(16)
	▽	Ethylene Glycol–n Hexane	Konnecke*
	▷	Triethylene Glycol–n Hexane	Konnecke*
	◁	Diethylene Glycol–n Hexane	Konnecke*
	▶	Ethylene Glycol–Benzene	Konnecke*
	◀	Diethylene Glycol–Benzene	Konnecke*
LARGE SYMBOLS	○	Tributyl Phosphate–Water	(79)
	●	Water–Anisole	(79, 101)
	□	Water 'Aroclor 1248'	(79)
	■	Benzene + Iso Octane (50:50)–Water	(82)
	△	Benzene + Liquid Paraffin (50:50)–Water	(82)
	▲	Benzene + Liquid Paraffin (75:25)–Water	(82)
	◀	Heptane + Liquid Paraffin (50:50)–Water	(82)

* Konnecke, H.G., Z. Physik Chem. (Leipzig), 211, 208, (1959)

(A DETAILED LIST OF THE FIGURE CORRELATIONS IS GIVEN ON THE FOLLOWING PAGE)

MULTIPLE LINEAR REGRESSION CORRELATIONS

Figures 7.1 to 7.13

Case No.	Description	Figure No. for correlation
Section 1.	(Series 2A, 2B, 2C, 2D)	
PROL 01	1st Stage Coalescence	7.1
PROL 02	2nd Stage Coalescence	7.2
PROL 03	3rd Stage Coalescence	7.3
PROL 04	4th Stage Coalescence	7.4
PROL 05	1st and 2nd Stage Coalescence	7.5
PROL	3rd and 4th Stage Coalescence	7.6
PROL	1st,2nd,3rd and 4th Stage Coalescence	7.7
Section 2.		
PROL 21	Two Component Systems for L = 0 cms.	7.8
PROL 22	Two Component Systems for L > 0 cms.	7.9
Section 3.		
PROL 31	Three Component Systems for L = 0 cms. (present work only,for Series 2B,2C,2D)	7.10
PROL 32	Three Component Systems for L > 0 cms.	7.11
Section 4.		
PROL 41	PROL 21 and PROL 31 for L = 0 cms.	7.12
PROL 42	PROL 22 and PROL 32 for L > 0 cms.	7.13

** NOTE Except for Section 1 Correlations,and unless specified otherwise,each of the correlations includes all of the relevant referenced data.

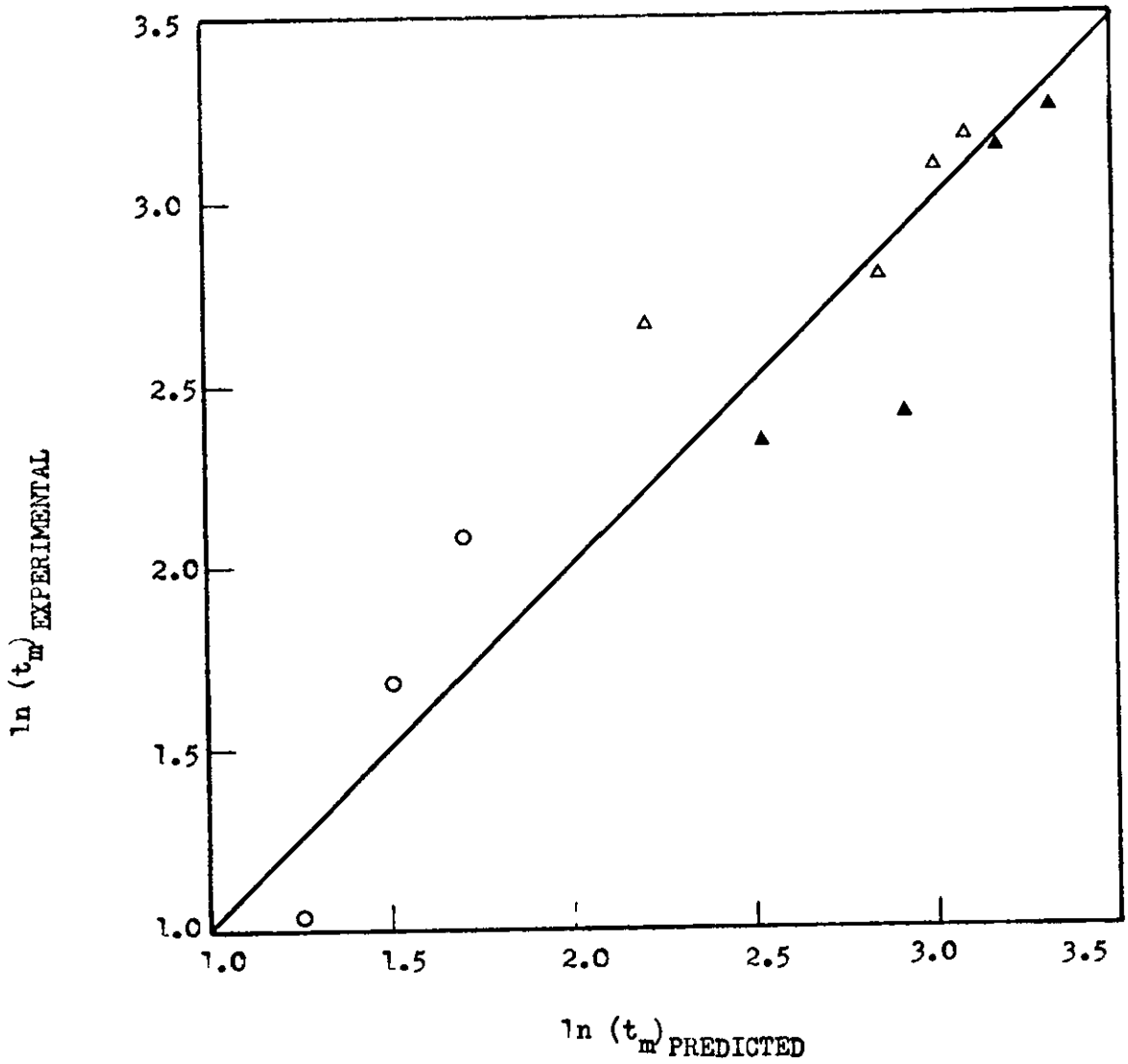

Case PROL 01

$$t_m = 28.6152\ (a^{1.0128}\ \mu_2^{3.8977}\ \Delta\rho^{1.4533}\ \gamma^{-0.8087})$$

Fig. 7.1 Correlation of mean rest-time (t_m) with physical variables

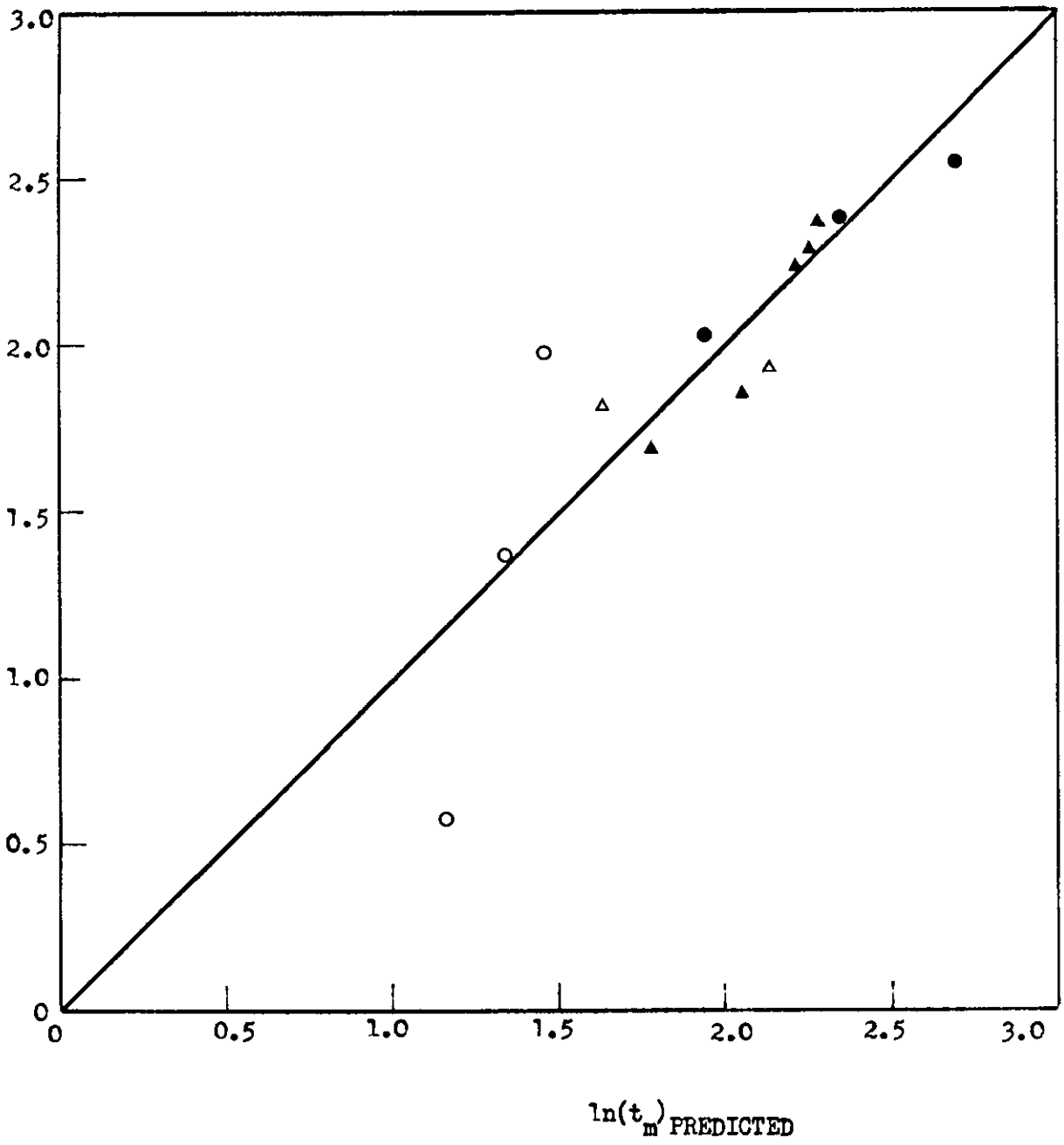

Case PROL 02

$$t_m = 20.1515\,(a^{1.4671}\ \mu_2^{2.0829}\ \Delta 2^{1.1271}\ \gamma^{-0.8255})$$

Fig. 7.2 Correlation of mean rest-time (t_m) with physical variables

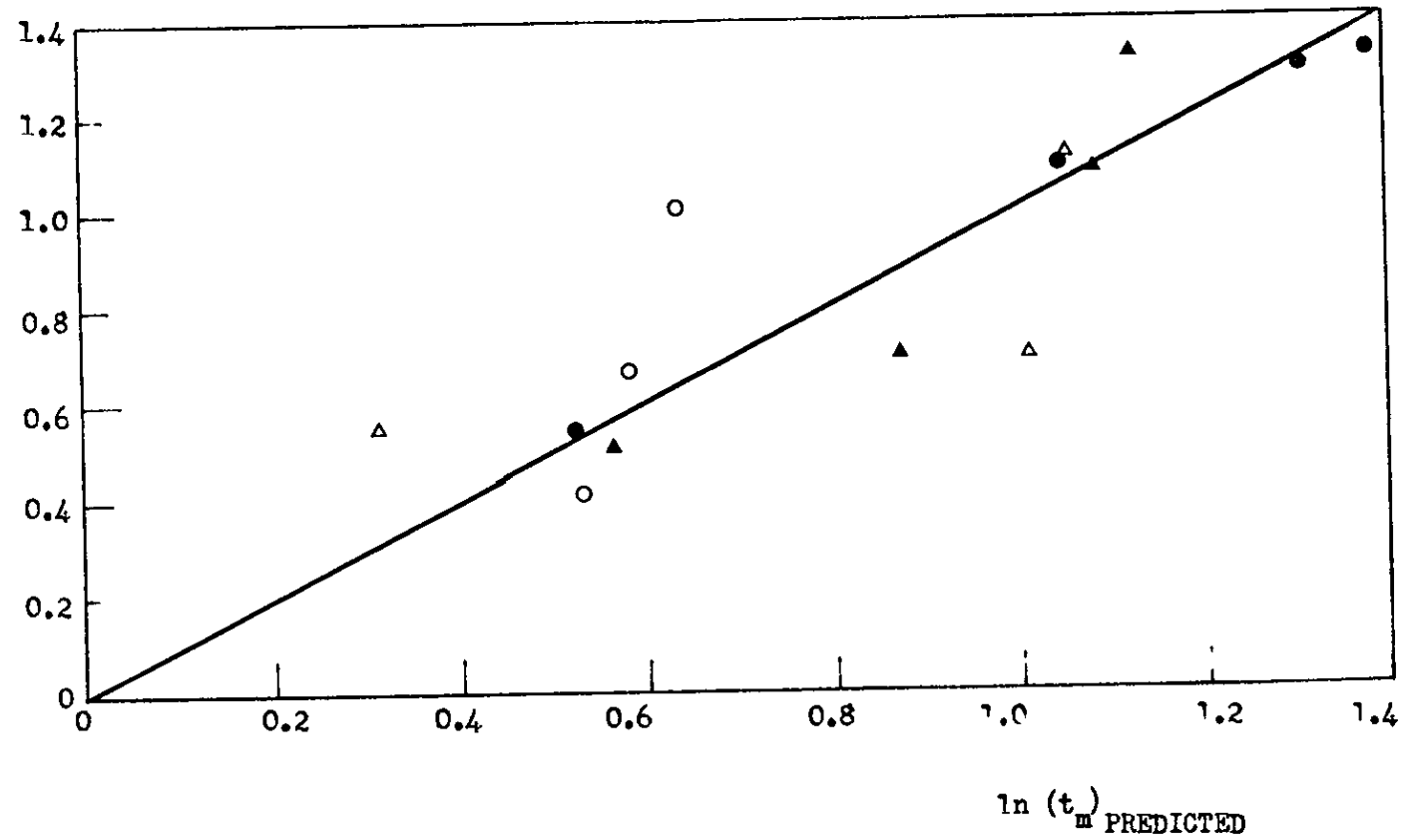

Case PROL 03

$$t_m = 21.3206\ (a^{2.2769}\ \mu_2^{2.0806}\ \Delta\rho^{1.0197}\ \gamma^{-0.4905})$$

Fig. 7.3 Correlation of mean rest-time (t_m) with physical variables

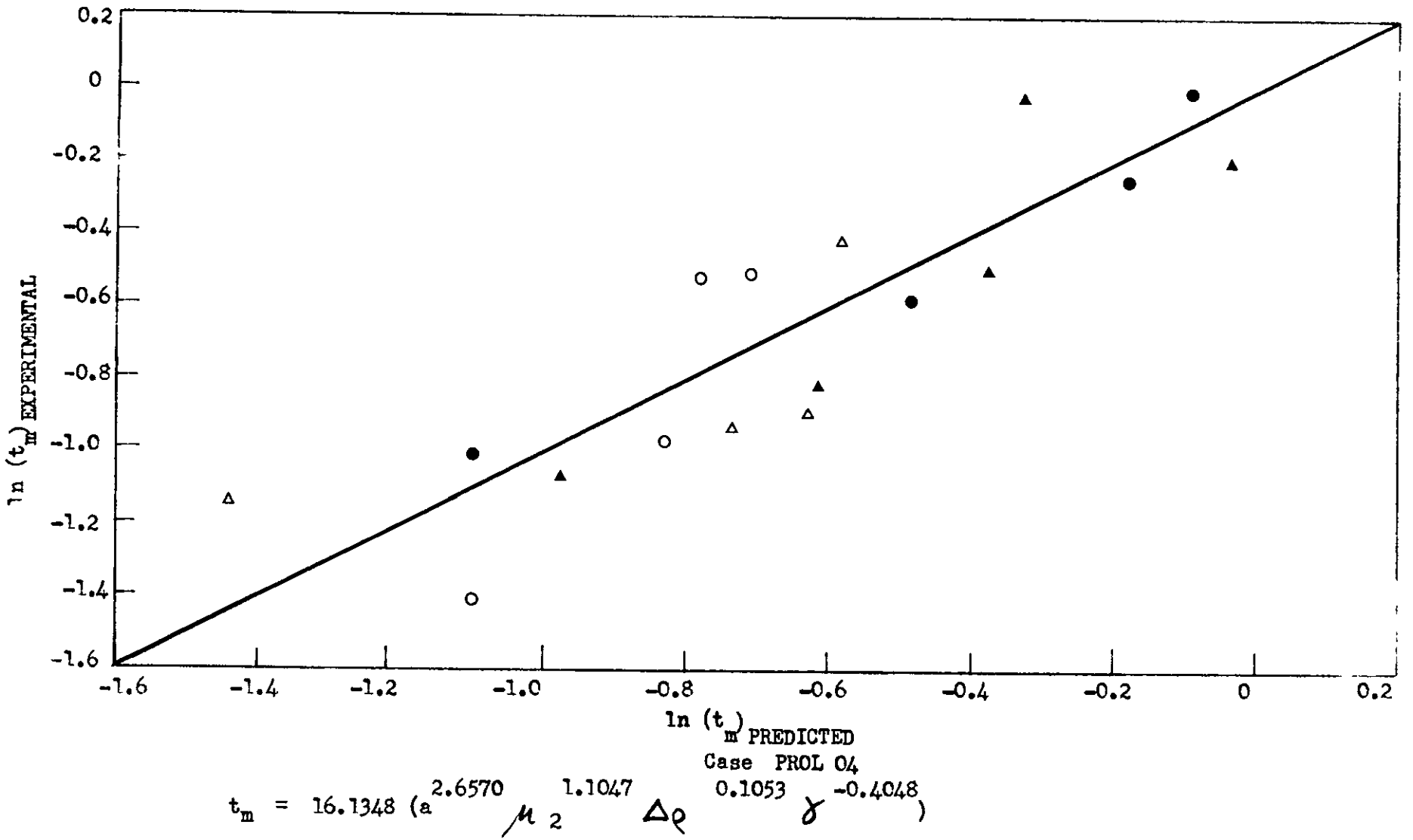

$$t_m = 16.1348\ (a^{2.6570}\ \mu_2^{1.1047}\ \Delta\rho^{0.1053}\ \gamma^{-0.4048})$$

Fig. 7.4 Correlation of mean rest-time (t_m) with physical variables

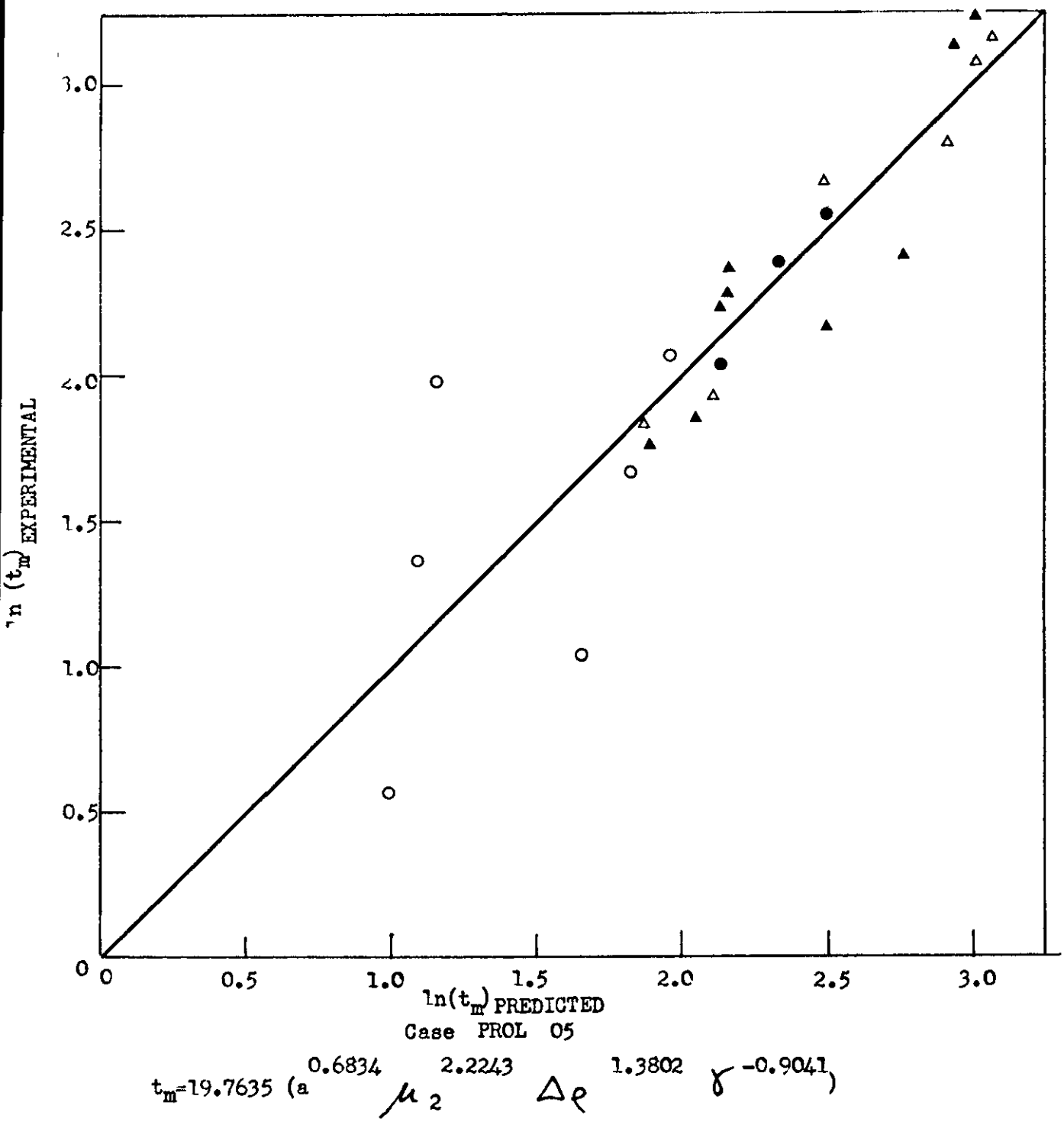

Fig. 7.5 Correlation of mean rest-time (t_m) with physical variables.

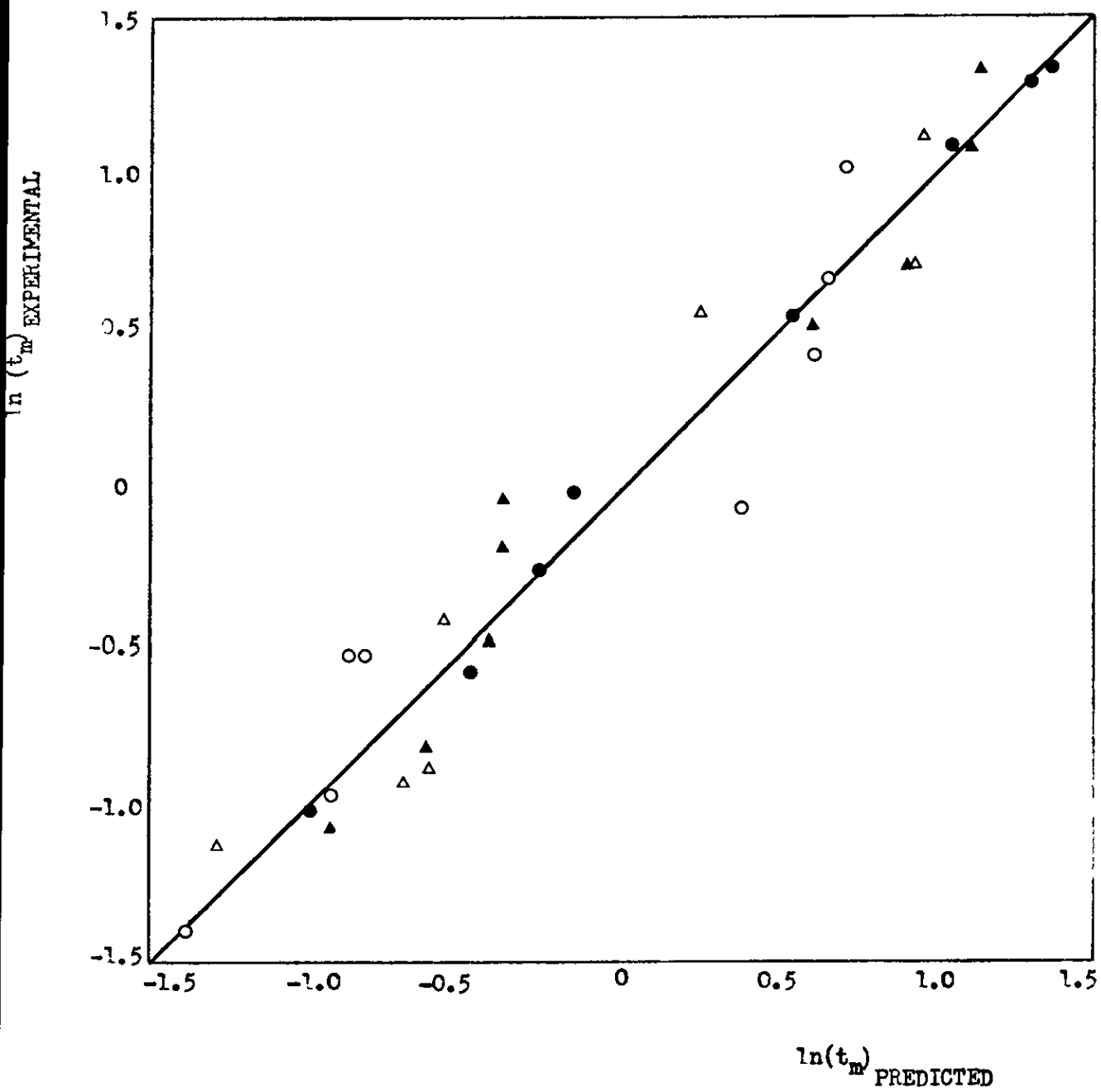

Case PROD 06

$$t_m = 15.8517\ (a^{2.2044}\ \mu_2^{1.2821}\ \Delta\rho^{0.3669}\ \gamma^{-0.4353})$$

Fig. 7.6 Correlation of mean rest-time (t_m) with physical variables

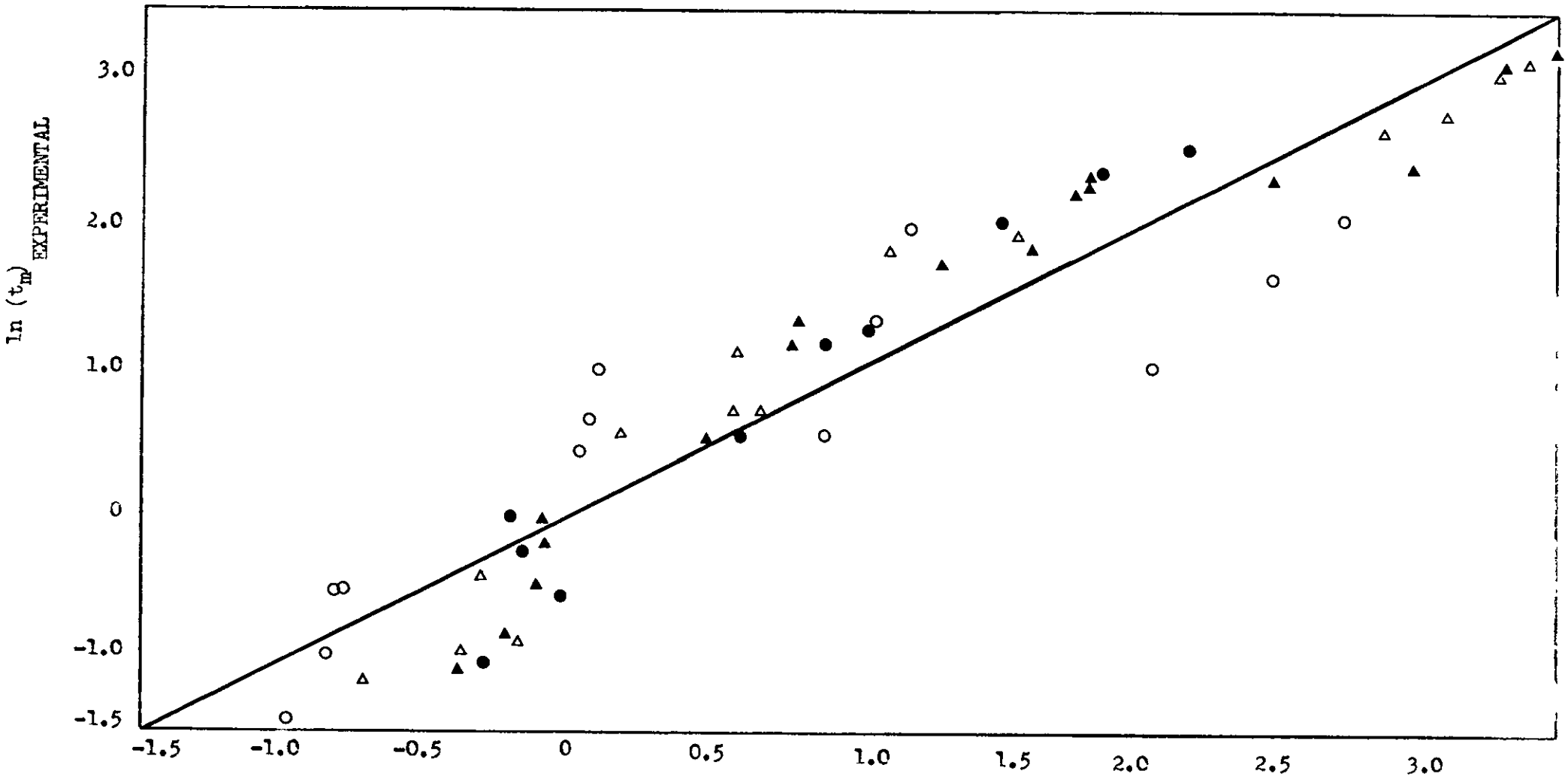

$$t_m = 10.7577\ (a^{1.2964}\ \mu_2^{0.7866}\ \Delta\rho^{0.1641}\ \gamma^{-0.6702})$$

Fig. 7.7 Correlation of mean rest-time (t_m) with physical variables

Case PROL 07

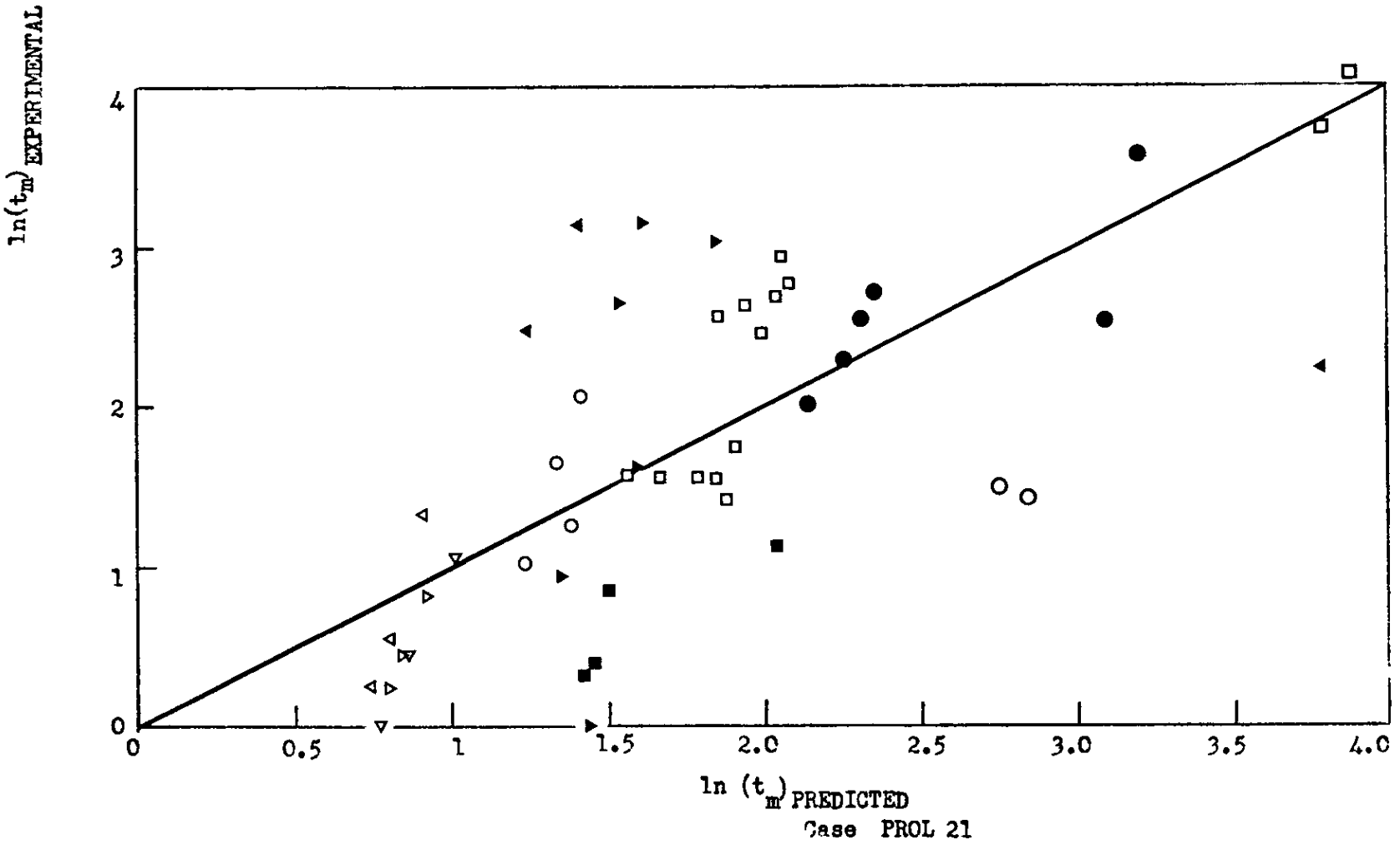

$$t_m = 4.5795\,(a^{0.4075}\,\mu_2^{0.4789}\,\Delta\rho^{-0.3100}\,\gamma^{-0.1565})$$

Fig. 7.8 Correlation of mean rest-time (t_m) with physical variables

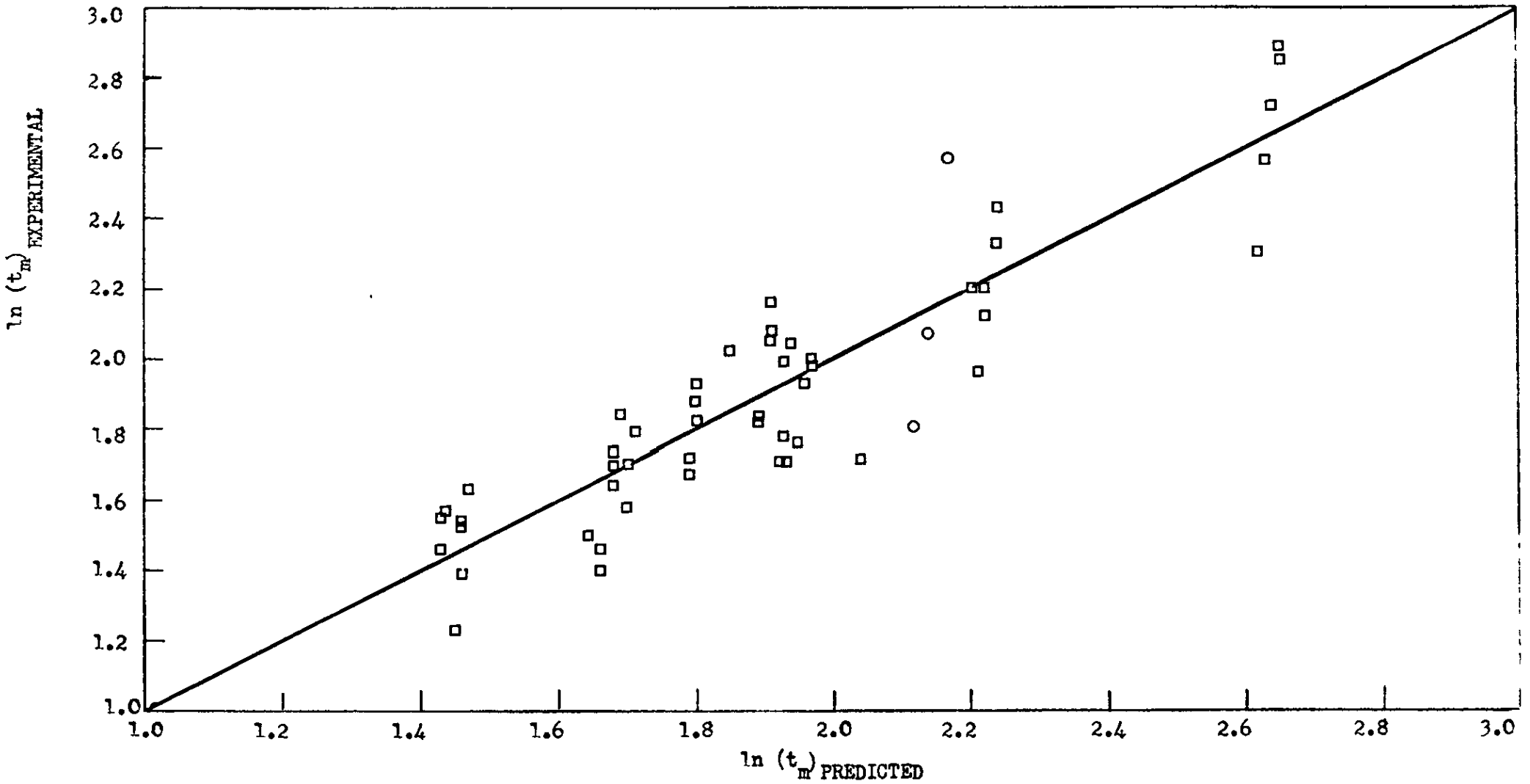

Case PROL 22

$$t_m = -3.2239\ (a^{1.6384}\ \mu_2^{0.3935}\ \Delta\rho^{-0.9748}\ \gamma^{1.7473}\ L^{-0.1096})$$

Fig. 7.9 Correlation of mean rest-time (t_m) with physical variables

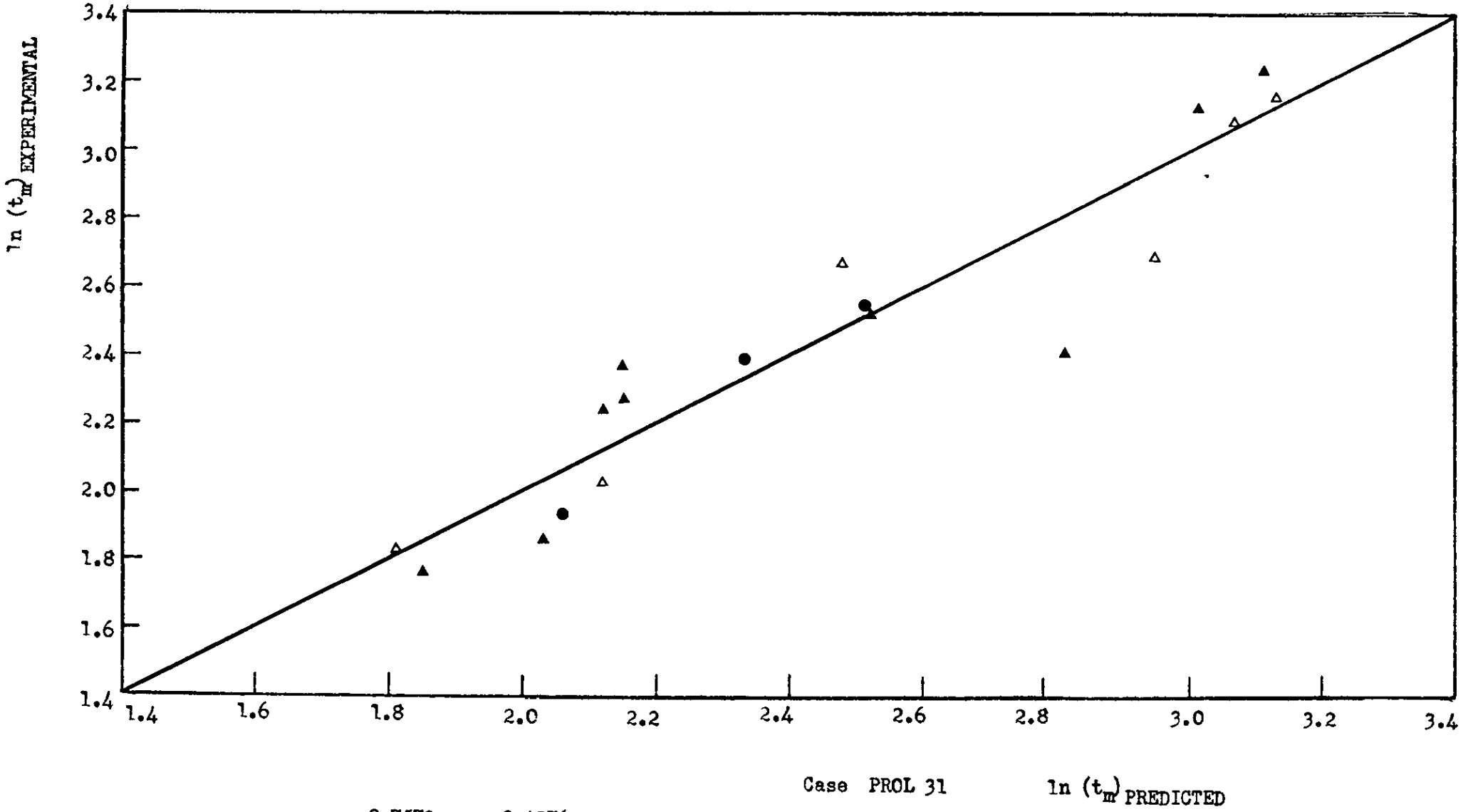

$$t_m = 2.0072\ (a^{0.7573}\ \mu_2^{-0.4276}\ \Delta\rho^{-0.2203}\ \gamma^{-0.2738})$$

Fig. 7.10 Correlation of mean rest-time (t_m) with physical variables

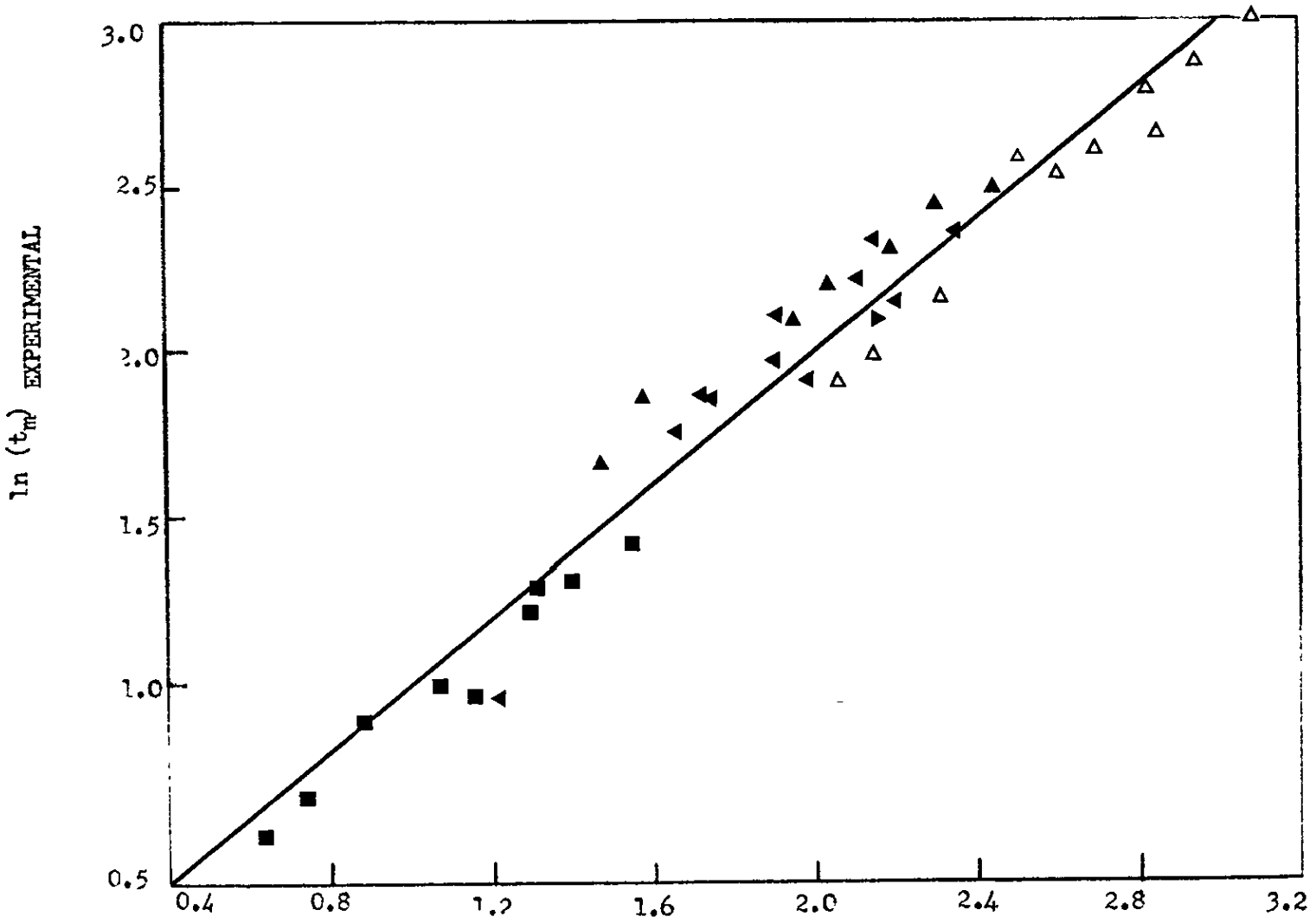

$$t_m = 12.4030\ (a^{1.4501}\ \mu_2^{0.8584}\ \Delta\rho^{0.1384}\ \sigma^{-1.1868}\ L^{0.1390})$$

Fig. 7.11 Correlation of mean rest-time (t_m) with physical variables

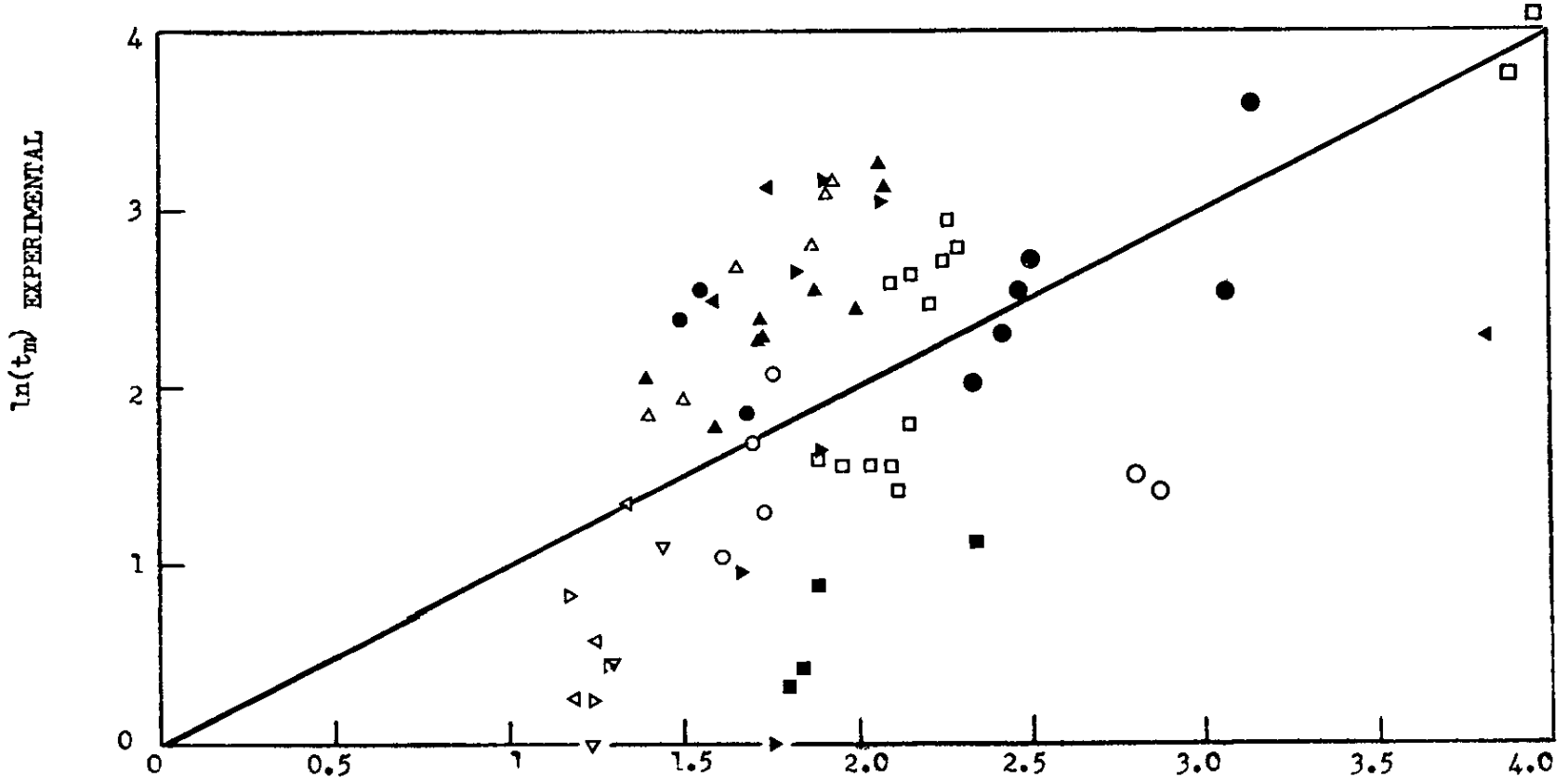

$$t_m = 4.4062\ (a^{0.3098}\ \mu_2^{0.4170}\ \Delta\rho^{-0.2320}\ \gamma^{-0.1059})$$

Fig. 7.12 Correlation of mean rest-time (t_m) with physical variables

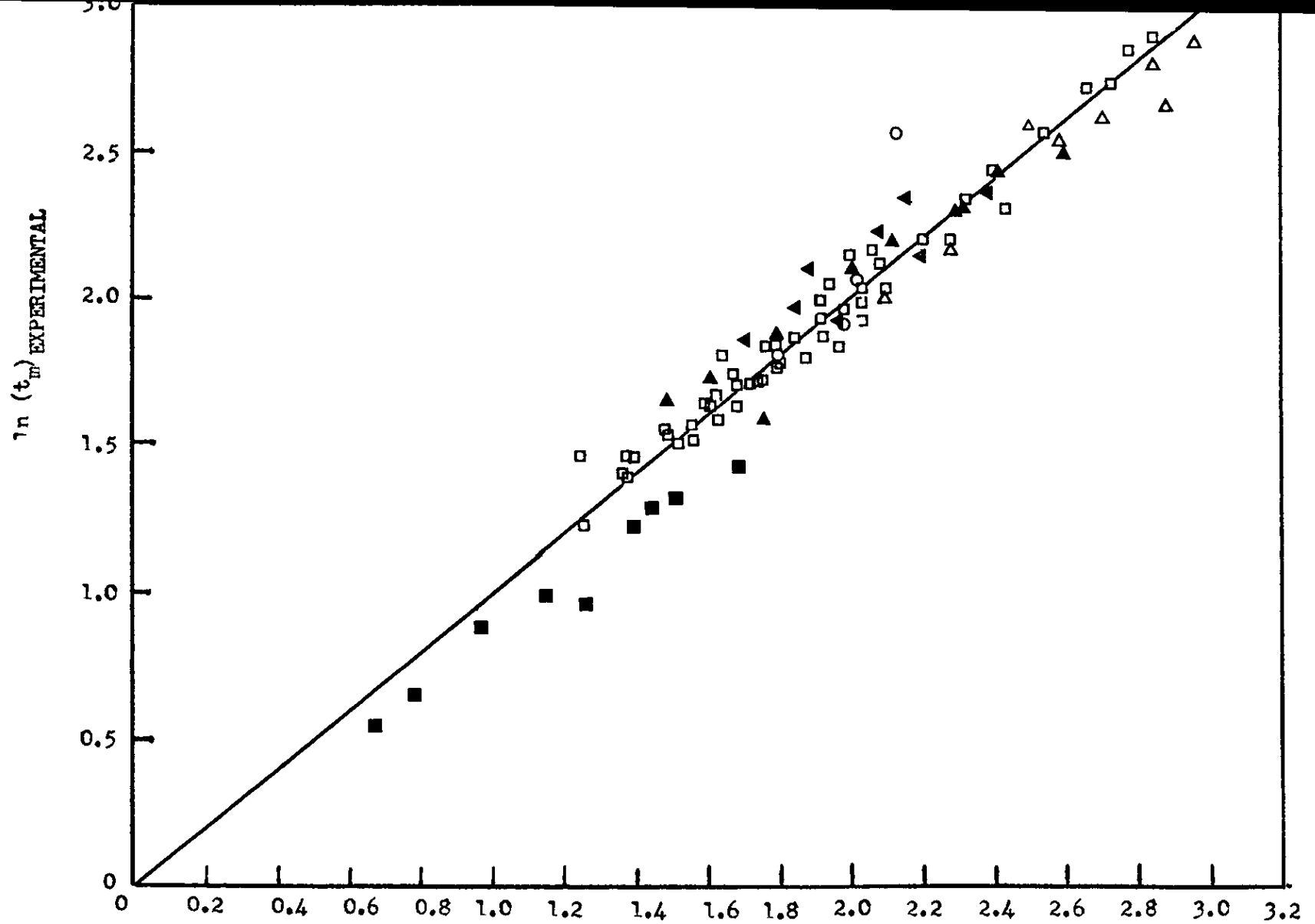

$$t_m = 11.1725\ (a^{1.5959}\ \mu_2^{0.7325}\ \Delta\rho^{-0.0126}\ \gamma^{-1.0248}\ L^{0.1669})$$

Fig. 7.13 Correlation of mean rest-time (t_m) with physical variables

CHAPTER 8

SCHLIEREN PHOTOGRAPHIC STUDY OF COALESCENCE

The aim of the photographic study was to observe the penetration of the fluid of the drop into the bulk aqueous phase.

A schlieren apparatus was readily available and this provides a convenient method of flow visualisation when density gradients exist in the flowing fluid. In the case under consideration, this was achieved by adding a small quantity of $CuCl_2$ to the droplet fluid.

8.1 Schlieren Method and Apparatus

The method of flow visualisation using schlieren techniques has been described in detail elsewhere (96) and can be summarised as follows:

The basis of the schlieren method is the deviation of some rays of light due to changes in the refractive index. This is because the velocity of light is related to the refractive index, e.g. in the case of a gas:

$$c = \left(\frac{1}{n}\right) c^*$$

where, c = velocity of light, c* = velocity of light in vacuo, and n = refractive index. If in the working section there is a gradient of refractive index (caused by density gradients) normal to the light rays, the light rays will be deflected because the light travels more slowly where the refractive index is larger.

The apparatus is illustrated in Fig. 8.1. Here the light source L, a 250W mercury vapour lamp, is focussed by a condenser lens C, on the slit S (the slit gap was 0.065 cm.). The heat filter F, is inserted as shown to protect the lens C. A plane mirror P_1 is used to 'fold' the light beam to obtain the experimentally more convenient Z-layout. The second plane mirror P_2 is used to 'fold' the beam from M_2 for focussing at the camera. M_1 and M_2 are concave mirrors, the latter one produces an image of the source in

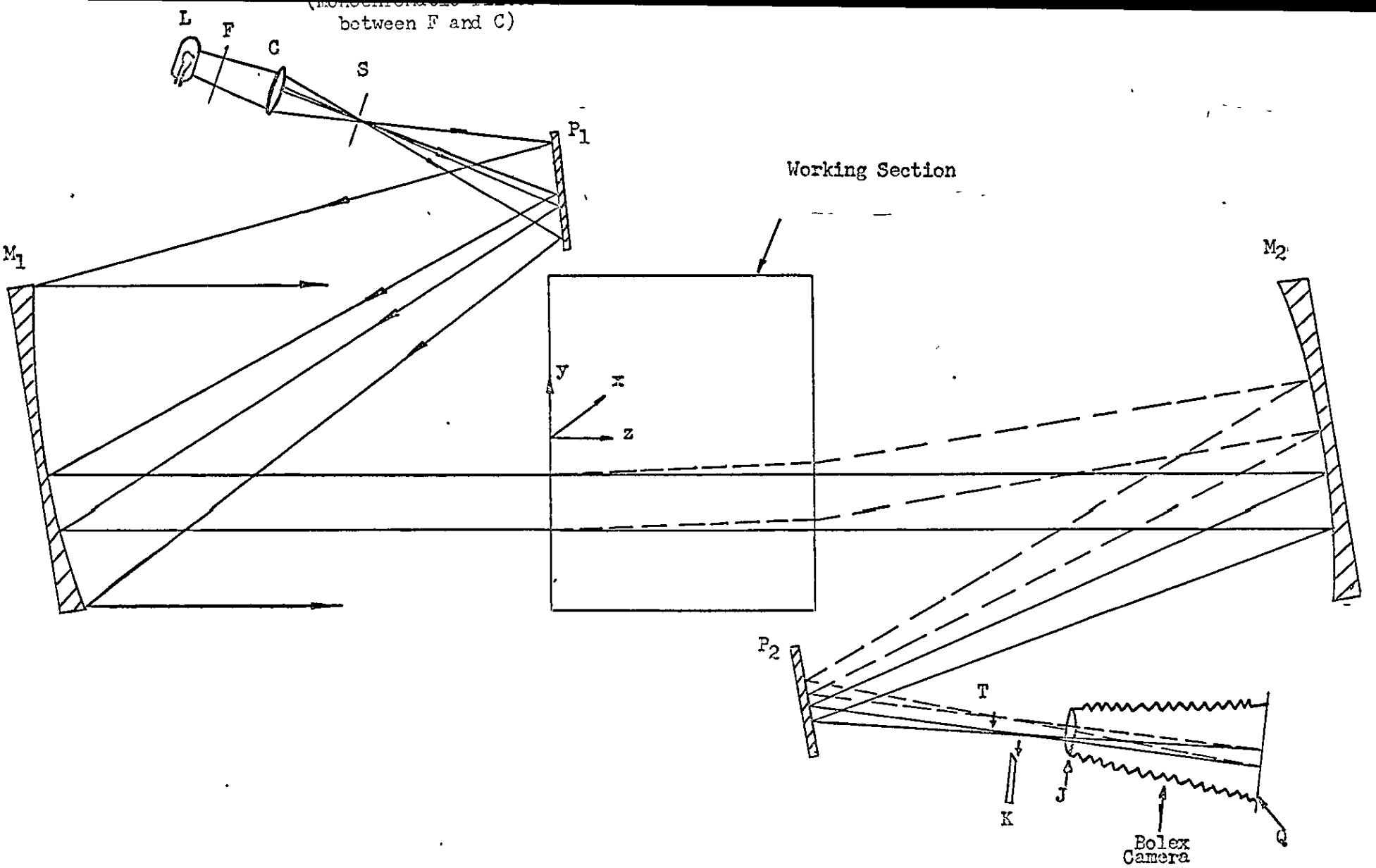

Figure 8.1 Sketch showing the arrangement of the Schlieren Apparatus
(Undisturbed rays shown full, disturbed lines shown broken)

its focal plane K. Beyond K,a focussing lens J is used to give an image of the object in the working section,on the photographic plate Q. Since the light is parallel between M_1 and M_2,the light from each point in the x - y plane may be considered to give an individual image of the source in the focal plane of M_2. If there is no gradient of refractive index (or if the gradient is uniform) over the working section,the individual images of the source will coincide. However,when the gradient in a small area differs from that in the rest of the field,the angular deflection ϵ will cause the corresponding image in the focal plane K to be moved approxiamtely by an amount $f_2 \epsilon$,where f_2 is the focal length of M_2. Irrespective of its direction,all light from a point in the object is brought to a focus at the corresponding point on the photographic plate. The image on the photographic plate is accordingly not displaced by the deflection of the rays produced by the refractive index gradients in the object.

To detect the displacement of the image of the source,the Toepler method is used (see ref. 96). A knife edge is placed at the focal plane K. The edge is adjusted so that in the absence of the optical disturbance,a fraction of the light from the image of the source (the fraction is normally set at 0.5) is cut-off from the focussing lens L,and the illumination is uniformly reduced. If,when the optical disturbance is introduced part of the image of the source is displaced,the illumination of the corresponding part of the image on the photographic plate Q,will decrease or increase by an amount proportional to $\epsilon_y f_2$,according to whether the deflection is towards or away from the opaque side of the knife edge. Displacement of the image of the source parallel to the knife edge produces no effect at Q, and the edge must then be set perpendicular to the direction in which the density gradients are to be observed.

The photographic and schlieren apparatus was mounted on optical

benches which were supported on adjustable columns.

8.2 Coalescence Cell

The coalescence cell, which is illustrated in Fig. 8.2, is made from standard 3" Q.V.F. pipe. The horizontal viewing section is fitted at each end with 3" plane glass windows (schlieren quality). These are mounted in a special flange arrangement and an exploded view of this is shown in Fig. 8.2. This method of mounting the windows should considerably reduce the possibility of the setting up of tangential stresses. A standard Q.V.F dip-pipe, I, is fitted to the vertical section of the glass-tee. Its purpose is to maintain an interface at the viewing level and accordingly, the end was ground flat and square. To permit the interface to be cleaned, the side of the glass-tee is fitted with an overflow pipe, C. All liquid contact surfaces were glass, PTFE and stainless steel (18/8/3 quality).

The coalescence cell was mounted independently of the schlieren apparatus on a rigid frame. In Photograph 8.P.1 the apparatus is shown fully assembled and the lay-out is given in Fig. 8.3.

8.3 Experimental

The schlieren image of the fluid motion at the interface was recorded with a Bolex cine camera.

Photographic Information

Camera	- Paillhard Bolex, Reflex, 16 mm cine.
Lens	- Meyer-Optik, f4.5/300 mm. (Special adaptor used)
Film	- Kodak 'Plus X'
Film speed	- 64 fps.
Film Exposure	- 1/216 second. Full aperture and neutral density filter.

Materials and Preparation

The bulk liquid components were prepared in the manner previously described in Chapter 4. The droplet phase material contained $CuCl_2$ (Analar Grade) and a solution was prepared with double-distilled water using 1 gm. of $CuCl_2$/litre of water. Both liquid phases were mutually saturated and

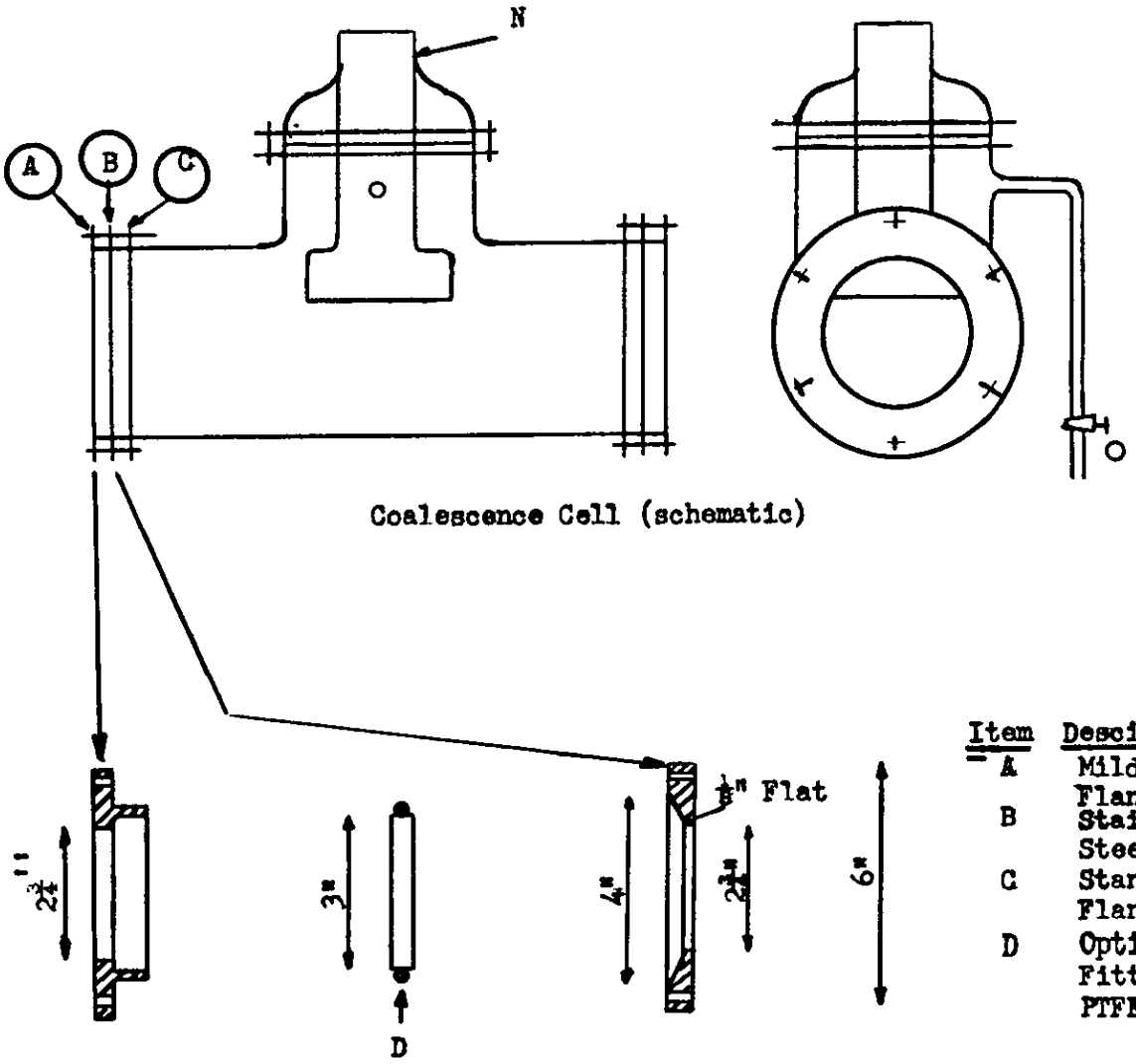

Figure 8.2 Coalescence Cell for Schlieren Photography

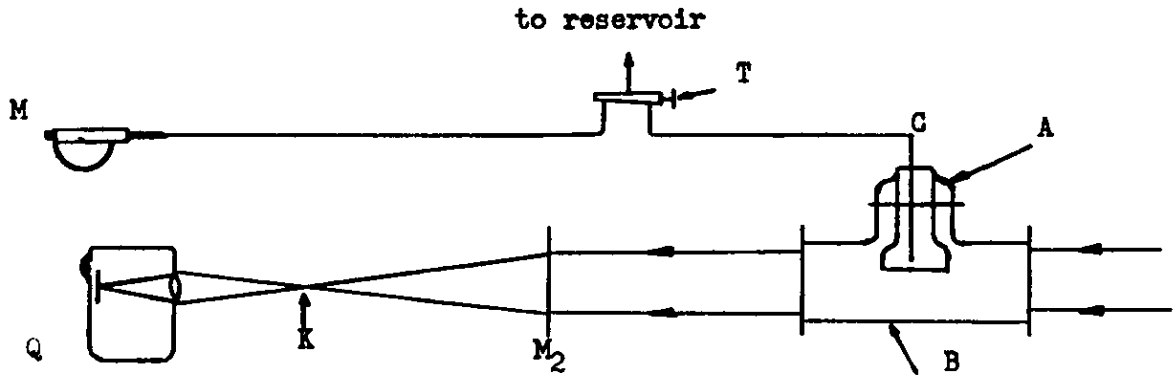

Figure 8.3 Layout for Schlieren Photography

PHOTOGRAPH 8.P.1

Schlieren Apparatus and Photographic Equipment

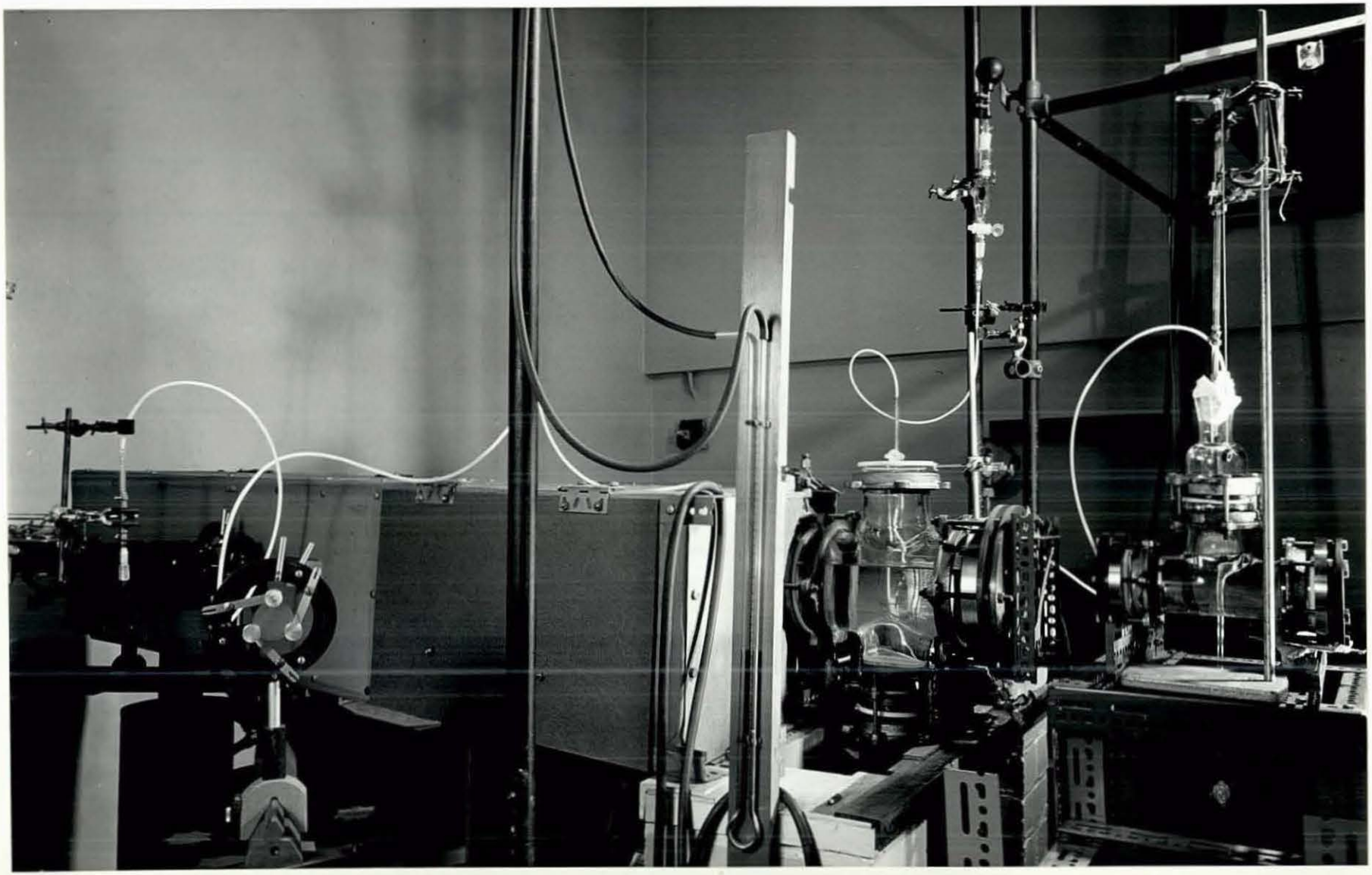

stored in glass receivers. The coalescence cell, associated glass-ware, PTFE and stainless steel parts were thoroughly cleaned in the manner described in chapter 4.

The complete apparatus was housed in a special dark room which was maintained at a constant temperature of approximately 25°C for the duration of theexperiments. Since the bulk liquid components were kept in this room a period of equilibration prior to actual experiments was not required.

Procedure

The coalescence cell, B, is filled with aqueous phase via the dip-pipe A until the optical windows are completely submerged. A quantity of light phase liquid is then poured gently on top of the aqueous phase until a level exists in the dip-pipe. Droplet formation is by means of a glass capillary, C, connected with PTFE tubing to the micrometer syringe M. The droplet injectionline, L to C, is completely filled with droplet phase liquid from the reservoir prior to insertion of the glass capillary into the dip-pipe. When the glass capillary is lowered into position in the dip-tube its vertical alignment, as well as that of the coalescence cell, is checked with a plumb-line. To form drops in the coalescence cell the three way tap, T, is moved to the open position (L to C) and the micrometer syringe adjusted. A number of trial drops are allowed to fall to the interface prior to an actual run so that the knife edge can be adjusted to its optimum position. The final adjustment is in practice found to be a compromise between the uniformity of screen illumination and the contrast of the schlieren image. Only the schlieren beam is used to illuminate the interface, all the other lights in the room being switched-off. A drop is formed by slowly turning the micrometer whilst simultaneously observing the calm interface through the camera. Without the aid of an assistant it is necessary to anticipate the arrival of the drop at the interface, although prior calibration of the micrometer syringe is a useful guide. Filming was continued until the fluid of the coalesced drop was well clear of the bulk interface.

8.4 Results

The coalescence of a water drop at a plane interface was investigated in the two systems heptane-water (system A) and 0.5M decanoic acid-heptane-water (system C). A range of fall height and drop size were studied. It was observed that unless the drop was formed close to the interface the motion of drop fluid in the lowererbulk aqueous phase was very irregular. Therefore the results presented in this section are mainly restricted to those cases where the interface disturbance caused by the impact of the drop was small.

The sequences presented in Photographs 8.P.2 and 8.P.3 show the penetration of the droplet fluid into the homophase, immediately after coalescence. The cases considered are:

Photograph 8.P.2: A water drop, 0.5995 cm. diameter, coalescing at the heptane-water interface, L = 0 cm.

Photograph 8.P.3 A water drop, 0.445 cm. diameter, coalescing at the 0.5M decanoic acid-heptane-water interface, L = 0 cm.

The extent of penetration of the droplet fluid into the homophase is given in Figs. 8.4 and 8.5 for systems A and C, respectively. It is seen that the rate of penetration of the droplet fluid passes through a maximum at a position which is close to the level of the bulk interface. This occurs at approximately 0.425 cm. and 0.2 cm. in the systems A and C, respectively. The curve for the 0.299 cm. drop in Fig. 8.5 at L = 2.5 cm. is seen to be lower than the corresponding curve for L = 0 cm.

As the droplet fluid progresses downwards through its homophase it eventually develops into a torroidal vortex. The trail which is left behind the vortex obscures the view of the later stages of coalescence. Photograph 8.P.4 shows the vortex formation resulting from four stages of coalescence of a 0.414 cm. drop in system A. The fourth stage is almost completely obscured by the vortex trail of the previous stage.

8.5 Interpretation and Discussion of Results

The main area of interest in Photographs 8.P.2 (frames 1 to 8)

PHOTOGRAPH 8.P.2

Penetration of Droplet Fluid into Bulk Aqueous Phase

System: Heptane-Water

$a_1 = 0.5995$ cm. $L = 0$ cm.

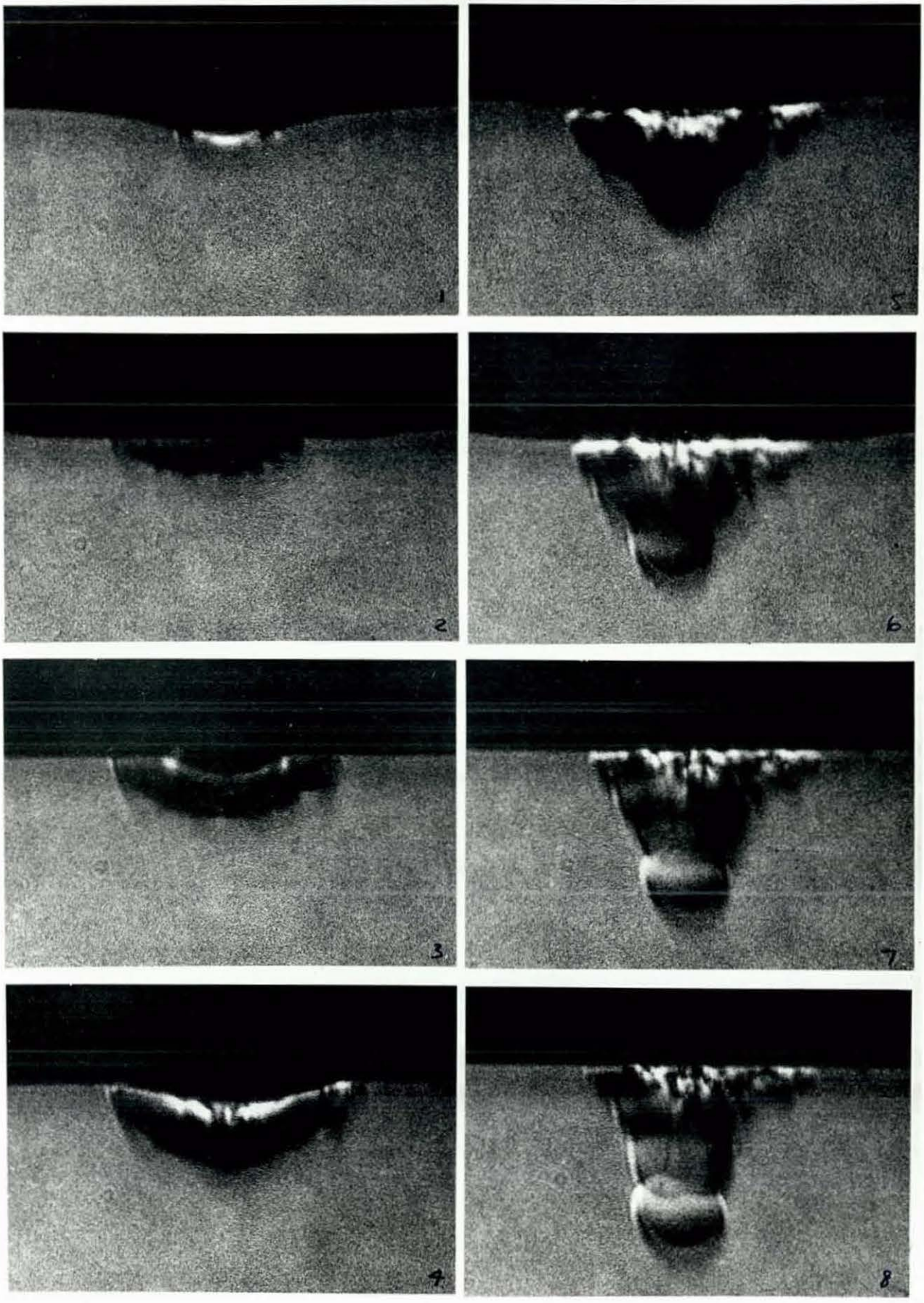
1
5
2
6
3
7
4
8

PHOTOGRAPH 8.P.3

Penetration of Droplet Fluid into Bulk Aqueous Phase

System: 0.5M Decanoic Acid-Heptane-Water

$a_1 = 0.4450$ cm. $L = 0$ cm.

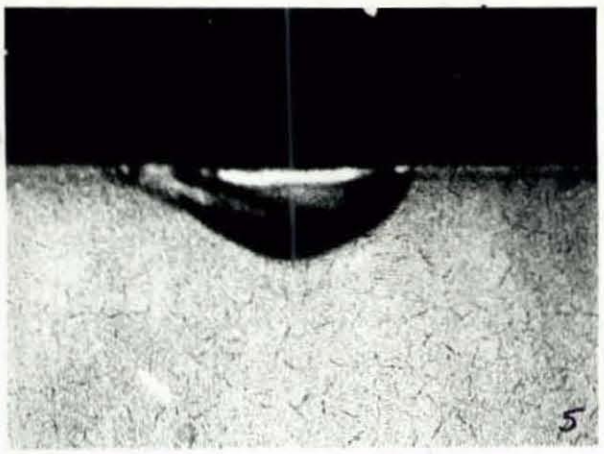
5

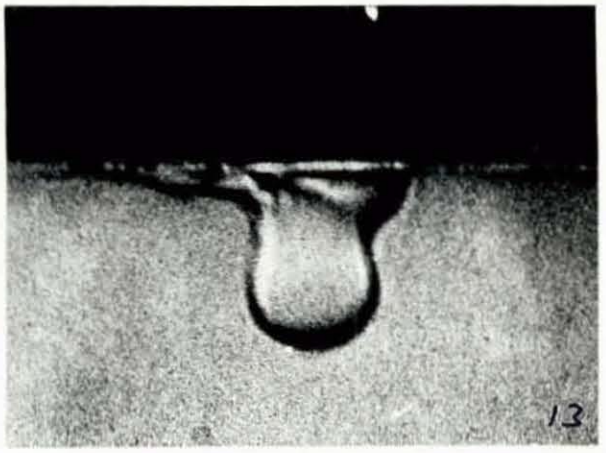
13

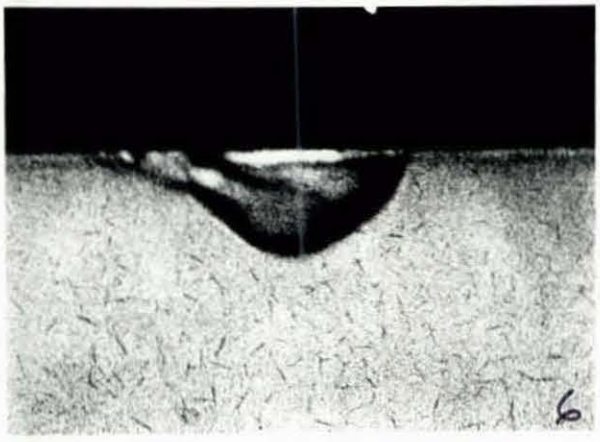
6

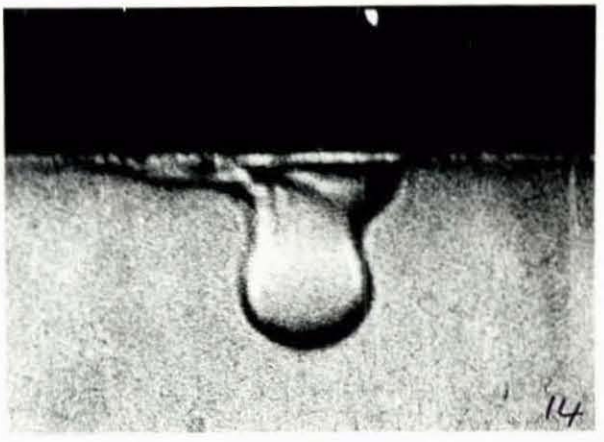
14

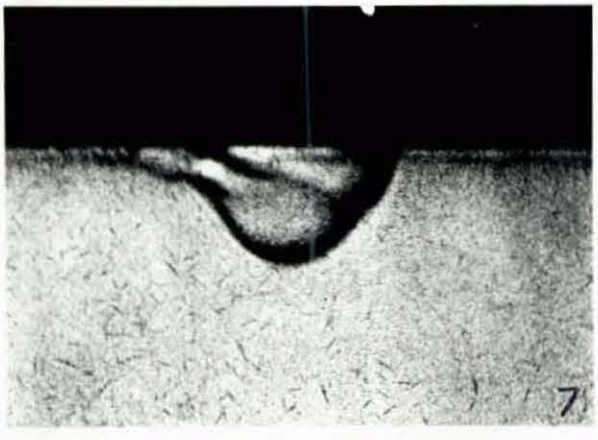
7

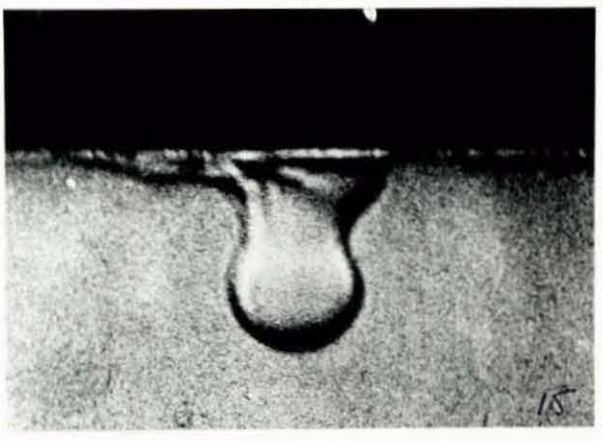
15

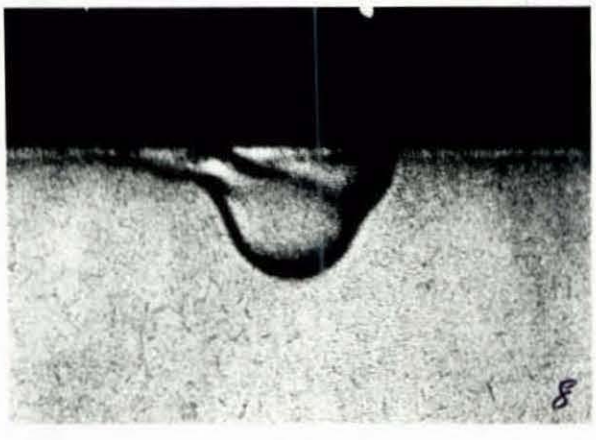
8

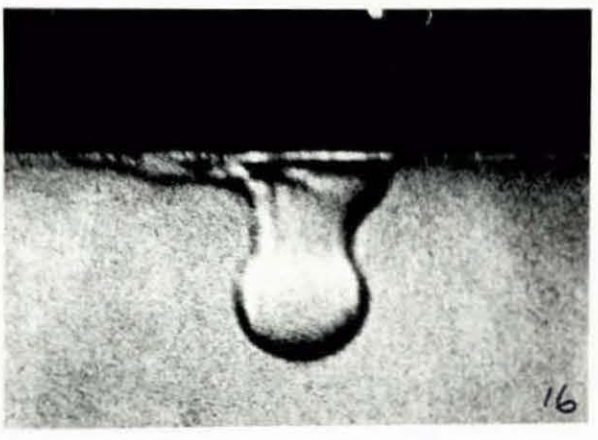
16

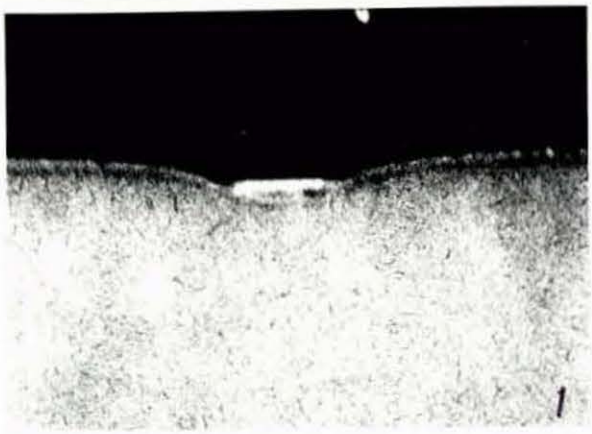
1

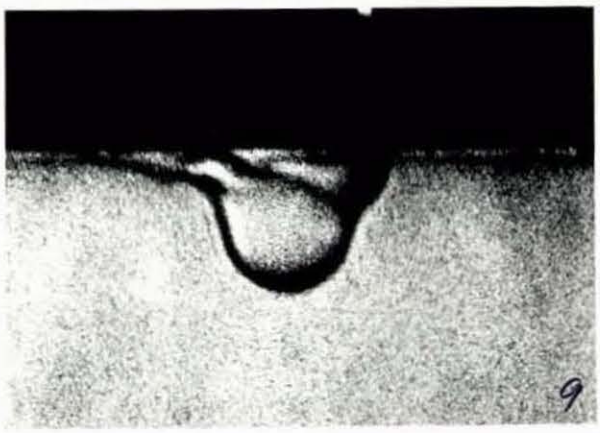
9

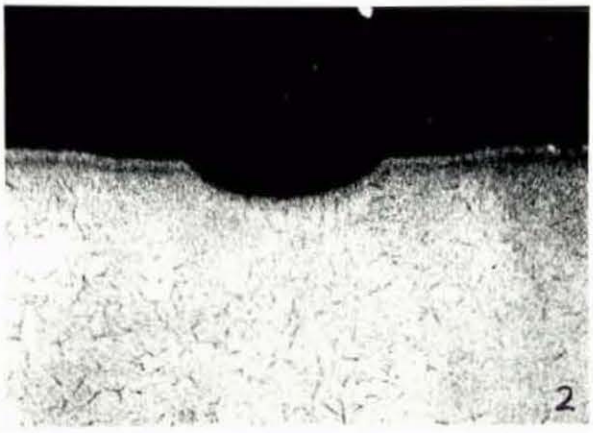
2

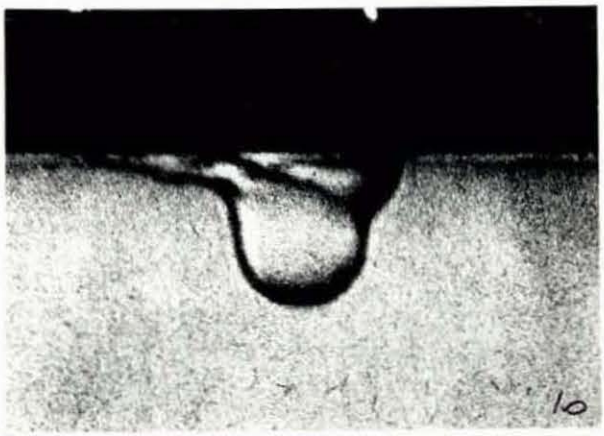
10

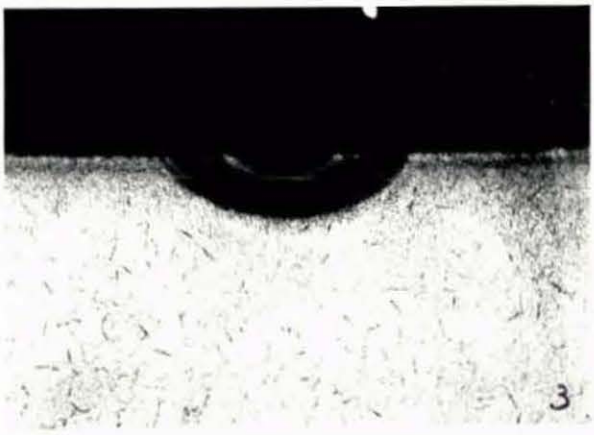
3

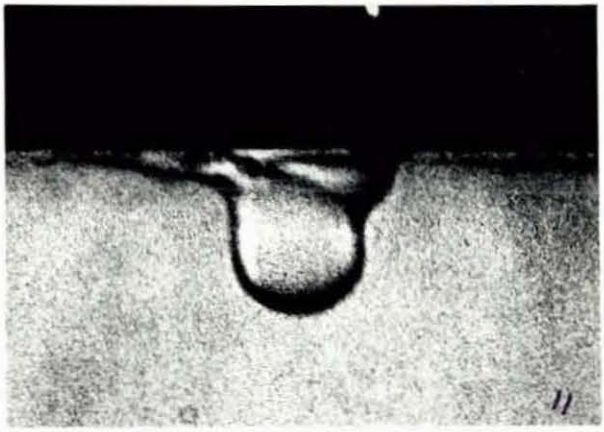
11

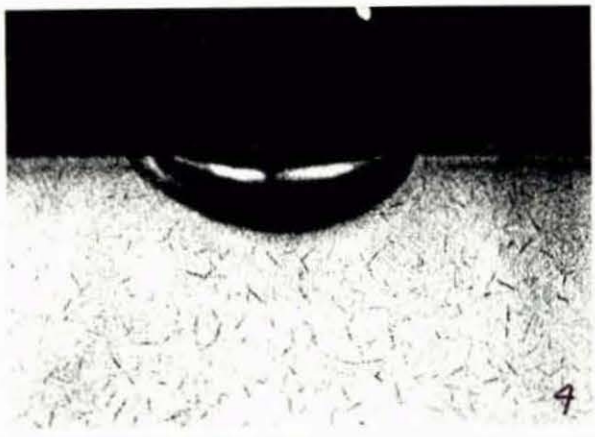
4

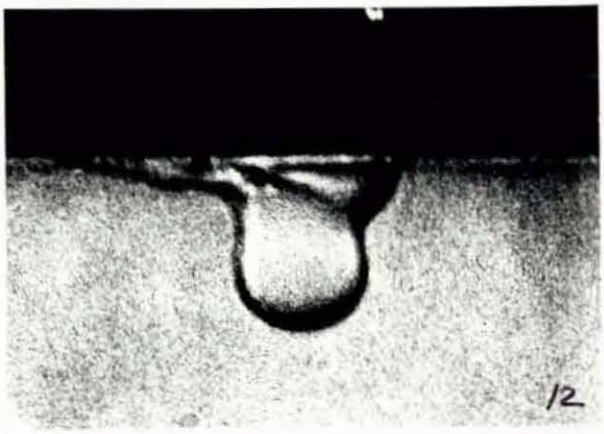
12

PHOTOGRAPH 8.P.4

Vortex Formation for Four Stages of Coalescence

System: Heptane-Water

a_1 = 0.4140 cm. L = 0 cm.

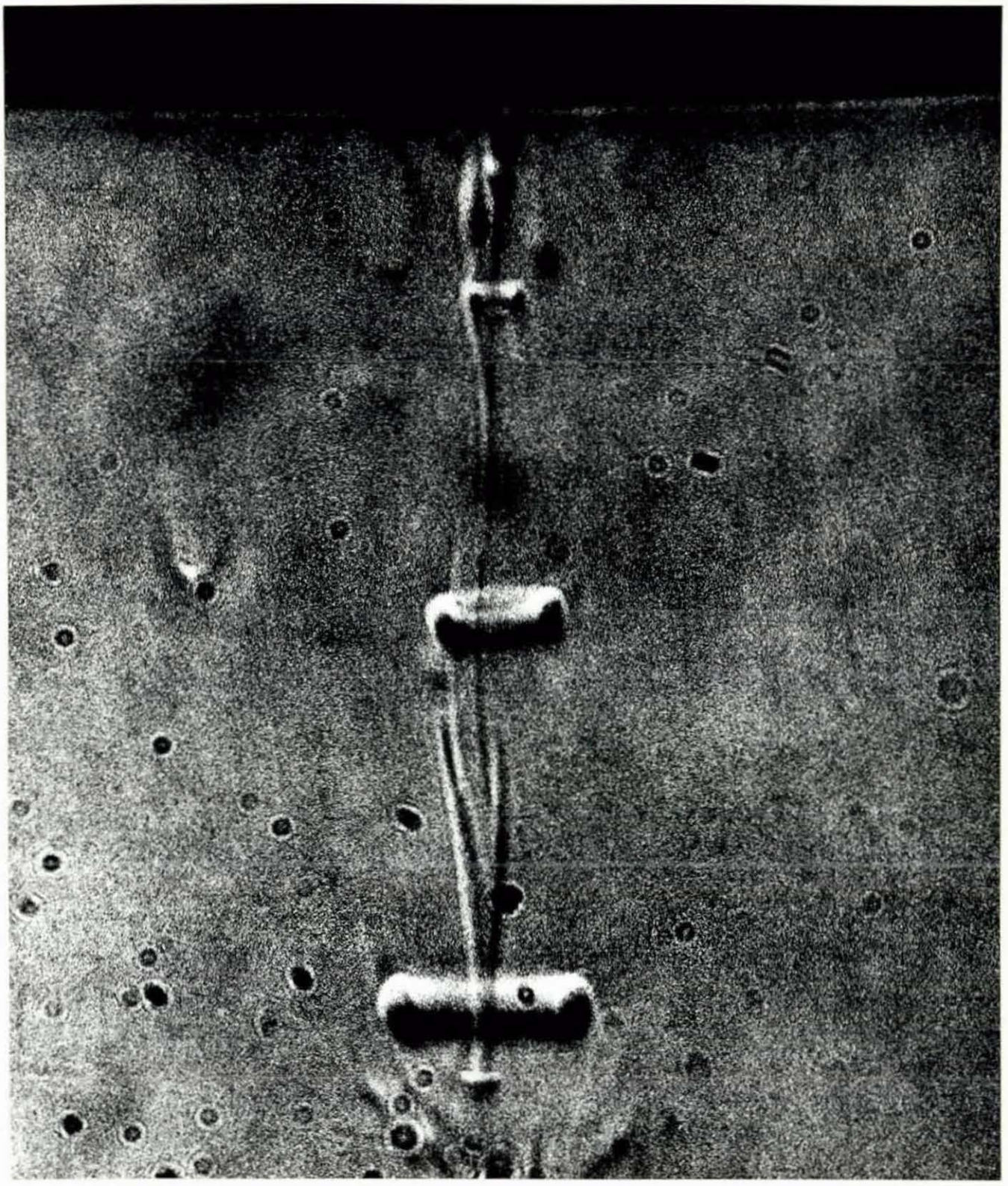

and 8.P.3 (frames 1 to 16) is concerned with the first few frames immediately after rupture of the phase-2 film has taken place. It is noticed that frames 1 to 4 in both photographs are practically identical in terms of sequence of events. These frames can be explained with reference to the high speed photographic work of Charles and Mason (16) and Lawson (82) as follows:

Frame 1: The drop is resting at the interface and the phase-2 film is on the point of rupture.

Frame 2: Rupture of the phase-2 film has taken place between frames 1 and 2 (time interval = 1/64 second). The liquid column formed from the drop is draining through the interface into the bulk phase (phase-1).

Frame 3: Instability has occurred and separation of the secondary drop has, or is about to take place.

Frame 4: The drop fluid minus the volume of fluid contained in the secondary drop has now drained completely throughthe interface. As the drop fluid expands into the homophase the bulk interface returns to its equilibrium level. The latter process is complete at frame 6 in 8.P.3 and at frame 7 in 8.P.2.

Charles and Mason (16) state that the hole in the phase-2 film expands very rapidly at speeds up to 300 cm./sec. Therefore this event takes place in an extremely short time,of the order of 1/1000 second for the size of drops considered in this work.

The time period between the initial rupture of the phase-2 film and the final separation of the secondary drop is less than the period between frames 1 and 3,i.e. less than 0.0312 seconds. Charles and Mason (16) and Lawson (82) who studied the coalescence of a large water drop at the benzene-water interface,photographically,found this period to be 0.030 and 0.0275 seconds,respectively.

It is interesting to note the presence of a 'light patch' at the dome of the interface depression in Frame 1. Reference to the tables on "Drop Shape Characteristics" in Appendix 4 shows that for the respective cases:

	System	a_1	$2x_c$	$h_{cap.}$
		cm.	cm.	cm.
Photograph 8.P.2	Heptane-Water	0.5995	0.4280	0.0476
Photograph 8.P.3	0.5% Decanoic Acid -Heptane-Water	0.4450	0.3434	0.0462

The dimensions $2x_c$, the maximum horizontal width of the phase-2 film, and $h_{cap.}$, the height of the phase-2 film, agree closely with those of the 'light patch' in frame 1. It is concluded therefore that this 'light patch' represents the extent of the phase-2 film.

The interpretation of the penetration characteristics of the droplet fluid after coalescence is best achieved by referring to the velocity profiles given in Figs. 8.6 (A and B) and 8.7 (A and B). They serve to give some idea of the way inwhich the liquid column drains throughthe interface. In Fig. 8.6 for the heptane-water system, the first profile (corresponding to frame 2 position) shows that the column drainage is greatest at the right-hand side of the film. This suggests that the initial rupture point occurred at the edge of the phase-2 film. Profiles 2 and 3 indicate that there is some, oscillatory motion set up in the liquid column. This is due to the unequal drainage of the liquid column caused by localised rupture of the phase-2 film. The oscillatory motion is superceded, and in profile 4, drainage from the centre of the column is greatly increased up to a maximum of 12.2 cm./sec. A similar process to that described above pertains in the 0.5% decanoic acid system.

The lower position of the curve at L = 2.5 cm. relative to that at L = 0 cm. in Fig. 8.5 is due to the way in which the drop fluid is dispersed in the bulk phase. This is because the disturbed motion of the interface caused by the impact of the drop considerably influences the way inwhich the liquid column drains through the interface.

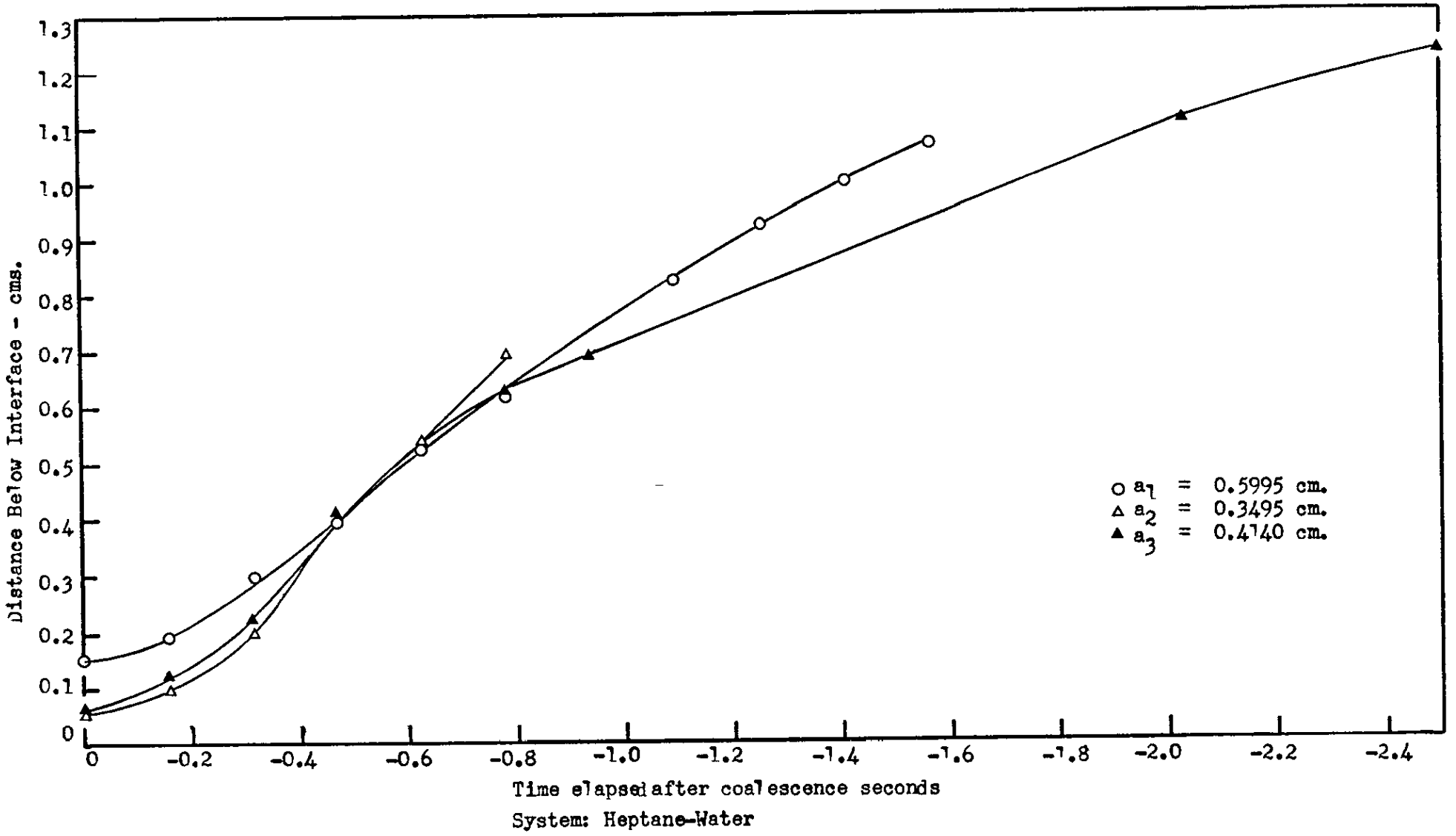

Fig. 8.4 Maximum Penetration of the Droplet Fluid into the Bulk Aqueous Phase as a Function of the Time which has Elapsed after Coalescence

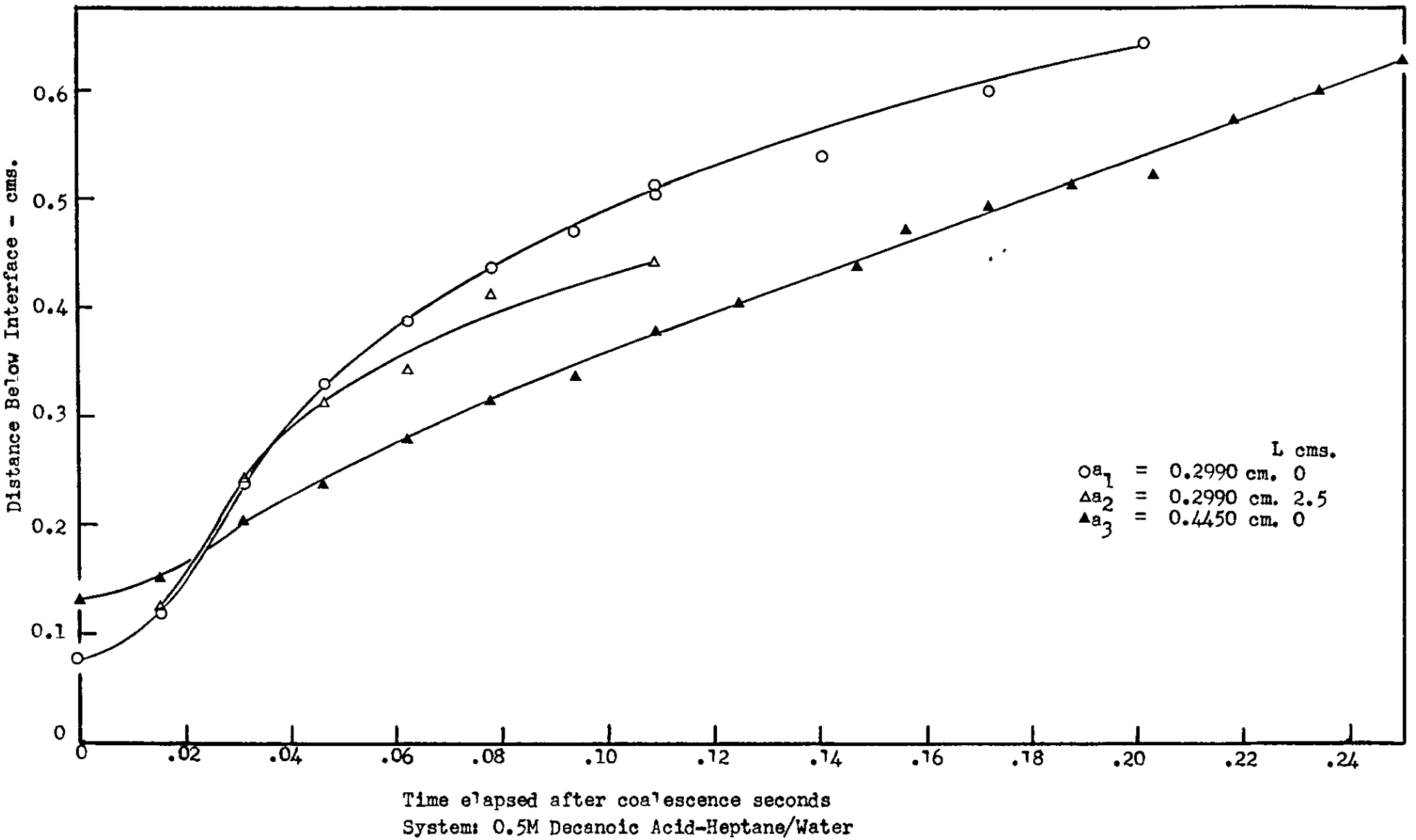

Fig. 8.5 Maximum Penetration of the Droplet Fluid into the Bulk Aqueous Phase as a Function of the Time which has Elapsed after Coalescence

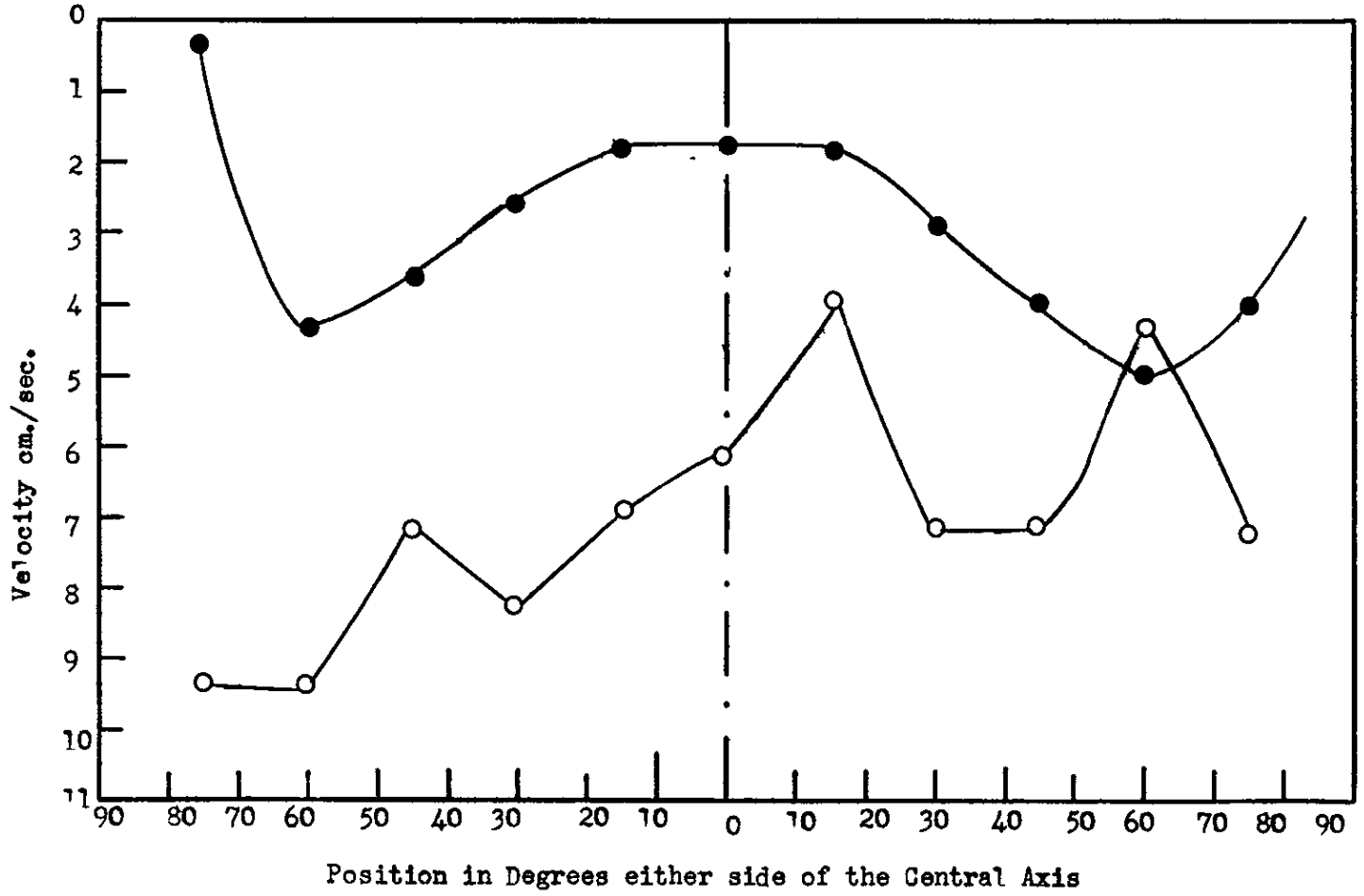

System: Heptane–Water a_1 = 0.5995 cms. L = 0 cms.

Fig. 8.6A Velocity Profile of Droplet Fluid in Aqueous Phase

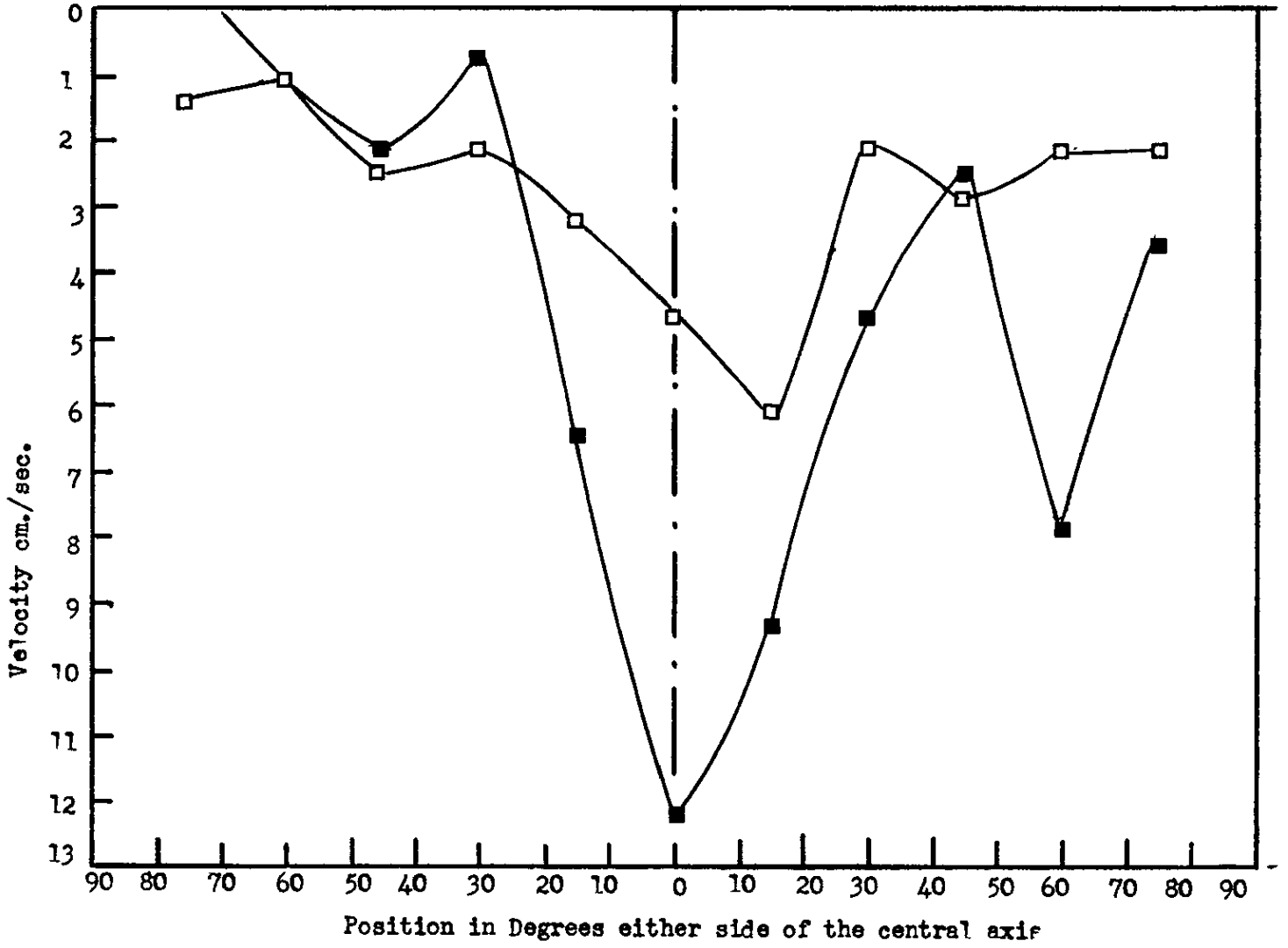

□ Position at Frame 4 (8.P.2)

■ Position at Frame 5 (8.P.2)

System Heptane-Water a_1 = 0.5995 cms. L = 0 cms.

Fig. 8.6B Velocity Profile of Droplet Fluid in Aqueous Phase

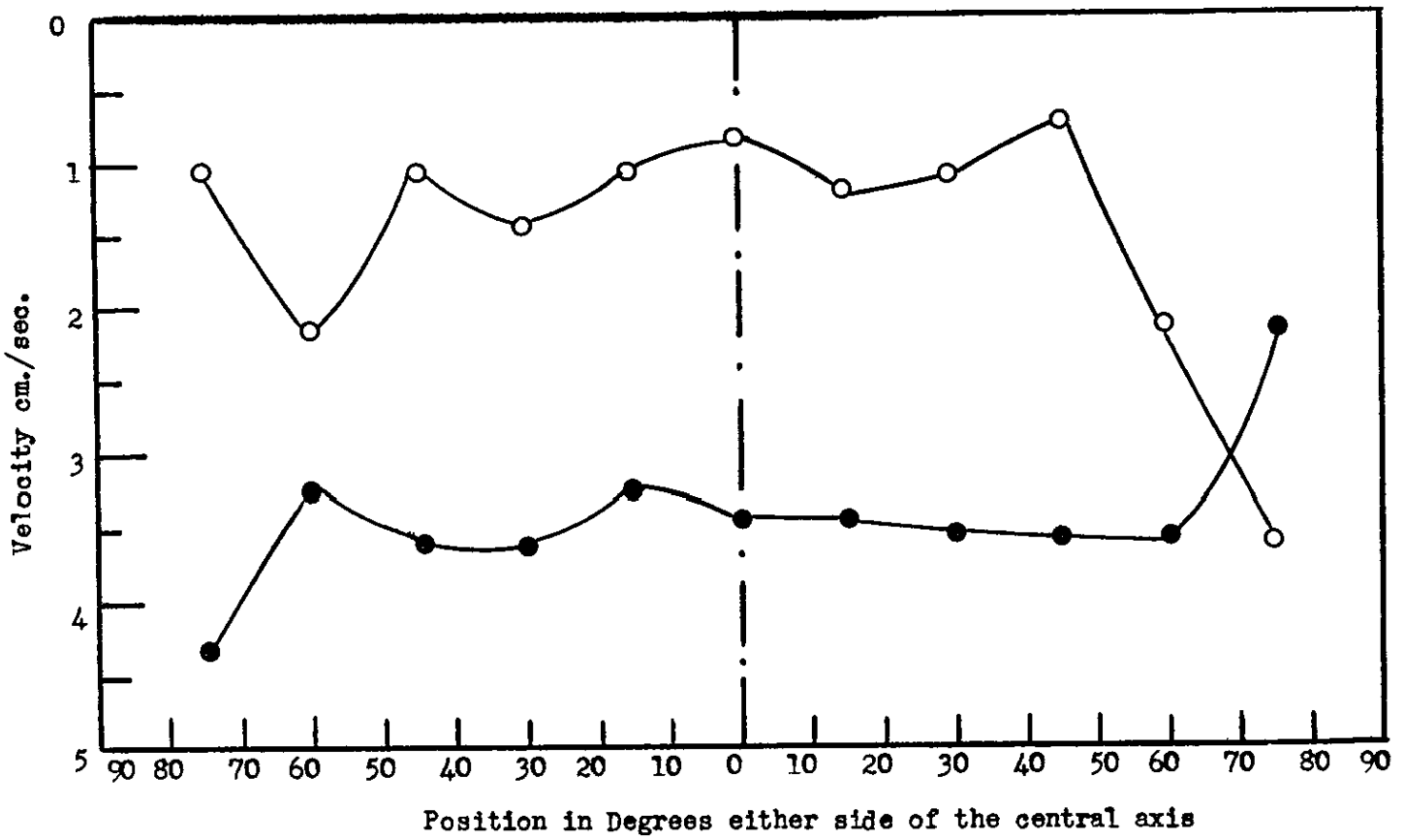

○ Position at Frame 2 (8.P.3)

● Position at Frame 3 (8.P.3)

System 0.5M Decanoic Acid a_1 = 0.445 cms. L = 0 cms.

Fig. 8.7A Velocity Profile of Droplet Fluid in Aqueous Phase

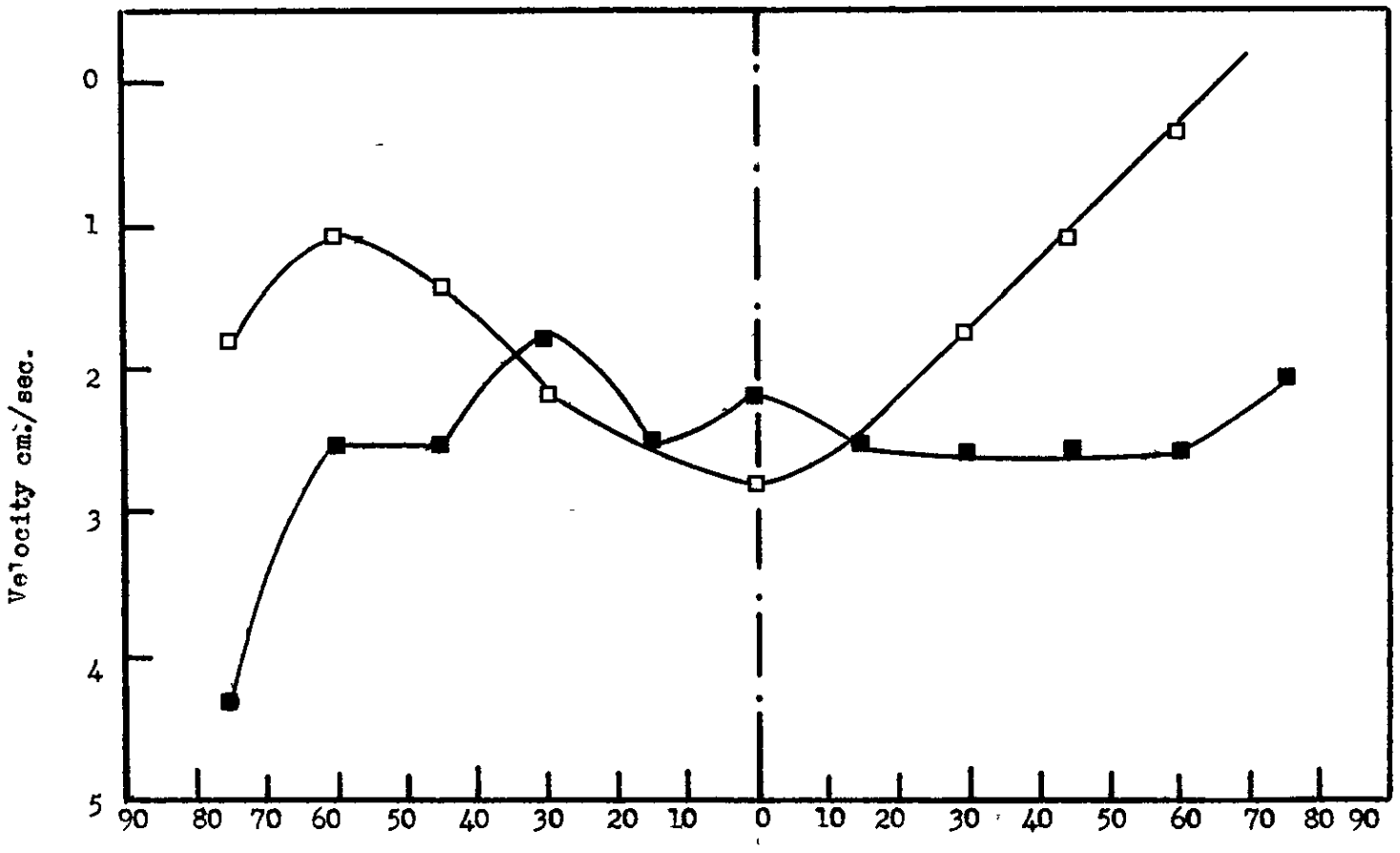

System 0.5M Decanoic Acid a_1 = 0.445 cm. L = 0 cms.

Fig. 8.7B Velocity Profile of Droplet Fluid in Bulk Aqueous Phase

CHAPTER 9

WAVE DISTURBANCES AT THE INTERFACE

Introduction

When a drop rests on a plane interface, it is separated from the interface by a film of phase-2 fluid. The upper surface of the film is inherently unstable in the presence of long wavelength disturbances, and provided the film thickness is less than a certain critical value, this will lead to rupture of the film.

The results of the investigation of coalescence of a single drop presented in Chapter 5, show that for a single size of drop in a given system, there is a distribution of coalescence rest-times. Previous workers in the field have also reported this behaviour for both purified and contaminated systems. It is important to realise, that when a drop is introduced into a system for the purpose of measuring its rest-time, a disturbance is also generated at the interface. This is especially so for large drops (i.e. greater than about 0.15 cm. diameter). The effect of increasing the fall height of the drop (up to a point where the terminal velocity is reached) is to increase the size of the disturbance at the interface. It was shown in Chapter 5, that increasing the fall height caused the coalescence rest-time to increase at all stages of coalescence. Lawson (82) has suggested that the fall height effect is essentially an equipment calibration factor. This is true in part, since a wave disturbance produced at the interface in this way will obviously be subject to the wall effect of the apparatus.

Practically all analyses to date have been based on idealised film drainage models. It is important therefore to examine the way in which disturbances at the interface can influence the coalescence process, and specifically, the drainage of the phase-2 film.

9.1 Impact of a Drop at the Interface

As part of the photographic investigation of the coalescence process, which is described in detail in Chapter 8, the profiles of the interface after

the impact of the drop and prior to coalescence, were determined (see Photograph 9.P.1). These were obtained by tracing the magnified image projected from the cine film (magnification 8.91X). The time interval between each frame is 1/64 second. Profiles for a range of drop size and fall height are presented in Figs. 9.1 to 9.13. In Figs. 9.1, 9.2, 9.4, 9.5, 9.6 and 9.11 a number of frames have been omitted from the sequences and this is indicated by a broken line. The sequence below the broken line describes the shape of the interface immediately prior to coalescence. For the purpose of analysis, the interface profiles may be treated as two-dimensional waves but in reality the disturbance is a three dimensional radial progressive wave.

The profiles presented in Figs. 9.1 to 9.13 can be divided into two groups:

(i) In this group, the interface deformation is mainly due to the weight of the drop. This is covered by the cases where the fall height of the drop is very small, i.e. L = 0 cm., Figs. 9.1, 9.2, 9.6 and 9.10.

(ii) Here the interface deformation is much greater than in (i). This is decribed by those cases for which $L > 0$ cm., i.e. at L = 2.5, 5.0, 8.5 and 13.5 cm.

For both groups (i) and (ii) the following sequence of events is observed to occur when the drop falls onto the interface; Fig. 9.2 will serve as an example:

(a) The impact of a 0.5995 cm. water drop causes the heptane-water interface to deform.

(b) The disturbance continues to grow in amplitude until it reaches a maximum about 4/64 second after impact. At this point, the amplitude of the wave is approximately 0.25 cm.

(c) The wave then decays rapidly (in approximately 5/64 second) spreading outwards over the surface of the interface.

PHOTOGRAPH 9.P.1

Impact of a Water Drop at the 0.5M Decanoic Acid-Heptane -Water Interface

a_1 = 0.4450 cm. L = 0 cm.

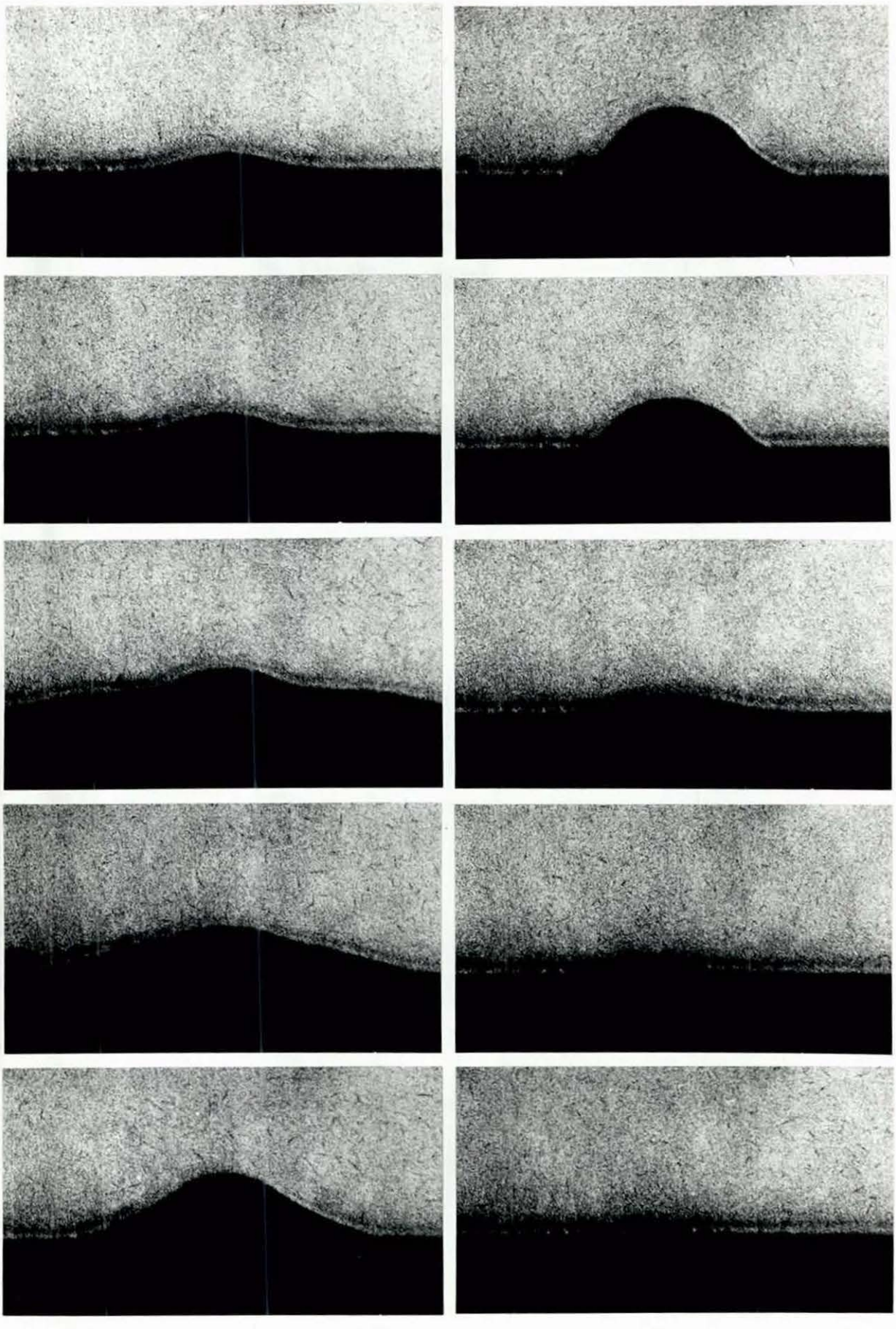

(d) After many frames have elapsed (equivalent to approximately 1 second) the interface is observed to be still in a disturbed condition. The disturbance, although not symmetrical due to the presence of the drop, is of long wave length compared to the size of the drop.

The discussion in this Chapter is concerned with those wave disturbances which can exist at the interface for periods long enough to influence the drainage of the phase-2 film. As we have just seen from the example above, the wave disturbance may still be present at the interface when the drop coalesces. Infact, it is present at the interface after coalescence of the primary drop.

It is interesting to note that in the exampleswhere L = 0 cm., e.g. Fig.9.1, there is a lack of symmetry in the lower sequences. This condition was checked by comparingwith profiles obtained under exactly the same conditions and at the same time. The same lack of symmetry was recorded. Since these were not attributable to tracing errors it must be concluded that the non-uniformity of the interface represents a wave disturbance. The amplitude of the disturbance for these cases is quite small in comparison to the size of the drop. It may, however, be extremely significant in comparison to the thickness of the draining phase-2 film.

Another interesting observation is revealed in Figs. 9.10 and 9.11 which may be important. In both cases, the drop-interface profile has moved slightly to the left in the lower sequence. The logical explanation for this occurrence would seem to be the existence of a wave disturbance.

The observations of the interface profiles suggest that the wave disturbance caused by the impact of the drop can exist for relatively long periods. It may still be present at the coalescence of the primary drop or even later stages of coalescence. To investigate this aspect more closely, the damping of wave disturbances is considered in the following section.

9.2 Damping of a Wave Disturbance

The method of computing the rate of viscous damping of surface waves was originally developed by Stokes (77). This method involves the assumptions that the flow be irrotational and that the velocity be very small at points distant from the interface. It produces results which are very similar to those which are obtained by solving the Navier-Stokes equations, even though the assumptions stated above are partially violated.

The method consists of equating the average rate of dissipation of energy, $\bar{\dot{E}}_w$, due to viscous effects, to the rate of change of energy contained in the progressive surface waves (78).

The damping of the waves is conveniently characterised by the damping factor, defined as:

$$\tau = \frac{\bar{\dot{E}}_w}{2\bar{E}_w} \qquad (9.2.1)$$

In the course of time, the energy of the wave decreases according to the law:

$$\bar{E}_w = \text{constant } (e)^{-2\tau t} \qquad (9.2.2)$$

Since the energy is proportional to the square of the amplitude, the latter decreases with time as $e^{-\tau t}$, i.e.

$$\alpha = \alpha_o e^{-\tau t} \qquad (9.2.3)$$

Using the equations for $\bar{\dot{E}}_w$ and $\bar{E}_w$, derived by Landau and Liftshitz (78) the damping factor is found to be:

$$\tau = 2\nu k^2 \qquad (9.2.4)$$

where:

$\nu = \frac{\mu_1 + \mu_2}{\rho_2 + \rho_1}$ = a pseudo kinematic viscosity (n.b. if the film is sufficiently thin, the disturbance can exist in both interfaces of the film)

$k = \omega^2/g$ = wave number

ω = frequency of wave.

$$\therefore \qquad \tau = 2\left[\frac{\mu_1 + \mu_2}{\rho_1 + \rho_2}\right]\frac{\omega^4}{g^2} \qquad (9.2.5)$$

This is the same result as obtained by Bankoff (6). Koussakov (76) computed the viscous damping factor by means of the Navier-Stokes equations and found for low viscosities:

$$\tau = \frac{2k^2\xi(\rho_1\mu_1 + \rho_2\mu_2)}{(\xi\rho_1 + \rho_2)(\rho_1 + \rho_2)} \qquad (9.2.6)$$

where $\xi = (\rho_1\mu_2/\rho_2\mu_1)^{\frac{1}{2}}$. If the viscosities of the two phases are small, Koussakov's result is very similar to that of Eqn. (9.2.5). On the basis of this comparison, the approximate method would appear to be satisfactory, provided the viscosities are low.

9.3 Decay of the Wave Energy

The surface disturbance created by a large drop falling onto a quiescent interface is gradually damped out by viscosity. Eqn. (9.2.5) indicates that at some zero time, which is a short time after the impact of the drop, the wave energy is equal to $\bar{E}_w$. If the wave energy decays to 50% of this value in time, $t_{\frac{1}{2}}$, then by Eqn. (9.2.2):

$$t_{\frac{1}{2}} = \frac{\ln 2}{2\tau} \qquad (9.3.1)$$

In a similar manner, $t_{0.99}$, the time for the wave energy to decay to 1% of its original value, i.e. 0.01 $\bar{E}_w$, is given by the expression:

$$t_{0.99} = 6.65\, t_{\frac{1}{2}} \qquad (9.3.2)$$

The value of the damping factor, τ, may be found from Eqn. (9.2.4), and $t_{\frac{1}{2}}$ can be calculated from Eqn. (9.3.1). In Fig. 9.14, $t_{\frac{1}{2}}$ is plotted against the frequency, ω, for a wide range of values of the kinematic viscosity,

ν . The curve for the heptane-water system is indicated at a value of ν = 0.00843 cm.^{2}/sec.

It was not possible to estimate values of the wave amplitude,or the frequencies,from Figs. 9.1 to 9.13. Eqn. (9.2.3) is used to estimate the amplitude of the disturbance at the heptane-water interface,t_{m1} seconds after the impact of the drop. t_{m1},is the mean coalescence time for the size of drop,where:

$$a_1 = 0.5995 \text{ cm. (as for Fig. 9.1)}$$
$$t_{m1} = 7.1 \text{ secs.}$$
$$\tau = (1.665 \times 10^{-4})\omega^4$$

It is assumed that the initial amplitude of the disturbance is α_o = 0.2 cm. Using Eqn. (9.2.3) it is found that for:

ω = 10 c.p.s. , α = 6.15 x 10^{-6} cm.

ω = 1 c.p.s. , α = 0.2 cm.

Discussion

The experimentally determined profiles given in Figs. 9.1 to 9.13 indicate that the interface is still in a disturbed condition for some time after the impact of the drop. This is true for all the cases investigated, at both high and low values of L. The curves for $t_{\frac{1}{2}}$ vs.ω ,presented in Fig. 9.14 reveal that the half-life decay time of the wave can be large for low viscosity systems (i.e.$\nu \leqslant$ 0.01 cm.^{2}/sec.). In the case of the systems studied in this work,it is possible for $t_{\frac{1}{2}}$ to be greater than the measured coalescence rest-time,and even greater than the overall rest-time,$\hat{t}$.

Knowing that the wave disturbance can continue to exist at the interface for long periods of time,the question is asked,"How does it influence the coalescence process ?" The work of Lang (78) has already shown that the upper surface of the phase-2 film is inherently unstable to long wave length disturbances and so the film may rupture in this way. Before rupture of the phase-2 film can occur though,it must thin down to a certain critical thickness,or below. The experimental evidence on film thickness is

small but the work of MacKay and Mason (88) has shown that in liquid-liquid systems the film thickness in the region of rupture may be less than 500 $\mathring{A}$.

The rate of attenuation of the wave disturbance is determined mainly by the value of the damping factor (see Eqn. (9.2.3)). If the amplitude of the wave disturbance is comparable,or greater than the thickness of the draining film,then it is reasonable to suggest that the wave motion will influence the drainage process of the film. The precise manner inwhich the wave motion interferes with the film is complex. This is because of interaction between wave fronts due to rebound at the walls of the apparatus. A common observation supporting this behaviour is that the drop is often observed to meander slightly whilst resting at the flat interface.

In summary,it is concluded that wave motion at the interface will have a significant effect on the rate of drainage of the phase-2 film, for at least the visible stages of coalescence. This would appear,in part, to be a logical explanation for the existence of the residence time distribution observed in single drop coalescence studies.

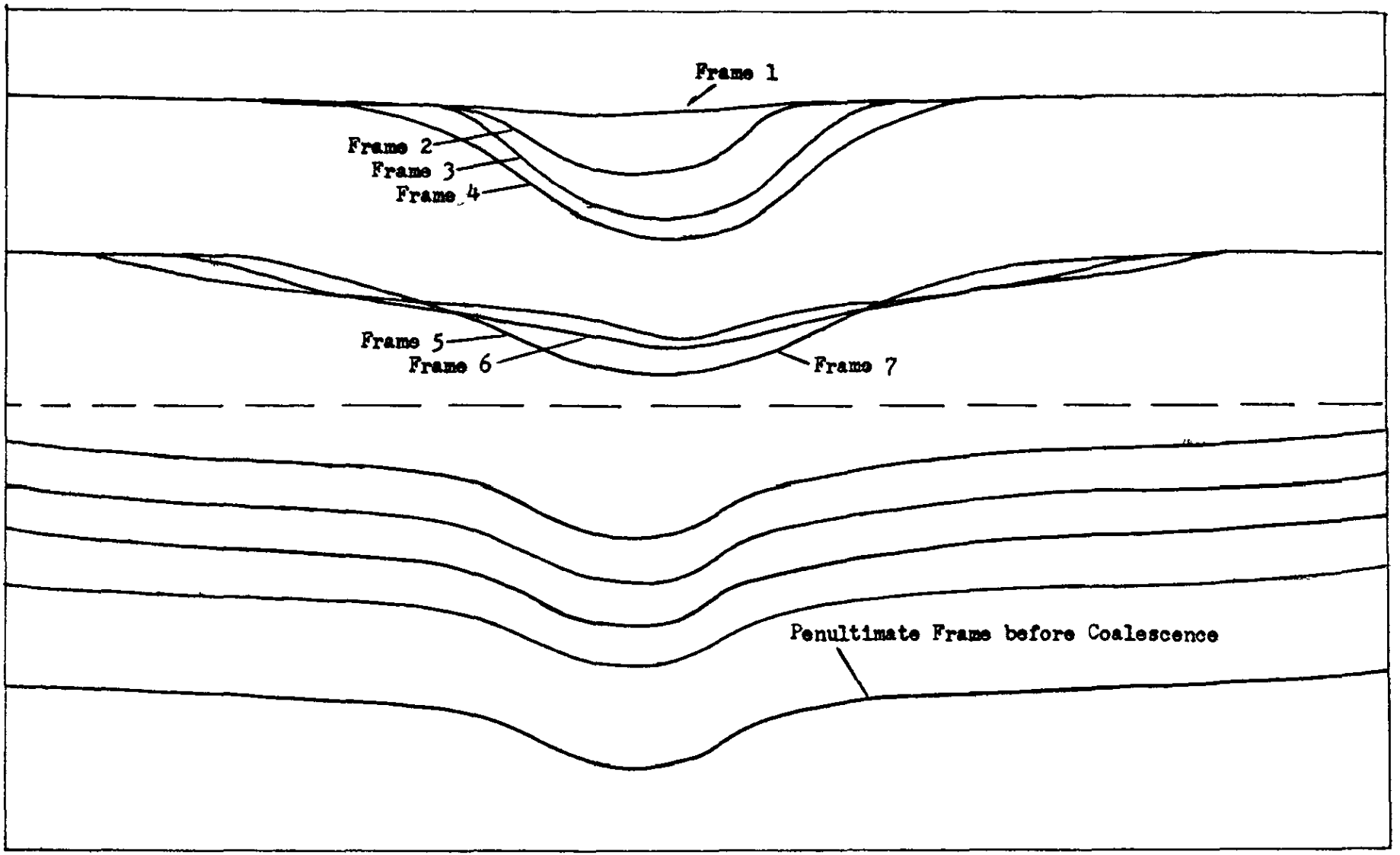

System: Heptane-Water

a_1 = 0.5995 cms. L = 0 cms.

Fig. 9.1 Drop-Interface Profiles

(All Profiles One Frame Apart unless indicated otherwise)

(1 Frame Difference = 0.0156 secs.)

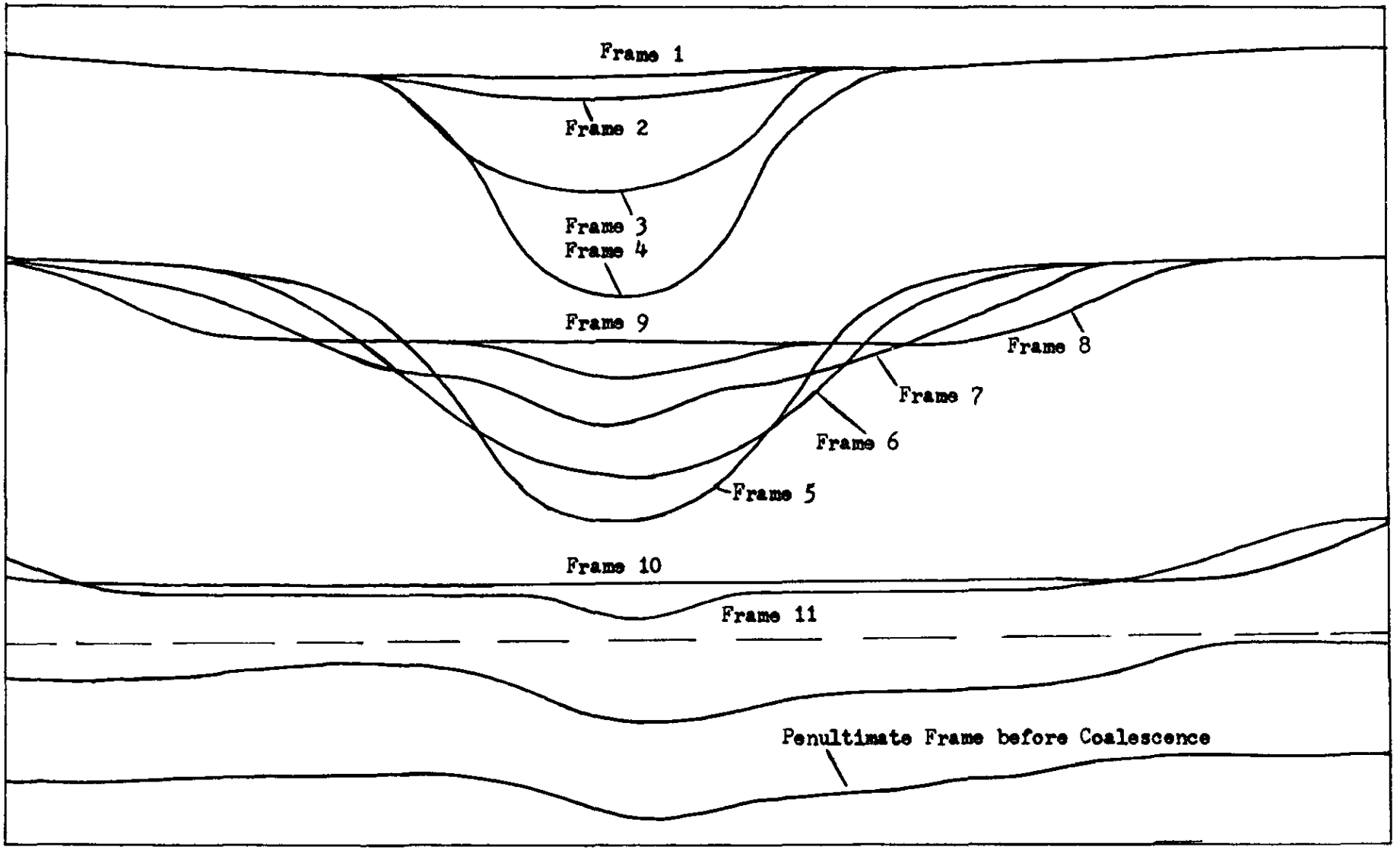

System: Heptane–Water a_1 = 0.5995cms. L = 2.5 cms.

Fig. 9.2 Drop-Interface Profiles

(All Profiles One Frame Apart unless indicated otherwise)

(1 Frame Difference = 0.0156 secs)

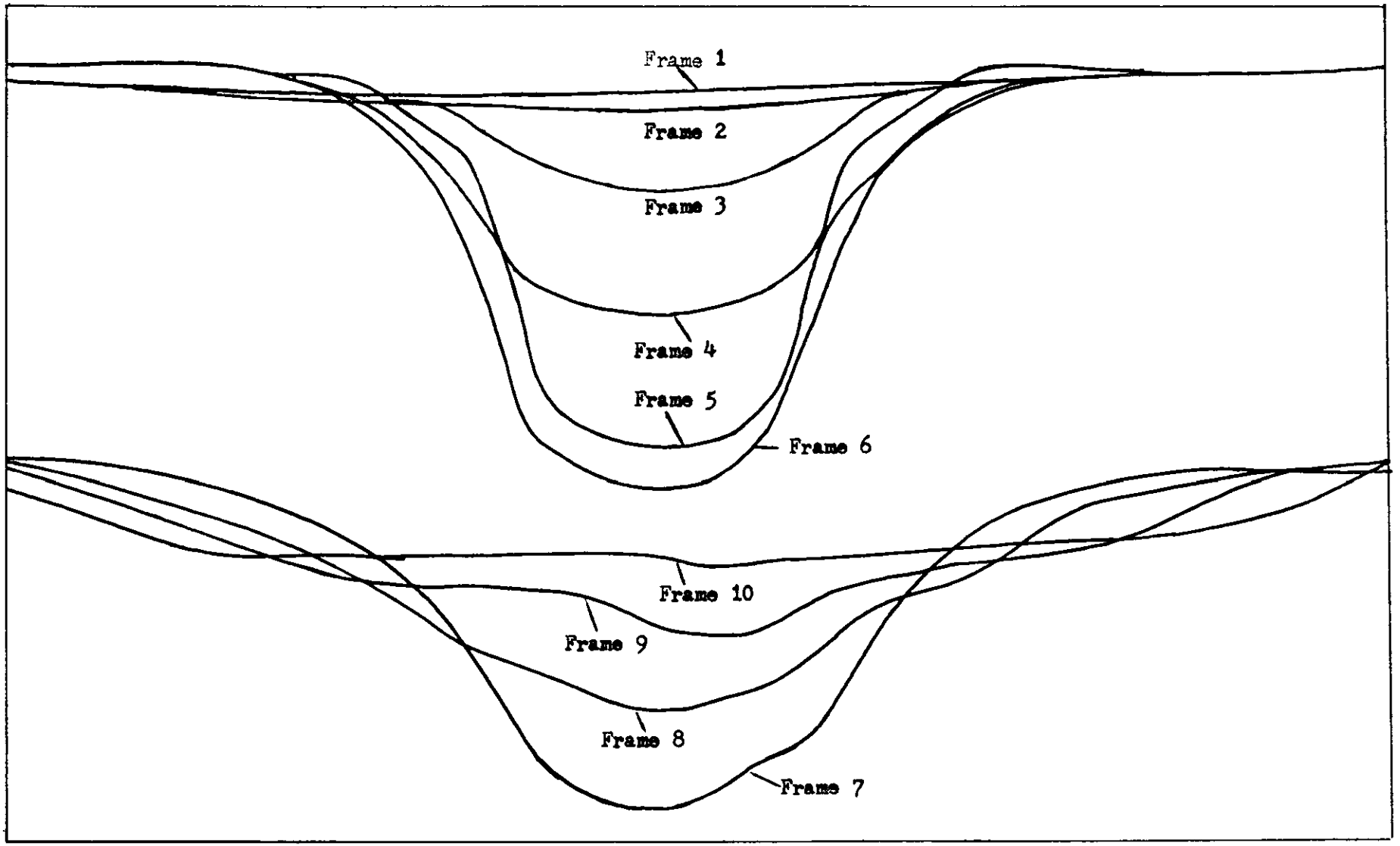

System: Heptane-Water a_1 = 0.5995 cms. L = 5.0 cms.

Fig. 9.3 Drop-Interface Profiles

(All Profiles One Frame Apart Unless Indicated Otherwise)

(1 Frame Difference = 0.0156 secs.)

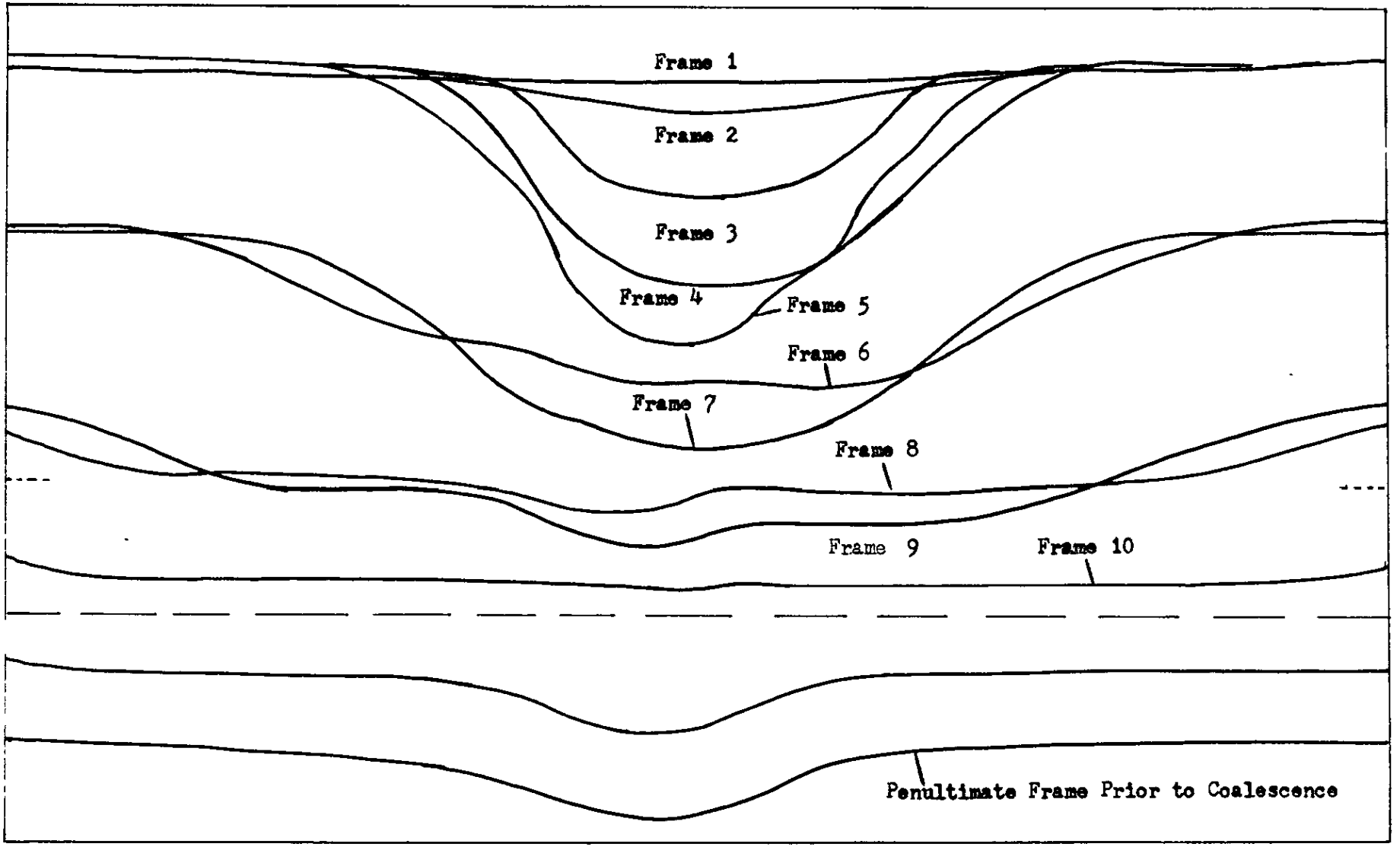

System: Heptane-Water a_1 = 0.5995 cms. L = 5.0 cms.

Fig. 9.4 Drop-Interface Profiles

(All Profiles One Frame Apart Unless Indicated Otherwise)

(1 Frame Difference = 0.0156 secs.)

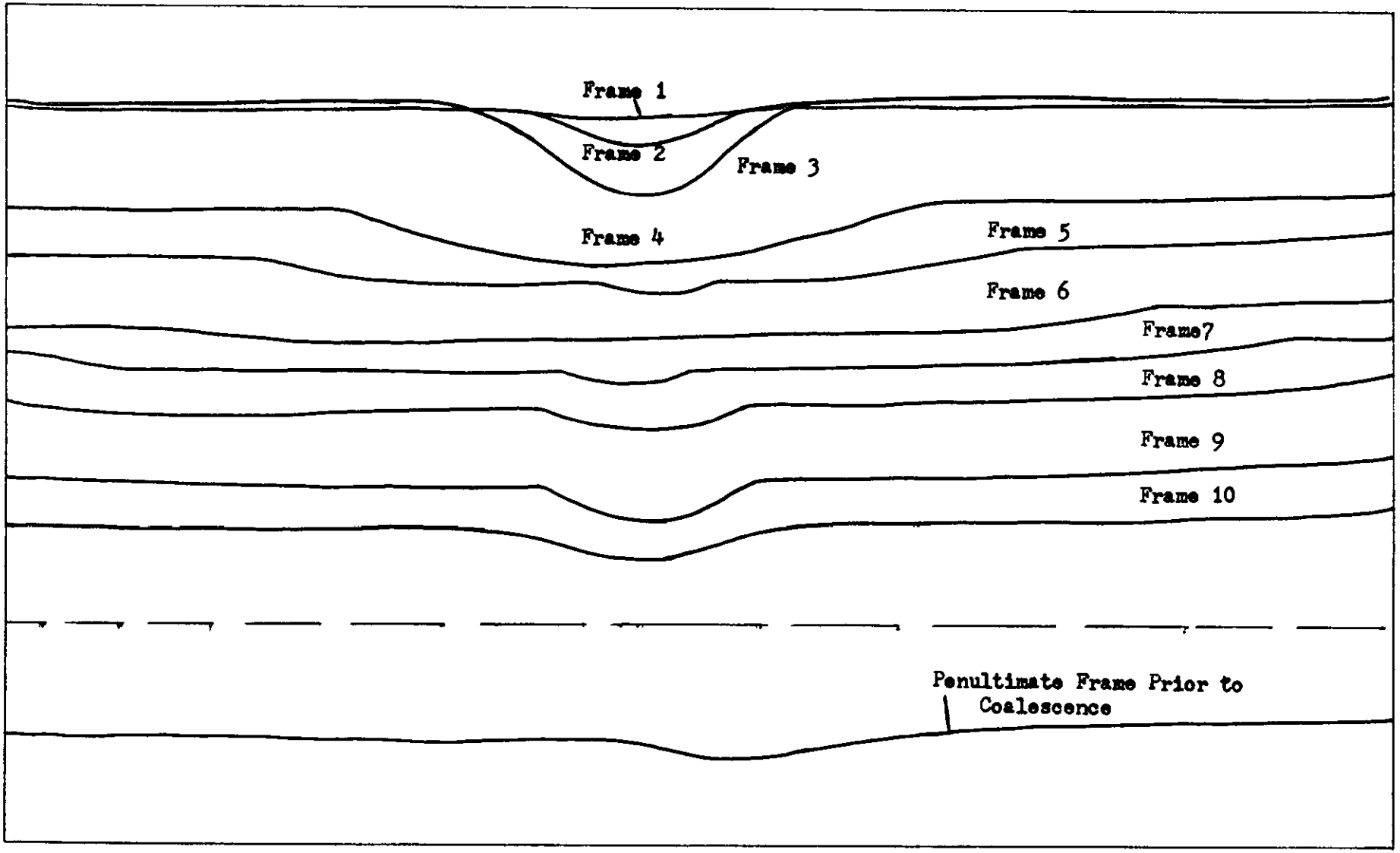

System: Heptane-Water

a_1 = 0.4140 cms. L = 0 cms.

Fig. 9.5 Drop-Interface Profiles

(All Profiles One Frame Apart Unless Indicated Otherwise)
(1 Frame Difference = 0.0156 secs.)

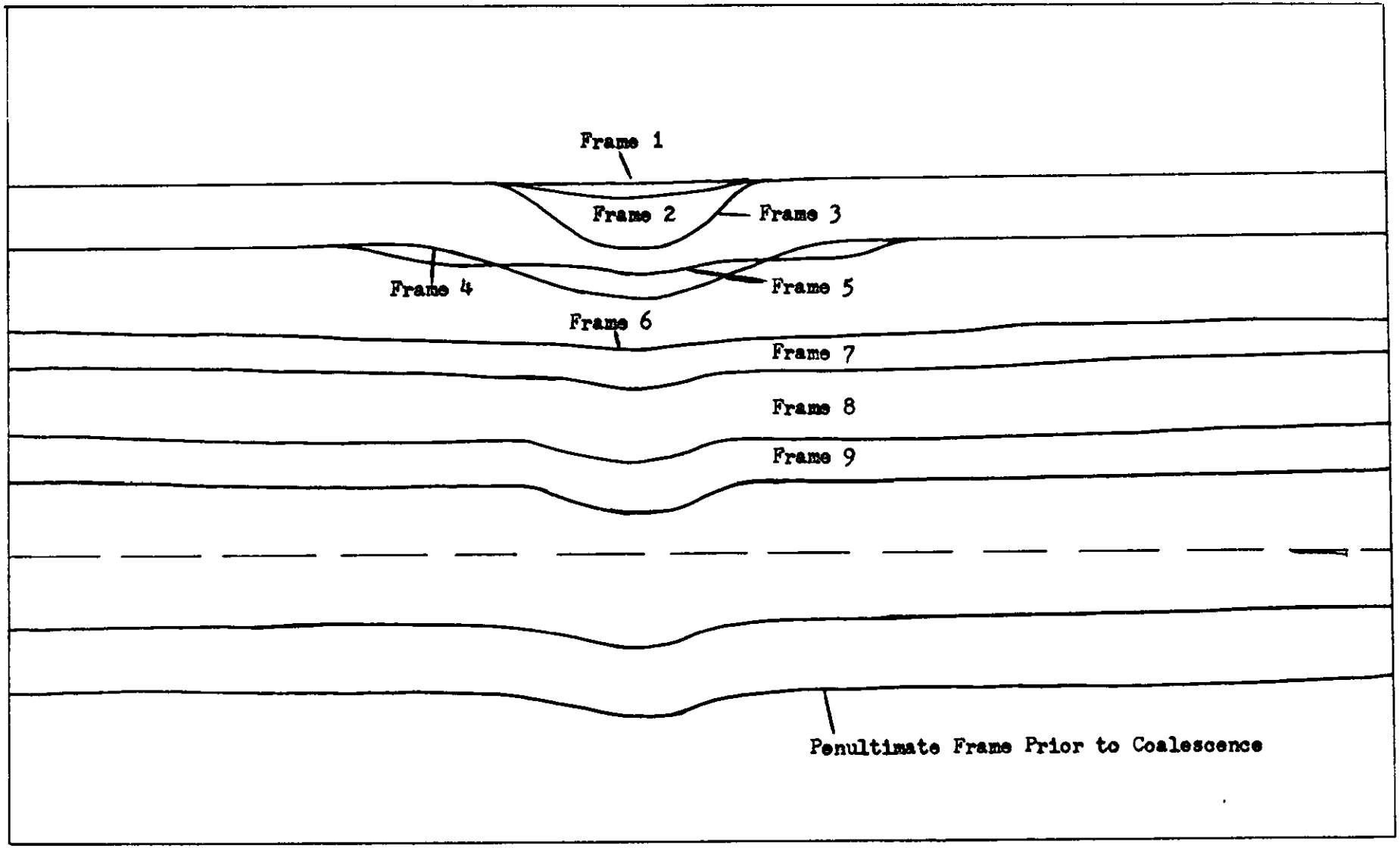

System 0.5M Decanoic Acid-Heptane/Water a_1 = 0.2990 cms. L = 0 cms.

Fig. 9.6 Drop-Interface Profiles

(All Profiles One Frame Apart Unless Indicated Otherwise)

(1 Frame Difference = 0.0156 secs.)

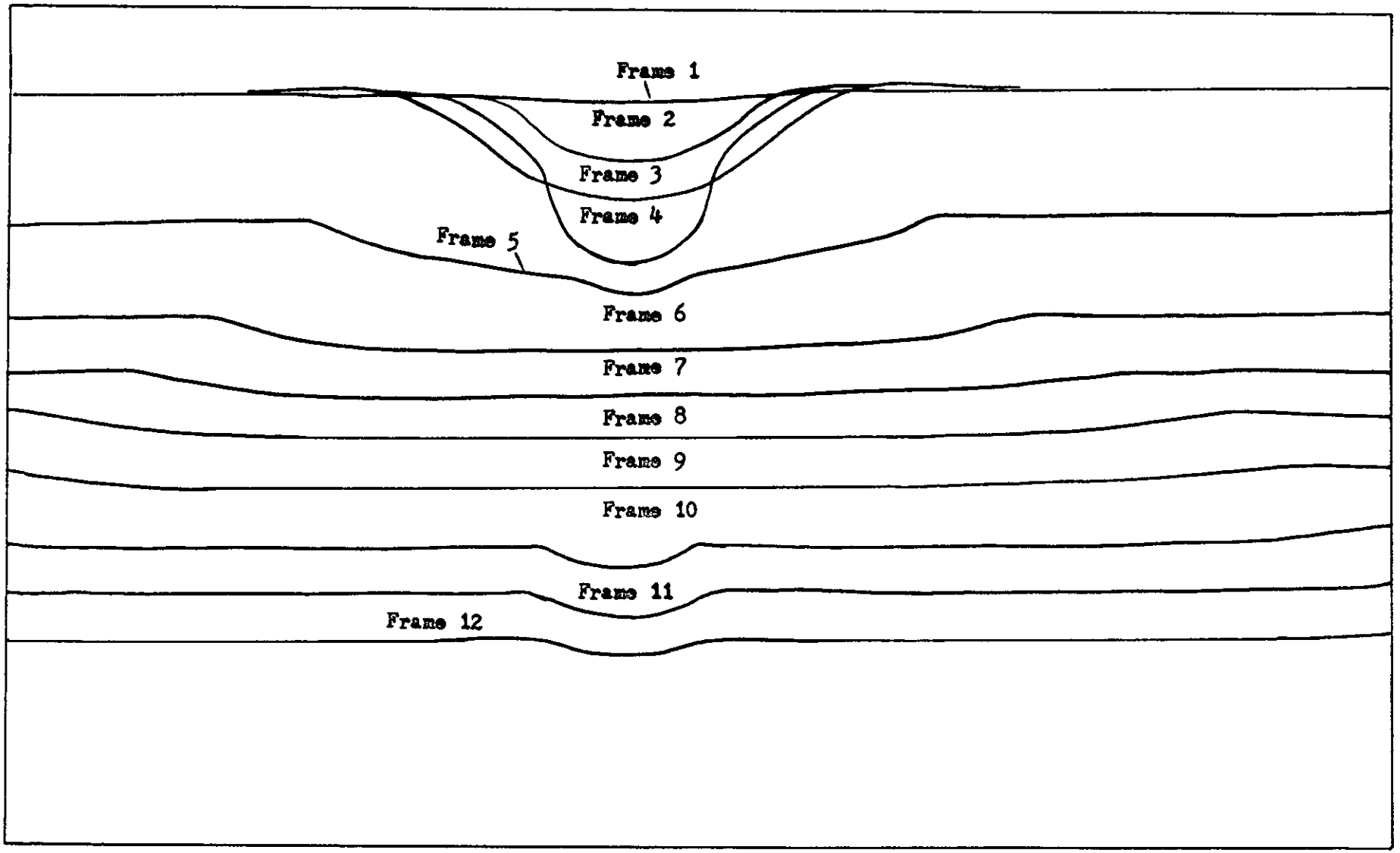

System 0.5M Decanoic Acid-Heptane/Water a_1 = 0.2990 cms. L = 5.0 cms.

Fig. 9.7 Drop-Interface Profiles

(All Profiles One Frame Apart Unless Indicated Otherwise Indicated)

(1 Frame Difference = 0.0156 secs.)

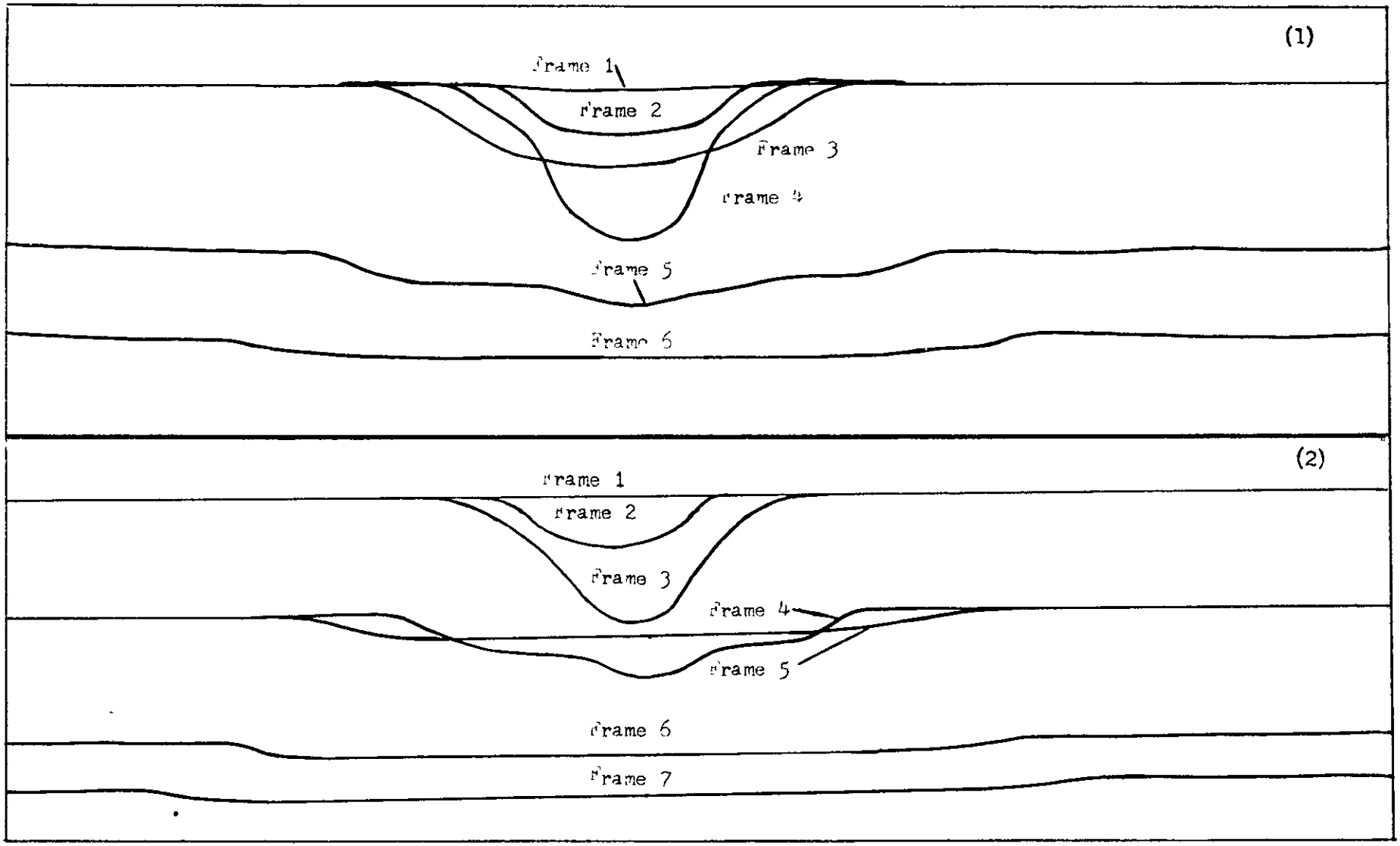

(1) a_1 = 0.2990 cms. L = 13.5 cms. System: 0.5M Decanoic Acid-Heptane/Water

Fig. 9.8 (1) Drop-Interface Profiles

(2) a_1 = 0.2770 cms. L = 13.5 cms. System 0.5M Decanoic Acid-Heptane/Water

Fig. 9.9 (2) Drop-Interface Profiles

All profiles one frame apart unless otherwise stated
1 frame difference = 0.0156 secs.

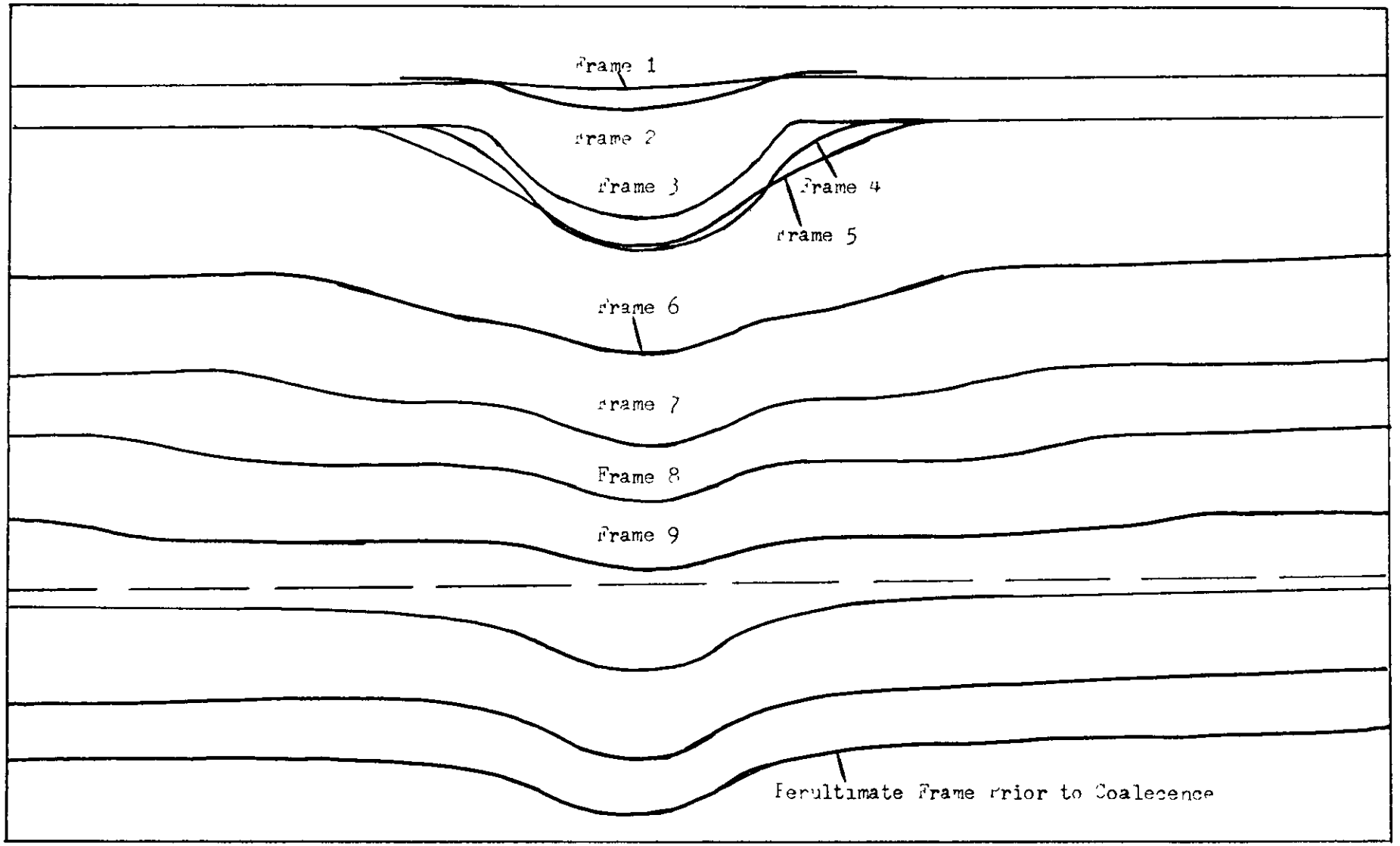

System: 0.5M Decanoic Acid-Heptane/Water

a_1 = 0.4450 cms. L = 0 cms.

Fig. 9.10 Drop-Interface Profiles

(All Profiles One Frame Apart unless Indicated Otherwise)

(1 frame Difference = 0.0156 secs.)

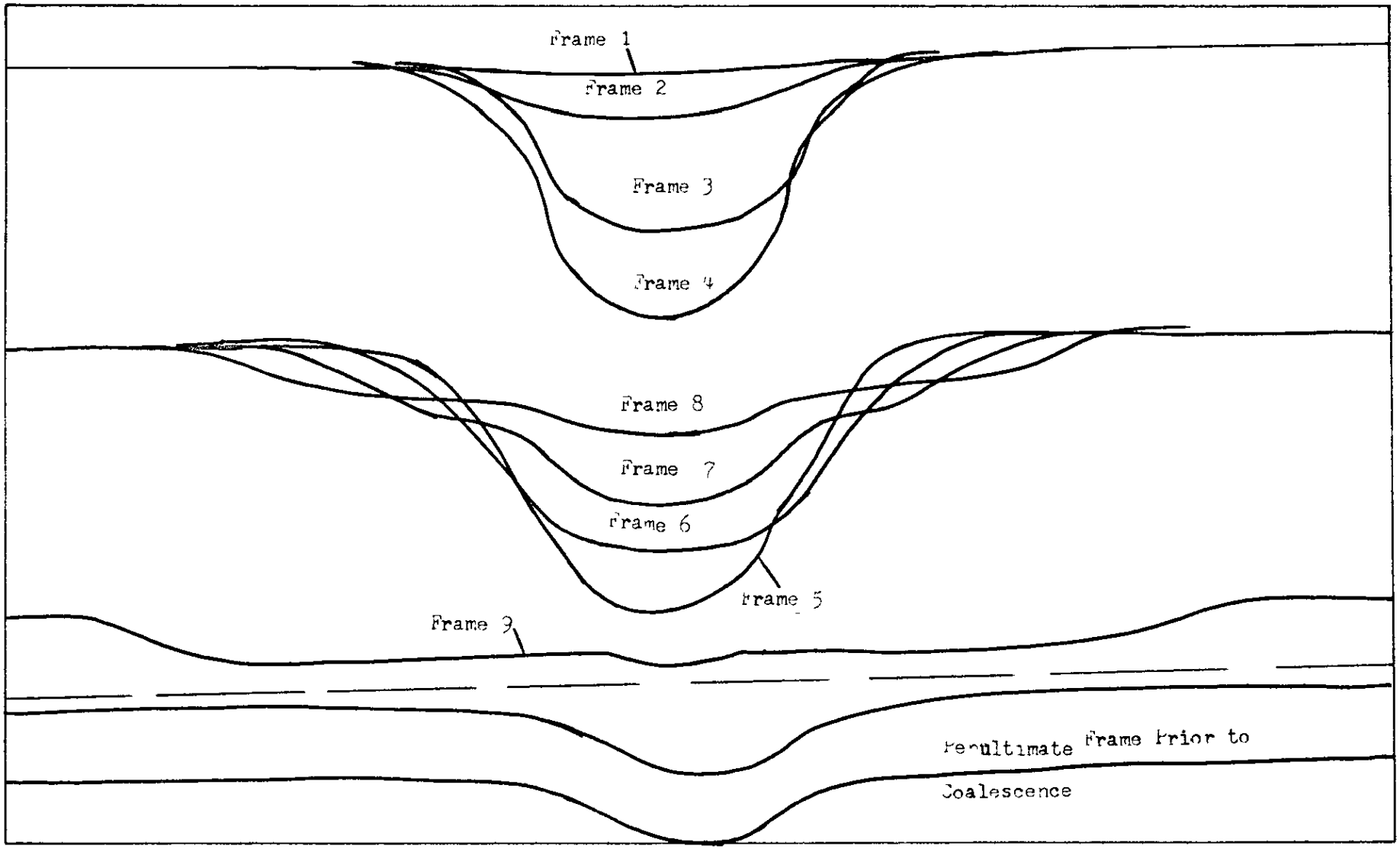

System: 0.5M Decanoic Acid-Heptane/Water a_1 = 0.4450 cms. L = 2.5 cms.

Fig. 9.11 Drop-Interface Profiles

(All Profiles One Frame Apart unless Indicated Otherwise)

1 Frame Difference = 0.0156 secs.

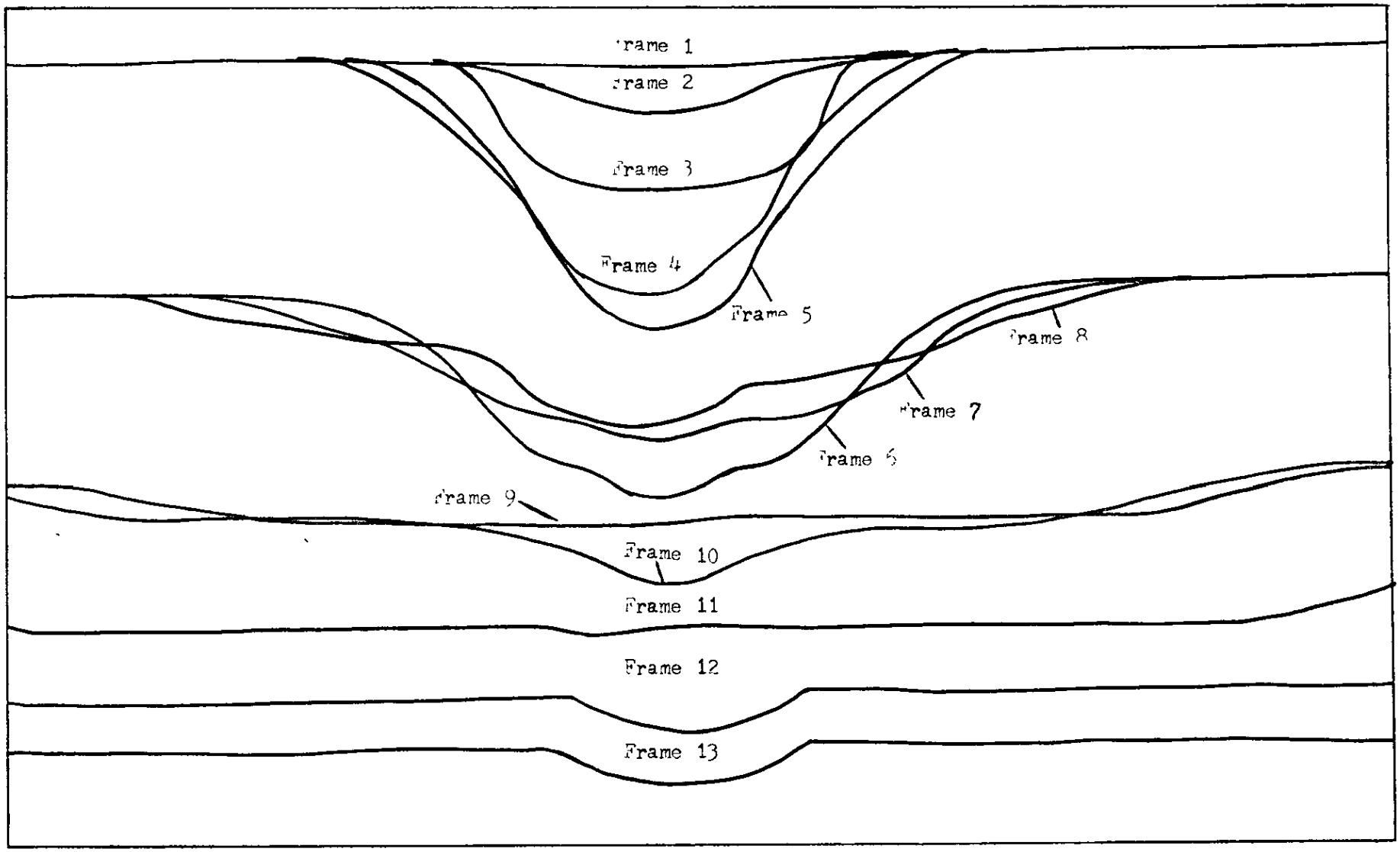

System: 0.5M Decanoic Acid-Heptane/Water a_1 = 0.4450 cms. L = 5.0 cms.

Fig.9.12 Drop-Interface Profiles

(All Profiles One Frame Apart Unless Indicated Otherwise)

(1 Frame Difference = 0.0156 secs.)

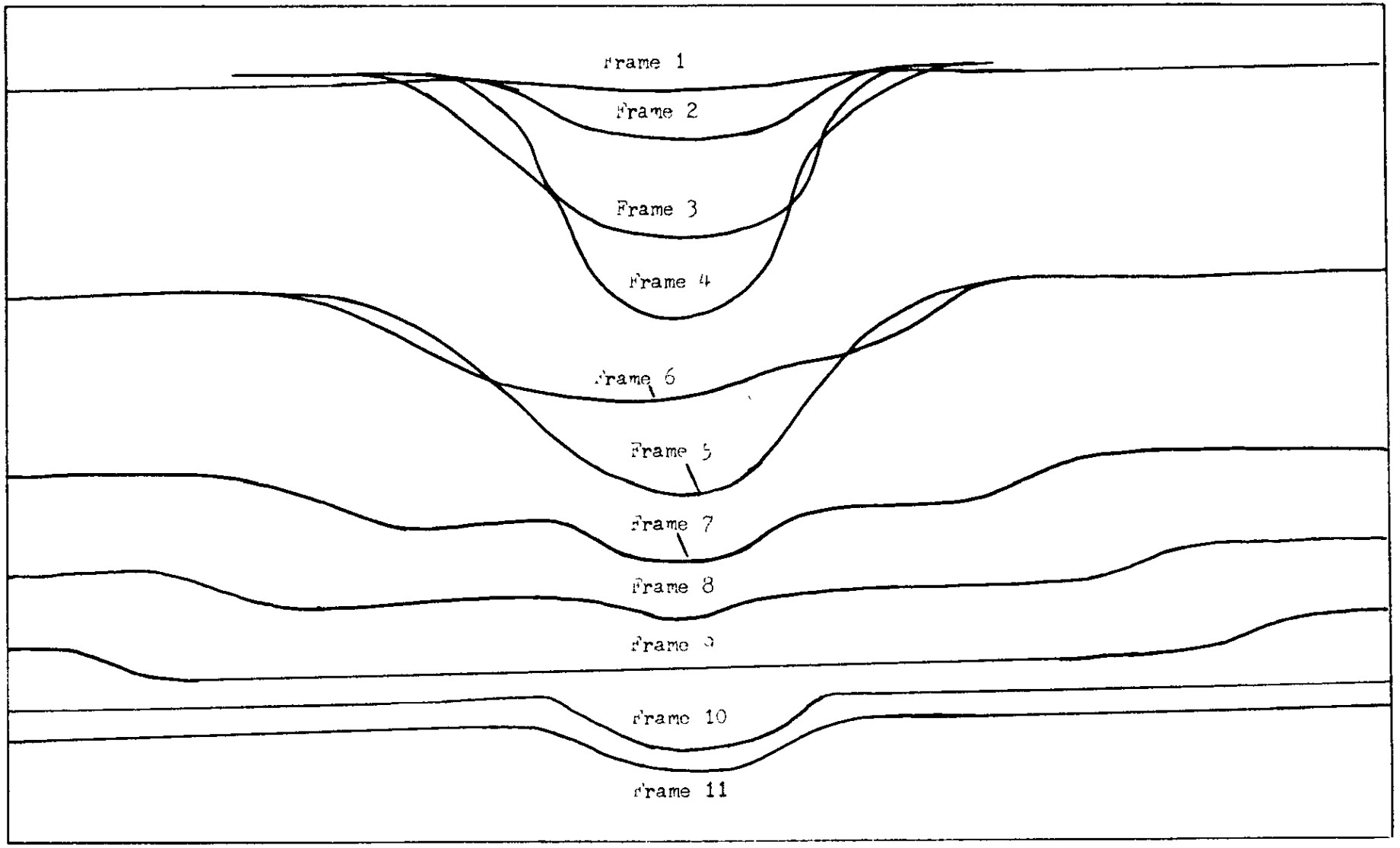

System: 0.5M Decanoic Acid-Heptane/Water a_1 = 0.4450 cms. L = 13.5 cms.

Fig.9.13 Drop-Interface Profiles

(All profiles [illegible] frame apart unless Indicated Otherwise)
1 frame difference = 2.0156 secs

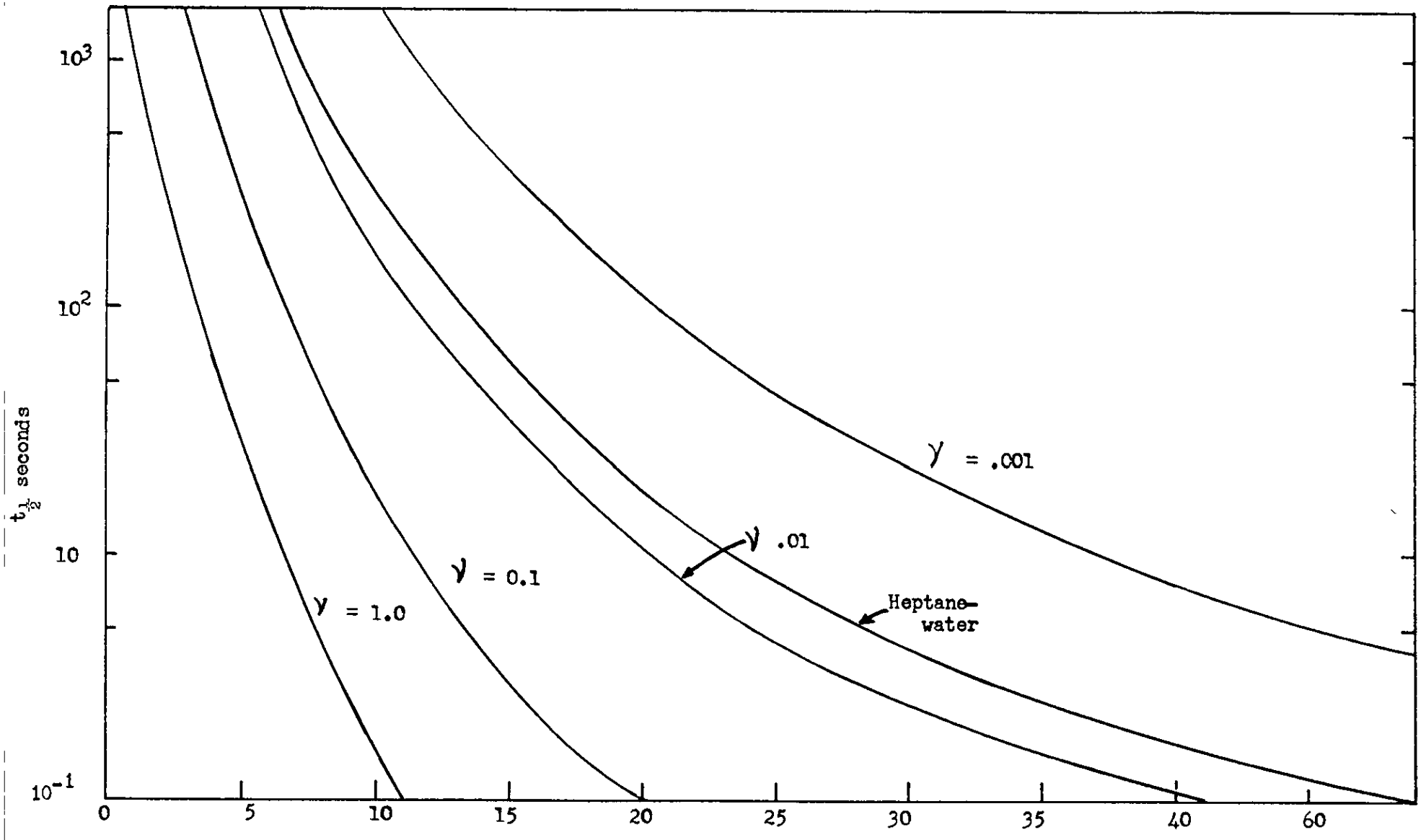

Fig. 9.14 Half life decay time ($t_{\frac{1}{2}}$) for gravity waves at an interface

CHAPTER 10

CONCLUSIONS AND SUGGESTIONS FOR FUTURE WORK

10.1 Conclusions

This study consists of a theoretical and experimental investigation of the coalescence of single droplets at a plane liquid-liquid interface. The conclusions which may be drawn from this work are as follows:

1. The values of t, t_m, $t_{\frac{1}{2}}$ and t_{max} increased with increasing size of drop. This trend was observed for all stages of coalescence.

   For the heptane-water system, there is a linear relation between the mean rest-time and size of drop at all stages of coalescence.

   There is a specific relationship between the mean rest-time and size of drop for a given stage in the coalescence process.

2. The rest-time distributions, for all stages of coalescence, in both two and three-component systems can be correlated by the following equations:

$$\ln \frac{N}{N_o} = -k(t - t_o)^{n1}$$

and

$$\ln \frac{N}{N_o} = -ct^{n2}$$

   The value of n_1 and n_2 in these equations increases with the stage of coalescence. However, the usefulness of the second equation, in the case of later stages of coalescence,

is limited because n_2 has high values.

An approximately linear relation is exhibited by the standard deviations between adjacent coalescence stage rest-time distributions.

3. The coalescence rest-time increased with increase in fall height of the primary drop. This increase occurred at all stages of coalescence in the heptane-water system.

The standard deviation of coalescence rest-time distributions is markedly reduced by increasing the fall height of the primary drop. This was observed for all stages of coalescence.

The droplet size of second and third stages of coalescence are dependent on the distance of fall of the primary drop on to the interface. However, there is not a simple relation between these variables. In the heptane-water case, the drop size increased whereas in the 0.5M decanoic acid/heptane-water case, it decreased.

4. There is a linear relation between the drop diameter ratio r_1, and the size of primary drop for the systems A and C. Thus, there is a linear relation between the size of drop before coalescence and the size of drop produced by coalescence.

The value of r_3 is approximately 0.5, independent of the system.

5. An expression for the rate of thinning of the continuous phase film has been developed. The model on which it is based is shown to lie somewhere between the parallel-plates model and the spherical-planar model. Comparison of predicted

drainage times with experimental coalescence rest-times suggests that a satisfactory agreement will be obtained for small drops (less than 0.01 cm. diameter).

6. A correlation between the mean rest-time t_m, and the physical variables a, $\Delta\rho$, μ_2, γ and L has been developed.

7. The phenomenon of "double drop" coalescence (i.e. the formation of a satellite drop with the secondary) only occurs when the values of the interfacial tension and the size of the primary drop are sufficiently large.

8. Disturbances of long wavelength and small amplitude can exist at the interface for appreciable periods. These time periods can be comparable to the coalescence rest-time, or much longer. The rest-time distribution may thus, be partly explained, on the basis of the effect of long wavelength disturbances on the rate drainage of the phase-2 film.

10.2 Suggestions for Further Study

1. The theoretical prediction of the rate of film drainage should be developed further, particularly for the case of large drops. A complication which will have to be allowed for is the effect of interface movement. The scope of this type of investigation would be greatly enhanced by undertaking a numerical solution of the full Navier-Stokes equations. This could be suitably accomplished by the recently developed Marker and Cell technique (MAC) (132), using a powerful high speed computer.

2. In view of the difficulties which have been experienced with experimental single drop studies, it is essential that the approach be simplified as much as possible. The main effort should be concentrated on the single drop situation rather than studying large numbers of drops. Experiments should be devised so that the rest-time, film thickness and rate of film drainage can be measured simultaneously. It is important that the experiments be tied in closely with a suitable theoretical treatment, e.g. as in 1. There will continue to be some need for carrying out further rest-time distribution studies, particularly for comparing effects in different systems. However, manual recording of single drop rest-times is notoriously slow and is a serious drawback to experimentation.

APPENDIX

APPENDIX 1

PHYSICAL PROPERTIES OF SOLUTIONS AT 25°C

System	Phase	Density $gm.cm.^{-3}$	Viscosity c.p.	Interfacial Tension dynes cm^{-1}
Heptane/Water	1	0.9968	0.9270	50.75
	2	0.6810	0.4158	
0.05M Decanoic Acid-	1	0.9935	0.9241	32.41
Heptane/Water	2	0.6833	0.4257	
0.5M Decanoic Acid-	1	0.9952	0.9286	22.54
Heptane/Water	2	0.7003	0.5194	
1.0M Decanoic Acid-	1	0.9964	0.8962	18.62
Heptane/Water	2	0.7232	0.6406	

APPENDIX 2

TABLES OF N/N_o AGAINST t

N = Number of drops which have not coalesced in time t

N_o = Total Number of drops assessed

t = coalescence time, seconds

The fraction N/N_o corresponds to a range of t up to the value of t given, e.g. in Series A1/1(i), $N/N_o = 0.9200$ corresponds to $0 < t < 2$ and $N/N_o = 0.7600$ corresponds to $2 < t < 4$, etc. The actual minimum and maximum values of t are given in Appendix 3.

In Series A1/1 the sample count ($N_o = 150$) is split into two parts to provide two distributions, namely; A1/1(i) which refers to the first part of the count ($N_o = 75$) and A1/1(ii) which refers to the second part of the count ($N_o = 75$). This also applies to the Series A1/2, A1/3, A1/5 and A1/6.

Contents

Series A1/1(i)

t_1	N/N_o	t_2	N/N_o	t_3	N/N_o	t_4	N/N_o
2	0.9200	1	0.9734	1.4	0.9867	0.3	0.8534
4	0.7600	2	0.9468	1.5	0.9601	0.4	0.5734
6	0.6934	3	0.9202	1.6	0.9201	0.5	0.2134
8	0.5734	4	0.8002	1.7	0.8669	0.6	0.0401
10	0.3868	5	0.6802	1.8	0.7069	0.7	0.0135
12	0.2535	6	0.5202	1.9	0.5603	0.9	0.0002
14	0.1869	7	0.4536	2.0	0.3603		
16	0.1069	8	0.3070	2.1	0.1870		
20	0.0537	9	0.2404	2.2	0.0537		
22	0.0137	10	0.0271	2.3	0.0137		
28	0.0004	11	0.0005	2.5	0.0004		

Series A1/1(ii)

t_1	N/N_o	t_2	N/N_o	t_3	N/N_o	t_4	N/N_o
4	0.9316	2	0.9726	1.4	0.9867	0.3	0.9452
6	0.8358	3	0.9452	1.7	0.9734	0.4	0.4932
8	0.7126	4	0.9178	1.8	0.9068	0.5	0.0960
10	0.5756	5	0.9041	1.9	0.7735	0.6	0.0139
12	0.4661	6	0.7946	2.0	0.5335	0.8	0.0002
14	0.3155	7	0.6576	2.1			
16	0.2334	8	0.3289				
18	0.1513	9	0.1646				
20	0.1239	10	0.0276				
22	0.1102	11	0.0002				
24	0.0692						
28	0.0144						
30	0.0007						

Series A1/2(i)

t_1	N/N_o	t_2	N/N_o	t_3	N/N_o	t_4	N/N_o
2	0.9867	2	0.9871	1.6	0.9734	0.3	0.9734
4	0.8934	3	0.9742	1.9	0.9334	0.4	0.6401
6	0.8402	4	0.9483	2.0	0.8401	0.5	0.2801
8	0.7870	5	0.9224	2.1	0.5868	0.6	0.0135
10	0.6937	6	0.8965	2.2	0.1468	0.8	0.0002
12	0.6004	6.5	0.8576	2.3	0.0402		
14	0.4804	7	0.8317	2.4	0.0002		
16	0.3738	7.5	0.7538				
18	0.2938	8	0.5980				
20	0.2005	8.5	0.4682				
22	0.1473	9	0.2734				
24	0.0807	10	0.0397				
26	0.0674	11	0.0009				
30	0.0408						
32	0.0142						
34	0.0009						

Series A1/2(ii)

t_1	N/N_o	t_2	N/N_o	t_3	N/N_o	t_4	N/N_o
2	0.9595	3	0.9865	1.6	0.9867	0.3	0.9468
4	0.6758	4	0.9730	1.8	0.9467	0.4	0.6002
6	0.5272	4.5	0.9190	1.9	0.8001	0.5	0.3202
8	0.4191	5	0.8785	2.0	0.5868	0.6	0.0402
10	0.3651	5.5	0.7975	2.1	0.3868	0.7	0.0002
12	0.2706	6	0.7300	2.2	0.0935		
14	0.1896	6.5	0.6895	2.3	0.0403		
16	0.1491	7	0.6085	2.4	0.0003		
18	0.1221	7.5	0.4599				
20	0.0816	8	0.3383				
22	0.0546	8.5	0.2708				
24	0.0276	9	0.1763				
26	0.0141	9.5	0.0547				
30	0.0006	10	0.0007				

Series A1/3(i)

t_1	N/N_o	t_2	N/N_o	t_3	N/N_o	t_4	N/N_o
2	0.8948	1	0.9869	0.8	0.9867	0.3	0.9868
4	0.7238	2	0.9475	1.2	0.9734	0.5	0.9336
6	0.5528	3	0.8694	1.6	0.9601	0.6	0.8670
8	0.3423	4	0.8168	2.0	0.9335	0.7	0.7337
10	0.2502	5	0.7387	2.2	0.9202	0.8	0.4671
12	0.1845	6	0.6861	2.4	0.8936	0.9	0.2005
14	0.1582	7	0.6335	2.6	0.8536	1.0	0.0272
16	0.1319	8	0.5678	3.0	0.8004	1.1	0.0006
18	0.1056	9	0.5152	3.2	0.7738		
22	0.0793	10	0.4495	3.4	0.6672		
24	0.0399	11	0.3969	3.6	0.5472		
26	0.0136	12	0.3188	3.8	0.4139		
42	0.0005	13	0.2662	4.0	0.2806		
		14	0.2005	4.2	0.0673		
		15	0.1479	4.4	0.0273		
		16	0.0558	4.6	0.0140		
		17	0.0164	8.6	0.0007		
		18	0.0033				

Series A1/3(ii)

t_1	N/N_o	t_2	N/N_o	t_3	N/N_o	t_4	N/N_o
2.5	0.9468	2	0.9734	1.8	0.9734	0.5	0.9865
5	0.7468	3	0.9334	2.0	0.9601	0.6	0.9730
7.5	0.6002	4	0.8802	2.2	0.9335	0.7	0.7839
10	0.4536	5	0.8270	2.4	0.9202	0.8	0.6353
12.5	0.3070	6	0.7337	2.6	0.9069	0.9	0.2570
15	0.2670	7	0.6671	2.8	0.8669	1.0	0.1219
17.5	0.2004	8	0.5871	3.0	0.7869	1.1	0.0409
22.5	0.1738	9	0.5339	3.2	0.6403	1.2	0.0139
27.5	0.1338	10	0.4273	3.4	0.5737	1.3	0.0004
30	0.0938	11	0.3873	3.6	0.4804		
32.5	0.0805	12	0.3341	3.8	0.3604		
35	0.0672	13	0.2809	4.0	0.2804		
37.5	0.0539	14	0.2676	4.2	0.1338		
40	0.0406	15	0.2410	4.4	0.0405		
42.5	0.0273	16	0.1344	4.6	0.0139		
50	0.0140	17	0.0678	5.2	0.0006		
62.5	0.0007	18	0.0146				
		19	0.0013				

Series A1/4

t_1	N/N_o	t_2	N/N_o	t_3	N/N_o	t_4	N/N_o
1	0.9200	2	0.9200	0.8	0.9867	0.6	0.9867
2	0.7734	3	0.8134	1.4	0.9734	0.7	0.9067
3	0.6668	4	0.6934	2.0	0.9601	0.8	0.6534
4	0.4935	5	0.6001	2.2	0.9468	0.9	0.3068
5	0.4269	6	0.5469	2.4	0.9335	1.0	0.1068
6	0.2669	7	0.4803	2.6	0.8935	1.2	0.0268
7	0.1736	8	0.4271	2.8	0.8535	1.3	0.0135
8	0.1204	9	0.3205	3.0	0.8003	2.1	0.0002
10	0.1071	10	0.1872	3.2	0.7072		
12	0.0405	11	0.1472	3.4	0.5739		
13	0.0139	12	0.1206	3.6	0.3606		
15	0.0006	13	0.0806	3.8	0.2273		
		14	0.0673	4.0	0.1340		
		15	0.0273	4.2	0.0274		
		17	0.0007	4.4	0.0008		

Series A1/5(i)

t_1	N/N_o	t_2	N/N_o	t_3	N/N_o	t_4	N/N_o
1	0.9734	2	0.9067	0.6	0.9868	0.4	0.9200
3	0.8934	3	0.6401	1.0	0.9602	0.5	0.8800
4	0.7601	4	0.5601	1.4	0.9070	0.6	0.5600
5	0.4801	5	0.4668	1.6	0.8538	0.7	0.2800
6	0.3735	6	0.3335	1.8	0.7738	0.8	0.0800
7	0.2669	7	0.2002	2.0	0.6272	0.9	0.0268
8	0.1869	8	0.0802	2.2	0.4672	1.0	0.0002
9	0.1337	10	0.0270	2.4	0.3072		
10	0.0937	11	0.0137	2.6	0.1339		
11	0.0804	13	0.0004	2.8	0.0273		
12	0.0404			3.0	0.0007		
13	0.0271						
14	0.0138						
19	0.0005						

Series A1/5(ii)

t_1	N/N_o	t_2	N/N_o	t_3	N/N_o	t_4	N/N_o
1	0.9734	1	0.9734	1.0	0.9867	0.3	0.9867
2	0.8801	2	0.9334	2.0	0.9067	0.4	0.9734
3	0.7868	3	0.9068	2.2	0.8535	0.5	0.9202
4	0.7336	4	0.7868	2.4	0.7069	0.6	0.6802
5	0.5336	5	0.7068	2.6	0.4403	0.7	0.3336
6	0.4403	6	0.6135	2.8	0.1603	0.8	0.1070
7	0.3337	7	0.4535	3.0	0.0537	0.9	0.0538
8	0.2537	8	0.2802	3.2	0.0271	1.0	0.0006
9	0.1471	9	0.1469	3.4	0.0005		
10	0.0939	10	0.1069				
11	0.0673	11	0.0269				
12	0.0407	13	0.0136				
16	0.0274	14	0.0003				
17	0.0008						

Series A1/6(i)

t_1	N/N_o	t_2	N/N_o	t_3	N/N_o	t_4	N/N_o
2	0.9734	2	0.9600	0.8	0.9867	0.2	0.9867
4	0.7868	2.5	0.8800	1.0	0.9467	0.3	0.8267
6	0.6935	3	0.8134	1.1	0.8667	0.4	0.3867
8	0.4802	3.5	0.5468	1.2	0.8001	0.5	0.0934
10	0.3602	4	0.3202	1.3	0.6135	0.6	0.0134
12	0.2402	4.5	0.2136	1.4	0.4535	0.7	0.0001
14	0.1469	5	0.1203	1.5	0.2802		
16	0.0937	5.5	0.0803	1.6	0.1202		
18	0.0804	6	0.0403	1.7	0.0670		
20	0.0538	6.5	0.0137	1.8	0.0270		
22	0.0272	8.5	0.0004	1.9	0.0137		
32	0.0139			2.0	0.0004		
36	0.0006						

Series A1/6(ii)

t_1	N/N_o
2	0.9468
4	0.8402
6	0.7336
8	0.5870
10	0.4270
12	0.3604
14	0.3338
16	0.2806
18	0.2673
20	0.2407
22	0.2007
24	0.1741
26	0.1608
28	0.1208
30	0.0942
34	0.0809
36	0.0676
38	0.0543
40	0.0410
44	0.0144
48	0.0011

Series A1/7

t_1	N/N_o	t_2	N/N_o	t_3	N/N_o	t_4	N/N_o
3	0.9460	1	0.9865	0.7	0.9867	0.2	0.9334
4	0.9055	2	0.9595	1.0	0.9601	0.3	0.7068
5	0.7299	3	0.8785	1.2	0.9468	0.4	0.3602
6	0.6083	4	0.7975	1.3	0.9335	0.5	0.0402
7	0.5408	5	0.6894	1.4	0.8803	0.6	0.0002
8	0.3922	6	0.5273	1.5	0.8271		
9	0.2301	7	0.2031	1.6	0.7471		
10	0.1085	8	0.0680	1.7	0.6271		
11	0.0545	9	0.0140	1.8	0.3605		
12	0.0410	10	0.0005	1.9	0.1605		
13	0.0140			2.0	0.1205		
14	0.0005			2.1	0.0139		
				2.2	0.0006		

Series A1/8

t_1	N/N_o	t_2	N/N_o	t_3	N/N_o	t_4	N/N_o
3	0.9606	3	0.9737	0.8	0.9867	0.1	0.9600
4	0.9212	4	0.8816	1.2	0.9734	0.2	0.6267
5	0.8160	5	0.8159	1.3	0.9601	0.3	0.2267
6	0.4082	6	0.5923	1.6	0.9468	0.4	0.0267
7	0.2635	7	0.3292	1.7	0.9335	0.5	0.0001
8	0.1320	8	0.1056	1.8	0.7202		
9	0.0926	9	0.0399	1.9	0.3602		
10	0.0269	10	0.0136	2.0	0.1602		
19	0.0138	11	0.0005	2.1	0.0269		
21	0.0007			2.2	0.0003		

Series B1/1

t_1	N/N_o	t_2	N/N_o	t_3	N/N_o
7.5	0.9867	3.5	0.9867	1.3	0.9734
10	0.9734	4.5	0.9734	1.4	0.9068
12.5	0.9601	5	0.9468	1.5	0.7735
15	0.9335	6	0.9068	1.6	0.4802
17.5	0.9202	6.5	0.8802	1.7	0.2136
20	0.8802	7	0.8270	1.8	0.0270
22.5	0.7869	7.5	0.7070	1.9	0.0137
25	0.5336	8	0.3470	2.0	0.0004
27.5	0.2803	8.5	0.0937		
30	0.1870	9	0.0004		
32.5	0.1204				
35	0.0271				
37.5	0.0005				

Series B1/2

t_1	N/N_o	t_2	N/N_o	t_3	N/N_o	t_4	N/N_o
2.5	0.9734	4	0.9468	1.3	0.9867	0.25	0.8534
5	0.9468	5	0.9068	1.7	0.9734	0.3	0.8134
7.5	0.9335	6	0.7202	1.8	0.8801	0.35	0.4001
10	0.8669	7	0.6402	1.9	0.6535	0.4	0.3735
12.5	0.7869	8	0.4936	2.0	0.3869	0.45	0.1069
15	0.6803	9	0.2270	2.1	0.1203	0.5	0.0803
17.5	0.5470	10	0.0537	2.2	0.0537	0.55	0.0137
20	0.4404	11	0.0137	2.3	0.0137	0.85	0.0004
22.5	0.2271	13	0.0004	2.5	0.0004		
25	0.1471						
27.5	0.0671						
30	0.0405						
32.5	0.0272						
37.5	0.0139						
50	0.0006						

Series B1/3

t_1	N/N_o	t_2	N/N_o	t_3	N/N_o	t_4	N/N_o
2.5	0.9867	3	0.9867	1.1	0.9867	0.15	0.9867
5	0.9335	4	0.9734	1.9	0.9734	0.25	0.9335
7.5	0.8935	5	0.9601	2.0	0.9601	0.3	0.9202
10	0.8535	6	0.8001	2.1	0.9468	0.35	0.8269
12.5	0.8402	7	0.5468	2.2	0.9202	0.4	0.7869
15	0.8136	8	0.4135	2.3	0.8402	0.45	0.4269
17.5	0.7470	9	0.3069	2.4	0.6136	0.5	0.3869
20	0.6804	10	0.2136	2.5	0.4003	0.55	0.0669
22.5	0.5471	11	0.1336	2.6	0.2537	0.65	0.0403
25	0.4671	12	0.0403	2.7	0.1204	0.75	0.0137
27.5	0.3605	13	0.0270	2.8	0.0538		
30	0.3073	14	0.0004	2.9	0.0138		
32.5	0.2140			3.0	0.0005		
35	0.1740						
37.5	0.1208						
40	0.0942						
42.5	0.0542						
45	0.0276						
50	0.0143						
60	0.0010						

Series B1/4

t_1	N/N_o	t_2	N/N_o	t_3	N/N_o	t_4	N/N_o
2.5	0.9872	8	0.8832	2.2	0.9871	0.35	0.9871
5	0.9744	9	0.7542	2.4	0.9742	0.45	0.9742
7.5	0.9488	10	0.6633	2.6	0.9613	0.55	0.8963
10	0.8208	11	0.5984	2.8	0.8964	0.6	0.9704
12.5	0.8080	12	0.5205	3.0	0.7406	0.65	0.6886
15	0.7952	13	0.4166	3.2	0.5199	0.7	0.6367
17.5	0.7696	14	0.2348	3.4	0.2083	0.75	0.2991
20	0.7568	15	0.0530	3.6	0.1044	0.8	0.2472
22.5	0.6927	16	0.0141	3.8	0.0395	0.85	0.1182
25	0.6543	18	0.0012	4.0	0.0006	0.95	0.0403
27.5	0.5646					1.05	0.0014
30	0.4877						
32.5	0.4365						
35	0.3853						
37.5	0.3084						
42.5	0.2572						
45.0	0.2316						
47.5	0.1547						
50	0.1419						
52.5	0.1035						
55	0.0779						
57.5	0.0651						
62.5	0.0395						
67.5	0.0267						
80	0.0139						

Series C1/1

t_1	N/N_o	t_2	N/N_o	t_3	N/N_o
2	0.9867	2.2	0.9867	1.0	0.9867
4	0.9601	2.4	0.9734	1.2	0.9335
5	0.9201	2.8	0.9601	1.3	0.8669
6	0.8935	3.0	0.9069	1.4	0.5869
7	0.8403	3.2	0.8003	1.5	0.2669
8	0.8003	3.4	0.7070	1.6	0.0536
9	0.7471	3.6	0.4670	1.7	0.0270
10	0.6671	3.8	0.3337	1.8	0.0004
11	0.5205	4.0	0.2137		
12	0.4539	4.2	0.1337		
13	0.3073	4.4	0.0805		
14	0.1473	4.6	0.0539		
15	0.0807	4.8	0.0273		
16	0.0141	5.2	0.0140		
18	0.0008	5.8	0.0007		

Series C1/2

t_1	N/N_o	t_2	N/N_o	t_3	N/N_o
2	0.9867	2.8	0.9867	1.4	0.9867
4	0.9601	3.8	0.9734	1.5	0.9201
6	0.8668	4.0	0.9468	1.6	0.8401
8	0.7468	4.2	0.8936	1.7	0.6268
10	0.7335	4.4	0.8003	1.8	0.3202
12	0.6269	4.6	0.7203	1.9	0.1469
14	0.4536	4.8	0.6137	2.0	0.0269
16	0.2270	5.0	0.4804	2.1	0.0009
18	0.0537	5.2	0.3871		
20	0.0404	5.4	0.2538		
22	0.0271				
24	0.0005				

Series C1/3

t_1	N/N_o	t_2	N/N_o	t_3	N/N_o
2	0.9468	3.6	0.9600	1.3	0.9600
4	0.8002	4.0	0.8400	1.4	0.8667
6	0.6136	4.2	0.7467	1.5	0.7467
8	0.5203	4.4	0.6801	1.6	0.4934
10	0.4270	4.6	0.5868	1.7	0.2934
12	0.2804	4.8	0.5468	1.8	0.1334
14	0.2004	5.0	0.4268	1.9	0.0801
16	0.1338	5.2	0.3735	2.0	0.0135
18	0.0806	5.4	0.2669	2.1	0.0002
20	0.0406	5.6	0.2136		
22	0.0006	5.8	0.1870		
		6.0	0.1337		
		6.2	0.0937		
		6.4	0.0671		
		6.8	0.0405		
		7.0	0.0272		
		7.2	0.0139		
		10.0	0.0006		

Series C1/4

t_1	N/N_o	t_2	N/N_o	t_3	N/N_o
2	0.9460	3.2	0.9867	1.6	0.9865
4	0.8920	4.2	0.9734	1.7	0.9730
6	0.8515	4.4	0.9468	1.8	0.8785
8	0.7705	4.6	0.9202	2.0	0.7570
10	0.6219	5.2	0.8936	2.1	0.6760
12	0.5409	5.4	0.7336	2.2	0.5004
14	0.4329	5.6	0.6803	2.3	0.3654
16	0.3113	6.0	0.6137	2.4	0.2709
18	0.2033	6.2	0.4804	2.5	0.1629
20	0.0953	6.4	0.4138	2.6	0.0684
22	0.0413	6.6	0.3338	2.8	0.0279
24	0.0278	7.0	0.2938	2.9	0.0144
26	0.0008	7.2	0.2805	3.3	0.0009
		7.4	0.2272		
		7.6	0.1606		
		7.8	0.1473		
		8.0	0.1340		
		8.4	0.1074		
		8.6	0.0808		
		9.2	0.0542		
		9.4	0.0276		
		9.6	0.0143		
		14.4	0.0010		

Series C1/5

t_1	N/N_o	t_2	N/N_o	t_3	N/N_o	t_4	N/N_o
2.5	0.9865	4	0.9867	2.0	0.9867	0.2	0.9867
5	0.9190	6	0.8801	2.2	0.9334	0.3	0.9601
7.5	0.8380	7	0.8135	2.4	0.8534	0.5	0.8268
10	0.7570	8	0.7335	2.6	0.7334	0.6	0.6668
12.5	0.6895	9	0.6669	2.8	0.6934	0.7	0.5335
15	0.5680	10	0.5336	3.0	0.5734	0.8	0.2802
17.5	0.4600	11	0.3736	3.2	0.4801	0.9	0.1469
20	0.4060	12	0.2670	3.4	0.3868	1.0	0.0269
22.5	0.3250	13	0.1737	3.6	0.3068	1.1	0.0003
25	0.2710	14	0.0804	3.8	0.2135		
27.5	0.2170	15	0.0404	4.0	0.1069		
30	0.1630	16	0.0138	4.2	0.0269		
32.5	0.1360	17	0.0005	4.6	0.0136		
35	0.0685			4.8	0.0003		
37.5	0.0280						
42.5	0.0010						

Series C1/6

t_1	N/N_o	t_2	N/N_o	t_3	N/N_o	t_4	N/N_o
5	0.9737	5	0.9734	3.0	0.9734	0.7	0.9868
7.5	0.8422	6	0.8534	3.5	0.8934	0.8	0.9736
10	0.7633	7	0.7734	4	0.8801	0.9	0.9472
12.5	0.6976	8	0.6801	4.5	0.8001	1.0	0.8551
15	0.5924	9	0.5735	5	0.7201	1.1	0.6447
17.5	0.3820	10	0.3869	5.5	0.6001	1.2	0.5921
20	0.2899	11	0.2669	6.0	0.4135	1.3	0.4079
22.5	0.2373	12	0.1603	6.5	0.2935	1.4	0.3027
25	0.1979	13	0.1070	7	0.1602	1.5	0.1449
27.5	0.1058	15	0.0804	7.5	0.0802	1.6	0.1055
30	0.0795	16	0.0671	8	0.0669	1.7	0.0792
32.5	0.0663	18	0.0405	9	0.0403	1.8	0.0529
35	0.0531	24	0.0272	14.5	0.0270	2.0	0.0397
42.5	0.0268	27	0.0139	45.5	0.0137	2.3	0.0265
70	0.0136	32	0.0006	53.0	0.0004	4.7	0.0133
75	0.0004					5.0	0.0001

Series D1/1

t_1	N/N_o	t_2	N/N_o	t_3	N/N_o
1	0.9730	2.5	0.9468	1.0	0.9867
2	0.7298	3.0	0.8135	1.1	0.9734
3	0.5271	3.5	0.6135	1.2	0.9068
4	0.3380	4.0	0.4135	1.3	0.8402
5	0.2029	4.5	0.2669	1.4	0.7202
6	0.1219	5.0	0.2269	1.5	0.5469
7	0.0814	5.5	0.1069	1.6	0.3069
8	0.0544	6.0	0.0537	1.7	0.1469
9	0.0274	6.5	0.0137	1.8	0.0937
10	0.0004	12.0	0.0004	1.9	0.0271
				2.0	0.0138
				2.5	0.0005

Series D1/2

t_1	N/N_o	t_2	N/N_o	t_3	N/N_o	t_4	N/N_o
2.5	0.9334	3	0.9867	1.8	0.9334	0.3	0.9334
5.0	0.7468	4	0.9335	2.0	0.8802	0.4	0.7334
7.5	0.5602	5	0.8269	2.2	0.6402	0.5	0.2802
10	0.4402	6	0.6936	2.4	0.4402	0.6	0.0536
12.5	0.3202	7	0.4536	2.6	0.2269	0.7	0.0403
15	0.1602	8	0.2536	2.8	0.0936	0.8	0.0003
17.5	0.0936	9	0.1336	3.0	0.0136		
20	0.0670	10	0.0536	4.2	0.0003		
22.5	0.0138	11	0.0136				
25	0.0005	14	0.0003				

Series D1/3

t_1	N/N_o	t_2	N/N_o	t_3	N/N_o	t_4	N/N_o
2.5	0.9730	3.5	0.9595	1.6	0.9865	0.3	0.9595
5	0.9055	4.0	0.9460	1.8	0.9730	0.4	0.8785
7.5	0.7569	4.5	0.9325	2.0	0.9325	0.5	0.5542
10	0.5948	5.0	0.8785	2.2	0.9055	0.6	0.2705
12.5	0.4867	6.0	0.8245	2.4	0.8110	0.7	0.0814
15	0.3651	6.5	0.7030	2.6	0.5138	0.8	0.0139
17.5	0.2706	7	0.6085	2.8	0.3111	1.1	0.0004
20	0.0950	7.5	0.5545	3.0	0.2030		
22.5	0.0410	8	0.3924	3.2	0.0544		
25	0.0140	8.5	0.2168	3.4	0.0409		
27.5	0.0005	9	0.1628	3.8	0.0275		
		9.5	0.1358	4.0	0.0140		
		10	0.0548	4.6	0.0005		
		10.5	0.0413				
		11	0.0278				
		14.0	0.0143				
		17.0	0.0008				

Series D1/4

t_1	N/N_o	t_2	N/N_o	t_3	N/N_o	t_4	N/N_o
2.5	0.9343	2	0.9869	1.8	0.9869	0.5	0.9737
5.0	0.8686	4	0.9738	2.2	0.9738	0.6	0.9344
7.5	0.7502	6	0.9475	2.8	0.9345	0.7	0.6713
10	0.5266	8	0.8686	3.0	0.8556	0.8	0.4477
12.5	0.4477	10	0.6581	3.2	0.7899	0.9	0.2767
15	0.3293	12	0.4608	3.4	0.6978	1.0	0.1320
17.5	0.2504	14	0.2372	3.6	0.5926	1.1	0.0663
20	0.1715	16	0.1583	3.8	0.4874	1.2	0.0270
25.0	0.0926	18	0.0662	4.0	0.4481	1.3	0.0007
27.5	0.0533	20	0.0399	4.2	0.3824		
30	0.0402	22	0.0268	4.4	0.3167		
32.5	0.0139	24	0.0005	4.6	0.2774		
37.5	0.0008			4.8	0.1985		
				5.0	0.1196		
				5.2	0.0803		
				5.4	0.0540		
				5.6	0.0147		
				6.0	0.0016		

Series A2/1

t_1	N/N_o	t_2	N/N_o	t_3	N/N_o	t_4	N/N_o
1.0	0.9867	1.4	0.9867	0.6	0.9734	0.2	0.9468
1.5	0.9734	1.4	0.9734	0.7	0.9334	0.3	0.3868
2	0.9668	1.5	0.9334	0.8	0.7068	0.4	0.0802
2.5	0.5735	1.6	0.7601	0.9	0.6002	0.5	0.0136
3	0.3735	1.7	0.5335	1.0	0.3202	0.6	0.0003
3.5	0.2002	1.8	0.3735	1.1	0.2269		
4	0.1336	1.9	0.3069	1.2	0.1737		
4.5	0.0804	2.0	0.2003	1.4	0.1337		
5	0.0404	2.1	0.1603	1.5	0.0805		
5.5	0.0138	2.2	0.1203	1.7	0.0672		
6	0.0005	2.3	0.1070	1.8	0.0539		
		2.4	0.0670	1.9	0.0273		
		2.6	0.0537	2.0	0.0140		
		2.9	0.0404	2.1	0.0007		
		3.0	0.0271				
		3.3	0.0138				
		3.4	0.0005				

Series A2/2

t_1	N/N_o	t_2	N/N_o	t_3	N/N_o	t_4	N/N_o
2	0.9734	2.0	0.9867	1.1	0.9734	0.3	0.8134
4	0.7601	2.6	0.9601	1.2	0.8801	0.4	0.3601
5	0.3335	2.8	0.9201	1.3	0.8135	0.5	0.0935
6	0.2402	3.0	0.8135	1.4	0.6669	0.6	0.0002
7	0.0936	3.2	0.7335	1.5	0.5736		
8	0.0536	3.4	0.6269	1.6	0.4270		
9	0.0270	3.6	0.5603	1.7	0.3470		
12	0.0004	3.8	0.4403	1.8	0.1870		
		4.0	0.3470	1.9	0.1204		
		4.2	0.2804	2.0	0.0538		
		4.4	0.2404	2.1	0.0405		
		4.6	0.2004	2.2	0.0139		
		4.8	0.1338	2.3	0.0006		
		5.0	0.1205				
		5.2	0.0939				
		5.4	0.0539				
		5.6	0.0273				
		5.8	0.0140				
		7.0	0.0007				

Series A2/3

t_1	N/N_o	t_2	N/N_o	t_3	N/N_o	t_4	N/N_o
2	0.9334	2	0.9867	1.1	0.9867	0.3	0.9867
4	0.8001	4	0.9201	1.6	0.9734	0.5	0.8801
6	0.5201	5	0.8268	2.2	0.9601	0.6	0.6935
8	0.3335	6	0.6668	2.5	0.9201	0.8	0.0802
10	0.2135	7	0.5202	2.6	0.8669	0.9	0.0002
12	0.1469	8	0.4002	2.7	0.7603		
14	0.1336	9	0.2402	2.8	0.6270		
16	0.1203	10	0.1602	2.9	0.4404		
18	0.0803	11	0.0936	3.0	0.2938		
20	0.0670	12	0.0136	3.1	0.0938		
22	0.0404	13	0.0003	3.2	0.0672		
26	0.0271			3.3	0.0006		
28	0.0138						
34	0.0005						

Series A2/4

t_1	N/N_o	t_2	N/N_o	t_3	N/N_o	t_4	N/N_o
1.0	0.9800	3	0.9800	1.2	0.9800	0.4	0.9000
3	0.9200	4	0.8200	1.6	0.9400	0.5	0.7200
4	0.9000	5	0.7400	1.8	0.8800	0.6	0.5000
5	0.8400	6	0.6200	2.0	0.7400	0.7	0.2400
6	0.6800	7	0.3600	2.2	0.6200	0.8	0.0800
7	0.4200	8	0.2200	2.4	0.5000	0.9	0.0200
8	0.2800	9	0.0400	2.6	0.3800	1.0	0.0000
9	0.2000	10	0.0200	2.8	0.2000		
10	0.1000	11	0.0000	3.0	0.0600		
11	0.0800			3.2	0.0400		
12	0.0600			3.4	0.0000		
15	0.0200						
19	0.0000						

Series A2/5

t_1	N/N_o	t_2	N/N_o	t_3	N/N_o	t_4	N/N_o
3	0.9600	3	0.9000	1.8	0.9800	0.3	0.9800
4	0.8800	4	0.7000	2.0	0.9600	0.4	0.9400
5	0.6000	5	0.5800	2.2	0.9400	0.5	0.8400
6	0.3000	6	0.4200	2.4	0.7200	0.6	0.5800
7	0.1800	7	0.2200	2.6	0.5800	0.7	0.3200
8	0.1600	8	0.1200	2.8	0.3200	0.8	0.0600
9	0.1200	9	0.1000	3.0	0.1400	0.9	0.0000
10	0.0800	10	0.0600	3.2	0.0400		
12	0.0600	11	0.0200	3.4	0.0200		
19	0.0400	12	0.0000	4.0	0.0000		
21	0.0200						
36	0.0000						

Series A2/6

t_1	N/N_o	t_2	N/N_o	t_3	N/N_o	t_4	N/N_o
1	0.8000	2	0.9800	1.2	0.9600	0.3	0.9800
3	0.7600	3	0.9600	1.4	0.8400	0.4	0.7600
4	0.6400	3.5	0.7800	1.6	0.5400	0.5	0.5400
5	0.4800	4	0.7000	1.8	0.4400	0.6	0.4600
6	0.4000	4.5	0.5200	2.0	0.4200	0.7	0.4400
7	0.2200	5	0.4400	2.2	0.3600	0.8	0.3800
8	0.1000	5.5	0.3200	2.4	0.3200	0.9	0.2400
9	0.0600	6	0.2400	2.6	0.2800	1.0	0.1200
10	0.0000	6.5	0.2000	2.8	0.1800	1.1	0.0200
		7.5	0.1200	3.0	0.0800	1.2	0.0000
		8.0	0.1000	3.2	0.0400		
		8.5	0.0200	3.8	0.0000		
		9	0.0000				

Series B2/1

t_1	N/N_o	t_2	N/N_o	t_3	N/N_o	t_4	N/N_o
5	0.9834	2.5	0.9834	1.4	0.9500	0.3	0.9500
10	0.9668	4.0	0.9335	1.5	0.9334	0.4	0.5500
20	0.8502	4.5	0.9169	1.6	0.8501	0.5	0.0500
25	0.7836	5.0	0.8503	1.8	0.5335	0.6	0.0000
30	0.5836	6.5	0.8337	1.9	0.2169		
35	0.3670	7	0.8004	2.0	0.0336		
40	0.1337	7.5	0.7838	2.1	0.0003		
45	0.0837	8	0.6338				
50	0.0504	8.5	0.3338				
60	0.0338	9	0.0672				
75	0.0005	9.5	0.0172				
		10	0.0006				

Series B2/2

t_1	N/N_o	t_2	N/N_o	t_3	N/N_o	t_4	N/N_o
5.0	0.8905	3	0.9864	1.6	0.9864	0.4	0.9864
7.5	0.8221	5	0.9592	1.7	0.9728	0.5	0.8769
10	0.6441	6	0.9182	2.6	0.9592	0.6	0.5756
12.5	0.4661	7	0.8772	2.8	0.9456	0.7	0.2195
15	0.3155	8	0.7951	3.0	0.8498	0.8	0.0552
17.5	0.2334	9	0.7815	3.1	0.7266	0.9	0.0142
20	0.1513	10	0.7405	3.2	0.3705	1.0	0.0006
22.5	0.0692	11	0.6173	3.3	0.1925		
25	0.0419	12	0.5215	3.4	0.0554		
27.5	0.0146	13	0.3298	3.5	0.0007		
32.5	0.0010	14	0.1244				
		15	0.0149				
		19	0.0013				

Series B2/3

t_1	N/N_o	t_2	N/N_o	t_3	N/N_o	t_4	N/N_o
2.5	0.9869	4	0.9867	2.2	0.9867	0.6	0.9734
5	0.9212	5	0.9601	2.4	0.9601	0.7	0.8134
7.5	0.8818	6	0.8935	2.6	0.9468	0.8	0.6001
10	0.6450	7	0.7602	3.4	0.8668	0.9	0.2935
12.5	0.4872	8	0.6402	3.6	0.7735	1.0	0.0269
15	0.3557	9	0.4669	3.8	0.4402	1.1	0.0136
17.5	0.2373	10	0.3203	4.0	0.1336	1.2	0.0003
20	0.1452	11	0.1870	4.2	0.0136		
22.5	0.0531	12	0.1070	4.4	0.0003		
25	0.0400	13	0.0804				
27.5	0.0006	14	0.0272				
		15	0.0006				

Series B2/4

t_1	N/N_o	t_2	N/N_o	t_3	N/N_o	t_4	N/N_o
2	0.9800	4	0,9800	1.8	0.9400	0.8	0.9200
3	0.9400	5	0.9400	2.2	0.9000	0.9	0.8400
4	0.9200	6	0.7800	2.6	0.8600	1.0	0.5000
6	0.8800	7	0.5400	3.2	0.8400	1.1	0.2000
7	0.7800	8	0.3800	3.4	0.8200	1.2	0.0800
8	0.6200	9	0.2800	3.8	0.7800	1.3	0.0200
9	0.4800	10	0.2000	4.0	0.6200	2.4	0.0000
10	0.2200	11	0.1200	4.2	0.3600		
11	0.0800	12	0.1000	4.4	0.1200		
12	0.0400	13	0.0400	4.6	0.0200		
13	0.0000	14	0.0200	4.8	0.0000		
		15	0.0000				

Series B2/5

t_1	N/N_o	t_2	N/N_o	t_3	N/N_o	t_4	N/N_o
10	0.9412	5.0	0.9616	2.2	0.9608	0.6	0.9804
15	0.9020	6	0.9232	2.6	0.9412	0.7	0.9020
20	0.6471	7	0.8848	2.8	0.9216	0.8	0.8040
25	0.4511	8	0.8464	3.0	0.8824	0.9	0.6276
30	0.2355	9	0.8272	3.2	0.8628	1.0	0.3737
40	0.1571	10	0.7696	3.4	0.8432	1.1	0.1375
45	0.0983	11	0.6927	3.6	0.8236	1.2	0.0395
50	0.0787	12	0.5775	4.0	0.8040	1.4	0.0199
55	0.0591	13	0.5391	4.2	0.7844	1.5	0.0003
70	0.0395	14	0.3468	4.4	0.5295		
85	0.0199	16	0.2507	4.6	0.2550		
100	0.0003	17	0.2123	4.8	0.0198		
		18	0.1162	5.0	0.0002		
		19	0.0393				
		20	0.0009				

Series B2/6

t_1	N/N_o	t_2	N/N_o	t_3	N/N_o	t_4	N/N_o
2.5	0.9600	4	0.9800	1.0	0.9800	0.7	0.9600
5	0.8000	6	0.8000	1.4	0.9400	0.8	0.9400
7.5	0.6000	8	0.5800	1.6	0.9000	0.9	0.9200
10	0.4200	10	0.2800	2.0	0.8800	1.0	0.8000
12.5	0.2800	12	0.2000	2.2	0.8600	1.1	0.4800
15	0.1800	14	0.0800	2.4	0.8400	1.2	0.0200
17.5	0.1400	16	0.0400	2.8	0.8200	1.3	0.0000
20	0.1200	22	0.0000	3.0	0.7800		
22.5	0.1000			3.2	0.7600		
25	0.0400			3.4	0.7400		
37.5	0.0200			3.6	0.7200		
52.5	0.0000			3.8	0.7000		
				4.0	0.6800		
				4.2	0.5800		
				4.4	0.2400		
				4.6	0.1200		
				4.8	0.0200		
				5.0	0.0000		

Series C2/1

t_1	N/N_o	t_2	N/N_o	t_3	N/N_o	t_4	N/N_o
2.5	0.9200	2	0.9867	1.3	0.9867	0.2	0.9600
7.5	0.8800	3	0.9467	1.4	0.9734	0.3	0.7734
10	0.7734	4	0.8801	1.5	0.9334	0.4	0.4268
12.5	0.6401	5	0.8269	1.6	0.8534	0.5	0.0268
15	0.4001	6	0.6269	1.7	0.7201	0.6	0.0002
17.5	0.2668	7	0.3336	1.8	0.4801		
20	0.1602	8	0.1203	1.9	0.3201		
22.5	0.1070	9	0.0403	2.0	0.1868		
25	0.0804	10	0.0137	2.1	0.0668		
27.5	0.0538	12	0.0004	2.2	0.0136		
30	0.0138			2.3	0.0003		
32.5	0.0005						

Series C2/2

t_1	N/N_o	t_2	N/N_o	t_3	N/N_o	t_4	N/N_o
2	0.9867	1.0	0.9868	1.1	0.9734	0.3	0.9734
3	0.9201	1.5	0.9342	1.2	0.9068	0.4	0.6668
4	0.8535	2.0	0.9079	1.5	0.8268	0.5	0.2535
5	0.7469	2.5	0.8816	1.6	0.6668	0.6	0.0002
6	0.6669	3.0	0.8684	1.7	0.4668		
7	0.6137	3.5	0.7763	1.8	0.3335		
8	0.4137	4.0	0.6053	1.9	0.2269		
9	0.3204	4.5	0.4869	2.0	0.1737		
10	0.2271	5.0	0.3817	2.1	0.1604		
11	0.1871	5.5	0.2896	2.2	0.1204		
12	0.1205	6.0	0.2107	2.3	0.1071		
13	0.0539	6.5	0.1186	2.4	0.0938		
14	0.0406	7.0	0.1054	2.5	0.0538		
15	0.0273	7.5	0.0660	2.7	0.0405		
18	0.0140	8.5	0.0528	3.0	0.0272		
27	0.0007	9	0.0396	3.2	0.0139		
		9.5	0.0264	3.3	0.0006		
		11.5	0.0132				
		13.5	0.0000				

Series C2/3

t_1	N/N_o	t_2	N/N_o	t_3	N/N_o	t_4	N/N_o
2.5	0.9867	1.0	0.9867	0.8	0.9867	0.3	0.9734
7.5	0.9335	4.0	0.9734	1.6	0.9067	0.4	0.6401
10	0.8803	4.5	0.9468	1.8	0.7467	0.5	0.3868
12.5	0.7870	5	0.9068	2.0	0.5067	0.6	0.0935
15	0.5737	5.5	0.8135	2.2	0.2934	0.7	0.0269
17.5	0.3871	6	0.6669	2.4	0.2001	0.8	0.0003
20	0.2005	6.5	0.5069	2.6	0.1068		
22.5	0.1205	7	0.3869	2.8	0.0668		
25	0.0805	7.5	0.3203	3.2	0.0268		
27.5	0.0405	8	0.2270	3.4	0.0135		
32.5	0.0139	8.5	0.1337	4.2	0.0002		
35	0.0006	9	0.0937				
		9.5	0.0804				
		10	0.0538				
		10.5	0.0405				
		13.5	0.0272				
		14.5	0.0139				
		18.0	0.0006				

Series C2/4

t_1	N/N_o	t_2	N/N_o	t_3	N/N_o	t_4	N/N_o
2.5	0.9800	1	0.9800	1.2	0.9800	0.4	0.9800
7.5	0.9400	4	0.7800	1.4	0.9600	0.5	0.8600
10	0.8400	5	0.6200	1.6	0.9400	0.6	0.7600
12.5	0.7800	6	0.4800	2.0	0.8800	0.7	0.4000
15	0.7400	7	0.3200	2.2	0.8400	0.8	0.3000
17.5	0.6600	8	0.2400	2.4	0.6800	0.9	0.1800
20	0.6400	9	0.1200	2.6	0.6400	1.0	0.1400
22.5	0.4600	10	0.1000	2.8	0.6000	1.1	0.0200
25	0.3800	11	0.0600	3.0	0.5400	1.2	0.0000
27.5	0.2400	13	0.0200	3.2	0.4800		
30	0.1800	16	0.0000	3.4	0.4200		
32.5	0.1200			3.6	0.2800		
35	0.0800			3.8	0.2400		
37.5	0.0400			4.0	0.2000		
45	0.0200			4.2	0.1800		
60	0.0000			4.4	0.1200		
				4.6	0.0800		
				4.8	0.0600		
				5.0	0.0000		

Series C2/5

t_1	N/N_o	t_2	N/N_o	t_3	N/N_o	t_4	N/N_o
5	0.9800	4	0.9800	3	0.9800	0.9	0.9400
10	0.8800	6	0.9600	3.4	0.9600	1.0	0.8800
15	0.6800	8	0.9400	3.8	0.9000	1.1	0.6800
20	0.5000	10	0.8600	4.2	0.8000	1.2	0.2800
25	0.3600	12	0.7400	4.4	0.5400	1.3	0.1600
30	0.2600	14	0.5200	4.6	0.3400	1.4	0.0200
35	0.1600	16	0.3400	4.8	0.2600	1.5	0.0000
40	0.1200	18	0.1600	5.0	0.0800		
45	0.1000	20	0.0600	5.2	0.0600		
50	0.0800	22	0.0000	5.4	0.0200		
55	0.0200						
85	0.0000						

Series D2/1

t_1	N/N_o	t_2	N/N_o	t_3	N/N_o	t_4	N/N_o
5	0.9067	3	0.9067	1.0	0.9867	0.3	0.8667
7.5	0.6934	4	0.8267	1.3	0.9601	0.4	0.4267
10	0.4401	5	0.6534	1.4	0.8935	0.5	0.0801
12.5	0.2535	6	0.3468	1.5	0.6669	0.6	0.0001
15	0.1202	7	0.1602	1.6	0.5203		
17.5	0.0670	8	0.1202	1.7	0.4403		
20	0.0404	9	0.1069	1.8	0.2937		
25	0.0138	10	0.0803	1.9	0.2137		
42.5	0.0005	11	0.0537	2.0	0.1737		
		12	0.0271	2.1	0.1604		
		16	0.0005	2.2	0.1338		
				2.3	0.0938		
				2.4	0.0672		
				2.5	0.0539		
				2.6	0.0406		
				3.0	0.0140		
				3.1	0.0007		

Series D2/2

t_1	N/N_o	t_2	N/N_o	t_3	N/N_o	t_4	N/N_o
2.5	0.9600	1	0.9867	1.0	0.9734	0.3	0.9867
5	0.8400	2	0.9734	1.4	0.9601	0.4	0.7734
7.5	0.7600	3	0.8934	1.6	0.8668	0.5	0.3868
10	0.5867	4	0.8001	1.8	0.7068	0.6	0.1068
12.5	0.4134	5	0.7335	2.0	0.4668	0.7	0.0802
15	0.2134	6	0.6402	2.2	0.3068	0.8	0.0669
17.5	0.0534	7	0.3736	2.4	0.1735	0.9	0.0137
20	0.0401	8	0.2670	2.6	0.1069	1.0	0.0004
22.5	0.0135	9	0.1204	2.8	0.0803		
27.5	0.0002	10	0.0538	3.0	0.0670		
		11	0.0272	3.4	0.0537		
		15	0.0139	3.6	0.0404		
		16	0.0006	3.8	0.0271		
				4.0	0.0138		
				4.2	0.0005		

Series D2/3

t_1	N/N_o	t_2	N/N_o	t_3	N/N_o	t_4	N/N_o
5	0.9867	4	0.9600	1.6	0.9867	0.4	0.9734
7.5	0.9734	6	0.8800	2.2	0.8401	0.5	0.7868
10	0.9601	8	0.6800	2.4	0.7735	0.6	0.5868
12.5	0.9069	10	0.3867	2.6	0.6802	0.7	0.3735
15	0.8669	12	0.1734	2.8	0.5202	0.8	0.2402
17.5	0.7336	14	0.0934	3.0	0.4269	0.9	0.0936
20	0.6270	16	0.0402	3.2	0.3336	1.0	0.0536
22.5	0.5070	18	0.0269	3.4	0.2804	1.1	0.0270
25	0.3470	20	0.0136	3.6	0.2272	1.2	0.0004
27.5	0.2804	24	0.0003	3.8	0.2006		
30	0.1738			4.0	0.1206		
32.5	0.1206			4.2	0.0940		
35	0.0806			4.4	0.0540		
37.5	0.0274			4.6	0.0141		
40	0.0142			5.0	0.0007		
50	0.0010						

Series D2/4

t_1	N/N_o	t_2	N/N_o	t_3	N/N_o	t_4	N/N_o
5	0.9388	4	0.9800	1.8	0.9600	0.4	0.9800
10	0.8164	6	0.7200	2.0	0.9400	0.5	0.9600
15	0.6532	8	0.4400	2.4	0.9000	0.6	0.9400
20	0.5512	10	0.2600	2.6	0.8800	0.7	0.8400
25	0.4084	12	0.1800	2.8	0.8400	0.8	0.5800
30	0.2452	14	0.1600	3.0	0.7600	0.9	0.3800
35	0.1840	16	0.1200	3.2	0.6600	1.0	0.2600
40	0.1228	18	0.1000	3.4	0.6400	1.1	0.1400
45	0.0820	22	0.0800	3.6	0.5200	1.2	0.1000
50	0.0616	26	0.0600	3.8	0.4400	1.3	0.0200
65	0.0208	30	0.0400	4.0	0.4000	1.4	0.0000
105	0.0004	32	0.0200	4.2	0.3600		
		34	0.0000	4.8	0.3000		
				5.0	0.2000		
				5.2	0.1400		
				5.4	0.1200		
				5.6	0.0800		
				5.8	0.0200		
				6.4	0.0000		

Series D2/5

t_1	N/N_o	t_2	N/N_o	t_3	N/N_o	t_4	N/N_o
10	0.8432	4	0.9400	1.6	0.9800	0.4	0.9800
15	0.5491	6	0.8200	2.0	0.9600	0.6	0.9600
20	0.3923	8	0.6600	2.2	0.9400	0.7	0.9400
25	0.2551	10	0.5200	2.6	0.9200	0.8	0.8200
30	0.1767	12	0.4000	2.8	0.9000	0.9	0.6000
35	0.0983	14	0.1600	3.0	0.8000	1.0	0.4800
45	0.0395	16	0.1000	3.2	0.6800	1.1	0.3600
50	0.0199	18	0.0800	3.4	0.6600	1.2	0.2600
100	0.0003	20	0.0600	3.6	0.5200	1.3	0.1600
		24	0.0400	3.8	0.4600	1.4	0.0800
		26	0.0200	4.0	0.3600	1.5	0.0400
		30	0.0000	4.2	0.3000	1.6	0.0000
				4.8	0.2200		
				5.0	0.1600		
				5.2	0.1200		
				5.4	0.1000		
				5.6	0.0800		
				5.8	0.0400		
				6.0	0.0000		

Series A3/1

t_1	N/N_o	t_2	N/N_o	t_3	N/N_o	t_4	N/N_o
1	0.9867	2.5	0.9867	1.3	0.9600	0.3	0.8534
2	0.9734	3	0.9734	1.4	0.8267	0.4	0.3201
3	0.9202	3.5	0.8668	1.5	0.6801	0.5	0.0535
4	0.8936	4	0.5468	1.6	0.4801	0.6	0.0269
5	0.8270	4.5	0.1868	1.7	0.3068	0.7	0.0003
6	0.6537	5	0.0535	1.8	0.1468		
7	0.3871	5.5	0.0135	1.9	0.0936		
8	0.1071	7	0.0002	2.0	0.0003		
9	0.0671						
10	0.0139						
12	0.0006						

Series A3/2

t_1	N/N_o	t_2	N/N_o	t_3	N/N_o	t_4	N/N_o
2	0.9867	2.5	0.9734	1.3	0.9867	0.3	0.6934
3	0.9734	3	0.9601	1.4	0.8401	0.4	0.2668
4	0.9468	3.5	0.9069	1.5	0.7735	0.5	0.0135
5	0.8402	4	0.8269	1.6	0.5869	0.6	0.0002
6	0.7736	4.5	0.6269	1.7	0.4136		
7	0.6670	5	0.3469	1.8	0.2270		
8	0.4937	5.5	0.1869	2.0	0.0937		
9	0.2804	6	0.1069	2.1	0.0537		
10	0.2138	6.5	0.0136	2.2	0.0271		
11	0.1338	7	0.0003	2.3	0.0138		
12	0.0806			2.4	0.0005		
13	0.0406						
15	0.0140						
16	0.0007						

Series A3/3

t_1	N/N_o	t_2	N/N_o	t_3	N/N_o	t_4	N/N_o
2	0.9600	3	0.9867	1.9	0.9600	0.4	0.8934
3	0.8534	4	0.9067	2.0	0.8400	0.5	0.5734
4	0.6134	4.5	0.8535	2.1	0.6267	0.6	0.2401
5	0.4668	5	0.7602	2.2	0.3467	0.7	0.0135
6	0.3868	5.5	0.6136	2.3	0.0934	0.9	0.0002
7	0.2668	6	0.3470	2.4	0.0001		
8	0.2136	6.5	0.2537				
9	0.1470	7	0.1737				
10	0.1070	7.5	0.1071				
11	0.0404	8	0.0405				
12	0.0271	8.5	0.0139				
13	0.0005	9	0.0006				

Series A3/4

t_1	N/N_o	t_2	N/N_o	t_3	N/N_o	t_4	N/N_o
2.5	0.9600	2.5	0.9867	1.8	0.9867	0.4	0.8667
5	0.8934	3	0.9734	1.9	0.9201	0.5	0.3067
7.5	0.8801	4.5	0.9468	2.0	0.7335	0.6	0.0134
10	0.7335	5.5	0.8802	2.1	0.4269	0.7	0.0001
12.5	0.6935	6	0.7602	2.2	0.1069		
15	0.5602	6.5	0.6936	2.3	0.0003		
17.5	0.3469	7	0.4670				
20	0.1203	7.5	0.3204				
22.5	0.0537	8	0.1471				
25	0.0271	8.5	0.0671				
27.5	0.0138	9	0.0271				
32.5	0.0005	9.5	0.0005				

Series C3/1

t_1	N/N_o	t_2	N/N_o	t_3	N/N_o	t_4	N/N_o
2	0.9867	3	0.9867	2.2	0.9867	0.4	0.9200
4	0.9734	4	0.9467	2.4	0.8267	0.5	0.7867
6	0.9334	5	0.8267	2.6	0.5601	0.6	0.4134
8	0.7734	6	0.7735	2.8	0.4935	0.7	0.1334
10	0.6534	7	0.5735	3.0	0.3602	0.8	0.0001
12	0.4668	8	0.4269	3.2	0.2269		
14	0.3868	9	0.3336	3.4	0.1603		
16	0.2802	10	0.2536	3.6	0.0803		
18	0.2270	11	0.1470	3.8	0.0403		
20	0.1337	12	0.0938	4.2	0.0137		
22	0.1204	13	0.0672	4.4	0.0004		
24	0.0672	14	0.0406				
26	0.0539	15	0.0140				
28	0.0273	19	0.0007				
32	0.0140						
34	0.0007						

Series C3/2

t_1	N/N_o	t_2	N/N_o	t_3	N/N_o	t_4	N/N_o
2	0.9867	3	0.9734	1.0	0.9868	0.4	0.9867
4	0.9067	4	0.9068	1.6	0.9736	0.5	0.8534
6	0.8134	5	0.8268	1.8	0.9604	0.6	0.3868
8	0.7067	6	0.7602	2.0	0.9472	0.7	0.1602
10	0.4402	7	0.5869	2.2	0.9072	0.8	0.0536
12	0.3736	8	0.4403	2.4	0.8006	0.9	0.0004
14	0.2803	9	0.2137	2.6	0.6406		
16	0.1470	10	0.0937	2.8	0.3740		
18	0.0804	11	0.0405	3.0	0.1474		
20	0.0272	12	0.0139	3.2	0.0674		
22	0.0139	15	0.0006	3.4	0.0408		
24	0.0006			3.6	0.0142		
				4.0	0.0009		

Series C3/3

t_1	N/N_o	t_2	N/N_o	t_3	N/N_o	t_4	N/N_o
3	0.9468	2	0.9867	1.4	0.9869	0.4	0.9867
4	0.8668	3	0.9734	1.6	0.9738	0.5	0.6934
5	0.7735	4	0.8268	1.8	0.9475	0.6	0.3868
6	0.6269	5	0.7202	2.2	0.9081	0.7	0.0535
7	0.4936	6	0.5736	2.4	0.7897	0.8	0.0135
8	0.4536	7	0.3870	2.6	0.6319	0.9	0.0002
9	0.3336	8	0.2537	2.8	0.4477		
10	0.2403	9	0.1604	3.0	0.1583		
11	0.2137	10	0.0804	3.2	0.0926		
12	0.1337	11	0.0272	3.4	0.0269		
13	0.1071	12	0.0006	3.6	0.0138		
14	0.0539			4.0	0.0007		
15	0.0273						
17	0.0140						
19	0.0007						

Series C3/4

t_1	N/N_o	t_2	N/N_o	t_3	N/N_o	t_4	N/N_o
4	0.9600	2	0.9871	1.2	0.9867	0.4	0.9867
6	0.9200	3	0.9352	2.2	0.9734	0.5	0.8801
8	0.7067	5	0.8703	2.4	0.9601	0.6	0.5068
10	0.4934	6	0.7924	2.6	0.8801	0.7	0.0335
12	0.3868	7	0.7145	2.8	0.7335	0.8	0.0669
14	0.2668	8	0.5197	3.0	0.5469	0.9	0.0137
16	0.1868	9	0.3249	3.2	0.3736	1.0	0.0005
18	0.1068	10	0.2211	3.4	0.2136		
20	0.0668	11	0.1302	3.6	0.1470		
22	0.0536	12	0.0783	3.8	0.0804		
26	0.0404	13	0.0264	4.0	0.0404		
30	0.0272	14	0.0135	4.2	0.0004		
32	0.0140	20	0.0006				
50	0.0008						

APPENDIX 3

CHARACTERISTICS OF COALESCENCE TIME DISTRIBUTIONS

Nomenclature

a_1, a_2, a_3, a_4 : Spherical drop diameter at the first, second, third and fourth stage of coalescence, respectively, cms.

L : Fall height of the primary drop to the interface

(N.B. Where L is reported as L = 0 cms. this means that the drop was formed very close to the interface and the distance of fall could not be measured accurately but was estimated to be between 0.2 and 0.3 cms.)

t_{m1}, t_{m2}, t_{m3}, t_{m4} : Mean coalescence rest-time for the first, second, third and fourth stage of coalescence, respectively, seconds.

$\sigma_1, \sigma_2, \sigma_3, \sigma_4$: Standard deviation of the coalescence rest-time for the first, second, third and fourth stage of coalescence, respectively, seconds.

t_{min} : minimum coalescence rest-time, seconds

t_{max} : maximum coalescence rest-time, seconds

$t_{\frac{1}{2}}$: the time for 50% of the drops to coalesce, seconds.

Heptane-Water

First Stage Coalescence

Study No.	a_1	L	t_{ml}	σ_1	t_{min}	t_{max}	$t_{\frac{1}{2}}$	$t_{ml}/t_{\frac{1}{2}}$	Number of Drops Assessed	Double-drop Coalescence
A1/1(i)	0.324	0	9.11	5.78	1.30	26.80	8.75	1.041	75	NO
A1/1(ii)	0.324	0	11.72	6.65	2.60	29.40	11.26	1.041	75	NO
A1/2(i)	0.324	2.5	14.07	8.17	1.70	33.10	13.80	1.020	75	NO
A1/2(ii)	0.324	2.5	8.63	6.57	1.20	28.05	6.50	1.328	75	NO
A1/3(i)	0.492	0	8.32	7.13	1.20	41.60	6.46	1.288	75	NO
A1/3(ii)	0.492	0	12.73	12.04	0.80	61.80	9.05	1.410	75	NO
A1/4	0.492	5.0	4.71	3.05	0.70	14.40	3.98	1.185	75	NO
A1/5	0.406	0.	5.82	3.00	0.75	18.00	5.20	1.120	75	NO
A1/6(i)	0.348	0	9.14	6.06	0.60	34.00	7.86	1.162	75	YES
A1/6(ii)	0.348	0	14.10	13.46	0.65	47.70	8.95	1.573	75	YES
A1/7	0.348	2.5	6.99	2.56	2.20	13.80	7.25	0.964	75	YES
A1/8	0.348	5.0	6.27	2.66	2.25	20.10	5.75	1.095	75	YES
A2/1	0.325	0	2.80	0.97	0.50	5.50	2.65	1.059	75	NO
A2/2	0.416	0	5.33	3.28	1.50	11.70	4.60	1.160	75	YES
A2/3	0.505	0	7.94	6.15	0.80	33.30	6.11	1.300	75	YES
A2/4	0.596	0	7.08	3.00	0.90	18.20	6.32	1.121	50	YES
A2/5	0.596	0	6.64	5.22	2.40	35.30	5.29	1.047	50	YES
A2/6	0.640	0	4.71	2.76	0.50	9.90	5.03	0.937	50	YES
A3/1	0.416	2.5	6.30	1.87	0.60	11.60	6.60	0.956	75	YES
A3/2	0.416	5.0	7.91	2.77	1.90	15.50	7.95	0.996	75	YES
A3/3	0.416	7.5	5.46	2.81	1.30	12.40	4.76	1.149	75	YES
A3/4	0.416	10.0	14.46	6.02	1.30	32.30	15.81	0.914	75	YES

Heptane-Water

Second Stage Coalescence

Study No.	a_2	t_{m2}	σ_2	t_{min}	t_{max}	$t_{\frac{1}{2}}$	$t_{m2}/t_{\frac{1}{2}}$	r_1
A1/1(i)	0.1229	6.28	2.56	0.50	10.65	6.31	0.995	0.3790
A1/1(ii)	0.1229	7.01	2.23	1.20	11.00	7.58	0.924	0.3790
A1/2(i)	0.1290	7.92	1.66	1.80	10.90	8.35	0.948	0.3980
A1/2(ii)	0.1290	7.06	1.83	2.60	9.60	7.36	0.960	0.3980
A1/3(i)	0.1540	9.16	4.63	0.90	17.20	9.15	1.001	0.3135
A1/3(ii)	0.1540	9.76	4.75	1.30	18.70	9.08	1.076	0.3135
A1/4	0.1610	6.83	3.92	1.20	16.00	6.61	1.033	0.3275
A1/5	0.1409	4.72	2.43	1.15	12.00	4.64	1.017	0.3465
A1/6(i)	0.1150	3.71	1.13	1.50	8.10	3.63	1.021	0.3302
A1/7	0.1341	5.65	1.92	0.90	9.20	6.10	0.926	0.3855
A1/8	0.1189	6.11	1.53	2.45	10.10	6.31	0.968	0.3418
A2/1	0.1230	1.77	0.43	1.30	3.30	1.72	1.031	0.3790
A2/2	0.1426	3.911	1.47	1.90	6.80	3.75	1.042	0.3430
A2/3	0.1558	7.22	2.41	1.90	12.10	7.10	1.018	0.3081
A2/4	0.1622	6.22	1.82	2.30	10.40	6.50	0.957	0.2721
A2/5	0.1622	5.54	2.22	2.10	11.00	5.50	1.008	0.2721
A2/6	0.1630	1.96	0.70	1.90	8.60	4.65	0.423	0.2546
A3/1	0.1450	4.00	0.63	2.20	6.60	4.06	0.983	0.3480
A3/2	0.1461	4.71	0.90	2.30	6.80	4.72	0.998	0.3519
A3/3	0.1431	5.73	1.23	2.90	8.80	5.73	0.999	0.3440

Heptane–Water

Third Stage Coalescence

Study No.	a_3	t_{m3}	ϵ_3	t_{min}	t_{max}	$t_{\frac{1}{2}}$	$t_{m3}/t_{\frac{1}{2}}$	r_2
A1/1(i)	0.0571	1.86	0.20	1.30	2.00	1.93	0.968	0.4665
A1/1(ii)	0.0571	1.887	0.34	1.30	2.30	2.06	0.916	0.4665
A1/2(i)	0.0593	2.05	0.14	1.50	2.30	2.14	0.958	0.4600
A1/2(ii)	0.0593	1.99	0.15	1.50	2.35	2.03	0.977	0.4600
A1/3(i)	0.0662	3.48	0.96	0.65	8.50	3.66	0.950	0.4300
A1/3(ii)	0.0662	3.43	0.69	1.60	5.10	3.56	0.964	0.4300
A1/4	0.0750	3.31	0.64	0.65	4.35	3.47	0.955	0.4660
A1/5	0.0631	2.19	0.55	0.40	3.20	2.15	1.018	0.4480
A1/6	0.0530	1.32	0.22	0.70	1.90	1.37	0.962	0.4610
A1/7	0.0601	1.65	0.27	0.60	2.10	1.75	0.942	0.4580
A1/8	0.0580	1.81	0.20	0.70	2.10	1.85	0.975	0.4880
A2/1	0.0573	0.94	0.28	0.50	1.90	0.93	1.018	0.4662
A2/2	0.0635	1.53	0.32	1.00	2.20	1.55	0.988	0.4460
A2/3	0.6650	2.77	0.33	1.00	3.20	2.87	0.965	0.4272
A2/4	0.6790	2.31	0.48	1.10	3.30	2.40	0.962	0.4080
A2/5	0.6790	2.59	0.36	1.70	3.80	2.68	0.966	0.4080
A2/6	0.6480	1.96	0.70	1.00	3.70	1.65	1.190	0.3980
A3/1	0.6580	1.55	0.19	1.20	1.90	1.59	0.975	0.4540
A3/2	0.6970	1.62	0.23	1.20	2.30	1.65	0.982	0.4775
A3/3	0.6830	2.09	0.13	1.80	2.30	2.15	0.973	0.4775
A3/4	0.6830	2.02	0.11	1.70	2.20	2.08	0.970	0.4775

Heptane–Water

Fourth Stage Coalescence

Study No.	a_4	t_{m4}	σ_4	t_{min}	t_{max}	$t_{\frac{1}{2}}$	$t_{m4}/t_{\frac{1}{2}}$	r_3
A1/1(i)	0.0285	0.39	0.11	0.20	0.80	0.41	0.921	0.5
A1/1(ii)	0.0285	0.36	0.10	0.20	0.70	0.39	0.882	0.5
A1/2(i)	0.0297	0.40	0.09	0.20	0.75	0.44	0.911	0.5
A1/2(ii)	0.0297	0.40	0.09	0.20	0.60	0.42	0.935	0.5
A1/3(i)	0.0331	0.81	0.68	0.25	1.00	0.79	1.020	0.5
A1/3(ii)	0.0331	0.78	0.17	0.45	1.20	0.83	0.937	0.5
A1/4	0.0375	0.83	0.18	0.50	2.00	0.83	0.988	0.5
A1/5	0.0315	0.59	0.12	0.30	0.90	0.62	0.945	0.5
A1/6(i)	0.0265	0.34	0.09	0.15	0.60	0.37	0.878	0.5
A1/7	0.0301	0.31	0.09	0.10	0.50	0.35	0.885	0.5
A1/8	0.0290	0.20	0.07	0.05	0.40	0.22	0.894	0.5
A2/1	0.0287	0.24	0.07	0.10	0.50	0.27	0.899	0.5
A2/2	0.0318	0.37		0.20	0.50	0.36	1.050	0.5
A2/3	0.0333	0.59	0.12	0.20	0.80	0.66	0.905	0.5
A2/4	0.0339	0.54	0.14	0.30	0.90	0.60	0.910	0.5
A2/5	0.0339	0.57	0.13	0.20	0.80	0.63	0.910	0.5
A2/6	0.0324	0.59	0.26	0.20	1.10	0.53	1.120	0.5
A3/1	0.0329	0.32	0.08	0.20	0.60	0.35	0.920	0.5
A3/2	0.0348	0.29	0.07	0.20	0.50	0.33	0.900	0.5
A3/3	0.0342	0.47	0.10	0.30	0.80	0.52	0.910	0.5
A3/4	0.0342	0.41	0.06	0.30	0.60	0.46	0.920	0.5

0.05M Decanoic Acid

First Stage Coalescence

Study No.	a_1	L	t_{ml}	σ_1	t_{min}	t_{max}	$t_{\frac{1}{2}}$	$t_{ml}/t_{\frac{1}{2}}$	Number of Drops Assessed	Double-drop Coalescence
B1/1	0.264	0	25.06	5.72	5.60	36.50	25.25	0.992	75	NO
B1/2	0.312	0	18.14	7.63	1.90	48.00	18.50	0.980	75	NO
B1/3	0.372	0	24.14	11.59	1.90	59.90	23.80	1.012	75	NO
B1/4	0.454	0	30.99	16.60	2.40	77.10	29.50	1.049	75	NO
B2/1	0.224	0	31.77	11.98	4.70	71.80	31.90	0.995	60	NO
B2/2	0.326	0	12.74	6.15	3.10	30.20	11.90	1.070	75	NO
B2/3	0.433	0	13.09	5.83	2.40	27.20	11.79	1.110	75	NO
B2/4	0.509	0	8.28	2.38	1.40	12.50	8.85	0.935	50	YES
B2/5	0.509	0	28.18	17.53	6.30	99.00	23.75	1.182	50	YES
B2/6	0.546	0	10.84	8.85	1.70	51.20	8.75	1.243	50	YES

0.05M Decanoic Acid

Second Stage Coalescence

Study No.	a_2	t_{m2}	σ_2	t_{min}	t_{max}	$t_{\frac{1}{2}}$	$t_{m2}/t_{\frac{1}{2}}$	r_1
B1/1	0.1062	7.51	1.03	3.30	8.90	7.80	0.962	0.4025
B1/2	0.1199	7.39	1.87	3.50	12.00	7.95	0.929	0.3840
B1/3	0.1340	7.87	2.32	2.10	13.70	7.28	1.081	0.3600
B1/4	0.1490	11.56	2.62	7.20	17.40	12.20	0.947	0.3280
B2/1	0.0936	7.63	1.63	2.10	9.50	8.46	0.903	0.4180
B2/2	0.1231	10.87	3.52	2.20	18.90	12.15	0.894	0.3780
B2/3	0.1458	8.88	2.44	3.70	14.70	8.74	1.017	0.3361
B2/4	0.1560	7.76	2.46	3.90	14.40	7.20	1.079	0.3064
B2/5	0.1560	12.80	3.98	4.80	9.60	12.70	1.009	0.3064
B2/6	0.1593	9.01	3.79	3.60	21.00	8.40	1.073	0.2920

0.05M Decanoic Acid

Third Stage Coalescence

Study No.	a_3	t_{m3}	σ_3	t_{min}	t_{max}	$t_{\frac{1}{2}}$	$t_{m3}/t_{\frac{1}{2}}$	r_2
B1/1	0.0510	1.54	0.13	1.25	1.90	1.59	0.968	0.4800
B1/2	0.0561	1.91	0.16	1.20	2.40	1.95	0.975	0.4685
B1/3	0.0610	2.35	0.43	1.00	2.90	2.47	0.950	0.4550
B1/4	0.0653	3.08	0.49	2.00	3.90	3.21	0.962	0.4280
B2/1	0.0457	1.73	0.16	1.30	2.00	1.83	0.944	0.4880
B2/2	0.0575	2.99	0.58	1.50	3.40	3.16	0.948	0.4660
B2/3	0.0645	3.65	0.39	2.10	4.20	3.76	0.972	0.4425
B2/4	0.0665	3.78	0.78	1.70	4.60	4.10	0.821	0.4265
B2/5	0.0665	4.12	0.71	2.10	4.80	4.42	0.932	0.4265
B2/6	0.0667	3.70	1.06	0.90	4.80	4.28	0.864	0.4190

0.05M Decanoic Acid

Fourth Stage Coalescence

Study No.	a_4	t_{m4}	σ_4	t_{min}	t_{max}	$t_{\frac{1}{2}}$	$t_{m4}/t_{\frac{1}{2}}$	r_3
B1/2	0.0281	0.34	0.09	0.20	0.80	0.36	0.935	0.50
B1/3	0.0305	0.42	0.10	0.10	0.70	0.45	0.941	0.50
B1/4	0.0326	0.69	0.13	0.30	1.00	0.71	0.980	0.50
B2/1	0.0228	0.36	0.06	0.20	0.50	0.42	0.855	0.50
B2/2	0.0288	0.56	0.14	0.30	0.90	0.62	0.899	0.50
B2/3	0.0323	0.77	0.12	0.50	1.10	0.83	0.930	0.50
B2/4	0.0333	0.98	0.22	0.70	2.30	1.00	0.976	0.50
B2/5	0.0333	0.89	0.17	0.50	1.40	0.97	0.918	0.50
B2/6	0.0334	1.01	0.12	0.60	1.20	1.10	0.925	0.50

0.5M Decanoic Acid

First Stage Coalescence

Study No.	a_1	L	t_{ml}	ϵ_1	t_{min}	t_{max}	$t_{\frac{1}{2}}$	$t_{ml}/t_{\frac{1}{2}}$	Number of Drops Assessed	Double-drop Coalescence
C1/1	0.232	0	10.76	3.38	1.30	17.05	11.15	0.965	75	NO
C1/2	0.232	2.5	12.48	4.79	1.40	22.00	13.50	0.925	75	NO
C1/3	0.232	5.0	9.03	5.50	1.00	21.70	8.50	1.061	75	NO
C1/4	0.314	0	12.40	5.93	0.70	24.30	12.80	0.967	75	NO
C1/5	0.382	0	18.08	10.18	2.30	42.10	16.50	1.116	75	NO
C1/6	0.428	0	18.03	11.17	2.50	72.50	16.20	1.112	75	NO
C2/1	0.208	0	14.42	6.27	2.50	30.40	13.90	1.039	75	NO
C2/2	0.324	0	7.78	3.94	1.50	26.60	7.66	1.014	75	NO
C2/3	0.387	0	16.27	5.98	0.90	34.20	15.85	1.026	75	NO
C2/4	0.449	0	21.85	10.58	1.50	58.10	22.20	0.985	75	NO
C2/5	0.488	0	23.53	14.93	1.50	80.60	20.00	1.171	50	NO
C3/1	0.324	2.5	13.18	6.40	1.80	33.00	11.60	1.135	75	NO
C3/2	0.324	5.0	10.42	4.98	1.60	22.90	10.10	1.031	75	NO
C3/3	0.324	7.5	7.76	3.57	2.10	18.20	7.07	1.099	75	NO
C3/4	0.324	10.0	11.90	6.95	2.30	48.60	10.20	1.168	75	NO

0.5M Decanoic Acid

Second Stage Coalescence

Study No.	a_2	t_{m2}	ϵ_2	t_{min}	t_{max}	$t_{\frac{1}{2}}$	$t_{m2}/t_{\frac{1}{2}}$	r_1
C1/1	0.0909	3.59	0.57	2.10	5.70	3.59	1.029	0.3920
C1/2	0.0889	5.12	1.02	2.70	8.20	4.98	1.028	0.3830
C1/3	0.0970	4.95	1.03	3.40	9.90	4.90	1.010	0.4185
C1/4	0.1092	6.44	1.59	3.10	14.35	6.24	1.031	0.3480
C1/5	0.1190	9.99	2.92	3.00	16.10	10.20	0.979	0.3115
C1/6	0.1230	9.87	4.56	4.80	31.90	9.40	1.050	0.2870
C2/1	0.0843	6.24	1.74	1.70	11.00	6.44	0.968	0.4050
C2/2	0.1110	4.65	2.15	0.90	13.60	4.43	1.048	0.3425
C2/3	0.1196	6.91	2.27	0.70	17.60	6.52	1.060	0.3086
C2/4	0.1239	6.28	2.77	0.70	15.70	5.83	1.079	0.2760
C2/5	0.1244	14.17	4.06	3.80	21.70	14.10	1.003	0.2546
C3/1	0.1079	8.00	3.00	2.20	18.40	7.50	1.068	0.3325
C3/2	0.1060	7.32	2.23	2.40	14.00	7.63	0.959	0.3275
C3/3	0.1052	6.40	2.28	1.40	11.50	5.31	1.209	0.3245
C3/4	0.1052	8.40	2.93	1.80	19.20	8.05	0.999	0.3245

0.5M Decanoic Acid

Third Stage Coalescence

Study No.	a_3	t_{m3}	ϵ_3	t_{min}	t_{max}	$t_{\frac{1}{2}}$	$t_{m3}/t_{\frac{1}{2}}$	r_2
C1/1	0.0438	1.37	0.14	0.90	1.70	1.43	0.962	0.4815
C1/2	0.0411	1.69	0.14	1.30	2.00	1.74	0.971	0.4740
C1/3	0.0522	1.56	0.18	1.20	2.00	1.60	0.976	0.5380
C1/4	0.0515	2.16	0.31	1.50	3.20	2.20	0.981	0.4710
C1/5	0.0551	3.13	0.65	1.90	4.70	3.15	0.994	0.4630
C1/6	0.0549	6.20		2.90	8.60	5.55	1.115	0.4460
C2/1	0.0408	1.75	0.20	1.20	2.20	1.79	0.979	0.4845
C2/2	0.0523	1.71	0.42	1.00	3.20	1.68	1.020	0.4700
C2/3	0.0554	2.03	0.49	0.60	4.10	2.20	0.925	0.4630
C2/4	0.0564	3.07	0.97	1.00	4.90	3.13	0.980	0.4550
C2/5	0.0561	4.23	0.45	2.80	5.20	4.44	0.952	0.4510
C3/1	0.0490	2.81	0.49	2.10	4.30	2.75	1.003	0.4550
C3/2	0.0543	2.63	0.44	0.80	3.90	2.70	0.974	0.5120
C3/3	0.0539	2.64	0.42	1.30	3.90	2.75	0.957	0.5120
C3/4	0.0539	3.03	0.48	1.10	4.10	3.05	0.994	0.5120

0.5M Decanoic Acid

Fourth Stage Coalescence

Study No.	a_4	t_{m4}	ϵ_4	t_{min}	t_{max}	$t_{\frac{1}{2}}$	$t_{m4}/t_{\frac{1}{2}}$	r_3
C1/5	0.0275	0.64	0.19	0.15	1.00	0.71	0.903	0.5
C1/6	0.0275	1.30	0.63	0.60	4.90	1.25	1.032	0.5
C2/1	0.0204	0.32	0.09	0.10	0.50	0.37	0.862	0.5
C2/2	0.0266	0.39	0.08	0.20	0.50	0.43	0.905	0.5
C2/3	0.0277	0.41	0.11	0.20	0.70	0.44	0.919	0.5
C2/4	0.0282	0.66	0.19	0.30	1.10	0.69	0.962	0.5
C2/5	0.0281	1.10	0.13	0.80	1.40	1.15	0.954	0.5
C3/1	0.0245	0.53	0.11	0.30	0.70	0.58	0.905	0.5
C3/2	0.0271	0.54	0.10	0.30	0.80	0.57	0.955	0.5
C3/3	0.0269	0.51	0.09	0.30	0.80	0.55	0.922	0.5
C3/4	0.0269	0.56	0.10	0.30	0.90	0.60	0.931	0.5

1.0M Decanoic Acid

First Stage Coalescence

Study No.	a_1	L	t_{ml}	ϵ_1	t_{min}	t_{max}	$t_{\frac{1}{2}}$	$t_{ml}/t_{\frac{1}{2}}$	Number of Drops Assessed	Double-drop Coalescence
D1/1	0.232	0	3.52	2.08	0.70	9.10	3.12	1.128	75	NO
D1/2	0.304	0	9.50	5.73	1.00	24.85	8.70	1.092	75	NO
D1/3	0.330	0	12.33	5.87	1.00	25.30	9.50	1.299	75	NO
D1/4	0.442	0	12.86	7.87	1.70	35.20	11.00	1.170	75	NO
D2/1	0.204	0	10.30	5.57	2.70	40.10	9.30	1.108	75	NO
D2/2	0.299	0	11.09	5.10	1.30	27.20	11.10	0.997	75	NO
D2/3	0.385	0	22.87	7.87	4.70	48.30	22.60	1.012	75	NO
D2/4	0.442	0	25.53	20.34	2.80	62.60	21.75	1.172	50	NO
D2/5	0.473	0	18.97	10.22	6.20	95.40	16.80	1.130	50	NO

1.0M Decanoic Acid

Second Stage Coalescence

Study No.	a_2	t_{m2}	ϵ_2	t_{min}	t_{max}	$t_{\frac{1}{2}}$	$t_{m2}/t_{\frac{1}{2}}$	r_1
D1/1	0.0908	4.01	1.37	2.30	11.80	3.75	1.070	0.3920
D1/2	0.1073	6.84	1.94	2.10	13.90	6.77	1.010	0.3535
D1/3	0.1120	7.53	2.24	3.00	16.80	7.70	0.978	0.3400
D1/4	0.1232	11.84	4.09	3.90	23.90	11.55	1.025	0.2795
D2/1	0.0830	5.83	2.49	2.30	15.30	5.45	1.070	0.4065
D2/2	0.1062	6.39	2.62	0.70	15.70	5.55	1.150	0.3560
D2/3	0.1192	9.41	3.34	2.30	22.00	9.20	1.023	0.3100
D2/4	0.1232	9.77	6.78	3.50	32.20	7.50	1.300	0.2795
D2/5	0.1242	10.70	5.43	2.60	29.40	8.20	1.308	0.2625

1.0M Decanoic Acid

Third Stage Coalescence

Study No.	a_3	t_{m3}	ϵ_3	t_{min}	t_{max}	$t_{\frac{1}{2}}$	$t_{m3}/t_{\frac{1}{2}}$	r_2
D1/1	0.0436	1.46	0.23	0.90	2.40	1.54	0.953	0.4810
D1/2	0.0507	2.27	0.47	1.60	4.10	2.34	0.975	0.4725
D1/3	0.0526	2.59	0.59	1.50	4.40	2.61	0.994	0.4696
D1/4	0.0563	3.88	0.87	1.60	5.80	3.78	1.028	0.4565
D2/1	0.0440	1.68	0.39	1.00	3.00	1.62	1.039	0.4850
D2/2	0.0504	2.03	0.56	0.80	4.10	1.97	1.031	0.4730
D2/3	0.0552	2.97	0.79	1.40	5.70	2.84	1.048	0.4635
D2/4	0.0562	3.81	1.17	1.60	6.30	3.65	1.045	0.4560
D2/5	0.0562	3.79	1.030	1.40	5.80	3.67	1.031	0.4525

1.0M Decanoic Acid

Fourth Stage Coalescence

Study No.	a_4	t_{m4}	σ_4	t_{min}	t_{max}	$t_{\frac{1}{2}}$	$t_{m4}/t_{\frac{1}{2}}$	r_3
D1/2	0.0254	0.41	0.10	0.25	0.70	0.44	0.953	0.5
D1/3	0.0263	0.49	0.132	0.20	1.00	0.51	0.975	0.5
D1/4	0.0282	0.76	0.17	0.40	1.20	0.77	0.994	0.5
D2/1	0.0220	0.34	0.08	0.20	0.50	0.38	1.039	0.5
D2/2	0.0252	0.44	0.13	0.20	0.90	0.46	1.031	0.5
D2/4	0.0281	0.82	0.21	0.30	1.30	0.83	1.045	0.5
D2/5	0.0281	0.97	0.26	0.30	1.50	0.98	1.031	0.5

APPENDIX 4

THE EXACT SHAPE OF A DEFORMED DROP

The exact shape of a deformed drop in an equilibrium position at the interface, can be calculated by the method of Princen (102), employing the Bashforth and Adams Tables (9). The calculated shape characteristics are shown in the figure below:

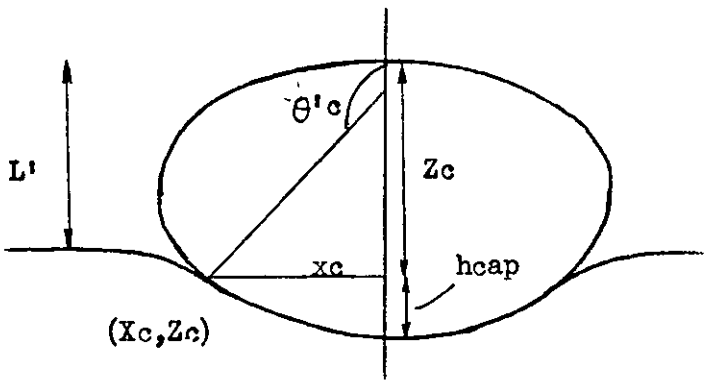

In addition, the following can also be calculated:

R = radius of spherical cap, cm.

L' = level of bulk interface far from the drop, cm.

$h_{cap} = R(1 + \cos \theta'_c)$ = height of spherical cap, cm.

$h_{drop} = h_{cap} + z_c$ = total height of drop, cm.

$A = 2\pi R h_{cap}$ = surface area of spherical cap ("contact" area), cm^2.

$V_{cap} = \frac{\pi}{3} h^2_{cap} (3R - h_{cap})$ = volume of spherical cap, cm^3.

V_c = volume of drop above the plane $z = z_c$, cm^3

θ'_c = angle of normal at (x_c, z_c)

$2X_{90^o}$ = maximum horixontal diameter, cm.

q = measure of deformation of the drop = $2X_{90^o}/h_{drop}$

p = R/b

and :

b = spherical drop diameter, cm.

F = Force causing drainage = $2\pi x_c \gamma \sin \theta'_c$, dynes

t_m = mean coalescence rest-time, seconds.

The tables of drop shape characteristics cover the systems A, B, C and D in this work and a number of other systems reported in the literature.

DROP SHAPE CHARACTERISTICS

(Series A2, B2, C2 and D2)

System	b	R	q	L'	x_c	z_c	θ'_c	h_{cap}	h_{drop}	$2X_{90^o}$	P	A	F	t_m
Heptane -Water	0.320	0.536	1.2735	0.3760	0.2420	0.4838	153.17	0.0576	0.5414	0.690	1.674	0.171	34.80	4.712
Heptane -Water	0.298	0.505	1.2495	0.3690	0.2140	0.4613	154.90	0.0476	0.5089	0.6350	1.693	0.151	28.95	6.640
Heptane -Water	0.2525	0.4405	1.200	0.3420	0.1608	0.3986	158.61	0.03016	0.42876	0.5146	1.745	0.0835	18.81	7.948
Heptane -Water	0.208	0.3745	1.1518	0.3066	0.1120	0.358	162.4	0.01753	0.3755	0.4326	1.800	0.0412	10.81	5.34
Heptane -Water	0.1625	0.3001	1.1088	0.2709	0.7345	0.291	165.81	0.0091	0.3001	0.3325	1.847	0.01714	5.74	2.804
0.05M Decanoic Acid	0.273	0.4551	1.279	0.2929	0.2082	0.4090	152.80	0.0504	0.4594	0.5872	1.668	0.1443	19.42	10.84
0.05M Decanoic Acid	0.2505	0.4230	1.2622	0.2945	0.1847	0.3835	154.00	0.04284	0.4263	0.5385	1.688	0.1140	16.51	8.28
0.05M Decanoic Acid	0.2165	0.3747	1.2178	0.2765	0.1438	0.3478	157.31	0.0290	0.3768	0.4585	1.730	0.06825	11.33	13.09
0.05M Decanoic Acid	0.1630	0.2935	1.1521	0.2439	0.08635	0.2880	162.82	0.01311	0.3011	0.3465	1.800	0.02435	5.21	12.74
0.05M Decanoic Acid	0.1120	0.2103	1.0911	0.1970	0.04315	0.2053	168.02	0.00441	0.2097	0.2285	1.879	0.00583	1.835	31.77

(Continued)

DROP SHAPE CHARACTERISTICS

(Series A2, B2, C2 and D2)

System	b	R	q	L'	x_c	z_c	θ'_c	h_{cap}	h_{drop}	$2X_{90°}$	P	A	F	t_m
0.5M Decanoic Acid	0.244	0.3993	1.3083	0.2705	0.196	0.3521	150.63	0.05127	0.4034	0.5271	1.635	0.1285	13.62	23.53
0.5M Decanoic Acid	0.2245	0.3751	1.2791	0.2634	0.1717	0.3365	152.40	0.04268	0.3792	0.4850	1.670	0.1008	11.22	21.85
0.5M Decanoic Acid	0.1935	0.3320	1.2303	0.2450	0.1328	0.306	156.32	0.02795	0.3340	0.4110	1.717	0.05825	7.545	16.27
0.5M Decanoic Acid	0.162	0.2820	1.1835	0.2288	0.0961	0.2658	160.00	0.0170	0.2828	0.3346	1.75	0.03009	4.64	7.28
0.5M Decanoic Acid	0.104	0.1940	1.104	0.1783	0.04268	0.1895	167.32	0.00474	0.1942	0.2143	1.867	0.0058	1.328	14.42
1.0M Decanoic Acid	0.2365	0.384	1.3273	0.260	0.1968	0.3346	149.2	0.0541	0.3887	0.5150	1.621	0.1306	11.80	18.97
1.0M Decanoic Acid	0.2210	0.3655	1.2930	0.2501	0.1731	0.3261	151.78	0.04215	0.3683	0.4765	1.654	0.09415	9.56	25.53
1.0M Decanoic Acid	0.1925	0.3275	1.2458	0.2328	0.1372	0.2996	155.19	0.0302	0.3298	0.4109	1.700	0.06179	6.726	22.87
1.0M Decanoic Acid	0.1495	0.2650	1.1753	0.2070	0.0871	0.2508	160.7	0.0149	0.2657	0.2915	1.774	0.0248	3.370	11.09
1.0M Decanoic Acid	0.1020	0.1898	1.110	0.1673	0.0433	0.1849	166.86	0.00497	0.1899	0.2085	1.8610	0.00592	1.148	10.30

DROP SHAPE CHARACTERISTICS

System	Reference	b	R	q	L'	x_c	z_c	Θ'_c	h_{cap}	h_{drop}	$2X_{90°}$	P	A	F	Temp. °C	t_m
Benzene -water	16	0.192	0.3562	1.085	0.3160	.0725	.3475	168.42	.007275	.35478	.3850	1.857	.01629	3.243	20	4.1
Benzene -water		0.208	0.3885	1.097	0.334	.08575	.3768	167.52	.00916	.38596	.4320	1.862	.0224	4.15	20	5.9
Benzene -water		0.272	0.4935	1.1404	0.3663	.1405	.4790	163.55	.0202	.4992	.5690	1.812	.06255	8.90	20	11.7
Benzene -water		0.302	0.5340	1.1650	0.4260	.1700	.5085	161.25	.0282	.5367	.6250	1.769	.0945	12.21	20	18.9
CCl4 -water	16	0.168	0.2917	1.206	0.2241	.1083	.2729	158.20	.02081	.2937	.3538	1.736	.03805	10.40	15	3.1
CCl4 -water		0.168	0.2916	1.2075	0.2241	.109	.2724	158.04	.02115	.29355	.3540	1.735	.0386	10.30	20	2.4
CCl4 -water		0.164	0.2917	1.206	0.1975	.106	.2670	158.20	.02081	.2878	.3461	1.778	.03805	9.025	25	1.5
CCl4 -water		0.162	0.2819	1.205	0.2140	.1045	.2637	158.22	.0205	.2842	.3425	1.740	.03621	8.680	30	1.4
Benzene -water	16	0.289	0.519	1.155	0.4276	.1560	.4970	162.58	.02379	.5218	.6035	1.797	.0779	10.61	15	16.1
Benzene -water		0.284	0.5095	1.15255	0.4196	.1541	.4873	162.38	.02385	.51115	.5776	1.795	.0765	10.44	20	14.8
Benzene -water		0.275	0.4935	1.1565	0.3774	.1509	.4712	162.11	.0238	.4950	.5720	1.794	.0737	10.10	30	13.8
Benzene -water		0.270	0.482	1.158	0.3920	.1492	.4605	161.86	.02395	.48445	.5600	1.788	.0725	10.10	40	13.2
n Heptane -water	16	0.232	0.4315	1.178	0.2179	.1350	.3800	160.2	.0255	.4055	.4780	1.860	.0691	14.48	20	3.6
Ethylene Glycol -n Hexane	*Konnecke	0.0965	0.1731	1.150	0.1488	.05176	.1660	162.63	.0079	.1739	.1999	1.795	.0086	1.562	20	3.0
Ethylene Glycol -n Hexane		0.0965	0.1729	1.1555	0.14105	.05655	.1652	162.05	.00841	.1736	.2004	1.790	.00913	1.669	40	1.6
Ethylene Glycol -n Hexane		0.0965	0.1731	1.15375	0.14125	.0526	.1654	162.24	.008255	.17366	.2002	1.795	.00899	1.582	60	1.0
Tri-Ethylene Glycol-n Hexane																

*Konnecke, H.G., Z. Physik Chem., (Leipzig), 211, 208, (1959).

(Continued)

DROP SHAPE CHARACTERISTICS

System	Reference	b	R	q	L'	x_c	z_c	Θ'_c	h_{cap}	h_{drop}	$2X_{90°}$	P	A	F	Temp. °C	t_m
Tri-Ethylene Glycol-n Hexane	Konnecke*	0.078	0.1391	1.1610	0.1141	.04355	.1329	161.69	.00704	.1399	.1625	1.783	.00615	0.845	20	2.3
Tri-Ethylene Glycol-n Hexane	Konnecke	0.078	0.1384	1.167	0.11215	.0445	.1320	161.15	.00740	.1394	.1628	1.775	.00643	0.835	40	1.6
Tri-Ethylene Glycol-n Hexane	Konnecke	0.078	0.1389	1.163	0.1139	.0439	.1329	161.45	.00720	.1401	.1630	1.780	.00628	0.796	60	1.3
Di-Ethylene Glycol-n Hexane	Konnecke	.075	0.1350	1.1498	0.1089	.0401	.1292	164.16	.00511	.1343	.1543	1.80	.00433	0.680	20	3.8
Di-Ethylene Glycol-n Hexane	Konnecke	.075	0.1349	1.150	0.1106	.04038	.1291	164.06	.005175	.13428	.1546	1.799	.004385	0.689	40	1.8
Di-Ethylene Glycol-n Hexane	Konnecke	.075	0.13475	1.1525	0.10875	.04115	.1288	162.37	.00632	.1351	.1558	1.795	.00534	0.760	60	1.3
Ethylene Glycol -Benzene	82	.085	0.1552	1.133	0.1282	.04272	.1491	164.91	.00534	.1544	.1750	1.829	.00521	0.5165	20	5.1
Ethylene Glycol -Benzene		.085	0.1540	1.1410	0.1254	.0440	.1478	163.48	.00636	.15416	.1760	1.810	.00615	0.5160	40	1.0
Ethylene Glycol -Benzene		.085	0.1535	1.1432	0.1291	.0444	.1473	163.27	.00650	.1538	.1760	1.805	.00626	0.567	60	2.6
Benzene -water	82	0.2075	0.3865	1.101	0.3281	.0880	.3745	167.17	.00965	.3842	.4230	1.863	.0234	4.24	25	4.7
Ethylene Glycol -Benzene	82	0.0975	0.1737	1.162	0.1358	.0544	.1658	161.58	.00889	.1747	.2030	1.780	.0097	0.802	25	23.5
Ethylene Glycol -Benzene		0.0795	0.1464	1.1320	0.1183	.03743	.1409	165.36	.00478	.1447	.1639	1.842	.0044	0.441	25	14.0
Ethylene Glycol -Benzene		0.0625	0.1231	1.08306	0.096	.02469	.1202	168.44	.00250	.1227	.1328	1.971	.001932	0.2282	25	20.9
Water -'Aroclor'	82	.114	0.2120	1.108	0.2059	.0503	.2042	166.5	.00585	.2101	.2325	1.859	.00779	3.02	25	206.0
Benzene -water	82	0.215	0.401	1.097	0.3389	.3843	.1632	167.03	.01025	.1735		1.865	.0258	1.890	25	6.0

*Konnecke, H.G., Z. Physik Chem. (Leipzig), 211, 208, (1959)

APPENDIX 5

FITTING OF MULTIPLE REGRESSION BY THE METHOD OF LEAST SQUARES

A.1. Mathematical Model and Least Squares Equations

The mathematical model relating the mean coalescence time to the physical variables of the system is given by Eqn. (7.2.1):

$$t_m = k\, a^p \mu_2^q \Delta\rho^r \gamma^s \qquad (A.1.)$$

A non-linear model of this type is referred to as being intrinsically linear (29) and it can be expressed by a suitable transformation of the variables, in a standard linear form. Taking logarithms to the base e of Eqn. (7.2.1):

$$\ln t_m = \ln k + p \ln a + q \ln \mu_2 + r \ln \Delta\rho + s \ln \gamma \qquad (A.2)$$

In the case where the fall height, L, is important Eqn. (7.2.2) is transformed to:

$$\ln t_m = \ln k + p \ln a + q \ln \mu_2 + r \ln \Delta\rho + s \ln \gamma + t \ln L \qquad (A.3)$$

If we put $y, x_1, x_2 \ldots x_5$ equal to $\ln t_m$, $\ln a$, $\ln \mu_2$, $\ln \Delta\rho$, $\ln \gamma$ and $\ln L$, respectively, the equations (A.2) and (A.3) may be re-written in the general manner as described by Davies (22):

$$y = b_o + b_1 x_1 + b_2 x_2 \ldots b_p x_p \qquad (A.4)$$

where $p = 4$ for Eqn. (A.2) and $p = 5$ for Eqn. (A.3). For sets of values satisfying this relationship exactly

$$y - b_o - b_1 x_1 - \ldots b_p x_p = 0 \qquad (A.5)$$

For any set of values $x_{1i}, \ldots, x_{pi}$ of the independent variables $x_1, \ldots, x_p$ we may derive an "expected value" Y_i of the "dependent" variable y from the relationship:

$$Y_i = b_o + b_1 x_{1i} + \ldots + b_p x_{pi} \qquad (A.6)$$

Observations obtained in practice will be more or less scattered about an exact relationship. To each observed set of values $x_{1i}, \ldots, x_{pi}$ will correspond an expected value of Y_i of the dependent variable y, but the observed value of y_i of y will not, in general, be equal to Y_i. The difference between the observed and expected values of y will be:

$$(y_i - Y_i) = (y_i - b_o - b_1 x_{1i} - \ldots b_p x_{pi}) \qquad (A.7)$$

The values of the constants $b_o, \ldots, b_p$ are as yet unknown. The problem is to derive those values for the constants which will give rise to the least disagreement, overall, between observation and expectation. As a measure of the overall disagreement we take:

$$Q = \sum_i (y_i - Y_i)^2 \qquad (A.8)$$

i.e. the sum of squares of the deviations of observed values of the dependent variable from those expected. In fitting by the method of least squares we aim to choose $b_o, \ldots, b_p$ so as to minimise Q. This may be done by the methods of the differential calculus. The partial deviations of Q with respect to $b_o, \ldots, b_p$ are each equated to zero, giving a set of simultaneous equations for the desired values of $b_o, \ldots b_p$.

We have that:

$$Q = \sum (y - b_o - b_1 x_1 - \ldots - b_p x_p)^2 \qquad (A.9)$$

where, for convenience, we have dropped the subscript i and the summation is understood to be over the n sets of observations $i = 1, \ldots, n$.

Differentiating with respect to b_o and equating to zero:

$$\frac{\partial Q}{\partial b_o} = -2\sum (y - b_o - b_1 x_1 - \ldots b_p x_p) = 0$$

$$\text{i.e. } nb_o = \sum y - b_1 \sum x_1 - \ldots - b_p \sum x_p$$

$$\text{or } b_o = \bar{y} - b_1 \bar{x}_1 - \ldots b_p \bar{x}_p \qquad (A.10)$$

For $k \neq 0$:

$$\frac{\partial S}{\partial b_k} = -2\Sigma x_k (y - b_o - b_1 x_1 - \ldots b_k x_k - \ldots - b_p x_p) = 0$$

i.e. $$b_o \Sigma x_k + b_1 \Sigma x_1 x_k + \ldots + b_k \Sigma x_k^2 + \ldots + b_p \Sigma x_p x_k = \Sigma y x_k \qquad (A.11)$$

Now $b_o = \bar{y} - b_1\bar{x}_1 - \ldots - b_p\bar{x}_p$, from Eqn. (A.10).

Hence, eliminating b_o, Eqn. (A.11) becomes:

$$b_1 \Sigma x_k (x_1 - \bar{x}_1) + \ldots + b_k \Sigma x_k (x_k - \bar{x}_k) + \ldots + b_p \Sigma x_k (x_p - \bar{x}_p) = \Sigma x_k (y - \bar{y}) \qquad (A.12)$$

Now $\Sigma x_k (x_1 - \bar{x}_1) \equiv \Sigma (x_k - \bar{x}_k)(x_1 - \bar{x}_1)$, the difference between the two expressions is $\bar{x}_k \Sigma (x_1 - \bar{x}_1)$, which is identically zero from the definition of $\bar{x}_1$. A similar modification may be made to the other summations involved in Eqn. (A.12) which thus becomes:

$$b_1 \Sigma (x_1 - \bar{x}_1)(x_k - \bar{x}_k) + \ldots + b_k \Sigma (x_k - \bar{x}_k)^2 + \ldots + b_p \Sigma (x_p - \bar{x}_p)(x_k - \bar{x}_k) = \Sigma (y - \bar{y})(x_k - \bar{x}_k) \quad (k = 1, \ldots, p)$$

or more concisely

$$b_1 C_{1k} + \ldots + b_k C_{kk} + \ldots b_p C_{pk} = C_{yk} \qquad (A.13)$$

$(k = 1, \ldots, p)$, where C_{1k} denotes $\Sigma (x_1 - \bar{x}_1)(x_k - \bar{x}_k)$, etc.

Eqn. (A.13) represents in fact a set of p simultaneous equations for the regression coefficients $b_1, \ldots, b_p$. Written out in more detail these take the form

$$\left.\begin{aligned} b_1 C_{11} + b_2 C_{12} + \ldots + b_p C_{1p} &= C_{y1} \\ b_1 C_{12} + b_2 C_{22} + \ldots + b_p C_{2p} &= C_{y2} \\ b_1 C_{13} + b_2 C_{23} + \ldots + b_p C_{3p} &= C_{y3} \\ \ldots \qquad \ldots \qquad \ldots & \\ b_1 C_{1p} + b_2 C_{2p} + \ldots + b_p C_{pp} &= C_{yp} \\ b_o = \bar{y} - b_1\bar{x}_1 - b_2\bar{x}_2 - \ldots b_p\bar{x}_p & \end{aligned}\right\} \qquad (A.14)$$

These equations, together with Eqn. (A.10), give the least squares estimates of the constants in the regression equation representing the dependence of

y on $x_1, \ldots, x_p$. The number of equations is equal to the number of constants to be estimated, i.e. $(p + 1)$, and the coefficients (apart from those in the equation of means defining b_o) form a symmetrical pattern, with sums of squares along the principal (N.W. - S.E.) diagonal, and sums of products elsewhere.

A.2 Solution of the Least Squares Equations

One form of solution of the equations is obtained by solving, not the original set of p equations, but the p sets of p equations obtained by successively substituting on the right of the original equations the sets of values (1, 0, 0, ..., 0), (0, 1, 0, ...0), (0,0,1 ...,0), ..., (0,0,0, ... , 1). The importance arises from the fact that this form of the solution gives as a by-product, the standard errors of the regression coefficients.

With for example, four independent variables, as in Eqn. (A.2), the Least Squares equations are

$$b_1 C_{11} + b_2 C_{12} + b_3 C_{13} + b_4 C_{14} = C_{y1}$$
$$b_1 C_{12} + b_2 C_{22} + b_3 C_{23} + b_4 C_{24} = C_{y2}$$
$$b_1 C_{13} + b_2 C_{23} + b_3 C_{33} + b_4 C_{34} = C_{y3}$$
$$b_1 C_{14} + b_2 C_{24} + b_3 C_{34} + b_4 C_{44} = C_{y4}$$

We replace these by four sets of equations

$$p C_{11} + q C_{12} + r C_{13} + s C_{14} = 1,0,0,0$$
$$p C_{12} + q C_{22} + r C_{23} + s C_{24} = 0,1,0,0$$
$$p C_{13} + q C_{23} + r C_{33} + s C_{34} = 0,0,1,0$$
$$p C_{14} + q C_{24} + r C_{34} + s C_{44} = 0,0,0,1$$

each set corresponding to a particular column of figures on the right. Let the solutions to the first set (right-hand sides 1,0,0,0 respectively) be

$$p_1 = C^{11}$$
$$q_1 = C^{21}$$
$$r_1 = C^{31}$$
$$s_1 = C^{41}$$

Let those to the second set be similarly

$$p_2 = C^{12}$$
$$q_2 = C^{22}$$
$$r_2 = C^{32}$$
$$s_2 = C^{42}$$

and so on for the third and fourth sets. We may write the four sets of solutions as the array of numbers

$$\begin{array}{cccc} C^{11} & C^{12} & C^{13} & C^{14} \\ C^{21} & C^{22} & C^{23} & C^{24} \\ C^{31} & C^{32} & C^{33} & C^{34} \\ C^{41} & C^{42} & C^{43} & C^{44} \end{array}$$

each set of solutions forming one column of the array.

The reader familiar with matrix algebra, will recognise this array as the inverse of the matrix of sums of squares and products formed by the coefficients on the left-hand sides of the original equations. Using the inverse matrix, the solutions to the original equations are given by:

$$\left.\begin{array}{rcl} b_1 &=& C^{11} C_{y1} + C^{12} C_{y2} + C^{13} C_{y3} + C^{14} C_{y4} \\ b_2 && C^{21} C_{y1} + C^{22} C_{y2} + C^{23} C_{y3} + C^{24} C_{y4} \\ b_3 && C^{31} C_{y1} + C^{32} C_{y2} + C^{33} C_{y3} + C^{34} C_{y4} \\ b_4 && C^{41} C_{y1} + C^{42} C_{y2} + C^{43} C_{y3} + C^{44} C_{y4} \end{array}\right\} \quad (A.15)$$

Thus, b_1 is obtained by summing the products of successive terms in the first row of the inverse matrix with the corresponding quantities on the right hand sides of the original equations, b_2 by using similarly, the second row of the matrix, and b_3 by using the third row.

A.3 Analysis of Variance

The sum of squares due to regression is given by

$$b_1 C_{y1} + b_2 C_{y2} + \ldots b_p C_{yp}$$

and is associated with p degrees of freedom. The residual sum of squares is:

$$C_{yy} - b_1 C_{y1} - b_2 C_{y2} - \ldots b_p C_{yp} \qquad (A.16)$$

and is associated with n- p- 1 degrees of freedom where n is the number of sets of observations used in deriving the regression equation. We may thus draw up an Analysis of Variance Table as follows:-

TABLE 5.A.1

ANALYSIS OF VARIANCE FOR MULTIPLE REGRESSION

Source of Variation	Degrees of Freedom	Sum of Squares	Mean Squares
Attributable to regression	p	$b_1C_{y1} + b_2C_{y2} + \ldots + b_pC_{yp}$	
Deviation from regression	n - p - 1	$C_{yy} - b_1C_{y1} - \ldots - b_pC_{yp}$	
Total	C_{yy}	n - 1	

The F-ratio calculated from this table may be used to test for the significance of the apparent dependence, but such a test of the combined dependence on all independent variables is not usually sufficient, since it tells nothing about the significance of particular terms in the regression equation.

A.4 Standard Errors and Confidence Limits

The residual sum of squares due to regression (i.e. Deviation from Regression in Table 5.A.1) gives an estimate of the residual variance based on n - p - 1 degrees of freedom, since in all p + 1 parameters have been

estimated. It should be noted, however, that the residual variance will only estimate the true "error" mean square if the regression equation is correctly formulated. If significant variables have been omitted, on if the true relationship is non-linear, the estimate will be biased.

The estimate of the residual variance is:

$$s^2 = \frac{1}{n - p - 1} (C_{yy} - b_1 C_{y1} - \ldots - b_p C_{yp}) \qquad (A.17)$$

As mentioned earlier, the standard errors of the estimated regression coefficients are obtained by way of the inverse matrix. Thus

$$\text{S.E. } (b_1) = s \sqrt{C^{11}}$$
$$\text{S.E. } (b_2) = s \sqrt{C^{22}}$$
$$\text{S.E. } (b_3) = s \sqrt{C^{33}}$$

etc.

Limits within which the true regression coefficients $b_1, \ldots b_p$ probably lie, i.e. the confidence limits, are calculated from the standard errors by means of the appropriate t - multipliers. Thus the $(1 - 2\alpha)$ confidence limits for b_1 are

$$b_1 \pm t_\alpha . s \sqrt{C^{11}} \qquad (A.18)$$

where t has the same number of degrees of freedom $(n - p - 1)$ as the estimate of s^2, i.e. on the residual scatter about the regression, on the number of observations available (which determines the appropriate t-multipliers) and also on the inverse matrix term C^{11}. This last depends on the spread of the observed x_1 - values, and also on the extent to which the variations in x_1 are correlated with variations in the other "independent" variables. The greater the spread, and the less the correlation, the smaller will be the value of C^{11}. Its reciprocal $1/C^{11}$, is in fact the residual sum of squares of the x_1-values about a regression of x_1 on the independent variables $x_2, \ldots, x_p$, and this is used to derive the standard error of b_1.

The significance of b_1 is measured by its ratio to its standard error, i.e. by:

$$t = b_1 / s \sqrt{C^{11}} \qquad (A.19)$$

The degrees of freedom for t are, as for t_α, n - p - 1.

For example, consider the case PROL 33 for which the calculated statistics are contained in Appendix 5. The residual sum of squares (i.e. "Deviation from Regression" in the computer print-out) is 2.25360 and this corresponds to (55 - 5 - 1) = 49 degrees of freedom. The estimated residual variance is thus

$$s^2 = \frac{1}{49} (2.2536) = 0.4599$$

giving $s = 0.6781$

Hence

$$S.E.(b_1) = 0.07557$$
$$S.E.(b_2) = 0.07362$$
$$S.E.(b_3) = 0.11480$$
$$S.E.(b_4) = 0.11959$$
$$S.E.(b_5) = 0.03915$$

95% confidence limits for the true regression coefficients are:

For
$$1 = 0.94123 \pm 2.011 \times 0.07557$$
$$2 = 0.92540 \pm 2.011 \times 0.07362$$
$$3 = 0.37633 \pm 2.011 \times 0.11480$$
$$4 = -1.59875 \pm 2.011 \times 0.11959$$
$$5 = 0.04132 \pm 2.011 \times 0.03915$$

while the calculated t - values for testing the significance of the b's are 12.4545, 12.5696, 3.7280, -13.3681 and 1.0553 respectively. The t - value for all of the coefficients except β_5 is significant at the 99% level. We see from the confidence limits that the estimate of β_5 is so imprecise that it is not unlikely that the true value is zero. The

t-value for β_5 fails, similarly, to reach the 0.05 significance level. The confidence limits for each of the other cases is presented in Table 5.A.2 and the significance at the 95% level is reported as "significant" or "not significant". If the regression coefficient is significant at the 99% level then it is reported as "highly significant".

A.5 Examination of Residuals

The residuals defined as the n differences $e_i = Y_i - \hat{Y}_i$, $i = 1,2, \ldots, n$ where Y_i is an observation and $\hat{Y}_i$ is the corresponding fitted value obtained by use of the fitted regression equation.

We can see from this definition that the residuals e_i are the differences between what is actually observed, and what is predicted by the regression equation - that is, the amount which the regression equation has not been able to explain. Thus e_i may be thought of as the observed errors if the model is correct. Now in performing the regression analysis certain assumptions have been made concerning the errors; the usual assumptions are that the errors are independent, have zero mean, a constant variance, σ^2, and follow a normal distribution. Thus if the fitted model is correct, the residuals should exhibit tendencies that confirm the assumptions that have been made, or at least, should not exhibit a denial of the assumptions.

The residuals can be examined graphically and the principal ways of plotting these are (29).

1. Overall
2. In time sequence, if the order is known
3. Against the fitted Y_i values
4. Against the independent variables

If we choose method (3) then the plot may be one of the forms indicated in Fig. (5.A.1)

(a)

(b)

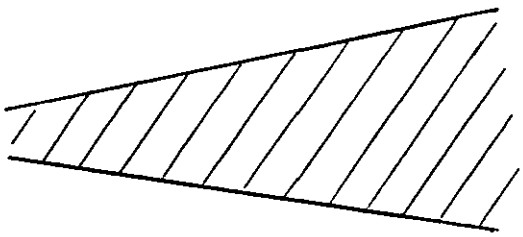

(c)

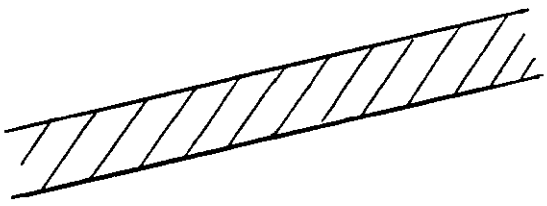

(d)

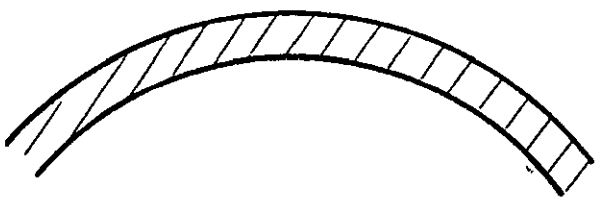

Fig. (5.A.1)

They represent:

(a) a "horizontal band" indicating no abnormality (the same form would be obtained for method (i))

(b) Variance not constant, as assumed; need for weighted least squares or a transformation on the observations Y_i before making a regression analysis

(c) Error in analysis; the departure from fitted equation is systematic

(d) Model inadequate - need for extra terms in the model, or need for a transformation on the observations Y_i before analysis

Figs. (5.A.2) to (5.A.4) show plots of e_i against Y_i for the cases PROL03, PROL 07 and PROL 41, respectively. Cases PROL 03 and PROL 41 clearly exhibit the trend shown in Fig. (5.A.1 (a)). Whilst the trend exhibited by case PROL 07 in Fig. (5.A.3) is not definitely of this latter type an overall plot of e_i does not indicate any abnormality. The examples shown in Figs. (5.A.2) to (5.A.4) are typical of the rest of the cases examined.

A.6 Prediction using the Regression Equation

The regression equation is of the form $y = b_o + b_1x_1 + \ldots + b_px_p$ where $b_o = \bar{y} - b_1\bar{x}_1 - \ldots - b_p\bar{x}_p$. We may therefore re-write the equation as:

$$y = \bar{y} + b_1 (x - \bar{x}_1) + \ldots + b_p (x_p - \bar{x}_p) \qquad (A.20)$$

remembering of course that,

$$y \equiv \ln t_m$$
$$x_1 \equiv \ln a$$
$$x_2 \equiv \ln \mu_2$$
$$x_3 \equiv \ln \Delta\rho$$
$$x_4 \equiv \ln \gamma$$
$$x_5 \equiv \ln L$$

Corresponding to any set of assigned values $(X_1, \ldots, X_p)$ of the independent variables $x_1, \ldots, x_p$, there is a predicted value Y of y which may be calculated from the equation. This value is subject to uncertainty, since it is derived by using coefficients which are themselves subject to uncertainty. The standard error of the estimate of Y is calculated by the computer program and 95% confidence limits are found in the same manner as for the regression coefficients.

TABLE 5.A.2

95% CONFIDENCE LIMITS FOR TRUE REGRESSION COEFFICIENTS

CASE		LIMITS	SIGNIFICANCE
PROL 01	β_1 =	1.0128 ± 0.4370	Highly significant
	β_2 =	fail	Not significant
	β_3 =	fail	Not significant
	β_4 =	fail	Not significant
PROL 02	β_1 =	1.4671 ± 1.2050	Highly significant
	β_2 =	2.0829 ± 3.8400	Not significant
	β_3 =	1.1271 ± 2.9630	Not significant
	β_4 =	-0.8255 ± 0.4080	Highly significant
PROL 03	β_1 =	2.2769 ± 1.1410	Highly significant
	β_2 =	2.0806 ± 2.4850	Not significant
	β_3 =	1.0197 ± 1.8460	Not significant
	β_4 =	-0.4905 ± 0.2600	Highly significant
PROL 04	β_1 =	2.6578 ± 1.0990	Highly significant
	β_2 =	1.1104 ± 2.1400	Not significant
	β_3 =	0.1053 ± 1.6200	Not significant
	β_4 =	-0.4048 ± 0.5400	Highly significant
PROL 05	β_1 =	0.6834 ± 0.2320	Highly significant
	β_2 =	2.2243 ± 2.1610	Significant
	β_3 =	1.3802 ± 1.6220	Not significant
	β_4 =	-0.9041 ± 0.3438	Highly significant
PROL 06	β_1 =	2.2044 ± 0.2237	Highly significant
	β_2 =	1.2821 ± 1.2750	Significant
	β_3 =	0.3669 ± 1.0550	Not significant
	β_4 =	-0.4353 ± 0.1590	Highly significant
PROL 07	β_1 =	1.2964 ± 0.1382	Highly significant
	β_2 =	0.7866 ± 1.9830	Not significant
	β_3 =	0.1641 ± 1.5770	Not significant
	β_4 =	-0.6702 ± 0.2755	Highly significant
PROL 21	β_1 =	0.4075 ± 0.4570	Not significant
	β_2 =	0.4739 ± 0.1512	Highly significant
	β_3 =	0.3100 ± 0.1820	Highly significant
	β_4 =	0.1565 ± 0.3840	Not significant
PROL 22	β_1 =	1.6384 ± 0.2350	Highly significant
	β_2 =	0.3935 ± 3.0650	Not significant
	β_3 =	-0.9748 ± 2.7150	Not significant
	β_4 =	1.7473 ± 4.520	Not significant
	β_5 =	-0.1096 ± 0.1492	Not significant

TABLE 5.A.2 (Continued)

CASE			LIMITS			SIGNIFICANCE
PROL 23	β_1	=	1.3939	±	0.3760	Highly significant
	β_2	=	0.5779	±	0.0966	Highly significant
	β_3	=	-0.0670	±	0.1354	Not significant
	β_4	=	-0.4326	±	0.2226	Highly significant
	β_5	=	-0.7072	±	0.2334	Highly significant
PROL 31	β_1	=	0.7573	±	0.1590	Highly significant
	β_2	=	-0.4276	±	fail	Not significant
	β_3	=	-0.2203	±	fail	Not significant
	β_4	=	-0.2738	±	fail	Not significant
PROL 32	β_1	=	1.4501	±	0.2308	Highly significant
	β_2	=	0.8584	±	0.1060	Highly significant
	β_3	=	0.1334	±	0.2432	Not significant
	β_4	=	-1.1868	±	0.3242	Highly significant
	β_5	=	0.1390	±	0.0601	Highly significant
PROL 33	β_1	=	0.9412	±	0.1519	Highly significant
	β_2	=	0.9254	±	0.1480	Highly significant
	β_3	=	0.3763	±	0.2303	Highly significant
	β_4	=	-1.5937	±	0.2400	Highly significant
	β_5	=	0.0413	±	0.0786	Not significant
PROL 41	β_1	=	0.3098	±	0.3796	Not significant
	β_2	=	0.4170	±	0.1519	Highly significant
	β_3	=	-0.2320	±	0.1848	Significant
	β_4	=	-0.1059	±	0.3710	Not significant
PROL 42	β_1	=	1.5959	±	0.1091	Highly significant
	β_2	=	0.7325	±	0.06345	Highly significant
	β_3	=	-0.0126	±	0.1390	Not significant
	β_4	=	-1.0248	±	0.2680	Highly significant
	β_5	=	0.1669	±	0.0292	Highly significant
PROL 43	β_1	=	0.6044	±	0.2286	Highly significant
	β_2	=	0.4641	±	0.0969	Highly significant
	β_3	=	-0.2360	±	0.1202	Highly significant
	β_4	=	-0.3572	±	0.2183	Highly significant
	β_5	=	-0.0398	±	0.0736	Not significant

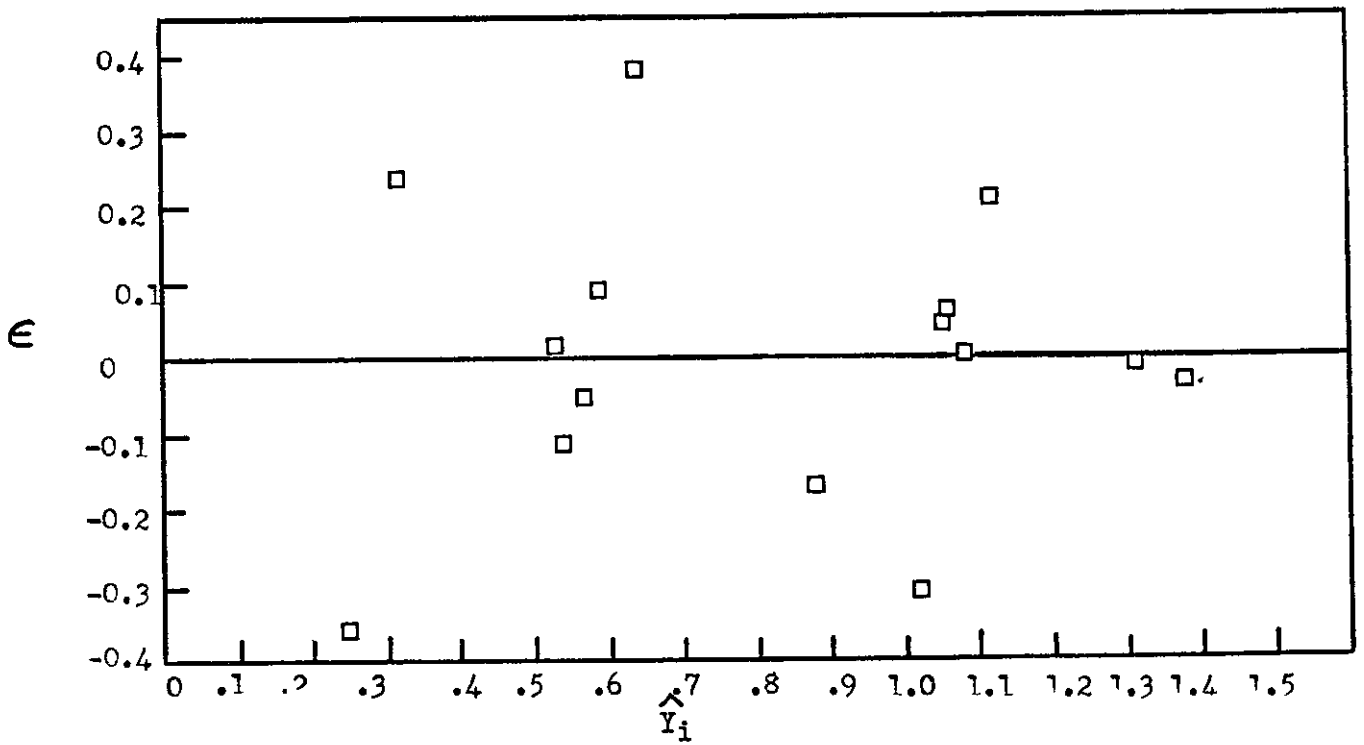

Case PROL 03

Fig. 5.A.2 Residual Plot

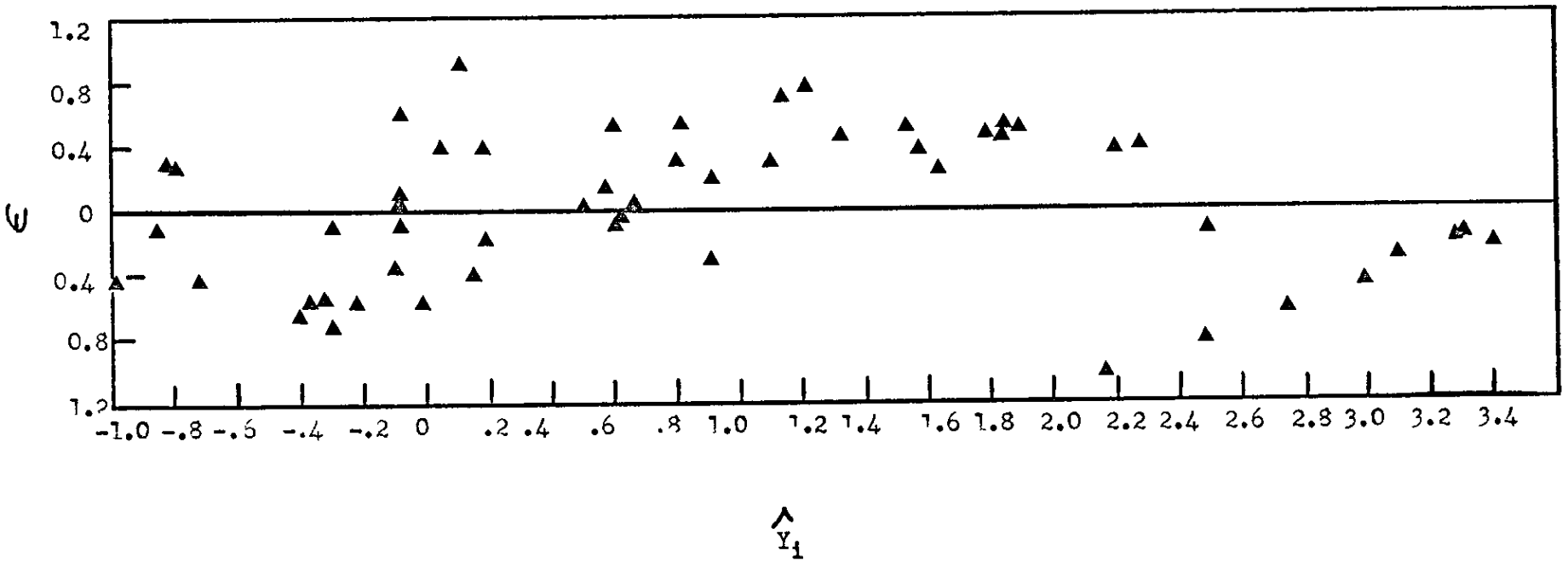

Case PROL 07

Fig. 5.A.3 Residual Plot

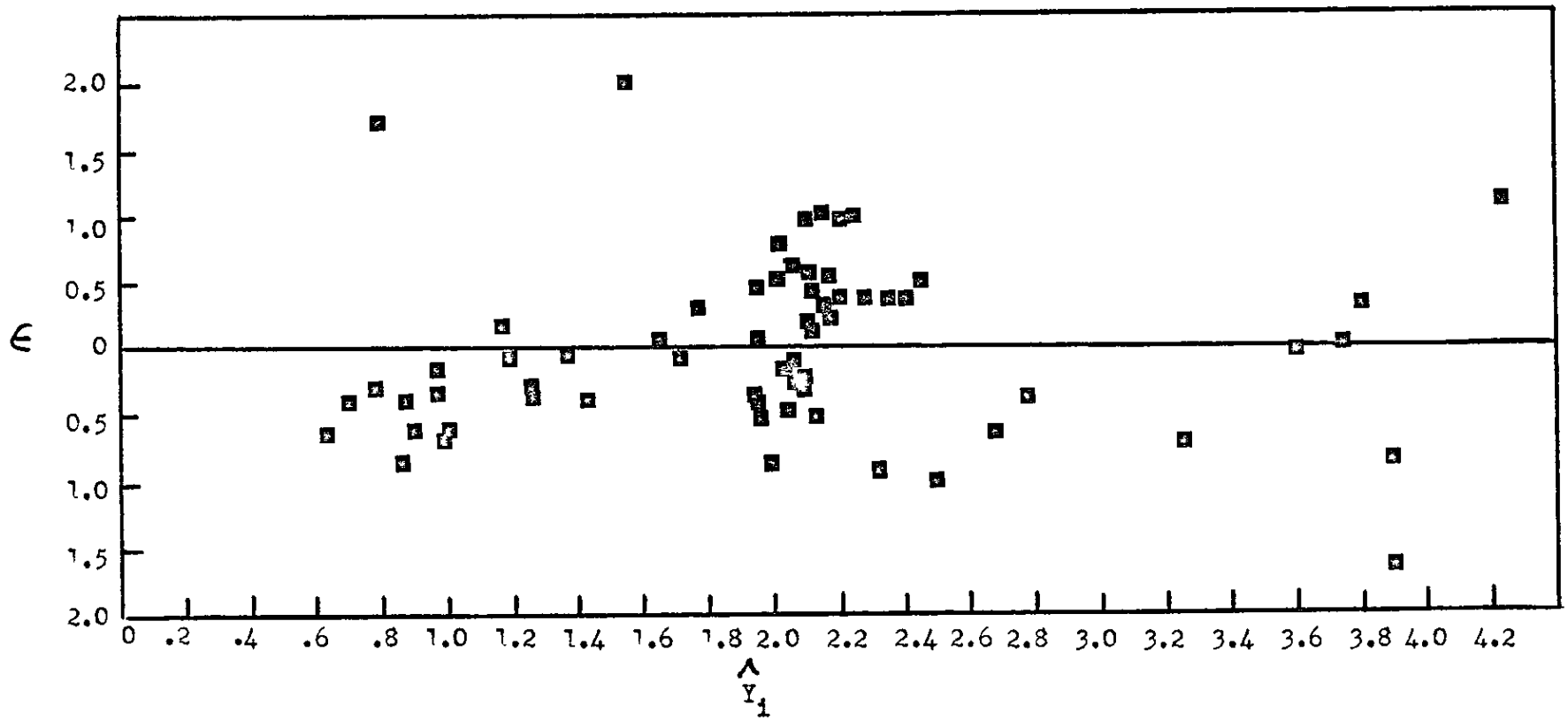

Case PROL 41

Fig. 5.A.4 Residual Plot

APPENDIX 5

COMPUTER PROGRAM

MULTRREGRE

Description

The multiple linear regression program consists of a modified program named REGRE, a special input subroutine named DATA, and four subroutines, namely, CORRE, ORDER, MINV and MULTR, from the I.B.M. Scientific Subroutine Package (64).

Input

One control card is required for each problem and is read by the main program, REGRE. This card is prepared as follows:

Columns	Contents	For Sample Problem
1-6	Problem number (may be alphameric)	Sample
7-11	Number of observations	00030
12-13	Number of variables	06
14-15	Number of selection cards	02

Data Cards - if the data field format exceeds 72 columns each row of data is continued on the second and third cards until the last data point is key punched. However, each row of data must begin on a new card.

Selection Card - the selection card is used to specify a dependent variable and a set of independent variables in a multiple linear regression analysis. Any variable can be designated as a dependent variable, and any number of variables can be specified as independent variables. Selection of a dependent variable and a set of independent variables can be performed over and over again using the same set of original variables. The Selection Card is prepared as follows:

Columns	Contents	For Sample Selection	Problem Selection
		2	2
1-2	Option code for table of residuals		
	00 if it not desired 01 if it is desired	01	01
3-4	Dependent variable designated for the forthcoming regression	01	01
5-6	Number of independent variables included in the forthcoming regression (the subscript numbers of variables are specified below)	04	05
7-8	1st independent variable included	02	02
9-10	2nd independent variable included	03	03
11-12	3rd independent variable included	04	04
13-14	4th independent variable included	05	05
15-16	5th independent variable included		06

Output

The output of the program for the multiple linear regression includes:

1. Means
2. Standard deviations
3. Correlation coefficients between the independent variables and the dependent variable
4. Regression coefficients
5. Standard errors of regression coefficients
6. Computed t-values
7. Intercept
8. Multiple correlation coefficients
9. Standard error of estimate
10. Analysis of variance for the multiple regression
11. Table of residuals (optional)

Designation of Variables

The variables included in the analysis were designated as follows:

t_m dependent variable number 1 (mean coalescence in seconds)

a independent variable number 2 (equivalent spherical drop diameter in cms.)

μ_2 independent variable number 3 (continuous phase viscosity in poise)

$\Delta\rho$ independent variable number 4 (phase density difference $(\rho_1 - \rho_2)$ in gm./cm.^{3})

χ independent variable number 5 (interfacial tension in dynes/cm.)

L independent variable number 6 (fall height to the interface in cms.)

Order of Data Processing for Multiple Regression Analysis

Section 1

Case	Description (Series 2A, 2B, 2C, 2D)	Fig. No. for Correlation
PROL 01	1st Stage coalescence	7.1
PROL 02	2nd Stage coalescence	7.2
PROL 03	3rd Stage coalescence	7.3
PROL 04	4th Stage coalescence	7.4
PROL 05	1st and 2nd Stage coalescence	7.5
PROL 06	3rd and 4th Stage coalescence	7.6
PROL 07	1st, 2nd, 3rd and 4th Stage coalescence	7.7
Section 2		
PROL 21	Two Component Systems for L = 0 cms.	7.8
PROL 22	Two Component Systems for L > 0 cms.	7.9
Section 3		
PROL 31	Three Component Systems for L = 0 cms. (present work only for Series 2B, 2C, 2D)	7.10
PROL 32	Three Component Systems for L > 0 cms.	7.11
Section 4		
PROL 41	PROL 21 and PROL 31 for L = 0 cms.	7.12
PROL 42	PROL 22 and PROL 32 for L > 0 cms.	7.13

```
      MASTERREGRE
C
C     ..... .....*.....
C
C        SAMPLE MAIN PROGRAM FOR MULTIPLE REGRESSION - REGRE
C
C        PURPOSE
C           (1) READ THE PROBLEM PARAMETER CARD FOR A MULTIPLE REGRES-
C           SION, (2) READ SUBSET SELECTION CARDS, (3) CALL THE SUB-
C           ROUTINES TO CALCULATE MEANS, STANDARD DEVIATIONS, SIMPLE
C           AND MULTIPLE CORRELATION COEFFICIENTS, REGRESSION COEFFI-
C           CIENTS, T-VALUES, AND ANALYSIS OF VARIANCE FOR MULTIPLE
C           REGRESSION, AND (4) PRINT THE RESULTS.
C
C        REMARKS
C           THE NUMBER OF OBSERVATIONS, N, MUST BE GREATER THAN M+1,
C           WHERE M IS THE NUMBER OF VARIABLES.  IF SUBSET SELECTION
C           CARDS ARE NOT PRESENT, THE PROGRAM CAN NOT PERFORM MULTIPLE
C           REGRESSION.
C           AFTER RETURNING FROM SUBROUTINE MINV, THE VALUE OF DETER-
C           MINANT (DET) IS TESTED TO CHECK WHETHER THE CORRELATION
C           MATRIX IS SINGULAR.  IF DET IS COMPARED AGAINST A SMALL
C           CONSTANT, THIS TEST MAY ALSO BE USED TO CHECK NEAR-
C           SINGULARITY.
C
C        SUBROUTINES AND FUNCTION SUBPROGRAMS REQUIRED
C           CORRE  (WHICH, IN TURN, CALLS THE SUBROUTINE NAMED DATA)
C           ORDER
C           MINV
C           MULTR
C
C        METHOD
C           REFER TO B. OSTLE,  STATISTICS IN RESEARCH , THE IOWA STATE
C           COLLEGE PRESS , 1954, CHAPTER 8.
C
C     ..........................................................
C
C     THE FOLLOWING  DIMENSIONS MUST BE GREATER THAN OR EQUAL TO THE
C     NUMBER OF VARIABLES, M..
C
      DIMENSION XBAR(40),STD(40),D(40),RY(40),ISAVE(40),B(40),
     1          SB(40),T(40),W(40)
C
C     THE FOLLOWING DIMENSION MUST BE GREATER THAN OR EQUAL TO THE
C     PRODUCT OF M*M..
C
      DIMENSION RX(1600)
C
```

```
C     THE FOLLOWING DIMENSION MUST BE GREATER THAN OR EQUAL TO
C     (M+1)*M/2..
C
      DIMENSION R(820)
C
C     THE FOLLOWING DIMENSION MUST BE GREATER THAN OR EQUAL TO 10..
C
      DIMENSION ANS(10)
C
C     ..................................................................
C
C        IF A DOUBLE PRECISION VERSION OF THIS ROUTINE IS DESIRED, THE
C        C IN COLUMN 1 SHOULD BE REMOVED FROM THE DOUBLE PRECISION
C        STATEMENT WHICH FOLLOWS.
C
C     DOUBLE PRECISION XBAR,STD,RX,R,D,B,T,RY,DET,SB,ANS,SUM
C
C        THE C MUST ALSO BE REMOVED FROM DOUBLE PRECISION STATEMENTS
C        APPEARING IN OTHER ROUTINES USED IN CONJUNCTION WITH THIS
C        ROUTINE.
C
C        ..........................................................
C
    1 FORMAT(A4,A2,I5,2I2)
    2 FORMAT(25H1MULTIPLE REGRESSION.....A4,A2//6X,14HSELECTION.....I2//
     1)
    3 FORMAT(9H0VARIABLE,5X,4HMEAN,6X,8HSTANDARD,6X,11HCORRELATION,4X,10
     1HREGRESSION,4X,10HSTD. ERROR,5X,8HCOMPUTED/6H   NO.,18X,9HDEVIATIO
     2N,7X,6HX VS Y,7X,11HCOEFFICIENT,3X,12HOF REG.COEF.,3X,7HT VALUE)
    4 FORMAT(1H ,I4,6F14.5)
    5 FORMAT(10H DEPENDENT)
    6 FORMAT(1H0/10H INTERCEPT,13X,F13.5//23H MULTIPLE CORRELATION  ,F13
     1.5//23H STD. ERROR OF ESTIMATE,F13.5//)
    7 FORMAT(1H0,21X,39HANALYSIS OF VARIANCE FOR THE REGRESSION//5X,19HS
     1OURCE OF VARIATION,7X,7HDEGREES,7X,6HSUM OF,10X,4HMEAN,12X,7HF VAL
     2UE/30X,10HOF FREEDOM,4X,7HSQUARES,9X,7HSQUARES)
    8 FORMAT(30H ATTRIBUTABLE TO REGRESSION   ,I6,3F16.5/30H DEVIATION F
     1ROM REGRESSION    ,I6,2F16.5)
    9 FORMAT(1H ,5X,5HTOTAL,19X,I6,F16.5)
   10 FORMAT(36I2)
   11 FORMAT(1H ,15X,18HTABLE OF RESIDUALS//9H CASE NO.,5X,7HY VALUE,5X,
     110HY ESTIMATE,6X,8HRESIDUAL)
   12 FORMAT(1H ,I6,F15.5,2F14.5)
   13 FORMAT(53H1NUMBER OF SELECTIONS NOT SPECIFIED.  JOB TERMINATED.)
   14 FORMAT(52H0THE MATRIX IS SINGULAR.  THIS SELECTION IS SKIPPED.)
C
C     ..........................#.....................................
C
```

```
C      READ PROBLEM PARAMETER CARD
C
  100 READ (5,1) PR,PR1,N,M,NS
C        PR.....PROBLEM NUMBER (MAY BE ALPHAMERIC)
C        PR1.....PROBLEM NUMBER (CONTINUED)
C        N.....NUMBER OF OBSERVATIONS
C        M.....NUMBER OF VARIABLES
C        NS.....NUMBER OF SELECTIONS
C
C      LOGICAL TAPE 13 IS USED AS INTERMEDIATE STORAGE TO HOLD INPUT
C      DATA.  THE INPUT DATA ARE WRITTEN ON LOGICAL TAPE 13 BY THE
C      SPECIAL INPUT SUBROUTINE NAMED DATA.  THE STORED DATA MAY BE USED
C      FOR RESIDUAL ANALYSIS.
C
       REWIND 13
C
       IO=
       X=0.0
C
       CALL CORRE (N,M,IO,X,XBAR,STD,RX,R,D,B,T)
C
       REWIND 13
C
C      TEST NUMBER OF SELECTIONS
C
       IF(NS) 108, 108, 109
  108  WRITE (6,13)
       GO TO 300
C
  109  DO 200 I=1,NS
       WRITE (6,2) PR,PR1,I
C
C      READ SUBSET SELECTION CARD
C
       READ (5,10) NRESI,NDEP,K,(ISAVE(J),J=1,K)
C        NRESI.....OPTION CODE FOR TABLE OF RESIDUALS
C                    0  IF IT IS NOT DESIRED.
C                    1  IF IT IS DESIRED.
C        NDEP.....DEPENDENT VARIABLE
C        K.....NUMBER OF INDEPENDENT VARIABLES INCLUDED
C        ISAVE.....A VECTOR CONTAINING THE INDEPENDENT VARIABLES
C                      INCLUDED
C
       CALL ORDER (M,R,NDEP,K,ISAVE,RX,RY)
C
       CALL MINV (RX,K,DET,B,T)
C
C      TEST SINGULARITY OF THE MATRIX INVERTED
```

```
C
      IF(DET) 112, 110, 112
  110 WRITE (6,14)
      GO TO 200
C
  112 CALL MJLTR (N,K,XBAR,STD,D,RX,RY,ISAVE,B,SB,T,ANS,M)
C
C     PRINT MEANS, STANDARD DEVIATIONS, INTERCORRELATIONS BETWEEN
C     X AND Y, REGRESSION COEFFICIENTS, STANDARD DEVIATIONS OF
C     REGRESSION COEFFICIENTS, AND COMPUTED T-VALUES
C
      MM=K+1
      WRITE (6,3)
      DO 115 J=1,K
      L=ISAVE(J)
  115 WRITE (6,4) L,XBAR(L),STD(L),RY(J),B(J),SB(J),T(J)
      WRITE (6,5)
      L=ISAVE(MM)
      WRITE (6,4) L,XBAR(L),STD(L)
C
C     PRINT INTERCEPT, MULTIPLE CORRELATION COEFFICIENT, AND STANDARD
C     ERROR OF ESTIMATE
C
      WRITE (6,6) ANS(1),ANS(2),ANS(3)
C
C     PRINT ANALYSIS OF VARIANCE FOR THE REGRESSION
C
      WRITE (6,7)
      L=ANS(8)
      WRITE (6,8) K,ANS(4),ANS(6),ANS(10),L,ANS(7),ANS(9)
      L=N-1
      SUM=ANS(4)+ANS(7)
      WRITE (6,9) L,SUM
      IF(NRESI) 200, 200, 120
C
C     PRINT TABLE OF RESIDUALS
C
  120 WRITE (6,2) PR,PR1,I
      WRITE (6,11)
      MM=ISAVE(K+1)
      DO 140 II=1,N
      READ (13) (W(J),J=1,M)
      SUM=ANS(1)
      DO 130 J=1,K
      L=ISAVE(J)
  130 SUM=SUM+W(L)*B(J)
      RESI=W(MM)-SUM
  140 WRITE (6,12) II,W(MM),SUM,RESI


      REWIND 13
  200 CONTINUE
      GO TO 1 0
  300 CONTINUE
      END

END OF SEGMENT, LENGTH   436, NAME  REGRE
```

MULTIPLE REGRESSION.....PROB 1

SELECTION . . 2

VARIABLE NO.	MEAN	STANDARD DEVIATION	CORRELATION X VS Y	REGRESSION COEFFICIENT	STD. ERROR OF REG.COEF.	COMPUTED T VALUE
2	-1. 27 9	.31712	[illegible].20298	1.01283	[illegible] 17842	5.67571
3	-5 24473	.17937	[illegible].66688	3.89770	97454.19637	[illegible].06.04
4	-[illegible] 36391	.24.52	- .39574	1.45338	35824.96272	[illegible].00.04
5	3.26719	43223	- .8[illegible]52	-0.80876	23697.796[illegible]1	-[illegible].00 03
DEPENDENT						
1	2.5 777	.69914				

INTERCEPT	28.61512
MULTIPLE CORRELATION	[illegible].98227
STD. ERROR OF ESTIMATE	[illegible].16919

ANALYSIS OF VARIANCE FOR THE REGRESSION

SOURCE OF VARIATION	DEGREES OF FREEDOM	SUM OF SQUARES	MEAN SQUARES	F VALUE
ATTRIBUTABLE TO REGRESSION	4	4.71626	1.179 6	41.18794
DEVIATION FROM REGRESSION	6	[illegible].17175	0.02863	
TOTAL	10	4.88801		

MULTIPLE REGRESSION.....PROB 2

SELECTION . 2

VARIABLE NO.	MEAN	STANDARD DEVIATION	CORRELATION X VS Y	REGRESSION COEFFICIENT	STD. ERROR OF REG.COEF.	COMPUTED T VALUE
2	-2.14221	2029	0.12518	1.46714	0.52215	2.80980
3	-5.27692	20075	0.29157	2.08292	1.66704	1.24947
4	-1.36447	.24843	-0.28526	1.12711	1.28786	0.87518
5	3.08219	.52921	-0.74000	-0.82551	0.17695	-4.66527
DEPENDENT						
1	1.93495	.51880				

INTERCEPT 20.15153

MULTIPLE CORRELATION .88091

STD. ERROR OF ESTIMATE .30072

ANALYSIS OF VARIANCE FOR THE REGRESSION

SOURCE OF VARIATION	DEGREES OF FREEDOM	SUM OF SQUARES	MEAN SQUARES	F VALUE
ATTRIBUTABLE TO REGRESSION	4	2.50637	0.62659	6.92890
DEVIATION FROM REGRESSION	8	0.72345	0.09043	
TOTAL	12	3.22982		

MULTIPLE REGRESSION.....PROB 3

SELECTION 2

VARIABLE NO.	MEAN	STANDARD DEVIATION	CORRELATION X VS Y	REGRESSION COEFFICIENT	STD ERROR OF REG.COEF.	COMPUTED T VALUE
2	-2.88743	15312	.38291	2.27698	.51233	4.44439
3	-5.31678	186 3	.15141	2.08 62	1.07593	1.93378
4	-1 30782	22441	- .15416	1.01970	.82772	1.23194
5	3 11098	56077	- .539	- .49 50	.1166.	-4.20559
DEPENDENT						
1	0.82435	.40035				

INTERCEPT 21 32 67

MULTIPLE CORRELATION .87294

STD. ERROR OF ESTIMATE .23108

ANALYSIS OF VARIANCE FOR THE REGRESSION

SOURCE OF VARIATION	DEGREES OF FREEDOM	SUM OF SQUARES	MEAN SQUARES	F VALUE
ATTRIBUTABLE TO REGRESSION	4	1 70997	0.42749	8.0 557
DEVIAT N FROM REGRESSION	10	0.53399	0.05340	
TOTAL	14	2 24396		

MULTIPLE REGRESSION.....PROL 4

SELECTION . 2

VARIABLE NO.	MEAN	STANDARD DEVIATION	CORRELATION X VS Y	REGRESSION COEFFICIENT	STD. ERROR OF REG COEF.	COMPUTED T VALUE
2	-3 58219	1446	.55496	2.65789	.50437	5.26971
3	-5 2978	18581	.128 5	1.11 47	.98094	1.13705
4	- 32371	.22857	- .21317	-.10539	0.74316	-.14182
5	3.1 25	.52651	-.36448	-.40484	.11794	-3.43269
DEPENDENT						
1	- 66389	.41191				

INTERCEPT	16.13483
MULTIPLE CORRELATION	0.87069
STD. ERROR OF ESTIMATE	0.23393

ANALYSIS OF VARIANCE FOR THE REGRESSION

SOURCE OF VARIATION	DEGREES OF FREEDOM	SUM OF SQUARES	MEAN SQUARES	F VALUE
ATTRIBUTABLE TO REGRESSION	4	2.05796	0.51449	9.40147
DEVIATION FROM REGRESSION	12	0.65669	0.05472	
TOTAL	16	2.71466		

MULTIPLE REGRESSION.....PROL 5

SELECTION . 2

VARIABLE NO.	MEAN	STANDARD DEVIATION	CORRELATION X VS Y	REGRESSION COEFFICIENT	STD. ERROR OF REG.COEF.	COMPUTED T VALUE
2	-1.63111	0.62237	-.46597	-.68348	.11212	-6.09611
3	-5.26216	0.18784	.45839	2.22436	1.03676	2.14549
4	-1.36422	0.23948	-.3031	1.38123	0.77723	1.77584
5	3.16695	0.4862	-.57313	-.90413	.16446	-5.49751
DEPENDENT						
1	2.1975	.66178				

INTERCEPT	19.76358
MULTIPLE CORRELATION	0.90449
STD. ERROR OF ESTIMATE	0.31054

ANALYSIS OF VARIANCE FOR THE REGRESSION

SOURCE OF VARIATION	DEGREES OF FREEDOM	SUM OF SQUARES	MEAN SQUARES	F VALUE
ATTRIBUTABLE TO REGRESSION	4	8.24054	2.06013	21.36252
DEVIATION FROM REGRESSION	19	1.83230	0.09644	
TOTAL	23	10.07284		

MULTIPLE REGRESSION.. ..PROL 6

SELECTION 2

VARIABLE NO.	MEAN	STANDARD DEVIATION	CORRELATION X VS Y	REGRESSION COEFFICIENT	STD. ERROR OF REG.COEF.	COMPUTED T VALUE
2	-3.25651	.38139	.9[illegible]97	2.20445	[illegible].10901	2[illegible].22261
3	-5.3 67	.18314	[illegible]. 1848	1.28219	[illegible].62123	2.[illegible]8395
4	-1.[illegible]1623	.2231	- .5523	[illegible].36693	[illegible].50091	.73252
5	3.10523	.53397	-[illegible].2[illegible].31	- .43539	[illegible].07756	-5.61755
DEPENDENT						
1	.3372	.85399				

INTERCEPT	15.8517[illegible]
MULTIPLE CORRELATION	0.970[illegible]1
STD. ERROR OF ESTIMATE	0.22167

ANALYSIS OF VARIANCE FOR THE REGRESSION

SOURCE OF VARIATION	DEGREES OF FREEDOM	SUM OF SQUARES	MEAN SQUARES	F VALUE
ATTRIBUTABLE TO REGRESSION	4	21.28138	5.32035	108.270[illegible]5
DEVIATION FROM REGRESSION	27	1.32677	0.04914	
TOTAL	31	22.60815		

MULTIPLE REGRESSION ....PROL 7

SELECTION. . . 2

VARIABLE NO.	MEAN	STANDARD DEVIATION	CORRELATION X VS Y	REGRESSION COEFFICIENT	STD. ERROR OF REG COEF.	COMPUTED T VALUE
2	-2.55991	0.95012	.89022	1.29647	0.06907	18.77164
3	-5.28761	0.18481	.21174	.78665	0.98982	.79474
4	-1.33683	0.22937	-.17044	.16413	0.78605	.20881
5	3.13172	0.51033	-.14068	-.67 21	0.13733	-4.88 13
DEPENDENT						
1	.96105	1.32727				

INTERCEPT 10.75771

MULTIPLE CORRELATION .93792

STD. ERROR OF ESTIMATE .478 7

ANALYSIS OF VARIANCE FOR THE REGRESSION

SOURCE OF VARIATION	DEGREES OF FREEDOM	SUM OF SQUARES	MEAN SQUARES	F VALUE
ATTRIBUTABLE TO REGRESSION	4	85.23450	21.30862	93.2352
DEVIATION FROM REGRESSION	51	11.65590	0.22855	
TOTAL	55	96.89039		

MULTIPLE REGRESSION PROL21

SELECTION . . 2

VARIABLE NO.	MEAN	STANDARD DEVIATION	CORRELATION X VS Y	REGRESSION COEFFICIENT	STD. ERROR OF REG.COEF.	COMPUTED T VALUE
2	-1.42491	0.65767	.06461	.40758	0.22817	1.78629
3	-4.7 948	1 66002	.62222	0.47893	0.07559	6.33511
4	-1 84835	1.3123	-.31051	-0.31003	0.09081	-3.41402
5	2.97814	.78677	.16539	-0.15653	0.19179	-0.81618
DEPENDENT						
1	1 85008	1.1499				

INTERCEPT	4.57951
MULTIPLE CORRELATION	0.733 8
STD. ERROR OF ESTIMATE	0.81687

ANALYSIS OF VARIANCE FOR THE REGRESSION

SOURCE OF VARIATION	DEGREES OF FREEDOM	SUM OF SQUARES	MEAN SQUARES	F VALUE
ATTRIBUTABLE TO REGRESSION	4	34.10878	8.52719	12.77898
DEVIATION FROM REGRESSION	44	29.36 45	0.66728	
TOTAL	48	63.46922		

MULTIPLE REGRESSION....PROL 22

SELECTION. . 2

VARIABLE NO.	MEAN	STANDARD DEVIATION	CORRELATION X VS Y	REGRESSION COEFFICIENT	STD. ERROR OF REG COEF.	COMPUTED T VALUE
2	-1 32063	.23.53	.84925	1.63847	2.11709	13.99325
3	-5.14004	.09143	- .04220	.39356	1.52866	0.25746
4	-2.09021	.22364	.09689	-.97485	1.35048	-0.72185
5	3.57080	.08316	.15393	1.74734	2.25621	0.77446
6	-9 50611	3615	.33740	- .10966	0.07439	-1.47414
DEPENDENT						
1	1 9 881	.37489				

INTERCEPT -3.22398

MULTIPLE CORRELATION 0.90511

STD. ERROR OF ESTIMATE 0.16674

ANALYSIS OF VARIANCE FOR THE REGRESSION

SOURCE OF VARIATION	DEGREES OF FREEDOM	SUM OF SQUARES	MEAN SQUARES	F VALUE
ATTRIBUTABLE TO REGRESSION	5	6.67784	1.33557	48.03799
DEVIATION FROM REGRESSION	53	1.47352	0.02780	
TOTAL	58	8.15136		

MULTIPLE REGRESSION.....PROL23

SELECTION. . 2

VARIABLE NO.	MEAN	STANDARD DEVIATION	CORRELATION X VS Y	REGRESSION COEFFICIENT	STD. ERROR OF REG COEF.	COMPUTED T VALUE
2	-1.36795	0.47493	[illegible].16264	1.39393	0.189[illegible]5	7.37319
3	-4.94469	1 1345	[illegible].56601	[illegible].57795	[illegible].04863	11.88535
4	-1.98 49	0.90238	-[illegible].28338	-[illegible].067[illegible]3	0.06812	-[illegible].98101
5	3.3[illegible]191	0.60771	0.15766	-[illegible].43263	[illegible].1124[illegible]	-3.84918
6	-9 2535	0.73249	-[illegible].11862	- .7 722	[illegible].1172[illegible]	-6.03442
DEPENDENT						
1	1.88219	.81867				

INTERCEPT 1.39833

MULTIPLE CORRELATION [illegible].79386

STD. ERROR OF ESTIMATE .5 989

ANALYSIS OF VARIANCE FOR THE REGRESSION

SOURCE OF VARIATION	DEGREES OF FREEDOM	SUM OF SQUARES	MEAN SQUARES	F VALUE
ATTRIBUTABLE TO REGRESSION	5	45.19450	9.03890	34.76696
DEVIATION FROM REGRESSION	1 2	26.51850	0.25999	
TOTAL	1 7	71.713[illegible]1		

MULTIPLE REGRESSION.....PROL31

SELECTION..... 2

VARIABLE NO.	MEAN	STANDARD DEVIATION	CORRELATION X VS Y	REGRESSION COEFFICIENT	STD. ERROR OF REG.COEF.	COMPUTED T VALUE
2	-1.69777	0.62950	0.93023	0.75739	0.07356	10.29529
3	-5.18969	0.15757	0.01228	-0.42760	38272.71601	-0.00001
4	-1.13477	0.23778	0.06034	-0.22039	22450.21774	-0.00001
5	2.91367	1.21869	0.17795	-0.27385	10179.85944	-0.00003
DEPENDENT						
1	2.45831	0.47912				

INTERCEPT	2.00729
MULTIPLE CORRELATION	0.94610
STD. ERROR OF ESTIMATE	0.17745

ANALYSIS OF VARIANCE FOR THE REGRESSION

SOURCE OF VARIATION	DEGREES OF FREEDOM	SUM OF SQUARES	MEAN SQUARES	F VALUE
ATTRIBUTABLE TO REGRESSION	4	3.49315	0.87329	27.73310
DEVIATION FROM REGRESSION	13	0.40936	0.03149	
TOTAL	17	3.90250		

MULTIPLE REGRESSION.....PROI 32

SELECTION..... 2

VARIABLE NO.	MEAN	STANDARD DEVIATION	CORRELATION X VS Y	REGRESSION COEFFICIENT	STD. ERROR OF REG.COEF.	COMPUTED T VALUE
2	-1.38901	0.20319	0.65326	1.45018	0.11348	12.77922
3	-4.14191	0.56810	0.72161	0.85843	0.05054	16.98540
4	-1.77561	0.31043	-0.47075	0.13840	0.10461	1.32292
5	3.78995	0.20365	-0.26351	-1.18582	0.15955	-7.43579
7	0.83068	0.73786	0.16617	0.13901	0.02955	4.70353
DEPENDENT 1	1.94755	0.62832				

INTERCEPT	12.40379
MULTIPLE CORRELATION	0.98116
STD. ERROR OF ESTIMATE	0.13082

ANALYSIS OF VARIANCE FOR THE REGRESSION

SOURCE OF VARIATION	DEGREES OF FREEDOM	SUM OF SQUARES	MEAN SQUARES	F VALUE
ATTRIBUTABLE TO REGRESSION	5	13.68171	2.73634	159.89278
DEVIATION FROM REGRESSION	31	0.53052	0.01711	
TOTAL	36	14.21223		

MULTIPLE REGRESSION.....PROB33

SELECTION..... 2

VARIABLE NO.	MEAN	STANDARD DEVIATION	CORRELATION X VS Y	REGRESSION COEFFICIENT	STD. ERROR OF REG.COEF.	COMPUTED T VALUE
2	-1.49005	0.41672	0.41505	0.94123	0.07557	12.45455
3	-4.68629	0.58992	0.23356	0.92540	0.07362	12.56969
4	-1.66401	0.32878	-0.09694	0.37633	0.11480	3.27800
5	3.50311	0.46353	-0.40198	-1.59875	0.11959	-13.36819
7	0.03207	1.30315	-0.27892	0.04132	0.03915	1.05531
DEPENDENT						
1	2.11472	0.62767				

INTERCEPT 14.07937

MULTIPLE CORRELATION 0.94555

STD. ERROR OF ESTIMATE 0.21446

ANALYSIS OF VARIANCE FOR THE REGRESSION

SOURCE OF VARIATION	DEGREES OF FREEDOM	SUM OF SQUARES	MEAN SQUARES	F VALUE
ATTRIBUTABLE TO REGRESSION	5	19.02058	3.80412	82.71301
DEVIATION FROM REGRESSION	49	2.25360	0.04599	
TOTAL	54	21.27418		

MULTIPLE REGRESSION.....PROL41

SELECTION..... 2

VARIABLE NO.	MEAN	STANDARD DEVIATION	CORRELATION X VS Y	REGRESSION COEFFICIENT	STD. ERROR OF REG.COEF.	COMPUTED T VALUE
2	-1.19821	0.65688	0.10870	0.30981	0.18993	1.63120
3	-4.83920	1.43398	0.53718	0.41708	0.07582	5.50060
4	-1.73725	1.14068	-0.24202	-0.23200	0.09236	-2.51201
5	2.96062	0.68069	0.14857	-0.10595	0.18579	-0.57029
DEPENDENT						
1	2.41349	1.04622				

INTERCEPT	4.40625
MULTIPLE CORRELATION	0.61580
STD. ERROR OF ESTIMATE	0.85050

ANALYSIS OF VARIANCE FOR THE REGRESSION

SOURCE OF VARIATION	DEGREES OF FREEDOM	SUM OF SQUARES	MEAN SQUARES	F VALUE
ATTRIBUTABLE TO REGRESSION	4	27.39458	6.84865	9.46794
DEVIATION FROM REGRESSION	62	44.84778	0.72335	
TOTAL	66	72.24236		

MULTIPLE REGRESSION.....PROL42

SELECTION..... 2

VARIABLE NO.	MEAN	STANDARD DEVIATION	CORRELATION X VS Y	REGRESSION COEFFICIENT	STD. ERROR OF REG.COEF.	COMPUTED T VALUE
2	-1.34699	0.22183	0.70354	1.59594	0.05510	28.96506
3	-4.87097	0.49403	0.43019	0.73253	0.03187	22.98541
4	-1.96897	0.30125	-0.18404	-0.01263	0.06980	-0.18094
5	3.65523	0.17727	-0.09071	-1.02481	0.13467	-7.60995
7	1.13439	0.84275	0.26284	0.16696	0.01468	11.37628
DEPENDENT						
1	1.92376	0.48556				

INTERCEPT 11.17259

MULTIPLE CORRELATION 0.97218

STD. ERROR OF ESTIMATE 0.11684

ANALYSIS OF VARIANCE FOR THE REGRESSION

SOURCE OF VARIATION	DEGREES OF FREEDOM	SUM OF SQUARES	MEAN SQUARES	F VALUE
ATTRIBUTABLE TO REGRESSION	5	21.16897	4.23379	310.11834
DEVIATION FROM REGRESSION	90	1.22870	0.01365	
TOTAL	95	22.39767		

MULTIPLE REGRESSION.....PROI43

SELECTION..... 2

VARIABLE NO.	MEAN	STANDARD DEVIATION	CORRELATION X VS Y	REGRESSION COEFFICIENT	STD. ERROR OF REG.COEF.	COMPUTED T VALUE
2	-1.10915	0.45850	0.20388	0.60442	0.11676	5.17580
3	-4.85755	0.99053	0.51370	0.46418	0.04918	9.43907
4	-1.87371	0.77227	-0.21715	-0.23605	0.06100	-3.86960
5	3.36988	0.56978	0.05352	-0.35720	0.11108	-3.21572
7	0.00889	1.50192	0.00262	0.03980	0.03740	1.06409
DEPENDENT						
1	1.96061	0.76561				

INTERCEPT 5.82817

MULTIPLE CORRELATION 0.64805

STD. ERROR OF ESTIMATE 0.59230

ANALYSIS OF VARIANCE FOR THE REGRESSION

SOURCE OF VARIATION	DEGREES OF FREEDOM	SUM OF SQUARES	MEAN SQUARES	F VALUE
ATTRIBUTABLE TO REGRESSION	5	39.87979	7.97596	22.73549
DEVIATION FROM REGRESSION	157	55.07799	0.35082	
TOTAL	162	94.95777		

General Nomenclature

a	Drop diameter
b	Drop radius
B	van der Waals constant
c	Coalescence constant in Eqn. (2.1.3)
c, c_b, c_o	Concentration; concentration in bulk of liquid; concentration when r is zero
c_i	Total ionic concentration
d	Deformation from parallel plates defined by Eqn. (2.4.13)
D, D_s	Diffusivity, surface diffusivity
F	Force on film due to buoyancy only
F_T	Total force on film
F_U	Upward surface tension force resulting from the deformation of the interface by the drop
F_D	Downward force equal to the weight of that part of the drop above the interface
G	Helmholtz free energy per unit of surface
h, h_o, h_1, h_2	Film thickness, film thickness corresponding to time t_o, t_1, t_2
H	Minimum separation distance = 2h
k	Coalescence constant in Eqn.(2.1.1),(2.1.2) and (2.1.4)
K	Specific conductivity of liquid
L	Length of fall of drop to the interface
m	Distance from the centre of the drop to the plane of the interface
n_1, n_2	Exponents in Eqns. (2.1.4) and (2.1.3), respectively
N	Number of drops not coalescing in time t
N_o	Total number of drops assessed
p	Viscosity ratio $= \mu_1/\mu_2$; angle between the radius positioned at the edge of the interface and m
P_o, P_R	Pressure in film at r = 0, pressure at edge of film at r = R

P_r, P	Pressure in film at any radial distance r, pressure on film
q	Degree of instabilty or growth constant
Q_r	Flow at any radius r in the film
r, r_o	Radius, radial co-ordinates; radius of liquid column at break-up
R, R'	Radius of disc or barrier ring, radius of deformed interface and deformed drop surface
R_A	Molal rate of production of A per unit volume
S	Specific surface expansion rate
$\hat{t}, t_1, t_2$	Coalescence rest-time for the overall, first, second, third and
t_3, t_4	fourth stages of coalescence, respectively
$\hat{t}_m, t_{m1}, t_{m2}$,	Mean coalescence rest-time for the overall, first, second, third
t_{m3}, t_{m4}	and fourth stages, respectively
$t_o, t_{\frac{1}{2}}$	Initial drainage period, half-life time or time for 50% of drops to coalesce
T	Temperature
u, u_r, u_t	Velocity of flow in the film, radial velocity in film at r, tangential velocity in general
u_s	Radial velocity at surface of film; Stokes velocity
V	Velocity of approach of opposite faces of film = dh/dt
x,	Vertical distance from axis of symmetry
y	Horizontal distance from axis of symmetry, distance along y-axis
z_o	Dimensionless parameter $\lambda_{opt}/2r$

Greek Symbols

α	Wave amplitude
β_1, β_2	Principal radii of curvature
ϵ	Dielectric constant
ζ	Electrokinetic potential
ξ	Film thickness at any radial distance r

λ Wavelength

ψ_o, ψ_G Interfacial potential

Γ Surface concentration

μ, μ_1, μ_2 Measurement, micron; dispersed phase viscosity, continuous phase viscosity

ρ, ρ_1, ρ_2 Density, dispersed phase density, continuous phase density

Density difference

θ_c' Angle of normal at (x_c, z_c), see Appendix 4

π_1, π_2 Dimensionless groups

γ Interfacial tension

$\Delta\gamma_o$ Difference in interfacial tension between the centre of the film $r = 0$ and periphery $r = R$

τ Shear stess in the interface defined by $\tau = \text{grad}\,\gamma$, hence $\tau_r = \mu(\frac{\partial u_r}{\partial r})$; interface age

σ Standard deviation of coalescence rest-time distribution

Bibliography

1. Allan,R.S. and Mason,S.G.,Trans. Faraday Soc.,57,2038,(1961).
2. Allan,R.S.,Charles,G.E. and Mason,S.G.,J. Colloid Sci.,16,150, (1961).
3. Allan,R.S. and Mason,S.G.,J. Colloid Sci.,17,383,(1962).
4. Andrews,S.P.S.,Int. Symposium on Distillation,Instn. Chem. Engrs., Brighton,73,(1960).
5. Appel,F.J. and Elgin,J.C.,I.E.C.,29,451,(1937).
6. Bankoff,S.G.,Phys. Fluids,2,576,(1959).
7. Bashforth,F. and Adams,J.C.,"An Attempt to Test the Theories of Capillarity",Cambridge University Press,1883.
8. Bingham,"Fluidity and Plasticity",p.30,McGraw Hill,1922. In Chemical Rubber Handbook.
9. Bird,Stewart and Lightfoot,"Transport Phenomena",Wiley,1960.
10. Black,W. and DeJongh,J.Ct.V.,Overbeek,J.Th.G. and Sparnaay,M.J., Trans. Faraday Soc.,56,1597,(1960).
11. Bowden,F.P. and Tabor,D.,"The Friction and Lubrication of Solids", Oxford University Press,p.272,1950.
12. Brown,A.H.,Ph.D. Thesis,University of Bradford,1967.
13. Brown,A.H. and Hanson,C.,Trans. Faraday Soc.,61,1754,(1965).
14. Idem,Paper presented to I.Ch.E. Symposium on Liquid-Liquid Extraction,University of Newcastle upon Tyne,April,1967.
15. Charles,G.E. and Mason,S.G.,J. Colloid Sci.,15,105,(1960).
16. Idem ibid.,15,236,(1960).
17. Idem ibid.,16,150,(1961).
18. Chappelear,D.C.,ibid.,16,186,(1961).
19. Cockbain,E.G. and McRoberts,T.S.,ibid.,8,440,(1953).
20. Davies,J.T. and Haydon,D.A.,Proc. 2nd Int. Congress on Surface Activity,I,p.281,400,Butterworths,London,1957.

21. Davies,J.T. and Rideal,E.K.,"Interfacial Phenomena",Academic Press,New York,p.44,1961.

22. Davies,O.,"Statistical Methods in Research and Production", Oliver and Boyd,3rd Edition,p.208,1961.

23. Derjaguin,B.V. and Kussakov,M.,Acta Physicochim,URSS,10,25,153, (1939).

24. Derjaguin,B.V.,Trans. Faraday Soc.,36,203,(1940).

25. Idem,J. Phys. Chem.,Moscow,14,137,(1940).

26. Idem.,Acta Physicochim,URSS,12,181,(1940).

27. Derjaguin,B.V. and Titijevskaia,A.S.,Abricossova,I.I. and Malkina,A.D.,Disc. Faraday Soc.,No.18,24,(1954).

28. DeVries,A.J.,Rec. Trav. Chim.,77,383,(1958).

29. Draper and Smith,"Applied Regression Analysis",John Wiley,1966.

30. Dupre,A.,"Theorie Meconiquede la Chaleur",Cantheir-Villiars, 350,Paris,1869.

31. Elton,G.A.H.,Proc. Roy. Soc.,A194,259,(1948).

32. Idem ibid.,A194,275,(1948)

33. Elton,G.A.H. and Picknett,R.G.,Proc. 2nd Int. Congress on Surface Activity,I,p.288,Butterworths,London,1957.

34. Evans,L.F.,I.E.C.,46,2420,(1954).

35. Ewers,W.E. and Sutherland,K.L.,Australian J. Sci. Res.,Ser.A., 5,697,(1952).

36. Fletcher,A.W.,Loughborough University of Technology Chemical Engineering Journal,2,35,(1966).

37. Fletcher,A.W. and Flett,D.S.,Paper presented to Int. Conf. on the Chemistry of Solvent Extraction of Metals,Harwell,Sept.,1965.

38. Frankel,S.P. and Mysels,K.J.,J. Phys. Chem.,66,190,(1962).

39. Freund,J.E.,"Modern Elementary Statistics",Prentice Hall,2nd Ed., p.184,1960.

40. Garner,F.H.,Trans. Instn. Chem. Engrs.,28,88,(1950).

41. Garner,F.H. and Skelland,A.H.P.,ibid.,29,14,(1951).

42. Garner,F.H. and Hale,A.R.,Chem. Eng. Sci.,2,157,(1953).

43. Garner,F.H. and Hammerton,D.,ibid.,3,1,(1954).

44. Gillespie,T. and Rideal,E.K.,Trans. Faraday Soc.,52,173,(1956).

45. Goldsmith,H.L. and Mason,S.G.,J. of Fluid Mech.,14,42,(1962).

46. Gossart,E.,Ann.Chim. et Phys.,4,391,(1895).

47. Green,H.,I.E.C.,Anal. Ed.,13,632,(1941).

48. Groothius,H. and Zuiderweg,F.J.,Chem. Eng. Sci.,12-13,288,(1960).

49. Idem,ibid.,19,63,(1964).

50. Hadamard,J.,Compt. Rend. Acad. Sci. (Paris),152,1735,(1911).

51. Hanson,C.,Brit. Chem. Eng.,10,34,(1965).

52. Hardy,W.B. and Bircumshaw,I.,Proc. Roy. Soc.,A108,1,(1925).

53. Hartland,S.,Trans. Instn. Chem. Engrs.,45,97,102,109,(1967).

54. Idem,Paper presented to I.Chem.E. Symposium on Liquid-liquid Extraction,Newcastle upon Tyne University,April,1967.

55. Idem,Trans. Instn. Chem. Engrs.,46,275,(1968).

56. Idem,Chem. Eng. Progress Symposium Series,"Unusual Methods of Separation",No. 91,Vol. 65,p.82-92,1969.

57. Idem.,Chem. Eng. Sci.,24,613,(1969).

58. Idem,ibid.,25,277,(1970).

59. Harkins and Brown,J. Amer. Chem. Soc.,41,499,(1919);Int. Crit. Tables,4,435,1928.

60. Hawksley,J.L.,Ph.D. Thesis,University of Birmingham,1963.

61. Haydon,D.A.,Nature,176,839,(1955).

62. Idem,Proc. Roy. Soc.,A243,483,(1958).

63. Hodgson,T.D.,Ph.D. Thesis,University of Wales,1966.

64. "I.B.M. System 360 Scientific Subtoutine Package",I.B.M. Technical Publications,112 East Post Road,White Plains,New York.

65. Ipsen,D.C.,"Units,Dimensions and Dimensionless Numbers",McGraw Hill,New York,1960.

66. Jeffreys,G.V. and Lawson,G.B.,Trans. Instn. Chem. Engrs.,43, 297,(1965).

67. Jeffreys,G.V. and Hawksley,J.L.,J. appl. Chem.,12,329,(1962).

68. Idem,A.I.Ch.E. Journal,11,No.3,413,(1965).

69. Johnson,H.F. and Bliss,H.,Trans. A.I.Ch.E.,42,331,(1946).

70. Katalinic,M.,Nature,127,627,(1931).

71. Idem,ibid.,136,916,(1935).

72. Keith,F.W. Jr. and Hixson,A.N.,I.E.C.,47,258,(1955).

73. Kitchener,J.A. and Prosser,A.P.,Proc. Roy. Soc.,A242,403,(1957).

74. Kitchener,J.A. and Govidan,K.P.,Ion Exchange Progress,2,5,(1963).

75. Kitchener,J.A. in "Recent Progress in Surface Science" (Ed: J.F. Danielli),Vol.1,p.51,Academic Press,1964.

76. Koussakov,M.,Acta Physicochim,URSS,19,286,(1944).

77. Lamb,H.,"Hydrodynamics",6th Edition,Cambridge University Press, p.77,1932.

78. Landau,L. and Liftshitz,E.,"Fluid Mechanics",Vol. 6,Pergamon Press,p.39,198,1959.

79. Lang,S.B.,Ph.D. Thesis,University of California,1962.

80. Lang,S.B. and Wilke,C.R.,J. Colloid Sci.,21,153,(1966).

81. Lawson,G.B.,M.Sc. Thesis,University of Manchester,1964.

82. Lawson,G.B.,Ph.D. Thesis,University of Manchester,1967.

83. Lee,J.C. and Lewis,G.,Paper presented to I.Chem.E. Symposium on Liquid-liquid Extraction,University of Newcastle upon Tyne, April,1967.

83* Lee,J.C. and Hodgson,T.D.,Chem. Eng. Sci.,23,1375,(1968).

84. Levich,V.G.,"Physicochemical Hydrodynamics",Prentice Hall,1962.

85. Linton,M. and Sutherland,K.L.,J. Colloid Sci.,11,391,(1956).

86. Idem,Proc. 2nd Int. Congress on Surface Activity,I,p.494, Butterworths,1957.

87. Lowes,L. and Tanner,M.C.,British Patent No. 909485,1962.

88. MacKay,G.D.M. and Mason,S.G.,J. Colloid Sci.,16,632,(1961).

89. MacKay,G.D.M. and Mason,S.G.,Can. J. Chem. Eng.,41,203,(1963).

90. Mahajan,L.D.,Phil. Mag.,10,383,(1930).

91. Idem,Kolloid-Z,65,20,(1933).

92. Marangoni,G.G.M.,11 Nuovo Cimento,Ser.2,34,404,(1872).

93. McAvoy,R.M. and Kintner,R.C.,J. Colloid. Sci.,20,189,(1965).

94. MacDonald,J.E.,J. Meteorology,11,478,(1954).

95. Meissner,H.P. and Chertow,B.,I.E.C.,38,856,(1946).

96. National Physical Laboratory,"Notes on Applied Science No. 31, Schlieren Methods",H.M.S.O.,1963.

97. Nielsen,L.E.,Wall,R. and Adams,G.,J. Colloid Sci.,13,441,(1958).

98. Nielsen,L.E.,unpublished derivation obtained from Reference(44).

99. Overbeek,J.Th.G. and Sparnaay,J.,Disc. Faraday Soc.,18,12,(1954).

100. Perry,(Editor),"Chemical Engineers Handbook",3rd Edition,p.175, McGraw Hill,1950.

101. Picknett,R.G.,Ph.D. Thesis,University of London,1957.

102. Princen,H.M.,J. Colloid Sci.,18,178,(1963).

103. Princen,H.M. and Mason,S.G.,J. Colloid Sci.,20,156,(1965).

104. Prokorov,P.,Disc. Faraday Soc.,18,41,(1954).

105. Rayleigh,Lord,Proc. London Math. Soc.,10,4,(1878).

106. Idem,Proc. Roy. Soc.,A28,406,(1879).

107. Idem,Phil. Mag.,34,145,177,(1892).

108. Idem,ibid.,48,321,(1899).

109. Rehbinder,P.A. and Wenstrom,Kolloid-Z,53,145,(1930).

110. Renolds,O.,Chem. News,44,211,(1881).

111. Idem,Phil. Trans. Roy. Soc.,A177,157,(1886).

112. Rubcynski,W.,Bull. Acad. polon. sci.,1,40,(1911).

113. Sawistowski,H. and Goltz,G.E.,Trans. Instn. Chem. Engrs.,41, 174,(1963).

114. Schotland,R.M. and Hale,J.L.,"Drop Coalescence",Geophys. Res. Dir.,AD-263,589,AFCRL - 842,July,(1961).

115. Scriven,L.E. and Sternling,C.W.,Nature,187,186,(1960).

116. Sheludko,A.,Kolloid-Z,155,39,(1957).

117. Idem,Z. Electrochem,61,220,(1957).

118. Sheludko,R. and Platikanov,D. and Menev,E.,Disc. Faraday Soc., 40,253,(1965).

119. Smith,A.R.,Caswell,J.E.,Larson,P.P. and Cavers,S.D.,Can. J. Chem. Eng.,41,150,(1963).

120. Sternling,C.V. and Scriven,L.E.,A.I.Ch.E. Journal,5,514,(1959).

121. Stewart,G. and Thornton,J.D.,Paper presented to I.Chem.E. Symposium on Liquid-liquid Extraction,University of Newcastle upon Tyne,April,1967.

122. Taylor,G.I.,Proc. Roy. Soc.,A201,192,(1950).

123. Tomotika,S.,Proc. Roy. Soc.,A150,302,(1935).

124. Treybal,"Liquid-Liquid Extraction",McGraw Hill,New York.

125. Van den Temple,M.,Rec. Trav. Chim.,72,419,(1953).

126. Idem,J. Colloid Sci.,13,125,(1958).

127. Verwey and Overbeek,"Theory of the Stability of Lyophobic Colloids",Elsivier,New York,1948.

128. Wark.I.W. and Cox,A.B.,Nature,136,182,(1935).

129. Watanabe,T. and Kusui,M.,Bull Chem. Soc. Japan,31,237,(1958).

130. Waterman,L.G.,Paper presented at A.I.Ch.E. Conference,San Francisco,May,1965.

131. Weber,C.,Z. Angew. Math. Mech.,11,136,(1931).

132. Welch,J.E.,Harlow,F.H.,Shannon,J.P. and Daly,B.J.,"The MAC Method",Los Alamos Scientific Laboratory,Los Alamos,New Mexico, Vol. LA - 3425,1966.

COALESCENCE IN THE SYSTEM DECANOIC ACID—HEPTANE—WATER

By R. M. EDGE, Ph.D.*† and M. GREAVES, B.Tech.*

SYNOPSIS

The coalescence of a water droplet with an oil–water interface has been studied for the three-component system *n*-decanoic acid—*n*-heptane—water. It was found that the coalescence occurred in the stagewise manner and coalescence-time distributions are presented for four stages. The coalescence-time distribution of all stages may be correlated by equations similar to those presented by other workers for the first stage of coalescence with binary systems.

The variation of both the mean residence time and the standard deviations of the coalescence time distributions with the diameter of the primary drop are discussed, and correlations are presented for a number of conditions

Introduction

Recently, solvent extraction has been used for the recovery and separation of common metals and attention has been given to the use of long-chain carboxylic acids as the extracting agent [1] The technique of liquid—liquid extraction requires that one of the phases be dispersed, and the eventual coalescence of the dispersed phase may impose limitations on the capacity and operation of the plant These features, associated with plant operation led to an investigation into the phenomena of coalescence and the system heptane-decanoic acid-water was chosen for this purpose

The stability of single droplets at an oil—water interface has been studied for both stabilized[2–5] and unstabilized droplets [5–9] Although correlations describing the distributions of coalescence times of primary drops at an interface exist for two phase, two component systems there is no consensus of opinion as to the actual mechanism of coalescence Thus at the present time no adequate theory exists for predicting coalescence times from a knowledge of the physical properties of the system Jeffreys and Hawksley[10] have formed an empirical equation which enables first and overall stage times to be estimated for two component systems from a knowledge of the physical properties of the system They were able to obtain good agreement with their experimental coalescence times but not with the coalescence times reported by other workers This was attributed in part to different designs of equipment

The process of coalescence in many systems takes place in a stepwise fashion called "partial coalescence". This phenomenon of partial coalescence was first noticed by Wark and Cox[11] during froth flotation experiments and by Mahajan[12] during experiments with drops at liquid—liquid interfaces Cockbain and McRoberts[2] observed partial coalescence only occasionally, as did Linton and Sutherland,[13] for drops coalescing with themselves and with an air—liquid interface Charles and Mason[6] reported partial coalescence in every case, after a series of experiments with a number of two-component, liquid—liquid systems These investigators carried out an extensive study of the process by high-speed cine photography and suggested that the mechanism of partial coalescence is as follows:

> "following the rupture of the film separating the drop and the interface, the primary drop is deflated by the excess internal pressure, until a column is formed (see Fig 1) The radius, R, of the column continues to decrease from the action of the excess pressure (γ/R) until, the circumference becomes less than the height, and a Rayleigh disturbance can grow From here on there is a race between drainage and the necking down process, the outcome of which determines the size of the secondary droplet or droplets"

Figure 1 shows two secondary droplets resulting from a partial coalescence stage and with the system heptane—water this process of "double-drop" coalescence was observed in every case. It has been shown[6] that the drop diameter ratio, secondary to primary, r, varies with the viscosity ratio, p, and passed through a maximum near $p = 1$ Jeffreys and Hawksley[9] showed r varied with p[9] and generally, the larger the value of r the larger the number of coalescence stages However, no clearly defined regions were found to correspond to a given number of coalescence stages, and it was concluded that other factors have to be taken into account. The application of an electric field between the drop and the interface has been investigated[6, 14] and its effect is to promote drop coalescence Brown and Hanson[14] found that a high-frequency oscillating electric field brought about single-staged and instantaneous coalescence when a certain critical voltage was reached

Cockbain and McRoberts found that coalescence was unlikely to occur until a certain time, t_0, had elapsed, which depended on the system and experimental conditions

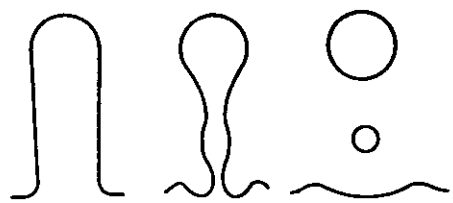

Fig 1 —*Simultaneous formation of two secondary droplets during partial coalescence (schematic)*

* Department of Chemical Engineering, University of Technology, Loughborough, Leicestershire

† *Present Address* Department of Chemical Engineering, University of Strathclyde, Montrose Street, Glasgow, C 1

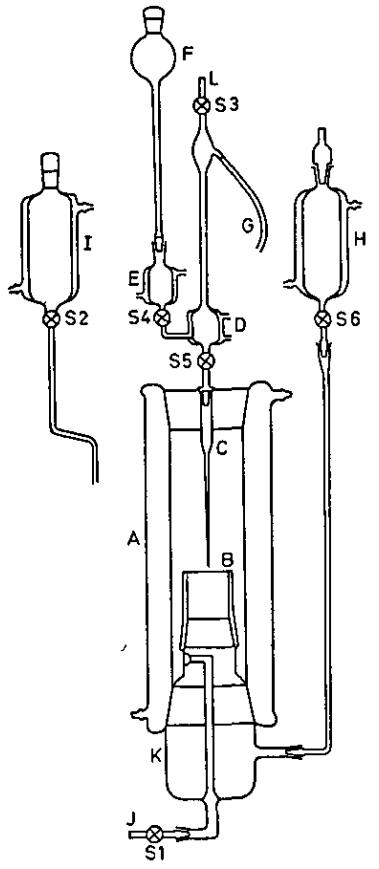

Fig 2—*Apparatus*

Gillespie and Rideal[7], whose results agreed with the above mechanism, suggested that a distorted drop profile previously observed by Derjaguin and Kussakov[15] for air—water systems could be applied to liquid—liquid systems They proposed the following equation †

$$\log\frac{N}{N_0} = -K(t-t_0)^{3/2} \quad . \quad . \quad (1)$$

to correlate their results

Elton and Picknett[3, 4] who studied the stability of droplets in the presence of electrolytes found that their results could not be correlated by equation (1) They proposed the equation

$$\log\frac{N}{N_0} = -ct^n \quad . \quad . \quad (2)$$

to correlate their results, where n has the value two for low electrolyte concentration and three for high electrolyte concentration

Coalescence time distributions for binary systems[8, 16] have also been correlated by

$$\log\frac{N}{N_0} = -K(t-t_0)^2 \quad . \quad . \quad (3)$$

and

$$\log\frac{N}{N_0} = -ct^4 \quad . \quad . \quad . \quad (4)$$

Equations (3) and (4) were used by Jeffreys and Lawson[17] to correlate coalescence time distributions for the ternary system acetone—benzene—water with mass transfer taking place

† *Symbols have the meanings given them on p.* 72.

Experimental

Apparatus

The apparatus used for the coalescence studies was made of glass and its construction is shown in Fig 2 To prevent seizure of glass to glass surfaces, PTFE sleeves were fitted to all ground glass joints and stopcock plugs were made of PTFE

The coalescence cell, A, consisted of a jacketed Pyrex tube, 42 cm long and 5 cm diam, fitted at each end with B55 ground glass joints The arrangement was such that the operation of the cell could be reversed to allow the study of the coalescence of rising droplets at a plane interface A method of interface renewal similar to that used by Charles and Mason[6] was employed The interface was maintained at the top of tube B, which was ground flat Various lengths of tube B were available to allow the interface to be positioned at a convenient height in the cell, A Drops were formed on a fine, drawn-out, glass capillary, C, approximately 18 cm long, the tip of which was ground flat and square The flow of liquid from the reservoir, D, to the capillary was controlled by a micrometer syringe connected to the reservoir by the PTFE tube, G The reservoir assembly was attached to a sliding frame which could be moved in a vertical direction A Perspex cabinet was used to enclose the coalescence apparatus and the whole assembly was mounted on an anti vibration stand The cell A and the various heavy and light phase reservoirs were enclosed in jackets maintained at 25 00°C ± 0 01 deg C In addition, fan-circulated air inside the Perspex cabinet was controlled at 25 00 ± 0 25 deg C

Cleaning

Prior to each series of observations the apparatus was thoroughly cleaned, in the following manner:

(1) All items of glassware and PTFE were degreased with acetone and rinsed with copious supplies of hot water

(2) The apparatus was filled with warm, concentrated chromic acid, freshly prepared, and allowed to stand for at least 24 h

(3) The apparatus was drained of chromic acid and vigorously rinsed with warm, freshly-distilled water for a prolonged period It was then dried in a hot-air oven During all the washing procedures and subsequent assembly great care was taken in handling the apparatus so as to prevent contamination

(4) Lastly, the apparatus was assembled in the Perspex cabinet, filled with distilled water, and left to stand overnight

Preparation of materials

The water used in all studies was double-distilled from potassium permanganate solution and stored in glass receivers The *n*-heptane used was to I P specification and was redistilled, except for experiments with the heptane—water, in which drop sizes of 0 162 and 0 264 cm were used

The decanoic acid was a "specially pure" grade, obtained in crystalline form from British Drug Houses Limited It was used without further purification All the solutions used were mutually saturated in glass receivers at 25°C

Filling and use of apparatus

After the double-distilled water had been drained from the apparatus, the saturated water phase was admitted to the reservoir, H, and a quantity was run through the coalescence cell, A, in order to purge any unsaturated water The drop

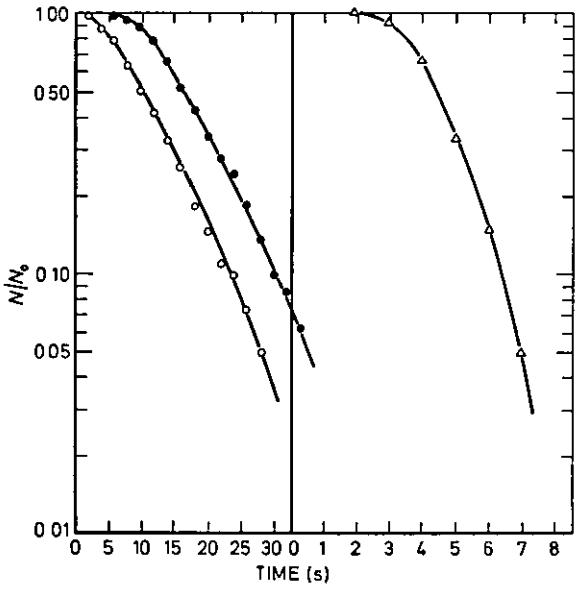

A

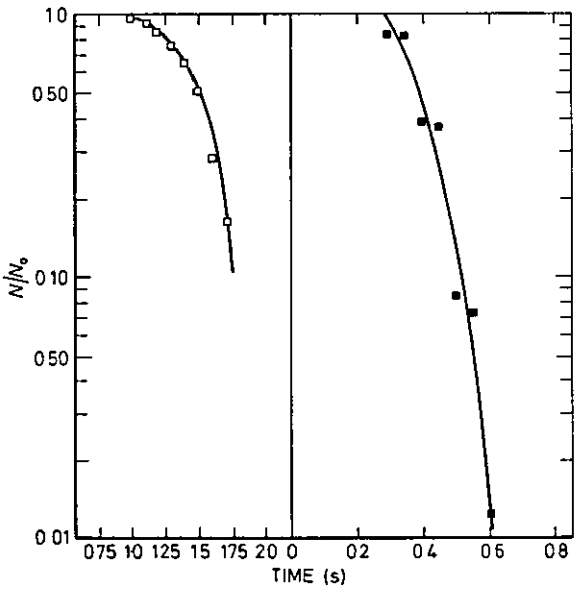

B

A Upper figure
● = overall stage
○ = first stage
△ = second stage
Drop size, a_1 = 0 172 cm

B Lower figure
□ = third stage
■ = fourth stage
Drop size, a_1 = 0 172 cm

Fig 3 —*Partial coalescence time distributions for system heptane–water*

forming arrangement was then lowered slightly so that the tip was just below the top of B With a suction bulb attached to L and s4 closed, the heavy-phase liquid was drawn up to a level just above s5 The suction bulb was removed and the drop forming arrangement was completely filled with liquid from the reservoir, F With s5 and s3 closed, the PTFE tube, G, and the micrometer syringe attached to it were also filled with liquid The light phase was then admitted to the coalescence cell from the reservoir I

The shape of the interface was adjusted by means of a suction bulb attached to H A water droplet was formed at the tip of the capillary by adjusting the micrometer syringe and its position relative to the interface was adjusted to that required by moving the frame supporting the drop forming device s5 was then closed and the whole apparatus together with its contents was allowed to come to equilibrium during a period of about 12 h

Before a series of readings was taken the interface was renewed and made plane, after which a short period was allowed for attainment of equilibrium The interface was subsequently adjusted after ten primary drops had been investigated and was renewed from time to time during a particular investigation

The coalescence was recorded on tape using a Ferguson " Model 3214 " tape recorder, each stage of coalescence being registered by a manually produced input signal The time between a drop arriving at the interface and the first stage of coalescence, and the times taken between the subsequent stages of coalescence, were determined with a stopwatch on playback of the tape

Reproducibility of coalescence times

Preliminary investigations of the coalescence time showed that there was a distribution about some mean value This is in accord with the findings of other workers in the field [2–4, 6–10 16] It was necessary therefore to determine the minimum drop count required to produce a reproducible distribution Coalescence-time distributions were determined for samples containing up to 300 drops for both a binary and ternary system It has been reported[6, 8] that the ratio $(t_m)_q/(t_{\frac{1}{2}})_q$ is the most reproducible characteristic of a particular distribution, and in fact, it was found that this ratio was reproducible with samples containing more than 50 drops However, this did not guarantee that the actual distribution curve was the same With a sample of 75 drops the distribution curve was reproducible and this was taken as the minimum drop count Generally, samples of this size have been used by other workers [3, 4, 6 8 9, 16]

Results

For both binary and ternary systems, partial coalescence was observed in every case In the binary system heptane—water there were four visible stages, whereas five or sometimes six were visible in the three-component system In the latter case, the droplet sizes of the fifth and sixth stages were extremely small and the coalescence time correspondingly was very short and could not be recorded manually

It should be mentioned that in the binary system, in which redistilled heptane was used (see Figs 3A and 3B), the first stage of coalescence took place by what is known as " double-drop " coalescence This was invariably the case though the satellite droplet was small in comparison with the parent droplet According to the theory proposed by Charles and Mason,[6] a Raleigh disturbance of the type illustrated in Fig 1 is responsible for this phenomenon Hawksley[8] has suggested that contamination of the system may result in double-drop coalescence, but this seems unlikely since this phenomenon was not observed with undistilled heptane

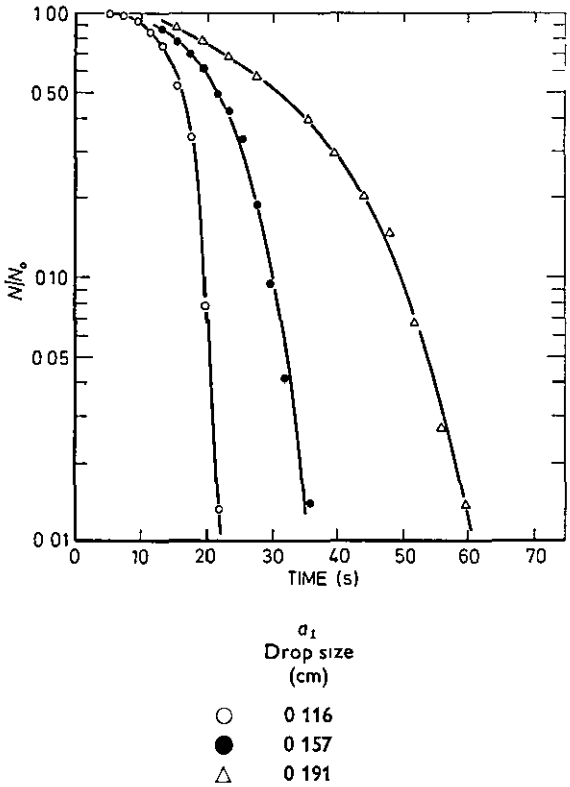

Fig 4 —*Overall coalescence time distributions for system 0 5M decanoic acid—heptane—water*

Coalescence times

The interval between the drop arriving at the interface and the first stage of coalescence, t_1, and the intervals between three further stages of coalescence, t_2, t_3, and t_4 respectively, were determined Typical results are presented in Fig 3 for heptane—water and in Figs 4–8 for the 0 5M decanoic acid—heptane—water system The values of t_m, the mean coalescence time, and $t_{\frac{1}{2}}$, the time for 50% coalescence, were calculated from the distributions obtained for each stage and the values of t_m are presented in Table I and Figs 9, 10, and 11. The overall mean coalescence time $\hat{t}_m$, defined as the sum of the partial coalescence times

The term

$$\sum_{q=1}^{4} (t_m)_q$$

is also presented in Table I and Table II lists values of $[(t_m)_q/(t_{\frac{1}{2}})_q]_{\text{Average}}$ and $[\hat{t}_m/\hat{t}_{\frac{1}{2}}]_{\text{Average}}$ where these ratios are the average values for the range of drop sizes which were investigated These are presented so that a comparison can be made with the values obtained by other workers (Table III), however, we do not regard them as very useful characteristics of the system because, by definition, they are dependent on a number of distributions thereby making their nature complex

In the system decanoic acid—heptane—water, the effect of increasing the concentration of the third-component (decanoic acid) is shown in Figs 12–15 The concentrations used were 0 05, 0 5, 1 0M and the droplet sizes were respectively 0 156, 0 157, and 0 152 cm equivalent spherical radius

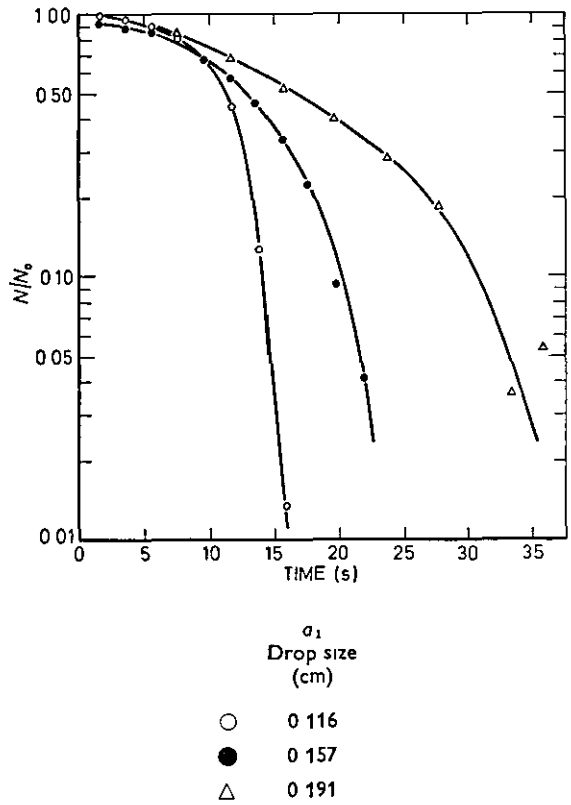

Fig 5 —*First stage coalescence time distributions for system 0 5M decanoic acid—heptane—water*

TABLE I —*Mean Coalescence Time for each Partial Coalescence Stage at Different Fall Heights for the Systems Heptane—Water and 0 5M Decanoic Acid—Heptane—Water*

System	Equivalent spherical radius of the drop (cm)	Distance of fall to the interface (cm)	$\hat{t}_m$ (s)	$(t_m)_1$ (s)	$(t_m)_2$ (s)	$(t_m)_3$ (s)	$(t_m)_4$ (s)
Heptane—Water	0 172	0	18 13	11 89	4 50	1 41	0 33
	0 174	2 5	14 44	6 84	5 63	1 66	0 31
	0 174	5 0	14 47	6 29	6 18	1 80	0 20
0 5 M Decanoic	0 116	0	15 66	10 73	3 56	1 37	*
Acid—Heptane—Water	0 119	2 5	19 51	12 53	5 08	1 90	*
	0 116	5 0	15 77	9 15	5 00	1 62	*

* Mean coalescence times were not recorded for this stage

TABLE II —*Values of the Ratios* $[(t_m)_q/(t_{\frac{1}{2}})_q]_{\text{Average}}$ *for each Partial Coalescence Stage and* $[\hat{t}_m/\hat{t}_{\frac{1}{2}}]_{\text{Average}}$ *for Overall Coalescence*

Decanoic Acid Concentration	System	Stage				
		Overall	1st	2nd	3rd	4th
0	Heptane—Water	1 10	1 27	1 12	1 01	1 04
0 05M	Decanoic Acid—Heptane—Water	1 04	1 10	1 03	1 02	1 05
0 5M	Decanoic Acid—Heptane—Water	1 06	1 12	1 11	1 05	1 06
1 0M	Decanoic Acid—Heptane—Water	1 18	1 18	1 14	1 06	1 12

Disscussion

Correlation of coalescence-time distribution

Previous workers have suggested that the distribution of $\hat{t}$, the overall coalescence-time, and of t_1, the coalescence-time of the first stage of the coalescence, may be correlated by equations which are of the form

$$\log \frac{N}{N_0} = -K(t-t_0)^n \qquad (5a)$$

or of the form

$$\log \frac{N}{N_0} = -ct^n \qquad (5b)$$

For both the heptane—water and the decanoic acid—heptane—water systems the distribution of the coalescence times of each stage of the coalescence can be represented by equation (5*a*) (Figs 16 and 17) However, with a sample containing only 70 drops, it is not possible to select particular values of t_0 and n from a range of connected values of these parameters and all of the distributions are correlated satisfactorily by equation (5*a*) with $t_0 = 0$ [*i e* by equation 5(*b*)] For example, the distributions of coalescence times for the system 0 5M decanoic acid—heptane—water are correlated satisfactorily by equation (5*b*) with n equal to 1 7, 3 57, and 5 1 for the first, second, and third stages of coalescence respectively However the usefulness of equation (5*b*) may be limited by the high values of n which are obtained for the latter stages of the coalescence Figure 16 and the values of n which are quoted above for equation (5*b*) illustrate how wide is the range of values of t_0 and n which are possible when only 70 results are avilable (the usual number analysed by other workers) Although the true values of n and t_0 in equation (5) may not be determined with accuracy, it is apparent that n increases with the stage of the coalescence

The distributions may also be correlated using arithmetic probability plots and an example is shown in Fig 18 Although this test of normality is insensitive[18] and the sample size is too small to allow any firm conclusions to be made, a number of features not immediately observable in Fig 16 and Fig 17 can be seen Several distributions are best represented by two straight lines Usually, the intersection of the lines is at $0\ 85 < N/N_0$ or $< 0\ 15$ and the one line exists only in a region where the accuracy of N/N_0 is not high, because of the small sample on which it is based However, it may be possible that certain distributions are best represented by the sum of two distributions It should be mentioned that if two normal distributions were involved, the two straight lines would in fact be replaced by a curve, lying near to the lines Generally, equation (5) correlates the results better than a normal distribution It is intended to repeat at least part of the investigation with increased sample sizes to determine the form of the correlation with more certainty

TABLE III —*Values of* $[(t_m)_1/(t_{\frac{1}{2}})_1]_{\text{Average}}$ *and* $[\hat{t}_m/\hat{t}_{\frac{1}{2}}]_{\text{Average}}$

	System	$\left[\frac{(t_m)_1}{(t_{\frac{1}{2}})_1}\right]_{\text{Average}}$	$\left[\frac{\hat{t}_m}{\hat{t}_{\frac{1}{2}}}\right]_{\text{Average}}$
Present Authors	Heptane—Water	1 27	1 10
Lawson[16]	Benzene—Water	1 09	1 04
Charles & Mason[6]	Benzene—Water	1 11	—
Hawksley[8]	Benzene—Water	1 04	1 01

Properties of coalescence time distributions

CORRELATION OF MEAN COALESCENCE TIMES

The mean coalescence times of the secondary and tertiary droplets are given in Fig 9 at three decanoic acid concentrations, as a function of the size of the primary drop, a_1 It

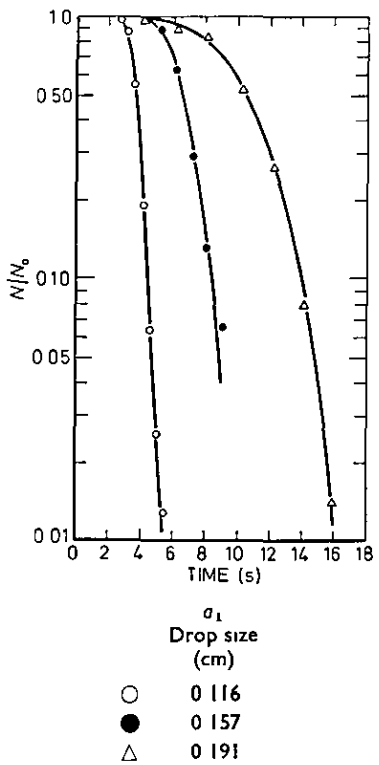

Fig 6 —*Second stage coalescence time distributions for system 0 5M decanoic acid—heptane—water*

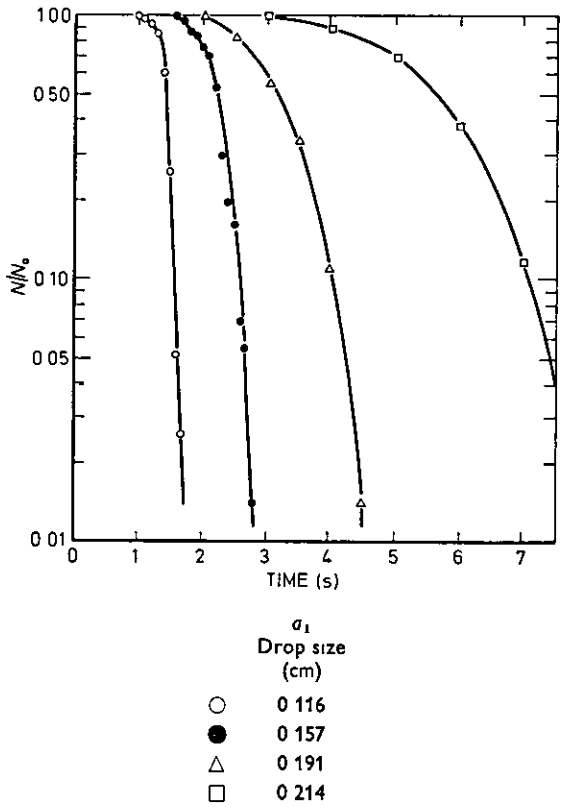

Fig 7—*Third stage coalescence time distributions for system 0 5M decanoic acid—heptane—water*

can be seen that, within the accuracy of the results, the relationship is linear for the third stage at the three concentrations investigated, and also for the second stage at the two highest concentrations employed The resultant curves for 0 5M and 1 0M solutions coincide for both the second and third stages of coalescence, whilst the third stage of coalescence with a 0 05M solution shows lower coalescence times than do the curves for the 0 5M and 1 0M solutions The results for the third stage of coalescence with a 0 05M solution suggest a minimum corresponding to $a_1 = 0\ 16$ cm, approximately The graphs obtained for the first stage of coalescence (Fig 10) are less well defined but with both the 0 5M and 1 0M solutions the mean coalescence time increases as the droplet size increases With the 0 05M solution a minimum is again suggested at a drop size similar to that at which the minimum in the second stage occurred The curves obtained for heptane—water are given in Fig 11, and for comparison Fig 9 is superimposed In this case, the curves for all stages indicate a minimum corresponding to a primary drop size, approximately, of $a_1 = 0\ 18$ cm It is intended to carry out further work to investigate this phenomenon

STANDARD DEVIATION OF COALESCENCE-TIME DISTRIBUTION

The standard deviation of the normal distribution which best fitted the coalescence-time distributions over the range $0\ 1 < N/N_0 < 0\ 9$ was determined for each stage of the coalescence It was found that for both 0 5M and 1 0M decanoic acid solutions the standard deviation for the third stage of the coalescence increased with increase in the standard deviation for the second stage of the coalescence The relationship was well described by the equation

$$\sigma_3 = 0\ 21\ \sigma_2 \qquad (6)$$

A similar relationship was obtained for the second and third stages of the coalescence with the heptane—water system although the correlation was less satisfactory However, it was expected that the correlation would be less satisfactory because several distributions obtained for this system were not adequately described by a single normal distribution

The standard deviation for the first stage of the coalescence was also found to increase with increase in the standard deviation for the second stage of the coalescence for both 0 5M and 1 0M decanoic acid solutions The relationship was linear for the 0 5M solution

With 0 5M and 1 0M decanoic acid solutions the standard deviation of the coalescence-time distribution could be related to the mean of the distribution Linear relationships were found for both the second and the third stages of the coalescence

These findings together with Fig 9 suggest that with the system decanoic acid—*n*-heptane—water and small drop-sizes there is a simple relationship between the drop size and the constants in the equations which describe the coalescence-time distributions Also that there is a linear relationship between the size of the drop before coalescence and the size of the drop which is subsequently produced by the coalescence

Effect of distance of fall

Although Jeffreys and Hawksley[9] and Lawson[16] have reported that the coalescence time increases with the distance of fall of the primary drop on to the interface, other workers have not found a satisfactory relationship A number of experiments carried out by us for heptane—water have also been inconclusive It is worth noting that immediately after formation, drops in free fall undergo oscillation from a prolate to an oblate spheroid This oscillation may be con-

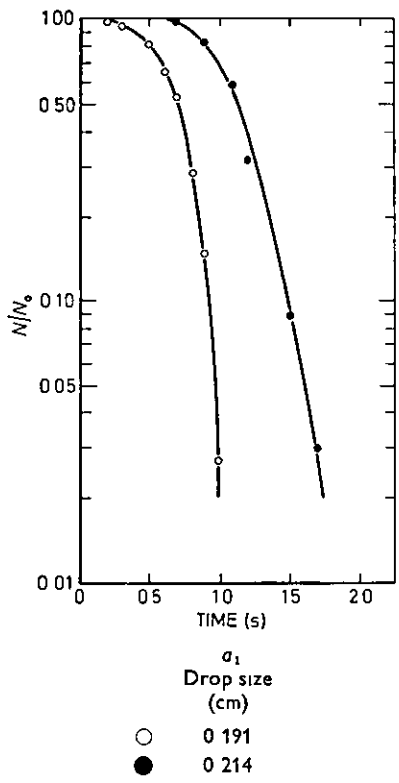

Fig 8—*Fourth stage coalescence time distributions for system 0 5M decanoic acid—heptane—water*

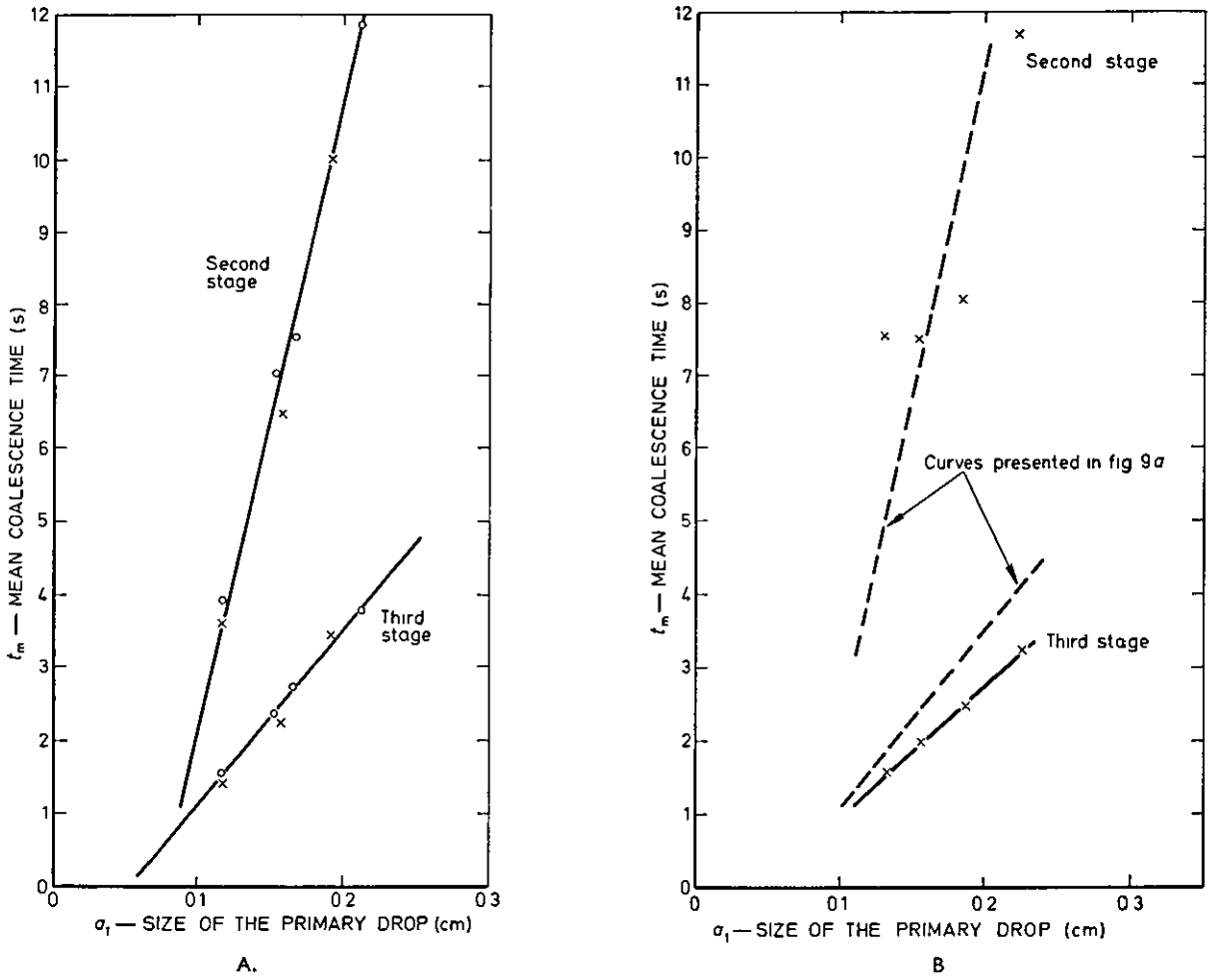

A Upper figure
× 0 5M decanoic acid
○ 1 0M decanoic acid
All drops formed at the interface

B Lower figure
0 05M decanoic acid

Fig 9 —*Mean coalescence times of the second and third stages of coalescence as a function of the size of the primary drop*

siderable with the purified, two-component systems investigated, especially when larger sizes of drop are being used As it is likely that the shape of the drop on arrival at the interface is an important factor in the coalescence, it is possible that the relationship between coalescence time and distance of fall will be oscillatory in form

Three fall heights, namely 0, 2 5, and 5 0 cm, were investigated for the system 0 5M decanoic acid—heptane—water, using drops having an equivalent spherical radius $a_1 = 0\ 116$ cm The results are quoted in Table I Using Fig 9, the mean coalescence times for the second and third stages of coalescence obtained with fall lengths of 2 5 and 5 0 cm are equal to those obtained for drops with $a_1 = 0\ 125$ and 0 135 cm formed at the interface It would appear therefore that when the primary drop is formed some distance from the interface, larger secondary and tertiary drops are produced than when the primary drop is formed at the interface The ratio of the standard deviations of the coalescence-time distributions of the second and third stages was found to be in agreement with that found for drops which were formed at the interface

Conclusions

For the systems heptane—water and decanoic acid—heptane—water the distribution of coalescence times for all stages of the coalescence may be represented by equations of the form

$$\log \frac{N}{N_0} = -K(t-t_0)^n$$

However, with a sample size of 70–80 drops, it has not been possible to select the actual correlation as a range of interconnected values of n and t_0 is possible

The mean coalescence times for all the stages of coalescence, with 0 5M and 1 0M solutions of decanoic acid in heptane, were found to increase with the size of the primary drop With 0 05M solution, a similar trend was shown by the later stages of the coalescence, but the early stages exhibited a minimum in the relationship With heptane and water all stages exhibited this minimum

The standard deviations of the coalescence time distributions of the third and fourth stages of coalescence are shown

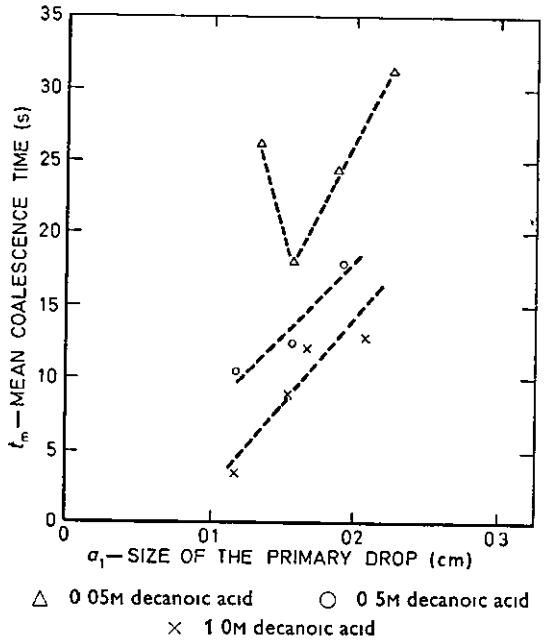

Fig 10 —*Mean coalescence time of the first stage of coalescence as a function of the size of the primary drop*

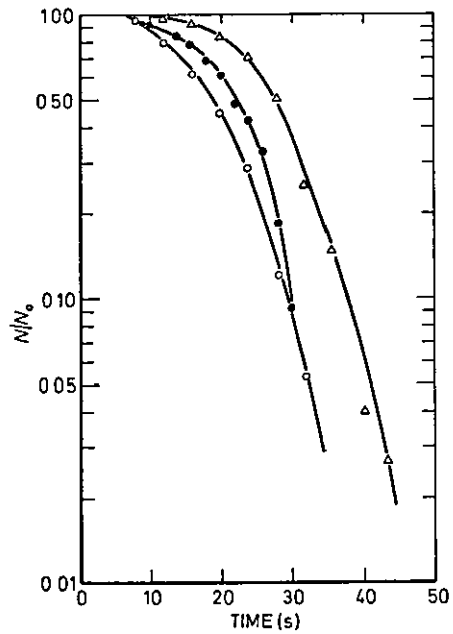

	a_1 Drop size (cm)	Concentration of decanoic acid
○	0 152	1 00M
●	0 157	0 50M
△	0 156	0 05M

Fig 12 —*Effect of acid concentration on the overall coalescence time distributions for the system decanoic acid—heptane—water*

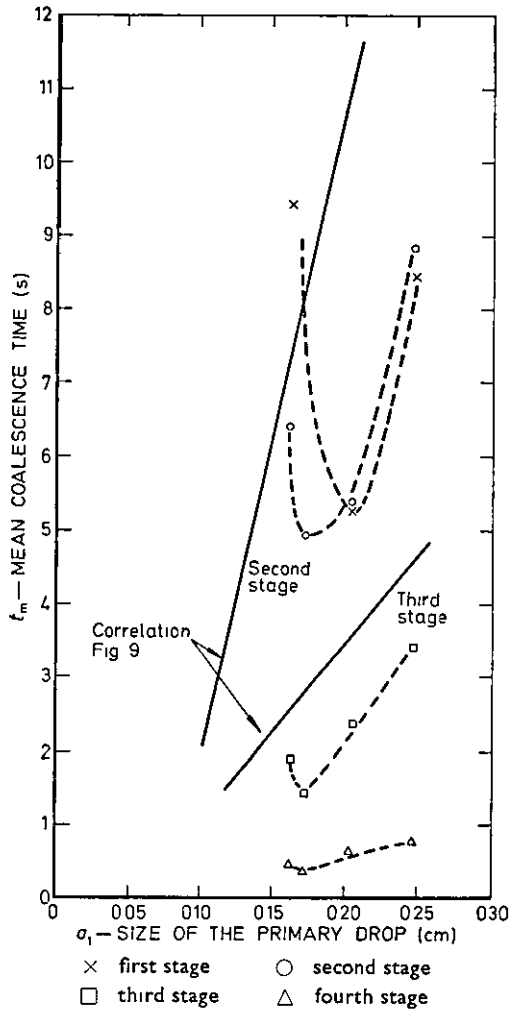

Fig 11 —*Relationship between the mean coalescence time and the primary drop size for the system heptane—water*

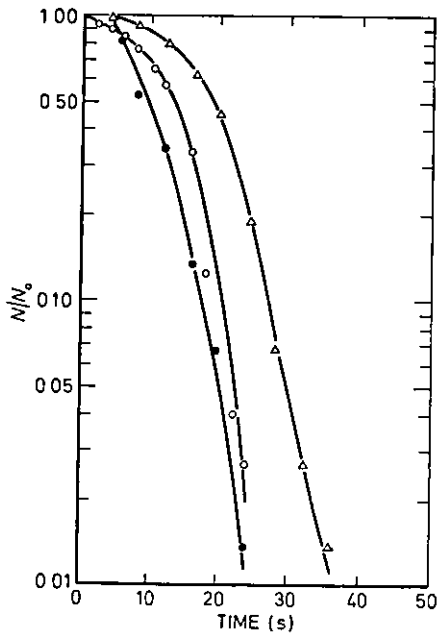

	a_1 Drop size (cm)	Concentration of decanoic acid
○	0 152	1 00M
●	0 157	0 50M
△	0 156	0 05M

Fig 13 —*Effect of acid concentration on the first stage coalescence time distributions for the system decanoic acid—heptane—water*

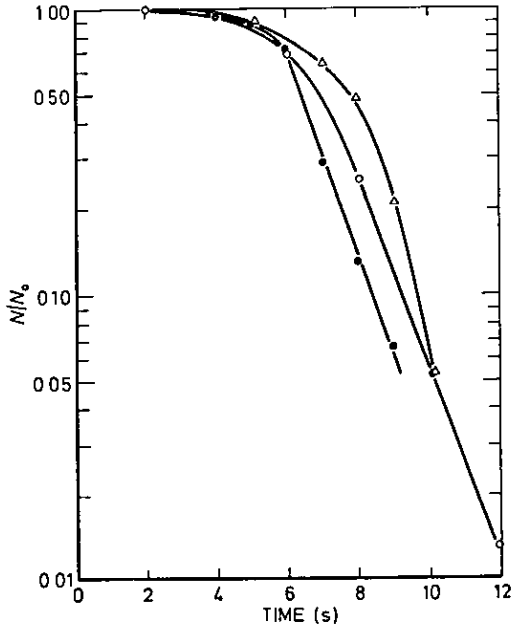

	a_1 Drop size (cm)	Concentration of decanoic acid
○	0 152	1 00M
●	0 157	0 50M
△	0 156	0 05M

Fig 14 —*Effect of acid concentration on the second stage coalescence time distributions for the system decanoic acid—heptane—water*

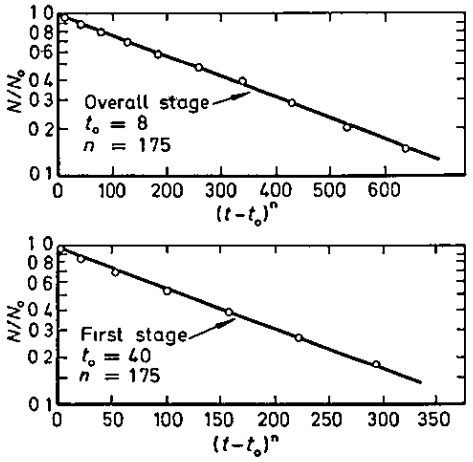

0 5M decanoic acid

Drop size, a_1 = 0 191 cm

Fig 16 —*Correlation of distributions for the system heptane—decanoic acid—water using equation (5a)*

to be related when 0 5M and 1 0M solutions of decanoic acid are used

Acknowledgment

The authors wish to acknowledge the financial support given by the Warren Spring Laboratory, Ministry of Technology, to carry out this work

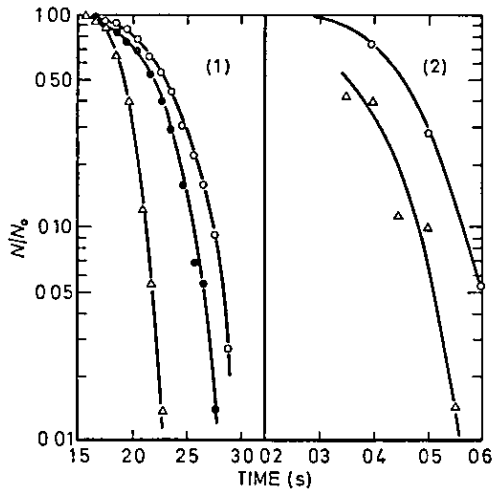

	a_1 Drop size (cm)	Concentration of decanoic acid
○	0 152	1 00M
●	0 157	0 50M
△	0 156	0 05M

Fig 15 —*Effect of acid concentration on* (1) *third stage,* (2) *fourth stage coalescence time distribution for the system decanoic acid—heptane—water*

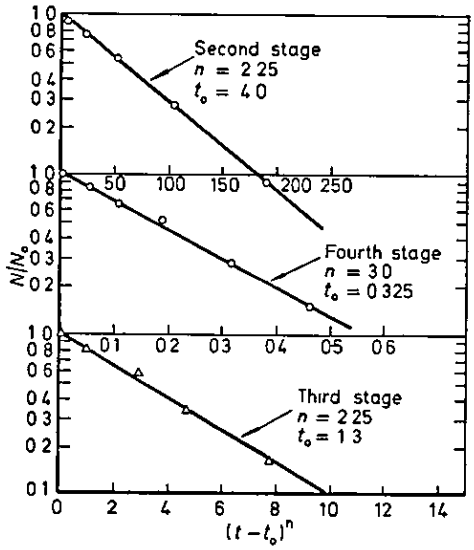

0 5M decanoic acid

Drop size, a_1 = 0 191 cm

Fig 17 —*Correlation of distributions for the system heptane—decanoic acid—water using equation (5a)*

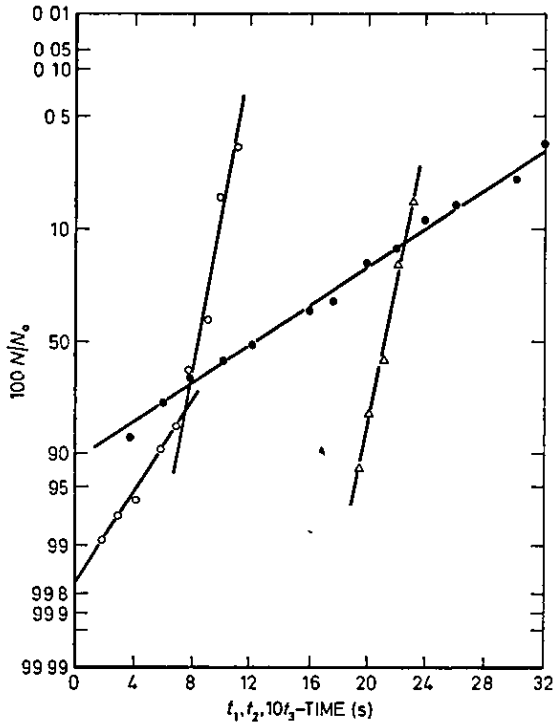

Fig 18 —*Correlation of coalescence time distributions for the system heptane—water using probability paper*

Symbols Used

a_1 = radius of primary drop

a_2 = radius of secondary droplet

n = power in equation (5)

c = a constant in equations (2), (4), and (5*b*)

K = a constant in equations (1), (3), and (5*a*)

N = number of drops not coalescing in time t

N_0 = total number of drops assessed

t_q = coalescence time for qth coalescence stages, where q is 1 to 4.

$\hat{t}$ = overall coalescence time $\left(= \sum_{q=1}^{4} t_q\right)$.

$(t_m)_q$ = mean colaescence time for qth coalescence stage, where q is 1 to 4

$\hat{t}_m$ = mean overall coalescence time $\left[= \sum_{q=1}^{4} (t_m)_q\right]$

$(t_{\frac{1}{2}})_q$ = half-life coalescence time for qth coalescence stage, where q is 1 to 4.

$\hat{t}_{\frac{1}{2}}$ = overall half-life coalescence time $\left[= \sum_{q=1}^{4} (t_{\frac{1}{2}})_q\right]$

t_0 = initial drainage period for the film between the drop and the interface Equal to the minimum value of t_q

$[(t_m)_q/(t_{\frac{1}{2}})_q]_{\text{Average}}$ = the average value of $(t_m)_q/(t_{\frac{1}{2}})_q$ for the range of drop sizes which were investigated

$[\hat{t}_m/\hat{t}_{\frac{1}{2}}]_{\text{Average}}$ = the average value of $\hat{t}_m/\hat{t}_{\frac{1}{2}}$ for the range of drop sizes which were investigated

R = radius of liquid column

M = molar concentration of decanoic acid in heptane

ρ = viscosity ratio $(= \mu_1/\mu_2)$

μ_1 = viscosity of droplet liquid

μ_2 = viscosity of liquid surrounding droplet

γ = interfacial tension

σ_q = standard deviation of the coalescence time distribution of the qth coalescence stage where q is 1 to 4

The above quantities may be expressed in any set of consistent units in which force and mass are not defined independently

References

1 Fletcher, A W *Loughborough University of Technology Chemical Engineering Society Journal*, 1966, **2**, 23

2 Cockbain, E G , and McRoberts, T S *J Colloid Sci* , 1953, **8**, 40

3 Elton, G A H , and Picknett, R G in "*Proceedings of the Second International Congress on Surface Activity*", 1957, Vol 1, p 288 (London Butterworths Scientific Publications)

4 Picknett, R G *Ph D Thesis*, 1958 University of London

5 Nielson, L E , Wall, R , and Adams, G *J Colloid Sci* , 1958, **13**, 441

6 Charles, G E , and Mason, S G *J Colloid Sci* , 1960, **15**, 105 *Idem ibid* , 236 *Idem ibid* , 245

7 Gillespie, T and Rideal, E K *Trans Faraday Soc* , 1956, **52**, 173

8 Hawksley, J L *Ph D Thesis*, 1963 University of Birmingham

9 Jeffreys, G V , and Hawksley, J L *J appl Chem* , 1962, **12**, 329

10 Jeffreys, G V , and Hawksley, J L *A I Ch E Jl*, 1965, **5**, 416

11 Wark, I W , and Cox, A B *Nature, Lond* , 1935, **136**, 182

12 Mahajan, L D *Kolloidzeitschrift*, 1934, **69**, 19

13 Linton, M , and Sutherland, K L *J Colloid Sci* , 1956, **11**, 391

14 Brown, A H , and Hanson, C *Trans Faraday Soc* , 1965, **61**, 1756

15 Derjaguin, B V , and Kussakov, M *Acta phys -chim URSS*, 1939, **10**, 25

16 Lawson, G B *M Sc Tech Thesis* 1965 University of Manchester

17 Jeffreys, G V , and Lawson, G B *Trans Instn chem Engrs*, 1965, **43**, T297

18 Freund, J E "*Modern Elementary Statistics*", 1960, 2nd Edition, p 184 (New York Prentice-Hall Inc)